AD-786 959

DESIGN AND STRENGTH OF AIRCRAFT AND HELICOPTERS

K. D. Mirtova, et al

Foreign Technology Division
Wright-Patterson Air Force Base, Ohio

18 September 1974

UNCLASSIFIED

Security Classification

DOCUMENT CONTROL DATA - R & D AD 786 959

(Security classification of title, body of abstract and indexing annotation must be entered when the overall report is classified)

1. ORIGINATING ACTIVITY (Corporate author)
Foreign Technology Division
Air Force Systems Command
U. S. Air Force

2a. REPORT SECURITY CLASSIFICATION
UNCLASSIFIED

2b. GROUP

3. REPORT TITLE

DESIGN AND STRENGTH OF AIRCRAFT AND HELICOPTERS

4. DESCRIPTIVE NOTES (Type of report and inclusive dates)
Translation

5. AUTHOR(S) (First name, middle initial, last name)

K. D. Mirtova and Zh. S. Chernenko

6. REPORT DATE	7a. TOTAL NO. OF PAGES	7b. NO. OF REFS
1972	679	14

8a. CONTRACT OR GRANT NO.	9a. ORIGINATOR'S REPORT NUMBER(S)
b. PROJECT NO	FTD-MT-24-406-74
c.	9b. OTHER REPORT NO(S) (Any other numbers that may be assigned this report)
d.	

10. DISTRIBUTION STATEMENT

Approved for public release; distribution unlimited.

11. SUPPLEMENTARY NOTES	12. SPONSORING MILITARY ACTIVITY
	Foreign Technology Division Wright-Patterson AFB, Ohio

13. ABSTRACT

01

DD FORM 1 NOV 68 1473

UNCLASSIFIED

Security Classification

EDITED MACHINE TRANSLATION

FTD-MT-24-406-74 18 September 1974

DESIGN AND STRENGTH OF AIRCRAFT AND HELICOPTERS

By: K. D. Mirtova and Zh. S. Chernenko

English pages: 655

Source: Konstruktsiya i Prochnost' Samoletov i Vertoletov, 1972, pp. 1-440

Country of Origin: USSR
Requester: FTD/PDXS
This document is a SYSTRAN machine aided translation, post-edited for technical accuracy by: Joseph E. Pearson
Approved for public release; distribution unlimited.

PREPARED BY:

TRANSLATION DIVISION
FOREIGN TECHNOLOGY DIVISION
WP-AFB, OHIO.

TABLE OF CONTENTS

All figures, graphs, tables, equations, etc. merged into this translation were extracted from the best quality copy available.

U. S. BOARD ON GEOGRAPHIC NAMES TRANSLITERATION SYSTEM

Block	Italic	Transliteration	Block	Italic	Transliteration
А а	*А а*	A, a	Р р	*Р р*	R, r
Б б	*Б б*	B, b	С с	*С с*	S, s
В в	*В в*	V, v	Т т	*Т т*	T, t
Г г	*Г г*	G, g	У у	*У у*	U, u
Д д	*Д д*	D, d	Ф ф	*Ф ф*	F, f
Е е	*Е е*	Ye, ye; E, e*	Х х	*Х х*	Kh, kh
Ж ж	*Ж ж*	Zh, zh	Ц ц	*Ц ц*	Ts, ts
З з	*З з*	Z, z	Ч ч	*Ч ч*	Ch, ch
И и	*И и*	I, i	Ш ш	*Ш ш*	Sh, sh
Й й	*Й й*	Y, y	Щ щ	*Щ щ*	Shch, shch
К к	*К к*	K, k	Ъ ъ	*Ъ ъ*	"
Л л	*Л л*	L, l	Ы ы	*Ы ы*	Y, y
М м	*М м*	M, m	Ь ь	*Ь ь*	'
Н н	*Н н*	N, n	Э э	*Э э*	E, e
О о	*О о*	O, o	Ю ю	*Ю ю*	Yu, yu
П п	*П п*	P, p	Я я	*Я я*	Ya, ya

* ye initially, after vowels, and after ъ, ь; e elsewhere. When written as ё in Russian, transliterate as yё or ё. The use of diacritical marks is preferred, but such marks may be omitted when expediency dictates.

FOLLOWING ARE THE CORRESPONDING RUSSIAN AND ENGLISH

DESIGNATIONS OF THE TRIGONOMETRIC FUNCTIONS

Russian	English
sin	sin
cos	cos
tg	tan
ctg	cot
sec	sec
cosec	csc
sh	sinh
ch	cosh
th	tanh
cth	coth
sch	sech
csch	csch
arc sin	$\sin^{-1}$
arc cos	$\cos^{-1}$
arc tg	$\tan^{-1}$
arc ctg	$\cot^{-1}$
arc sec	$\sec^{-1}$
arc cosec	$\csc^{-1}$
arc sh	$\sinh^{-1}$
arc ch	$\cosh^{-1}$
arc th	$\tanh^{-1}$
arc cth	$\coth^{-1}$
arc sch	sech^{-1}
arc csch	csch^{-1}
rot	curl
lg	log

GREEK ALPHABET

Alpha	A	α		Nu	N	ν		
Beta	B	β		Xi	Ξ	ξ		
Gamma	Γ	γ		Omicron	O	o		
Delta	Δ	δ		Pi	Π	π		
Epsilon	E	ε	ϵ	Rho	P	ρ	ϱ	
Zeta	Z	ζ		Sigma	Σ	σ	ς	
Eta	H	η		Tau	T	τ		
Theta	Θ	θ	ϑ	Upsilon	T	υ		
Iota	I	ι		Phi	Φ	φ	ϕ	
Kappa	K	κ	ϰ	Chi	X	χ		
Lambda	Λ	λ		Psi	Ψ	ψ		
Mu	M	μ		Omega	Ω	ω		

Design and strength of aircraft and helicopters. Voskoboynik M. S., Lagosyuk G. S., Milen'kiy Yu. D., Mirtov K. D., Oskin D. P., Skripka M. L., Ushakov V. S., Chernenko Zh. S. Publishing House "transport", 1972, pages 1-440.

This manual sets forth the sequence of the design and construction of flight vehicles; it relates the conditions of their loading, the selection of rational shapes and structure diagrams; it examines the general questions of design, strength and operation of the basic parts of flight vehicles, their reliability, durability and effectiveness.

This manual corresponds to a course program on the design and strength of flight vehicles, the mastery of which is necessary for the understanding and the resolution of questions on the design and strength of aircraft and helicopters which can be encountered in the practical activity of a mechanical engineer during the operation of flight vehicles and engines of civil aviation

This manual was written by the instructors of the departments of design and strength of flight vehicles of the Riga and Kiev institutes of engineers of civil aviation. It is intended for the students of higher educational institutions, and also can be used by the flight and technical-engineering personnel of production subdivisions. Figures - 260, Tables - 14, Bibliographical references - 14.

Introduction, chapters 1-4, 6, 9-14 were written by M. S. Voskoboynik, Yu. D. Milen-kiy,

K. D. Myrtles, D. P. Osokin, M. L. Skripka and V. S. Ushakov; chapters 5, 7 and 8 were written by G. S. Lagosyuk, K. D. Mirtov, D. P. Osokin, M. L. Skripka, V. S. Ushakov and Zh. S. Chernenko.

INTRODUCTION

§ 1. PROBLEMS AND STRUCTURE OF THE COURSE

This course on the design and the strength of flight vehicles is an applied engineering discipline. It sets forth the rules of aircraft and helicopter design and the methods of determining their strength.

The present manual covers the materials of this discipline necessary for the mechanical engineer with respect to the operation of the flight vehicles and engines of civil aviation.

For mastery of this discipline it is necessary to have knowledge of the course on the basics of aviation technology, which is studied in the first semester. Illuminated in it is the history of the development of civil aviation, the classification of flight vehicles is presented, the most contemporary designs of aircraft and helicopters is discussed, the prospects for their development are indicated.

Of great value for understanding of the questions of the design and strength of flight vehicles is the preliminary study of such engineering disciplines as aviation materials science, strength of materials, machine parts, aerodynamics, etc. For

these purposes it is also necessary to have knowledge of specific sections of mathematics and mechanics.

Since the course on the design and strength of flight vehicles can be studied in parallel with the course on the aerodynamics of flight vehicles, or with a certain foreknowledge, sufficient attention is given in this manual to the examination of the aerodynamic bases of the layout of flight vehicles.

For better understanding of the operation of flight vehicle parts the questions of design and strength are presented together. Design work in a number of cases is explained with the aid of approximate methods of calculation.

In studying flight vehicle parts the technical requirements and the principles of designs and strength rating are examined first, then on the basis of this design specimens are studied.

In connection with this, the material in this manual is set forth in a sequence which corresponds to the program of the course structure:

1) the conditions of flight vehicle loading;

2) the design and the strength of the airframe;

3) the design and the strength of the systems and mechanisms;

4) questions of design and evaluation of the effectiveness of flight vehicles.

§ 2. OPERATIONAL AND TECHNICAL REQUIREMENTS IMPOSED ON A FLIGHT VEHICLE

For the creation of a new flight vehicle a clear formulation of requirements, which it should satisfy, is necessary.

The contemporary level of the development of aviation technology and the prospects for its perfection should be thoroughly taken into account in the requirements. The thorough consideration and validity of these requirements are necessary to ensure the complete conformity of the flight vehicle to its purpose.

During the designing the technical assignment and the summary of the operational and technical requirements for a new flight vehicle are worked out by the customer organization and are coordinated with the office designers.

The operational and technical requirements are divided into two groups:

1) the requirements imposed on the aviation engineering data, the loading and the equipment of the flight vehicle. They pertain to each actual aircraft and helicopter being designed and are determined by its purpose and the missions to be carried out.

During the designing it is necessary to attain the best possible indices with respect to the most important aviation engineering data for the flight vehicle in question. This should be ensured by the application of the most advanced achievements in science and technology and should not operate due to an impermissible reduction in any other indices;

2) technical requirements imposed on the design. They are more general and can pertain to specific classes of flight vehicles. These requirements will be further examined in connection with the design parts being studied.

The design aircraft and helicopter airframes can be divided into the following basic groups:

airframe: wing, empennage, fuselage, engine mounts;

power-distribution systems and mechanisms: landing gear, control systems and mechanisms;

fixed equipment: high-altitude, deicing and others.

The technical requirements imposed on a design can be classified in the following manner:

1) the requirements ensuing from the purposes of the design which express the necessity for the correspondence of the design to its purpose. For example, a wing should create lift, the landing gear should ensure the possibility of the aircraft to move along the ground, etc.;

2) the strength requirements which express the necessity for ensuring with the least design weight of its sufficient strength and rigidity, the absence of vibrations, the presence of the proper service life, reliability and durability;

3) the operational requirements directed at ensuring simplicity and convenience of technical operation;

4) the technological requirements directed at ensuring simplicity and low cost of manufacture and design repair, the application in its manufacture of materials which are not in short supply.

In our course in describing the design parts we will adhere to the following sequence of presentation: a) purpose; b) the most important technical requirements determined by the purpose; c) the examination of the design as a result of the fulfillment of the technical requirements.

The more completely all requirements are satisfied, the higher will be the quality of flight vehicle design, the fewer defects and

failures will arise and the more economical will be the operation of the flight vehicle.

It is necessary to emphasize the special importance of the unconditional satisfaction of a specific level of strength requirements. For their fulfillment it is necessary to know the forces which act on flight vehicles in all possible cases of their operation.

The requirements imposed on flight vehicle design are in many respects connected with each other and sometimes are contradictory. With development of technology they are more precisely refined and changed.

§ 3. DESIGN, CONSTRUCTION AND OPERATION OF A FLIGHT VEHICLE

Let us briefly examine the basic stages in the design and construction of a flight vehicle and its service life after it is accepted into operation.

1. Preliminary Design

Upon obtaining the technical assignment for the design of a flight vehicle and the summary of the technical requirements, the experimental designer office (OKB) [OKB] outlines its basic features and parameters and carries out the preliminary design.

The aviation engineering properties of a flight vehicle are determined by selecting:

1) the power system;

2) the external (aerodynamic) configuration;

3) the airframe design;

4) equipment.

In selecting the power system and the aerodynamic configuration the most promising types of engines and the latest results in aerodynamic research are employed. In developing the design of the airframe and in selecting the equipment the latest achievements in these areas are employed and the experience in the design and operation of flight vehicles similar in purpose is considered.

The preliminary design is sometimes simultaneously worked out in several versions.

The work of the design office in creating the preliminary design includes the following elements:

a) determining of the basic parameters of the flight vehicle, the selection of the engines and equipment;

b) development of the general drawings, configuration drawing, drawings of individual parts;

On the configuration drawing executed on a large scale, the basic parts of the design, load and equipment are shown. By means of this drawing their mutual arrangement is agreed upon and the interests of all the design groups are tied together. The configuration drawing is utilized as the basis for positioning the center of gravity. The aim in positioning the center of gravity is the arranging of the loads and parts, in which the center-of-gravity position (c.g.) of the flight vehicle corresponds to the stability and controllability requirements;

c) the preliminary aerodynamic rating based on wind-tunnel test data (usually a limited number of them);

d) the stress analysis of the individual parts (incomplete for the most responsible design parts in the sense of strength);

e) the manufacture of a mock-up (full size) of the design sections. In the mock-up there is included the flight deck, part of the passenger salon, the adjoining wing parts, the engine installation, etc. The mock-up is accepted by the mock-up commission, which includes pilots, equipment engineers, etc.

The preliminary design by the OKB workers is defended before a special commission and is accepted as basis for further work, if the design is approved.

2. Technical Design and Construction of an Experimental Model

The work of the design office and the plant which constructs the experimental model of a flight vehicle includes the following:

a) the preparation of the working drawings;

b) the carrying out of the complete aerodynamic research and rating program;

c) the stress analysis;

d) the construction usually of not less than three specimens of the flight vehicle - two for flight tests and one for the strength test;

e) the design strength test.

3. Flight Tests

The flight tests are carried out in the following sequence:

a) the plant tests;

b) the tests carried out by the customer organization.

After termination of the testing and finishing (elimination of design deficiencies) in the case of the positive conclusion of their results a decision can be made with respect to series construction and the acceptance of the flight vehicle for operation.

4. Series Construction

The series design office (SKB) [СКБ] works on the preparation for series construction. During the process of its work the SKB sometimes introduces changes in the design connected with the characteristics of the manufacturing technology during series construction and subsequently taking operating experience into account. All the changes are coordinated with the experimental design office and the customer. A complete stress analysis is performed and all the drawings are carried out, the technological tooling up is worked out.

The acceptance of the prepared flight vehicles is carried out by the representatives of the customer organization. After a specific number of flight vehicles has been turned out, specimens of them are put through more complete flight tests and are checked for strength.

5. Operation of a Flight Vehicle and Its Service Life

During the operation of a flight vehicle and during its repair observation of the state of the design is carried out, defects and the periods of time it takes them to arise are detected.

For earlier detection of changes in the state of an inventory of a specific type of flight vehicle under operation conditions scheduled flight vehicles are employed which have flown more hours, and leaders, the increased accrued operation time of which is determined by a special program.

For definitizing the service life of an airframe and substantiating of its prolongation fatigue tests both of new flight vehicles and those having a specific accrued operating time are carried out. On the basis of such tests the maintenance and repair periods are established, the necessary modifications (changes in design) are determined, that is, those that are necessary for increasing the service life of the individual parts.

The service life of contemporary flight vehicles is mainly determined by economic principles. This is explained by the following.

If modifications connected with improving the aviation engineering properties (due to the construction of more highly developed engines, an increase in the number of passenger seats etc.) are not introduced, then in the course of time flight vehicles of the type in question in accordance with their data fall considerably behind the level of new types and therefore are transferred to routes where there is not as much freight or as many passengers to carry.

When a flight vehicle has a long service life the expenditures on repair are increased; thus, the time arrives when its further use and the prolongation of its service life become unfavorable and the flight vehicle is removed from operation.

CHAPTER 1

CONDITIONS OF FLIGHT VEHICLE LOADING

To ensure flight safety the design of flight vehicles first of all should be sufficiently durable and rigid under the effect on it of the loads which are encountered in operation. It is necessary that the strength and rigidity should be ensured during the entire service life of the flight vehicle and that these be attained with the least possible design weight of this flight vehicle.

For establishing the strength requirements connected with this and their definitization taking into account the development of aviation technology in research organizations work is being systematically carried out on the study of the values, directions and recurrence of the loads which act on design parts under operational conditions.

The results of these works are systematized, generalized and set forth in the stress standards of flight vehicles (see § 7 of the present chapter).

The fulfillment of the requirements for stress standards is checked by rating the design and by tests carried out in laboratories and in flight.

When evaluating the strength of a flight vehicle the following types of operational loading conditions are examined:

1) maneuvering flight;

2) flight in turbulent air;

3) motion along airfield during takeoff, landing and taxiing.

To the basic loads which act on parts of a flight vehicle under these conditions, the following can be added:

a) loads from the forces of surplus pressure in pressurized sections;

b) loads connected with oscillations and large deformations in design parts (oscillations caused by the lack of balance of an engine; oscillations due to acoustic effects; the increase in deformations and oscillations in carrying surfaces during the interaction of aerodynamic and elastic forces, etc.);

c) power effects arising during the heating of a structure (in the engine zone, during supersonic flight).

The effect of loads on the design is exhibited and is considered during the testing of the strength depending differently on their magnitude and number of repetitions.

The greatest loads possible in operation but which are rarely encountered, can cause residual deformations and even structural failure. They are accepted as the basis when evaluating the dimensions of the design necessary to ensure strength and they are examined as applied one time.

Lesser loads, but repeatedly encountered during the service life, can lead to structural fatigue failures. They are decisive in determining the longevity of the design.

Along with the loads, when evaluating strength the factors which can affect the strength, the rigidity and the longevity of the design should be considered: the wear of the parts, the effect of the medium (different types of corrosion), variation in the properties of materials due to heating, radiation, etc.

§ 1. FORCES ACTING ON A FLIGHT VEHICLE

In examining the forces acting on a flight vehicle or its parts in flight and on the ground, the method of kinetostatics based on the application of the d'Alembert principle, is used.

Briefly, the d'Alembert principle is formulated as follows: a moving body can be considered as being in equilibrium, if in the number of forces acting on it we include the force of inertia.

By using the method of kinetostatics, it is possible to comparatively simply determine the loads acting on a design which is in motion, and from the loads - to determine the stresses in its elements.

In carrying out stress analysis, all forces acting on a flight vehicle and its parts, are usually divided into two types:

1) mass forces - are forces which act on the mass elements and are proportional to the mass. They include the gravitational forces and the inertia forces;

2) surface forces - are forces applied to the surface of a vehicle. The surface forces include aerodynamic forces, engine thrust, reaction of the earth during landing, the forces of interaction between the individual parts of the design.

Let us examine a translationally moving aircraft (Fig. 1.1).

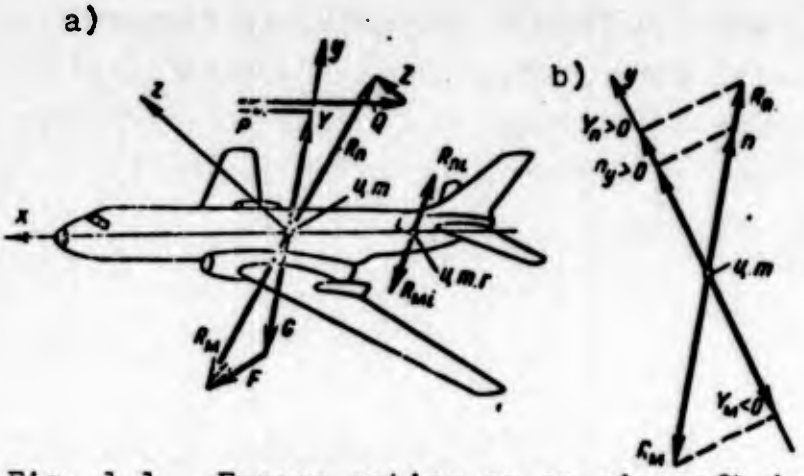

Fig. 1.1. Forces acting on an aircraft in curvilinear flight.

The resultants $R_п$ and $R_м$ of the surface and mass forces applied to an aircraft and to load i located in it, pass respectively through the center of gravity of the aircraft (c.g.) and the center of gravity of the load (l.c.g.).

According to d'Alembert's principle, under the effect of these forces both the aircraft and the load can be considered as being in equilibrium.

Then for the aircraft as a whole it is possible to write

$$\bar{R}_п + \bar{R}_м = 0,$$

whence it follows that

$$\bar{R}_п = -\bar{R}_м, \quad R_п = R_м,$$

where $\bar{R}_п$ is the resultant of the surface forces obtained by the summation of the vectors of the resultant of the aerodynamic forces and engine thrust; $\bar{R}_м$ is the resultant of the mass forces obtained by the vectorial summation of the gravitational and inertia forces of the aircraft; $R_п$ and $R_м$ are the absolute values of vectors $\bar{R}_п$ and $\bar{R}_м$.

For any load i located in an aircraft, we will similarly obtain:

$$\bar{R}_{пi} = -\bar{R}_{мi}, \quad R_{пi} = R_{мi},$$

where $\bar{R}_{п\,i}$ - is the resultant of the surface forces of load i, equal to the vectorial sum of the reactions of load attachment; $\bar{R}_{м\,i}$ - is the resultant of the mass forces of load i, equal to the vectorial sum of the gravitational force and the inertia force of the load; $R_{п\,i}$ and $R_{м\,i}$ - are the absolute values of vectors $\bar{R}_{п\,i}$ and $\bar{R}_{м\,i}$.

Let us dwell on two cases of aircraft motion: in curvilinear flight and in horizontal rectilinear uniform flight. We will consider them as the motion of a particle - the center of gravity of an aircraft, at which all forces acting on the aircraft are applied. This corresponds to the assumption that the aircraft motion is translational.

1. Curvilinear Flight

Let us draw the wind coordinate axes x, y, z through the center of gravity of an aircraft. At this point the surface and mass forces are applied (Fig. 1.1a).

The surface forces are: Y - lift; P - engine thrust; Q - drag; Z - lateral force; $R_п$ - is the resultant of the surface forces.

The mass forces are: G - weight; F - inertia force; $R_м$ - is the resultant of the mass forces.

From the force diagram given in Fig. 1.1a, it follows that

$$\bar{R}_п = \bar{Y} + \bar{P} + \bar{Q} + \bar{Z}; \quad \bar{R}_м = \bar{G} + \bar{F}.$$

The surface force $\bar{R}_п$ can be represented by the acceleration $\bar{a}_п$

$$\bar{R}_п = \frac{G}{g}\bar{a}_п.$$

The vector of complete acceleration of motion is

$$\bar{a}=\bar{a}_{\text{и}}+\bar{g},$$

where $\bar{g}$ is the vector of acceleration due to gravity. Hence

$$\bar{a}_{\text{и}}=\bar{a}-\bar{g}$$

and

$$\bar{R}_{\text{и}}=\frac{G}{g}(\bar{a}-\bar{g}).$$

This expression can be obtained, by examining mass force $\bar{R}_{\text{м}}$ and taking into account that

$$\bar{G}=\frac{G}{g}\bar{g} \text{ и } \bar{F}=-\frac{G}{g}\bar{a}.$$

Then

$$\bar{R}_{\text{и}}=\frac{G}{g}(\bar{g}-\bar{a}).$$

Since

$$\bar{R}_{\text{и}}=-\bar{R}_{\text{м}},$$

then

$$\bar{R}_{\text{и}}=\frac{G}{g}(\bar{a}-\bar{g}).$$

[и=and]

2. Horizontal Rectilinear Uniform Flight

During horizontal rectilinear flight at a constant velocity only weight G will be the mass force, and included in the number of surface forces will be thrust P, drag Q and lift Y.

If P does not give a projection on the y-axis, then

$$\bar{P}=-\bar{Q}$$

and

$$\bar{R}_{\text{п}}=\bar{Y}.$$

Since $\bar{R}_{\text{п}}=-\bar{R}_{\text{м}}$, the absolute values of the resultants of the surface and mass forces in this type of flight will be equal to the weight of the aircraft:

$$R_{\text{п}}=R_{\text{м}}=G.$$

The above examined conditions are also valid for the surface and mass forces which act on a helicopter.

§ 2. THE CONCEPT OF G-FORCE

For comparison of the forces acting on an aircraft and its parts in curvilinear and in horizontal rectilinear uniform flight, the concept of g-force is introduced.

1. Total G-Force

Total g-force at the center of gravity of a flight vehicle is the ratio of the resultant of the surface forces to its weight.

Total g-force - is a vector quantity, since it is assumed that it is the ratio of the vector $\bar{R}_n$ to the absolute value of weight G, i.e.,

$$\bar{n} = \frac{\bar{R}_п}{G} = -\frac{\bar{R}_м}{G}.$$

Vector $\bar{n}$ is directed in the same way as vector $\bar{R}_n$.

The absolute value of the total g-force can be determined from the expression

$$n = \frac{R_п}{G} = \frac{R_м}{G}.$$

In other words, the absolute value of the total g-force can be calculated from the value of the resultants either of surface, or mass forces.

Let us express g-force through acceleration.

Since the resultant of the surface forces is:

$$\bar{R}_a = \frac{Q}{g}\bar{a}_a = \frac{Q}{g}(\bar{a}-\bar{g}),$$

then the total g-force is

$$\bar{n} = \frac{1}{g}\bar{a}_a = \frac{1}{g}(\bar{a}-\bar{g}).$$

To elucidate the meaning of the concept of g-force, let us examine three possible representations of the g-force of an aircraft.

1. On the basis of an examination of horizontal rectilinear uniform flight, it is possible to say that the total g-force of an aircraft shows, by how many times the surface forces acting in flight with acceleration, are more or less than the surface forces in horizontal rectilinear uniform flight.

2. From the expression of total g-force it is evident that the quantity of g-force gives a comparison of the mass forces in the flight in question with the weight of the aircraft. Consequently, the total g-force characterizes the apparent change in the weight of the aircraft (increase or a decrease) in a flight with acceleration (curvilinear or rectilinear unsteady). The aircraft is seemingly "overloaded" (or "unloaded") due to the adding of the inertia forces to the gravitational forces.

3. As is evident from the expression of g-force via accelerations, the total g-force is

$$\bar{n} = \frac{\bar{a}_a}{g}.$$

Thus, g-force can be examined as a measure of that acceleration $\bar{a}_n = \bar{n}g$, which the surface forces[1] acting on the aircraft cause.

---

[1]It is necessary to note that sometimes, by mixing the concepts of g-force and acceleration incorrectly represent g-force in the form of a number multiplied by the magnitude g.

The concept of g-force can also be applied to the forces acting on a helicopter and on individual aircraft and helicopter components and on loads accomodated in them (i.e., in the aircraft or helicopter).

For example, the expression for the total g-force of a load which has a weight G, is written in the following manner:

$$\bar{n}_i = \frac{\bar{R}_{ni}}{G_i},$$

where $\bar{R}_{n\,i}$ is the resultant of the surface forces acting on the load.

The total g-force expressed via accelerations, is determined from the formula

$$\bar{n}_i = \frac{1}{g}\bar{a}_{ni} = \frac{1}{g}(\bar{a}_i - \bar{g}),$$

where $\bar{a}_i$ - is the acceleration of load i; $\bar{a}_{n\,i}$ is the acceleration due to the force $\bar{R}_{n\,i}$.

From the obtained formulas it is evident that the total g-force depends not only on the acceleration of motion $\bar{a}$, but also on the acceleration due to gravity $\bar{g}$.

2. G-Forces in the Direction of Coordinate Axes

Frequently, not the total g-force is examined, but its component in the direction of some axis.

The g-force in the direction of an axis is called the projection of the total g-force n in the direction of this axis.

From Fig. 1.1b it follows that the quantity of g-force in the direction of the y-axis will be determined according to the formula

$$n_y = n\cos(\bar{n}, \bar{y}).$$

Since $n = \frac{R_п}{G}$, and $R_п\cos(\bar{n}, \bar{y}) = Y_п$, where $Y_п$ is a projection of vector $\bar{R}_п$ on the y-axis, i.e., a scalar value, then

$$n_y = \frac{Y_п}{G}.$$

By analogy:

$$n_x = \frac{X_п}{G}.$$

The g-force in the direction of a specific axis as the projection of a vector on an axis can be positive, negative or equal to zero.

If in determining n_y we proceed from the expression of the total g-force via accelerations:

$$\bar{n} = \frac{\bar{a}_п}{g} = \frac{1}{g}(\bar{a} - \bar{g}),$$

then the projection of vector $\bar{n}$ on the y-axis will be found as an algebraic sum of the projections on the same axis of the vectors comprising $\bar{n}$.

Since $\frac{1}{g}(a_y - g_y) = \frac{1}{g}[a\cos(\bar{a}, \bar{y}) - g\cos(\bar{g}, \bar{y})]$, then

$$n_y = \frac{a_{пy}}{g} = \frac{a_y}{g} - \cos(\bar{g}, \bar{y}).$$

Let us note certain conditions connected with the application of a concept of g-force in the direction of a coordinate axis.

1. The sign of the g-force in the direction of the y-axis is determined by the sign $Y_п$ - the projection of the resultant of the surface forces on this axis, and its absolute value

$$|n_y| = \frac{|Y_п|}{G} = \frac{|Y_м|}{G}.$$

2. Most frequently the g-force of an aircraft is examined in the direction of the wind axis y. Experience shows that during maneuvering flight and during flight in turbulent air the g-force in the direction of the y-axis is the greatest.

3. Sometimes g-force in the direction of the y-axis is simply called "g-force" or "load factor". This terminology is inaccurate.

4. Strictly speaking, for an aircraft $Y_п$ - a projection of a surface force is equal to the sum of the projections of the air forces of the wing and of the elevator unit and the thrust force on the y-axis. During the approximate determination of n_y the air force of the elevator unit and the projection of thrust force are not considered. The projection of the surface force is taken equal to the lift force of the wing. The inaccuracy in the value of n_y can be great in those cases when the thrust is directed at a considerable angle to the velocity (especially for aircraft having great engine thrust), and then, when the area of the elevator unit is comparable with the wing area.

5. The g-force of an aircraft in the direction of wind axis x is:

$$n_x = \frac{X_п}{G}.$$

This type of g-force arises, for example, during the acceleration of a flying aircraft.

3. Expressing total G-Force Via G-Forces in the Direction of the Coordinate Axes

If the g-forces in the directions of three mutually perpendicular coordinate axes n_x, n_y, n_z, are known then the total g-force can be defined as vector $\bar{n}$ having projections n_x, n_y, n_z.

The absolute value $\bar{n}$ is found from the formula

$$n = \sqrt{n_x^2 + n_y^2 + n_z^2}.$$

§ 3. EXPERIMENTAL STUDY OF G-FORCES. MEASUREMENT OF G-FORCES

The determination of g-forces by theoretical methods encounters a number of difficulties. Thus, especially in determining the maximum values of g-forces for stress analysis, a great role is played by the measurement of g-forces directly on flight vehicles in flight and also during their motion along the ground.

For measuring g-forces g-force instruments called accelerometers (acceleration indicators), and also g-force recorders - accelerographs - are employed.

The first investigations of g-forces in flight were carried out in 1918 by V. P. Vetchikin who utilized for this purpose conventional spring scales with weights (bobs).

Let us examine the operating principle of g-force instruments as illustrated by the simplest instrument design (Fig. 1.2a). In housing 1, in which a liquid is poured, on spring 2 weight (bob) 3 with apertures is suspended. The indicator shows the weight (bob) displacement on a scale of 4. The resistance of the liquid passing through the apertures in the weight (bob) damps the oscillations which distort the instrument readings.

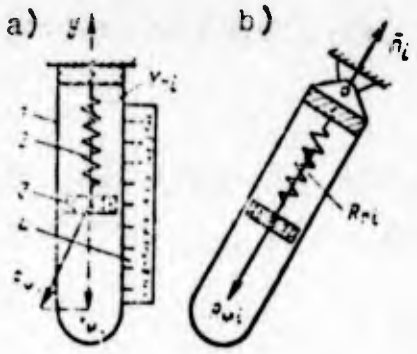

Fig. 1.2. The simplest accelerometer: a) upon being stationarily secured the instrument shows the component of the total g-force acting along its axis; b) with hinged suspension the instrument shows the total g-force at the point of its attachment.

Let the instrument be mounted at point i of an aircraft.

If the instrument is hinged suspended, then during the aircraft motion its longitudinal axis is situated in the direction of the line of the effect of the resultant of the mass forces. In this case the instrument indicates the total g-force $\bar{n}_i$ (Fig. 1.2b).

The total g-force at any point is determined by the acceleration of this point and by the acceleration due to gravity:

$$\bar{n}_i = \frac{\bar{P}_{mi}}{G_i} = \frac{1}{g}(\bar{a}_i - \bar{g}).$$

The g-force of the weight (the bob) of the instrument situated at point i of the aircraft, will be equal to the g-force of point i (let us assume, that $\bar{a}_{гр} = \bar{a}_{i\ сам} = \bar{a}_i$).

During uniform motion or when at rest on the weight (bob) of the instrument the mass force - the weight of the weight (bob) $R_{м\ i} = G_i$ and the surface force - the spring tension $R_{п\ i}$ act. In this case $R_{п\ i} = G_i$ and

$$n_i = \frac{R_{пi}}{G_i} = 1.$$

Due to the effect of the weight of the weight (bob) the spring is deformed by a constant value Δl_G. During curvilinear aircraft motion the weight (bob) will be under the effect of the resultant of the mass forces of the weight (bob) $R_{м\ i} \neq G_i$

In this case surface force is $R_{п\ i} \neq G_i$, and the deformation of the spring is $\Delta l_R \neq \Delta l_G$.

If the deformation of the spring obeys Hooke's law, then the deformations are proportional to values of $R_{п\ i}$. Therefore

$$n_i = \frac{R_{пi}}{G_i} = \frac{\Delta l_R}{\Delta l_G},$$

i.e. the weight (bob) displacement is proportional to the g-force.

However, the hinged suspension of the instrument is inconvenient in practice (the rocking of the instrument, the large overall dimensions necessary for accommodating the instrument etc.). Usually they use instruments fixed in the direction of any axis.

Let the instrument be mounted stationarily in the direction of the y-axis (see Fig. 1.2a). Only force $Y_{п\ i}$ caused by component $R_{м\ i}$ directed along the y-axis will affect in curvilinear flight the displacement of the weight (bob) and the deformation of the spring. The instrument in this case shows the g-force in the direction of the axis of the instrument, i.e.

$$n_{yi} = \frac{Y_{пi}}{G_i} = \frac{\Delta l_y}{\Delta l_G},$$

where Δl_y is the deformation of the spring due to the action of force $Y_{м\ i}$.

The motion of the weight (bob) of the instrument downward will correspond to a positive g-force in the direction of the y-axis.

The zero point of the instrument scale corresponds to the absence of spring tension, a g-force equal to unity - corresponds to the deformation of the spring of a fixed, vertically positioned instrument, under the effect of the weight of the weight (bob).

Of greatest interest are the g-forces of an aircraft n_y in the direction of the lift force (in the direction of the wind axis y). The g-force instrument is fastened stationarily (its y_1-axis is approximately situated along a normal to the chord plane), and the g-forces measured by it, differ from the g-forces in direction of lift force. However, this difference is small, since in flight regimes the angles of attack lie within a narrow range (from -2 to +15°), where the direction of the lift force differs little from the direction of the normal to the chord plane.

Contemporary g-force instruments are based on the same operating principle, but have a design which makes it possible to record g-forces with respect to time, synchronously with the recording of flight velocity and flight altitude.

When it is necessary to determine the total g-force the g-force instruments are mounted in the directions of the main body axes of flight vehicle x_1, y_1 and z_1. The component g-forces with respect to the three axes x_1, y_1, z_1 are measured synchronously, and then the value n is calculated from the formula

$$n = \sqrt{n_{x_1}^2 + n_{y_1}^2 + n_{z_1}^2}.$$

In studying g-forces the instruments are placed both close to the center of gravity of the flight vehicle and in other places, because during complex maneuvering flight and as a result of the elastic structural deformations the g-forces at the different points of the flight vehicle differ greatly.

Certain statistical data on g-forces are given in Table 1.1.

Table 1.1

Cases in which g-forces are encountered	Greatest value	Order of the time of the effect, s
Pullout from a dive.....	8-9 (to 11)	1

Going into a dive.....	-4	1
Single uncontrolled ("spinning") roll...	3	Several s
The spin.....	1.5-2	The same
Flight in turbulence.....	4	0.1
Landing, landing run, takeoff run.....	3-5	0.1
Landing of a seaplane on water.....	7	0.1
Opening of a parachute with a change in velocity of from 60 to 5 m/s.....	5	0.5
Ejection of a pilot.....	16	0.1

The Effect of G-Forces on the Human Body

The human body's ability to endure g-forces depends first of all on the magnitude of the acting g-force. Small and infrequently repeated g-forces (<2-3) do not have a noticeable effect on the efficiency of a pilot in the pilot's cabin, even if they act over a period of several seconds. With an increase in the magnitude of the g-force or time of its action, there is a displacement in the internal organs, a deterioration in blood circulation and a disruption in vision. With a further increase in the g-forces loss of consciousness occurs, and then injury to the internal organs and the skeleton. The important factors determining the maximum magnitude of g-force which can be endured by a person are the direction, duration and repetition of the effect of g-force, and also the individual characteristics of the organism and its state.

§ 4. MANEUVERING FLIGHT

Let us examine for certain typical types of maneuvering flight the derivation of the expressions of the magnitude of g-force via the parameters which characterize flight conditions.

1. Determining G-Force n_y Via Velocity and the Parameters of the Flight Trajectory

Let us express the g-force at the center of gravity of an aircraft with respect to the direction of lift force n_y during curvilinear flight in a vertical plane via flight velocity V and the parameters of the trajectory of the center of gravity: the radius of curvature r and the slope angle of a tangent to the horizon θ.

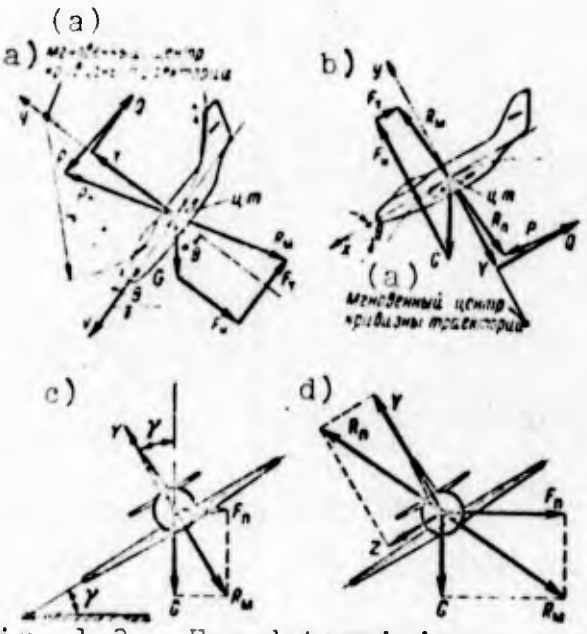

Fig. 1.3. For determining n_y: a) during pullout from a dive or a glide; b) when going into a dive or a glide; c) during an accurate turn; d) during a turn with sideslip.
Key: (a) Instantaneous center of curvature of trajectory.

Figure 1.3a in accordance with d'Alembert's principle shows the forces acting on an aircraft in the case of a pullout from a dive or the transition from a glide to horizontal flight.

Earlier it was obtained, that

$$n_y = \frac{Y_\text{п}}{G}.$$

Since the components of mass force $Y_\text{м}$ are expressed directly via V, r and θ, for solving the posed problem let us express $Y_\text{п}$ via these components.

By projecting the forces on the y-axis, we will obtain $Y_\text{п} = G\cos\theta + F_\text{ц}$, but $F_\text{ц} = \frac{G}{g}\cdot\frac{V^2}{r}$; thus $Y_\text{п} = G\left(\cos\theta + \frac{V^2}{gr}\right)$. As a result

$$n_y = \cos\theta + \frac{V^2}{gr}.$$

If the tangent to the trajectory at the center of gravity is parallel to the horizon, then $\theta=0$, $\cos\theta=1$ and

$$n_y = 1 + \frac{V^2}{gr}.$$

For rectilinear horizontal flight when $r=\infty$, $n_y=1$.

Let us proceed to the case when lift force has a direction opposite to the direction of the y-axis (for example, when going into a dive or making a transition to a glide). The forces which act on an aircraft are shown in Fig. 1.3b. By projecting the forces on the y-axis, we obtain

$$Y_a = G\cos\theta - \frac{GV^2}{gr} = G\left(\cos\theta - \frac{V^2}{gr}\right).$$

In this case of the g-force is

$$n_y = \cos\theta - \frac{V^2}{gr}.$$

For the horizontal inverted flight $\theta=180°$, $\cos\theta=-1$ and $n_y=-1$. The flight-path curvature $1/r$ can be expressed via velocity with respect to V and angular velocity $\omega=d\theta/d\tau$ in the following manner:

$$\frac{1}{r} = \frac{d\theta}{dS} = \frac{d\theta}{d\tau}\cdot\frac{d\tau}{dS} = \frac{\omega}{V}.$$

Then the above obtained expressions for n_y during a maneuver in the vertical plane can be transformed in the following manner:

$$n_y = \cos\theta \pm \frac{V\omega}{g}.$$

From the last expression it follows that the value of g-force, which can be attained during a maneuver in the vertical plane, depends on angle θ, flight velocity with respect to trajectory V and the angular rate of turn of the aircraft ω.

2. G-Forces During Turning

During an accurate turn (Fig. 1.3c) the resultant of the centrifugal force and the weight is balanced by the lift Y.

From the equation of the projections on the vertical $Y \cos \gamma - G = 0$, we find $Y = \frac{G}{\cos \gamma}$.

Then the g-force in an accurate turn is equal to

$$n_y = \frac{Y}{G} = \frac{1}{\cos \gamma}.$$

In a turn with sideslip (Fig. 1.3d - external sideslip) an aerodynamic force of resistance to sideslip Z arises. G-force is determined from the formula

$$n_z = \frac{Z}{G}.$$

§ 5. FLIGHT IN TURBULENT AIR

During the flight of a flight vehicle in turbulent air considerable g-forces n_y arise, caused by the encounter with vertical gusts. These g-forces are perceived as "turbulence".

1. Reasons for the Emergence of Vertical Gusts

The turbulent state of the air medium is the result of air motions caused by a difference in temperatures and pressures in its different sections. In this case, in particular, vertical currents and the gusts with different velocity arise. The gusts are customarily called currents, whose velocity rapidly builds up, i.e., which have a high gradient W/h (Fig. 1.4a).

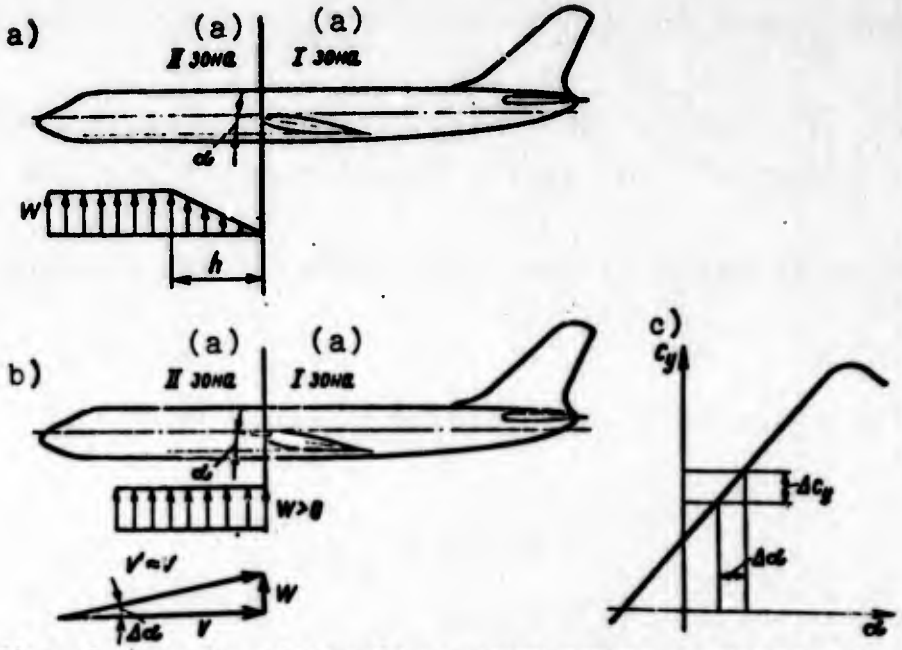

Fig. 1.4. An aircraft encountering a vertical current: a) entry into the current with a gradient of W/h; b) entry into a sharply limited current; c) variation in c_y with respect to α. Key: (a) zone.

The main reasons for the formation of vertical currents and gusts are:

a) nonuniform heating of the earth's surface. Gusts caused by the nonuniform heating of the earth's surface ("convective currents" or "thermals"), are propagated to altitudes of 2,000-3,000 m and they have velocities of up to 10 m/s;

b) variation in the relief of the terrain. When moving masses of air encounter mountains gusts arise with speeds of up to 20 m/s which extend up to altitudes of 1,500-2,000 m above the level of the mountain peaks;

c) air circulation in clouds. During the formation of powerful cumulus clouds which extend up to altitudes of 4,000-5,000 m, vertical gusts of considerable velocity arise: in the surface layer, outside the cloud - up to 10 m/s, and in cloud - up to 15 m/s. The vertical gusts in a thunderstorm front attain velocities

of 20-50 m/s; therefore aircraft flights in this zone are dangerous and prohibited;

d) jet streams. Vertical currents caused by jet streams, can attain velocities exceeding 10 m/s.

2. Determination of n_y of an Aircraft During Flight in Turbulent Air

Let us find the g-force n_y of an aircraft which is carrying out horizontal rectilinear uniform flight, at the moment of its entry into a sharply limited vertical ascending current of air which has a constant velocity $W>0$ (Fig. 1.4b).

We assume that an aircraft goes from a zone of nonturbulent atmosphere (zone I) into a zone of a vertical current (zone II), without giving way to the effect of the current.

Table 1.2 gives the parameters which characterize the flight conditions and the wing loading of an aircraft in zones I and II.

Table 1.2

Parameters	Zone I	Zone II
Angle of attack of the wing.....	α	$\alpha+\Delta\alpha$
Lift coefficient of the wing.....	c_{yI}	$c_{yII}=c_{yI}+\Delta c_y$
Lift force of the wing.....	Y_I	$Y_{II}=Y_I+\Delta Y$
Vertical velocity of the gust.....	0	$W>0$
Flight velocity.....	V	$V'\approx V$

Since the flight velocity is considerably greater than the velocity of a vertical gust, then angle $\Delta\alpha$ is small; therefore it is possible to consider that

$$\Delta\alpha \approx \operatorname{tg}\Delta\alpha = \frac{W}{V};$$

$$V' \approx V.$$

Assuming, that surface force $Y_п$ is equal to the lift force of the wing (disregarding the lift force of the elevator unit and the projection of engine thrust force on the y-axis), it is possible to write

$$Y_п \approx Y = c_y S q;$$

where $q = \frac{\rho V^2}{2}$ — ram pressure in the flight in question.

Taking into account that the g-force is

$$n_y = \frac{Y_п}{G},$$

we will obtain for the moment of the entry of the wing into zone II

$$n_y = \frac{c_{yI} S q}{G} = \frac{(c_{yI} + \Delta c_y) S q}{G}.$$

Since $c_{yI} Sq = Y_I = G$, then

$$n_y = 1 + \frac{\Delta c_y S \frac{\rho V^2}{2}}{G}.$$

From figure 1.4b and c it is apparent that

$$\Delta c_y = c_y^\alpha \Delta\alpha \approx c_y^\alpha \frac{W}{V}.$$

Introducing the expression for Δc_y into formula n_y and taking into consideration that the vertical gusts can be both ascending and descending, we will obtain

$$n_y = 1 \pm 0{,}5 c_y^\alpha \rho W V \frac{S}{G}.$$

In the real atmosphere the vertical velocity of the gusts acting on an aircraft, increases from the gust boundary gradually, in section h (Fig. 1.4a).

Thus, at the moment when the wing encounters the maximum value of gust velocity, the aircraft is already acquiring velocity V_y in the direction of the gust effect and, consequently, the velocity of the wing's encounter with the vertical current will be equal to $W-V_y$. This leads to a decrease in g-force n_y.

To account for this fact in the above obtained expression for n_y a correction is introduced: the factor $k<1$ is introduced in the second term.

Then the formulas for g-force during flight in turbulent air take the form:

$$n_y = 1 \pm 0{,}5kc_y^{\alpha}\rho WV\frac{S}{G}.$$

Taking into account that V=aM (where a - the velocity of sound, M - the Mach number of the flight), we will obtain:

$$n_y = 1 \pm 0{,}5kc_y^{\alpha}\rho WaM\frac{S}{G}.$$

The magnitude of coefficient k depends both on the gradient of the increase in the gust velocity W/h and on the aerodynamic inertial and elastic characteristics of the aircraft.

The value of k can be approximately determined by the formula

$$k = 1 - \frac{\rho g c_y^{\alpha} h}{4G/S}.$$

The flight test data showed that the vertical gusts causing considerable g-forces, have gradient sections h of from 20 to 70 m.

Examining the flight of aircraft in turbulent air, it is necessary to still note the following.

The encounter with the ascending gust is dangerous also by the fact that the total angle of attack $\alpha+\Delta\alpha$ can turn out to be close to critical and the emergence of the buffeting phenomenon and losses in the stability of the aircraft are possible. This danger is increased at high altitudes, where flight occurs at great angles of attack.

§ 6. FLIGHT AT HIGH VELOCITIES

Figure 1.5 depicts the boundaries of the region of the possible employment of winged flight vehicles at high velocities which approach escape velocities.

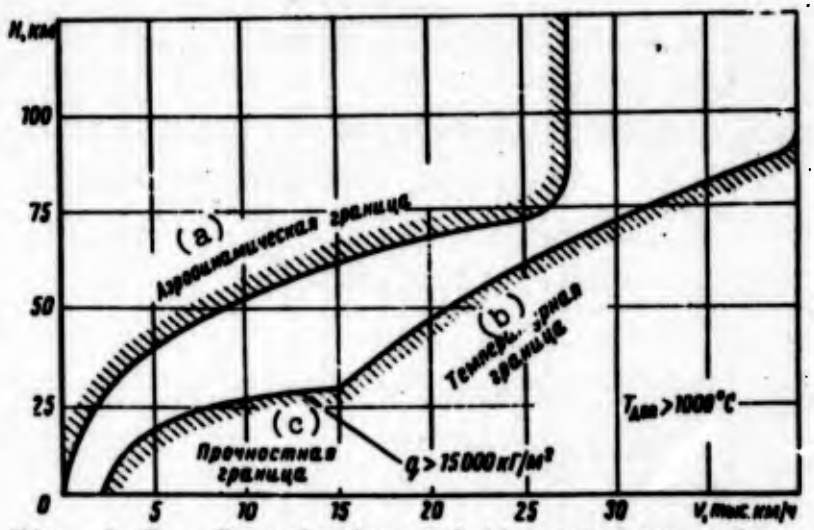

Fig. 1.5. Boundaries of the regions of the utilization of winged flight vehicles. Key: (a) Aerodynamic boundary; (b) Temperature boundary; (c) Strength boundary. Abbreviations: кГ/м^2=kgf/m^2; тыс. км/ч= thous. km/h.

The strength boundary - the line q=const separates the zone of low altitude and high velocities, where the flight is virtually impossible due to the high values of ram pressure. First, the

aerodynamic loads on the skin are great, which requires a considerable increase in the weight to ensure the strength; second, due to the increase in drag, engines with too great thrust are necessary for flight.

The line T=const is the temperature boundary of the zone of too high kinetic heating. For flight at high velocities it is necessary to create designs from heat-resistant materials and to complicate the equipment by introducing means for heat shielding and cooling.

The line c_y=const - the aerodynamic boundary - limits from above the zone in which it is possible to carry out the flight of winged vehicles at a constant altitude, without exceeding the permissible (sufficiently distant from $c_{y\ max}$) value of c_y.

From Fig. 1.5 it follows that at high velocities flight at a constant altitude is feasible at high altitudes within the limits of the "corridor" limited by the permissible values of q, T and c_y. For Fig. 1.5 the strength boundary $q_{доп}$=15,000 kgf/m^2 is conditionally accepted,

$$T_{доп} = 1000^\circ\text{C}, \quad \frac{G}{c_y S} = 800 \text{ kgf/m}^2.$$

Let us examine the forces and g-forces acting on a flight vehicle. In this case the curvature of the earth and the flight-path curvature of the flight vehicle at H=const determined by it should be taken into account (at velocities remote from the escape velocities, the path curvature which corresponds to constant-level flight, does not play a significant role).

During flight beyond the effect of the atmosphere along an arc of the great circle r (Fig. 1.6a) Y=0; therefore $Y_м=F_н-G=0$, where the centrifugal force $F_н = \frac{G}{gr} V_{кр}^2$. Hence $\frac{G}{gr} V_{кр}^2 - G = 0$.

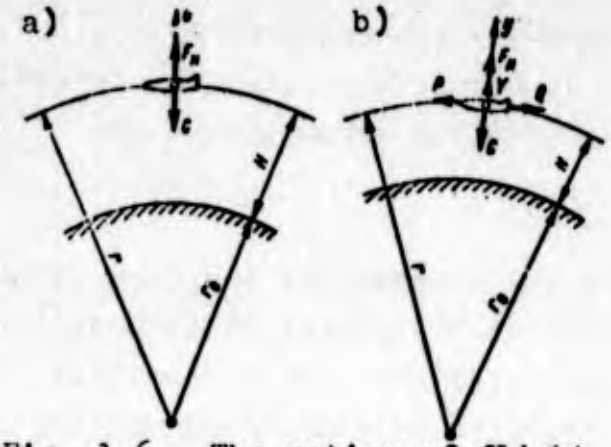

Fig. 1.6. The motion of flight vehicles at the great velocities: a) outside the atmosphere; b) in the atmosphere.

Then the formula for determining circular or first escape velocity $V_{кр1}$ - the velocity at which a flight vehicle can fly in a circular orbit without the presence of aerodynamic lift - will take the form:

$$V_{кр1} = \sqrt{gr}.$$

Near the earth where $g_0=9.81$ m/s^2; $r_0=6379$ km - the radius of the earth at the equator, we will obtain

$$V_{кр1 0} = 7{,}912 \text{ km/s}.$$

At altitude H=const (Fig. 1.6b)

$$r = r_0 + H, \quad g = g_0\left(\frac{r_0}{r}\right)^2,$$

$$V_{кр1} = V_{кр1 0}\sqrt{\frac{r_0}{r}}.$$

At a flight speed of $V<V_{кр1}$ aerodynamic lift is necessary

$$Y = G - F_ц = G - \frac{G}{g}\cdot\frac{V^2}{r} = G\left(1 - \frac{V^2}{gr}\right).$$

Since $gr=V^2_{кр1}$, then

$$Y = G\left(1 - \frac{V^2}{V^2_{кр1}}\right).$$

The g-force is

$$n_y = \frac{Y}{G} = 1 - \frac{V^2}{V^2_{кр1}}.$$

At flight velocity $V=V_{кр}$ we have $n_y=0$, which corresponds to a state of weightlessness.

§ 7. REQUIREMENTS IMPOSED ON STRENGTH AND THE STRENGTH STANDARDS OF AIRCRAFT

The strength standards of an aircraft are a summary of the basic mandatory requirements imposed on the strength, rigidity and longevity of a design, which should be observed during rating and strength tests[2].

In strength standards of aircraft a number of cases of the loading of an aircraft, probable in operation and most dangerous for the strength of its parts is examined. These cases are selected on the basis of flight tests, laboratory and theoretical investigations, and also of materials which generalize the operating experience of aircraft. The determination of loads in different cases is carried out taking into account the purpose of the aircraft, its flight weight, maximum flight velocity and other factors. In all cases of loading the strength standards indicate the methods for determining loads on an aircraft and its part, and also their direction and distribution.

For each case of loading the operational g-force or operating load is assigned by the strength standards.

Operational g-force $n^э$ is the greatest probable g-force during operation (which is possible to be encountered in practice). In the majority of cases the strength standards examine g-force in the direction of lift force. Sometimes strength standards give the values of the operating load on a part of the aircraft design

[2]Strength standards are routinely reexamined and brought up to date. Taking into account the differences in technical requirements and operating conditions, the strength standards of different countries for military and for civil aircraft have differences. There are also strength standards for helicopters, airframes, and other flight vehicles.

$P^э$ - greatest load probable during operation. As the basic indices of the level of requirements imposed on the strength of aircraft during its creation maximum and minimum (the greatest negative) operational g-forces $n^э_{max}$ and $n^э_{min}$ are assigned (through them the strength standards express the values of $n^э$ for different load cases).

Along with this the maximum values of the velocity characteristics of a flight vehicle are established, up to which design strength should be ensured. For aircraft the basic ones of these are: $q_{max\ max}$ - is the rated maximum (super-maximum) ram pressure and $M_{max\ max}$ - the rated maximum Mach number.

These maximum values are brought about by the necessity for putting a limit on the flight properties in order to reduce the design weight. The limiting of q and V can be connected with the necessity for limiting the air pressure on the skin or g-force during turbulence, with the flutter danger; the limiting of M - with ensuring the stability of subsonic aircraft and with limiting the kinetic heating of supersonic aircraft.

With the effect of $n^э$ and $P^э$ there should not be residual deformations and losses of stability of the power elements of the design.

With respect to cases of loading rated destructive g-force $n^р$ or rated destructive load $P^р$ on an aircraft design part are determined. Before attaining the values $n^р$ and $P^р$ the design should not be destroyed.

The values $P^р$ and $n^р$ are connected with $P^э$ and $n^э$ by the dependences:

$$P^р = fP^э; \quad n^р = fn^э,$$

where f is the safety factor.

Let us examine in detail the requirements for strength and rigidity which the design state should satisfy under the effect of $P^э$ and $P^р$:

1) under the effect of $P^э$:

the maximum stresses[3] (local, at the most loaded points of the design) should not cause the residual deformations $\varepsilon_p \geq 0.2\%$;

there should not be losses in stability and such structural distortions, which lead to distortion of the aerodynamic shapes or disruption of the operation of control.

The strength condition takes the form:

$$P^э < P_{доп} \text{ или } \sigma^э < \sigma_{доп},$$
[или=or]

where $\sigma^э$ - the operational stress (from the effect of the load), in accordance with which the strength is checked; sometimes this can be tangential $\tau^э$, or reduced (with respect to the third theory of strength) stress $\sigma^э_{прив}$; $P_{доп}$, $\sigma_{доп}$ - are the permissible load and stress. These are permissible characteristics of design strength determined by the aforementioned requirements; permissible stress is taken equal to yield point $\sigma_т = \sigma_{0.2}$ (or $\tau_т$), and for elements which lose stability, - to critical stress $\sigma_к$ (or $\tau_к$);

2) before the attainment of $P^р$ the final destruction of design parts should not occur; they should retain the ability to withstand an increase in load.

The strength conditions are:

---

[3]The maximum stresses arise in concentrators; thus the deformation $\varepsilon_p = 0.2\%$ is local; it is possible to consider in practice that the total structural distortions before this obey Hooke's law.

$P^p \leqslant P_{разр}$, or $\sigma^p \leqslant \sigma_{разр}$,

where σ^p (or τ^p, $\sigma^p_{прив}$) - is the rated stress (due to the effect of P^p); $P_{разр}$, $\sigma_{разр}$ - are the strength characteristics during design failure: destructive load and stress; destructive stress is equal $\sigma_в$ (or $\tau_в$), and for the elements which lose stability, is taken on the basis of the tests, within the limits of from $\sigma_н$ to $\sigma_в$ (or from $\tau_н$ to $\tau_в$).

The reduced requirements are reflected in the values of the safety factor f taken in stress standards.

In parts whose dimensions are selected according to the strength condition, the stress from P^p will be $\sigma^p=\sigma_в$; with $P^э$ it will be equal to $\sigma^э=\sigma_в/f$. For fulfilling conditions $\sigma^э<\sigma_т$, it is necessary that it be $\sigma_в/f<\sigma_т$, or $f>\sigma_в/\sigma_т$. For contemporary aviation metals $\sigma_в/\sigma_т\leq 1.3$. The least permissible value $f=1.3$ is substantiated by this.

For the basic cases of loading f is given within the limits of from 1.5 to 2 depending on how frequently the case is encountered and for the strength of which parts it is decisive. An increase in f is specified for especially important parts, for design elements, the strength characteristics of which have considerable variance and in certain cases for purposes of increasing the rigidity of the design parts.

In fulfilling the requirements for the strength standards and the rigidity standards of flight vehicle design it is necessary to ensure and to estimate its longevity, reliability and durability. These questions are examined in chapter 13.

The strength standards examine the flight and landing cases of loading. Most important among them are the flight cases A, A', B, C, D, D' and the case of a three-point landing E (cases B and C are

examined with the ailerons deflected). These cases of loading can be called basic, since precisely these are usually decisive for the strength of different aircraft components. As is shown in Fig. 1.7, they cover a wide range of values of angles of attack, operational g-forces and aircraft flight velocities.

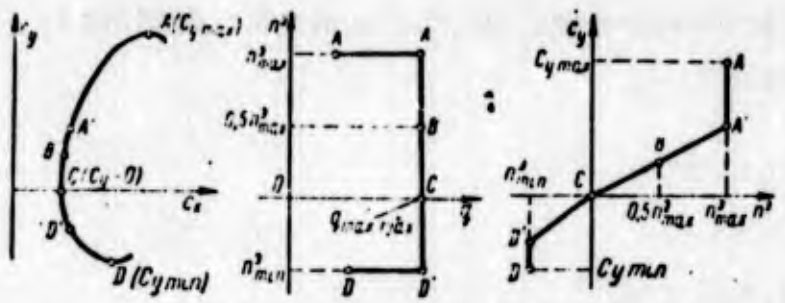

Fig. 1.7. Cases of loading with aircraft strength standards.

The basic flight cases of loading are A, A', B, C, D, D'. For maneuvering and limitedly maneuvering aircraft the conditions of loading, which correspond to these cases of strength standards, are encountered during curvilinear maneuvering flight. For nonmaneuvering aircraft of civil aviation these conditions are most probable during flight in turbulent air.

In flight cases the strength standards assign the g-force $n^э$, and also q or c_y for determining the wing lift force.

A summary of the values characterizing the basic flight cases of loading of strength standards of an aircraft, is given in Table 1.3.

Table 1.3

Case of loading	Parameters			
	$n^э$	c_y	q	f
A	$n^э_{max}$	$c_{y\,max}$	—	1,5
A'	$n^э_{max}$	—	$q_{max\,max}$	1,5
B	$0,5n^э_{max}$	—	$q_{max\,max}$	2,0
C	0	0	$q_{max\,max}$	2,0
D	$n^э_{min}$	$c_{y\,min}$	—	1,5
D'	$n^э_{min}$	—	$q_{max\,max}$	1,5

For finding the loads on a wing and for determining the non-given parameters in flight cases of loading dependence $Y^э=n^эG=c_ySq$ is employed.

Along with the examined cases of loading there is still a considerable quantity of cases, which are decisive for the strength of individual parts. They are presented in the chapters dedicated to specific parts of the design.

§ 8. CHARACTERISTICS OF HELICOPTER LOADING

1. Forces Acting on a Helicopter in Flight

Surface and mass forces (Fig. 1.8) act on a helicopter in curvilinear flight.

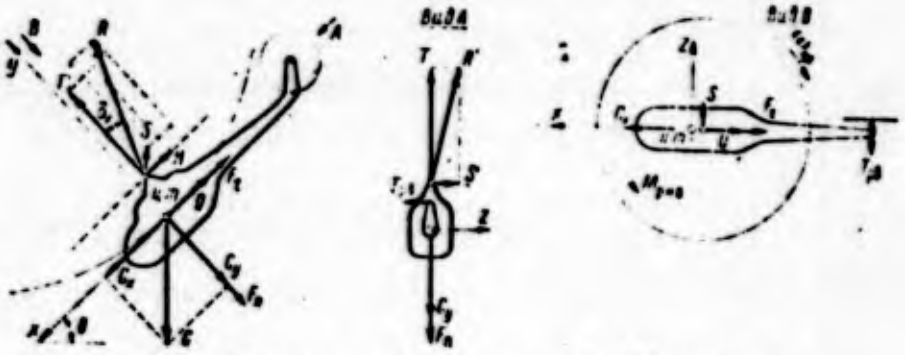

Fig. 1.8. Forces acting on a helicopter.

Surface forces: R - is the resultant of the aerodynamic forces of the rotor (NV) [HB], directed along the axis of the cone of rotation of the rotor; Q - is the drag of a helicopter (it is approximately considered applied at the center of gravity of the helicopter); $T_{р.в}$ - is the thrust of the tail rotor (RV) [PB] which balances the reactive torque $M_{р.н.в}$.

Mass forces: G - is the weight of the helicopter; F_n; F_t - are the inertia forces.

In a body coordinate system (along the helicopter axes) force R is apportioned into three components: the rotor thrust force T directed along the axis of the shaft (perpendicular to the plane of rotation of the rotor), longitudinal force H and lateral force S.

Forces H and S act in the plane of rotation of the rotor. The thrust force of the rotor T differs insignificantly in magnitude from the total aerodynamic force R, since angle δ_x is small and changes within the limits of from 0 to 6°. This makes it possible in the calculations to assume T≈R.

2. Loads Acting on a Helicopter, and Their Standardization

Loads acting on a helicopter, are assigned a g-force magnitude.

The basic conditions pertaining to g-forces (their determination, measurement, etc.) investigated for aircraft, also remain valid for helicopters.

The flight speed of a helicopter is comparatively low (V_{max}=300-350 km/h). Therefore, the drag and the longitudinal force of the rotor are usually small: Q<0.2 G; H<0.2 T.

Hence, it follows that for the strength of a helicopter of basic value as for an aircraft, is the g-force which acts in the direction of the y-axis. Its magnitude is determined by the magnitude of rotor thrust

$$n_y = \frac{T}{G}.$$

The strength standards of helicopters (as with aircraft) examine the loading of helicopters in flight, during landing, and also during operation under ground conditions.

The norms assign the characteristic cases of helicopter loading, and also the magnitude of operational g-force $n^э$ (the greatest actually possible during helicopter operation), the value of the safety factor f, the values of the rotor revolutions and the flight speed of a helicopter in the case under examination.

One of the characteristic flight cases of the loading of a helicopter is maneuvering flight - the pull-out of a helicopter from a glide. In this case it is considered that $n^э_{max}=3$; $f=1.5$; the number of rotor revolutions $n_{н.в}=1.2(n_{н.в})_{ном}$; $V=1.15\ V_{max}$; rotor thrust $T=n^э_{max}G$; longitudinal force $H^э=0.15\ T^э$ and lateral force $S^э=0.075\ T^э$.

For helicopters the maximum operational g-forces determined by the aerodynamic possibilities of the rotor, are comparatively low, since in the case of large g-forces flow separation arises on the rotor. The calculated g-forces usually do not exceed $n^р=4-6$.

CHAPTER 2

EXTERNAL SHAPES OF WINGS AND ROTORS

§ 1. THE PURPOSE OF A WING AND THE MOST IMPORTANT TECHNICAL REQUIREMENTS IMPOSED ON IT

The basic purpose of a wing is the creation of the lift force required for all normal flight regimes characteristic to an aircraft, with least possible expenditure of thrust by the engine set-up. Furthermore, the wing plays an important role in the stabilization and the controllability of an aircraft and can be utilized for the accommodation and the attachment of a number of units (landing gear, fuel tanks, engine set-up).

The wing is the most important part of an aircraft design.

The considerable part of the weight and of the total drag of an aircraft is exerted on a portion of the wing. Usually for subsonic aircraft the weight of a wing is

$$G_к = (0{,}07 \div 0{,}16)\,G_0; \quad G_к = (0{,}35 \div 0{,}45)\,G_{кн},$$

where G_0 is the takeoff weight of an aircraft; $G_{кн}$ - the design weight of aircraft.

In flight regimes, close to V_{max}, the ratio of the wing drag coefficient $c_{x\ н}$ to the aircraft drag coefficient $c_{x\ сам}$ is coefficient:

$$\frac{c_{xн}}{c_{xсам}} = 0{,}3 \div 0{,}5.$$

A reduction in wing weight and its drag leads to a decrease in G_0 and $c_{x\ сам}$, brings about a decrease in the required thrust and fuel consumption and, consequently, an increase in the economic efficiency of the aircraft.

It is necessary to keep in mind that the necessity for the fulfillment of additional wing functions - the ensuring of stabilization and especially of the accommodation of units - sometimes considerably affects wing design.

Let us examine the most important technical requirements imposed on a wing, and the means by which they are accomplished.

Aerodynamic requirements. The external shapes and the geometric dimensions of a wing should ensure the obtaining of the flight properties which correspond to the purpose of aircraft. In this case the interference of the wing with the other parts of the aircraft should be considered.

The basic aerodynamic requirements are the following:

1) a low value of wing drag characterized by the product $(c_x S)_н$ in the basic flight regimes, - is attained by selecting of profiles with low c_x, by selecting a rational wing planform, by limiting the wing area S and by improving the state of the external wing surface (the roughness of the skin is decreased, lapped joints, the projection of rivet heads and other irregularities which increase c_x are not permitted);

2) a high $M_{крит}$ value - critical Mach number for transonic aircraft and the least possible variation in c_x and c_y with respect to M during the transition to supersonic flight velocities - is ensured by employing special high-speed profiles of low thickness ratio, swept wings in plan, and low-aspect-ratio-wings;

3) a sufficiently large value of the product $c_{y\ max}S$ which characterizes the ability of the wing to create the necessary lift for flight at low velocities, and the possibility of increasing it as a result of lift increasing devices on the wing are attained by installing profiles which have a high $c_{y\ max}$ value, by selecting a wing area sufficient to ensure the necessary takeoff and landing properties; by selecting a planform which ensures good layout, sufficient area and high efficiency of the mechanization being employed (increase in the chords of the center section, small sweepback (0-20°); sometimes by the application of a biplane wing design;

4) a high value of the maximum lift-drag ratio $K_{max}=(c_y/c_x)_{max}$, necessary for increasing the range and ceiling of an aircraft, is attained by employing profiles which have large values of K_{max}, and high-aspect-ratio-wings; by ensuring a good state of the external wing surface; by employing a special layout of the external shapes of the aircraft (wing and fuselage);

5) the ensuring of stabilization and controllability in all permissible aircraft flight regimes.

This requirement is reflected on the entire aerodynamic layout of the aircraft, being basic for determining the shapes, dimensions and the arrangement of the empennage and the ailerons; it also affects the external shapes and arrangement of the wing.

Layout requirements are connected with the possibility of accommodating loads and units in the wing (tanks, landing gear,

engine set-up, etc.) under the condition of an insignificant increase in wing drag by secondary structures or by the deterioration in the state of its surface due to the presence of doors, hatch covers, etc. On high-speed aircraft this condition sometimes makes it necessary to forgo installing engines in the wing and attaching landing gear supports to the wing.

Furthermore, when coupling the wing with other aircraft components the arrangement of their structure diagrams should not be disrupted.

Requirements imposed on the strength and rigidity of a wing. A wing should possess the least possible design weight, sufficient strength, longevity and rigidity for ensuring the safety of the aircraft in all permissible operating regimes.

It is necessary to ensure a rigidity of wing design sufficient so that the critical velocities at which the phenomena of excessive wing twisting (overtwisting, divergence), loss in aileron efficiency (reversal), self-excited wing oscillations (flutter) arise, exceeded the flight velocities specified for operation. These phenomena are examined in detail in chapter 6.

Operating requirements. It is necessary in creating a wing to ensure the operational quality of the production technique of its design. For this the design should make possible the simple and rapid execution of all monitoring and maintenance operations. It is necessary to ensure good access to all important parts of the wing and to the units accommodated in it, the simplicity of installing and removing them, to provide for hatches and joints on the wing, and it is necessary to take measures to protect the surface of the wing from the effect of the external medium and from random damages during operation.

Technological requirements. This group of requirements pertains to the production and the repair of the technological efficiency in

a wing design. It specifies for the taking of measures to ensure low labor input and simplicity in manufacture and repair, precise execution of the external wing contours, the possibility of employing comparatively inexpensive, plentiful materials and semi-finished products, etc.

The technical requirements imposed on a wing, to a considerable extent are mutually contradictory. For example, the small thickness of the wing profile is favorable from the viewpoint of the aerodynamics of a high-speed aircraft, but in ensuring the necessary strength a thin wing turns out to be heavier. The operating requirement of the presence of hatches in a wing contradicts the requirement for ensuring strength with less weight; even well fitted hatch covers detract from the aerodynamic characteristics of the wing.

In designing it is necessary to take into account the type and the purpose of the aircraft, its operating conditions, by subordinating the selection of the parameters and the structural shapes of the wing to the condition best satisfying the most important requirements imposed on the particular aircraft.

§ 2. LAYOUT OF THE EXTERNAL SHAPES OF A WING

By the layout of the external shapes of a wing - by aerodynamic layout is understood the selection and the mutual tying together of the external wing contours and the coupling of the wing with the fuselage.

The purpose of aerodynamic layout is the realization first of all of aerodynamic requirements imposed on the wing. At the same time all the other technical requirements should also be taken into consideration.

The aerodynamic layout of the wing is included in the complex of the aerodynamic layout of the entire aircraft. Thus, in the final selection of the wing parameters the shapes and the arrangement of the other aircraft components should be taken into account.

1. External Wing Shapes

External wing shapes are characterized:

a) by the profiles of the wing sections;

b) by the wing contour in plan;

c) by the wing contour in a front view;

d) by the dimensions of the wing and by the lay-out diagram of its parts (monoplane, biplane).

The external wing shapes of a contemporary aircraft are the result of a prolonged process of refining them. The development of the external shapes of a wing is connected with improving the flight characteristics of aircraft, by introducing into aircraft construction new materials and improving the structure diagrams and the designs.

The requirements imposed at the present time on an aircraft, are so complex that the external shapes of the wings of an aircraft being designed are established as a result of special research.

Let us examine considerations concerning the effect of the basic parameters, characterizing the external shapes of a wing, on the properties of the wing and the aircraft.

Profiles of Wing Cross Sections

The shape of a profile (Fig. 2.1) is characterized by the contours of the upper and lower outlines and the following basic

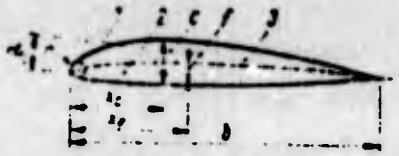

Fig. 2.1. Geometric characteristics of: c - the maximum thickness; f - the maximum concavity; r - the radius of curvature of the leading edge; b - chord length; x_c and x_f - the distances from the leading edge of the profile to the maximum thickness and the maximum concavity: 1 - aerodynamic chord; 2 - geometric chord; 3 - the center line of the profile.

dimensionless parameters: the relative thickness $\bar{c}=c/b$; the relative distance of the maximum thickness with respect to the chord $\bar{x}_c=x_c/b$; the center-line camber (curvature) $\bar{f}=f/b$; the relative distance of the maximum concavity with respect to the chord $\bar{x}_f=x_f/b$; the relative radius of curvature of the leading (trailing) edge $\bar{r}=r/b$.

Profiles are usually assigned for the wing sections taken in accordance with flight or perpendicular to the aerodynamic center axis. The length of chord b is measured in accordance with the arrangement of the cross section.

An aerodynamic chord of a profile (zero-lift chord) is a chord passing through the trailing edge of a profile parallel to direction of flow at which $c_y=0$. The curvature of a profile increases the angle α_0 between the geometric and aerodynamic chords (Fig. 2.2). For a symmetric profile the geometric and aerodynamic chords coincide and $\alpha_0=0$. The types of profiles of wing cross sections (Fig. 2.3) and their parameters are selected in accordance with the outlined flight data of the aircraft.

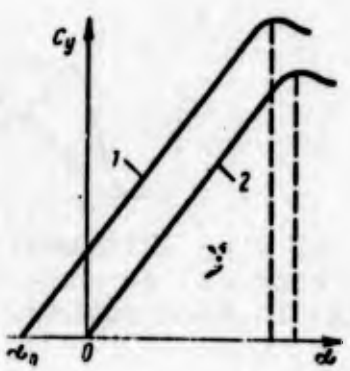

Fig. 2.2. The effect of the concavity of a profile on the dependence $c_y=f(\alpha)$ and the magnitude of zero-lift angle: 1 - for an unsymmetric profile; 2 - for a symmetric profile. For symmetric profiles $\alpha_0=0$.

For the wings of subsonic aircraft (M<0.8) comparatively thick lift profiles with a rounded leading edge are employed. The average values of the most important parameters of these profiles are: $\bar{c}$=0.1-0.18; $\bar{x}_c$=0.2-0.37; $\bar{f}$=0-0.035.

Wings with such profiles have high values of $c_{y\ max}$ and low profile drag which during subsonic flow depends little on the profile thickness (Fig. 2.4a). The profile thickness ensures acceptable volumes for the accommodation in a wing of fuel, landing gear, engines and sufficient structural height of the wing.

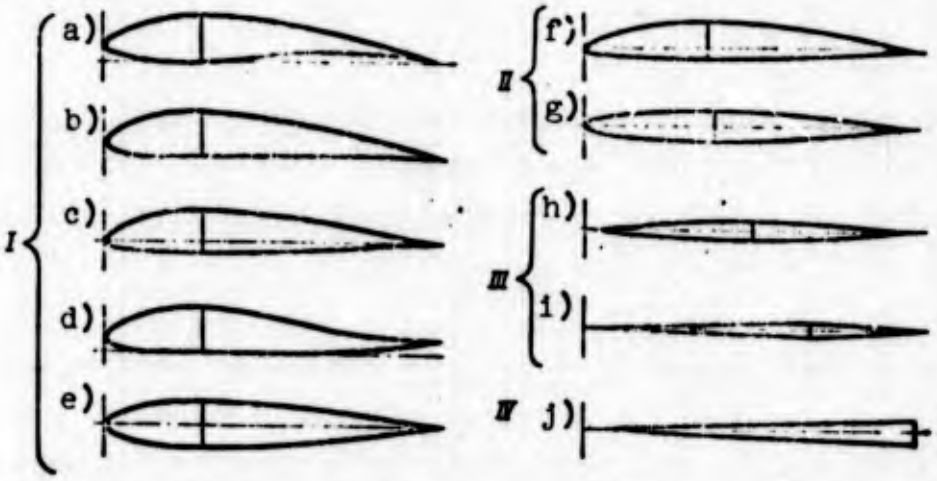

Fig. 2.3. Types of wing profiles for different flight velocities: I - subsonic flight velocities: a) convex-concave (very low flight velocity); b) plane-convex; c) biconvex unsymmetric; d) S-shaped; e) biconvex symmetrical; II - transonic flight velocities: f) biconvex unsymmetric; g) biconvex symmetrical; III - supersonic flight velocities; h) arc; i) diamond-shaped; IV - hypersonic flight velocities; j) tapered.

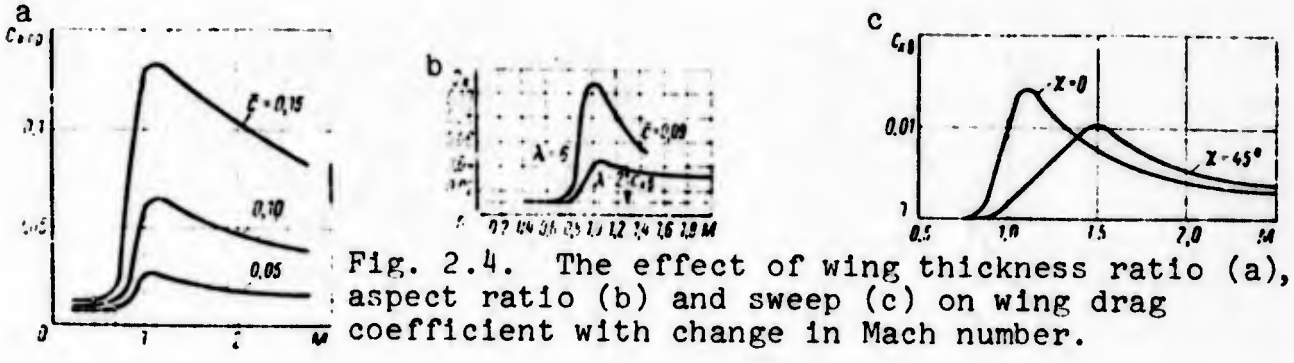

Fig. 2.4. The effect of wing thickness ratio (a), aspect ratio (b) and sweep (c) on wing drag coefficient with change in Mach number.

For the wings of transonic and supersonic aircraft[1] special thinner symmetrical profiles are employed.

An increase in the aerodynamic efficiency of a delta wing can be attained by employing, for the purpose of decreasing the included drag, the bending downward of the leading edge of the airfoil profile which increases in the direction from the root toward the wing tip (conical wing camber).

The values of the most important parameters of profiles for the wings of transonic aircraft are $\bar{c}$=0.09-0.16; $\bar{x}_c$=0.3-0.4; $\bar{f}$=0-0.035, for wings of supersonic aircraft - $\bar{c}$=0.02-0.-5; $\bar{x}_c$>0.5; $\bar{f}$=0.

Wings with these types of profiles possess high values of $M_{крит}$ and low wave drag when making the transition over the speed of sound. The essential deficiencies in thin wings are the low values of $c_{y\ max}$. A decrease in the thickness ratio in the case of short wing chords decreases the internal volumes of a wing and the structural height of the wing beam, which leads to an increase in its design weight.

The effect of profile thickness on wing weight can be explained in the following manner. If a wing is represented as a beam with height H loaded with bending moment $M_{изг}$, then the force in the beam zones is (see Chapter 3, § 6)

$$P = \frac{M_{изг}}{H}.$$

If it is assumed that in a specific cross section $H \approx \bar{c}b$ the destructive bending moment is $M^{р}_{изг}$, and the rupture stress is $\sigma_{разр}$,

---

[1] Aircraft which can attain M>1 are considered transonic aircraft, but in normal operation fly at M<1.

Supersonic aircraft have a supersonic cruising flight regime M>>1. Aircraft with M>5 are hypersonic aircraft.

then the cross-sectional area of the wing beam zone required to ensure the strength is

$$F = \frac{M^{P}_{изг}}{\bar{c} b \sigma_{разр}}.$$

It is evident from this expression that with assigned b an increase in $\bar{c}$ leads to a decrease in the required F and, consequently, also in the weight of the beam.

Wing Contour in Plan

The trapezoidal wing planform usually with the rounded tips (Fig. 2.5a) has the greatest distribution.

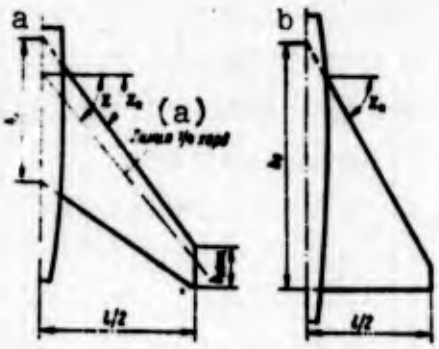

Fig. 2.5. Plan view and the basic dimensions of swept (a) and delta (b) wings.
Key: (a) 1/4 chord line.

The trapezoidal wing is characterized by the aspect ratio $\lambda = l^2/S$, by the taper $\eta = b_0/b_{конц}$ and by a sweep angle with respect to the aerodynamic center axis of (1/4 chord) - χ.

The wing is called swept when $\chi > 20°$.

A trapezoidal low aspect-ratio wing with great taper which has a trailing edge perpendicular to the longitudinal axis of the aircraft, is called a delta wing (Fig. 2.5b).

For delta wings and for a-l wings of supersonic aircraft the sweep is characterized by the angle with respect to the leading edge $\chi_п$.

The aspect ratio λ is the most important parameter of a wing.

An increase in the aspect ratio of wings of subsonic aircraft leads to a decrease in the coefficient of induced drag and to an increase in the lift/drag ratio K_{max} as follows from the expression

$$c_{xi} = \frac{1}{\pi k_1 \lambda} c_y^2,$$

where k - is the coefficient which considers the wing planform, the magnitude of its area occupied by the fuselage, and its arrangement with respect to the height of the fuselage.

This leads to a decrease in fuel consumption, and consequently to an increase in the flight range.

The negative consequences of an increase in λ are:

a) an increase in the weight of the wing due to an increase in bending moment (Fig. 2.6) and a decrease in the design height of the wing; a decrease in its rigidity;

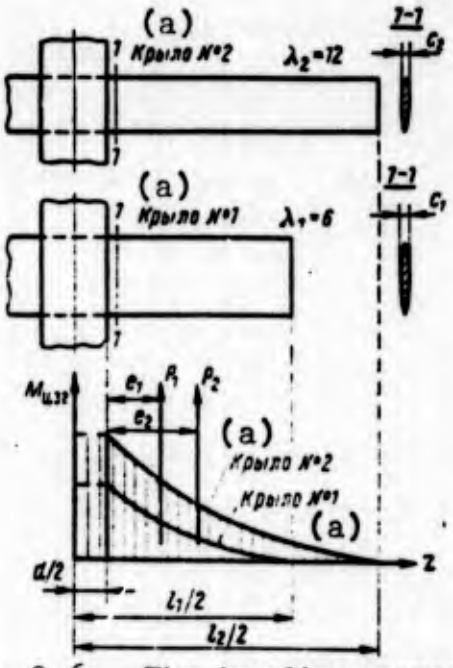

Fig. 2.6. The bending moments increase with an increase in λ: $P_2e_2>P_1e_1$.
Key: (a) Wing No.

b) a deterioration in maneuverability as a result of an increase in the mass moment of inertia of the aircraft relative to the longitudinal axis - I_x due to the variance in wing mass.

The values of λ are selected for each aircraft type taking into account the aforementioned aspects.

For nonmaneuverable subsonic transport aircraft with unswept wings λ=6-13, with swept wings - λ=5-8.

In certain cases to attain the outlined flight data it is necessary to increase λ even at the expense of an increase in wing weight. Thus, for instance, the record aircraft in its time with respect to flight range was the ANT-25 aircraft which had a wing with λ=13.1. The aspect ratio of the wings of performance-type gliders and sailplanes attains 25.

Maneuvering sport subsonic aircraft with unswept wings have lower aspect ratios - λ=5-7.

This is explained by the fact that in a maximum velocity regime, which is the basic one for these aircraft, the fraction of c_{xi} in c_x of an aircraft is insignificant (small α and c_y, and this means, also small c_{xi} correspond to regime V_{max}) and an increase in λ does not give a significant gain in c_x. At the same time by limiting λ acceptable maneuvering properties of the aircraft are attained, and the weight of the wing is reduced.

When selecting supersonic aircraft wing aspect ratios the following considerations are also taken into consideration:

a) the coefficient of induced drag c_{xi} of a supersonic flow depends little on the aspect ratio and in an approximate calculation the effect of λ is disregarded:

$$c_{xi} = \frac{\sqrt{M^2-1}}{3,8} c_y^2;$$

b) a considerable decrease in the aspect ratio leads to an increase of $M_{крит}$ and to a decrease in the increase in c_x due to the wave drag when $M>M_{крит}$ (see Fig. 2.4b);

c) in wings with low aspect ratios the values of c_y^2 and $c_{y\ max}$ are attained at large angles of attack - 25-30°. This is a deficiency, since with a limited layout of the landing gear at a

value $\alpha_{\text{пос}}$ a small value $c_{y\ \text{пос}}$ leads to a worsening of the landing properties of the aircraft;

d) for wings having supersonic profiles with small thickness ratios $\bar{c}$, it is very important that the employment of low aspect ratios leads to a reduction in the weight, and to an increase in the rigidity and the volumes of the root parts of the wing.

Taking the above cited aspects into account for supersonic aircraft wings of comparatively low aspect ratios are employed: λ=1.5-4.0.

When selecting the taper η both the positive and negative effect of the magnitude of taper on the properties of the wing and the aircraft are taken into account.

The positive effect of an increase in taper:

a) the effectiveness of lift-increasing (high-lift) devices on a wing (various types of slots and flaps) is increased, since its effect is propagated in this case by the large wing area;

b) the volumes of the root part of the wing is increased, which facilitates landing gear retraction, the accommodation of the tanks, etc.;

c) the weight is decreased and the rigidity of the root part of the wing is increased as a result of the increase in the structural height and the chord of the most loaded root cross sections.

The negative effect of increasing the taper η:

a) the tendency toward tip stall is increased, the stability and controllability in flight at large angles of attack drops off;

b) aileron effectiveness is decreased.

In wings of contemporary aircraft with different purpose the magnitude of taper is η=1-4.5.

Small sweep angles χ are sometimes employed for purposes of displacing the mean aerodynamic chord (MAC) of a wing to ensure the necessary position of the center of gravity in an aircraft.

The basic purpose of employing swept wings with χ=20-60° is to improve the aerodynamic properties of a wing at large Mach numbers:

a) in swept wings $M_{\text{крит}\chi}$ increases in comparison with $M_{\text{крит}\chi=0}$ of an unswept wing. The increase in the $M_{\text{крит}\chi}$ number of a swept wing is approximately characterized by the dependence

$$M_{\text{крит}\chi} = \frac{M_{\text{крит}\chi=0}}{\cos\chi}.$$

The employment of swept wings makes it possible to fly at large M numbers without the emergence of shock stall on the wing;

b) wing sweep also makes it possible to get through a shock stall more smoothly and to decrease the maximum value of $c_{x\,в}$. The nature of the effect of χ on the dependence of $c_{x\,в}$ on M is shown in Fig. 2.4c. The usually employed sweepback (χ>0) leads to an increase in the directional and lateral stability of an aircraft and to an increase in the critical rates of flutter and divergence.

However, swept wings also possess the deficiencies:

a) in wings with sweepback premature wing-tip stall occurs. This leads to a deterioration in the stability and controllability at large angles of attack, in particular during takeoff and during landing;

b) with an increase in sweepback $c_{y\ max}$ and K_{max} decrease, effectiveness of the high-lift devices is reduced which increases $c_{y\ max}$;

c) sweepback leads to the complication of production and to an increase in wing design weight.

For supersonic aircraft the delta wing planform is also employed.

The positive aerodynamic properties of sweepback, low aspect ratio and low thickness ratio are well combined in the delta wing.

In spite of the low thickness ratios delta wings can have in the root part comparatively large volumes and a design height, which facilitates layout and ensures the weight advantages of delta wings as compared with wings of another planform. The deficiency of a delta wing is the reduction in $c_{y\ пос}$ due to low aspect ratio.

Table 2.1 gives a brief summary of the basic qualitative data on the effect of the parameters characterizing wing contours in plan, on the properties of the aircraft.

Table 2.1

Parameters	Effect of an increase in the parameter	
	Positive	Negative
λ	Decrease in c_{xi}	1. An increase in $M_{изг}$ and the weight, a decrease in wing rigidity. 2. Decrease in $M_{крит}$. 3. Deterioration in the maneuvering properties of an aircraft due to the distribution in wing mass.
η_1	1. Decrease in $M_{изг}$ and weight and an increase in wing rigidity.	1. An increase in the tendency toward tip stall.

2. An increase in the effectiveness of wing high-lift devices. 3. An increase in the volumes of the wing root part.	2. A decrease in aileron effectiveness.
1. An increase in $M_{крит}$. 2. A decrease in $c_{x\ в}$ during the transition through the speed of sound.	1. An increase in the tendency toward tip stall. 2. A decrease in the effectiveness of wing high-lift devices. 3. Complication of production and an increase in wing weight.

Wing Contour in Front View

The basic parameter characterizing the front view of a wing is the wing dihedral angle ψ.

The magnitude and the sign ψ (in Fig. 2.7 $\psi>0$) are selected mainly from the condition of obtaining the necessary relationship between the directional and lateral stability depending on the magnitude of the sweep angle, the mutual arrangement of the wing and fuselage with respect to height and the parameters of the rudder unit.

Fig. 2.7. Explanation of a dihedral wing.

Sometimes layout considerations have an effect on the selection of the magnitude of angle ψ, for example the necessity for lowering the wing to reduce the height of the landing gear or for raising it to increase the height of the propeller blade tips above the ground or the height of the airscoops when mounting the engines on the wing.

2. Mutual Arrangement of the Wing and Fuselage

The mutual arrangement of the wing and fuselage is characterized:

a) by the longitudinal arrangement of the wing relative to the fuselage;

b) by the arrangement of the wing with respect to the height of the fuselage;

c) by the angle of the wing setting - by the angle between the geometric chord of a profile cross section and the fuselage center line;

d) by the coupling of the wing and fuselage surfaces.

In establishing the wing arrangement with respect to the fuselage it is necessary to consider that the basic load-bearing elements of the central part of the wing should pass through the fuselage and be fastened to it, without disturbing the layout of the passenger and cargo compartments.

The Longitudinal Arrangement of a Wing Relative to the Fuselage

The positioning of the mean aerodynamic chord of the wing - MAC - relative to the remaining aircraft components determines the position of the center of gravity of the aircraft - the center-of-gravity location with respect to the MAC (Fig. 2.8) characterized by magnitude $\bar{x}_{\text{ц.т}}=x_{\text{ц.т}}/b_A$ 100%. This is considered when selecting the longitudinal position of the wing relative to the fuselage.

Fig. 2.8. The position of the center of gravity of an aircraft (c.g.) relative to the leading edge of the mean aerodynamic chord (MAC) of the wing characterizes the position of the center of gravity of the aircraft.

The Arrangement of a Wing with Respect to the Height of the Fuselage

The arrangement of a wing with respect to the height of a fuselage can be in the middle, down, or up position. The three monoplane aircraft configurations shown in Fig. 2.9 correspond to this.

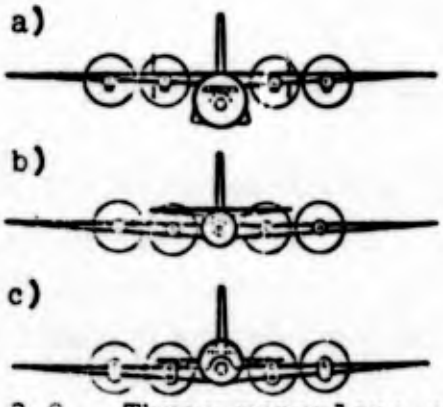

Fig. 2.9. Three monoplane configurations: a) high wing monoplane; b) midwing monoplane; c) low wing monoplane.

The middle wing position is the best from the point of view of aerodynamics, since it ensures the least harmful mutual wing and fuselage effect.

However, an essential deficiency of the midwing monoplane is the complexity in the positioning of the cabins and the cargo compartments in that part of the fuselage through which the wing passes.

The middle wing arrangement is encountered on military aircraft.

The upper wing arrangement makes it possible to obtain the least reduction in the $c_{y\ max}$ of the wing due to the effect of the fuselage and increases the lateral stability of the aircraft. Furthermore, the high wing monoplane provides: simpler, than for the midwing monoplane, coupling of the load-bearing elements of the wing with the fuselage; convenience in loading and unloading cargo aircraft because of the low position of the fuselage (Fig. 2.10a); a sufficient downward view. In the high wing monoplane configuration it is easier to provide, with the engines in the wing, sufficient distance of the propeller blade tips from the ground.

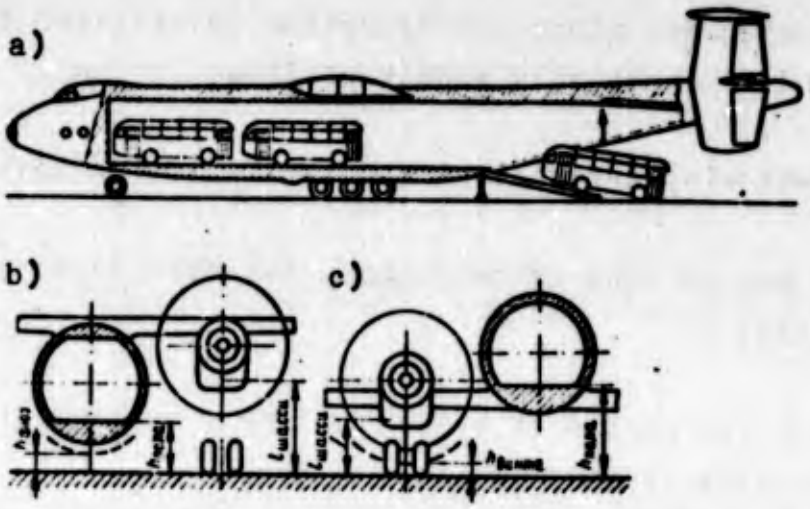

Fig. 2.10. A comparison of the layouts of a high wing monoplane and a low wing monoplane: a) the employment of a high wing monoplane configuration for a cargo aircraft makes it possible to lower the floor level and facilitates loading-unloading operations; b) and c)-the arrangement of the fuselage, engines and landing gear on a high wing monoplane and a low wing monoplane; with complete compression of the landing gear the following are necessary $h_{фюз} \geq 400$ mm and $h_{винта} \geq 200$ mm.
[фюз=fus; пола=floor; щасси=landing gear; винта=propeller].

Among the deficiencies of the high wing monoplane are the following:

a) the difficulty in the arrangement of the main landing gear struts - upon attaching the struts to the wing it is necessary to make them long, which leads to an increase in the weight of the landing gear and impedes their retraction; in attaching the main landing gear struts to the fuselage the track of the landing gear is narrow, and the need for retracting them into the fuselage complicates its design;

b) the complication of the design: in an emergency belly landing the fuselage of a high wing monoplane experiences great dynamic loads; therefore it is necessary to reinforce it and to increase the design weight;

c) the inconvenience of servicing high positioned engine installations.

A high wing monoplane configuration is utilized for passenger aircraft, and is especially widely utilized for cargo aircraft.

The lower wing arrangement has the following advantages:

a) the possibility of retracting the main landing gear struts into the wing;

b) during an emergency belly landing a considerable portion of the impact energy is absorbed by the wing;

c) high-lift devices can also be employed on the subfuselage part of the wing, which contributes to an improvement in the takeoff and landing properties of the aircraft;

d) convenience in servicing of low positioned engine installations;

e) the simplicity in coupling the load-bearing elements of a wing with fuselage.

Included among the deficiencies of a low wing monoplane are the following:

a) an increase in c_x of the aircraft and a reduction in $c_{y\ max}$ of the wing;

b) blocking of the downward view by the wing;

c) during the operation of engines situated close to the ground, the danger arises of the sucking of foreign objects into the engines;

d) the danger of the wing tip catching on the ground during landing with bank.

Low wing positioning is widely employed for passenger and training-sport aircraft.

Figure 2.10b shows the characteristics of the mutual positioning of the fuselage, engine, propellers and landing gear for high wing monoplane and low wing monoplane configurations.

Wing Setting Angle

The angle of incidence $\phi_{уст}$ (wing setting angle) is usually measured between the geometric chord of a profile of the lateral or axial (in the plane of symmetry of the aircraft) wing section and the fuselage center line, with which the flow direction actually coincides which corresponds to $c_{x\ фюз\ min}$ (Fig. 2.11).

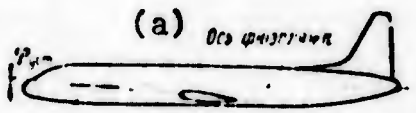

Fig. 2.11. Wing setting angle $\phi_{уст}$.
Key: (a) Fuselage center line.

To ensure the least aircraft drag it is desirable to take the wing setting angle equal to the angle of attack in the main flight regime: $\phi_{уст} \approx \alpha_{полета}$. In this case in the basic flight regime the fuselage center line will be located in the line of flight and the fuselage will create the least drag.

For transport aircraft the main flight regime is that with the angle of attack, close to the angle of the maximum L/D ratio, for fighters it is the regime of maximum velocity.

Deviations from the rule in question are encountered which are explained by the difficulties connected with the layout of the landing gear and the ensuring of the magnitude of the ground angle of attack of the wing (or the angle of attack of wing at rest), necessary with respect to takeoff and landing conditions.

The usual values of the wing setting angle are $\phi_{уст}=1\text{-}4°$.

Coupling of Wing and Fuselage Surfaces

In the coupling of a wing and fuselage roundings are employed which smooth the joint and fillet contours (Fig. 2.12), filling the channels between the wing and the fuselage. They are not introduced in calculating wing area. Their shape is selected by wind-tunnel tests.

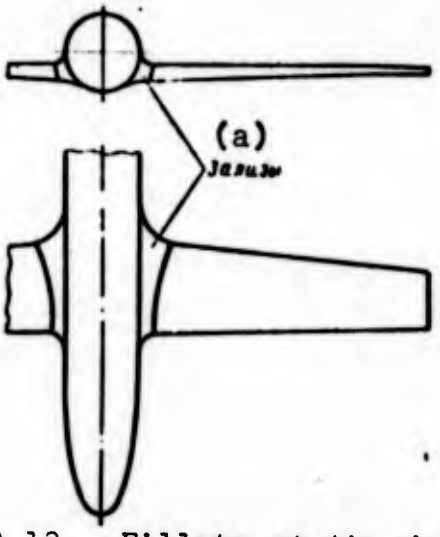

Fig. 2.12. Fillets at the joining of the wing with the fuselage which reduce interference drag.
Key: (a) Fillets.

When correctly laid out fillets eliminate the formation of vortices in flight regimes, give the reduction in c_x due to interference, however, increase c_x due to friction.

If near the fuselage the wing chord plane is normal to the surface of the fuselage, then the interference is lwo (Fig. 2.13) and fillets are not required. In this case it is sufficient to ensure the smooth coupling of the wing with the fuselage.

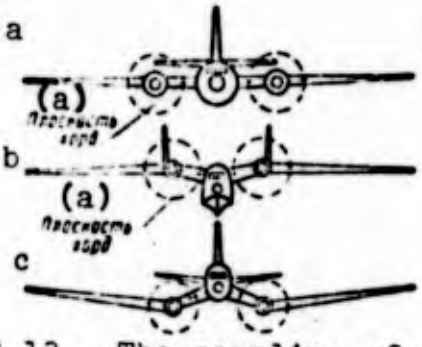

Fig. 2.13. The coupling of the wing with the fuselage in the midwing monoplane configuration (a), in the gull-wing configuration (b) or the inverted gull-wing configuration (c) reduces the interference drag.
Key: (a) Chord plane.

Let us dwell on the characteristics of the coupling of the wing with the fuselage in a transonic aircraft.

In the joint zone, there where the greatest curvature

of the mating surfaces coincides, a considerable increase in the local flow velocities flowing around the aircraft occurs, and as a consequence a decrease in $M_{крит}$ and an increase in $c_{x\ в}$.

To prevent this it is necessary that the maximum thickness of the lateral wing section not coincide with the fuselage midsection cross section (Fig. 2.14).

Fig. 2.14. When the position of maximum thickness distance of the lateral wing section and the midsection cross section of the fuselage coincide the wave drag of the aircraft sharply increases. Key: (а) Fuselage midsection.

The "area rule" is a generalization of this position, which it is possible to formulate in the following manner: to reduce the increase in the local flow velocities in the case of mutual coupling of aircraft components the cross-sectional area distribution of the entire aircraft over its length should be the same, as for a solid of revolution with the least drag.

For observance of this rule the areas of the transverse cross sections of the fuselage and the engine nacelles should be decreased at the section where they couple with the wing. This has been done, in particular, on the Tu-104 aircraft. Figure 2.15 shows the general shape of the B-58 "Hustler" aircraft, in the layout of which the area rule was also employed.

In coupling the swept wing with the fuselage measures are taken to reduce the "central effect", which manifests itself in the fact that the plane-parallel flow around the central parts of the wing does not make it possible to realize the sweep effect.

For this an increase in the sweep of the leading edge of the wing is employed (Fig. 2.16) in the section which adjoins the

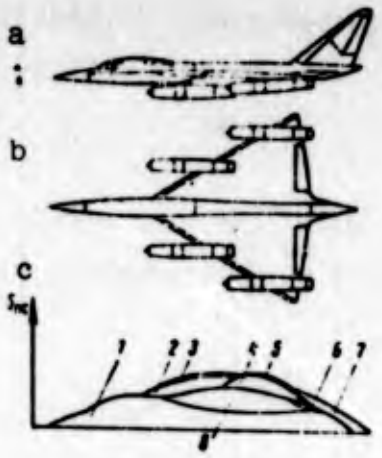

Fig. 2.15. Side view of the aircraft (a), bottom view (b) and the distribution of the cross-sectional areas (c) along the length of the supersonic B-58 aircraft, in the layout of which the "area rule" is used: 1 - fuselage; 2 - internal engine nacelles; 3 and 5 - pylons; 4 - external engine nacelles; 6 - fillet; 7 - empennage; 8 - wing.

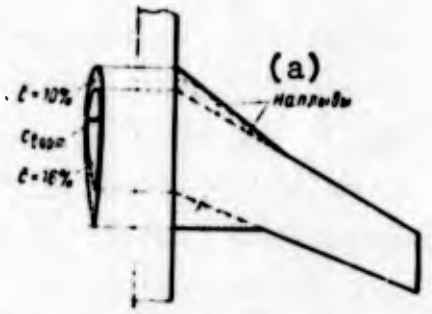

Fig. 2.16. "Extension" on the leading edge compensates for the decrease in the sweep effect of the wing section which adjoins the fuselage.
Key: (a) Extensions.

fuselage ("extension"), and the positioning at these sections of profiles with a more forward arrangement of the minimum pressure (usually this is attained by displacing the maximum thickness forward).

"Extensions" in front and in back are also employed for purposes of increasing the chords of the central wing part (see Fig. 2.16), and consequently, its volume (for example, for landing gear retraction) and area (for increasing the effectiveness of the high-lift devices). Furthermore, the employment of "extensions" makes it possible without varying the design height of the wing beam ($c_{борт}$=const), to reduce the thickness ratio $\bar{c}$ of the lateral profile, which is necessary for increasing the $M_{крит}$ of the central part of the wing.

3. Measures for Preventing Tip Stall

When large angles of attack appear for tapered wings with $\chi \geq 0$ flow separation begins at the tips (usually nsymmetric) and extends further along the wing. This phenomenon is dangerous, since

it leads to a sharp deterioration in stability and controllability, in the loss of aileron effectiveness, the going into a spin, etc., and at the larger magnitudes of wing taper and sweep it arises earlier, at lesser angles of attack.

Let us examine the measures used to prevent tip stall on wings at flight angles of attack.

Unswept Wings

The following design measures are finding employment for tapered unswept wings:

a) the magnitude of taper η is limited;

b) special selection of the profiles and their angles of setting is accomplished - aerodynamic and geometric twist;

c) on the tip sections of a wing slats are installed with a length somewhat exceeding the aileron length, automatically (under the effect of air forces) opening at large angles of attack;

d) a slight forward sweep is imparted to the wing, in which the flow separation begins near the wing root and manifests itself less sharply.

Let us examine the effect of wing twist on tip stall in more detail.

Geometric twist. If the geometric chords of wing sections do not lie in one plane, then the wing is called geometrically twisted (Fig. 2.17a).

The angle of geometric twist ϕ_r - is the rotation of the tip chord relative to the root chord (chord of the axial or lateral

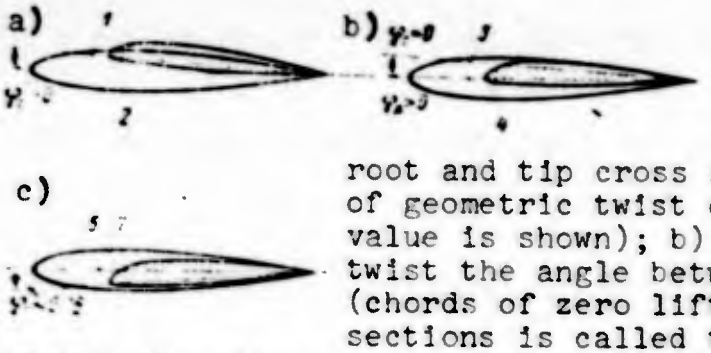

Fig. 2.17. Geometric and aerodynamic twist of a wing: a) the angle between the geometric chords of the root and tip cross sections is called the angle of geometric twist of the wing (a positive angle value is shown); b) in the absence of geometric twist the angle between the aerodynamic chords (chords of zero lift) of the root and tip cross sections is called the angle of aerodynamic twist of the wing (a positive angle value is shown); c) a combination of positive aerodynamic twist with negative geometric twist is employed to prevent tip stall at large angles of attack; 1, 6 - geometric chords of the tip cross sections; 2, 7 - geometric chords of the root cross sections; 3 - aerodynamic chord of the tip cross section; 4 - aerodynamic chord of root cross section; 5 - aerodynamic chords of root and tip cross sections ($\phi_A > 0$).

cross section) is considered positive in direction for increasing the angle of attack:

$$\alpha_{0\,tip} = \alpha_{0\,root} - \varphi_A.$$

Aerodynamic twist. If in the absence of geometric twist the aerodynamic chords of the wing cross section profiles do not lie in one plane, then the wing is called aerodynamically twisted (Fig. 2.17b).

The aerodynamic twist is achieved when the profiles of different cross sections possess different center-line camber $\bar{f}$.

The angle of aerodynamic twist ϕ_A is measured as the angle between the root and tip aerodynamic chords and also is considered positive in the direction of an increase in α.

The wings of contemporary aircraft can have both aerodynamic and geometric twist.

To prevent tip stall at a wing tip more lifting profiles are installed - profiles with more camber and therefore with higher $c_{y\,max}$ and α_0 (positive aerodynamic twist) and negative geometric

twist is imparted. In this case usually for unswept tapered wings geometric and aerodynamic twists are combined so that the aerodynamic chords of the root and tip cross sections are approximately parallel (Fig. 2.17c).

This is explained by the fact that if we impart only a positive aerodynamic twist to the wing, i.e., if we install a more lifting profile at the wing tip, then it is possible not to obtain the desired effect, if $\alpha_{кр\,крит}$ of the tip profile will be less than the $\alpha_{кр\,крит}$ of the root profile.

but if in addition we decrease the setting angle of the tip profile, i.e., if we impart a negative geometric twist to the wing, $\alpha_{кр\,крит}$ of the tip cross section will increase (Fig. 2.18) and at the tip profile a considerable angle of attack reserve of up to $\alpha_{кр\,крит}$ is formed as compared with the root profile.

Fig. 2.18. Negative geometric twist, by increasing the critical angle of attack of the wing-tip section, ensures a sufficient reserve with respect to stall (reserve of angle of attack: $\alpha_{кр\,крит} - \alpha_{кр\,корн}$) of a more lifting tip profile: 1 - c_y of tip profile; 2 - c_y of tip cross section with negative geometric twist; 3 - c_y of root profile.

The application of twist leads to the fact that the separation of vortices from the wing at large angles of attack arises earlier not at the wing tips, in the zone where the ailerons are located, but in the central part where it does not lead to so considerable a disruption in lateral stability and controllability.

Swept Wings

Transonic and supersonic aircraft have, as a rule, wings with sweep which possess an increased tendency toward tip stall.

Characteristic for a wing with $\chi>0$ is the motion of the boundary layer of the wing from middle toward the tip of the wing and the accumulation of the boundary layer at the tips causes tip stall at comparatively small angles of attack (5-8°).

Tip stalls can cause for swept wings the appearance not only of transverse, but also of longitudinal destabilizing moments, since the wing tips are moved away from the center of gravity of the aircraft along the longitudinal axis.

For preventing tip stalls in swept wings there are employed along with the already examined measures (a combination of aerodynamic and geometric twists, limitation of the magnitude of taper, and slats) also special measures for retarding the motion of the boundary layer toward the wing tip and for removing the swirling air layer from the wing before its impingement on the ailerons. Included among these are:

a) the mounting of stall fences of low height (Fig. 2.19) on the upper wing surface, whose plane (the fences) is parallel to the plane of symmetry of the aircraft;

b) the formation of a projection on the tip part of a wing, a "tooth" or of small slots in the leading edge of the tip part of a wing parallel to the flow - "notches", and sometimes both (Fig. 2.20).

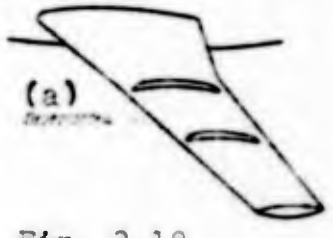

Fig. 2.19

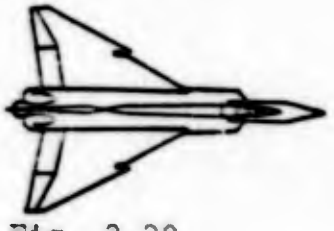

Fig. 2.20

Fig. 2.19. Stall fences on the upper surface of a swept wing prevent the accumulation of a boundary layer on wing tip sections and they displace the separation zone to its middle part.
Key: (a) Stall fences.

Fig. 2.20. "Tooth" and "notch" combination on a delta-wing airplane.

Wing Dimensions

The above examined considerations concerning the external shapes of a wing are considered when laying out a wing and when determining its dimensions.

The basic magnitudes characterizing the dimensions of a wing are: S - wing area; l - wing span; b_0 and $b_{конц}$ - the lengths of the axial and tip chords; c_0 and $c_{конц}$ - wing thicknesses along the axis of the symmetry of an aircraft and at the tip.

Wing area S is the most important parameter determined during the designing of an aircraft depending on its purpose and on the technical requirements imposed on it.

Also included in the wing area S is the section of wing located within the fuselage.

There are different methods for calculating S. Subsequently, we will use the method indicated in Fig. 2.21b) In determining S the area of the fillets is not considered.

Let us analyze certain formulas of aerodynamic calculation, into which wing area enters.

The velocity of horizontal flight at an assigned height at an assigned value of thrust P or of power $N_{энв}$ of an engine is

$$V=\sqrt{\frac{2P}{\rho C_x S}}=\sqrt{\frac{2\mu_{пр}P}{\rho C_x}} \qquad (2.1)$$

or

$$V=\sqrt[3]{\frac{150N_{энв}\eta_в}{\rho C_x S}}=\sqrt[3]{\frac{150\mu_{нв}\eta_в P}{\rho C_x}}, \qquad (2.2)$$

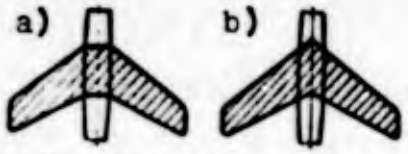

Fig. 2.21. Methods of determining wing area.

where $\mu_P = P/G$ - is the thrust-weight ratio of the aircraft; $\mu_N = N_{экв}/G$ - is the power-weight ratio; $p = G/S$ - load per unit wing area, kgf/m^2.

Landing velocity

$$V_{пос} = \sqrt{\frac{2G}{\rho c_{y\,пос} S}} = \sqrt{\frac{2p}{\rho c_{y\,пос}}}. \qquad (2.3)$$

Length of takeoff run

$$l_{взл} \approx k_1 \frac{G_0}{S} \frac{G_0}{P_0} = k_1 \frac{p_0}{\mu_{P_0}} \qquad (2.4)$$

or

$$l_{взл} \approx k_2 \frac{G_0}{S} \frac{G_0}{N_0} = k_2 \frac{p_0}{\mu_{N_0}}, \qquad (2.5)$$

where P_0 and N_0 are the thrust and the power during takeoff; G_0 - is the takeoff weight; $p_0 = G_0/S$; k_1, k_2 - are coefficients.

From formulas (2.1) or (2.2) it follows that to increase V it is desirable to decrease $c_x S$.

It is known that

$$c_x S = c_{x\,к} S + \Sigma c_{x\,вр} S_{вр}. \qquad (2.6)$$

where $c_{x\,вр}$ - is the coefficient of parasite drag (the drag coefficient of the nonlifting aircraft components - fuselage, empennage, engine nacelles installations, etc.); $S_{вр}$ - is the area of the midsection cross section of the nonlifting aircraft components; $c_{x\,к}$ - is the value of the drag coefficient of the wing in the flight regime in question.

A decrease in S leads, as is evident from (2.6), to a decrease in $c_x S$ due to a decrease in the fraction of wing drag and to an increase in the flight velocity.

However, it follows from formulas (2.3), (2.4) and (2.5) that a decrease in S will cause also an increase in the landing velocity $V_{пос}$ and in the length of the takeoff run $L_{разб}$. Furthermore, a reduction in wing area leads to a deterioration in the characteristics of horizontal aircraft maneuvering.

To sum up, it is necessary to select the wing area of a specific aircraft type so that an improvement in some flight qualities (for example V_{max}) would not lead to a sharp deterioration in other qualities (for example $V_{пос}$, $L_{разб}$).

A contradiction in the requirements is to a certain extent resolved by the application of wing high-lift devices (flaps of various types, etc.) and by the fact that in the case of a decrease in S certain flight characteristics of an aircraft (for example takeoff run length) can be ensured, by compensating for a reduction in wing area by an increase in thrust (thrust augmentation).

When determining wing area the load per unit wing area $p=G/S$ is taken into account.

The effect of p on certain flight data is evident from formulas (2.1)-(2.5).

The magnitude of load per unit wing area is selected during designing to be such, so as to fulfill the technical requirements imposed on the most important flight properties and to ensure acceptable takeoff-and-landing characteristics of the aircraft. In this case the effect of p on aircraft operational economy is taken into account.

According to statistics for contemporary aircraft the usual values of load per unit area p_0 which correspond to takeoff weight, have the following values:

for the passenger and cargo aircraft of local lines p_0=150-300 kgf/m^2;

for heavy main-line transport aircraft p_0=350-600 kgf/m^2.

The possibility of employing higher values of load per unit wing area for heavy main-line transport aircraft is explained by the fact that for their takeoff airfields are employed which have long runways.

The increase in the level of load per unit area explained by increasing the cruising velocities of transport aircraft, led to the fact that the monoplane wing configuration even a long time ago was considered the most favorable and is most widely employed. It is examined in essence below.

For aircraft in which for the purpose of operating from small airfields the least possible values of landing velocity and takeoff run length should be provided and high cruising velocity is not required, a considerable decrease in the load per unit area and an increase in the wing area can turn out to be rational. The employment of a biplane configuration makes it possible in this case to have the least aircraft wing span.

Table 2.2 presents the values of p_0 for certain aircraft of civil aviation.

Table 2.2

Aircraft	[illegible]	An-2 (biplane)	An-14A	[illegible]	An-24	Il-14M	An-10A	Tu-134	Tu-154	Il-62
$p_0\left[\frac{kgf}{m^2}\right]$	54.6	77	82.5	178.5	265	435	444	345	421	560

For comparison let us point out that for the Po-2 biplane aircraft the load per unit area on the wing was equal to 27.8 kgf/m^2.

In designing an aircraft the magnitude of wing area S can be determined from the weight of the aircraft found by approximate calculation and from the selected load per unit area p_0

$$S = \frac{G_p}{p_0}.$$

The values of λ, η, $\bar{c}$ and of other parameters established on the basis of the above cited considerations make it possible to find the geometric dimensions of a wing (see Fig. 2.5).

Span is

$$l = \sqrt{\lambda S}.$$

The dimensions of the tip and the axial chords of a tapered wing planform can be determined, by simultaneously solving the following two equations:

$$S = \frac{b_0 + b_{конц}}{2} l;$$

$$b_0 = \eta b_{конц}.$$

To sum up,

$$b_{конц} = \frac{2S}{l(\eta + 1)}.$$

Wing thickness:

along the axis of symmetry of the aircraft $c_0 = \bar{c}_0 b_0$;

at the tip $c_{конц} = \bar{c}_{конц} b_{конц}$.

§ 3. HELICOPTER ROTORS

1. General Characteristics

The rotor (NV) [HB] is the most important part of a helicopter. The main purpose of a rotor is to create lift force in all flight regimes and forces which ensure the translatory displacement of a helicopter in the assigned directions. Moreover, the rotor creates stability for the helicopter and is employed to control it.

The requirements which are placed at the basis of the creation of a rotor design, ensue from its purpose and are determined by considerations of aerodynamics, strength, rigidity and the savings with respect to design weight, and also by the conditions of production and operation. They are similar to the requirements imposed on the wing examined in detail in § 1.

The basic parts of a rotor are the hub and blades. By the method of attaching of the blade to the hub and the hub to the shaft which rotates the rotor, rotors can be subdivided into three types:

1) with hinged suspension of the blade (Fig. 2.22a, b);

2) on a universal joint (Fig. 2.22c);

3) with rigid attachment of the blades (Fig. 2.22d).

At the present time on some light helicopters rotors with a spring blade attachment are employed which can be considered a variety of the first type of rotor.

Rotors with hinge attachment of the blades have received the greatest application.

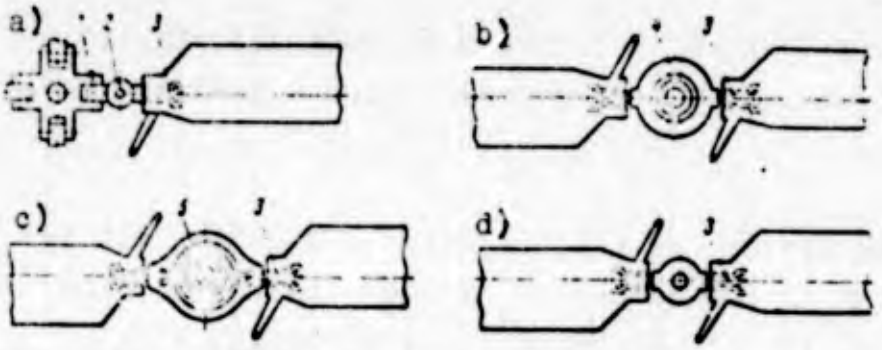

Fig. 2.22. Types of rotors a) with hinged suspension of blades; b) with general drag hinge; c) on a universal joint; d) with rigid attachment of the blades: 1 - flapping hinge (GSh); 2 - drag hinge (VSh); 3 - feathering hinge (OSh); 4 - general flapping hinge; 5 - universal joint.

Each rotor blade of this type has three hinges: the flapping hinge (GSh) [ГШ], the drag hinge (VSh) [ВШ] and the feathering hinge (OSh) [ОШ].

Because of the presence of the flapping hinge the blade can accomplish so-called flapping motion upward and downward.

The flapping angle β is limited designwise by stops.

The drag hinge makes it possible for the blades to accomplish oscillations in the plane of rotation. The angles of lag or lead of a blade are also limited by stops. The feathering hinge makes it possible for the blade to be turned around the axis which passes through its span, varying its setting angle (blade pitch).

Let us examine the basic parameters which determine the technical properties of a rotor.

2. Parameters Which Determine the Properties of a Rotor

a. The external shapes of the blade are characterized by the type of cross section profiles of the blade and by the contour of the blade in plan.

The obtaining of high values of lift and maximum velocity in horizontal flight at the assigned engine power, etc. depends on the external blade shapes.

Thus, the blade profile should possess great L/D ratio, little variation in the position of the center of pressure in the working range of the angles of attack of the blade cross sections, high values of $c_{y\ max}$, $\alpha_{крит}$ and $M_{крит}$, to ensure the capacity to transfer into the autorotation regime in a large range of angles of attack and the possibility of simple design and technological execution of the blade.

To a sufficient degree these requirements are satisfied by the shapes used for aircraft wings: the NACA 00 biconvex symmetrical series and the unsymmetric shapes of the NACA230 series with $\bar{c}$=0.06-0.18. At the blade tips high-speed profiles are frequently installed (for example, TsAGI (Cent. Inst. of Aerohydrodynamics im N. Ye. Zhukovskiy) P-57-9 profiles with a high $M_{крит}$ value. Sometimes special profiles are created which possess the above enumerated properties.

The shape of a blade in plan can be rectangular (untapered), tapered and mixed (Fig. 2.23).

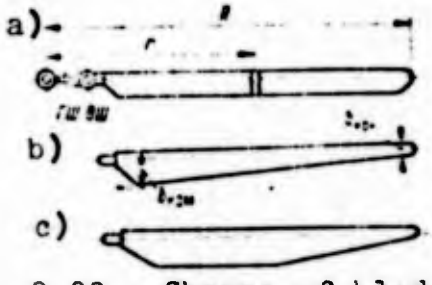

Fig. 2.23. Shapes of blades in plan: a) rectangular (untapered); b) tapered; c) mixed.

The effect of blade shape on thrust magnitude is slight in comparison with the effect of other parameters.

b. Geometric blade twist. Usually the rotor blades of helicopters, analogous to aircraft wings, have negative geometric twist, so that near the root the angles of attack are greater than at the tip. This gives a more uniform distribution of the aerodynamic forces along the blade and decreases the inductive

rotor losses, caused by the nonuniformity of the flow distributions.

This twist also leads to stall delay at the blade tip going along the flow, and increases the $M_{крит}$ of the tip profiles, which makes it possible to increase the flight velocity of the helicopter.

c. The area swept by the rotor $F_{ом}$ - the area of the circle, which the blade tips describe. $F_{ом}$ is analogous in its value to the area of an aircraft wing.

d. The load per unit area on the area swept by the rotor p. The load on a square meter of area being swept is one of the most important parameters which determine the flight properties of a helicopter, and is computed according to the following formula

$$p = \frac{G}{F_{ом}},$$

where G - is the flight weight of a helicopter, kg.

In contemporary helicopters the load per unit area is p=12-45 kgf/m^2.

e. Rotor solidity ratio - is the abstract number which indicates, which part of the area swept by a rotor, is filled by blades:

$$\sigma = \frac{F_{д}z}{F_{ом}},$$

where $F_{д}$ is the blade area; z is a number of blades.

The magnitude of σ depending on the helicopter configuration is selected within the limits of from 0.03 up to 0.09.

With an increase in helicopter weight the rotor solidity ratio increases.

f. The diameter of the rotor $D_{н.в}$ is selected depending on the weight of the helicopter G and on the necessary load p on the area swept by the rotor:

$$D_{н.в} = \sqrt{\frac{4G}{\pi p}}.$$

Besides the diameter, the following parameters are frequently employed: radius of blade tip - R (Fig. 2.23a), radius of blade element - r, relative radius of blade element - $\bar{r}=r/R$.

For obtaining great thrust at a comparatively low expenditure of power large-diameter rotors are employed on helicopters, which rotate at limited circular speeds which prevent flow separation from the blade tips.

g. Blade setting angles and rotor pitch.

The setting angle of a blade element is the angle ϕ formed by the chord of an element and by the plane of rotation of the rotor head.

For different blade elements the setting angles will be different.

The pitch of the rotor is arbitrarily estimated by the setting angle of the blade element, the relative radius of which is $\bar{r}=0.7$.

h. Number of rotor blades.

The most advantageous rotors which satisfy the requirements for equilibrium and which possess sufficiently good efficiency, are the rotors which have a number of blade more than two. Three-bladed, four-bladed and five-bladed rotors are employed.

i. Weight of a rotor blade has a substantial effect on the characteristics of blade flapping. Thus, the weight of a rotor is in a definite relationship with the weight of the helicopter.

In a single-rotor helicopter for obtaining a good weight coefficient it should be 9-15% of the total flight weight of the helicopter.

j. Characteristics of the operational regime of a rotor. Depending on the position of the rotor in the airflow two basic operational regimes are distinguished: axial and oblique flow.

Axial flow occurs during vertical flight and during "hovering", when the counterflow is directed along the axis of the rotor. The position of a blade of a rotating rotor relative to the flow impinging on the rotor, does not vary, thus, the aerodynamic forces also do not vary.

In horizontal or in inclined flight there is oblique airflow around a rotor. In this case the airflow can be resolved into two flow components: along the rotor axis and in the plane of rotation (Fig. 2.24).

Fig. 2.24. Resolution of the flight velocity vector for two components.
Key: (a) Plane of rotations of the hub.

The ratio of the rate of flow, lying in the plane of rotation, to the blade tip velocity is the coefficient which characterizes the operational regime of the rotor:

$$\mu = \frac{V \cos \alpha_{пл}}{\omega R}.$$

Sometimes μ is called the characteristic of the flight regime of a helicopter.

For horizontal flight when the angle of attack $\alpha_{H.B}$ of a rotor is small and its cosine is close to unity, it is possible to assume that

$$\mu = \frac{V'}{\omega R}.$$

In the case of vertical flight or "hovering" $\mu=0$.

During horizontal flight at maximum velocity μ can attain a value of 0.35-0.4.

Under the conditions of oblique flow a continuous variation occurs in the position of the blade relative to the velocity vector of the flow impinging on the rotor. The nature of the flow about the blades and the forces which arise in this case depend on this.

For determining the blade position the concept of blade azimuth is introduced.

The azimuth, or the angle of azimuthal blade position ψ is the angle between the zero line and the longitudinal axis of a blade at a given instant (Fig. 2.25).

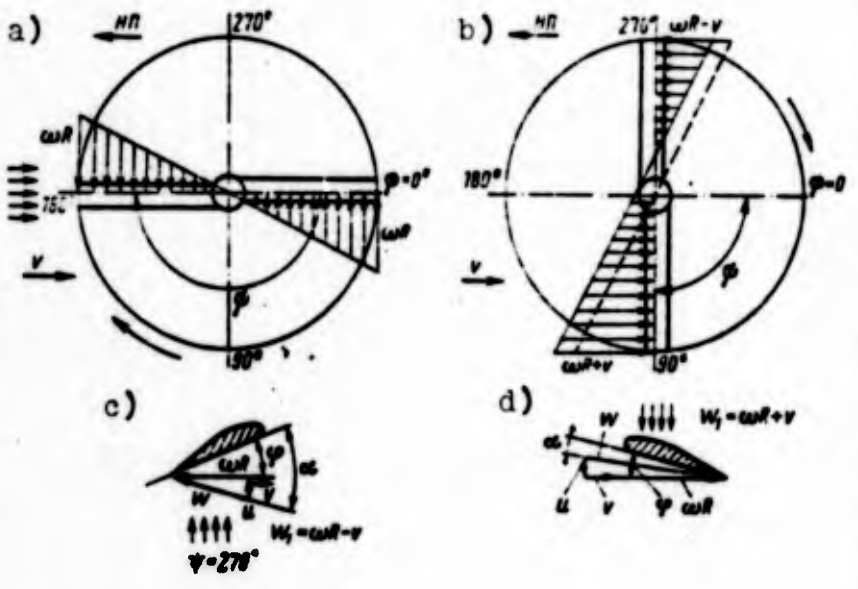

Fig. 2.25. Airstream velocity and variation in the angles of attack of the blade cross section during flapping: a, b) horizontal flight: velocity of the airstream flowing around the blade in different azimuthal positions; c) flapping downward; d) flapping upward; variation in the angles of attack of the blade cross section during flapping motions.

Azimuth is reckoned from 0 to 360° in the direction of rotor rotation.

3. The Purpose of Flapping, Drag and Feathering Hinges of the Blade Attachment

During the horizontal flight of a helicopter the airflow blows around its rotor at an angle to its axis of rotation (oblique flow). Because of this for blade elements in different positions the flow velocities and the angles of attack vary with respect to azimuth.

As is evident from Fig. 2.25, in positions $\psi=90°$ and $\psi=270°$ the horizontal components of the total flow velocity are identical (not allowing for the induced rates), since in one case the tip velocity ωR and the velocity of the impinging flow are summed, and in another they are deducted (Fig. 2.25 does not show the induced rates which are insignificant in magnitude).

The total flow velocity is greater for a blade which is going against the flow ($\psi=90°$), than for a blade which is going with the flow ($\psi=270°$).

Because of this the aerodynamic force created by the blade during its motion against the flow, will be greater than during motion with the flow. With rigid attachment of the blades this distinction in the aerodynamic forces creates a transverse moment M_x (Fig. 2.26) on the rotor which tends to turn the helicopter.

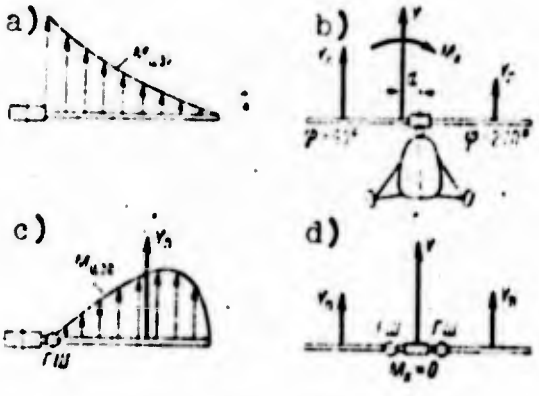

Fig. 2.26. Bending moment of the blade and the tilting moment of rotor thrust: a, c) bending moment with rigid and hinged blade attachment; b, d) tilting moment of rotor thrust.

To eliminate the tilting moment of rotor thrust in the oblique flow regime a flapping hinge (Fig. 2.26d) is positioned at the site where the blade is attached to the head.

Since the magnitude of aerodynamic force varies with azimuth, the blade which has a flapping hinge, along with rotation accomplishes oscillatory (flapping) motion. Because of this the blade elements obtain a supplementary velocity u due to the flapping motion directed upward during the motion against the flow and downward during motion with the flow. Being summed with the flow velocities W_1 (see Fig. 2.25c, d), velocity u leads for the blade, going against the flow, to a decrease, and for the blade going with the flow, to an increase in the angles of attack and, therefore, to an increase in the aerodynamic forces. As a result the equalizing of the aerodynamic forces occurs automatically and the tilting moments are mainly removed.

Furthermore, the flapping hinge relieves the root part of the blade of considerable bending moments (Fig. 2.26c).

The drag hinge is intended for relieving the blade root from the effect of the bending moments in its plane which appear from the inertia loads and drag forces.

The feathering hinge makes it possible to vary the blade setting angle in controlling the helicopter.

CHAPTER 3

GENERAL QUESTIONS OF THE DESIGN AND STRENGTH OF WINGS AND ROTORS

§ 1. LOADS ON A WING

1. Determining Loads

In calculating the strength and in analyzing the operation of a wing design the surface and mass forces acting on the wing and the units fastened to it in flight and also during the motion of the aircraft over the ground (figure 3.1) are examined.

The calculated destructive magnitudes of forces which correspond to g-forces n^p are subsequently examined.

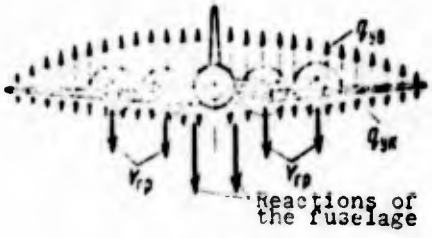

Figure 3.1. Loads acting on the wing.

Surface loads. The following are included among these:

a) the distributed air loads (the forces of pressure and rarefaction) applied directly to the wing skin;

b) the surface loads acting on the units attached to the wing: engine thrust, the reactive moments of the propellers,

the landing-gear loads arising during the motion of the aircraft over the ground, etc. These loads are transmitted to the wing through the assemblies connecting the units with the wing.

Mass loads. Mass loads include the following:

a) the distributed loads acting on the masses of the wing design and applied directly to each of its elements;

b) the distributed loads acting on the fuel and tank masses accommodated in the wing and being transmitted to its design through the tank attachments;

c) mass loads which act on compact masses of the units and weights attached to a wing (engines, landing gears). It is possible to examine these loads in determining the forces in wing cross sections as concentrated, applied at the centers of gravity of the corresponding masses. They are transferred to the wing through the unit and weight attachment devices.

It is necessary to note that the latter two types of loads with respect to the design of the wing itself are surface loads.

In examining wing equilibrium fuselage reactions are included among the number of surface forces acting on it.

As the initial values for calculating with respect to the stresses standards the air and mass loads are determined in the direction of the y-axis:

a) surface load due to air forces

$$Y_в^р = n^р G;$$

b) mass load of the wing design

$$Y_к^р = n^р G_к;$$

c) mass forces of the loads on the wing

$$Y_{гр}^{р} = n^{р} G_{гр}.$$

With respect to the stress standards it is permissible to take the directions of the mass forces acting on the wing and the units fastened to it as parallel to the direction of the resultant of the wing air forces.

The thrust of the engines situated on a wing acts on the wing through the engine suspension attachment devices.

For every engine

$$P_{дв}^{р} = jP_{дв}^{э},$$

where $P_{дв}^{э}$ - is the thrust during flight in the regime of the case of loading in question; f - the safety factor.

Determining of air forces. Let us first examine how the resultant of the air load and its components with respect to the wind axes y and x and the body axes of the wing n and t are directed with respect to the profile - in accordance with $Y_в$, $X_в$, $N_в$, $T_в$ (figure 3.2).

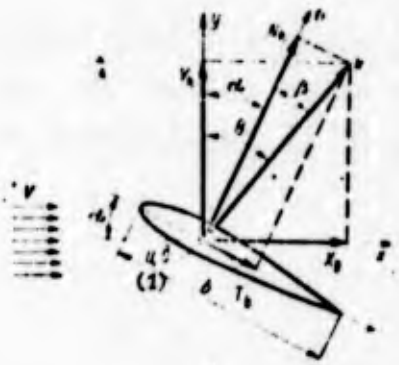

Figure 3.2. Resultant of the air forces and its components with respect to the wind (x, y) and the body (n, t) axes. Key: (1) c.p. (center of pressure).

The magnitude of the resultant of the calculated destructive air load R is determined from known formula[1]

[1]In the subsequent formulas for simplying the notation the superscript "p" is not shown for designating the calculated destructive loads.

$$R = fc_R \frac{\rho V^2}{2} S,$$

where

$$c_R = \sqrt{c_x^2 + c_y^2}.$$

For determining the magnitude of each of the components of resultant R it is possible to employ the relationships:

$$\frac{R}{Y_a} = \frac{c_R}{c_y}; \quad \frac{N_a}{Y_a} = \frac{c_n}{c_y};$$

$$\frac{T_a}{Y_a} = \frac{c_t}{c_y}; \quad \frac{X_a}{Y_a} = \frac{c_x}{c_y},$$

where

$$c_n = c_y \cos\alpha + c_x \sin\alpha,$$

$$c_t = c_x \cos\alpha - c_y \sin\alpha.$$

It is apparent from figure 3.2, that

$$\beta = \theta - \alpha; \quad \operatorname{tg}\theta = \frac{X_a}{Y_a} = \frac{c_x}{c_y};$$

$$\operatorname{tg}\beta = \frac{T_a}{N_a} = \frac{c_t}{c_n}; \quad R = \frac{Y_a}{\cos\theta}.$$

Angle β is positive with small α and can be negative with large α (positive and negative). Figure 3.3, for example, shows the positions of the resultant of the air wing forces R at different angles of attack.

As an examination of wind-tunnel test results shows, angles β and θ are small. Thus, in the approximate calculations for all stress standard loading cases, except case C, it is possible to assume that

$$c_R \approx c_n \approx c_y; \quad c_t = 0; \quad c_x = 0$$

and accordingly

$$R \approx N_a \approx Y_a; \quad T_a = 0.$$

For case C it is possible to assume that

$$c_y = 0; \quad c_n = 0; \quad c_R = c_t = c_x$$

and accordingly

$$Y_a = 0; \quad N_a = 0; \quad R = T_a = X_a$$

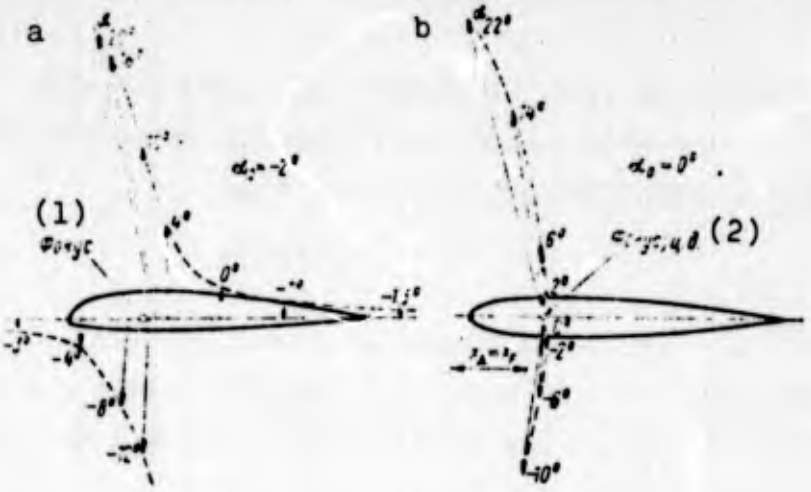

Figure 3.3 Slope magnitude (in scale) and the point of application (center of pressure) of the resultant air wing force with unsymmetric (a) and with symmetric (b) profile at different angles of attack.
Key: (1) Aerodynamic center; (2) Aerodynamic center, c.p. (center of pressure).

On this basis, subsequently for all flight loading cases, except case C, the total rated destructive air wing loading is calculated in accordance with stress standards according to the following formula

$$Y_a = n^r G$$

and is considered to be acting in the direction of the n-axis (perpendicular to the geometric wing chord) (see figure 3.2) close to the direction of the least flexural wing rigidity.

All the drawn conclusions and formulas of the resolution of the air forces on the components are also valid for the mass forces, if it is assumed that the resultants of the aerodynamic and mass forces are parallel ($R||R_M$).

2. Distribution of Air Forces Along a Wing Span

The distribution of the air loading along a wing span is a function of the external shapes of the wing and the flight velocity.

The rated destructive linear air wing loading can be defined as the air force which acts on a section of a wing which has chord b and a unit length along the span:

$$q_{y_3} = fc_y bq \text{ kgf/m},$$

where $q=\rho V^2/2$ - is the dynamic pressure, kgf/m^2; c_y - is the lift coefficient of the wing cross section being examined; b - is the chord of the cross section being examined.

From expression $Y_в=n^рG=fc_{y\ к}Sq$ it is possible to determine the value of the dynamic pressure

$$q = \frac{n^рG}{fc_{yк}S},$$

where $c_{y\ к}$ - is lift coefficient of the wing.

After substituting the obtained value of q in expression for $q_{yв}$ and taking into account that the wing area is $S=b_{ср}l$ (where $b_{ср}$ - the mean geometric chord of the wing), we will obtain

$$q_{yв} = \frac{n^рG}{l} \cdot \frac{c_y b}{c_{yк} b_{ср}}. \qquad (3.1)$$

It is readily noticeable that the right side of expression (3.1) contains two factors:

the first $n^рG/l$ represents the average linear air loading;

the second $c_y b/c_{y\ к} b_{ср}=\bar{f}$ can be called the relative circulation. It considers the effect on the load distribution of the variation along the wing span of value c_y and of the chords dimensions.

In summation, the linear rated destructive load is

$$q_{y_B} = \frac{n^p G}{l} \bar{\Gamma}. \qquad (3.2)$$

Relative circulation $\bar{\Gamma}$ changes along the span depending on the wing planform, on the twist and the Mach number.

From a comparison of formulas (3.1) and (3.2) it is evident that linear load $q_{y\ B}$, relative circulation $\bar{\Gamma}$ and the product $c_y b$ are proportional to each other. Consequently, the laws of the distribution of these values along a wing span with specific ρ and V are also proportional.

This makes it possible to find distribution $q_{y\ B}$ along the span from the calculational data of circulation distribution carried out by the methods of theoretical aeromechanics, or from the distribution of c_y found from the results of wind-tunnel tests of a drained wing.

Figure 3.4a gives (according to the data of TsAGI (Cen. Ints of Aerohydrodynamics im. N. Ye. Zhukovskiy)) the curves for determining the $\bar{\Gamma}$ of plane tapered unswept wings with different η.

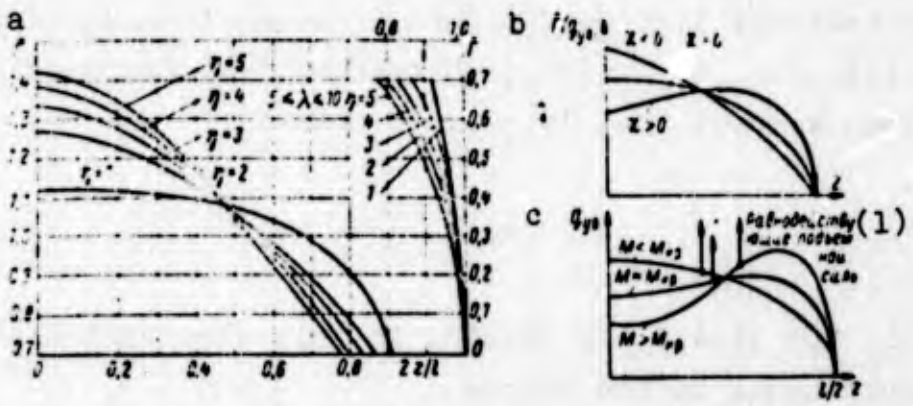

Figure 3.4. Distribution of the relative circulation along the span of a tapered unswept wing (a) and the effect of sweep on it (b) and Mach number (c).
Key: (1) Resultant of lift force.

The curves were plotted under the assumption of the linear dependence of c_y on α. However, practice shows that it is possible to use them also at angles of attack, close to critical (i.e., in cases of A and D loading).

Wing sweep and air compressibility can have a considerable effect on the distribution of circulation $\bar{\Gamma}$ and on linear air loading $q_{y\ в}$.

The nature of this effect is shown in the diagrams of figure 3.4b and c.

By employing suitable wing layout (selection of profiles, twist), it is possible to a certain extent to compensate for this effect.

3. Approximate Methods of Distributing Air Loading Along a Wing Span

Tapered Wings

As the results of the wind-tunnel tests show, for a rationally laid out tapered wing it is possible in approximate stress analyses and in analysis of the operation of the wing design to consider that the lift coefficient c_y along the span does not change, i.e., $c_{y\ к}=c_{y\ сеч}=c_y$. Therefore, from expression (3.1), taking into account that $\int b_{ср}=S$, we obtain

$$q_{y\text{в}}=\frac{n^{y}G}{S}b.$$

Thus, the linear air loading in this case varies along the span proportional to the chords.

In accordance with this law of distribution $q_{y\ в}$ the loading on a wing section limited by chords a-a and b-b in figure 3.5, is determined by the following formula:

$$\Delta Y_в = fc_y \Delta S \frac{\rho V^2}{2} = \frac{Y_в}{S} \Delta S_ч \qquad (3.3)$$

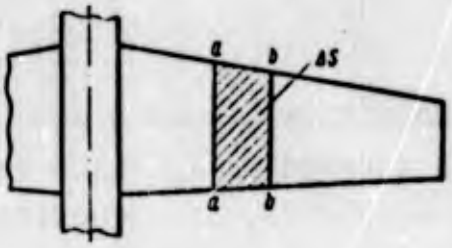

Figure 3.5. For determining the air loading on a wing section ΔS.

The linear drag $q_{x\ в}$ is also calculated on the basis of the assumption concerning the proportionality of the wing to its chords. This law of distribution of air loading is based on the assumption that

$$c_{x\,в} = c_{x\,сеч} = c_x;$$

then

$$X_в = fc_x S \frac{\rho V^2}{2} \text{ and } q_{xв} = fc_x b \frac{\rho V^2}{2},$$

whence

$$q_{xв} = \frac{X_в}{S} b.$$

The linear aerodynamic moment $m_в$ relative to the axis passing through the leading edge of a profile, is determined from the following formula

$$m_в = fc_{m\,сеч} b^2 \frac{\rho V^2}{2} \text{ kgf-m/m}$$

where $c_{m\ сеч}$ - the moment coefficient of the cross section relative to the leading edge of the profile.

As has already been indicated, the components X of wing loadings can be disregarded in all cases, except C, since they are small in comparison with the Y loads.

Delta Wings

For a low aspect-ratio delta wing the following approximate laws of distribution of linear air loading along the wing span can be accepted.

Subsonic flow. In the case of subsonic flow around a low-aspect wing the lift coefficient of cross section $c_{y\ сеч}$ increases from the wing root toward the wing tip. Therefore, in approximate calculations it is assumed, that $c_{y\ сеч} b_{сеч} = c_{y\ к} b_{ср} = \text{const}$.

In this case the linear air loading is constant along the wing span and can be determined by the formula

$$q_{ув} = \frac{n^{э} G}{l}.$$

Supersonic flow. In this case it is approximately assumed that $c_{y\ сеч} = c_{y\ к}$ and the linear air loading is distributed along the span proportional to the chords:

$$q_{ув} = \frac{n^{э} G}{S} b.$$

4. Distribution of the Mass Forces of Wing Design and of Tanks With Fuel

The mass forces of a wing are the distributed loading obtained as a result of the addition of the weight forces and the inertia forces. The distribution of these forces does not depend on the angle of attack, but is determined by the wing design.

Statistical formulas of the weight distribution of a wing exist however, for the sake of calculational simplicity it is approximately possible to assume that the law of distribution of the mass forces along the span of a wing coincides with the accepted in calculating the law of distribution of aerodynamic forces:

$$q_{yk} = q_{yB}\frac{Y_k}{Y_B}.$$

Since $Y_k = n^p G$, and $Y_B = n^p G$,

$$q_{yk} = q_{yB}\frac{G_k}{G}.$$

This assumption is justified by the fact that G_k is small in comparison with G and the error of the result of this approximate calculation is small.

The linear load $q_{y\ k}$ is applied along the line of the centers of gravity of the cross sections of the primary wing structure (c.g.). The center-of-gravity position of each cross section (figure 3.6a) is characterized by the coefficient

$$\bar{x}_T = \frac{x_T}{b} = 0{,}40 \div 0{,}45.$$

The mass forces of the tanks with the fuel give on the wing span section a linear loading whose intensity is determined in the general case by the expression

$$q_6 + q_T = n^p(F_6\gamma_6 + F_T\gamma_T),$$

where γ_6 and γ_T - are the volumetric weights of the tank material and the fuel; F_6 and F_T are the cross-sectional areas (see figure 3.6b).

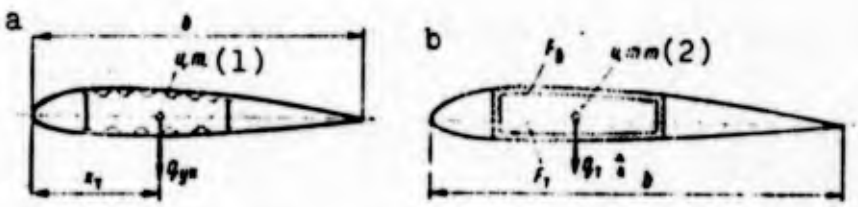

Figure 3.6. The distributed mass forces of the wing design are applied at the center of gravity of the wing cross section (a), and the distributed mass forces of the fuel are applied at the center of gravity of the area F_T (b).

Key: (1) c.g.; (2) Fuel c.g.

The linear loading $q_т$ is applied along the line of the centers of gravity of the fuel. The center of gravity of the fuel at individual cross sections (fuel c.g.) is defined as the center of gravity of the area $F_т$; loading $q_б$ can be considered applied in conjunction with $q_т$. If the tanks are included in the wing lifting design, then it is possible to consider their weight included in $G_к$ and not to consider the mass forces separately.

In the case of C in approximate calculation the mass forces of the wing and the tanks with the fuel are not considered.

5. Direction of Linear Loads

Earlier it was assumed that the mass loads act parallel to the air loads ($q_к || q_в$).

On this basis for the air and mass forces:

$$\frac{q_x}{q_y}=\frac{X}{Y}=\frac{c_x}{c_y};\quad \frac{q_n}{q_y}=\frac{N}{Y}=\frac{c_n}{c_y};\quad \frac{q_t}{q_y}=\frac{T}{Y}=\frac{c_t}{c_y}.$$

Since for all cases of loading, except case C, it is usually assumed, that $c_R \approx c_n \approx c_y$, $c_t=0$, then the basic distributed loads for wing strength analysis are the loads in the direction of the y-axis, i.e., $q_{y\ в}$ and $q_{y\ к}$.

In further calculations, except special cases, only these components of the distributed loads will be examined.

6. Determining the Center-of-Pressure Position (c.p.)

The point of intersection of the resultant of the air force applied to a wing or to its elementary section, with the corresponding chord (for the entire wing - with its mean aerodynamic chord) is called the <u>center of pressure</u> (c.p.).

Its position is characterized by the center-of-pressure coefficient (see figure 3.3)

$$\bar{x}_д = \frac{x_д}{b}.$$

As is known,

$$\bar{x}_д = -\frac{c_m}{c},$$

where c_m - is the coefficient of the aerodynamic moment of the profile relative to its leading edge. Coefficient c_m is considered positive, when the moment acts on increasing the angle of attack; c_{m0} - is a moment coefficient when $c_y=0$.

If x_F - is the distance from the leading edge to the aerodynamic center of the profile and

$$\bar{x}_F = \frac{x_F}{b} = -\frac{dc_m}{dc_y} = \text{const},$$

then

$$c_m = -\bar{x}_F c_y + c_{m0}$$

and

$$\bar{x}_д = \bar{x}_F - \frac{c_{m0}}{c_y}.$$

Since for unsymmetric profiles $c_{m0}<0$, then with a decrease in α and c_y the c.p. is displaced backwards, further from the aerodynamic center as is shown in figure 3.3a.

For symmetrical profiles $c_{m0}=0$; therefore for them the center of pressure coincides with the aerodynamic center (figure 3.3b).

At transonic flight velocities with an increase in Mach number the center of pressure is displaced backwards and when $M\approx1.3$-1.4 it is at a distance from the leading edge of the profile of up to $\bar{x}_д=0.46$-0.47.

In wing sections with ailerons the displacement of the position of the c.p. caused by aileron deflection is taken into account.

Aerodynamic wing characteristics are either taken from wind-tunnel tests, which is the most advisable, or for them the characteristics of a mean profile having a thickness ratio are approximately taken:

$$\bar{c}_{ср} = \frac{c_{ср}}{b_{ср}},$$

where $b_{ср}=S/l$ - is the mean geometric chord; $c_{ср}=(c_0+c_{конц})/2$.

The air force acting on a wing, is considered applied at the center of pressure of the mean aerodynamic chord b_A:

$$b_A = \frac{2}{S}\int_0^{l/2} b^2 dz = \frac{2}{3}\cdot\frac{1+\eta+\eta^2}{\eta(1+\eta)}\cdot b_0.$$

It is also possible to find the magnitude of b_A and its position graphically.

7. Determining the Position of the Total Linear Load Along a Chord

In each wing cross section the position of the points of the application of linear loads $q_{y\ в}$ and $q_{y\ к}$ along the chord is determined by the coefficients $\bar{x}_д$ and $\bar{x}_т$.

For the stress analysis of a wing it is advisable to combine the two distributed linear loads - the air load $q_{y\ в}$ and the mass load $q_{y\ к}$ - into one total load $q_y=q_{y\ в}-q_{y\ к}$.

Let us introduce the concept of the center of application of the total distributed load. Let us call the center of load (c.l.) the point on the chord of a cross section, through which the total linear load q_y passes.

Its coordinate $x_н$ and value $\bar{x}_п=x_н/b$ are determined from the moment equation of the linear loads being examined (figure 3.7) relative to the leading edge of the profile:

$$\bar{x}_{\text{ц}} = \frac{x_{\text{ц}}}{b} = \frac{q_{y\text{в}}\bar{x}_{\text{д}} - q_{y\text{н}}\bar{x}_{\text{т}}}{q_{y\text{в}} - q_{y\text{н}}} = \frac{q_{y\text{в}}\bar{x}_{\text{д}} - q_{y\text{н}}\bar{x}_{\text{т}}}{q_y}.$$

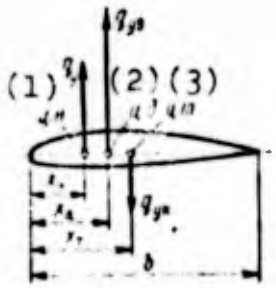

Figure 3.7. Towards determining of the position of the center of loads.
Key: (1) c.l. (center of loads); (2) c.p.; (3) c.g.

If values $\bar{x}_{\text{д}}$ and $\bar{x}_{\text{т}}$ for different wing sections are constant, and the laws of distribution of $q_{y\text{ в}}$ $q_{y\text{ н}}$ are proportional, then, since

$$q_{y\text{в}} = \frac{n^{\text{э}}G}{S}b; \quad q_{y\text{н}} = \frac{n^{\text{э}}G_{\text{н}}}{S}b; \quad q_y = \frac{n^{\text{э}}G}{S}\left(1 - \frac{G_{\text{н}}}{G}\right)b,$$

position $\bar{x}_{\text{н}}$ is determined from the expression

$$\bar{x}_{\text{н}} = \frac{\bar{x}_{\text{д}} - \bar{x}_{\text{т}}\dfrac{G_{\text{н}}}{G}}{1 - \dfrac{G_{\text{н}}}{G}}.$$

8. Characteristics of Load Determination and Distribution in Individual Loading Cases

Above we examined the general sequence of determining wing loads and their distributions along the span. This sequence can be applied to the calculation for case of A of stress standards, which is one of the most important for a wing.

The determination and distribution of loads in different cases of loading has its own peculiarities. Let us dwell on their main peculiarities.

The Effect of the Fuselage and Other Secondary Structures Located on a Wing on the Load Distribution Along the Span of a Wing in Cases A' and B

The presence of the fuselage, the engine arrangement and other secondary structures on the upper side of a wing changes the linear load distribution. This can sometimes have a strong effect at low angles of attack which correspond to loading cases A' and B.

The effect of the fuselage and different secondary structures manifests itself in the fact that on wing cross sections where there are secondary structures or a fuselage, $q_{y\ в}$ decreases, and in the sections where there are none, it increases.

As wind-tunnel tests show, with the rational coupling of the wing with the fuselage in the form of a midwing monoplane set-up and the successful layout of the secondary structures their adverse effect on distribution $q_{y\ в}$ can be almost completely eliminated.

Taking Aileron Deflection Into Account

In the event of aileron deflection, besides the load which acted before deflection, additional loads arise (figure 3.8):

1) the distributed air load due to aileron deflection (on the wing parts opposite the ailerons) $q_э$, which has the resultant $P_э$;

2) the inertia forces which arise as a result of accelerated turning of an aircraft - distributed q_ε and concentrated $Y_{\Gamma p_\varepsilon}$

3) the distributed damping air load q_ω which counteracts the turning of an aircraft, proportional to ω_x - the angular rate of turning.

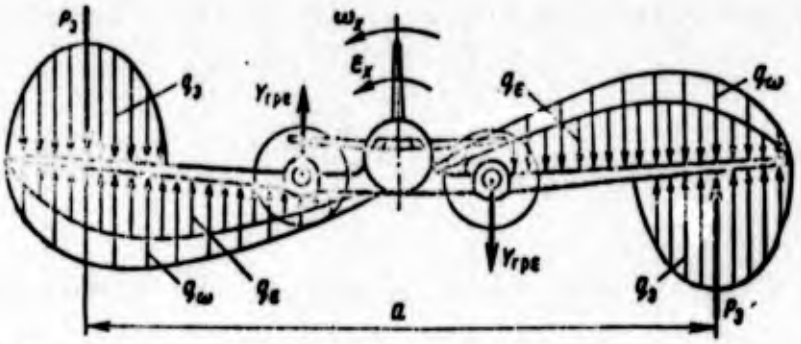

Figure 3.8. Additional surface and mass loads arising as a result of aileron deflection.

Let us examine the causes of the appearance of these loads.

During aileron deflection an additional air distributed load $q_э$ arises which acts on the wing sections where the ailerons are situated. The resultant moment of this load relative to the x-axis

$$M_x = P_э a$$

causes angular acceleration $\varepsilon_X = M_X / I_X$.

Connected with this is the appearance of additional mass loads:

a) distributed load, whose intensity for the cross section with coordinate z is

$$q_i = \frac{q_{G_к}}{g} z\varepsilon_x,$$

where $q_{G_K} = \frac{G_к}{S} b$ - the linear weight of the wing design;

b) concentrated loads

$$Y_{гр_i} = \frac{G_{гр}}{g} z\varepsilon_x.$$

The presence of angular acceleration ε_x leads to an increase in the angular rate of turning of an aircraft relative to the x-axis:

$$\omega_x = \int_0^t \varepsilon_x dt.$$

For a turning wing the velocity of the air-stream impinging on a wing at the cross section with coordinate z, is composed of velocity V, equal to the flight velocity, and to velocity

$$u = z\omega_x.$$

As a result an increase in the angle of attack of the wing cross section is obtained at $\Delta\alpha = u/V$ and coefficient c_y changes at the cross section just as in the case when a wing encounters in horizontal flight an ascending airflow with magnitude:

$$\Delta c_y = \frac{dc_y}{d\alpha} \cdot \frac{u}{V}.$$

The additional distributed damping air load on a wing corresponds to this:

$$q_\omega = \Delta c_y b \frac{\rho V^2}{2} = \frac{1}{2} \cdot \frac{dc_y}{d\alpha} \rho V z \omega_x.$$

These types of additional loads must be examined, when they are especially great, for example in the case of a sharp aileron deflection, which is provided for in the flight of a maneuvering aircraft. In this case it is necessary to consider that greatest values of q_ε and q_ω do not coincide with time (first ε is the greatest, and $\omega = 0$). For maneuvering aircraft this case can be calculated for certain wing parts.

With respect to stress standards load cases B and C are examined for a wing with deflected ailerons. In these cases the aileron deflection angles are small (usually the angle of deflection

is $\delta_э$=2-5°) and it is possible to consider that additional loads in the opposite direction which arise upon aileron deflection in a projection on the y-axis are mutually balanced. It is necessary to consider only the effect of the deflected ailerons on the position of $q_{y\ в}$ along the chord or on the linear air moments of the wing $m_в$.

In case B it is assumed, that the effect of aileron deflection produces only a center-of-pressure displacement on the wing section occupied by the ailerons (figure 3.9a).

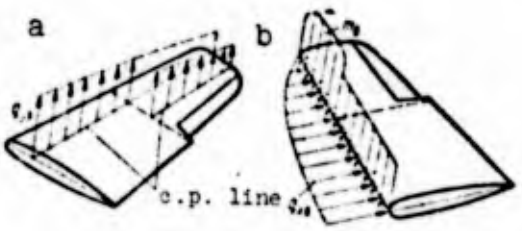

Figure 3.9. Effect on the nature of aileron deflection wing loading in cases B (a) and C (b).

In case C linear load $q_{x\ в}$ acts on the wing.

The air force in the direction of the y-axis gives q_y=0, but forms linear aerodynamic moment $m_в$.

If we designate the coefficients of the cross section moment by $c_{m0\ сеч}$, then the linear moment (relative to the axis, parallel to z) is

$$m_в = \int c_{m0сеч} b^2 q_{max\ max}.$$

Aileron deflection only affects a variation in the c_{m0} of the profile at the wing section where the ailerons are located. This leads to a change in this section in the value of $m_в$ (figure 3.9b).

The effect of aileron deflection on the value of $q_{x\ в}$ is not considered.

The conditions of loading examined here are dangerous due to the possibility of the presence of the large torsional moments in the wing cross sections.

Unsymmetric Loading Wing

The strength of a wing is also checked in flight under the effect of unsymmetric loading. In cases A, A' and B one half-wing with a full load is examined which corresponds to a case of loading, and another with a load of 20% less for nonmaneuvering and limited maneuvering aircraft.

The unsymmetrical loading of a wing can be dangerous for the design elements of its attachment to the fuselage.

Characteristics of Wing Loading in Landing Cases

Wing strength should also be checked for landing loading cases. In this case loads are considered which act on the landing gear from the ground and which are transferred to the wing through the landing gear wing attachment, and also the air load and the mass forces which act on the wing design and the units and weights attached to it. In these cases the stress standards are assigned for wing value f=1.65, larger than for the landing gear (1.5).

§ 2. FORCES IN THE WING CROSS SECTIONS

1. Basic Assumptions

The wing design of a monoplane aircraft can be considered as a simple beam with cantilevers, which under the effect of distributed and concentrated loads is bent and twisted. The assemblies attaching the wing to the fuselage, usually located near the sides of the fuselage are usually the wing supports.

Just as for the conventional beams examined in structural mechanics, the deformation of a wing beam section can be represented in the form of a combination of section bending which is accompanied by the turning of its transverse cross sections relative to their neutral axes, and the twisting which takes place in the form of turns of the cross sections relative to the axis (normal to the cross sections) of rigidity (a.r.) of the section.

The axis of the rigidity of a design section is the straight line which possesses that property, which in the passage of transverse force through it the section is not twisted.

The center of rigidity is the point of the intersection of the axis of rigidity with the cross-sectional plane.

It is possible to consider that the wing beam whose design does not have spar fractures in plan possesses a single rectilinear axis of rigidity which plays the role of an elastic axis. We will subsequently accept this assumption.[1]

In the presence of such fractures it is necessary to consider the difference in the positions of the axes of rigidity of the different wing parts - the fracture of the elastic axis. For example, for the wing shown in figure 3.10, load P does not cause twisting of section I of the wing, since it passes through its axis rigidity, but will twist section II.

Figure 3.10. Force P does not cause twisting of section I of the wing, section II is subjected to twisting.

[1]For an unswept wing the axis of rigidity is frequently considered parallel to the z-axis.
The position of the axis of rigidity along the chord is determined mainly by the arrangement of the spars and by their flexural rigidity. The calculation of the position of the axis of rigidity is further examined in § 8.

Experiments show that a change in the arrangement of the ribs relative to the elastic axis of a wing beam (for example, with respect to flight or at right angles to the aerodynamic center line) does not have a substantial effect on the stresses in transverse wing sections. This pertains both to straight (unswept) wings and to swept wings (except for the root sections, which constitute 0.2-0.3 of a semispan).

To facilitate and simplify the calculational analysis of wing design operation, we make the following assumptions which do not distort the physical picture of wing operation:

1. In the calculations let us examine a plane wing (the angle of twist is $\varphi=0$) with a dihedral angle equal to zero ($\psi=0$), i.e., we assume, that the wing chords lie in one horizontal plane determined by the chord of the mean profile.

2. The cross sections with the plane perpendicular to the axis of rigidity are usually taken as calculated cross sections. In examining the forces and the stresses in a wing design, let us consider that the main central axes of the wing cross sections usually constitute a small angle with the profile chord and the axis normal to it. In connection with this, we will approximately assume, that the axis of smallest inertial moment of the cross section is parallel to the profile chord.

3. Let us utilize the assumptions adopted earlier in examining wing loads:

$$N_в = Y_в,\ T_в = 0 \text{ in all cases, except C;}$$

$$N_в = 0,\ T_в = X_в \text{ in case C.}$$

These assumptions make it possible to represent the deformation of the wing as a combination of simple bending due to the N forces (in case C - due to the T forces) with torsion (figure 3.11).

The torsional moment will be created by the N loads which give moment M relative to the axis of rigidity (in case C - by moment M_0). The torsional moment due to the T forces is small; therefore it can be disregarded. Figure 3.11 shows the usual directions of the external forces and moments.

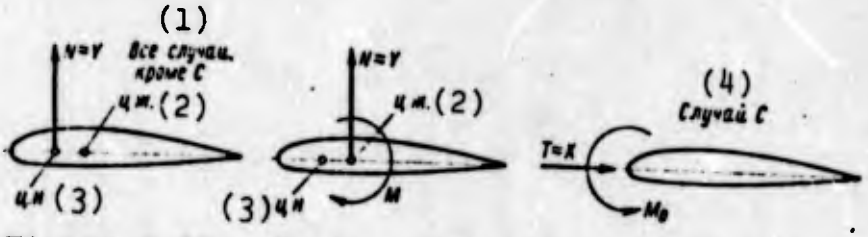

Figure 3.11. It is possible to reduce the system of external loads to forces N≈Y(T≈X in case C) applied to the axis of rigidity and to those which cause pure bending of the wing, and to the moment M which twists the wing relative to the axis of rigidity. Key: (1) All cases, except C; (2) Center of rigidity (tszh.=c.r.); (3) c.l. (center of loads); (4) case C.

2. Forms of Forces in a Wing Cross Section

The forces in a cross section are the resultants (static equivalents) of internal forces - the stresses in the load-bearing elements of the cross section in question.

In determining the forces in design elements we will use the method of cross sections employed in structural mechanics. This method is based on the examination of the equilibrium of a conceptually cut off design part. If an entire design is in equilibrium, then each of its parts should be in equilibrium. Applying the equation of equilibrium to the cut off part, let us determine the forces in the cross section.

Let the wing under the effect of the mass and surface forces be in equilibrium. Let us conceptually cut off the end part of a wing with the plane of cross-section I-I (figure 3.12). The

external loads of the end part of the wing due to the air and mass forces can be reduced to the resultant P applied at the center of loads of the cut off part - at point 0.

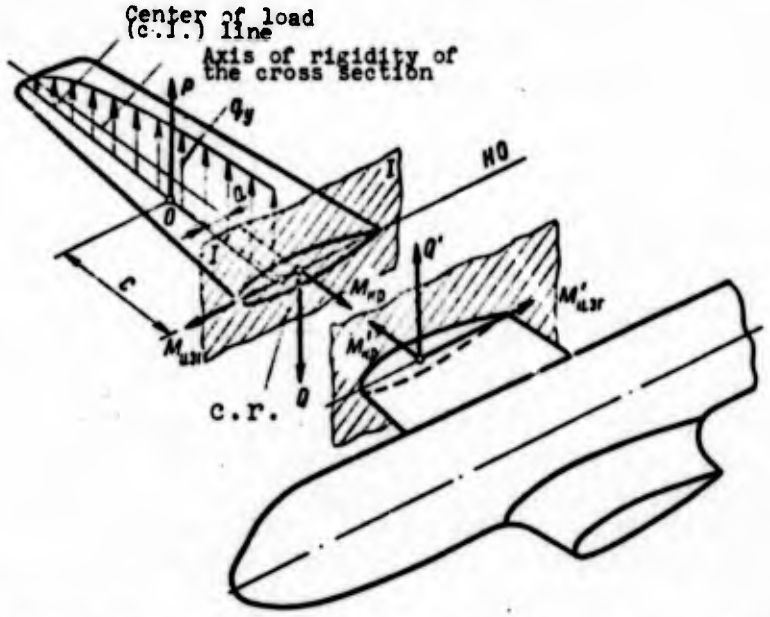

Figure 3.12. The effect of the external load on the cut-off part of a wing is balanced in cross section I-I by the internal forces Q, $M_{изг}$ and $M_{кр}$ - by the resultants of the normal and tangential stresses arising in the elements of the cross section under the effect of load P. Forces Q', $M'_{изг}$ and $M'_{кр}$ act from the cut-off part on the root part.

Force P, obviously, is balanced by the internal forces in cross section I-I, since the cut off part of the wing in question, just as the whole wing, is in a state of equilibrium. In this case the forces in cross section I-I, which balance the external forces, reduce to three forces: to transverse force Q, to bending moment $M_{изг}$ and to torsional moment $M_{кр}$ determined from examining the equilibrium of the cut off part of the wing:

$$Q = P;$$

$$M_{изг} = Qc;$$

$$M_{кр} = Qa.$$

The vectors of the forces Q, $M_{изг}$, $M_{кр}$ are always directed opposite to the vectors of the resultant external loads, which produce them.

The vectors of the forces Q and $M_{изг}$ lie in the plane of the cross-section.

The vector of force $M_{кр}$ is directed along the axis of rigidity.

Forces Q, $M_{изг}$, $M_{кр}$ in the cross section I-I represent the effect of the remaining part of the wing on the cut-off part in question; on the other hand, forces Q', $M'_{изг}$, $M'_{кр}$ in the cross section of the remaining part of the wing represent the effect of the cut-off part of the wing on the remaining part ($Q'=Q$; $M'_{изг}=M_{изг}$; $M'_{кр}=M_{кр}$).

3. Determining Forces Q, $M_{изг}$ and $M_{кр}$ in the Cross Sections of a Wing Beam

The projection diagram q_y and the position of the center load line, the values of the mass forces of concentrated loads and the points of their application, the values and the points of application the concentrated surface loads (figure 3.13) are the initial ones for determining Q, $M_{изг}$ and $M_{кр}$.

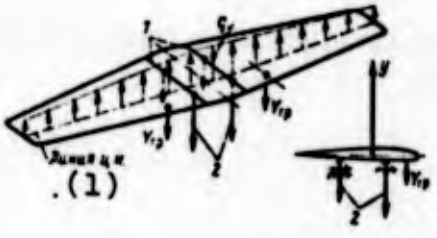

Figure 3.13. Design diagram of a wing: 1 - inside (side) wing ribs; 2 - reactions.
Key: (1) Center of load (c.l.) line.

It is usually assumed, that on the wing section occupied by the fuselage, the distributed load is received directly by the fuselage.

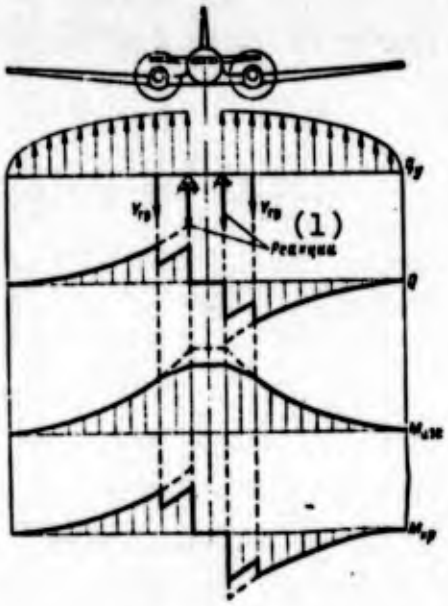

Figure 3.14. Loading diagram and view of the diagrams of q_y, Q, $M_{изг}$ and $M_{кр}$ of an unswept wing.
Key: (1) Reactions.

Figure 3.14 shows a wing loading and balancing diagram and a diagram of q_y, Q, $M_{изг}$ and $M_{кр}$ of an unswept wing.

Procedures known from structural mechanics are utilized for determining forces.

Let us determine transverse force Q, integrating the diagram q_y along the span (along z) and taking the concentrated loads Y_i (the sign is determined by the direction relative to the y-axis) into account:

$$Q_z = \int_{z_2}^{z} q_y dz + \Sigma Y_i.$$

The bending moment $M_{изг}$ is determined by iterated integration:

$$M_{изг.z} = \int_{z_2}^{z} Q dz.$$

If the axis of rigidity is parallel to z, then the torsional moment $M_{кр}$ is found in the following manner:

$$M_{кр.z} = \int_{z_2}^{z} q_y (x_н - x_ж) dz + \Sigma Y_i (x_i - x_ж),$$

where $x_н$, $x_ж$, x_i - the current values of abscissas x (along the chord) of the center of load, the axis of rigidity and the points of application of the concentrated loads.

It is possible to carry out integration graphically, by the planimetric method or by the numerical method.

The presence of concentrated loads and fuselage reactions causes discontinuities in the diagrams of Q and $M_{кр}$ and fractures in the diagram of $M_{изг}$.

4. The Approximation Method of Determining Forces in Wing Cross Sections

Assuming that q_y is distributed along the span proportional to the wing chords, i.e., that

$$q_y = \frac{n^p(G - G_к)}{S} b,$$

then the determination of the forces Q, $M_{изг}$ and $M_{кр}$ is considerably simplified.

The forces in the cross sections of an unswept tapered wing are found in the following manner:

1) The wing diagram is drawn to scale in plan. The position of the center of load line is determined, and it is plotted on the wing plan (figure 3.15a);

2) the calculated cross section I-I, parallel to the x-axis, is drawn.

The position of the center of rigidity[2] is determined and the axis of rigidity of the cross section in question will be plotted on the wing plan;

---

[2]The position of the center of rigidity of the wing cross section can be approximately determined by the formula $x_ж = \frac{\sum H_i^2 x_i}{\sum H_i^2}$, where H_i - the height of the i-th spar; x_i - the distance of the i-th spar from the leading edge.

3) the forces are determined. If q_y is distributed along the span proportional to chords, then the resultant of the distributed load for the cut-off part of the wing is determined on the basis of formula (3.3) as for a section limited by the chords. It is proportional to the area of the cut-off part of the wing $S_{отс}$:

$$P = \frac{Y}{S} S_{отс} = \frac{n^{э}(G - G_{к})}{S} \cdot \frac{b_{I-I} + b_{конц}}{2} l_{отс}.$$

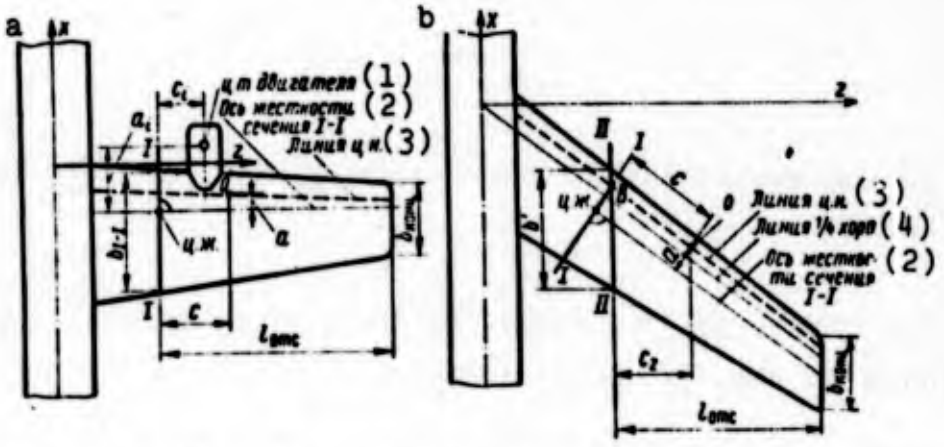

Figure 3.15. Diagrams for determining the forces in the cross section of an unswept (a) and a swept (b) wing.
Key: (1) c.g. of the engine; (2) Axis of the rigidity of cross section I-I; (3) Center of load (c.l.) line; (4) 1/4 chord line.

The transverse force Q_{I-I} is determined by the formula

$$Q_{I-I} = P - n^{э}\Sigma G_{гр}.$$

Let us find the bending moment $M_{изг\ I-I}$.

Point O of the application of the resultant of the distributed load for the cut-off part of the wing P lies on the center of load line and is located from cross section I-I a distance of c (see figure 3.15a), where c - is the distance along the z-axis from cross section I-I to the center of gravity of the cut-off wing area (trapezoid):

$$c = \frac{l_{отс}}{3} \cdot \frac{b_{I-I} + 2b_{конц}}{b_{I-I} + b_{конц}}.$$

The distances of c_i from the points of application of the mass forces of the concentrated loads to cross section I-I are determined from the drawing.

Thus,

$$M_{изг_{I-I}} = Pc - n^p \Sigma G_{гр_i} c_i;$$

$$M_{кр_{I-I}} = Pa \pm n^p \Sigma G_{гр_i} a_i,$$

where a and a_i - are the distances from the points of application of force P and of the mass forces of the loads to the axis of rigidity of cross section I-I.

In determining the forces in the cross sections of a swept tapered wing the following is considered. For a swept wing the longitudinal load-bearing elements of the wing are considerably sloped toward the z-axis; thus, the z-axis and the axis of rigidity of the wing beam are not parallel. It is approximately possible to assume the 1/4 chord line parallel, and to take the calculated cross sections perpendicular to this line.

These characteristics determine the differences in the technology of determining the forces in the cross sections of swept wings as compared with unswept wings.

The sequence of determining forces in the cross sections of swept wings is such:

1) the wing diagram is drawn to scale in plan; the position of the center of load line is determined and it will be plotted on the wing plan (figure 3.15b);

2) the calculated cross section I-I is drawn perpendicular to the 1/4 chord line; the position of the center of rigidity is

determined and the axis of rigidity of the cross section in question will be plotted on the wing plan;

3) the forces are determined.

An auxiliary cross section II-II parallel to the x-axis is drawn through the point of intersection of the calculated cross section with the center of load line (point B). It is possible to consider that the value of the resultant of distributed load P fitting on the area cut off by the auxiliary cross section II-II, is equal to the load on the area cut off by the calculated cross section I-I, since point B lies on the center of load line.

In the absence on the cut-off part of the wing of concentrated loads the transverse force at cross section I-I is found with the formula

$$Q_{I-I} = P = \frac{n^y(G - G_к)}{S} \cdot \frac{b' + b_{конц}}{2} l_{отс.}$$

Let us find bending moment $M_{изг\ I-I}$.

Point O of the application of the resultant of the distributed load is located on the center of load line and is located along the z-axis from cross section II-II a distance of

$$c_z = \frac{l_{отс}}{3} \cdot \frac{b' + 2b_{конц}}{b' + b_{конц}}.$$

Then $M_{изг\ I-I} = Pc$, where c - the distance from point O (point of application of P) to cross section I-I; c is determined from the drawing.

The torsional moment $M_{кр\ I-I}$ is:

$$M_{кр\ I-I} = Pa,$$

where a - is the distance from point O (point of application of P) to the axis of rigidity; a is determined from the drawing.

If, besides the distributed load, concentrated forces are applied to the cut-off part of the wing, then they should also be taken into account in calculating Q, $M_{изг}$ and $M_{кр}$ at cross section of I-I.

§ 3. WING STRUCTURE DIAGRAM

The structure diagrams and the designs of wings and rotors of domestic aircraft and helicopters are the result of the great collective work of the designers, strength-of-materials specialists and technologists. The leading role in their development was played by the investigations the design ideas of V. N. Belyayev, S. V. Ilyushin, M. L. Mil, A. N. Tupolev, A. M. Cheremukhin and many other Soviet designers and scientists.

A wing design is a complex engineering structure. The analysis of the operation of this type of design and its stress analysis without definite simplifications are onerous and complex.

The load-bearing elements of a design are called the elements; they play the main role in ensuring its strength and rigidity.

The combination of load-bearing elements which ensures the strength and the rigidity of a design under the loads acting on it is called the design structure diagram. By making substantiated assumptions it is possible to represent the structure diagram of a real design in the form of an approximate calculated diagram, which represents a rather simple system of load-bearing elements convenient for the calculation and analysis of its operation.

In a conventional wing design the load-bearing elements are as follows (figure 3.16):

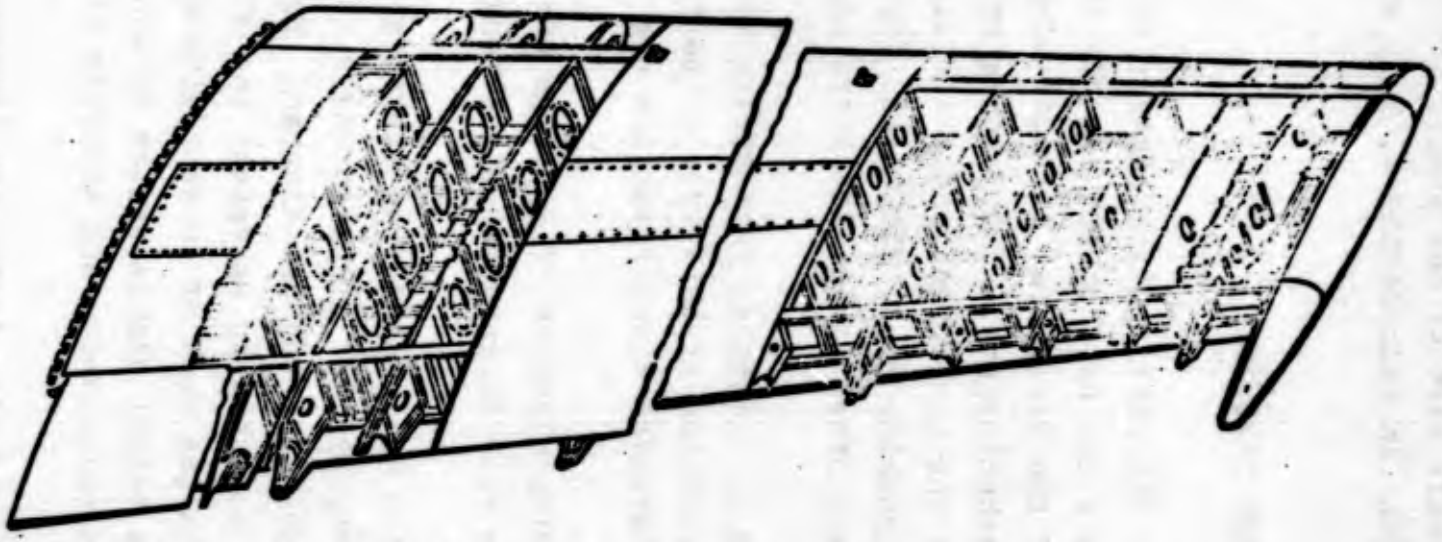

Figure 3.16. Design of a typical monoplane wing.

a) the skin;

b) the longitudinal assembly - the spars and stringers;

c) the transverse assembly - the ribs;

d) the joints - riveted, bolted, welded or adhesive.

The wing of a monoplane-aircraft can be considered as a beam which under the effect of loads operates in flexure, shear and torsion.

The part of a wing beam limited by the front and rear spars, is called the box (or two-spar beam). Let us examine, which load-bearing elements of a contemporary monoplane wing with a rigid skin receive the following forces: $M_{изг}$, Q and $M_{кр}$ (figure 3.17).

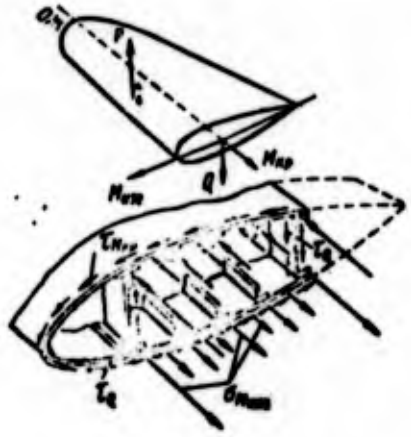

Figure 3.17. Forces in a wing cross section and the stresses corresponding to them in the load-bearing elements.

In the general case it is possible to say that the bending moment $M_{изг}$ in a given wing section is received by the caps (flanges) of the spars, by the rigid skin and by the stringers in which in this case normal stresses σ (of different sign in the upper and lower panels) arise.

The normal stresses in spar webs are disregarded since they are small.

The transverse force Q is mainly received by the spar webs. The torsional moment $M_{кр}$ is received by the skin and the spar

webs which form a closed outline. Tangential stresses τ arise due to the transverse force and the torsional moment in corresponding elements.

The path of forces in a wing structure diagram. Let us examine the sequence of the transfer of forces along the elements of a wing structure diagram.

The basic load for a wing is the air load.

The mass load due to the weight and the inertia forces of the design acts in the form of forces distributed over each design element. These forces are transmitted further in conjunction with the forces arriving on an element from the air load; thus, we will not dwell further on the transfer of these mass forces.

The air load (figure 3.18) is directly received by the skin supported on stringers, ribs and spars.

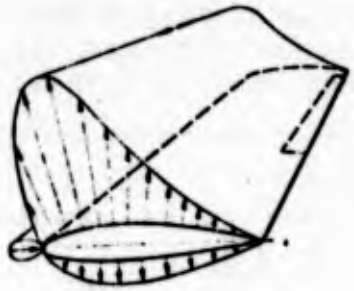

Figure 3.18. Air load on a wing surface.

The load is transmitted to ribs in the form of a linear load q_H distributed along the length of a rib and of concentrated forces from stringers R_H (they are partially shown in figure 3.19a) through coupling elements (rivets, welded or adhesive joints).

In the general case loads are also transferred to ribs due to the weights and structures fastened to a wing.

The resultants of the air and mass forces ΔR, loading the ribs, are applied in the centers of the distributed loads for the appropriate cross sections (figure 3.19b).

The ribs transfer the loads received by them to the spar webs.

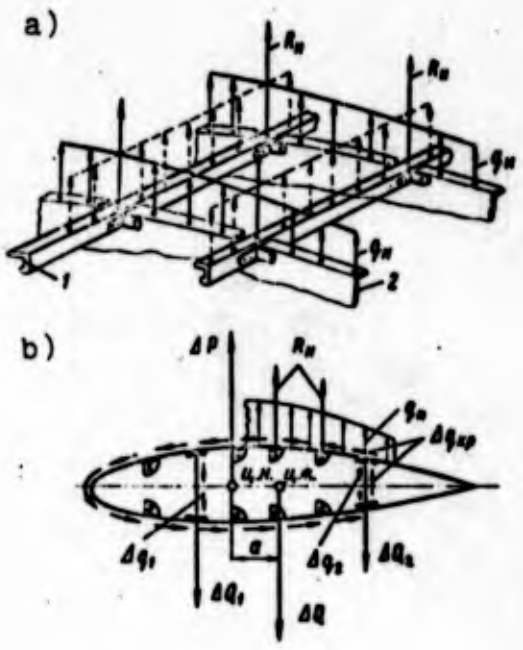

Figure 3.19. Diagram of the loading and balancing of a rib: 1 - stringer; 2 - rib.

The reactions of the spar webs balancing each rib ΔQ_1 and ΔQ_2 acting in the form of flows of tangential forces Δq_1 and Δq_2 (transferred through the rivets in the angle pieces joining a rib and webs), yield the resultants $\Delta Q=\Delta P$ applied at the centers of rigidity of the corresponding cross sections of the wing beam. The moments $\Delta M_{кр}=\Delta Pa$ arising (see figure 3.19b) are transmitted in the form of tangential forces $\Delta q_{кр}$ to the skin and to the webs which form a closed contour.

Let us note that in figure 3.19b reactive (balancing) flows Δq_1, Δq_2 and $\Delta q_{кр}$ are depicted which act from the direction of the spar webs and the skin to the rib. Flows of reverse direction act from the direction of the rib to the webs and the skin.

The loads ΔP transmitted by the ribs to the spar webs in the form of flows Δq_1 and Δq_2, and also the loads transmitted by the skin directly to the spars, cause in the web cross sections transverse forces Q_1 and Q_2 (figure 3.20a), which gradually increase irregularly from one rib to the next in the direction from the wing tip to the wing root.

All loads received by the webs, are transmitted by them to the units fastening the wing spars to the fuselage or to the wing center section.

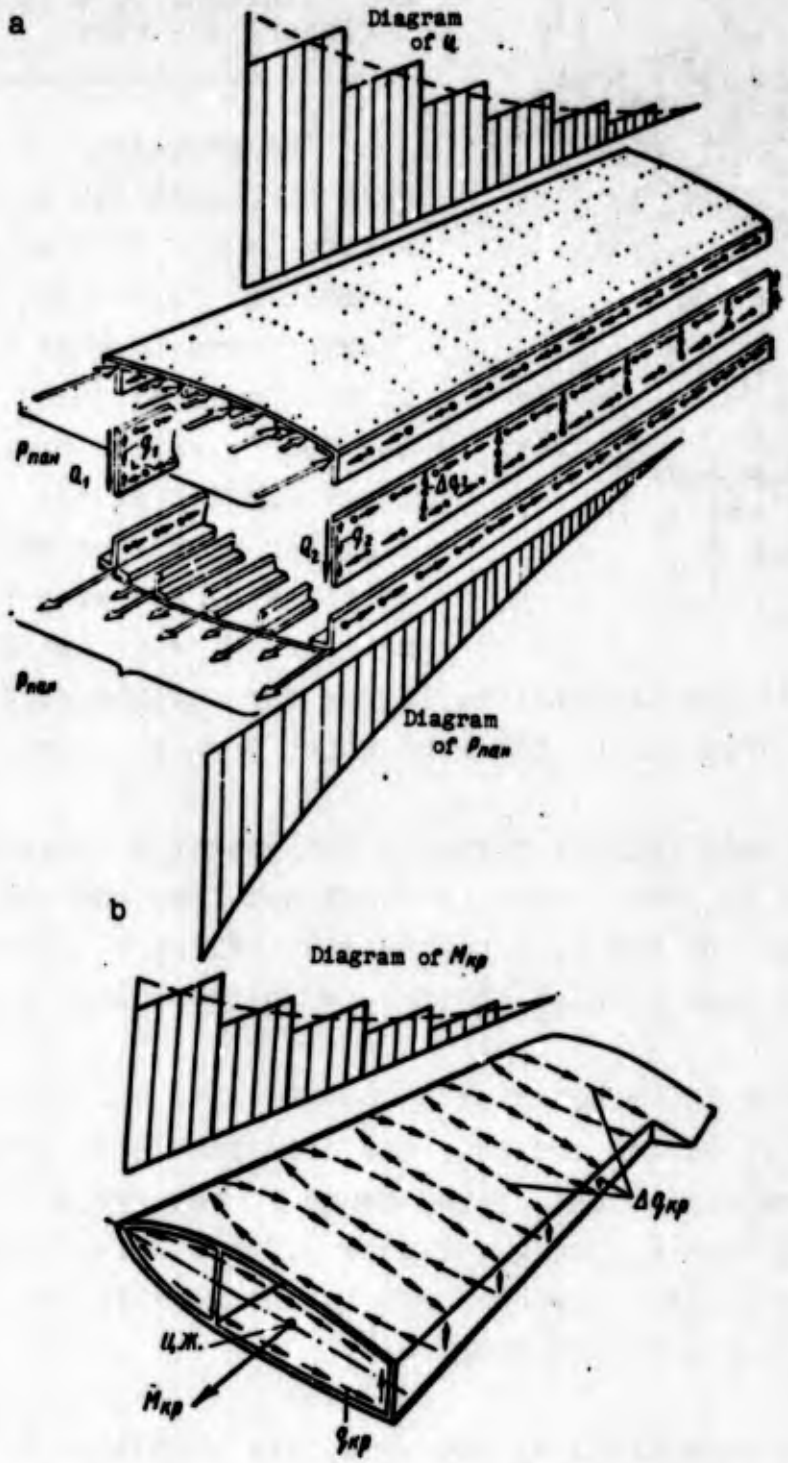

Figure 3.20. Diagram of the emergence of axial forces in the box (caisson) panels (a) and the loading of the contour with torsional moment (b).

Figure 3.20a (at the top) shows the intermittent change in the transverse force along the wing span. There the broken line represents the diagram of transverse forces, which is usually obtained by calculation without taking the discrete application of loads to the webs into account.

With the wall loading in question flows of tangential forces q_1 and q_2 arise in their transverse cross sections. According to the law of pairing of tangential stresses the same flows arise on the upper and lower boundaries of the webs, i.e., along the riveted joints connecting the webs with the spar flanges (see figure 3.20a). These flows yield axial forces (gradually building up from wing tip to wing root) in the upper and lower wing panels, which include the spar flanges, stringers and skin. In this case one of the panels (in this case the upper one) undergoes compression, and the other (the lower one) undergoes tension.

Figure 3.20a (at the bottom) shows a diagram of the axial forces in the panel along the wing span.

The internal tension and compression forces in the panels $P_{пан}$ in each wing cross section form a pair of forces whose moment is the wing bending moment in the given cross section.

At the side of the fuselage this moment is transmitted to the assemblies attaching the wing to the fuselage or to the center section.

The moments $\Delta M_{кр}$ transmitted by the ribs to the closed contour in the form of flows $\Delta q_{кр}$, being accumulated intermittently from the wing tip to wing root (figure 3.20b), cause torsional moment[3] in the wing cross sections.

---

[3]If the axes of rigidity of the different cross sections do not coincide, then the transverse force also affects the torsional moment.

The torsional moment $M_{кр}$ is transmitted to those same assemblies attaching the wing to the fuselage or to the center section and is balanced by the flow $q_{кр}$ acting from the direction of these assemblies.

In figure 3.20b (at the top) the broken line shows the torsional moment diagram, plotted as is usually done, disregarding the discrete transfer of loads to the closed contour.

Let us note that a simplified diagram of the transfer of forces from the skin to the webs was given above; it is valid for a wing with a skin which itself has low flexural rigidity. In a wing with a more rigid skin the transfer of the air load from the skin to the webs both through the ribs as well as passing by them is possible.

In summation, the purpose and the operation of the load-bearing elements of a wing can be described in the following manner.

The skin gives to the wing its streamlined shape; it receives the air load, operating in this case in lateral flexure and as a membrane, in tension ("chain stresses"); it operates in tension or compression and in shear, participating in the bending and the torsion of the wing beam.

The spars. The spar flanges, operating in tension or compression, receive part of the bending moment. The spar webs receive the transverse force; they together with the skin receive the torsional moment, operating in this case in shear.

The stringers together with the skin receive part of the bending moment, operating in this case in tension or compression; they transmit the air load from the skin to the ribs, operating

in transverse bending. The stringers, being skin supports, increase its critical stresses and reduce the local deformations.

The ribs preserve the assigned shape of the wing profile, transmit the loads incident on them (from the air and mass forces) to the spars and the skin; being supports of the skin and the stringers, they increase their critical stresses.

The joints connect the basic load-bearing elements with each other and transmit the forces from some parts of the structure diagram to others.

Along with the load-bearing elements in question which form the structure diagram ensuring the total strength of the wing beam, the wing design has a number of parts not related to this structure diagram: the wing tips, fillets, strips or covers which cover slots in the planes of the wing joints, auxiliary webs in front of the ailerons, etc.

The design of these parts carries the local loads incident on them, it transmits them to the basic load-bearing elements; for this it should possess the necessary strength.

Types of wing structure diagrams. Of the three forces $M_{изг}$, Q and $M_{кр}$ acting in the transverse wing sections, bending moment $M_{изг}$ can be called the main force, since the weight of the load-bearing elements receiving $M_{изг}$, constitutes approximately 50% of the total wing weight.

Depending on which load-bearing elements mainly receive the bending moment, the wing structure diagrams are divided into two types: spar and monocoque wings.

A wing structure diagram is called a spar wing, if the bending moment is mainly received by the spar flanges (figure 3.21a).

The spar wing has powerful spar flanges, comparatively weak stringers and thin skin.

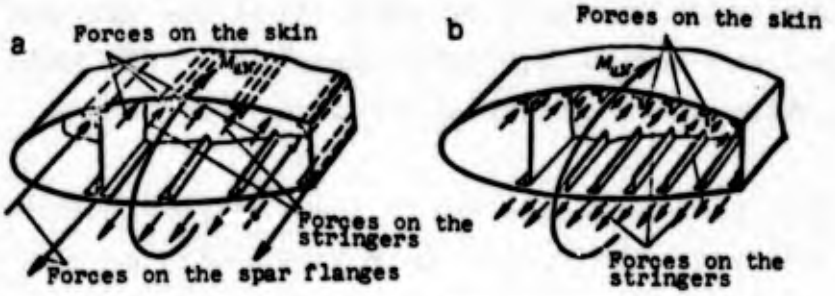

Figure 3.21. Spar (a) and monocoque (b) wing structure diagrams.

A wing structure diagram is called a monocoque wing, if the bending moment is mainly received by the skin and stringers (figure 3.21b).

The monocoque wing has a powerful stringer setup, thick skin and comparatively weak spar flanges (the cross-sectional areas of the flanges are of the same order as the cross-sectional areas of the stringers).

Let us carry out a brief comparison of the structure diagrams in question with respect to certain of the most important properties.

Design weight. In monocoque wings the skin material is utilized more rationally, which can lead to a decrease in the design weight of the entire wing. Investigations show that the advantage of the monocoque setup from the point of view of weight increases with an increase in aircraft weight, sweep angle, wing aspect-ratio, and with a decrease in the thickness ratio of a wing profile.

Rigidity. Monocoque wings as compared with spar wings possess greater rigidity in flexure and torsion.

Reliability and durability. In a monocoque wing the failure of a part of the load-bearing elements as a result of fatigue failures or random damages does not lead to the immediate failure of the entire design. In a spar wing the failure of even one of the spar flanges, as a rule, leads to the rapid failure of the entire design.

Thus, with respect to these properties monocoque wings are more favorable than spar wings.

Production and operational design technological effectiveness. From this viewpoint spar wings are more favorable. In spar wings the skin and stringers assume little participation in the operation of the wing flexure. Thus, in spar wings it is possible to make cut-outs (hatches) in the skin for the installation and inspection of fuel equipment, bays for the retraction of landing gear, for the installation and inspection of control cables, etc., without considerably reducing the bending strength of the wing. To preserve wing strength in torsion in this case are comparatively simple design measures accomplished which do not lead to a substantial increase in wing weight.

In monocoque wings cutouts in the skin should be mandatorily covered with heavier load-carrying covers secured by screws and bolts, and these covers should be capable of transmitting both shear forces as well as axial forces.

All this makes it difficult to accomodate loads and equipment within the wing, and also to inspect equipment and service it during operation.

Furthermore, spar wings are simpler than monocoque wings with respect to the attachment of removable parts to the center section or the fuselage.

Purely longeron (with the skin not receiving $M_{изг}$) and purely monocoque structure diagrams (without clearly expressed spar flanges) are rarely encountered at the present time; they can be considered as limited structure diagrams.

A comparison of spar and monocoque structure diagrams which was carried out shows that each of them possesses its own advantages and deficiencies.

Therefore, sometimes certain sections of a wing design (for example, the wing tip part), are made in accordance with the monocoque setup and others (for example, in the zone of a landing gear well) - are made in accordance with the spar setup.

§ 4. EXAMPLES OF WING DESIGN IN CONTEMPORARY AIRCRAFT

The variety and the contradictoriness of the requirements imposed on aircraft wings, do not make it possible to create a "universal" wing design possessing all the desired qualities and suitable for an aircraft of any type and purpose. Thus, in designing a wing it is necessary to select the requirements to be imposed on it which are most important for the given type of aircraft, which are also satisfied primarily by means of choosing the appropriate aerodynamic and internal layout, structure diagram and wing design.

Structure diagrams of wings, the purpose and operation of their load-bearing elements have been examined in the preceding section. Below as illustrated by different designs certain types of wings of contemporary high-speed aircraft, and also biplane and semicantilever (strutted) wing setups employed in low-speed small-engine aviation are examined.

The characteristic example of the monocoque design characteristic of the wings of medium and heavy passenger aircraft is the wing of the IL-18 aircraft (figure 3.22), consisting of

a center section and two removable parts - the cantilevers. The main load-carrying part of the wing is the box formed of spars (three in the center section and two in the removable part), the interspar panels consisting of the skin reinforced with stringers, and the middle parts of the ribs.

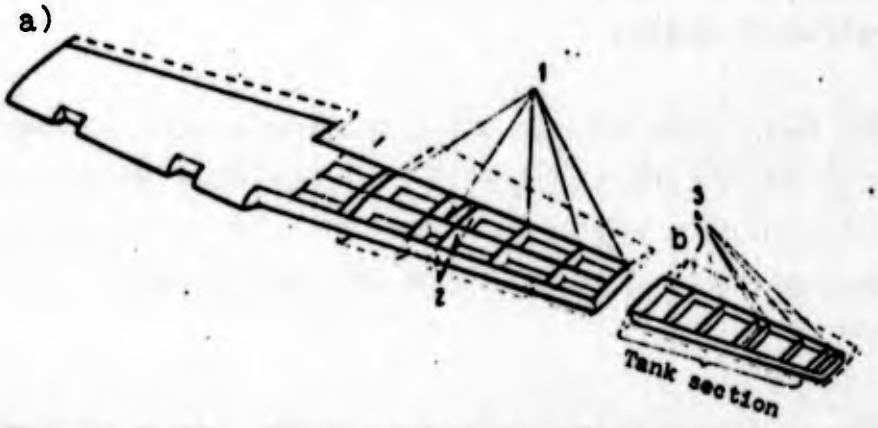

Figure 3.22. Wing of the IL-18 aircraft only the reinforced ribs are shown): a) center section; b) the removable part of the wing; 1 - flap suspension assemblies; 2 - main landing strut attachment units; 3 - aileron suspension assemblies.

The box receives the aerodynamic and mass distributed loads, and also the concentrated loads applied to the assemblies attaching the engine nacelles, the landing gear, the flaps and ailerons, and it operates in flexure, shear and torsion.

Concentrated loads are transmitted to the box through the reinforced ribs shown in figure 3.22. The internal volumes of the box are employed for the installation of flexible cell fuel tanks. The box of the removable part of the wing is hermetically sealed and represents a tank compartment.

The beam type spars are located at 13, 39, and 65% of the wing chord.

The middle spar in the center section increases wing rigidity during flexure and torsion and is employed for attaching the landing gear strut assemblies.

The upper and lower spar flanges are formed by pressed angle profiles which have a small cross-sectional area. In connection with this, the bending moment received by the spars is comparatively small.

The main part of the wing bending moment is received by the interspar stringers and the skin. The spar webs are supported by profile struts which increase the critical stresses of the webs during shear. Part of the struts is employed for securing the ribs.

The center section panels have stringers of trapezodal, T-shaped and H-shaped cross sections. The attachment of the detachable panels employed for the installation of the fuel tanks is carried out with the T-shaped and H-shaped stringers.

In the design of the removable part of the wing lightened stringers of trapezoidal and angular cross sections are employed. The quantity of stringers in the upper and lower panels is identical, but the stringers of the upper panels which operate in compression have large cross-sectional areas. All stringers are parallel to the middle spar of the center section. The pitch of the stringers in all wing cross sections is 140-145 mm. The cross-sectional areas of the stringers and their number decrease toward the wing tip.

The working skin of the box part of the wing has a thickness of from 1 to 6 mm.

The wing ribs in the region where the flexible fuel tanks are situated are made in the form of two flange-beams which

operate individually in flexure under the effect of the load which is transmitted from the skin. The ribs of the tank-section of the removable part of the wing are one-piece (in height) beams consisting of flanges and webs with apertures to make them lighter in weight.

The pitch of the ribs of the box part of the wing is equal to 450 mm.

The reinforced ribs of the center section which receive the concentrated loads, have a continuous web reinforced by struts.

The nose and tail sections of the center section and the removable parts of the wing are not included in the basic structure diagram of the wing beam. They receive only the local aerodynamic loads.

The butt joining of the removable parts of the wing with the center section is accomplished with bolts installed along the closed contour of the box.

Wing design ensures the possibility for the broad application of contemporary progressive methods of panel assembly and group press riveting. To increase the service life of a wing the skin, spars, stringers and ribs are manufactured from D16T aluminum alloy which has better characteristics of fatigue strength, than the high-strength alloys of the V-95 type.

The swept monocoque wing of the TU-124 aircraft represented in figure 3.23 and figure 3.24 consists of a center section, two middle parts and two removable parts. Just as in the IL-18 aircraft wing design, the acting loads are received by a box formed by two spars, by the interspar panels and ribs. Between the ribs of the center section and the middle parts of the wing flexible fuel tanks are installed. The box of the removable part of the wing is partially hermetically sealed and is employed as a tank-section.

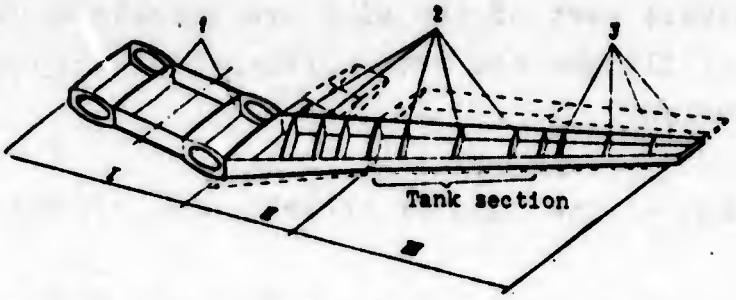

Figure 3.23. The swept monocoque wing of the TU-124 aircraft (only the reinforced ribs are shown): I - center section; II - middle part of the wing; III - removable part of the wing; 1 - inside ribs; 2 - flap suspension assemblies; 3 - aileron suspension assemblies.

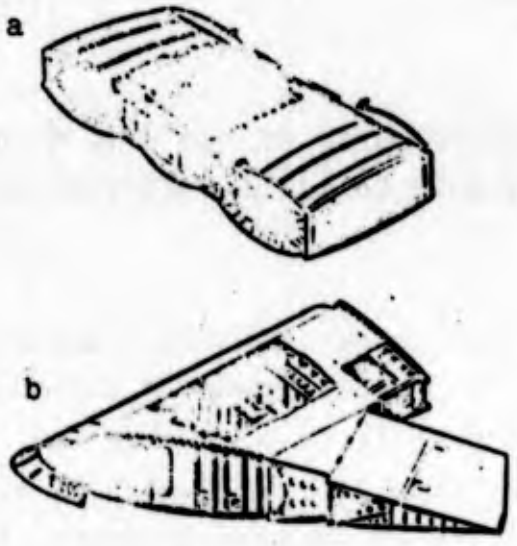

Figure 3.24. Center section (a) and the middle part (b) of the TU-124 wing.

The spar flanges located at 14 and 55% of the chord have noticeably larger cross-sectional areas than the stringers, but nevertheless the main portion of the bending moment is received by the interspar wing panels.

The spars - are of the beam type, with the exception of the center section spar sections in the area where the engine air intake ducts transit. These spar sections are made in the form of massive frames stamped from AK-8 alloy. Here, in view of the absence of a web the transmission of the transverse force and the torsional moment is accomplished by the operation of the upper and lower frame flanges in flexure, which requires their reinforcement and leads to a certain increase in spar weight.

The skin and the stringers of the upper panels operating in compression are made from high-strength V95AT aluminum alloy. The lower panels operating in tension, for which the ensurance of fatigue strength is important, are made from D16AT duralumin. The skin plates have a different thickness. The thickest skin (4 mm) is installed in the root part of the wing near the rear spar in the most loaded section of a swept wing.

The stringers are parallel to the rear spar. Powerful trapezoidal and H-shaped stringers in the center section and the middle part of the wing are replaced by angle stringers in the tip part.

At the joint of the swept part of the wing with the center section the longitudinal assembly endures fracture. Here the bending moment from the swept part is transferred to the center section in the form of bending and torsional moments. For the transmission of the latter to the skin it was necessary to insert a reinforced rib. Reinforced ribs were also installed at the sites of the attachment of the landing gear, the flaps and the ailerons.

All wing ribs (both reinforced and standard) - of the beam type, are installed perpendicular to rear wing spar.

With this arrangement of the ribs of a swept wing their length and weight are less than in the case when the ribs are located along the flow.

In the design in question chemical milling of the wing skin and the spar webs is broadly employed; the depth of the chemical milling attains 1.5-2.2 mm. This gives a reduction in the weight, at the same time preserving the strength of the skin near the riveted joints where its thickness is not reduced.

The wings of light aircraft in the majority of cases have spar design. The rigid skin of these types of wings participates in the wing's operation in torsion, and the bending moment is completely received by the spars. The employment of the monocoque type design at a relatively small magnitude of bending moment caused by the small dimensions of the wing and by the light weight of the aircraft, turns out to be unsuitable. The need to insert riveted joints makes it necessary in this case to employ a skin with a thickness greater than is required in accordance with the condition of strength during wing bending, which makes the wing weight characteristics worse. Spar wings have in this case the best weight data.

A long with the standard, monoplane, cantilever wing, most commonly employed in contemporary aviation, in which the loads acting on it are received by the internal elements of the framework (by the spars, the stringers, and the skin), those wing setups are also employed which have external (located in the flow) load-bearing elements which participate in the operation of the wing in flexure and torsion.

These setups which occupied the predominant position in the beginning of the development of aviation are encountered at the present time in two versions: the biplane setup and the monoplane semicantilever (strutted) setup.

The employment of the biplane and monoplane semicantilever setups turns out to be advisable for light low-speed aircraft with small wing loading per unit area which have nonretracting landing gear, since it yields, in this case, a reduction in the design weight (due to less wing weight) and a reduction in cost.

The biplane wing cell is a three-dimensional framework loaded with the aerodynamic and mass loads applied to it. The basic idea of the design consists in the employment of a large

design height of the biplane box characterized by the ratio h/l (figure 3.25a). If monoplane cantilever wings have $h/l=c/l=$ $=0.015-0.025$ then for biplane wings $h/l=0.14-0.2$.

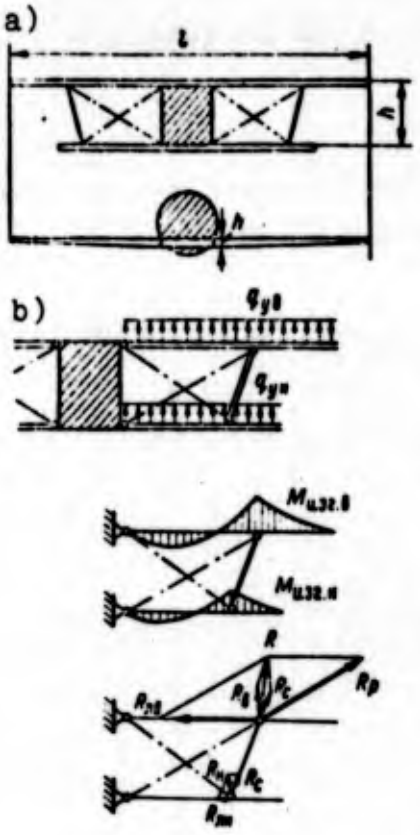

Figure 3.25. Biplane: a) its comparison with the cantilevered monoplane with respect to the magnitude of the ratio h/l; b) the loading of the biplane cell elements.

Since an increase in the design height leads to a weight reduction in the framework flanges, then the employment of the biplane design yields a certain reduction in weight as compared with the monoplane cantilever setup.

Another advantage of the biplane in comparison with the monoplane is its lesser wing span (with equal area and aspect ratio). This determines the lesser overall dimensions and the lesser rolling-moment inertia of the aircraft (the x-x axis) which provides biplanes with better maneuvering properties.

At the same time the biplane design possesses a significant deficiency which prevents the possibility of its application for contemporary high-speed aircraft. This deficiency is the great drag of the biplane box due to the mutual effect of the upper and lower wings and by the presence in the flow of framework elements (struts, bracing wires). Furthermore, in operation the biplane design proves to be more complex than the monoplane design, since it requires frequent checking and regulation of the position of the wings.

The biplane design was rather broadly employed in aircraft construction right up to the middle of the 30's, especially for maneuverable fighters, and attained the greatest aerodynamic and weight refinement in the form of a single-strut sesquiplane (lower wing shorter than upper).

At the present time the biplane design is employed for light low-speed aircraft of special application aviation.

The biplane wing cell of the contemporary AN-2 sesquiplane (figure 3.26) consists of upper and lower wings, carrying and supporting strip-braces and struts connecting the wings.

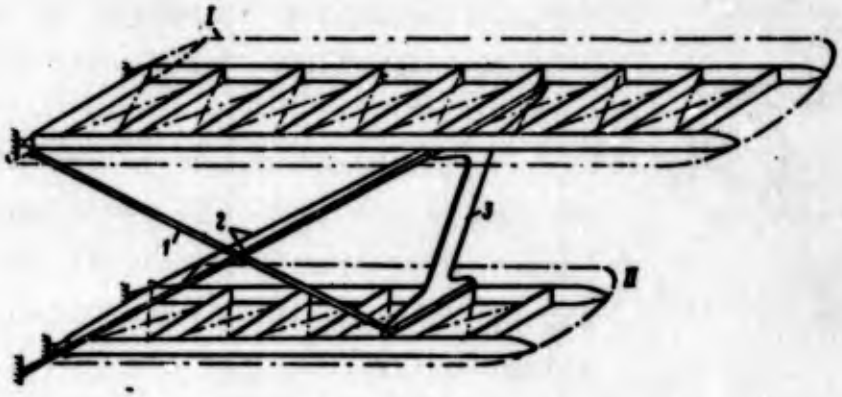

Figure 3.26. Biplane wing cell of the AN-2 sesquiplane (only the reinforced ribs are shown): I - the upper wing; II - lower wing; 1 - supporting brace; 2 - carrying braces; 3 - strut.

Each wing is a plane horizontal framework formed by two spars reinforced with ribs and internal braces. As long as the wings are connected with each other, they can operate only in flexure in the horizontal plane, since the attachment of the wings to the fuselage is accomplished with the aid of hinged wing root fittings which do not transmit the moments acting in the vertical plane. All braces have been pretensile-stressed, which eliminates their sagging with a change in direction of a load acting during operation.

The entire three-dimensional framework as a whole operates in vertical bending and torsion. In this case tensile or compressive forces act in its individual elements. Thus, for instance, the carrying braces in the main flight cases operate in tension under the effect of a load received by the upper wing, and a load from the lower wing transmitted along the strut to the brace attachment assemblies. The supporting braces are also loaded with negative g-forces when the aircraft is parked on the ground.

On the wing spars, which are beams having two supports each, comparatively small bending moments act (figure 3.25b), but in the brace attachment assemblies longitudinal compressive loads $R_{л.в}$ and $R_{л.н}$ which attain considerable magnitudes, are transmitted to the spars.

The struts operate in compression, transmitting loads R_c from one wing to the other. Force R_p stretches the carrying braces.

In connection with low flight velocities and the relieving of torsion from the wings a light linen skin is employed which receives only local aerodynamic loads.

The semicantilever monoplane design occupies an intermediate position between the biplane and the cantilever monoplane. The presence of an external load-bearing element - the strut,

increasing the design height h/l (figure 3.27a), makes it possible to reduce the wing weight, but at the same time leads to an increase in drag. In comparison with the biplane, the semicantilever monoplane has greater $c_{y\ max}$, less c_x and greater L/D ratio as a result of the fact that there is no harmful mutual effect of the wings, characteristic of the biplane setup.

Contemporary semicantilever monoplanes are constructed mainly in accordance with the high wing monoplane setup. The semicantilever low wing monoplane design is employed considerably more rarely since in this case the struts situated above the wing, operate in the most important loading cases A and A' in compression and are heavier. Furthermore, with upper positioning of the strut the aerodynamic characteristics of the wing deteriorate somewhat.

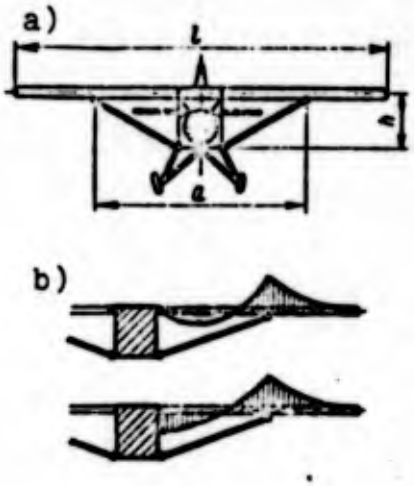

Figure 3.27. Semicantilever monoplane: a) its setup (front view); b) diagrams of the bending moments in the case of hinged and moment attachment of the wing to the fuselage.

The attaching of the wing to the fuselage can be hinged or it can be accomplished in the form of moment assemblies. Depending on the type of attachment the form of the diagram of bending moment received by the wing spars (figure 3.27b) varies.

The strut attachment assemblies are situated in such a way, so as to ensure less weight of the wing with the struts. According to statistics a/l=0.5-0.6 (Fig. 3.27a). If the struts are fastened to each wing spar, then they operate in flexure and during wing torque, and the middle part of the wing is relieved of torsional moment, which at low flight velocities makes it possible to use a light linen skin.

The wing design of semicantilever monoplanes is similar to the design of biplane wings.

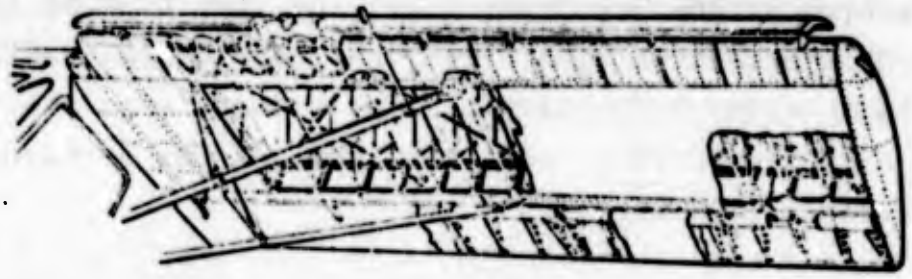

Figure 3.28. Wing of the YAK-12 aircraft.

Let us examine it as illustrated by the wing of the YAK-12 aircraft (figure 3.28). The wing - two-spar - has a metallic framework and a flexible linen skin. The spars are located at 14 and 65% of the wing chord and are connected with each other by ribs and tubular spacers. In the interspar sections between the spacers diagonal strip braces are installed which are pretensile-stressed and which form in conjunction with the spars and the spacers a plane framework which operates in flexure in the horizontal plane. The assemblies attaching the wing to the fuselage are hinged, and they do not transmit the bending moment acting in the vertical plane.

The V-shaped strut connecting both spars with the assembly on the fuselage, relieves the wing in the case of vertical flexure. The load-carrying triangle formed by the strut tubes and by the reinforced wing rib situated in the plane of the strut attachment assemblies, receives the loads arising during wing torque. To increase the critical force during compression of the strut counter-struts are installed, which connect the middle part of the strut with the assembly on the first wing spar.

The ribs - of the framework type - ensure the preservation of the shape of the profile and transmit the loads received by the skin fastened to them to the wing spars.

The section of the root part where the fuel tank is located, and the leading nose up to the first spar have a rigid skin. The rigid duralumin skin of the leading edge ensures more precise preservation of the profile shape and improves the aerodynamic characteristics of the wing.

§ 5. BASES OF THE REDUCTION COEFFICIENT METHOD

During the stress analysis of aviation designs, the basic type of which is calculation for the effect of the destructive loads, the method of reduction coefficients is employed, which takes into account the difference between the mechanical characteristics and the operating conditions of the individual design elements.

This method was introduced into ship-building practice by I. G. Bubnov, and into aircraft construction - by V. N. Belyayev (TsAGI (Cen. Ints of Aerohydrodynamics im. N. Ye. Zhukovskiy)).

The difference in the mechanical properties already exists in the initial, unloaded state of elements, if they are made from materials with different values of elastic modulus E. This difference in the mechanical properties increases in proportion to the increase in load when the deformation of a part of the elements deviates from Hooke's law due to the transition into the plastic deformation region (the stresses exceed the limit of proportionality) and certain elements whose stress attained the critical value lose stability.

The fundamental characteristics of the mechanical properties of load-bearing elements employed in calculation are their tension-compression diagrams.

Figure 3.29 shows as an illustration the real and schematized diagrams of a load-bearing element (duralumin stringer).

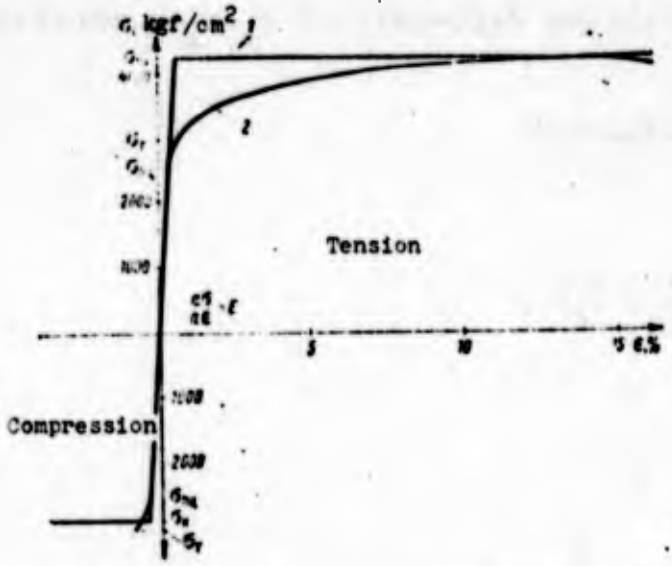

Figure 3.29. Tension-compression diagrams of a load-bearing element (example): 1 - schematized; 2 - real.

In order in the calculation in tension or compression of a design made from heterogeneous elements to use the usual strength of material formulas, valid only within the effective limits of Hooke's law (up to the limit of proportionality), it is possible to arbitrarily replace all these elements with fictitious elements having a single rectilinear diagram $\sigma=f(\varepsilon)$.

Usually the replacement process is carried out by reducing to a straight line Hooke's law of the real diagram which corresponds to the strongest and most rigid design element of the wing panel, in a spar wing - to a spar flange.

To account for the disparity in elements their real areas are arbitrarily replaced by reduced areas:

$$F_{\text{ред}} = \varphi F,$$

where $F_{\text{ред}}$ - is the reduced cross-sectional area of an element; F - is the real cross-sectional area of an element; φ - is the reduction coefficient.

Hence

$$\varphi = \frac{F_{\text{ред}}}{F}.$$

In this case the condition is put that the fictitious and real elements, the diagrams $\sigma=f(\varepsilon)$ of which are depicted in figure 3.30c, with identical relative deformations $\varepsilon_ф=\varepsilon_д=\varepsilon$ receive the identical load:

$$P = \sigma_ф F_{реа} = \sigma F.$$

Hence follows that

$$\frac{\sigma}{\sigma_ф} = \frac{F_{реа}}{F}.$$

Since

$$\frac{F_{реа}}{F} = \varphi,$$

then

$$\varphi = \frac{\sigma}{\sigma_ф}.$$

If the fictitious element has a rectilinear diagram - the diagram of Hooke's law

$$\sigma_ф = E\varepsilon,$$

then the connection of the stresses and deformations of the real element and after loss of stability or after its transition beyond the limit of proportionality can be expressed by the formula

$$\sigma = \varphi E\varepsilon.$$

Let us examine the sequence of calculation by the reduction coefficient method of a tensioned or compressed wing panel - of a statically indeterminable system consisting of heterogeneous elements with respect to their mechanical properties, in which the assigned force P acts. The elements are connected with each other so that their longitudinal deformations are identical.

Figure 3.30 shows the stresses in the elements of real and reduced panels.

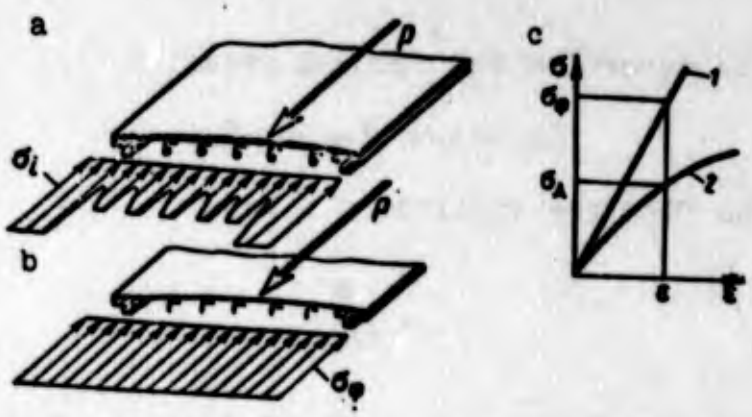

Figure 3.30. Stress in the elements of a real (a) and reduced (b) panel; fictitious (1) and real (2) diagrams $\sigma=f(\varepsilon)$ (c).

It is necessary to determine the stresses σ_i in the system elements.

Let us present P in the following manner:

$$P = \sigma_1 F_1 + \sigma_2 F_2 + \ldots,$$

or, since

$$\sigma_i F_i = \sigma_\phi F_{i\text{пред}} = \sigma_\phi \varphi_i F_i,$$

then

$$P = \sigma_\phi F_{1\text{пред}} + \sigma_\phi F_{2\text{пред}} + \ldots = \sigma_\phi \varphi_1 F_1 + \sigma_\phi \varphi_2 F_2 + \ldots$$

Then

$$\sigma_\phi = \frac{P}{\Sigma F_{i\text{пред}}};$$

$$\sigma_i = \varphi_i \sigma_\phi.$$

In the general case it is necessary to find the values of φ_i by the method of successive approximations, since for determining φ_i from diagram $\sigma=f(\varepsilon)$ it is necessary to know ε or σ_ϕ, and for determination ε or σ_ϕ, it is necessary to know the reduction coefficient or to assign it a value.

It is possible to determine σ_i in the following order:

1. Let us assign the values of φ_1, φ_2, ...

2. Let us determine the reduced areas:

$$F_{1\text{пед}} = \varphi_1 F_1; \quad F_{2\text{пед}} = \varphi_2 F_2 \ldots$$

3. Let us find the fictitious stress

$$\sigma_\phi = \frac{P}{\Sigma F_{i\text{пед}}}.$$

4. Let us determine from σ_ϕ found from the diagrams of the type shown in figure 3.30c, the real stresses of the first approximation σ_1, σ_2 ....

5. Let us compute the reduction coefficients of the first approximation φ_1, φ_2 as the relations σ_1/σ_ϕ, σ_2/σ_ϕ, ...

The calculation is repeated until for each element the assigned values of φ_i and the values of φ obtained from calculation are virtually identical.

The values of σ_i obtained in this case will be final.

With a rational selection of the initial values of φ necessary number of calculation repetitions decreases.

The initial values of φ are selected taking into account the properties of the materials and the cross sections of the load-bearing elements, the load-bearing setup of the design, the type of deformation (tension, compression etc.) and the magnitudes of the anticipated stresses. Thus, in rating a wing for flexure the selection of the initial values of φ is based on the following considerations.

Loading cases A or A' are usually decisive in estimating the strength (rated) for the load-bearing elements which ensure wing strength during flexure.

In a rationally designed wing in these cases of loadings the spar flanges and the skin with stringers operate at stresses, close to destructive.

As the rupture stresses there are assumed: in tension - the ultimate strength $\sigma_в$ (or $k\sigma_в$ taking into account the local weakening of the stretched members), in compression - the critical stress $\sigma_к$.

Thus in rating for cases A and A' the reduction coefficient is assumed for each element equal to the ratio of the rupture stress of the element $\sigma_{разр\ i}$ ($\sigma_{в\ i}$ or $\sigma_{i\ к}$) to the rupture stress of the flange ($\sigma_{вп}$ or $\sigma_{кп}$):

$$\varphi_i = \frac{\sigma_{разр\,i}}{\sigma_{разр\,п}}.$$

In other loading cases $M_{изг}$ is usually considerably less than in cases A or A'; thus, in rating for these cases it is assumed, that in the tensioned and compressed zones the limit of proportionality $\sigma<\sigma_{пп}$ is not exceeded, and in the compressed zone $\sigma<\sigma_к$, g.e. and the real and fictitious diagrams are linear.

In this case according to Hooke's law

$$\sigma_i = E_i\varepsilon_i \text{ and } \sigma_ф = E_п\varepsilon_ф.$$

Since earlier it was agreed, that the deformations of the real and fictitious element were equal to: $\varepsilon_i=\varepsilon_ф=\varepsilon$, then

$$\varphi_i = \frac{E_i}{E_п}.$$

It is necessary to employ the same values of φ_i in all cases when the calculation is carried out for the effect of the

operating loads in which the design should operate within the limits of Hooke's law.

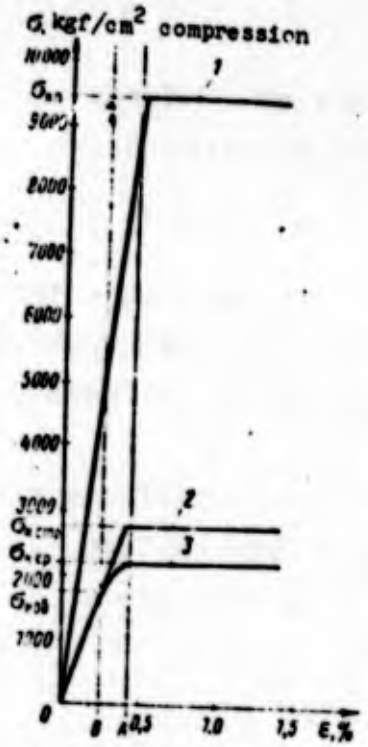

Figure 3.31. Schematized diagrams of the load-bearing elements of a compressed wing panel: 1 - flange; 2 - stringer; 3 - skin.

For explaining the principles of selecting the initial values of φ it is possible to examine the schematized diagrams of the load-bearing elements of a compressed wing panel (skin and stringers of duralumin, flange of Chromansil). Figure 3.31 shows the deformations which correspond to loading cases A and B.

The values of φ_1 for the individual elements which correspond to the above expressed considerations, are given in Table 3.1.

Table 3.1

Elements	Cases A and A'		The remaining loading cases
	Tensioned zone	Compressed zone	Tensioned and compressed zones
Flanges	$\varphi = 1$	$\varphi = 1$	$\varphi = 1$
Stringers	$\varphi = \frac{\sigma_{к\,стр}}{\sigma_{в1}}$	$\varphi = \frac{\sigma_{к\,стр}}{\sigma_{вн}}$	$\varphi = \frac{E_{стр}}{E_н}$
Skin	$\varphi = \frac{\sigma_{к\,обш}}{\sigma_{вн}}$	$\varphi = \frac{\sigma_{к\,ср}}{\sigma_{вн}}$	$\varphi = \frac{E_{обш}}{E_н}$

The critical stresses of stringers $\sigma_{к\ стр}$ and the average critical stresses of the reinforced skin $\sigma_{к\ ср}$ which are included in the expressions of φ of table 3.1 are defined in the manner that was discussed in chapter 4, § 3 and 4.

The approximate methods of rating a wing design based on assumptions which considerably simplify the calculation and which facilitate its execution, are examined below. These methods of calculation possess clarity and simplicity and at the same time rather correctly reflect the purpose and the operation of the design elements. It is important for the operator-engineer to know how to use them.

§ 6. TWO-FLANGE BEAM

The approximate rating of a wing in flexure is based on taking the so-called two-flange beam as the calculation system of the wing. Let us examine the peculiarities of this system also frequently employed in calculating of other design parts of aircraft and helicopters.

It is known from strength of materials that the H-shaped beam cross section is the most advantageous in a weight regard during operation in flexure. The broad application of the types of beam cross sections in aircraft construction is explained by this.

Let us examine the distribution of normal (σ due to $M_{изг}$) and tangential (τ due to Q) stresses in an H-shaped beam cross section load with forces lying in its longitudinal plane of symmetry (figure 3.32a).

Calculational formulas of strength of materials are:

$$\sigma = \frac{M_{изг}}{I} z, \quad \tau = \frac{QS_z}{Ib},$$

where I - is the inertia moment of beam cross section relative to the neutral axis; z - is the distance from the neutral axis to the fiber in question; S_z - is static moment of the cross-hatched part of the cross section; b - is the width of the beam at the z level.

Figure 3.32. H-shaped beam: a) distribution of the normal and tangential stresses in the cross section; b) schematization of the cross section.

The diagrams of σ and τ in figure 3.32a correspond to these formulas.

From an examination of the indicated diagrams and the calculational formulas it follows that:

a) the greatest normal stresses arise in the flanges; if their areas are significant, then $M_{изг}$ is mainly received by the flanges;

b) the greatest tangential stresses τ act in the cross section sections, closer to the neutral axis - in the web; transverse force Q is mainly received by the web.

The designer's tendency is naturally in the direction of in the very best manner to employ the operation of the flanges for normal, and of the webs - for tangential stresses.

The ultimate of this refinement is the setup of a two-flange beam with concentrated flanges and a thin web. It is possible to assume for it that the flanges completely receive the bending moment, and the web - the transverse force. The approach to this setup is advantageous from the viewpoint of weight economy, since evenly distributed stresses act in the flanges and in the web, which ensures the full-valued employment of the material.

The carrying out of the design calculation as of a two-flange beam leads to considerable simplification in the calculational operations.

The schematization of the H-shaped beam cross section is shown in figure 3.32b. For the schematized two-flange beam the web area is

$$F_{ст} = H\delta_{ст}.$$

The inertia moment of the cross section we disregard (the inherent inertia moments of the flanges and of the web) is

$$I = \frac{F_п H^2}{2}.$$

From a direct examination of a two-flange beam it is possible to record:

the force in the flange

$$P = \frac{M_{изг}}{H};$$

the stress in it

$$\sigma = \frac{P}{F_п} = \frac{M_{изг}}{F_п H}.$$

The more the flanges are spaced, the thinner they are, the closer is their stressed state to pure tension and compression.

By assuming that the transverse force is received only by the web section with a height H in the form of evenly distributed stresses, we will obtain

$$\tau = \frac{Q}{F_{ст}}.$$

In employing these formulas to the calculation of real beams it is necessary to keep in mind that there can be cases (in unsuccessful designs), when small forces due to the transverse force incident on flanges, and the small fractions of the bending moment incident on the webs, can cause dangerous stresses in them. The cases presented in figure 3.33 can serve as an example.

Figure 3.33a shows the result of the unsuccessful selection of web material.

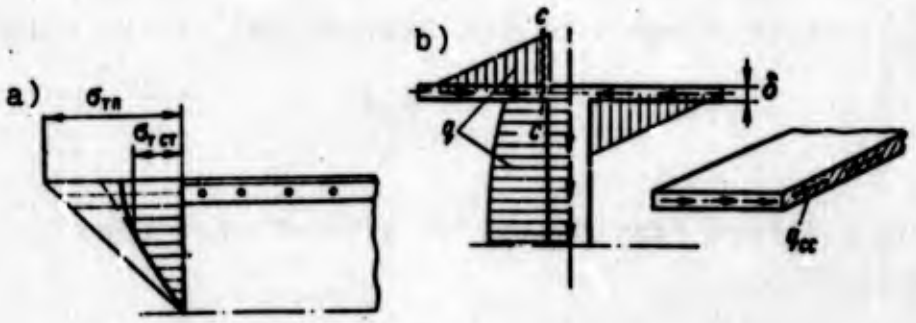

Figure 3.33. Examples of the unsuccessful design of an H-shaped beam: a) unsuccessful selection of web material; b) unsuccessful flange shape.

The stress distribution between the web and the flange is determined by the ratio of the absolute values of:

$$\frac{\sigma_{ст}}{\sigma_{т}} = \frac{E_{ст}}{E_{т}}.$$

If

$$\frac{E_{ст}}{E_{т}} > \frac{\sigma_{т.ст}}{\sigma_{тт}},$$

that the web will obtain plastic deformations earlier than the flange.

Figure 3.33b gives an example of an unsuccessful flange shape. Due to too small a thickness of δ large stress values are obtained in the c-c cross section:

$$\tau_{ск} = \frac{q_{ск}}{\delta}.$$

Let us examine the effect on forces in the cross-section elements of the nonparallelism of the flanges of a two-flange beam which is characterized by angle α (figure 3.34a). Usually in aircraft designs this angle is small and it is possible to assume that

$$r = \frac{H}{\alpha},$$

where α - is in radians.

In figure 3.34a Q and $M_{изг}$ - are the forces acting from the direction of the left cut-off part on the right part in question.

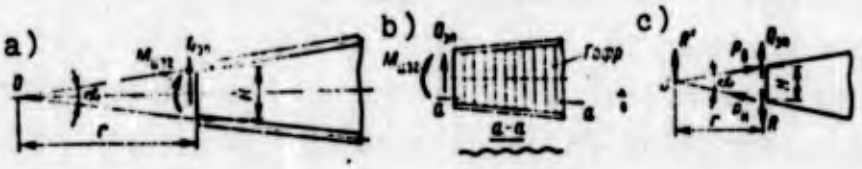

Figure 3.34. The effect of the nonparallelism of the flanges of a two-flange beam on the distribution of $M_{изг}$ and Q between its elements.

Let us consider the effect of the nonparallelism of the flanges on the distribution of $M_{изг}$ and Q between the beam elements.

Let us assume as for a two-flange beam with parallel flanges, that the flanges can receive forces only along their axis, and the web receives forces parallel to the cross section.

It is possible to base these assumptions on the fact that the flanges in view of their low rigidity in flexure, cannot receive forces directed across their axis.

The property of a web to only receive forces parallel to the cross section, can be explained by an example of a thin

corrugated web with wave crests, parallel to the cross section (figure 3.34b), which does not resist the forces directed along the beam axis.

Acceptability of such assumptions is confirmed by experimental results.

In accordance with these assumptions the transverse force and the bending moment are distributed between the web and the flanges in the manner shown in figure 3.34c: Q is transmitted directly to the web, $M_{изг}$ is transmitted in the form of the pair of forces R and R' ($\bar{R}'=\bar{P}_в+\bar{P}_н$), which are applied in accordance with the potentiality of the design receiving them.

The resultant of forces $P_в$ and $P_н$ received by the flanges, should pass through O - the point of intersection of the flange axes. This determines the site one of the forces of the pair (R'); the other force (R) should lie in the plane of the cross-section:

$$R = R' = \frac{M_{изг}}{r} = \frac{M_{изг}}{H} a.$$

Let us connect force R applied in the plane of the web, with force Q. The force obtained as a result of the summation, can be called the reduced transverse force $Q_{прив}$ in contrast to the transverse force taken from the calculation of the transverse forces or from the diagram of $Q_{эп}$. It is determined by the following formula

$$Q_{прив} = Q_{эп} - R = Q_{эп} - \frac{M_{изг}}{H} a.$$

Force R' applied at point O, will cause only longitudinal forces in the flanges. Their values can be found from an equilibrium triangle of forces $P_в$, $P_н$ and R'.

In view of the smallness of the angle

$$P_1 \approx P_2 = P = \frac{R}{a} = \frac{M_{изг}}{H}.$$

Thus, the forces in the flanges in this case are approximately expressed by the same formula, as for a beam with parallel flanges:

$$P = \frac{M_{изг}}{H}.$$

From a comparison of the calculational formulas it follows that the calculation of a beam with nonparallel flanges for $M_{изг}$ can in the first approximation be carried out in accordance with the formulas for beams with parallel flanges. It is necessary to carry out the calculation of the webs in shear taking into account the effect of the bending moment on the variation in the magnitude of the transverse force.*

This method of calculation is also employed for a wing beam. The wing in the front view is a beam which narrows toward the tip. The conicity of wing is considered by introducing $Q_{прив}$. into the calculation.

§ 7. APPROXIMATE CALCULATION OF A WING IN FLEXURE

1. Schematization of the Cross Section

For the approximate calculation of a wing for normal stresses due to bending moment the real wing cross section (figure 3.35a) is replaced by a cross section having the form of a rectangle

---

*If $M_{изг}$ is caused by the force applied at point O in the left cut-off part, then the forces reduce to the forces P and $Q_{прив}=0$.

with the width of panels B and the working height H (figure 3.35b). Width B is assumed equal to the distance between the outmost spars.

The mean working height of the cross section is taken as H. Approximately for a two-spar wing

$$H = \frac{H_1 + H_2 + 0{,}95\bar{c}b}{3},$$

and for a multispar wing

$$H = \frac{\Sigma H_i}{m};$$

where b - is the chord of the cross section in question; $\bar{c}$ - is the thickness ratio of the profile; m - is the number of spars; H_i - the distance between the centers of gravity of the flanges (the working height of the spar) - is measured from the drawing.

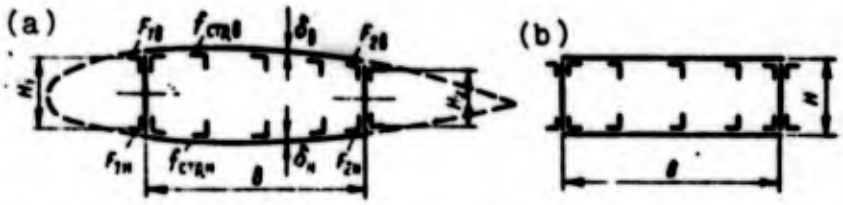

Figure 3.35. Real (a) and schematized (b) wing cross sections.

The nose and tail parts of the cross section (in figure 3.35a are designated by the broken line) are not considered in calculating for $M_{изг}$.

The calculational setup for a cross section in the approximate calculation of a wing in flexure is the two-flange beam with a working height of H.

The reduced areas of the panels limited by the outermost spars, in which are included the spar flanges, the stringers,

the skin are taken at the cross-sectional areas of the flanges of this beam $F_в$ and $F_н$. The sum of the cross-sectional areas of the spar webs is included in the cross-sectional area of web $F_{ст}$.

2. Determining the Forces in Panels

For the cross-sectional setup in question the forces in the panels, as the forces in the flanges of a two-flange beam, are found from known $M_{изг}$ and H,

$$P = \frac{M_{изг}}{H}.$$

3. Calculation of a Panel

Panels are calculated in tension or compression with the employment of the method of reduction coefficients.

Usually the cross-sectional area of each panel is reduced by reduction to the diagram of Hooke's law for the main load-bearing element of a panel - the spar flange.

The distribution of the fictitious stresses with respect to the reduced area of a panel is considered to be uniform:

$$\sigma_ф = \frac{P}{F_{прд}} = \frac{M_{изг}}{HF_{прд}}.$$

The reduction coefficients of the flanges are $\varphi_п = 1$. Therefore

$$F_{прд} = \Sigma F_в + \Sigma f_{стр}\varphi_{стр} + B\delta_{обш}\varphi_{обш}.$$

For each panel (upper and lower) are taken their magnitudes of the areas (thicknesses) and of the reduction coefficients of the flanges, stringers and skin are taken to be $F_п$, $f_{стр}$, $\varphi_{стр}$, $\delta_{обш}$, $\varphi_{обш}$.

The real stresses in the panel elements are determined from the formula

$$\sigma_i = \varphi_i \sigma_\phi.$$

Thus, for a flange $\sigma_п = \sigma_\phi (\varphi_п = 1)$; for a stringer $\sigma_{стр} = \varphi_{стр} \sigma_\phi$; for the skin $\sigma_{обш} = \varphi_{обш} \sigma_\phi$.

When selecting the values of the reduction coefficients one ought to be guided by the instructions given in § 5.

The obtained formulas are employed for calculating of the wing panels of any load-bearing designs.

The assumption that panels operate in uniform tension or compression, is sufficiently well founded for cases A and A', when the operation of all the elements corresponds to the horizontal sections of the diagram $\sigma = f(\varepsilon)$.

During the operation of the beam in the elastic region the distance from the neutral axis as is shown in figure 3.36 affects the stress level.

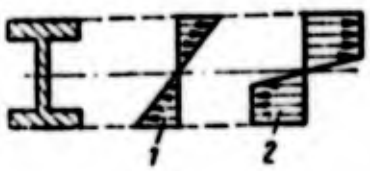

Figure 3.36. The effect of the distance of the elements from the neutral axis for normal stresses: 1 - within the elastic limits; 2 - beyond the elastic limits in the plastic flow region.

The effect of the difference in the over-all spar heights $H_{раб\ i}$ from H during operation in the elastic region can be taken into account, by employing the formula

$$\sigma_{ri} = \sigma_\phi \frac{H_{раб\ i}}{H}.$$

For the remaining elements not connected by webs, the effect of the difference in height is less, since as a result of the

deformability of the wing design between spars during bending flattening of the wing occurs, as the more distant elements approach the neutral axis.

Let us examine the peculiarities of determining the normal stresses in the elements of the wing cross sections of the maximum structure diagrams - the monocoque and spar wings.

Monocoque wing. In this case the areas of the spar flanges practically do not differ from the areas of the stringers. Thus, it is necessary to consider spar flanges as stringers and to assume $\varphi_{стр}=1$.

Then for each panel

$$F_{рез} = n_{стр} f_{стр} + B\delta_{обш}\varphi_{обш},$$

where $n_{стр}$ - is the number of stringers in a panel (including the spar flanges): $\varphi_{обш}$ - is the reduction coefficient of the skin.

For a tensioned panel

$$\varphi_{обш} = \frac{\sigma_{в\,обш}}{\sigma_{в\,стр}}.$$

for a compressed panel

$$\varphi_{обш} = \frac{\sigma_{к\,ср}}{\sigma_{к\,стр}}$$

where $\sigma_{к\ стр}$ - is the critical stress in a stringer; $\sigma_{к\ стр}$ - is the average critical stress in a reinforced skin.

Even if the skin, and the stringers are made from duralumin, then for a compressed panel it is possible to consider that in conjunction with each stringer with the same stresses a connected strip of skin by a width of $2c=(25-30)\delta_{обш}$ (for stringers with large $\sigma_{к\ стр}$ the magnitude of 2c is less) operates. Then

$$\varphi_{обш} \approx \frac{2c}{t_{стр}} \leqslant 1,$$

where $t_{стр}$ - is the stringer pitch.[5]

The fictitious stress in a panel is determined by the already known formula

$$\sigma_{ф} = \frac{M_{изг}}{HF_{ред}}$$

or by the formula

$$\sigma_{ф} = \frac{M_{изг}}{HB\delta_{пр}},$$

where $\delta_{пр}$ - is the reduced panel thickness: $\delta_{пр}=\delta_{обш}\varphi_{обш}+(f_{стр}/t_{стр})$.

Spar wing. Let us examine the two-spar wing in which the bending moment is received only by the spars.

In this case

$$M_{изг} = M_1 + M_2,$$

where M_1 and M_2 - are the bending moments received by the first and second spars respectively.

On the other hand, from a condition of joint spar operation (equality of the curvature of their elastic lines) we will have:

$$\frac{M_1}{I_{ред1}} = \frac{M_2}{I_{ред2}},$$

where $I_{ред\ 1}$ and $I_{ред\ 2}$ - are the reduced inertia moments respectively of the first and second spars.

By simultaneously solving the obtained equations, we find:

---

[5]Determination of the critical stresses $\sigma_{к\ стр}$, $\sigma_{к\ ср}$ is examined in chapter 4, § 1.

$$M_1 = M_{изг}\frac{I_{ред1}}{I_{ред1}+I_{ред2}};$$

$$M_2 = M_{изг}\frac{I_{ред2}}{I_{ред1}+I_{ред2}}.$$

For a multispar wing

$$M_i = M_{изг}\frac{I_{рединг}}{\Sigma I_{рединг}}.$$

After determining the bending spar moments M_i, we find the stress in the flanges

$$\sigma_i = \frac{M_i}{H_i F_{пi}}.$$

4. Strength Testing

In concluding the calculation it is necessary to check for all the cross-sectional elements the fulfillment of the strength condition in the case of the design destructive load. If a cross section is loaded with pure flexure (or the tangential stresses can be disregarded), then the strength condition takes the form:

$$\sigma_i^p \leqslant \sigma_{разр\,i},$$

where σ_i^p - is the acting stress due to the design destructive load P^p; $\sigma_{разр\ i}$ - is the destructive normal stress of the element.

The coefficient of the strength excess is

$$\eta_i = \frac{\sigma_{разр\,i}}{\sigma_i}.$$

The critical stresses of the main load-bearing elements are taken for the compressed zone as destructive stresses:

for a spar setup of a wing $\sigma_{разр} = \sigma_{к\ п}$;

for a monocoque setup $\sigma_{разр} = \sigma_{к\ стр}$.

For elements of the tensioned zone $\sigma_{раз\ i}=k\sigma_{в\ i}$, where k - is the coefficient which considers the local weakening of the tensioned elements of the rivet holes (usually k=0.9).

The calculation for the effect of the operational load is carried out in the same sequence as the examined calculation for P^{p}. The difference consists in the fact that, since the design should operate within the elastic limits, it is necessary to find the values of the reduction coefficients from the expression

$$\varphi_i = \frac{\dot{E}_i}{E_\phi},$$

during strength testing the following requirement is examined:

$$\sigma_i \leqslant \sigma_{прид\ i},$$

where $\sigma_{прид\ i}$ - is the maximum stress permissible in accordance with the condition of the absence of noticeable residual deformations or deformations which considerably disturb the design shape. Usually is accepted the arbitrary yield point $\sigma_т$ or $\sigma_{к\ обш}$ (for the compressed zone) for $\sigma_{прид\ i}$.

These questions of strength testing are examined in chapter 4, § 1-3 taking into account in more detail the joint effect of the normal and tangential stresses.

5. Determining the Dimensions of the Wing Cross Section Elements

Let us examine the determination of the dimensions of the cross-sectional elements receiving $M_{изг}$.

The dimensions of the main load-bearing elements (spar flanges, skin and stringers) in the majority of wing cross sections are determined by the magnitude of the bending moment in the case of A or A'.

In order to show how the forces and the arrangement of the load-bearing elements in a wing cross section affect the necessary

dimensions of the elements, let us examine the approximate design calculation of a cross section. The elements selected in accordance with it are subsequently checked in the final verifying calculation of the wing design.

In a rationally designed wing with calculated destructive loads of the decisive case the stress loads in the load-bearing elements should be close to destructive. However, it is necessary to consider that the found dimensions of the elements are the smallest possible and the need for increasing them can arise to ensure the fatigue life (see chapter 13).

The initial data for the calculation are:

the drawing of the cross section profile;

the calculated destructive value of $M_{изг}$ in the cross section;

the mechanical characteristics of the materials selected for the manufacture of the main load-bearing elements.

The calculation is made in this sequence.

1. Selection of the type of structure diagram; the arrangement of the spars and the determination of their heights.

Select the value of the coefficient $\kappa = \frac{M_{изг.л}}{M_{изг.о}}$, characterizing the distribution of the total bending moment $M_{изг}$ between the spars ($M_{изг.л}$) and the structural skin ($M_{изг.о}$).

If κ=0.7-0.9 - the setup is close to the spar setup, when κ=0.1-0.3 - close to the monocoque setup.

It is necessary to keep in mind that the type of structure diagram of the section of the design wing is determined

by the magnitude of coefficient κ. Thus, in selecting the magnitude of κ it is necessary to consider the characteristics of the internal layout of wing in this section.

The arrangement of the spars is carried out taking into account the layout and strength requirements imposed on the wing.

The arrangement of the spars is characterized by the following data.

The relative position of the spar along the chord $\bar{x}_i = x_i/b$, where b - is the chord, and x_i is - the distance of spar i from the leading edge.

In a wing with two spars $\bar{x}_1 \approx 0.2$; $\bar{x}_2 \approx 0.6$; in a wing with three spars $\bar{x}_1 \approx 0.15$; $\bar{x}_2 \approx 0.4$; $\bar{x}_3 \approx 0.65$. This determines the width B of the box.

2. The schematization of the cross section. The wing beam cross section is examined as a cross section of a two-flange beam with a width of B and a height of H.

For each spar the working height - is the distance between the centers of gravity of the flanges $H_i \approx (0.8\text{-}0.95)(H_{i\ \text{заб}}$, where $H_{i\ \text{заб}}$ is the overall height of the spar (with respect to the overall dimensions of the wing cross section profile).

The working height of the skin panels is $H_{об} \approx 0.95\bar{c}b$, where b and $\bar{c}$ are the chord and the thickness ratio of the cross section profile.

The beam cross section height

$$H = \frac{\Sigma H_i}{m},$$

where m - is the number of spars (in a two-spar wing $H_{об}$ is taken into account in the number H_i).

3. Determination of the reduced areas of the wing panels (skin, stringers, flanges). Upper (compressed) panel

$$F_{\text{ред.в}} = \frac{M_{\text{изг}}}{H\sigma_{\text{кп}}},$$

where $\sigma_{\text{кп}}$ - is the critical stress in the spar flange.

For heavy profiles it is possible to take $\sigma_{\text{кп}}=\sigma_{\text{в}}$. For relatively weak profiles of T-shaped or angular cross section $\sigma_{\text{кп}}\approx(0.7\text{-}0.9)\sigma_{\text{в}}$.

The lower (tensioned) panel

$$F_{\text{ред.н}} = \frac{M_{\text{изг}}}{Hk\sigma_{\text{вп}}},$$

where $\sigma_{\text{вп}}$ - is the ultimate strength of the spar flange material; $k=0.9$ - the coefficient which takes into account the weakening of the lower panel elements with the rivet holes.

4. Determination of the reduced areas of the panel elements. The reduced area of the entire cross section of each panel $F_{\text{рвд}}$ is distributed between the spar flanges (F) and the structural skin with stringers ($f_{\text{ред}}$) in accordance with accepted magnitude of the ratio of κ:

$$\kappa = \frac{F}{F_{\text{ред}}};\quad \frac{f_{\text{ред}}}{F_{\text{ред}}} = 1-\kappa.$$

5. The selection of the stringer pitch $t_{\text{стр}}$ and of the rib pitch $t_{\text{н}}$. Usually for load-bearing designs, close to a spar setup, $t_{\text{стр}}$=120-240 mm; for load-bearing designs, close to a monocoque setup, $t_{\text{стр}}$=80-160 mm.

The rib pitch is $t_{\text{н}}$=350-1,000 mm depending on the dimensions of the wing and its load-bearing design. For wings, close to a monocoque setup (with powerful stringers), the rib pitch is usually greater than for wings, close, to a spar setup.

It is necessary to keep in mind that the magnitudes of the critical stresses of the spar flanges and the stringers depend on the rib pitch.

6. Determining the dimensions of the spar flanges. For more effective use of the flange material it is advantageous to distribute the total areas of the upper and lower flanges between spars proportional to the spar heights:

$$F_{в1} = F_в \frac{H_1}{\Sigma H_1}; \quad F_{н1} = F_н \frac{H_1}{\Sigma H_1}.$$

The profiles of the flange cross sections are determined from the found values of the areas.

7. Determining the dimensions of the skin and stringers:

a) the skin and the stringers of the upper (compressed) panel.

The reduced thickness of the upper skin.

$$\delta_в = \frac{f_{ред.в}}{B\varphi_{стр.в}},$$

where

$$\varphi_{стр.в} = \frac{\sigma_{к\,стр.в}}{\sigma_{к\,в}}.$$

The critical stress of the stringer in the first approximation is $\sigma_{к\ стр} \approx \sigma_{пц} - 0.8\sigma_в$, and smaller values pertain to corner profiles, and large values - to the more powerful profiles of the Z-shaped, H-shaped, U-shaped cross sections.

The thickness of the upper skin is $\delta_{обш\ в} = (0.5\text{-}0.55)\delta_в$; the cross-sectional area of the stringer is

$$f_{стр.в} = \frac{f_{ред.в} - B\delta_{обш.в}\varphi_{обш.в}}{n_в\varphi_{стр.в}} \quad \text{where} \quad \varphi_{обш.в} = \frac{\sigma_{к\,ср}}{\sigma_{к\,в}};$$

$n_в$ - is the number of stringers in the upper panel.

A rationally selected skin should have a value $\frac{\varphi_{общ.в}}{\varphi_{стр.в}}$ close to unity (but not greater);

b) the skin and the stringers of the lower (tensioned) panel. Their dimensions are determined from formulas similar to those used for the compressed elements of the upper panel:

The thickness of the lower skin

$$\delta_{общ.н} = (0{,}6 \div 0{,}65)\delta_в;$$

$$\varphi_{общ.н} = \frac{\sigma_{в.общ.н}}{\sigma_{в.н}}$$

From the obtained values of $\delta_{общ}$ and $f_{стр}$ the closest (which correspond to the standards) sheet thicknesses in a stringer profile cross section are selected, for which it is possible from the reference data to determine $\delta_{к\ стр}$ and, if it is necessary, to calculate more refined values of $\delta_{общ.в}$ and $f_{стр.в}$.

The skin operates not only in normal stresses during wing flexure, but also in normal stresses during local flexure (during the transfer of the air forces) and in tangential stresses (due to wing torsion). Thus, it is necessary to increase by 20-30% the skin thickness (upper and lower) obtained from the calculation in normal stresses during wing flexure.

§ 8. APPROXIMATE CALCULATION OF A WING IN SHEAR AND TORSION

In an approximate calculation in shear and torsion the effect of the transverse force Q situated at the center of rigidity of the cross section (c.r.), and the effect of the torsional moment $M_{кр}$ (figure 3.37) are examined separately.

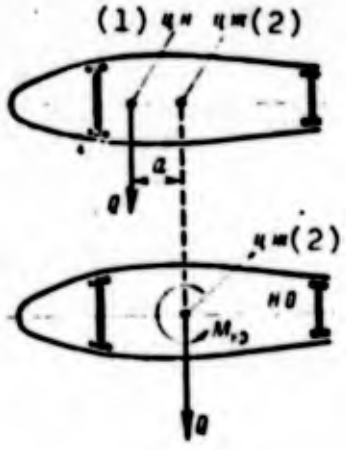

Figure 3.37. Transverse force and torsional moment in a wing cross section. Key: (1) c.l. (center of loads); (2) c.r. (center of rigidity).

The approximate method of calculation gives a sufficiently correct representation of the role of the spar webs and the skin during the operation of the wing in shear and torsion.

1. Determining the Tangential Stresses τ_Q from the Transverse Force Applied at the Center of Rigidity of a Cross Section

The basic assumption made in the approximate determination of τ_Q, consists in assuming that transverse force Q passing through the center of rigidity of a cross section, causes tangential stresses only in the webs. Let us disregard the tangential stresses arising in this case in the upper and lower skin.

As was already mentioned, the spars making up a wing beam work together. Thus, transverse force Q passing through the center of rigidity of the cross section is distributed between the spars proportional to their flexural rigidities.

On this basis for a two-spar wing

$$\frac{Q_1}{Q_2} = \frac{(EI)_1}{(EI)_2} = \frac{I_{пр.1}}{I_{пр.2}};$$

$$Q_1 + Q_2 = Q.$$

Hence

$$Q_1 = Q\frac{I_{пр.1}}{I_{пр.1} + I_{пр.2}}; \quad Q_2 = Q\frac{I_{пр.2}}{I_{пр.1} + I_{пр.2}}.$$

For a multispar wing

$$Q_i = Q\frac{I_{пр.i}}{\Sigma I_{пр.i}}.$$

The linear tangential force in a web due to the transverse force is

$$q_{Q_i} = \frac{Q_i}{H_i},$$

where H_i - is a working height of a spar.

The tangential stresses in the webs are

$$\tau_{Q_i} = \frac{q_{Q_i}}{\delta_{ст\,i}} = \frac{Q_i}{F_{ст\,i}},$$

where $F_{ст\,i}$ - is the web cross-sectional area; $F_{ст\,i} = H_i \delta_{ст\,i}$; $\delta_{ст\,i}$ - is the web thickness.

If the wing is tapered, then the following is introduced into the formulas

$$Q_{прив} = Q_{эк} - R,$$

where

$$R = \frac{M_{изг}}{H} a.$$

The taper (conicity) of a wing is characterized from the front by the angle a, which is approximately found with the formula

$$a = \frac{\Sigma a_i}{m},$$

where a_i - is the angle between the axes of the flanges of the i-th spar; m - is the number of spars.

2. Determining the Position of the Center of Rigidity of a Cross Section

We find the center of rigidity of a wing cross section as the point through which the resultant Q of the Q_i forces passes.

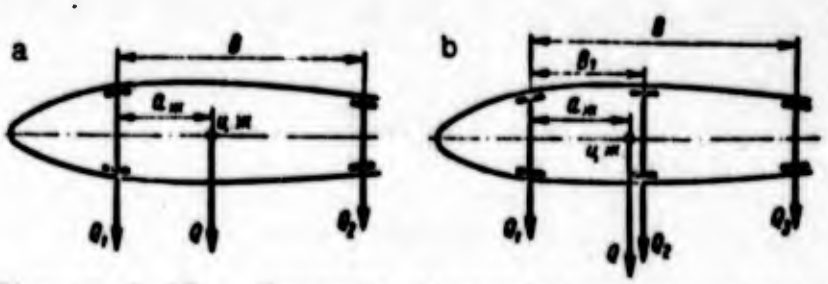

Figure 3.38. Towards determining the position of the center of rigidity of a two-spar (a) and a three-spar (b) wing.
[ц.ж. = c.r. (center of rigidity)].

In particular, for a two-spar wing (figure 3.38a) the condition of equality of the moments with respect to the first spar from force $Q=Q_1+Q_2$ and its components Q_1 and Q_2 has the form:

$$Q_2 B = Q a_ж,$$

where $a_ж$ - is the distance from the forward spar to the center of rigidity.

Hence

$$a_ж = B\frac{Q_2}{Q} = B\frac{I_{пр.2}}{I_{пр.1}+I_{пр.2}}.$$

For a three-spar wing (figure 3.38b) we will similarly obtain

$$a_ж = \frac{Q_2 B_1 + Q_3 B}{Q} = \frac{I_{пр.2} B_1 + I_{пр.3} B}{I_{пр.1}+I_{пр.2}+I_{пр.3}}.$$

3. Determining Tangential Stresses Due to Torsional Moment

Accurate calculations show that the effect of taper (conicity) (nonparallelism of the longitudinal elements) on the distribution of forces due to $M_{кр}$ is insignificant. Therefore, $M_{кр}$ is determined without taking taper (conicity) into account:

$$M_{кр} = Qa,$$

where $Q=Q_{эп}$ - is the diagram value of the transverse force (without correcting for taper (conicity); a - is the distance from the force effect line Q to the center of rigidity of the cross section (see figure 3.37).

In the calculation for $M_{кр}$, it is necessary to introduce all sections of the wing cross section which have a closed contour.

The cross sections of the trailing part of a wing are usually not a closed contour, since the ailerons or the lift-increasing devices on the wing are situated there.

The leading edge of a wing, if it does not have a cut-out, is introduced into the calculation.

The operation of the internal webs for $M_{кр}$ are disregarded, since the tangential stresses due to torsion are usually small in them. It is assumed, that $M_{кр}$ is received by the external closed contour.

The determination of $\tau_{M_{кр}}$ is carried out in accordance with the formulas for calculating torsion during free distortion:

$$q_{M_{кр}} = \frac{M_{кр}}{\omega_к} = \frac{M_{кр}}{2F_к};$$

$$\tau_{M_{кр}} = \frac{q_{M_{кр}}}{\delta_i}.$$

In calculating $\tau_{M_{кр}}$ for each element its value of δ_1 is taken.

The area of contour $F_к$ is computed according to trapezoid formulas. The leading edge part is rectified with respect to a trapezoid shape, equivalent to the area of leading edge (figure 3.39a). Thus, for a two-spar wing

$$F_{\text{к}} = A\frac{H_0 + H_{\text{лев}}}{2} + B\frac{H_{\text{лев}} + H_{\text{прав}}}{2}.$$

When it is desirable to take into account the presence of several closed contours in the cross section the total torsional moment can be approximately distributed between them proportional to their torsional rigidities c:

$$M_{\text{кр}i} = M_{\text{кр}}\frac{c_i}{\Sigma c_i}.$$

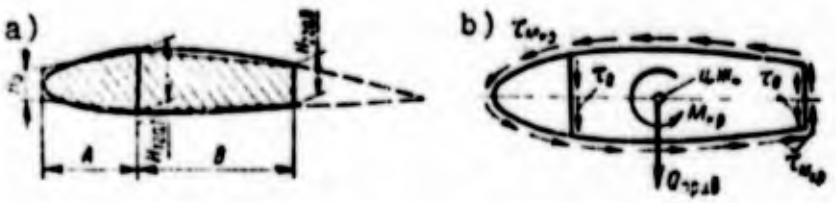

Figure 3.39. Towards calculating a wing in shear and torsion: a) the area of the cross section contour; b) transverse force, torsional moment and the tangential stresses in cross section the elements corresponding to them.
[u.м. = c.r. (center of rigidity)].

Here

$$c_i = \frac{\omega_{\text{к}i}^2}{\frac{1}{G}\sum_j \frac{s_j}{\delta_j}} = \frac{4F_{\text{к}i}^2}{\frac{1}{G}\sum_j \frac{s_j}{\delta_j}},$$

where s_j - is the length of the section of the perimeter of the contour in question with a web thickness of δ_j.

Then linear tangential force in each contour is

$$q_{M_{\text{кр}i}} = \frac{M_{\text{кр}i}}{2F_{\text{к}i}}.$$

The magnitude of $q_{M_{\text{кр}}}$ of the internal web is found as the difference in the values for adjacent contours.

4. Summation of the Linear Tangential Forces and Stresses

The total linear tangential force in the element of the contour is

$$q_i = q_{Q_i} \pm q_{M_{кр}}.$$

The total tangential stress is

$$\tau_i = \frac{q_i}{\delta_i} = \tau_{Q_i} \pm \tau_{M_{кр}}.$$

Figure 3.39b shows the forces in the cross section and the stresses due to them.

For testing the correctness of the calculation it is possible to utilize the condition

$$\Sigma \tau_{Q_i} F_{ст\,i} = Q_{внеш}.$$

5. Strength Testing

The condition of strength of elements operating in shear,

$$\tau_i^p \leqslant \tau_{разр\,i}.$$

The coefficient of strength excess is

$$\eta_i = \frac{\tau_{разр\,i}}{\tau_i^p}.$$

For a web load only with τ, the condition of strength in shear is the main one. For the skin it should be taken into account, that it works together for σ and τ.

The strength testing of the webs and the skin is given in detail in chapter 4, § 1-4.

§ 9. WING DEFORMATIONS AND CHARACTERISTICS OF THE OPERATION OF ITS ROOT PART

Wing deformations are characterized by sagging of the y of its cross sections and by the angles of twist φ.

A wing is considered to be a beam fixed to the side of the fuselage, the wing axis of rigidity is taken as its elastic axis z.

From the stress analysis data, it is possible to calculate the following values for wing cross sections:

$$y'' = \frac{d^2y}{dz^2} = \frac{M_{изг}}{E_\phi I_{ред}},$$

where E_ϕ - is the elastic modulus for a fictitious rectilinear diagram $\sigma = f(\varepsilon)$; $I_{ред}$ - is the reduced moment of inertia of the entire cross section.

If we schematize a wing as a two-flange beam with a height H and with equal reduced flange (panels) F areas, then

$$I_{ред} \approx F\frac{H^2}{2}.$$

The deviation (slope angle of the tangent to the bent axis) is defined as the integral of function y'':

$$\frac{dy}{dz} = y' = \int_{z_{борт}}^{z} \frac{M_{изг}}{E_\phi I_{ред}} dz.$$

Sagging is calculated as the integral of function y':

$$y = \int y' dz.$$

Usually there are no expressions for $M_{изг}$, E_ϕ and $I_{ред}$ from z and integration is carried out planimetrically, graphically, and numerically.

Relative angle of twist (for a single-closed contour)

$$\theta = \frac{M_{кр}}{\omega_к^2} \oint \frac{ds}{G\delta} \quad \frac{рад}{см},$$

where $\oint$ - the curvilinear integral is taken along the length of the cross section contour; $\omega_к$ - is the doubled area of tne contour; δ - is the thickness of the skin.

The total angle of twist in the z section from the side is

$$\varphi = \int_{z_{опр}}^{z} \theta dz.$$

Integration is carried out numerically or graphically.

The deformations found in this way do not take into account the deformations in the subfuselage part of the wing.

In calculating the deformation of a swept wing, it is necessary to carry out integration along its elastic axis lying in the plane of flexure.

In determining torsional strains it is necessary to take into account the difference in the values of shear modulus G of different wing elements.

Let us proceed to an examination of certain characteristics of the operation of the root part of the wing.

The following assumptions are usually made in the calculation:

a) the wing (like other thin-walled structures of the framework) works in shear and torsion under conditions of free warping of the cross sections;

b) the deformation caused by the effect of bending moments themselves obey the law of plane cross sections and do not affect the warping of the cross sections.

Experiments and theoretical investigations confirm the validity of these assumptions for a wing tip section of conventional design.

With regard to a wing root part, the constraining of warping, which leads to the appearance of additional normal stresses in the cross sections during operation in shear and torsion has an effect on its stressed state during elastic operation of the wing.

This aspect is explained by the setup in figure 3.40a. Additional normal forces in the flanges, arising in the sealing of a wing section due to the constraining of warping caused by torsion, are shown in the setup. A wing cross section along the plane of symmetry of an aircraft is under such conditions of complete constraining of warping in the case of symmetrical wing loading.

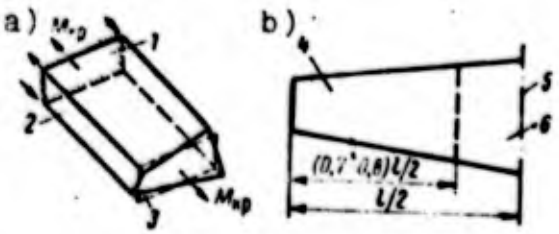

Figure 3.40. Characteristics of the operation different wing sections in torsion: 1 - sealing; 2 - constraining of warping; 3 - free warping; 4 - zone of free warping; 5 - complete constraining of warping; 6 - partial constraining of warping.

The adjoining wing section operates under conditions of partial constraining warping (figure 3.40b).

The distribution of forces in wing cross section elements in the zone of complete constraining of warping is similar to the force distribution between bolts or rivets in assembly joints, the method of calculation of which (the center of rigidity method)

was proposed by the famous Russian engineer V. G. Shukhov. The method of calculating a wing in constrained torsion was developed in 1932 by V. N. Belyayev.

It is necessary to note that with the onset of plastic deformations the aforementioned additional stresses in the root part elements of a wing are reduced. On the basis of this in calculating for the effect of calculated destructive load in case A and A' it is possible to approximately not take into account the effect of warping constraint and deviations from the law of plane cross sections.

As investigations have shown, in the elastic operation of a swept two-spar or monocoque wing design considerable additional stresses arise near the root due to deviation of the bending deformations from the law of plane cross sections.

These additional stresses exceed in magnitude the stresses from warping constraint so much, that it is possible to disregard the latter in a swept wing design.

§ 10. DESIGN CHARACTERISTICS AND OPERATION OF THE ROOT SECTIONS OF A SWEPT WING

Swept wing designs are carried out on the basis of the same load-bearing setups, as unswept wing designs.

For cross sections situated rather distant from the root section, the operation and the stress analysis of the load-bearing setup of a swept wing in no way differ from the operation and the design of an unswept wing.

The design and the load-bearing setup of a swept wing have differences as compared with an unswept wing only in the root section.

The root section of a swept wing we will call the section which is directly adjacent to the fuselage and which enters into the fuselage.

The effect of breaks (in plan) and the differences in the length of longitudinal elements (spars, stringers and skin sections operating in normal stresses) affect the stress distribution in root section cross sections.

The load-bearing setup of a swept wing root section depends mainly on the conditions of the internal layout of the wing and fuselage (the loaction of the loads and of the compartments, the type of landing gear retractions, etc.).

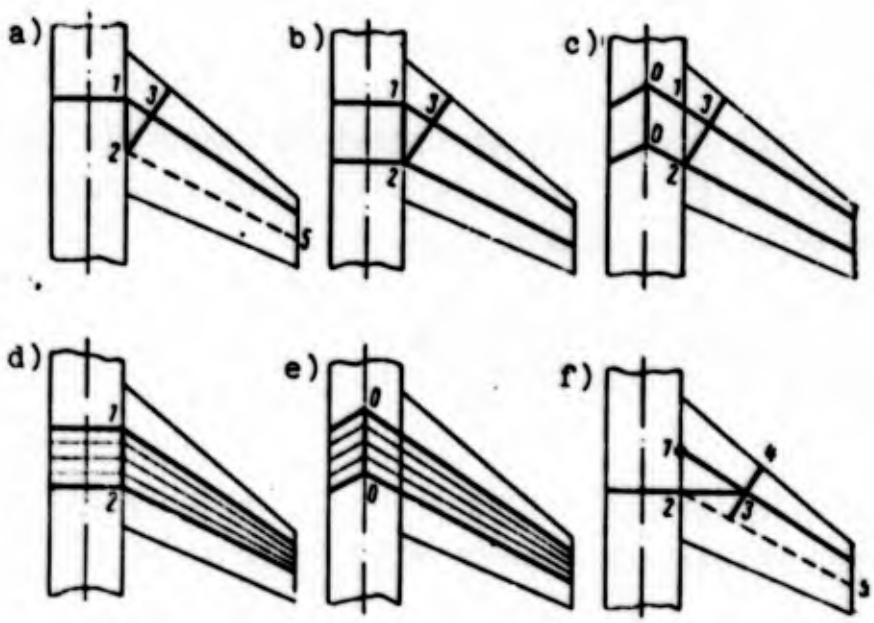

Figure 3.41. Examples of the load-bearing setups of swept wings with different root section designs.

Figure 3.41 depicts several examples of swept wing load-bearing setups with different root section designs:

a) a one-spar wing with a break in the spar axis at the sides of the fuselage: 1-2 - side setup and 2-3 - root setup, reinforced ribs; 2-5 - auxiliary spar;

b) a two-spar wing with a break in the spar axes at the sides of the fuselage: 1-2 - side setup and 2-3 root setup, reinforced ribs;

c) a two-spar wing with a break in the spar axes at the axis of symmetry: 2-3 root setup and 0-0 - axial setup, reinforced ribs;

d) monocoque wing with a break in the panel axis at the sides of the fuselage: 1-2 - side setup, reinforced rib;

e) monocoque wing with a break in the panel axis at the axis of symmetry: 0-0 - an axial setup, reinforced rib;

f) a one-spar wing with a semicantilever beam (internal strut): 2-3 - a semicantilever beam, 3-4 - a root setup, reinforced rib, 2-5 - auxiliary spar.

The operation of the root section elements in each of the setups being examined differs in its characteristics.

The operation of the reinforced ribs situated at the break of the axes of the elements of the longitudinal assembly - the spars and stringers at the joint of the swept part of the wing - is one of them.

As is shown, for example, in the setup in figure 3.42, the forces $P_{л}$ transmitted from the spar flanges of the swept wing break down into the components $P_{н}$ loading the rib in its plane, and $P_{ф}$ transmitted to the spar flanges (lying beyond the break) of the central part of the wing which enters into the fuselage.

The loads of the $P_{н}$ type acting on the ribs situated at the boundary of the break in axes of the longitudinal elements, are very considerable - in magnitude they are close to the forces in the spar flanges.

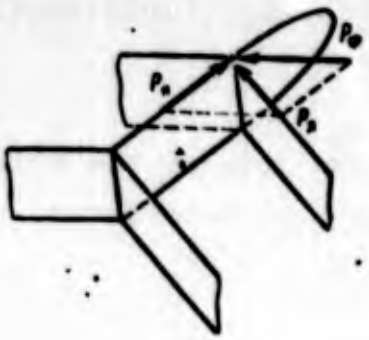

Figure 3.42. Loading of a rib situated at the joining of spars (situated at an angle) with forces in their flanges.

The side ribs in setups 1-2 of a, b, d and those ribs situated in the plane of symmetry of the aircraft in setups 0-0 of c and d shown in figure 3.41 are similarly loaded.

The root ribs (2-3 in setups a, b, c and 3-4 in setup f) serve in a spar design wing to remove the tangential forces due to torsional moment from the skin of the wing cantilever.

The design and the operation of the ribs of the root part of a swept wing are examined in detail in chapter 4, § 5.

In the present section let us examine the operation of the longitudinal elements and the skin in the root part of a swept wing which has a break at the axes of these elements on the sides of fuselage, and the method for the approximate verifying calculation of the wing in the root cross section.

We will call the cross section perpendicular to the wing axis and passing through point 2 of the rear spar attachment root cross section 2-3 (figure 3.43a).

Let us examine the part of the two-spar swept wing with spars of identical cross section limited on the right and on the left by lines 2-3 and 2'-3'. In this part the length of the longitudinal load-bearing elements and the sections of the skin connected to them included between the root cross sections, decreases from the front spar to the rear spar. But with equal cross sections the short elements (for example 2-2') in tension

and compression possess less flexibility than the long ones (for example 3-1-1'-3'). This fact leads in the bending of the root part of the swept wing to an increase in the normal stresses in the shorter elements of the root section situated nearer to the rear spar, and to a decrease in the normal stresses in the longer the elements lying nearer the front spar.

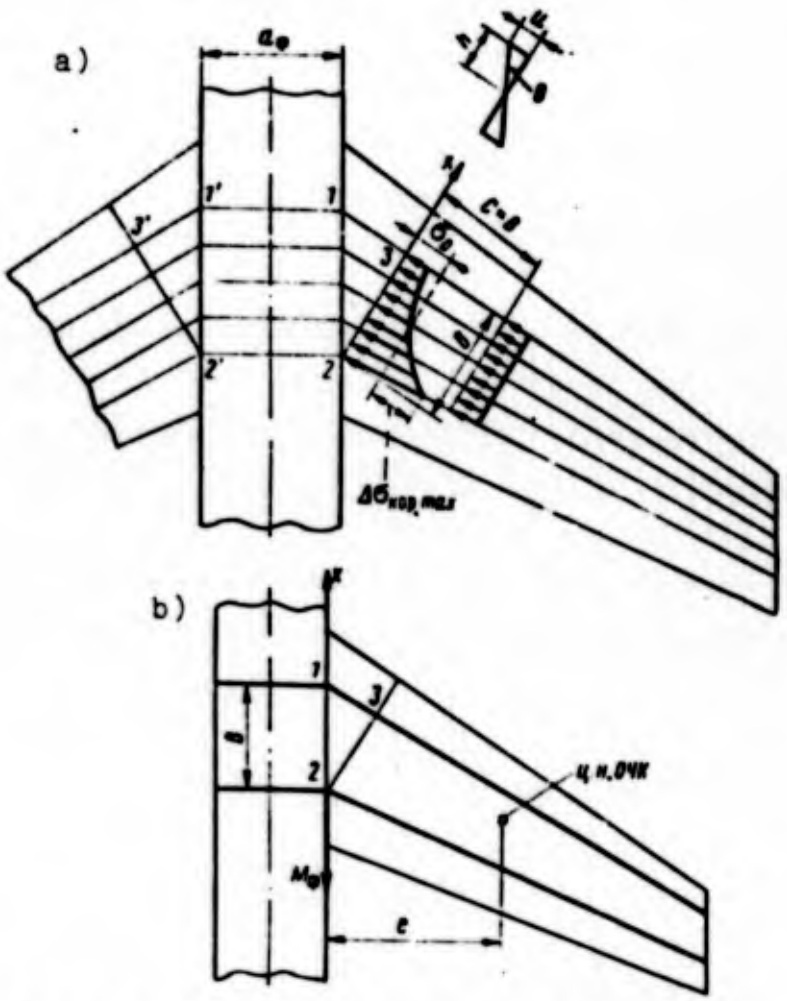

Figure 3.43. Two-spar swept wing: a) diagrams of the normal stresses in the elements of the root cross section and far from it; b) towards determining the stresses in a side cross section.

Figure 3.43a shows a diagram of the change in the stresses $\sigma_{\text{нор } i}$ in the elements of root cross section 2-3. These stresses can be presented as the sum $\sigma_{\text{нор } i}=\sigma_0\pm\Delta\sigma_{\text{нор } i}$, where σ_0 -

are the stresses obtained without taking sweep into account; $\Delta\sigma_{\text{нор } i}$ - are the additional stresses in fiber i caused by the sweep effect.

In proportion to the distance from the root cross section toward the wing tip the additional stresses decrease. In the cross sections located at distance from the root of $C \geq B$ (see figure 3.43a), the additional stresses decrease so much that it is possible to calculate these cross sections just like the cross sections of an unswept wing.

1. Determining the Normal Stresses in a Root Cross Section

During the deformation of a swept wing which occurs under the effect of bending moment, an element of the root section (spar flange, stringer, skin element) will experience elongation u (figure 3.43a).

Let us express this elongation via stress $\sigma_{\text{нор } i}$. For this let us distinguish from the root triangle 1-2-3 a certain element ab (figure 3.44) which has a cross-sectional area of $\Delta F_{\text{нор } i}$.

This element will be loaded by force

$$\Delta P_{\text{нор}i} = \sigma_{\text{нор}i}\Delta F_{\text{нор}i}. \qquad (3.1)$$

Let us approximately assume, that along the length of the element the force is constant. Then the deformation is

$$u_i = \frac{\sigma_{\text{нор}i}}{E_i} l_{ab} = \frac{\sigma_{\text{нор}i}}{E_i} x_i \operatorname{tg}\chi, \qquad (3.2)$$

where x_i - is the distance to the element in question calculated from point 2 in the direction of the auxiliary x-axis; χ - is the

mean sweep of the longitudinal assembly: $\chi=\Sigma\chi_i/m$ (χ_i - is the sweep of the i-th spar; m - is the number of spars).

The element of the fuselage part of the wing bc (figure 3.44) which in the general case has another cross-sectional area $\Delta F_{\Phi\ i}$, will be loaded with force $\Delta P_{кор\ i}\cos\chi$, which causes the deformation

$$u_2 = \frac{\Delta P_{кор\,i}\cos\chi}{\Delta F_{\Phi i} E_i}\cdot\frac{d_\Phi}{2} = \frac{\sigma_{кор\,i}}{E_i}\cdot\frac{\Delta F_{кор\,i}}{\Delta F_{\Phi i}}\cdot\frac{d_\Phi}{2}\cos\chi. \qquad (3.3)$$

The displacement of point a caused by the elongation of element abc (figure 3.44) is found using the following formula

$$u = u_1 + u_2\cos\chi = \frac{\sigma_{кор\,i}}{E_i}\left(x_i\operatorname{tg}\chi + \frac{\Delta F_{кор\,i}}{\Delta F_{\Phi i}}\cdot\frac{d_\Phi}{2}\cos^2\chi\right). \qquad (3.4)$$

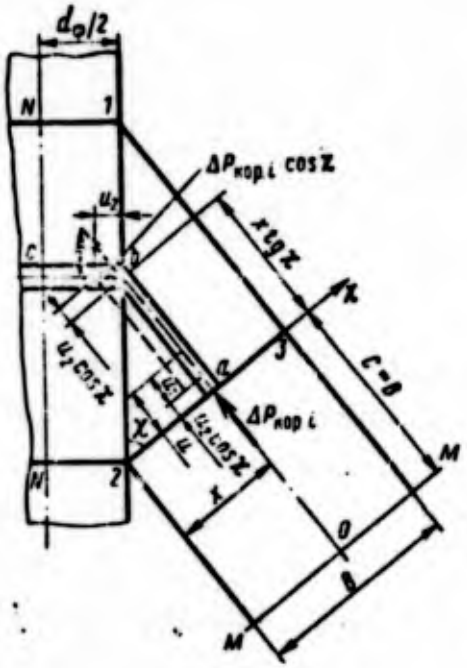

Figure 3.44. Determining the deformations of root section elements of a swept wing.

The elasticity of the cantilever makes possible the warping of the root cross section. This can be taken into account by increasing the deformed length of the element. It is possible to approximately assume that the deformation is propagated over length oa, equal to B, assuming the stress over its extent to be constant.

Then expression (3.4) will take the form:

$$u = \frac{\sigma_{кор}}{E_i}\left(x_i \operatorname{tg}\chi + \frac{d_\Phi}{2}\cdot\frac{\Delta F_{кор}}{\Delta F_{\Phi i}}\cos^2\chi + B\right) = \frac{\sigma_{кор} B}{E_i} I_i,$$

where

$$I_i = \bar{x}_i \operatorname{tg}\chi + \frac{d_\Phi}{2B}\cdot\frac{\Delta F_{кор}}{\Delta F_{\Phi i}}\cos^2\chi + 1; \qquad (3.5)$$

$$\bar{x}_i = \frac{x_i}{B}.$$

When there is a difference in the mechanical properties of the cross section elements it is assumed that $F_i = \varphi_i E$ and according

$$u = \frac{\sigma_{кор} B}{\varphi_i E} I_i. \qquad (3.6)$$

The stress in element i, which is included in the composition of the unswept wing cross section remote from the setting in site can be found by the method of reduction coefficients from the expression

$$\sigma_i = \varphi_i \frac{P}{F_{ред}}, \qquad (3.7)$$

where P - is the force in the panel; $F_{ред} = \Sigma \varphi_i \Delta F_i$.

It is necessary to note that the reduction coefficient φ_i and the reduced area $F_{ред}$ only take into account the difference in the mechanical properties of different elements (the difference in material, transition beyond the limit of proportionality). With this type (usual) of treatment of the reduction coefficients the expression (3.7) is valid, if during bending of the wing the cross sections remain plane and in the wing compartments adjacent to the cross section in question the lengths of the longitudinal elements are identical, and the cross-sectional areas of the elements do not vary.

For the root section of a wing these assumptions, generally speaking, are not applicable.

For a swept wing this is evident from expression u (3.6), where in the factor $\bar{l}_i$ (3.5) the first term takes into account the additional length of the element (caused by sweep), the second is the difference in the element cross sections and its continuation in the fuselage part of the wing, the third is the deformability of the cantilever in the section of its length C=B. Even when $\chi=0$, i.e., in an unswept wing, the second and third terms remain in expression $\bar{l}_i$.

For calculating the stresses in the root cross section the assumption is introduced that the bending strains in the root section occur in such a way that cross sections M-M and N-N, which limit this section, remain plane.

In connection with this formula (3.7) must be changed for calculating the stresses in the root cross section, after introducing the reduction coefficient $\varphi_{\text{кор } i}$ into it which takes into account along with the difference in the mechanical properties of the elements the above examined additional factors which affect the deformations in the root section. Accordingly, the reduction coefficients $\varphi_{\text{кор } i}$ should enter into the reduced area $F_{\text{кор } i}$.

The normal stress in the root cross section element is

$$\sigma_{\text{кор } i} = \varphi_{\text{кор } i} \frac{P}{F_{\text{ред кор}}}, \qquad (3.8)$$

where $F_{\text{ред.кор}} = \Sigma \varphi_{\text{кор } i} \Delta F_{\text{кор } i}$.

The reduction coefficient $\varphi_{\text{кор } i}$ is inversely proportional to the magnitude of $\bar{l}_i$. It is possible to represent it in the following form:

$$\varphi_{\text{кор } i} = \varphi_i \varphi_{\chi i},$$

where

$$\varphi_{\chi i} = \frac{\bar{l}_0}{\bar{l}_i}.$$

Here $\bar{l}_0$ - relating to B the reduced length of the axial longitudinal element of the panel (having constant cross section); $\bar{l}_0 = 0{,}5 \lg \chi + \frac{d_\Phi}{2B} \cos^2 \chi + 1$; $\bar{l}_i$ - relating to B the reduced length of element i; with respect to (3.5)

$$\bar{l}_i = \bar{x}_i \lg \chi + \frac{d_\Phi}{2B} \cdot \frac{\Delta F_{\text{кор } i}}{\Delta F_{\Phi i}} \cos^2 \chi + 1.$$

Expression $\varphi_{\text{кор } i}$ shows that stress $\sigma_{\text{кор } i}$ varies along coordinate $\bar{x}$ according to hyperbolic law, attaining the greatest value at the rear spar when $\bar{x}=0$.

Coefficient $\varphi_{\text{кор } i}$ can be called the generalized reduction coefficient which takes into account not only the mechanical properties of the element via the usual reduction coefficient φ_i, but also the characteristics of its location and operation in the root part of the swept wing (by means of coefficient $\varphi_{\chi i}$).

It is not difficult to see that within the limit when $\chi=0$ for an unswept wing with constant section cross sections of the longitudinal elements along the length of root $\varphi_{\chi i}=1$, $\varphi_{\text{кор } i}=\varphi_i$.

Formula (3.8) is valid for the spar-type monocoque and intermediate wing load-bearing designs.

2. Determining Normal Stresses in a Side Cross Section

The normal stresses in the elements of side cross section 1-2 (figure 3.43b), i.e., the stresses in the elements of the fuselage part of the wing, can be approximately determined by the formula

$$\sigma_{\phi \text{поз} i} = \frac{M_\Phi}{H \Sigma \Delta F_{\Phi i} \varphi_{\Phi i}} \varphi_{\Phi i},$$

where $M_{ф}$ - is the bending moment in side cross section 1-2 of the wing; $M_{ф}=M_{1-2}=P_{очк}e$; $P_{очк}$ - is the resultant of all loads on the detachable wing sections (ОЧК+ОСhК) applied to the center of loads (c.l.) of the detachable wing sections (ОЧК=ОСhК).

The magnitudes of H, $\Delta F_{ф\ i}$ and $\varphi_{ф\ i}$ have the same sense, as for cross section 2-3 but are calculated for cross section 1-2.

3. Determining Tangential Stresses in a Root Cross Section

The approximate definition of tangential stresses τ_{Q} and $\tau_{M_{кр}}$ in a root cross section is carried out in the same was as in the cross section of an unswept wing.

A characteristic of the calculation here is only the fact, that the distribution of the transverse force between the webs and the determination of the position of the center of rigidity of cross section 2-3 are carried out taking the sweep effect into account:

$$Q_i = Q_{2-3}\frac{M_i}{\Sigma M_i} = Q_{2-3}\frac{I_{\text{ред.кор}i}}{\Sigma I_{\text{ред.кор}i}},$$

where Q_{2-3} - is the transverse force in the wing root section.

The reduced inertia moments of spar cross sections $I_{\text{ред.кор}\ i}$ are determined taking the generalized reduction coefficients of the flanges $\varphi_{кор\ i}$ into account.

§ 11. CHARACTERISTICS OF THE DESIGN AND OPERATION OF LOW ASPECT-RATIO OF DELTA WINGS

Single-spar, multispar and monocoque load-bearing designs (figure 3.45) are employed for low aspect-ratio delta wings. Let us examine the variants of these designs.

Single-spar wings can exist in these variants:

1) the main and auxiliary spars are located at constant percents of wing chords (figure 3.45a) in a fan-shaped manner;

2) the main and auxiliary spars are situated perpendicular to the fuselage axis (figure 3.45b);

3) wing with a semicantilever beam (internal strut) (figure 3.45c).

This design is similar to the design of a single-spar swept wing with an internal strut. It can be convenient from the viewpoint of layout (retraction of the landing gear into the wing).

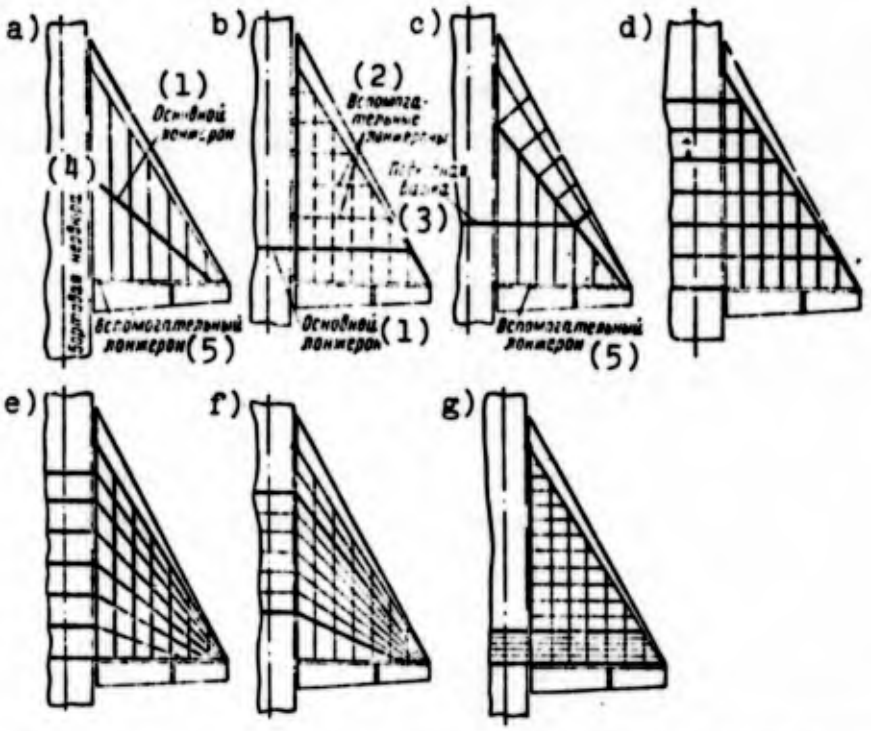

Figure 3.45. Examples of delta wing load-bearing designs.
Key: (1) Main spar; (2) Auxiliary spars; (3) Semicantilever beam; (4) Side rib; (5) Auxiliary spar.

Multispar wings can be made in two variants:

1) a wing with parallel spars (figure 3.45d);

2) a wing with spars positioned in a fan-shaped manner (figure 3.45e).

The general advantage of multispar wings in comparison with single-spar wings is their great rigidity. Their deficiency is the passage through the fuselage of a large number of spars, which complicates the fuselage layout.

Monocoque delta wings differ from the corresponding unswept and swept wings by the fact that the load-bearing panels occupy a small part of the root chords which have large dimensions. Only in this case is it possible to ensure, with light weight, a rather reduced panel thickness which makes it possible to remove the high critical stresses from them. Monocoque delta wings are made in the following variants:

1) a wing with a break in the elements of the load-bearing panel at the side (figure 3.45f);

2) a wing with parallel elements in the load-carrying panel (figure 3.45g).

The basic difference in the designs shown in figure 3.45 consists in the arrangement of the elements of the longitudinal assembly of the spars and stringers.

If the spars are situated at constant percents of the chords (in a fan-shaped manner) and the wing surface is tapered (conical), then the spar flanges and the stringers are rectilinear, since they proceed along the generatrix.

In this case it is possible to install one of the spars along the line of the maximum profile cross section thicknesses, completely employing the possible design height.

However the longitudinal elements have great length, and due to the break in their axes at the fuselage it is necessary to insert a side rib which is highly loaded (see chapter 4, § 5).

If in the wing design the elements are parallel and directed along the wing span, then they have less length and do not disrupt the design of the side ribs. Multispar wings of these types of designs are the lightest and most rigid, but the curvilinearity of the longitudinal elements complicates the technology of their manufacture.

A characteristic of the operation and calculation of load-bearing designs of short wing aspect-ratio is the fact that the effect of the setting in is propagated over the whole wing, and not only on the root section, as occurs in wings of high and intermediate aspect-ratios.

Furthermore, in delta low aspect-ratio wings the effects of nonparallelism in plan of the longitudinal load-bearing elements and of elasticity of the ribs, whose length is commensurate with the span of the aircraft wing, considerably affect the stress distribution in the wing cross section.

As a result the deformations of such wings deviate from the law of plane cross sections in flexure, which makes it necessary to examine delta wings not as continuous beams, but as systems of jointly operating beams.

An accurate consideration of the indicated facts is complex and onerous, since the task reduces to the solution of a repeatedly statically indeterminable system.

As calculations and experiments show, the flexural rigidity of the ribs, the torsional rigidity of the skin outlines and the rigidity of the attachments of the spars to the fuselage have a great effect on the force distribution between the spars.

If the rigidities of the ribs and skin are low, then the spars operate as a system of beams not connected with each other. In this case the longer spars will be more intensely loaded.

To equalize the spar loading conditions it is advantageous to increase the rigidity of the skin and ribs and to ensure the rigidity of the spar attachments proportional to the flexural rigidities of the spars themselves.

Assuming that the rigidities of the spar-to-fuselage attachments are proportional to the flexural rigidities of the spars and the rigidity of the connections between the spars is rather great, then it is possible to approximately distribute the bending moment and the transverse force in the side cross section between the spars proportional to their flexural rigidities. Let us examine the approximate calculation of a delta wing with parallel spars.

Basic assumptions.

1. Only the spar flanges operate in normal stresses.

2. The skin and spar webs operate only in shear.

3. The rigidity of the ribs is not too great due to their low height and great length. Thus, it is possible not to consider the effect of the ribs on the redistribution of the forces between the spars, i.e., to consider the rib sections as hinged connected with the spars and transmittting the load incident on them only to the nearest spars.

4. The torsional rigidity of the skin (during torsion relative to the axes parallel to the x-axis) ensures the spar connection so much that in root wing section the bending moment is distributed between the spars which have moment attachment proportional to their flexural rigidities. In the absence of this type of connection the longer spars are loaded somewhat more than this is obtained in the case of the distribution of the moments proportional to the flexural rigidities.

These assumptions correspond to the physical pattern of the operation of a delta wing and their validity is satisfactorily confirmed by the results of accurate calculations.

In the general case part of spars has moment attachments to the fuselage, and part - is hinged. As a calculated cross section let us take the cross section at the side of the fuselage.

Calculational sequence.

1. *Determining external loads.* The linear load distributed along the span of a delta wing due to the air forces and the mass forces of the design during supersonic flow, if found with the following formula

$$q_y = \frac{n^p(G - G_н)}{S} b.$$

It is possible to assume that the load from these forces is distributed along the wing chord according to rectangular law. Then the specific load (per unit area) is:

$$p = \frac{q_y}{b} = \frac{n^p(G - G_н)}{S} = \text{const.}$$

2. *Distribution of external loads between the spars.* It is assumed, that on each spar there is a distributed load from the (from the front and from the back) skin section adjacent to this spar.

In figure 3.46a these skin sections for spars No. 2 and 3 are shaded.

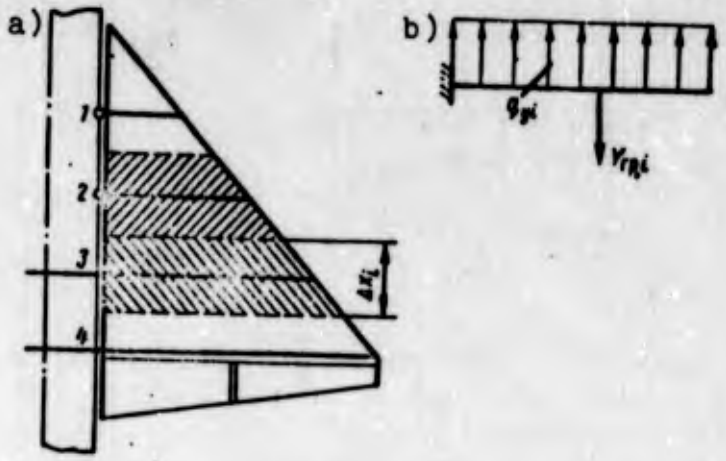

Figure 3.46. Determining loads on the spars of a delta wing.

Then the linear load of spar i (figure 3.46b) is

$$q_{yi} = p\Delta x_i,$$

where Δx_i - is the width of the section from which the load is transmitted to spar i (see figure 3.46a).

If there are concentrated loads in a wing (landing gear, engines, fuel tanks, etc.), then the mass forces from them $Y_{гр\ i}$ should be applied to the assemblies attaching these loads to the spars (see figure 3.46b).

3. *Determining bending moment* $M_{изг}$ *and transverse force* Q *in a side cross section.* The M_{0i} and Q_{0i} forces, are determined in the side cross section for all spars, including hinged supported ones, which are also examined as cantilever beams (figure 3.47a).

Then the total forces in a side wing cross section are:

$$Q = \Sigma Q_{0i};\quad M_{изг} = \Sigma M_{0i}.$$

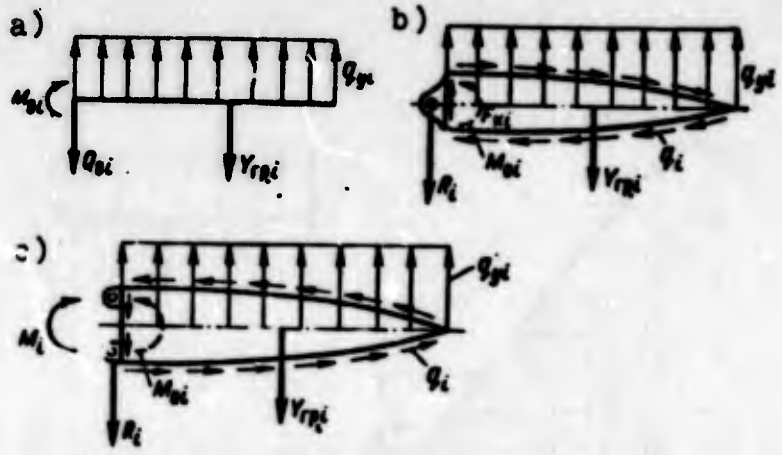

Figure 3.47. Determining forces in side spar cross sections of a delta wing and balancing spars.

4. *Balancing spars with a hinge attachment* (determining reactions). The reaction of a hinge is

$$R_i = Q_{oi}.$$

The moment from loads acting on a spar with a hinge attachment (figure 3.47b), can be balanced only by the reactive flow of tangential forces q_1 transmitted to a spar from the skin through the coupling joint which attaches the skin to the spar.

The magnitude of this flow is

$$q_i = \frac{\Delta M_i}{2F_{ni}},$$

where ΔM_1 - is the reactive moment of the skin acting as M_0 in the web plane; $F_{н\ i}$ - is the area of a contour receiving moment ΔM_1 (area of a spar web).

It is easy to see that for a spar with a hinge attachment

$$\Delta M_i = M_{oi}.$$

5. *Determining the bending moment in a side cross section between spars with a moment attachment.* According to the adopted assumptions,

$$M_i = M_{max} \frac{I_{peat}}{\Sigma I_{peat}}.$$

6. *Balancing spars with a moment attachment* (determining reactions). From the equilibrium conditions of a spar with a moment attachment (figure 3.47c) we have:

$$R_i = Q_{0i};$$
$$\Delta M_i = M_i - M_{0i},$$

where ΔM_1 - is the reactive moment from the direction of the skin, which loads (or unloads) a spar with a moment attachment.

The physical pattern of the redistribution of forces between spars is explained in figure 3.48a, in which the setup of the loading of a spar with a moment attachment due to the spar with the hinge attachment situated next to it as represented.

As is evident, the redistribution of the forces is accomplished by the skin which operates in this case in shear during torsion relative to the axis parallel to the x-axis (normal to the spar planes).

7. *Determining tangential stresses in the skin.* Let us find the torsional moments in the cross sections parallel to the spars (normal to the x-axis) which load the skin with flows of tangential forces (figure 3.48b). For the cross section between spars i and i+1 we will have:

$$M_{i,\,i+1} = \sum_{1}^{i} \Delta M_i.$$

Linear tangential force and tangential stress are found with the following formulas:

$$q_{i,\,i+1}=\frac{M_{i,\,i+1}}{2F_{\kappa i,\,i+1}};\quad \tau_{i,\,i+1}=\frac{q_{i,\,i+1}}{\delta_{i,\,i+1}},$$

where $F_{\kappa\ i,\ i+1}$ - the area of the contour of the cross section in question; $\sigma_{i,\ i+1}$ - is the thickness of the skin in this cross section.

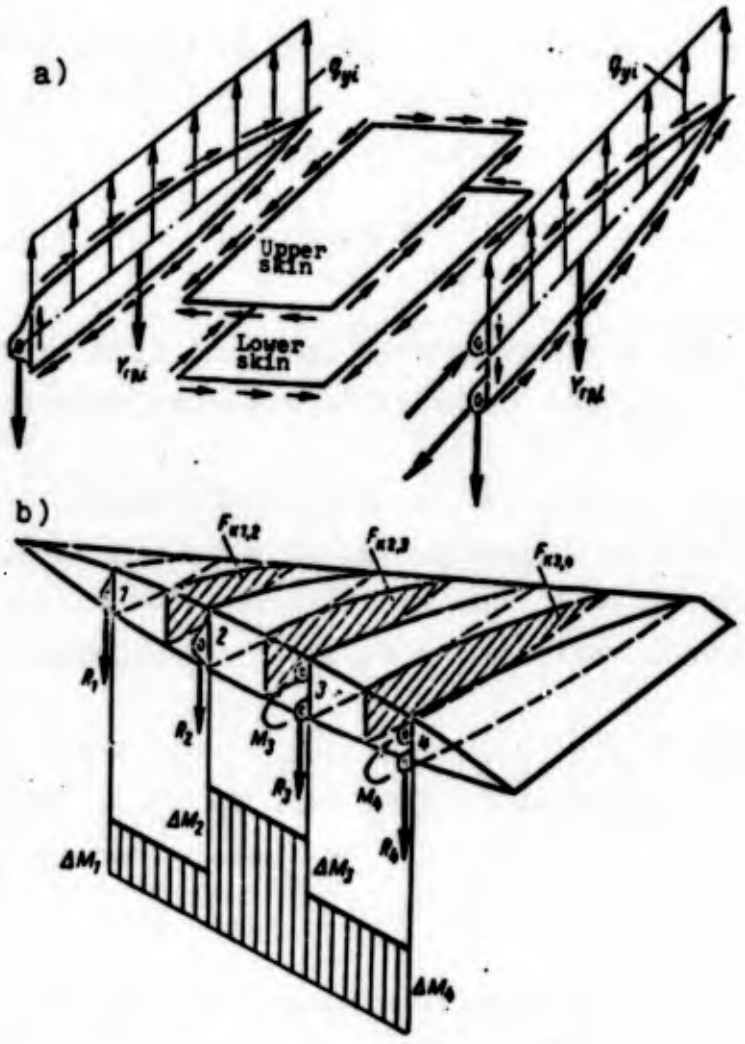

Figure 3.48. Towards determining tangential stresses in the skin of a delta wing.

For example, for the cross section between the second and third spars (see figure 3.48b):

$$M_{2,3}=\Delta M_1+\Delta M_2;\quad q_{2,3}=\frac{M_{2,3}}{2F_{\kappa 2,3}}.$$

From an examination of the operation of a delta wing parallel spars it follows that in this wing the side rib should have a continuous web so that the closure of the contour in the wing cross sections, parallel to the spars would be ensured.

8. *Strength testing.* The strength testing of spar flanges, spar webs, the web of a side rib and the skin is carried out by conventional methods (see chapter 4).

§ 12. LOADS ON A ROTOR BLADE AND THE FORCES IN ITS CROSS SECTIONS

1. The Loads Acting on a Blade in Flight

In flight the blades are loaded with air and mass forces.

For the sake of simplicity in blade stress analysis let us break down the load system into two groups:

1) the loads which ensure moment balance relative to the flapping hinge and which act in the plane of the least blade rigidity - in the flap plane (figure 3.49a). The following pertain to these: air load $Y_в$; load due to the blade design weight $Y_к$; centrifugal force $N_{цб}$, and also inertia force $Y_β$ due to angular acceleration during the flapping motion of the blade relative to the flapping hinge. These loads are balanced by the reaction R of the hub in the flapping hinge;

2) loads which ensure equilibrium of the moments with respect to the drag hinge and which act in plane rotation of the rotor (figure 3.49b). The following pertain to these: drag $Q_л$ (directed counter to the rotation, tangent to the circle which the center of pressure of the blade describes); inertia $N_{ин}$ due to the vibrations relative to the drag hinge (giving moment directed opposite to the angular acceleration); centrifugal force $N_{цб}$ and Coriolis force $F_{кор}$ due to the flapping motion of the blade relative to the flapping hinge.

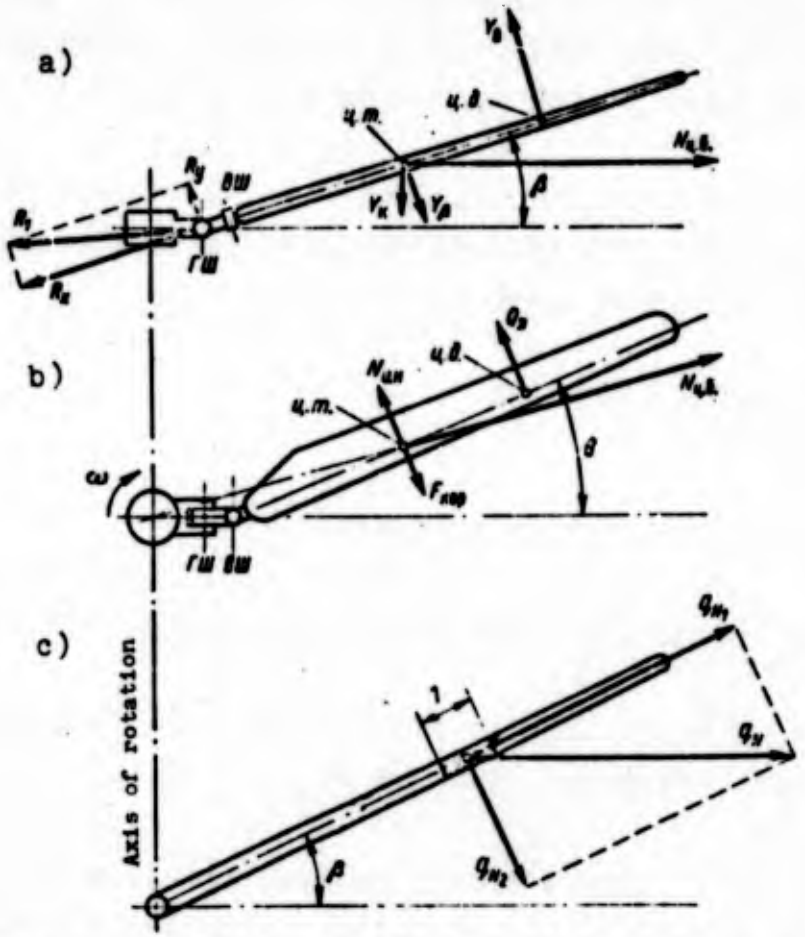

Figure 3.49. Forces acting on a rotor blade: a) in the flapping plane; b) in the plane of rotor rotation; c) components of the linear centrifugal force.
[ВШ = drag hinge; ГШ = flapping hinge; ц.т. = c.g.; ц.д. = c.p.]

For blade strength the most significant are the loads acting in the plane of its least rigidity. Thus of the two groups of loads let us examine only the first one, i.e., the loads which ensure the equilibrium of the moments with respect to the flapping hinge.

The loads and forces due to them let us examine approximately without taking the effect of blade elasticity into account.

2. Determining Loads and Their Distribution Along the Span of a Blade

The magnitude and the distribution of linear loads along the span of a blade depend on a number of factors: the aerodynamic characteristics of the profile, the setting angle, the shape of the blade in plan, the blade twist and the speed of the flow, flowing around, due to the azimuthal position of the blade.

The latter factor leads to the fact that in contrast to an aircraft wing in one and the same flight regime the magnitude and the distribution of the load along the span of the blade vary cyclically.

First let us examine the air load.

The magnitude of the load on one blade is

$$Y_л = \frac{fn^э G}{z} = \frac{n^р G}{z},$$

where $n^э$ - is operational g-force; $n^р$ - is the calculated destructive g-force; G - is the weight of the helicopter; z - is the number of rotor blade; f - is the safety factor.

The operational g-force $n^э$ depends on the nature of the curvilinear motion in flight cases, its magnitude is assigned the strength standards.

In testing the static strength in flight cases it is recommended that the following be taken $n^э$=3-4; f=1.5.

The linear air load is

$$q_{уд} = \frac{n^р G}{zR}(\bar{\Gamma}_{пл} + \bar{\Gamma}_э).$$

where $n^p G/zR$ - is the mean linear air load along the blade radius; $\bar{\Gamma}_{пл}$ - is the coefficient characterizing the linear load distribution along the radius of a plane blade taking into account the distribution of the lift coefficients, the position of the blade with respect to azimuth, the variation in the chord along the blade radius and the characteristics of the flight regime $\mu=V/\omega R$; $\bar{\Gamma}_{э}$ - is the coefficient which considers the effect of blade twist on the air load distribution.

Values $\bar{\Gamma}_{пл}$ and $\bar{\Gamma}_{э}$ are taken from rotor wind-tunnel tests or are approximately determined by calculation. For a rectangular blade composed of profiles with identical aerodynamic characteristics, in the case of axial airflow

$$\bar{\Gamma}_{пл} = 3\bar{r}^2,$$

where $\bar{r}=r/R$ - is the relative radius of the blade.

Let us examine the mass loads.

1. The load due to blade design weight is

$$Y_к = n^p G_л,$$

where $G_л$ - is the weight of one blade.

The linear mass load is

$$q_{yк} = n^p q_л,$$

where $q_л$ - is the linear weight of the blade.

The load distribution $q_{yк}$ is analogous to the distribution of the linear weight of the blade.

2. The centrifugal force is

$$N_{об} = \int \frac{G_л}{g} r_{ц.т.} \omega^2,$$

where $r_{ц.т.}$ - is the radius of the center of gravity of the blade; ω - is the angular rate of rotor rotation.

The linear load is

$$q_N = f\frac{q_n}{g}\omega^2 r,$$

where r - is the radius of a blade element to the axis of rotation.

For blade stress analysis the linear load q_N is decomposed into two components (figure 3.49c) which act along and perpendicular to the blade axis in the plane of its least rigidity:

$$q_{N_1} = q_N \cos\beta \approx f\frac{q_n}{g}\omega^2 r;$$

$$q_{N_2} = q_N \sin\beta \approx f\frac{q_n}{g}\omega^2 r\beta.$$

Under the effect of q_{N_1} the blade operates in tension, q_{N_2} is the transverse load of the blade relieving it from the effect of aerodynamic forces.

3. The inertia load from the flapping motion of the blade relative to the flapping hinge is

$$q_\beta = f\frac{q_n}{g}\cdot\frac{d^2\beta}{dt^2}r,$$

where β - is the blade flapping angle.

The distribution of these forces along the blade radius depends not only on r and q_n, but also on the position of the blade with respect to azimuth (factor $d^2\beta/dt^2$).

Angle β depends on the magnitude of the acting forces and their law of distribution along the radius. It is possible to determine it from the equilibrium condition of the blade relative to the flapping hinge.

In the case of axial airflow there are no angular accelerations of the flapping motion relative to the flapping hinge and the inertia force is $q_\beta = 0$.

4. The total (surplus) linear load is

$$q_y = q_{ya} - q_{yk} - q_{N_z} - q_\beta.$$

Figure 3.50 shows the nature of the variation in q_y and of its components.

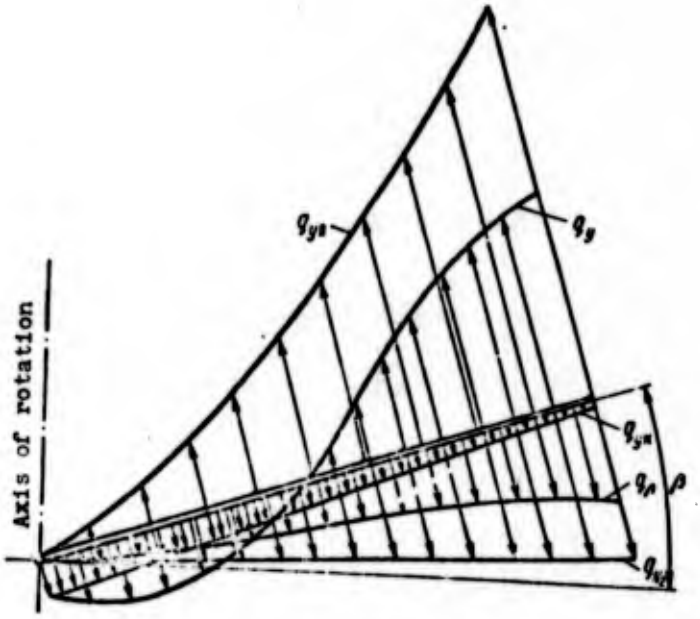

Figure 3.50. Diagrams of the total linear load q_y and its components.

The forces acting on a blade in the flapping plane, differ significantly in value. The lift of a blade is usually 12-15 times greater than its weight, the centrifugal force is 10-12 times greater than the lift.

3. Forces in Blade Cross Sections

Under the effect of air and mass forces, forces arise in the blade cross sections: transverse Q and axial N forces, bending $M_{изг}$ and torsional $M_{кр}$ moments.

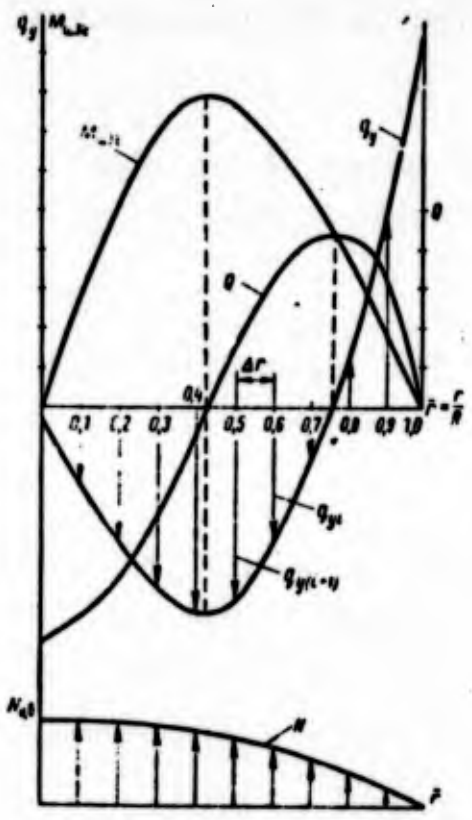

Figure 3.51. Diagrams of the total linear loads, bending moments, transverse and axial forces.

The diagram of the total linear load q_y (figure 3.51) is the initial value for determining Q and $M_{изг}$.

Then the transverse force Q in a certain cross section located a distance of from the axis of rotation is found with the formula

$$Q = \int_r^R q_y dr.$$

The bending moment in this cross section is determined by iterated integration

$$M_{изг} = \int_r^R Q dr.$$

In practice it is possible to replace integration with summation, breaking the blade down into a number of sections with length Δr (see figure 3.51). For every section q_y is determined on its boundaries and then the increase in the transverse force is found with the formula

$$\Delta Q = \frac{q_{yi} + q_{y(i+1)}}{2} \Delta r.$$

The magnitude of the transverse force in the cross section in question is found by consecutive summation of ΔQ from the blade tip

$$Q = \Sigma \Delta Q.$$

After plotting the diagram of transverse force Q the values of the bending moments $M_{изг}$ are determined in the same sequence and its diagram is plotted.

The equality to zero of the bending moment in the drag hinge is the test for the correctness of the plotting of the diagrams of $M_{изг}$ and Q.

Analysis of the calculations shows that the maximum values of the bending moments are obtained at a distance (0.35-0.5) R from the axis of rotation.

The center of pressure and the center of gravity of a blade cross section in the general case do not coincide with the center of rigidity. Thus $q_{ув}$, $q_{ук}$ and q_{N_2} twist the blade (figure 3.52).

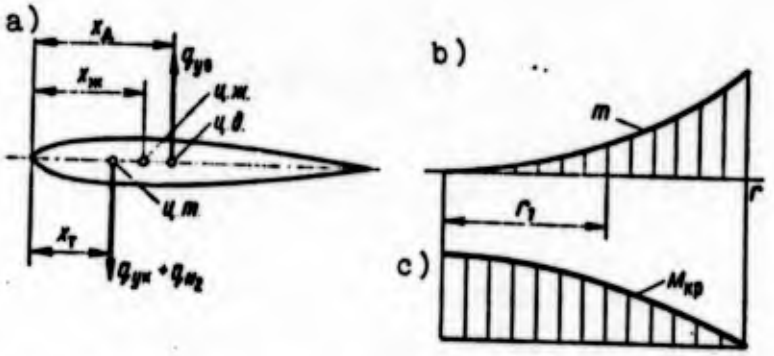

Figure 3.52. Blade twisting: a) loads causing blade twisting; b) diagram of linear torsional moment; c) twisting moment diagram.
[ц.ж. = c.r.; ц.д. = c.p.; ц.т. = c.g.]

The torsional moment in any cross section is determined by integration (summation) of the linear torsional torque from the blade tip

$$M_{кр} = \int_r^R m dr,$$

where $m=q_{yв}(x_д-x_ж)+(q_{yн}+q_{N_2})(x_ж-x_т)$. Here $x_д$, $x_т$, $x_ж$ - are distances from the leading edge of an airfoil profile to the center of pressure, the center of gravity, and the center of rigidity of the cross section.

The longitudinal force in a blade cross section is determined by the expression

$$N = \int_r^R q_{x_1} dr.$$

The type of the diagram of N is represented in figure 3.51.

Considerable (in magnitude) longitudinal (axial) forces $N_{цб}$ acting on a blade, and the presence of elastic deformations in the plane of lesser rigidity lead to a variation in the load distribution and to a decrease in the forces due to blade flexure and torsion.

CHAPTER 4

DESIGN AND ANALYSIS OF WING PARTS AND HELICOPTER ROTOR BLADES

The wings of contemporary flight vehicles usually consist of a rigid skin and the longitudinal and transverse load-bearing elements.

A wing design under the operating conditions characteristic to it should satisfy the set of requirements examined in chapter 1, § 7, including the extremely important requirements of sufficient strength and rigidity with the least weight and the necessary service life. The fulfillment of these requirements is in direct dependence on how effectively they are satisfied in the design of all wing parts.

From these positions let us examine purpose, the design and the operation of the main wing parts.

§ 1. GENERAL QUESTIONS OF THE DESIGN AND ANALYSIS OF AIRPLANE DESIGN COMPONENTS

1. Requirements for the Technological Effectiveness of Production, Repair and Operational Effectiveness

Wings, rotor blades and other parts of the airframes of flight vehicles are tubular thin-walled designs: riveted thin plates and thin-walled sections.

In working out designs the basic requirements of the technological effectiveness of production and repair are taken into account: the preservation of design continuity with respect to the accomplished models, the duplicatability of uniform assemblies and parts, the employment of standardized parts, the limitation of the requirements imposed on manufacturing precision, the possibility of employing effective technological methods, the limitedness of the assortment of materials and semi-finished products etc.

Considerable attention should be allotted to the realization of the requirements of operational technological efficiency: ensuring convenience of access to assemblies and units during maintenance, ease of dismantling, mutual interchangeability, the possibility of employing existing equipment for maintenance, etc.

2. Theoretical Weight and Specific Strength

The need for observing the requirements of technological effectiveness stimulates the uniformity and the standardization of designs.

However, the requirement (mandatory for aviation designs) for ensuring the necessary properties with the least weight leads to greater individuality in design solutions, following the trend to bring a design closer to minimum weight. In connection with this, let us dwell on the principles of determining so-called theoretical design weight.

Theoretical design weight is defined as the minimum weight which is obtained with the maximum employment of the strength properties of a material in a load-bearing setup resulting from the layout of a design. As was noted in chapter 3, § 6, the most rational load-bearing setup is the two-flange beam. The stresses in the cross sections for it are connected with the forces by the following dependences:

$$\sigma = \frac{M_{изг}}{HF}, \quad \tau = \frac{Q}{H\delta}.$$

If $M_{изг}$ and Q are the calculated destructive loads, then the strength of the material will be maximally utilized, when in tensioned and compressed flanges the stresses are respectively equal to $\sigma_в$ and $\sigma_н$, and in a web - to $\tau_{разр}$. The required areas of tensioned and compressed flanges and the web thickness are determined by the formulas:

$$F_{пр} = \frac{M_{изг}}{H\sigma_в}; \quad F_{пс} = \frac{M_{изг}}{H\sigma_н}; \quad \delta = \frac{Q}{H\tau_{разр}}.$$

Then the theoretical weight of a beam section of length dz at specific weights of the flange material $d_п$ and of the web material $d_с$ will be:

$$dG_{теор} = \left[\left(\frac{M_{изг}}{H\sigma_в} + \frac{M_{изг}}{H\sigma_н}\right) d_п + \frac{Q}{H\tau_{разр}} d_с\right] dz.$$

The linear theoretical weight of a beam is

$$q_{теор} = \frac{M_{изг}}{H}\left(\frac{d_п}{\sigma_в} + \frac{d_п}{\sigma_н}\right) + \frac{Q}{H}\frac{d_с}{\tau_{разр}}.$$

The magnitudes $\frac{\sigma_в}{d}, \frac{\sigma_н}{d}, \frac{\tau_{разр}}{d}$ are called the specific strength of a material with different types of stressed state.

The rigidity characteristic of a material is the specific rigidity E/d, where E is the modulus of normal elasticity.

The theoretical weight of a beam with a length l is

$$G_{теор} = \int_0^l q_{теор} dl.$$

The structure of the expression for theoretical weight shows that to attain minimum design weight it is necessary: 1) to find and to employ the rational load-bearing setup; 2) to employ the materials with the highest possible specific strength characteristics.

3. Aviation Materials

When selecting a material for wing components and other parts of an aircraft airframe it is necessary to consider all the requirements imposed on the aircraft, but first of all the strength and the rigidity of the design with the least weight must be ensured.

The basic criteria of the suitability of a material from this point of view are: the high value of the specific strength and specific rigidity characteristics which ensure less flight vehicle weight.

In the design of civil aircraft intended for intense and prolonged operation, it is necessary to also consider the capacity of a material to resist repeated loads. The higher it is the longer is the service life of the aircraft, and the greater is its economic effectiveness.

In the airframe design of contemporary subsonic aircraft aluminum alloys of the D16 and V95 type and 30KhGSA and 30KhGSNA are predominantly employed.

Table 4.1 gives the mechanical and physical characteristics of the most widely employed aviation materials at room temperature.

For the design of supersonic aircraft which undergo kinetic heating, materials which do not have a decrease or which have only a slight decrease in their mechanical properties during heating to temperatures of 150-400°C are necessary.

Table 4.1

Material	Ultimate strength $\sigma_в$, kgf/mm^2	Elastic modulus E, kgf/mm^2	Elongation of rupture δ, %	Specific weight d, g/cm^3	Specific strength $\sigma_в/d$	Specific rigidity E/d	Note
D16AT	44	$7 \cdot 10^3$	13	2.8	15.5	2500	High fatigue life
AK4-1	40-42	$7.2 \cdot 10^3$	7-12	2.8	14-15	2570	Slight reduction in mechanical characteristics during heating up to 150-170°C
B95T	60-62	$7 \cdot 10^3$	6	2.85	21.7	2460	
Titanium alloys of the VT20 and OT4-2 type	100-120	$12 \cdot 10^3$	7-15	4.45	23-27	2700	High heat resistance
30KhGSA	140	$2 \cdot 10^4$	5	7.83	17.8	2550	
30KhGSNA	170	$2 \cdot 10^4$	5	7.77	21.9	2580	
Pine wood	8.3	$9.2 \cdot 10^2$	-	0.5	16.6	1840	

With an increase in temperature the strength of the D16 and V95 type alloys drops off sharply and at temperatures above 150-200°C they can no longer be employed as structural (design) materials.

At 300°C the strength of D16AT is decreased by 3 times, for V95T - by 5 times.

The AK4-1 alloy is in the best position. It can be employed in the design of supersonic aircraft with a flight M number of up to 2-2.2. For aircraft intended for flight at large M numbers, in the manufacture of wing, fuselage, and empennage components and other elements subjected to considerable kinetic heating, it is necessary to employ titanium alloys or heat-resistant steels of the

VlT stainless steel type, although at low temperatures they are inferior in specific strength to other materials.

4. Strength Conditions and Strength Characteristics of Design Elements

The general strength requirements established in the strength standards (chapter 1, § 7) determine the need for the testing of the design strength under calculated destructive $P^{р}$ and operational $P^{э}$ loads. The main one is, as a rule, the strength condition for $P^{р}$, in general form expressed by the dependences:

$$\sigma^{р} \leqslant \sigma_{разр}, \qquad (4.1)$$

$$\tau^{р} \leqslant \tau_{разр}. \qquad (4.1')$$

Respectively, the strength condition for $P^{э}$ takes the form:

$$\sigma^{э} \leqslant \sigma_{доп}, \quad \tau^{э} \leqslant \tau_{доп}. \qquad (4.2)$$

For thin-walled aviation design elements the magnitudes of those destructive stresses $\sigma_{разр}$ and $\tau_{разр}$ and those permissible stresses in operation $\sigma_{доп}$ and $\tau_{доп}$ are determined not only by the mechanical characteristics of the material, but also by the design shapes and by the manufacturing technology of the elements.

Tensioned elements. Included among these are the flanges, stringers, the skin of a tensioned wing panel, etc. Under strength condition (4.1) for tensioned elements it is assumed, that

$$\sigma_{разр} = k\,\sigma_{в},$$

where k - the reduction coefficient; $\sigma_{в}$ - the ultimate tensile strength of the material.

The reduction coefficient can be represented in the following manner:

$$k = k_1 k_2.$$

where k_1 - the coefficient which considers the decrease in the cross-sectional area of element with holes for rivets or bolts; k_2 - the coefficient which considers the stress concentration. For cross sections where it is possible to disregard taking into account the reduction in area ($F_{раб}=F$), $k_1=1$. In the remaining cases $k_1=F_{раб}/F<1$, where $F_{раб}=(0.89-0.96)F$ depending on the diameter of the rivets, the dimensions and the type of element.

Coefficient k_2 depends on the plasticity of the material, the diameter and the quality of the holes. For aviation structures made from duralumin and steel $k_2=0.85-0.95$.

Hence the range of variation in the reduction coefficient is $k=0.76-0.95$.

In each actual case it is necessary to select it taking into account the factors in question which affect its magnitude.

If in the cross section of a tensioned element (for example in the skin) shear stress τ is also acting, strength testing is carried out according to the third theory of strength. As a criterion of the stressed state it is assumed that $\sigma_{прив}=\sqrt{\sigma^2+4\tau^2}$. The strength condition has the form:

$$\sigma_{прив} < \sigma_{разр}. \qquad (4.3)$$

where $\sigma_{разр}=k\sigma_в$.

Plates which lose stability in compression and in shear. These can be sections of spar webs, wing skin and other structural (design) elements. Depending on which type of stresses is decisive, the strength condition has the form:

$$\sigma^p < \sigma_к \text{ or } \tau^p < \tau_к.$$

For thin rectangular plates with large values of b/δ the critical stresses do not exceed the limit of proportionality or the elastic limit close to it and are determined by expressions of the Euler formula type, valid within the limits of the applicability of Hooke's law.

$$\sigma_э \text{ or } (\tau_э) = \kappa \frac{0{,}9E}{\left(\frac{b}{\delta}\right)^2}, \qquad (4.4)$$

where κ - the coefficient which considers the support conditions and the nature of the external loads applied along the plate boundaries; b - the characteristic, usually the lesser dimension of the rectangle; δ - the thickness of the plate.

For thicker plates for which formulas (4.4) give values of $\sigma_э$ and $\tau_э$, which exceed the limits of proportionality, the critical stresses can be found from empirical formulae of the form:

$$\sigma_к (\text{или } \tau_к) = \sigma_в (\text{или } \tau_в) \frac{1+\nu}{1+\nu+\nu^2}, \qquad (4.5)$$

[или=or]

where

$$\nu = \frac{\sigma_в}{\sigma_э} \left(\text{или } \frac{\tau_в}{\tau_э} \right).$$

As is shown in Fig. 4.1, these empirical formulas give for thick plates critical stresses, close to the ultimate strengths $\sigma_в$ or $\tau_в$, and for thin plates - those close to Eulerian critical stresses.

During the simultaneous effect of compression and shear stresses on a plate, the condition of the onset of loss in stability has the form:

$$\frac{\sigma}{\sigma_к} + \left(\frac{\tau}{\tau_к}\right)^2 = 1.$$

where $\sigma_к$ and $\tau_к$ - the critical stresses in the event of separate loading with compression or with shear.

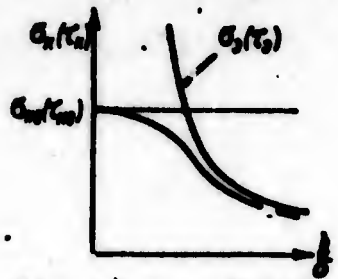

Fig. 4.1. Critical stresses in a plate.

Hence it is possible to find:

the critical normal stress taking into account the effect of τ:

$$\sigma_{к\tau} = \sigma_к \left[1 - \left(\frac{\tau}{\tau_к}\right)^2\right] \qquad (4.7)$$

and the critical tangential stress taking into account σ:

$$\tau_{к\sigma} = \tau_к \sqrt{1 - \frac{\sigma}{\sigma_к}}. \qquad (4.8)$$

Compressed rods. They include the flanges and stringers of compressed wing panel, etc.

The strength condition is:

$$\sigma^p < \sigma_к. \qquad (4.9)$$

The holes in compressed rods filled with rivets, practically do not effect $\sigma_к$. The values of $\sigma_к$ are usually found from the curves of $\sigma_к = f(l)$ (where l - the length of a rod) obtained from the buckling tests of standard profiles.

For long rods the general loss of stability - the buckling of a rod axis - is decisive. If the cross section of a rod does not change its shape and the loss in stability occurs within the limites of the applicability of Hooke's law, $\sigma_к$ is expressed by the Euler formula

$$\sigma_э = \frac{E\pi^2}{\lambda^2}, \qquad (4.9')$$

where $\lambda=\mu l/i$; μl - the reduced length of a rod, equal to the length of the half-wave curve, along which the buckling occurs; μ considers the supporting conditions. For hinged supports $\mu=1$, in the event of elastic fastening (it is simulated in the testing of the near-face rod ends) $\mu=0.5$; and $i=\sqrt{I/F}$ - the radius of inertia during bending.

For shorter rods the compression failure can sometimes begin beyond the elastic limit in the form of both general and local loss in stability.

In the latter case the ratio b/δ affects $\sigma_к$ for the rod cross section. Then $\sigma_к$ is found from experimental curves, and in the absence of them - by the empirical formula

$$\sigma_к=\sigma_{к0}\frac{1+\nu}{1+\nu+\nu^2}, \qquad (4.10)$$

where $\sigma_{к0}$ - the critical stress in the local loss of stability; for thin-walled profiles it is defined as the critical stress in the least stable plate-like element included in the composition of the profile, and it depends on the b/δ of this plate; $\nu=\sigma_{к0}/\sigma_э$.

§ 2. SPARS

A spar - a longitudinal beam or a truss, capable of operating independently in flexure in its plane.

The number and the arrangement of the spars along the wing chord depend on the dimensions of the aircraft and the wing layout characteristics. Usually the arrangement of the spars is characterized by the following averaged data of the values $\bar{x}=x_1/b$; in a wing with two spars $\bar{x}_1=0.17-0.2$; $\bar{x}_2=0.58-0.62$; in a wing with three spars $\bar{x}_1=0.15-0.18$; $\bar{x}_2=0.38-0.42$; $\bar{x}_3=0.63-0.67$ (Fig. 4.2a).

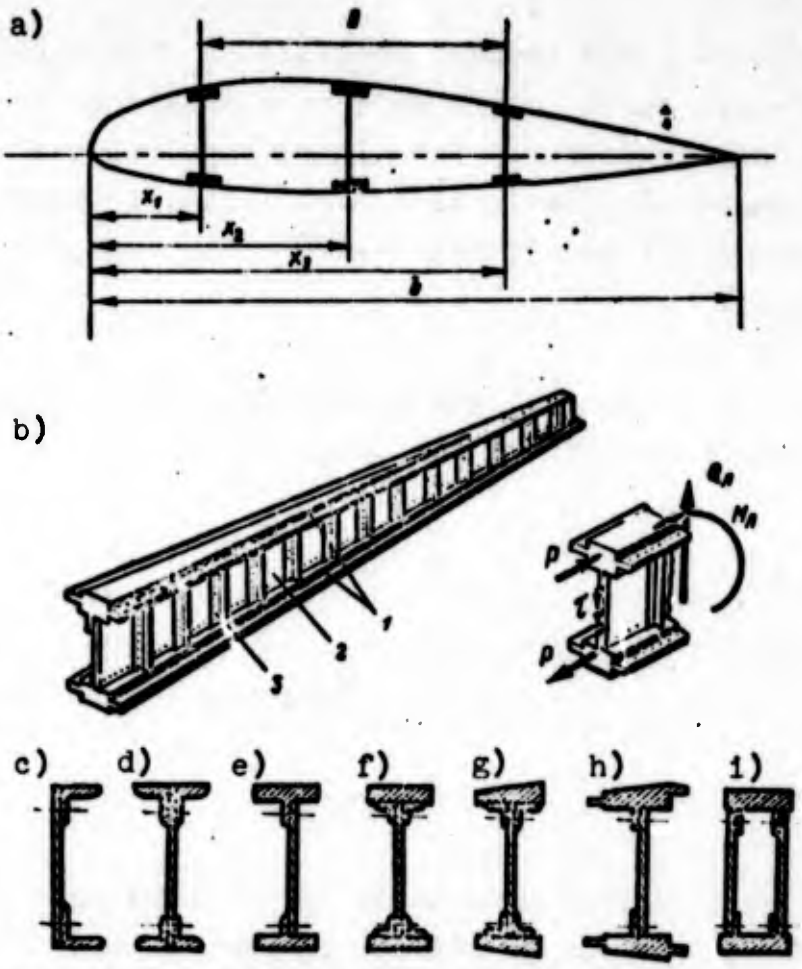

Fig. 4.2. Beam spars: a) the arrangement of the spars along the wing chord; b) spar of H-shaped cross section and the operation of its elements; c-i) beam spars cross sections; 1 - flanges; 2 - web; 3 - strut.

A spar is called a beam spar, if a web serves for receiving the transverse force, and a truss spar, if a truss lattice is employed for this purpose and like the web, connecting the flanges (caps).

Beam spars are usually employed in the designs of contemporary wings.

1. Design and Operation of Beam Spars

Beam spars are made in the form of a two-flange beam with a thin web reinforced with struts. The general form of this type of

spar of H-shaped cross sections is shown in Fig. 4.2b. Figure 4.2c through i shows the possible cross sections of a beam spar. The two flange setup of a spar ensures the most effective employment of the flange and web material, and consequently, the minimum design weight.

Spar flanges operate in tension and compression due flexural moment, a web - in shear due to transverse force (see Fig. 4.2b).

Spar flanges should meet both the general requirements imposed for aviation structures (strength and rigidity, light weight, long service life, technological effectiveness, etc.) as well as special requirements, namely:

convenience in connecting the skin and the web;

maximum utilization of the design (over-all) spar height;

minimum losses in the flange cross-sectional area for holes for rivets and bolts.

The requirements for convenience in connecting the skin and the web and of utilization of the height are most simply accomplished as a result of the employment of flange angle and T-shaped cross sections (see Fig. 4.2c, d and e).

When necessary for reinforcing a flange to angles it is possible to rivet a strip (see Fig. 4.2f). This type of design is technologically simple, makes it possible to mill the strips, fitting their transverse cross section shape to the wing profile (see Fig. 4.2g), and to vary the cross-sectional area of the flange along the length right up to the transition for one angle at the spar tip.

Further refinement of flange design has led to the creation of a profiled cross section with lugs for fastening the skin and

the web (see Fig. 4.2k). This type of flange completely meets all three special requirements. It is usually made from a pressed profile, which for preserving the conditions of uniform strength of the flange along the length of the spar is subjected to mechanical processing. The processing of the flange surface should be done with great care. The presence of scratches, especially transverse scratches, leads to a considerable reduction in the service life of a flange with repeated loads.

The spar web has a constant thickness in height, since the tangential forces in the web cross section are almost constant. Therefore in riveted spars the web is usually manufactured from sheets of D16 or V95 type alloys.

With a constant wing chord or center section it is possible to employ seamless-rolled spars whose web is made together with the flanges (spars of the center section of the AN-24). The advantage of these types of spars as compared with riveted spars is less weight and greater fatigue life.

The joining of the web with the flanges of a unit-construction spar is carried out for the most part with rivets and sometimes with bolts. Usually the diameter of the rivets and the bolts does not exceed 6 mm.

The struts are intended for attaching the ribs to the spar, for reducing the free section of the web to increase the critical shearing stress $\tau_{кр}$, for counteracting the coming together of the spar flanges upon the loss of stability of the web due to tangential stresses and during bending of the spar.

Struts are usually manufactured from the duralumin profiles of angle cross section. They are fastened with rivets to the web and to the spar flanges (Fig. 4.3).

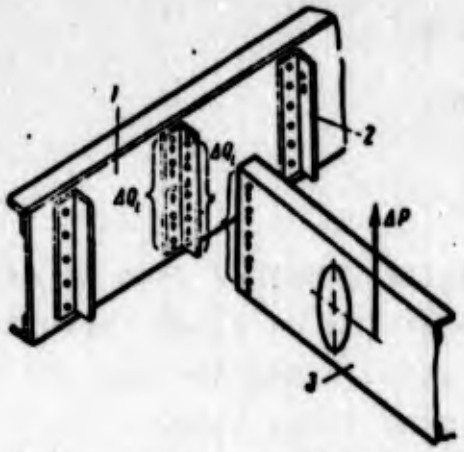

Fig. 4.3. Load transfer from the rib to the spar web: 1 - spar; 2 - strut; 3 - rib.

The strut interval is equal to 10-25 cm (the rib interval - 50-100 cm). A decrease in the strut interval increases the $\tau_к$ of the web without increasing its thickness.

The struts attaching the ribs, by receiving the forces ΔQ incident on them from the load on rib ΔP transmit them through the rivets to the spar web.

The web loosing stability, is capable of withstanding a further increase in load, if it rests on a rod contour rigid in flexure in the web plane. After the loss of stability under the effect of $\tau_к$ the web continues to operate in shear, receiving tangential stresses, and additionally operates also in tension in the direction of the wave crests which were formed during the loss of stability.

If a web is very thin, then $\tau_к \approx 0$. The tensile stresses directed at an angle of $\alpha \approx 45°$ to the spar axis (Fig. 4.4a) are:

$$\sigma_{ст} = 2\tau,$$

where $\tau = q/\delta$ - the nominal stresses due to the linear tangential force in the web q.

Additional compressive forces S and N arise in the flanges and struts; furthermore, the flanges and the extreme struts are loaded with additional transverse loads $q_п$ and q_c which cause their bending:

$$q_n = q_c = \frac{1}{2}\sigma_{cr}\delta = \tau\delta;$$

$$S = q_c\frac{H}{2} = \frac{1}{2}\tau H\delta;$$

$$N = q_n l = \tau l\delta.$$

Expressions σ_{cr} and $q_n = q_c$ are easily obtained from an examination of the equilibrium of the forces acting on a web strip directed at an angle of 45° and having a unit width along the web and the flange. From q_c and q_n S and N are found (Fig. 4.4b)

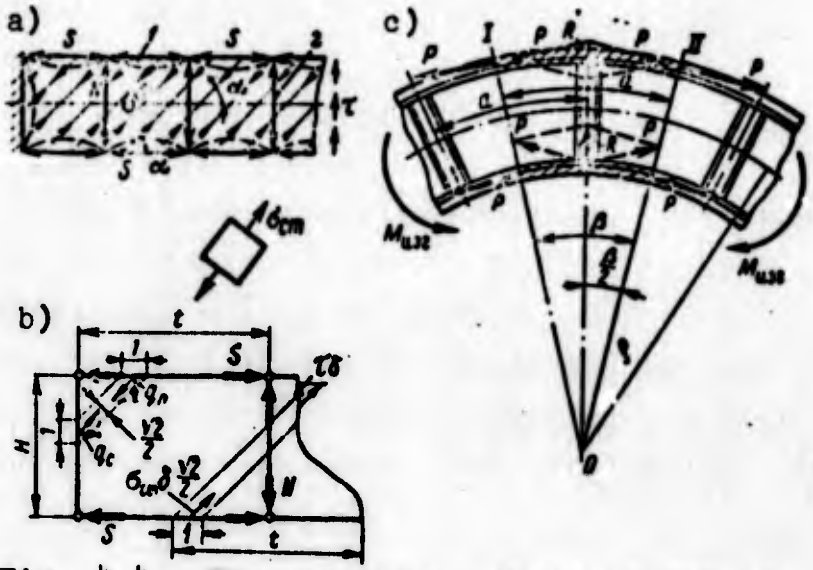

Fig. 4.4. The operation of spar elements: a) diagram of the operation of a spar after the loss in stability of the web in shear: 1 - flange; 2 - strut; b) forces and stresses after the loss of web stability; c) radial forces during bending.

By employing the operational capacity of the web after a loss in stability, it is possible to make it somewhat lighter. However, in this case it is necessary to additionally reinforce the spar flange and struts.

For this spar webs (up to 1-1.5 mm), operating in shear, a loss in stability is permissible in the case of loads greater than operational loads ($P \geq P^3$).

A loss in stability of the thicker webs and the webs of the tank-sections is not permissible up to the calculated destructive load P^p, since the breaking off of the rivet heads and spar failure, and in the tank-sections - the breakdown of hermeticity - are possible.

With the bending of a spar radial forces arise in it which tend to draw the flanges together. The spar struts prevent this drawing together.

Let us examine the equilibrium of spar section I-II subjected to bending (Fig. 4.4c).

The forces of P acting in the flanges of the section with the presence of spar curvature, cause the radial forces R received by the struts.

From the equilibrium condition

$$R = 2P \sin \frac{\beta}{2},$$

where $\beta = a/\rho$.

At a low value of β it is possible to assume $\sin \beta/2 \approx \beta/s$, then

$$R = P \frac{a}{\rho}.$$

Usually the deformation of a spar during its bending is insignificant; therefore ρ is great, the radial force R in the strut is small and it is possible not to take it into account.

However, if the web of this type of spar loses stability due to tangential stresses and the strut is also loaded with force N, the joint effect of forces N and R must be considered and it is necessary to check the strut for longitudinal bending.

If a beam is made especially curvilinear, for example the beam of the engine mount, then in the sections of its greatest curvature the radial forces R are considerable. In these sections it is necessary to place the struts with a cross section and with small spacing.

2. Testing the Strength of Beam Spar Elements

The strength of spars, as a rule, is checked for loading case A (or A') and D (or D').

Tensioned flange. The fulfillment of the strength condition for tensioned elements is checked with formula (4.1). For flanges of the type shown in Fig. 4.2d, in determining $\sigma_{разр}$ it is assumed that $k_1=1$ and $k=0.95$. A tensioned flange should also be mandatorily checked for compression in the D case.

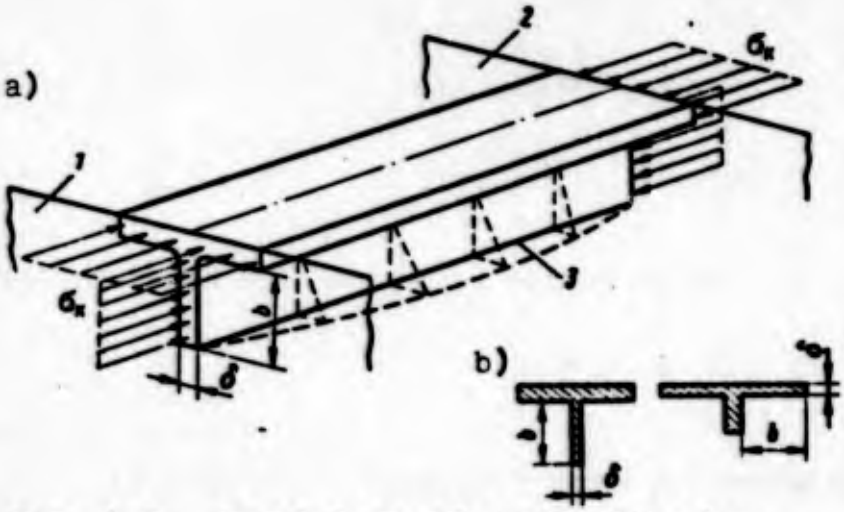

Fig. 4.5. Local loss of stability of a flange element: 1, 2 - ribs; 3 - free side.

Compressed flange. Critical flange stress $\sigma_{кп}$ is usually defined as the critical stress $\sigma_{кр}$ of the local loss in stability taking place in the shape shown in Fig. 4.5. The general loss in spar flange stability is hindered as a result of the attachment of the skin and web to it. In accordance with formula (4.10) $\sigma_к \approx \sigma_{кр}$.

For the duralumin and steel profiles of T-shaped and angle cross section it is possible to determine the stresses $\sigma_{кр}$ of a

local loss in stability from the curves of $\sigma_к = f)b/\delta)$ available in reference literature. The dimensions b and δ - the height and the thickness of the flange element (web or cap), the local loss in stability of which is most probable (Fig. 4.5b). In the absence of curves it is possible to determine $\sigma_{кО}$ from the empirical formula of the critical normal stress in a plate:

$$\sigma_{кО} = \sigma_в \cdot \frac{1+\nu}{1+\nu+\nu^2}; \qquad (4.10')$$

where $\nu = \frac{\sigma_в}{\sigma_э}$; $\sigma_э = k\frac{0{,}9E}{(b/\delta)^2}$.

The flange element which loses stability, is examined as a plate, three sides of which are freely supported, and the fourth, parallel to the load, is free (see Fig. 4.5). In this case

$$k = 0{,}425 + \frac{1}{(a/b)^2},$$

where a - the rib interval.

The reinforcing effect of the spar web (the skin), fastened to the flange is slight and is not taken into account in this case.

In order to maximally employ the design height of a spar, it is desirable to take b/δ of the flange large, but it is necessary to check that the flange does not lose stability when operating in compression.

For a flange the empirical dependence (4.10') is valid at values $b/\delta > (4\text{-}5)$.

When $b/\delta < 4$ the web of the profile (cap) practically does not lose stability, it operates in pure compression. The experiments with rods which do not lose stability in compression, show that $\sigma_{сж} = \sigma_в$ of the material. Consequently, for purposes of increasing $\sigma_к$ and of reducing the spar weight, it is advantageous to select

the dimensions of a compressed flange fomm condition $b/\delta<4$, especially with large values of $F_п$.

In testing the strength of this type of flange it is recommended that it be taken that $\sigma_к=\sigma_в$. A compressed flange should also be checked in tension in case A.

Spar web. In accordance with the strength condition in general form according to formula (4.1)

$$\tau^р = \tau_{разр},$$

where $\tau^р=q_{ст}/\delta_{ст}$ - the total tangential stress in a web from Q and $M_{кр}$; $\tau_{разр}$ - the tangential breaking stress. According to experimental data $\tau_{разр}=(0.3-0.5)\sigma_в$.

Depending on the web thickness and the requirements imposed on it, the testing of its strength is carried out differently.

For thin webs ($\delta_{ст}\leq$1-1.5 mm), the loss in stability of which is permissible when $P>>P^э$, the strength conditions are the following:

$$\text{when } P^э \quad \tau^р \leqslant \tau_к;$$
$$\text{when } P^р \quad \tau^р \leqslant \tau_{разр}.$$

For thick webs ($\delta_{ст}\geq$1.5-2 mm) and webs of tank-sections, the loss in stability of which is not permitted up to $P=P^р$, the strength condition is:

$$\tau^р \leqslant \tau_к.$$

The critical web stress, if loss in stability occurs within the limits of elasticity, can be determined on the basis of formula (4.4):

$$\tau_к = k\frac{0{,}9E}{(b/\delta)^2}. \qquad (4.11)$$

where $k = 5{,}6 + \frac{3{,}8}{\left(\frac{a}{b}\right)^2}$ for a plate, all four sides of which are freely supported; b - always the smaller side of the plate (a/b>1).

For spars with frequently positioned struts usually b is the strut interval.

If in the calculation $\tau_к$ is obtained higher than the limit of proportionality, then it is necessary to determine $\tau_к$ from the empirical formula (4.5) of the critical tangential plate stress:

$$\tau_к = \tau_в \frac{1+\nu}{1+\nu+\nu^2},$$

where $\nu = \tau_в/\tau_э$; $\tau_в = \sigma_в/2$; $\tau_э$ is determined from formula (4.4).

An increase in $\tau_к$ of a web is possible both by thickening it and by installing additional struts between the ri[illegible].

Load on a rivet. For a web which does not lose stability up to $P^р$, from the equilibrium condition of a spar section it is possible to determine the rivet load from formula

$$T = \frac{q_{ст} t}{n},$$

where $q_{ст}$ - the total flow of forces in a web due to Q and $M_{кр}$; t - the rivet interval in one row; n - the number of rows of rivets in a riveted seam.

For a web which loses stability when $P \geq P^э$, the load on a rivet T is determined approximately by the same formula.

With respect to load T taking into account the number of shear planes of the rivet its diameter is selected (from the handbook) and the web is checked for crumpling.

3. Design Characteristics of Truss Spars

Truss spars are manufactured from Chromansil tubes by welding them or from Chromansil and duralumin profiles - employing rivets and bolts. In this case the strut flanges are made continuous.

During the calculation a truss spar is schematized as a rod system with hinged joints.

The local additional bending stresses resulting from the rigidity of the welded and riveted joints, are not taken into account.

However the presence of these stresses can lead as a result of the effect of repeated loads to the appearance of cracks, especially in a welded zone.

In designing truss spars, as a rule, the following aspects are taken into account:

the rod axes of the truss should intersect at one point (Fig. 4.6a);

it is desirable to place diagonal braces as longer elements so that in the basic loading case they operate in tension (Fig. 4.6b).

Truss spars as compared with beam spars do not have any weight or rigidity advantages. At the same time they are more complex with respect to manufacturing technology, they are multicomponent; thus, they are not too frequently encountered in recent times.

However, their employment is possible on supersonic aircraft which undergo kinetic heating. The truss design, during heating, experiences less thermal stresses, than the solid beam design.

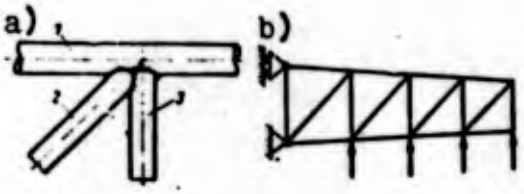

Fig. 4.6. Joint and diagram of a truss spar: 1 - flange; 2 - diagonal brace; 3 - strut.

§ 3. STRINGERS

1. Design and Operation

Stringers are longitudinal wing elements fastened to the skin. Usually the stringer interval $t_{стр}$ in a wing load-bearing setup, close to a monocoque setup, is equal to 80-160 mm and in a load-bearing setup, close to a beam setup, is 120-240 mm.

Stringers participate in a wing design in the transmission of the air load from the skin to the ribs and in conjunction with the skin receive part of the wing bending moment.

The loading setups of stringers (and skin) loaded with the forces of a transverse air load and with normal stresses due to $M_{изг}$ are shown in Fig. 4.7a, b, c. If the skin is less rigid in flexure than the stringers, then the air load is transmitted from skin sections I partially to the stringers, and from them to the ribs. Stringers are more frequently manufactured from pressed and more rarely from bent profiles.

The shapes of stringer cross sections are distinguished by their great diversity (Fig. 4.8). The selection of the shape of a stringer cross section is determined by many factors, for example by the magnitude of the critical stresses of the general and local loss in stability, by the ease in joining them with the skin and ribs, etc.

In contrast to the flanges of beam spars both local and general loss of stability (with a large rib interval) can occur in stringers during compression. In the latter case the stringer bulges along the normal to the skin, and, as a rule, inside the wing.

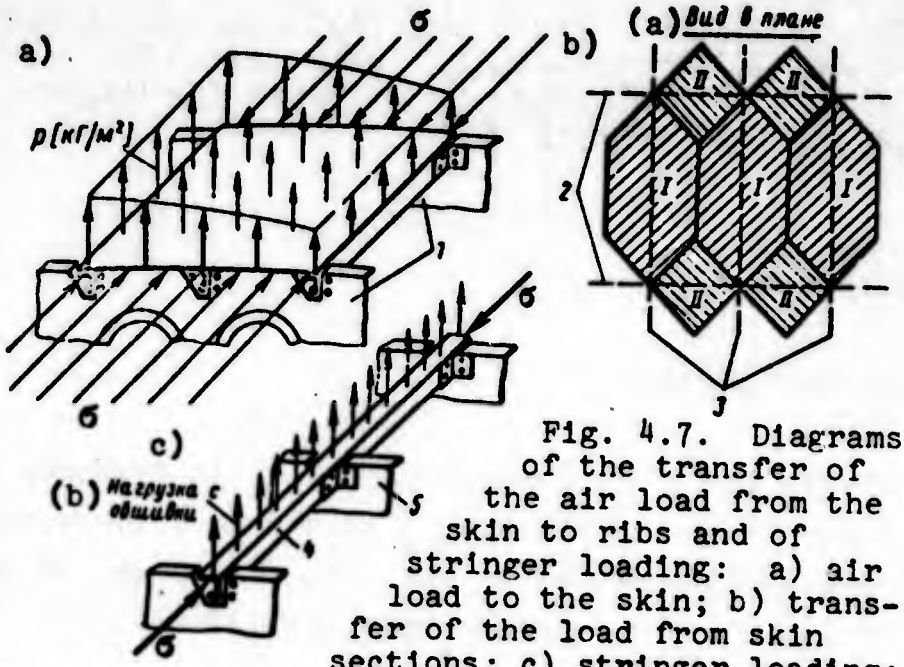

Fig. 4.7. Diagrams of the transfer of the air load from the skin to ribs and of stringer loading: a) air load to the skin; b) transfer of the load from skin sections; c) stringer loading; 1, 2, 5 - ribs; 3, 4 - stringers.
Key: (a) View in plan; (b) Load from the skin. [кГ/м^2=kgf/m^2].

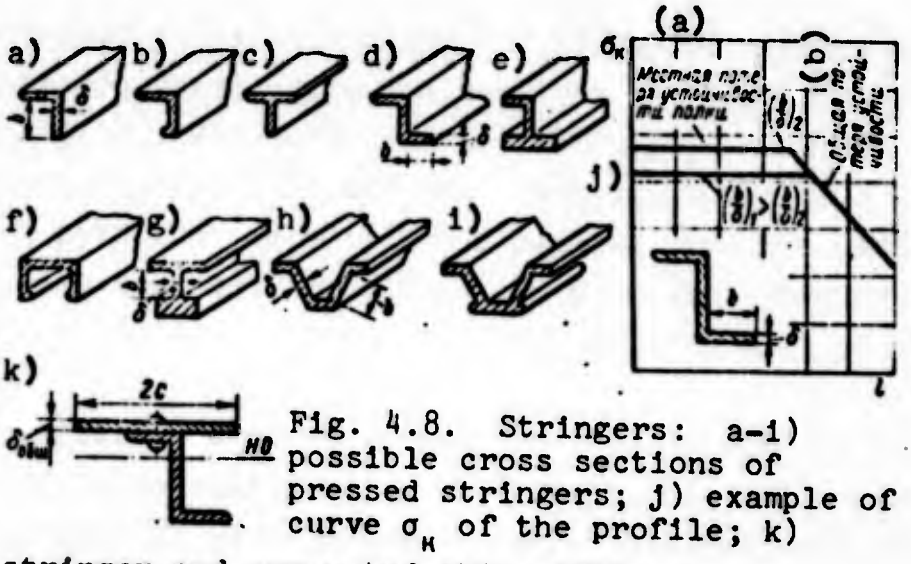

Fig. 4.8. Stringers: a-i) possible cross sections of pressed stringers; j) example of curve $\sigma_к$ of the profile; k) stringer and connected skin width.
Key: (a) Local loss of stability in the cap; (b) General loss of stability.

To increase the critical stress $\sigma_{кО}$ of the local loss of stability it is necessary to support the free edge of the profile section which loses stability, as a plate. This is attained by local thickening of the free edge - with "bulbs" (Fig. 4.8b and c).

To increase the critical stress $\sigma_к$ of the general loss in stability of the profile and to increase its flexural rigidity, it is necessary, for reinforcing the skin, to employ an increase in the profile section part at a distance from the skin (Fig. 4.8e, g, h, i). Since this reinforcement supports the vertical web of the profile, then $\sigma_{кО}$ of this profile is also increased. Thus, the wing stringers of medium and heavy aircraft are usually manufactured from the profiles shown in Fig. 4.8e, g, h, i.

Angle cross section stringers, more convenient and simpler from the point of view of joining them with the skin and ribs, are utilized in the design of the leading and trailing wing parts of the same aircraft and in the wings of light aircraft.

Bent stringers are made from sheet material of small thickness. They are employed mainly in the designs of the nonload-bearing sections of light wings, in the designs of flaps, control surfaces and ailerons.

2. Strength Testing

The calculations and tests show that the main stresses for a stringer are the normal stresses due to the $M_{изг}$ of the wing. Thus, the strength conditions respectively for tensioned and compressed stringers under the effect of $P^{р}$ have the form:

$$\sigma^{р} \leqslant k\sigma_{в\,стр};\quad \sigma^{р} \leqslant \sigma_{к\,стр}. \qquad (4.12)$$

where k=0.8-0.9 - the reduction coefficient of a stringer with holes.

The critical stress in a stringer necessary for strength testing is usually determined from experimental curves $\sigma_{к\ стр}=f(l)$

taking the effect of b/δ into account. The distance between the ribs (rib interval) is taken as l. There are curves $\sigma_к$ in reference literature for the profiles of aviation assortment (Fig. 4.8j) plotted from tests of faced rods. If they are employed for determining $\sigma_{к\ стр}$, then it is necessary to take into account that they do not reflect the supporting effect of the skin, which gives understated results, if the loss in stability is not local.

The supporting effect of the skin with a general loss in stability can be taken into account by calculating with the Euler formula (4.9') or with empirical formula (4.10), by examining, in the determination of I and F, the cross section of the stringer together with the connected width 2c of the skin (Fig. 4.8k), where $2c=(25-30)\ \delta_{обш}$. In this case the bending occurs relative to the neutral axis НО, which passes through the center of gravity of this cross section parallel to the skin.

§ 4. THE SKIN

1. Design and Operation

The wing skin is intended for creating and retaining the external shape of the wing. The skin operates:

1) by receiving the air load and transmitting it to the ribs and spars;

2) by receiving $M_{кр}$ together with the spar webs and part of $M_{изг}$ in the wing beam system.

A metallic skin section, which is comparatively thick and is reinforced by stringers, between two adjacent ribs and spars can be examined as a rather rigid plate. The transverse bending stresses due to the air load in it are insignificant.

The sections of linen and very thin metallic skin weakly reinforced by stringers are similar to a membrane fastened to fixed supports (ribs, spars).

From the air load this type of skin operates in tension like a membrane; membrane (chain) stresses arise in it which must be considered in calculating the skin.

The participation of the skin as a load-bearing element of a wing beam in receiving $M_{изг}$ in the tensioned zone depends on its thickness and ultimate strength: in the compressed zone - from the thickness and the critical stress determined by the design of the reinforced skin.

Until a compressed skin loses stability, the stress in it is the same as in the stringers (if $E_{обш}=E_{стр}$).

After the loss of skin stability the stress in it is distributed unevenly: in the immediate proximity of the stringers it is equal to the stringer stress, and in the middle of the span - to the critical skin stress $\sigma_{к\ обш}$.

The torsional moment $M_{кр}$ is received by the closed contour formed by the skin and the spar webs. Consequently, the skin of a contemporary wing is subjected to the simultaneous effect of normal and tangential stresses due to $M_{изг}$ and $M_{кр}$.

The metallic skin, attaining at the wing root of very heavy aircraft 12-18 mm, is manufactured from sheet duralumin. Toward the wing tip, for purposes of reducing the weight, the thickness of the skin is gradually reduced with retention of uniform strength. This is attained both by employing plates of different thickness and by their mechanical and chemical milling.

The cutting out of a skin pattern is accomplished in such a way that the longitudinal joints go along the spar flanges and only in

the case of a very large wing chord - additionally along the stringers (Fig. 4.9a, b, c, d). The transverse joints are accomplished along the rib flanges or along joint strips; in the case of small skin thickness a lap joint with an under support is permitted (Fig. 4.9e, f, g).

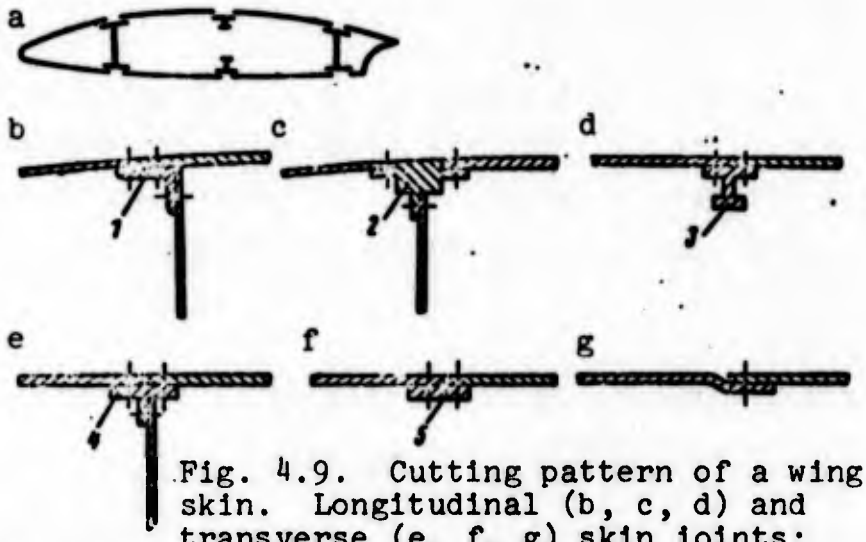

Fig. 4.9. Cutting pattern of a wing skin. Longitudinal (b, c, d) and transverse (e, f, g) skin joints: 1, 2 - spar flange; 3 - stringer; 4 - rib flange; 5 - joint strip.

The joining of a metallic skin with stringers and ribs is carried out with rivets, this type of joint is most reliable. Recently panels, in which the skin and stringers are one piece, have been broadly employed.

The advantage of such panels as compared with riveted panels is less weight and greater fatigue life.

In less load wing sections glued or glue-welded skin joints with stringers and ribs are employed.

For purposes of increasing corrosion resistance the skin of contemporary aircraft is anodized and is coated on top with a thin layer of special varnishes.

2. Strength Testing

The strength testing of skin is carried out for the joint effect of σ and τ.

Tensional zone. The strength testing of tensional skin is carried out only for the effect of P^p. The strength condition with respect to the third theory of strength is:

$$\sigma^p_{прив} = \sqrt{(\sigma^p_{обш})^2 + 4(\tau^p_{обш})^2} \leqslant k\sigma_в, \qquad (4.13)$$

where k≈0.9 - the weakening (reduction) coefficient of skin with holes; $\sigma^p_{обш}$ and $\tau^p_{обш}$ - normal and tangential stresses at one point of the cross section of the skin under the effect of P^p.

Compressed zone. Strength testing of compressed skin is carried out under the effect of $P^э$ and the effect of P^p. Testing under the effect of P^p is the main one.

Duralumin skin up to 3-4 mm in thickness with a conventional stringer reinforcement should not lose stability up to $P^э$.

The strength condition under the effect of $P^э$ is:

$$\sigma^э_{обш} = \frac{\sigma^p_{обш}}{f} \leqslant \sigma_{к\ обш\tau^э}, \qquad (4.14)$$

where $\sigma_{к\ обш\ \tau^э} = \sigma_{к\ обш}\left[1 - \left(\frac{\tau^э_{обш}}{\tau_{к\ обш}}\right)^2\right]$ – determined from formula (4.10);

$$\sigma_{к\ обш} = 4\frac{0{,}9E}{(b/\delta)^2};\ \tau^э_{обш} = \frac{\tau^p_{обш}}{f} = \frac{\tau^p_{M_{кр}}}{f};$$

$\tau_{к\ обш}$ is determined from formula (4.11).

Here $\sigma_{к\ общ}$ and $\tau_{к\ общ}$ - the critical stresses in the skin section with separate loading of it with normal and tangential stresses.

The strength condition for the same skin under the effect of P^p expresses the requirement for stabilization of the entire panel as a whole (although the skin between the stringers has lost stability):

$$\sigma^p_{общ} \leqslant \sigma_{к\ ср\ кр}. \qquad (4.15)$$

where $\sigma_{к\ ср\ кр} = \sqrt{\sigma_{к\ стр} \cdot \sigma_{к\ общ\ кр}}$ - the average critical stress in the panel;

here $\sigma_{к\ общ\ кр} = \sigma_{к\ общ}\left[1-\left(\frac{\tau^p_{общ}}{\tau_{к\ общ}}\right)^2\right]$. A duralumin skin with a thickness of more than 4-5 mm should not lose stability up to P^p.

The strength condition for this type of skin is

$$\sigma^p_{общ} \leqslant \sigma_{к\ общ\ кр}. \qquad (4.16)$$

3. Skin With Stringer Reinforcement

The stringer reinforcement of the skin - the most broadly employed.

The effectiveness of the stringer and skin combination can be estimated by the specific strength of a reinforced skin panel under compression: $\sigma_{к\ пан}/d$ - by the ratio of the critical stress of the panel to the specific weight of its materials.

If the panel consists of m stringers which have an area of $f_{стр}$ and an interval $t_{стр}$, and of a skin with a width of $B=mt_{стр}$ and a thickness of $\delta_{общ}$, then the critical force of the panel is

$$P_{к\ пан} = m(\sigma_{к\ ср}\delta_{общ}t_{стр} + \sigma_{к\ стр}f_{стр}),$$

where $\sigma_{к\,ср} = \sqrt{\sigma_{к\,общ}\sigma_{к\,стр}}$ - the average critical stress of the reinforced skin, in which the loss of stability of the panel as a whole occurs - the skin with the stringers.

The reduction coefficient of the reinforced skin is

$$\varphi_{общ} = \frac{\sigma_{к\,ср}}{\sigma_{к\,стр}} = \frac{2c\delta_{общ}}{f_{стр}},$$

where $2c \approx (25\text{-}30)\ \delta_{общ}$ - the attached width (the width of the skin section operating in conjunction with a stringer).

The cross-sectional panel area is

$$F_{пан} = m(f_{стр} + \delta_{общ} l_{стр}) = B\delta_{прг} l_{стр},$$

where $\delta_{прг} = \delta_{общ} + \frac{f_{стр}}{l_{стр}}$ - the geometric reduced thickness of the skin. The cited reduced width is $\delta_{пр} = \delta_{общ}\varphi_{общ} + \frac{f_{стр}}{l_{стр}}$.

The critical stress in the panel is

$$\sigma_{к\,пан} = \frac{P_{к\,пан}}{F_{пан}} = \sigma_{к\,стр}\frac{\varphi_{общ} + \dfrac{f_{стр}}{\delta_{общ} l_{стр}}}{1 + \dfrac{f_{стр}}{\delta_{общ} l_{стр}}} = \frac{\delta_{пр}}{\delta_{прг}}$$

From this expression it follows that the greatest value of $\sigma_{к.пан}$ is obtained when $\phi_{общ}=1$, i.e., when $\sigma_{к\ общ}=\sigma_{к\ стр}$.

Usually $\frac{f_{стр}}{\delta_{общ} l_{стр}} = 1-2$.

4. Three-Layered Skin

A three-layered skin consists of two external carrying layers and one internal light layer - the filler (Fig. 4.10). The carrying layers are manufactured from the same materials, as a conventional skin, and porous plastics (foam) with a specific weight of

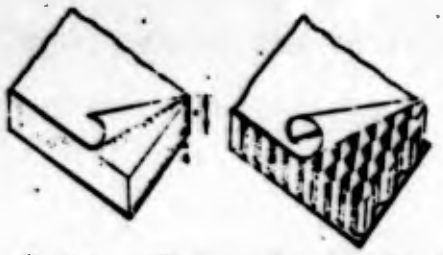

Fig. 4.10. Three-layered skin.

0.05-0.2 g/cm^3 or more frequently honeycombs cell of the same specific weight made from metallic foil with a thickness of 0.05-0.2 mm are employed as the filler. The honeycomb filler is usually manufactured from the same material, as the carrying layers. Steel honeycomb filler is obtained by soldering corrugated foil, duralumin filler - obtained by cementing. The steel honeycomb filler is soldered to the external layers, the duralumin and foam fillers are cemented.

The filler in effect does not render resistance to the tensile and compressive forces acting in the transverse cross section of the skin. These forces are received by the carrying layers. The filler possesses a specific rigidity in the direction perpendicular to the skin, and a rigidity in shear. Thus the filler ensures the joint operation of the carrying layers both in the case of local bending and under the effect of normal and tangential forces in the skin cross section. This substantially increases the flexural rigidity, $\sigma_н$ and $\tau_н$ of the three-layered skin as compared with a single-layer skin; thus a three-layered skin does not require stringer reinforcement and frequently placed ribs. A wing with this type of skin can be lighter. Furthermore, it possesses good thermal insulation properties, which is important for a supersonic aircraft. The high flexural rigidity of a three-layered skin contributes to the retention of aerodynamic wing shapes at high flight velocities. A three-layered skin is manufactured almost without riveted joints, which increases its fatigue strength and improves the surface condition of the wing.

However, the manufacturing and repair technology of a three-layered skin is complex. The mating of skin sections with each other and with other design elements of the wing is complicated, since it is necessary to ensure the joining of not only the carrying layers, but also of the filler.

§ 5. RIBS

Ribs are transverse load-bearing elements of a wing.

The ribs of an unswept wing, and also of swept and delta low aspect-ratio wings are situated along the flow and, therefore, at right angle to the spar postioned perpendicular to the axis of the aircraft (Figs. 3.16; 3.26 and 3.45). In the swept part of a high aspect-ratio-wing in the sections situated at a distance from the wing tip and root, ribs are usually placed perpendicular to one of the spars to reduce their length; only the tip rib and the center section ribs are placed along the flow.

In accordance with their purpose and design formulation ribs are divided into normal and reinforced ribs.

Normal ribs serve to preserve the given shape of the wing profile and to transmit the air load incident on them from the adjacent skin section, to the wing beam. Moreover, they reinforce the skin and the stringers, increasing the critical stress.

Usually the rib interval is t_H=350-1,000 mm. In a monocoque load-bearing wing setup the rib interval is greater than in the spar.

The ribs, just like the spar struts (see § 2), resist wing flattening (the coming together of the compressed and tensioned panels) during flexure. They are loaded in this case by the radial forces from the stringers and the skin connected to them. However, these forces are considerable only where the chord plane has a break (in the case of variation in the dihedral angle).

It should be noted that, if the skin together with the spars represents a tube possessing great inherent (frame) rigidity in the cross-sectional plane, then the role of the normal ribs is

diminished, a considerable part of the air load is transmitted from the skin directly to the spars, bypassing the ribs.

Reinforced ribs, fulfilling the same functions, as normal ribs, have as their main purpose the transmission to the wing beam of the loads acting on them from assemblies installed in the wing (engines, landing gear, lift-increasing devices, etc.), or the redistribution of the internal forces between the wing elements at wing joint sites, in the root and side cross sections and near the edges of large cutouts in the skin. All this determines the sites where the reinforced ribs are situated.

1. Rib Design and Operation

Air loads transmitted from the skin to a rib, and loads applied to a reinforced rib, act in the rib plane and tend to shift (along the vertical) and to turn it relative to the wing beam.

A rib is balanced by the forces acting from the direction of the webs and the skin on the coupling elements, which attach the rib to them.

It is necessary to note the following:

1) air loads are transmitted to a rib in the form of forces normal to the skin surface; in this case the skin loaded by rarefaction forces the rivets attaching it to the rib cap to operate in tension;

2) the loads on a rib form a force and a moment, causing shearing and turning of the rib due to the deformation of the skin, webs and coupling elements by which the rib is fastened to them. By disregarding the flexibility of the latter, it is possible to consider as the center of rotation the center of rigidity of that wing beam cross section near which the rib is located;

3) the reactions of the skin and the webs balancing the rib act in the direction of their greatest rigidity, i.e., at tangents to the contour of the box formed by them.

The rivets which attach the rib to them operate in shear.

Figure 4.11 shows a diagram of the balancing of a reinforced rib and the transmission of forces from the rib to the wing beam.

Beam ribs are the most broadly employed type of ribs. They are more rigid and their design is lighter and more technologically effective in comparison with truss ribs.

Examples of the designs of normal and reinforced ribs are represented in Fig. 4.12a, b, c.

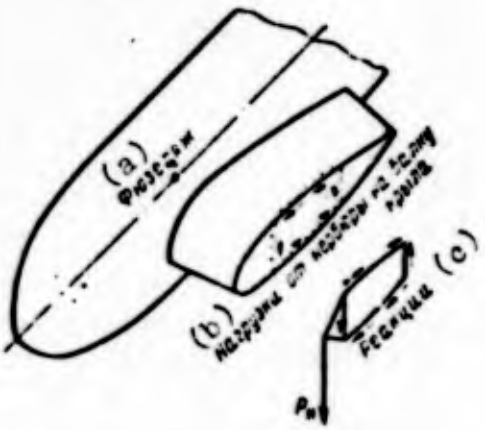

Fig. 4.11. Rib balancing. Key: (a) Fuselage; (b) Loads from the rib on the wing beam; (c) Reactions.

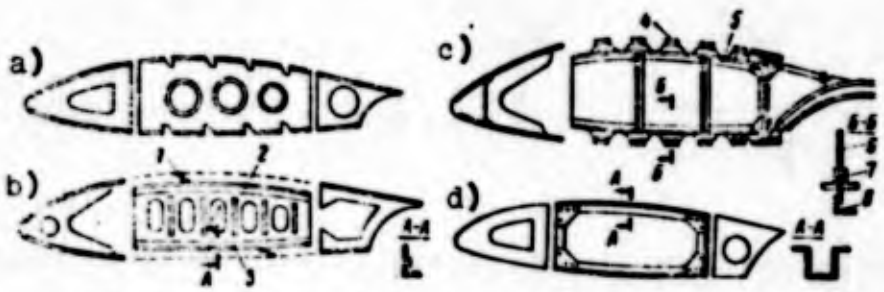

Fig. 4.12. Designs of normal and reinforced ribs: a) stamped beam design; b) beam design with flanges on the interspar part; c) beam reinforced design; d) frame (flange) design; 1 - stringer; 2 - ridge; 3, 5, 7 - the rib flanges; 4, 8 - compensators; 6 - rib web.

Ribs, as a rule, consist of three parts: leading-edge, interspar and trailing-edge parts. The simplicity of the design of beam ribs is explained by the fact that many of their parts are manufactured by stamping from sheet material.

A normal rib is connected with the skin by means of the flanges obtained during stamping (see Fig. 4.12a and 4.13a). Since cut-outs are made in a rib at the bottom and top for stringers, the role of the flanges in this type of rib is performed by the skin. If this is insufficient due to the small thickness of the skin, then flanges of usually angle cross section are riveted to the rib web.

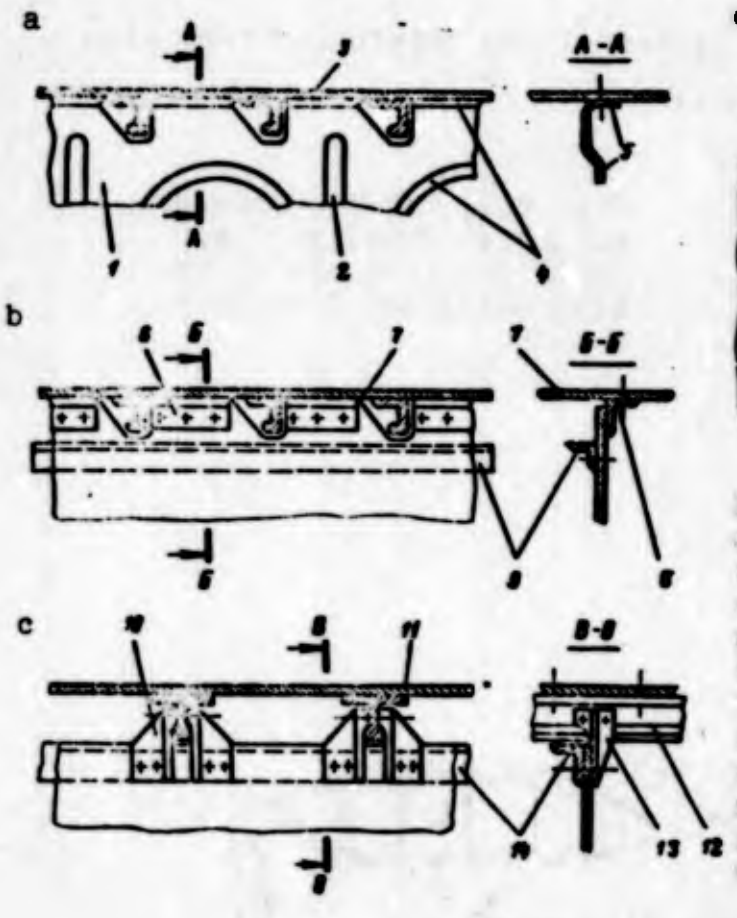

Fig. 4.13. Diagrams of the attachment of skin to ribs (a, b, c) and of a reinforced rib to a spar: 1 - web; 2 - ridge; 3, 7, 11, 16 - skin; 4, 5 - flange; 6, 8, 10, 13, 15 - compensators; 9, 14, 22 - rib flanges; 12 - stringer; 17 - fitting; 18 - spar flange; 19 - spar web; 20 - the strut; 21 - rib web.

Frequently the rib web thickness is made greater than is required due to strength conditions. Then holes with flanging are stamped in it to lighten it. The flanges on the hole contours, and also the ridge (Fig. 4.12b) increase the rigidity of the rib webs.

The joining of the skin with a rib in a number of cases is carried out with the aid of so-called compensators (Fig. 4.13b, d), which makes it possible to more accurately hold the assigned wing profile shape. Sometimes for purposes of improving the skin surface or decreasing the volume of riveting work the skin is fastened only to the stringers (Fig. 4.12b, c and 4.13c).

In such designs the transmission of both the air loads (along normals to the skin contour) and reactions in balancing a rib (along tangents to the skin contour) to the rib occurs via the stringers and compensators.

The ribs are fastened to the spar webs by means of struts (see Fig. 4.3).

Reinforced beam ribs have more powerful flanges and webs; their webs are reinforced by struts (see Fig. 4.12c).

The concentrated loads acting on reinforced ribs, create in their cross sections, especially near the spars, great concentrated moments and transverse forces. This requires extremely good attachment of both the rib web and its flanges to the spar, usually by means of special fittings (Fig. 4.13d).

Frame (flange) ribs are employed as normal ribs in such cases when this is necessary due to the design conditions, for example, at the sites of the accommodation of fuel tanks in the wing (Fig. 4.12d). Since the flanges of a frame rib are separated, then each operates in flexure as a beam of low height. The air load from the upper skin is transmitted to the upper rib flange, and to the lower rib flange from the lower skin. A conventional beam rib operates as a beam with full design height similar to a spar (Fig. 4.14).

The height of a frame rib flange is low; therefore it is possible to obtain the required moment of inertia of its cross

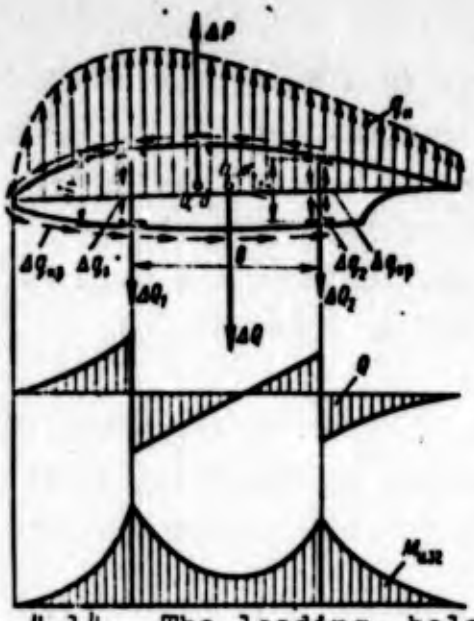

Fig. 4.14. The loading, balancing and operation in shear and flexure of a normal rib.

section only as a result of a considerable increase in the flange width and the thickness of its elements. In summation, the weight of a frame rib is greater than a beam rib.

Truss ribs are employed mainly in the designs of light aircraft wings with a linen skin. It is possible to employ them on prospective (future) aircraft in accordance with the same considerations, as truss spars.

2. Calculating Rib Strength

Let us examine the sequence of rib strength calculation.

The main load for rating a normal rib is the air load which is transmitted from a wing strip with a width equal to the rib interval $t_{нер}$. The resultant of the air load on a rib is (see Fig. 4.14)

$$\Delta P = q_y l_{нер},$$

where q_y - the value of the linear air load (distributed along the wing span) of the rib in question.

In designing reinforced ribs the air load is considered just as for normal ribs, but the main loads for them are those loads, for receiving of which they are specially placed: from the landing gear attachment assemblies, the engines or from the load-bearing elements of the wing. The loads are determined from an examination of the basis of these designs for the rib being rated.

In rating the ribs the relieving of their mass forces of the design is not taken into account.

The subsequent sequence in designing is common for normal and reinforced ribs. Let us analyze it as illustrated by a normal rib on which air load ΔP is acting.

All three sections of the rib are connected with each other and the rib is examined as one whole.

A rib is examined as a beam which rests along its contour on the skin and spar webs.

The load on the rib is introduced in the form of force $\Delta Q=\Delta P$ applied at the center of rigidity of the wing beam cross section at that site where the rib is located, and which turns the rib relative to the center of rigidity of moment $\Delta M_{кр}$. Force ΔQ and moment $\Delta M_{кр}$ represent additions to the transverse force and torsional wing moment created by the rib.

The reactive tangential force flows which balance a rib (see Fig. 4.14) are determined with the formulas:

$$\Delta q_i = \frac{\Delta Q_i}{H_{pi}} = \frac{\Delta Q}{H_{pi}} \cdot \frac{I_i}{\Sigma I_i}; \quad \Delta q_{кр} = \frac{\Delta M_{кр}}{2F_к},$$

where ΔQ_i - the load on the web of the i-th spar due to force ΔQ; I_i - the moment of inertia of the i-th spar; $F_к$ - the total area of the contours of the leading-edge and interspar part of the cross section.

The flow $\Delta q_{M_{кр}}$ in the web of the leading-edge spar and in the skin of the trailing-edge section of the cross section is assumed approximately equal to zero.

For plotting the diagrams of Q and $M_{изг}$ of the rib we load it with load $q_н$, equivalent to ΔP and distributed in accordance with the diagram of the pressure distribution along the wing chord.

The approximate form of the diagram of Q and $M_{изг}$ due to $q_н$ and the reactive tangential forces is given in Fig. 4.14.

Using the values of Q and $M_{изг}$ the web and the flanges of the rib are checked for strength in the same way as the corresponding spar elements.

3. Characteristics of the Design and Operation of the Ribs of the Root Part of a Swept Wing

Root rib. In swept wings of spar load-bearing design reinforced root rib 2-3 (Fig. 4.15b) is necessary for transmitting torsional moment from the removable part of the wing to the center section.

The basic load for the root rib is the torsional wing moment. It is removed by the rib from the skin via the riveted joint and is transmitted in the form of a pair of forces to assemblies 2 and 3.

Figure 4.15a shows the flow of tangential forces due to torsional moment, the reactions $R_{нк}$ which balance the rib and the form the transverse force and bending moment diagrams.

The values of the transverse force and the bending moment for the rib cross sections in the section between the spars are determined by the formulas:

$$Q_x = R_{нк} - q_{м_{кр}} H_x;$$

$$M_x = R_{нк} x - 2q_{м_{кр}} F_x,$$

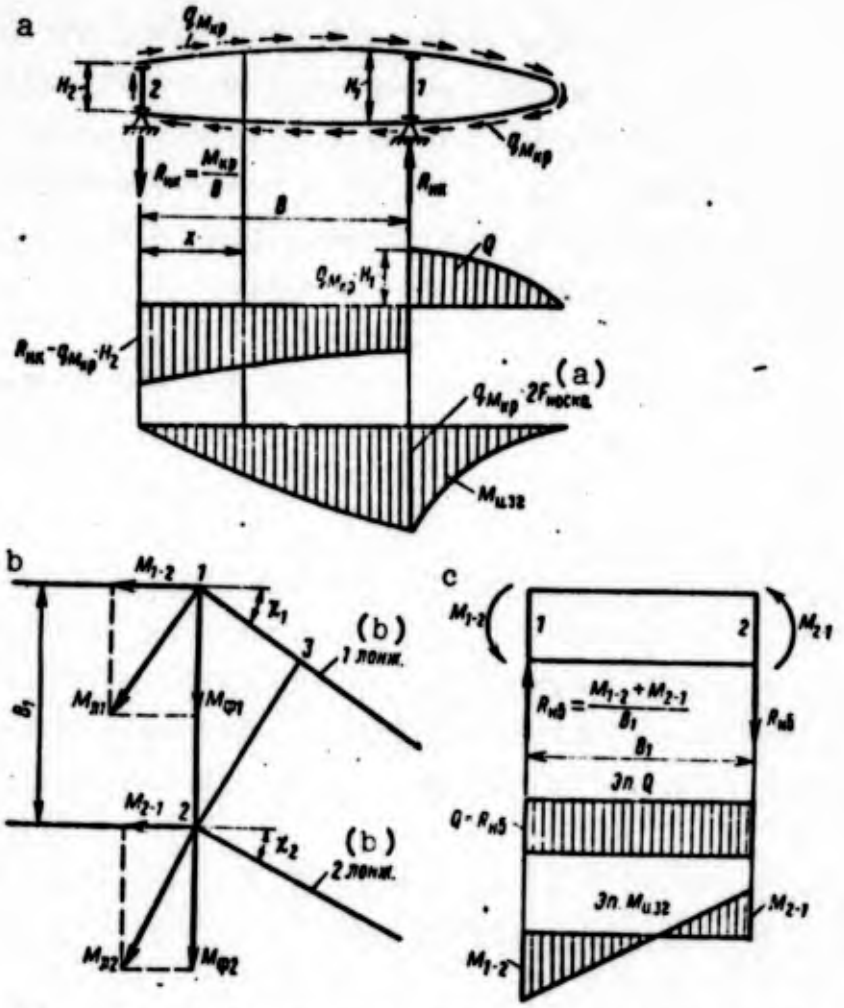

Fig. 4.15. The loading and operation of the root (a) and side (b and c) reinforced ribs of the swept wing of a spar load-bearing setup.
Key: (a) leading edge; (b) spar.

where H_x - the height of the rib in the cross section with coordinate x; $F_x \approx x\frac{H_2+H_x}{2}$ - the area of the section of the rib contour from H_2 to the cross section; H_2 - the height of the rib at the second spar.

The flow of tangential $q_{M_{кр}}$ is assumed constant along the rib contour, and in the web of the leading-edge spar - it is assumed equal to zero.

In the absence of a root rib the forces in the skin are transmitted to the side rib and will cause its loading both by the forces

situated in the rib plane and those directed along the normal to it. This is impermissible in a spar setup wing where the skin ends at the side rib, since the forces normal to the rib plane, will bend it in the plane of least rigidity. In a monocoque wing the forces, normal to the side rib plane, are transmitted to the continuation of the wing box passing through the fuselage.

Side rib. Let us examine the loading and the operation of the side wing rib of the spar load-bearing setup depicted in Fig. 4.15b.

A fracture in the longitudinal load-bearing elements of a swept wing occurs in the majority of cases at the side of the fuselage. In connection with this the bending moments of the wing spar near the fracture load not only the spars of the fuselage part of the wing, but also the side rib with concentrated moments.

Figure 4.15b shows the resolution of the vectors of bending moment $M_{л1}$ and $M_{л2}$ in assemblies 1 and 2.

Moments $M_{ф1}$ and $M_{ф2}$ are received by the spars of the fuselage part of the wing. Moments M_{2-1} and M_{1-2} load side rib 1-2.

From an examination of Fig. 4.15c it is evident that the large forces Q and $M_{изг}$ in the cross sections of side rib require the thickening of its web and powerful flanges which approach (with large χ) along their cross sections the web and the flanges of the spars of the fuselage part of the wing.

§ 6. DESIGN AND OPERATION OF A WING IN THE REGION OF A CUTOUT IN THE SKIN

For access to the fuel tanks, units of the fuel system and the control units, for the retraction of the landing gear cut-outs are made in the wing skin. These cutouts disrupt the continuity of the

skin and stringers and thereby affect the operation of the wing. The degree of the effect depends on the size of cutout and its design shape.

Small cutouts in wing, as a rule, are compensated for, by ensuring wing strength by installing a rigid frame with an easily removable cover with locks or framing with a power cover held by screws along the contour of the cutout. The second method of compensation is employed in cases when the cover covering the cutout is rarely removed in operation.

In both cases of compensation the cutouts practically do not affect the total wing strength, since those forces which must be transmitted through the cutout section of the panel are transmitted through the compensating element.

The design which compensates for the cutout should satisfy not only the strength requirement, but also the rigidity requirement. It is desirable that the rigidity of a frame or load-bearing cover be the same as the rigidity of the cutout section of the panel. Otherwise a stress concentration arises - an increase in the stresses either in the elements adjacent to the cutout if the compensating structure is readily deformed, or in the compensating structure if its rigidity is excessive.

When this requirement is not met the fatigue life of the wing is reduced.

Large cutouts are compensated for and not compensated for.

Compensation for large cutouts is accomplished by inserting detachable load-bearing panels, similar in construction to the adjacent wing section. The reliable joining of the detachable panels with the wing restores the disrupted load-bearing couplings and ensures the full-valued transmission of forces due to bending and torsion (Fig. 4.16).

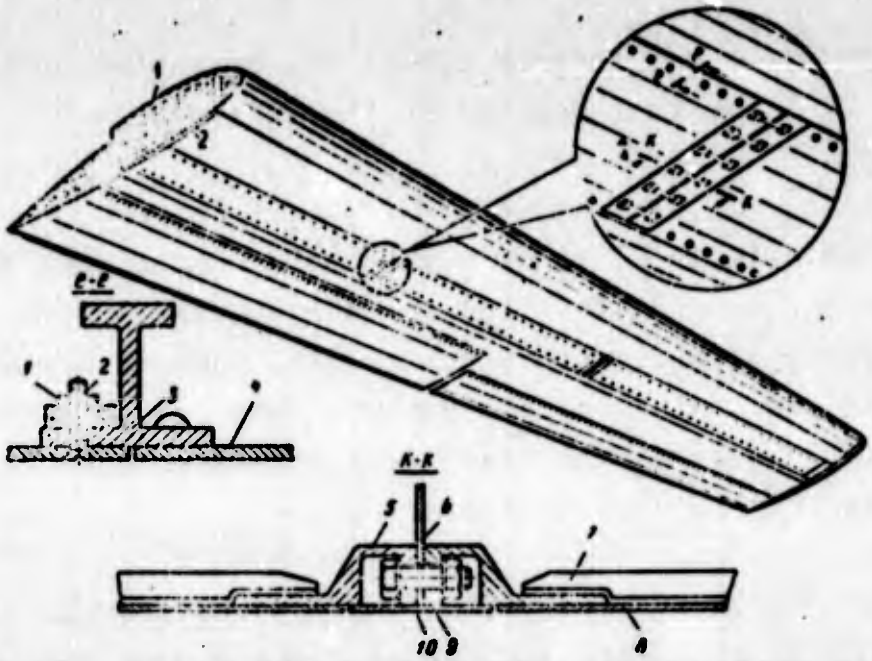

Fig. 4.16. Detachable load-bearing panels which compensate for a large cutout in a wing: 1 - floating nut; 2 - screw; 3, 7 - stringers; 4, 8 - skin; 5 - joint profile; 6 - web of detachable rib; 9 - overlapping strip; 10 - bolt.

It is not always possible to compensate for large cutouts in a wing: for example, a cutout under the landing gear which retracts into the wing. The installing of a frame along the contour of a large cutout is unfavorable in a weight regard.

If a large cutout is not compensated for, then the stressed state of the wing in the cutout section and near it varies considerably.

Let us briefly examine the operation of a two-spar wing with a cutout in the lower skin under the effect of forces Q, $M_{изг}$ and $M_{кр}$.

Transverse force Q (passing through the center of rigidity) loads the spar webs. Since the webs are continuous, then a cutout in the skin does not affect the forces in them due to Q.

Bending moment $M_{изг}$ loads the panels with axial forces. If the skin and the stringers do not participate in receiving the

axial force (the load-bearing setup of the wing is a purely spar design), then the nature of wing operation does not change. If the skin and the stringers participate in receiving the axial force, then in the cutout where they are interrupted, a redistribution of the forces occurs between the panel elements.

In cross section 2-2 (Fig. 4.17a) rather distant from the cutout, the skin, the stringers and the spar flanges which are parts of the composition of the panel, receive forces $P_{обш}$, $\Sigma P_{стр}$, $P_{п1}$ and $P_{п2}$ in accordance with the values of their reduced areas.

The edges of the cutout are limited by ribs. The flexural rigidity of a rib in the chord plane is insignificant; thus the stresses in the skin and the stringers $\sigma_{обш}$ and $\sigma_{стр}$ at the edges of a cutout are equal to zero and in cross section 1-1 the forces are transmitted only through the spar flanges.

If we arbitrarily assume that $M_{изг}$ in a wing section between cross sections 1-1 and 2-2 does not change, then the force in the flange of the first spar along cross section 1-1 will be

$$P_1 = P_{п1} + \frac{P_{обш} + \Sigma P_{стр}}{2}.$$

Expression P_2 - the force in the flange of the second spar - has a similar form.

The transmission of axial forces from the spars to the skin and stringers occurs within the limits of the so-called zone of inclusion due to the tangential forces q in the skin.

The zone of inclusion of the skin and the stringers operating in σ as investigations have shown, takes the form of an area limited by a curve of the type shown in Fig. 4.17a. It is usually assumed, that C=B, where B - the distance between the continuous elements (spars).

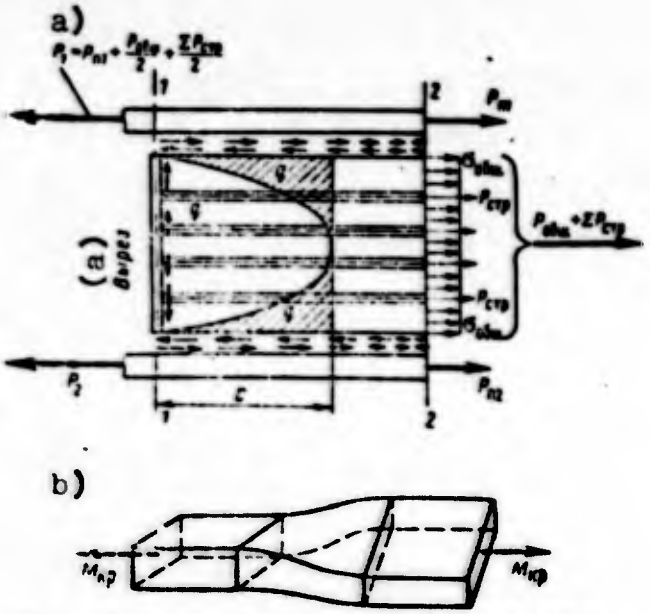

Fig. 4.17. Large uncompensated cutout in a wing: a) redistribution of forces due to $M_{изг}$ between load-bearing elements of a wing in the cutout region; b) wing deformation in the cutout section due to $M_{кр}$.
Key: (a) Cutout.

Torsional moment up to the cutout, where the contour is closed, loads the skin and the spar webs with a flow of tangential forces. At the cutout the rib removes the flow of tangential forces due to $M_{кр}$ from the upper and lower skins and additionally loads the spar webs. The spars begin to operate in flexure. Finally, the torsional moment acting on the wing, causes flexural torsion in the wing section with the cutout.

The nature of wing deformation in the cutout section is shown in Fig. 4.17b. The presence of an uncompensated cutout during wing bending and torsion makes it necessary to:

install reinforced ribs at the edge of the cutout;

reinforce the spar flanges and webs;

reinforce the skin in the region of the cutout to receive additional tangential forces q and for earlier inclusion of the skin.

Everything that has been said about wing operation in the cutout region due to Q, $M_{изг}$ and $M_{кр}$ also completely pertains to the zone near the wing joint with point attachment and to the section of the fuselage with an uncompensated cutout.

§ 7. DESIGN AND OPERATION OF A WING AT A JOINT

For satisfying the operational and technological requirements aircraft wings are made jointed.

The wings of low weight aircraft usually have two joints, the wings of heavy aircraft - up to four joints.

Increasing the number of joints simplifies the manufacture and repair technology of a wing. However, the larger the joints, the more complex is the wing design and greater is its weight. The designs of attaching one part of a wing to another at a joint can be reduced to two types: point attachment and contour attachment.

The initial loads on attachment assemblies are the loads which act on the parts being joined together. But to ensure sufficient reliability designwise of complex assembly joints aircraft strength standards introduce the additional safety factor $f'=1.25$. Thus, the calculated loads for the assembly joints of the components are $P_{узла}=1.25P_{дет}$.

1. Point Attachment

Point attachment is employed on wings of the spar load-bearing type of setup. The load-bearing elements of these types of wings delivering forces to a joint are only spars. Joint assemblies are also attached to them (Fig. 4.18a, b, c, d, e).

The skin, stringers and reinforced (joining) rib at a wing joint operate as in the zone of an uncompensated cutout. At the joint of a swept wing an additional redistribution of the forces between load-bearing elements occurs, which is carried out by the root and side ribs; their operation was examined earlier.

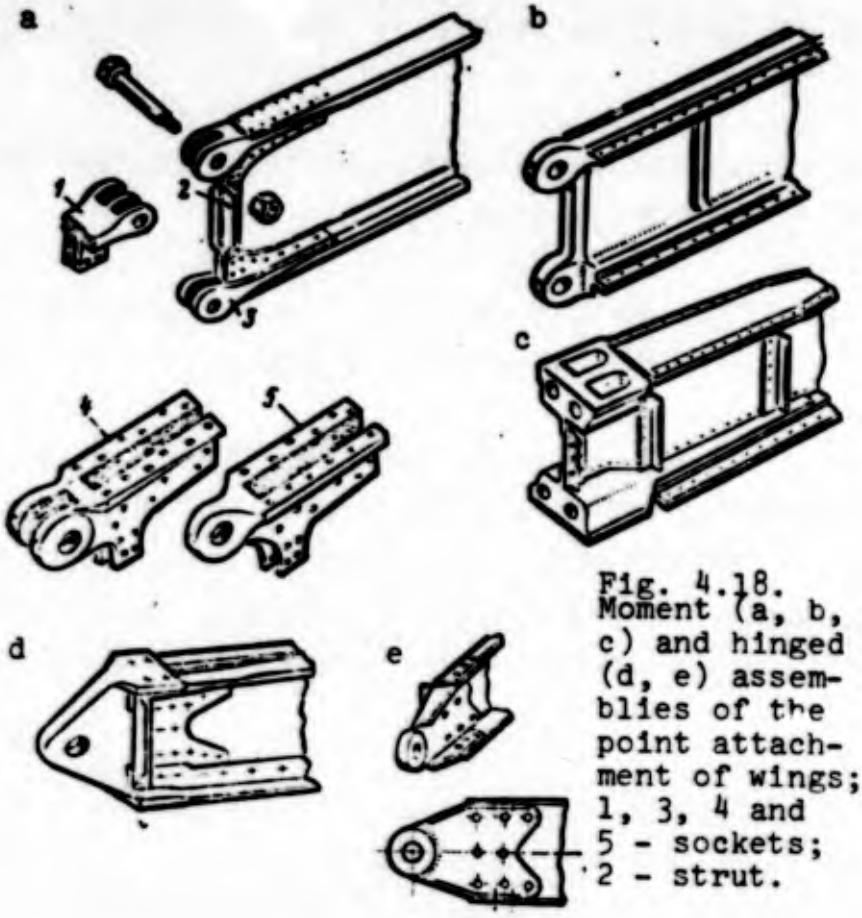

Fig. 4.18. Moment (a, b, c) and hinged (d, e) assemblies of the point attachment of wings; 1, 3, 4 and 5 - sockets; 2 - strut.

The joint assemblies transmitting forces and bending moment, are usually called moment assemblies (Fig. 4.18a, b, c). The assemblies transmitting only forces, are called hinged, or momentless assemblies (Fig. 4.18d, e).

The number of moment and momentless assemblies in a wing joint is determined by its load-bearing setup. Thus, the detachable part of a wing is fastened to the center section in a one-spar cantilever wing with one moment assembly and one momentless assembly; this type of attachment is called a three-point attachment; in a two-spar cantilever wing - by two moment assemblies, this type of attachment is called a four-point attachment (Fig. 4.19a).

The design of a broadly employed type of moment assembly is represented in Fig. 4.18a. Its basic elements are: two sockets made from high-strength steel, a reinforced strut and bolts.

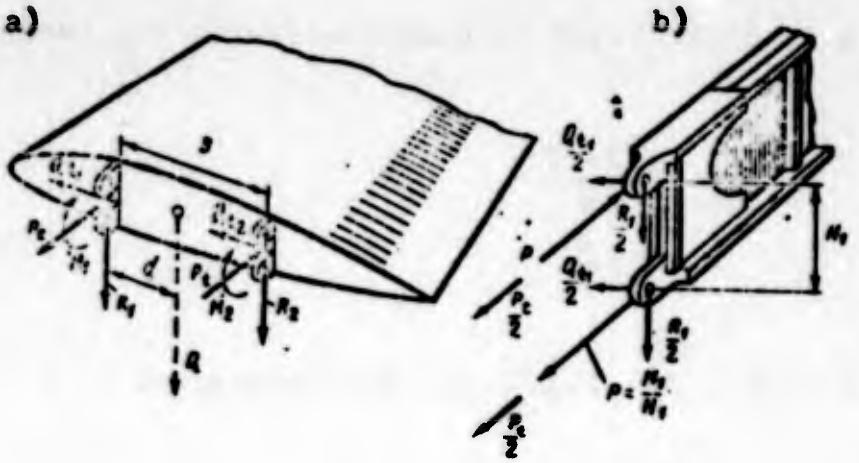

Fig. 4.19. Towards rating a point attachment: a) forces in the moment assemblies of a point attachment of a detachable wing section; b) distribution of forces between the sockets of an assembly.

The joint assembly depicted in Fig. 4.18b, is made of one forging together with the flanges and the web. The assembly positioned under it (see Fig. 4.18c) has duralumin sockets and steel bolts operating in tension.

Milled and welded momentless joint assemblies are depicted in Fig. 4.18d, e.

Let us examine the sequence in determining the loads on the attachment assemblies of unswept and swept wings with spar-type load-bearing setups.

Unswept wing. The following rated destructive forces act in the joint plane of an unswept wing: $M_{изг}$; Q; Q_t and M_t. In determining Q taper is not taken into account, since the center section does not have it. In the rating of point attachment assemblies the determining of forces Q_t and M_t acting in the chord plane is mandatory.

Let us examine the distribution of the indicated forces between assemblies as illustrated by a two-spar wing (Fig. 4.19a). The additional safety factor f; is introduced into the calculation.

The bending moment $M_{изг}$ is distributed proportional to the inertia moments of the spars. For example for assembly 1:

$$M_1 = f' M_{изг} \frac{I_1}{I_1 + I_2}.$$

Transverse force Q is distributed in accordance with the lever rule:

$$R_1 = f'Q\frac{B-d}{B};$$

$$R_2 = f'Q\frac{d}{B}.$$

Force $Q_t = Q\frac{c_t}{c_y}$ and moment $M_t = M_{кр}\frac{c_t}{c_y}$ are distributed as follows:

$$Q_{t1} \approx Q_{t2} \approx f'\frac{Q_t}{2};$$

$$P_t = f'\frac{M_t}{B}.$$

The distribution of forces between the sockets for the front spar assembly is given in Fig. 4.19b.

The distribution of R_1 and Q_{t1} is approximate, based on the assumption of equal rigidity of the sockets.

Swept wing. In this case let us examine the distribution of forces between the assemblies as illustrated by a one-spar wing (three-point attachment).

The attachment assemblies of the swept detachable part of the wing to the unswept center section are usually made so that the axes of the joining bolts are perpendicular to the axes of the center section spar (Fig. 4.20).

The moment in the joint (relative to the axis parallel to the chord of the joint) is

$$M = f'M_\phi = f'P_{\text{оч}}c.$$

In a one-spar wing this moment is completely received by the moment assembly joining the center section spars and the detachable part.

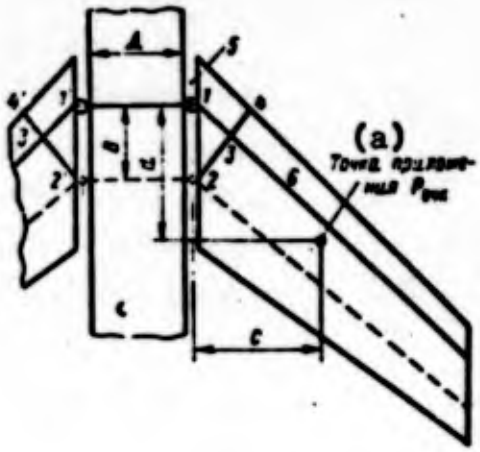

Fig. 4.20. Design of a swept wing of the spar-type load-bearing setup at the joint: 1-2 - side rib; 2-3-4 - root rib; 5 - joining bolt axis; 6 - spar.
Key: (a) Point of application of $P_{очк}$

The transverse force as for an unswept wing, is distributed in accordance with the lever rule between moment assembly (R_1) and hinged assembly (R_2). However, if in an unswept wing each of the forces R_1 and R_2 is less than f'Q, then in a swept wing $R_2 = f'Q\frac{d}{B} > f'Q$.

The distribution of moment M_t between the assemblies occurs as for an unswept wing. Force Q_t is not distributed. It is approximately assumed, that it is received by the front assembly as more rigid.

The breakdown of the forces between the sockets of a moment assembly is similar to that given in Fig. 4.19b.

2. Contour Attachment

Contour attachment is employed in the designs of monocoque wings.

In contour attachment the joint assemblies are positioned along the outline of the box cross section, by carrying out the load-bearing connection of the wing elements, in this manner going into the joint: the skin, stringers, flanges and spar webs. Thanks to this the load-bearing elements near the joint completely participate in the operation in normal and tangential stresses.

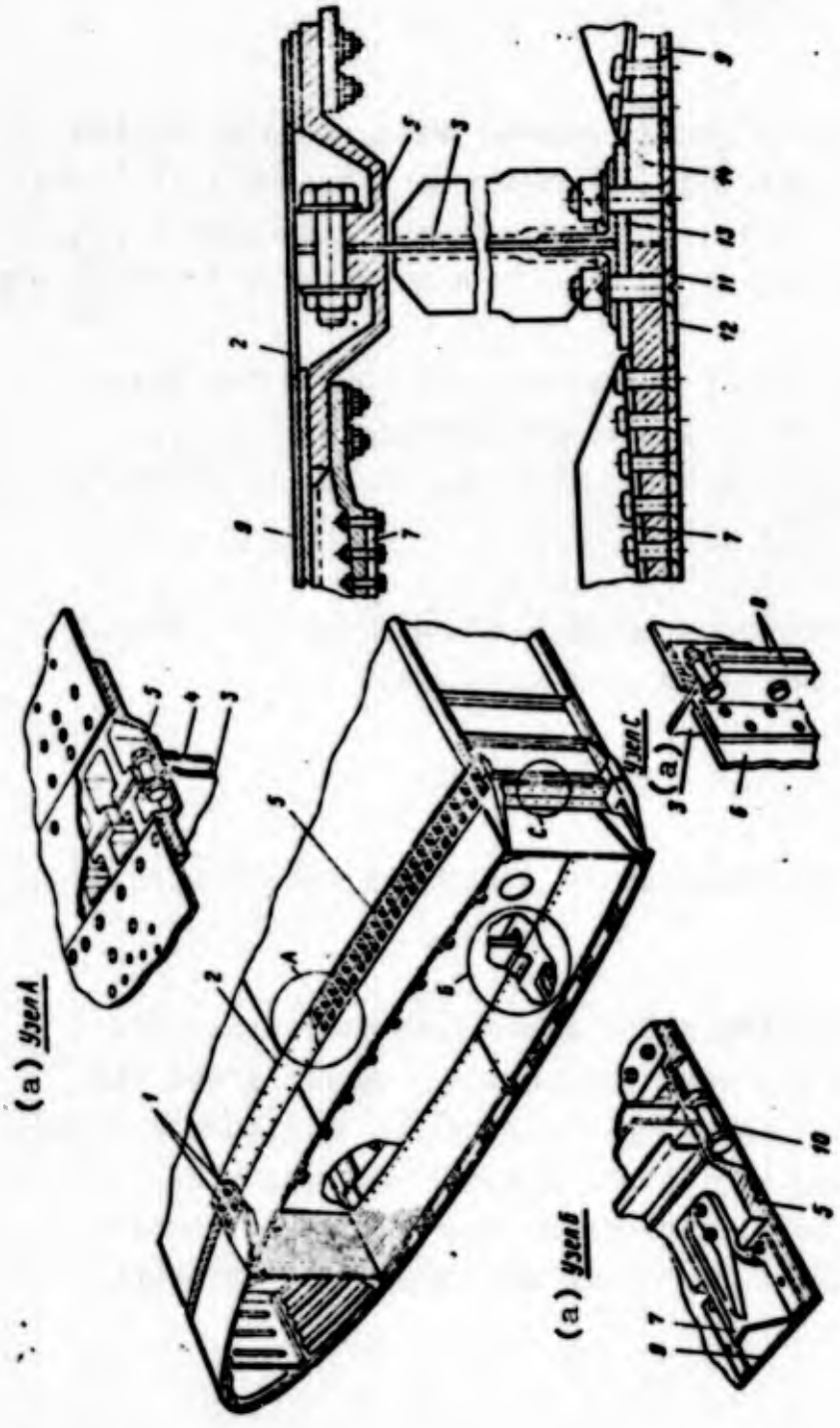

Fig. 4.2.. Contour attachment: 1 - pinch bolts of the spar flange; 2 - overlapping strip; 3 - web of a detachable rib; 4 - rib; 5 - joint profile; 6 - spar web; 7 - stringer; 8 - joint struts; 9 - skin; 10 - pinch bolt of a panel operating in tension; 11 - joint bolt of a panel operating in shear; 12 and 13 - lower and upper joint strips; 14 - joint plate. Key: (a) Assembly.

A contour attachment is usually made from joint profiles fastened to the panels of the wing parts being connected, the joint struts fastened to the spar webs, and pinch bolts 1, 10 (Fig. 4.21).

Sometimes underneath instead of joint profiles joint plates and strips 14, 12 and 13 are installed.

For tight fitting of the wing parts being joined their faces are milled.

Due to technological considerations the width of the well in a joint profile is made somewhat larger than the diameter of the bolt; therefore the bolts securing

the panels do not receive shear; they are loaded only with the axial forces for which they are designed.

The torsional moment in a joint is transmitted by the bolts fastening the spar webs. These bolts have a high-quality fit. For transmitting part of $M_{кр}$ further to the skin two ribs are installed at the joint.

In a contour attachment design where joint strips with joint plates are employed the bolts operate in shear.

Let us examine the sequence of determining the loads on the bolts of a contour attachment due to $M_{изг}$, $M_{кр}$ and Q (moment M_t and force Q_t in this case are not taken into account due to their small effect on each joint bolt).

A diagram of the forces in a joint reduced to the center of rigidity (c.r.) is shown in Fig. 4.22a.

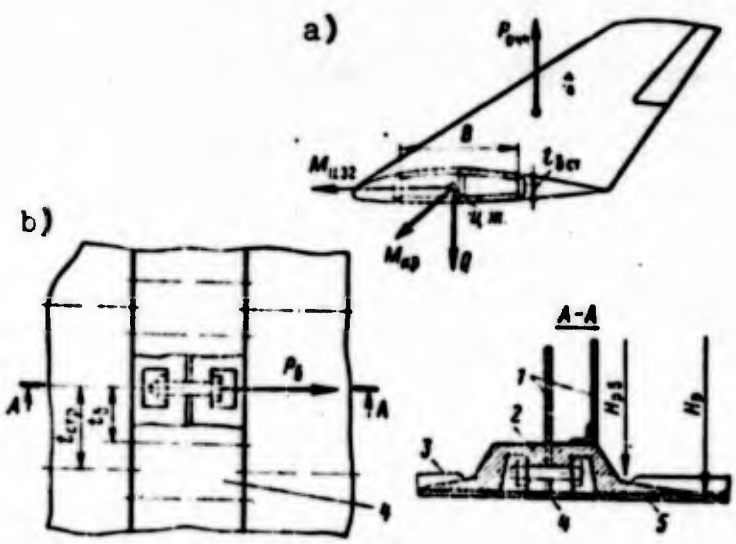

Fig. 4.22. Towards the rating of a contour attachment: a) forces in the joint; b) loading of a panel bolt (bottom view); 1 - rib; 2 - joint profile; 3 - stringer; 4 - overlapping strip; 5 - skin.

The tensile load on one panel bolt due to $M_{изг}$ (Fig. 4.22b) is

$$P_б = f' \frac{H_р}{H_{р.б}} \left(\sigma_{обш} \delta_{обш} l_б + \sigma_{стр} f_{стр} \frac{l_б}{l_{стр}} \right).$$

The tensile load on one spar flange bolt is

$$P_{б.п} = f' \frac{H_{р.п}}{H_{р.б.п}} \cdot \frac{\sigma_п F_п}{n}.$$

Here $\delta_{обш}$ and $f_{стр}$ - the thickness of the skin and the cross-sectional area of the stringer; $\sigma_{обш}$, $\sigma_{стр}$ and $\sigma_п$ - the normal calculated rupture stresses in the skin, stringers and spar flanges; $H_р$, $H_{р.п}$, $H_{р.б}$ and $H_{р.б.п}$ - respectively the working heights of a panel, a spar flange, panel bolts and flange bolts (see Fig. 4.22b); $F_п$ - the cross-sectional area of a spar flange; $t_б$ and $t_{стр}$ - the panel bolt interval and the stringer interval; n - the number of flange attaching bolts.

The shearing load on one spar web attaching bolt is

$$T = f' q_{ст i} t_{б\,ст},$$

where $q_{ст\ i} = q_{Qi} \pm q'_{M_{кр}}$ - the total flow of forces in spar web i; $q_{Qi} = Q_i/H$ - the flow of forces in spar web i due to $Q_i = Q\frac{I_i}{\Sigma I}$; $q'_{M_{кр}} = M_{кр}/BH$ - the flow of forces in spar web i due to $M_{кр}$; $t_{б\ ст}$ - the flange attaching bolt interval (see Fig. 4.22a); $H_{р\ i}$ - the working height of spar i.

§ 8. CHARACTERISTICS OF THE DESIGN AND THE RATING OF ROTOR BLADES

1. Design Characteristics of Rotor Blades

The load-bearing elements of a blade, just like those of a wing, are the spars, the ribs, the stringers and the skin. However, the blade design has its own characteristics caused by its loading and attachment.

For more convenient attachment of the blades to the hub they are made in accordance with a single-spar setup.

A spar operates in tension due to the longitudinal forces, in flexure, shear and torsion due to the transverse loads. The remaining elements (ribs, stringers and skin) ensure the preservation of the shape of the blade profile and the transmission of the aerodynamic loads to the spar.

Blades are mixed, wooden and metallic in construction.

Metallic olades have received broad application; they have high reliability in operation, sufficient strength, prolonged service life and comparatively light weight.

At first metallic blades were of riveted construction.

Subsequent refinement of metallic blades proceeded along the path of improving spar design and the methods of joining metallic parts with each other, in particular the replacement of riveted and bolt joints by adhesive joints. The employment of adhesive joints in blades reduced the stress concentration to a minimum and made it possible to improve the fatigue characteristics and to increase blade service life.

At the present time all-metal blades consisting of a spar, individual shaped compartments (sections) not connected with each other, root part, tip and root fairings (Fig. 4.23) have obtained wide acceptance.

The spar is made in the form of a steel tube with a cross section of circular or oval shape (Fig. 4.23b) or in the form of a pressed duralumin beam (Fig. 4.23c).

Cold-rolled tubes made from high-grade alloy steel of the 30KhGSA or 40KhNMA type quenched and tempered to $\sigma_в$=110-130 kgf/mm^2 are being employed. The external and internal surfaces of the tube are polished.

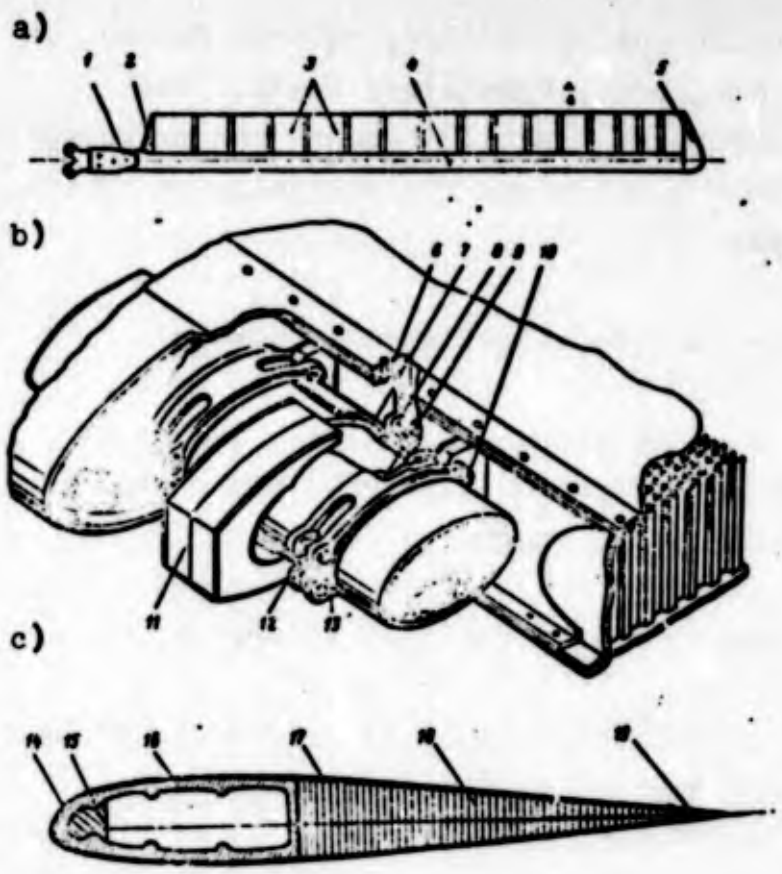

Fig. 4.23. Design of a metallic blade: a) blade in assembled form; b) attachment of the rear section to the spar; c) cross section of metallic blade with duralumin spar; 1 - root part; 2 - root fairing; 3 - profiled sections; 4 - spar; 5 - tip fairing; 6 - rear socket; 7 - journal; 8 - tubular spar; 9 - clamp; 10 - clamp attachment to rear section; 11 - foam-plastic unit; 12 - cross piece; 13 - strip; 14 - safety covering; 15 - weight compensator; 16 - spar; 17 - skin; 18 - honeycomb filler; 19 - stringer.

The duralumin spar is a beam with an internal cavity of constant cross section. On the outside the beam is machined in accordance with the theoretical contour of the blade.

Both steel and duralumin spars undergo work hardening which increases the fatigue life of the blade.

The spar cross section along the blade varies in accordance with the variation in bending moment and axial force.

The profiled sections of the blade are fastened to the spar and transmit aerodynamic loads to it which act on the sections.

Each blade section with a tubular spar consists of leading and trailing sections. In a blade with a box-shaped duralumin spar there is no leading section, the spar itself replaces it (see Fig. 4.23c).

Recently sections consisting of a thin upper and lower skin with an internal honeycomb filler made from metal foil (see Fig. 4.23b) or fiberglass laminate foil have been receiving broad application.

The attaching of the sections to the spar is made employing glue or special clamps (see Fig. 4.23b), which makes it possible to avoid apertures in the spar where fatigue cracks arise with alternating loads. The employment of individual sections in the design makes it possible in production to readily ensure blade twist, and in the case of damage to one of the sections to replace it, without replacing the entire blade.

The root part of a spar is usually made thick at the root end of the blade; this is necessary for attaching the blade to the hub.

A rotor blade has a pneumatic system for signaling spar damage. The internal cavity of the spar is filled with air up to a pressure which exceeds the pressure at which the signal indicator begins to operate. In the case of the appearance of cracks on the spar the pressure in it drops and the visual signal indicator begins to operate.

To prevent blade flutter in the leading edge of a spar (see Fig. 4.23c) or the leading edge part of a blade section weight compensators are installed. Moreover, at the end of each spar under the tip fairing a balancing weight is installed which serves to equalize the blade static moments relative to the axis of rotation of the rotor. The weight consists of a set of steel plates (Fig. 4.24).

Recently for manufacturing even larger rotor blades new plastic materials have been employed, the physicomechanical properties of which make it possible to obtain blades with a considerably greater safe service life.

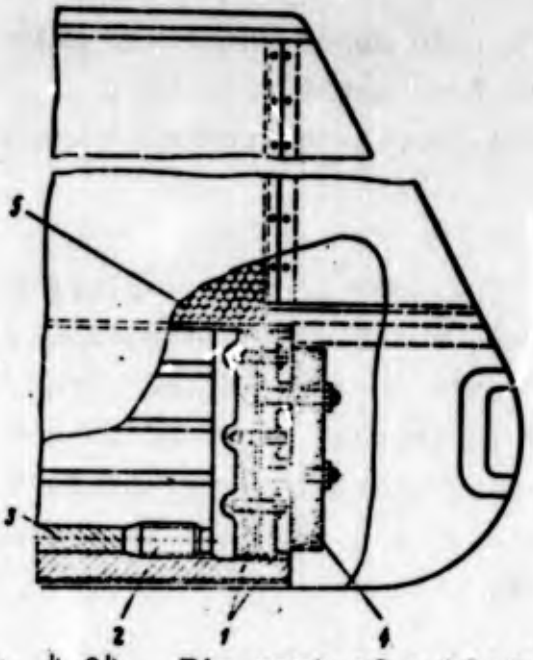

Fig. 4.24. Tip part of a blade: 1 - signaling system plug; 2 - screw stop; 3 - weight compensator; 4 - balancing plates; 5 - tip part of the section.

The design of these types of blades is similar to the design of a metal blade with a box-shaped duralumin spar.

2. Characteristics of Blade Stress Analysis

Of all the possible loading cases the most dangerous for blade strength are the following:

a) blade bending due to its impact against the droop stop upon the dropping of the blade when the air moving up through the blade ceases to support it at the moment of its stopping, when centrifugal forces are practically absent;

b) blade loading in a low flight velocity regime when the flight velocity is 3-8% of the blade tip speed ($\mu=V/\omega R=0.03-0.08$)

c) blade loading during flights at cruising and maximum velocities.

Blade analysis upon its dropping on the droop stop. When a rotor blade drops it impacts about its droop stop. As a result of the accelerations imparted sections of a blade are loaded with mass forces.

The calculated bending moment in any cross section, which arises upon the dropping of the blade on the stop, can be found with the following formula

$$M_{max} = fn^2 G'_3 r_{n.t.}$$

where $G'_{л}$ - the weight of a cut-off part of a blade; $r_{ц.т}$ - the distance from the center of gravity of the cut-off part of the blade to the calculated cross section; f - the safety factor; $n^{э}$ - the g-force. With respect to the results of blade tests for drop it is recommended that it be assumed that $n^{э}=4-4.5$.

Strength testing is carried out or the necessary dimensions of the blade cross section elements are determined with respect to the magnitude of bending moment in a cross section.

Blade analysis in various helicopter flight regimes. During helicopter flight constant and variable stresses due to blade bending are added to the constantly acting stresses due to centrifugal forces in the blade. This combination of stresses is serious for blade fatigue design strength.

Especially significant are the variable loads in low and high velocity regimes (cases [b] and [c]). Due to the transverse loads and the centrifugal forces which yield moment equilibrium with respect to the flapping hinge, the blade experiences flexure and tension (Fig. 3.49). The magnitudes of the transverse loads are variable and periodically repeat themselves during each revolution of the rotor, and the centrifugal forces are constant.

As was already mentioned (see § 12, chapter 3), the maximum bending moment is obtained in the cross section near the center of the span, and the maximum axial forces - near the blade root (see Fig. 3.51). In the blade root $M_{изг}$ is insignificant (in the flapping hinge $M_{изг}=0$), and it is possible to assume that up to distance 0.1R the blade spar experiences only tension alone due to the centrifugal forces.

On other blade sections the stresses due to tension and flexure are summed algebraically.

To the normal stresses computed from the known bending moment (as in wing design) are added the tensile stresses $\sigma_{рас}$ due to effect component $N_{цб}$ directed along the blade. The stress in the longitudinal blade element i:

$$\sigma_{рас\,i} = \frac{\varphi_i N}{F_{ред.в} + F_{ред.н}},$$

where N - the longitudinal force in the blade cross section due to the effect of the centrifugal force; $F_{ред.в}$ and $F_{ред.н}$ - the reduced cross-sectional areas of the elements of the upper and lower panels; φ_i - the reduction coefficient of the element.

Thus, in a panel tensioned due to flexure the stresses are usually greater than in a compressed panel, since they are summed with the stresses due to force N.

Usual strength testing by comparing $\sigma^р$ with the destructive stresses is carried out, as for a wing, with respect to the calculated destructive stresses $\sigma^р$ (found from $M_{изг}$ and N): in tension with $k\sigma_в$, in compression with $\sigma_н$.

Determining of fatigue service life of a blade is carried out by the methods examined in chapter 13.

CHAPTER 5

AILERONS AND EMPENNAGE

The empennage: the stabilizer, fin, control surfaces (rudder and elevators), and also the ailerons (in interaction with wing) are the organs of stability and controllability of an aircraft, which ensure stability and controllability (including balancing) relative to the x-, y-, and z-axes in all flight regimes permissible for a given aircraft.

By aircraft stability is understood the ability to return to the original flight regime after the cessation of the effect of external perturbing forces which caused its deviation, by controllability is understood the possibility of changing the flight regime in accordance with the pilot's volition or in accordance with the indications of an automatic control device, by balance is understood the balancing of the moments of all forces relative to the appropriate axis.

For helicopters the functions of the organs of stability and controllability are fulfilled by the rotor and the tail rotor, and sometimes also by design components patterned after aircraft components - stabilizer, fin etc.

For aircraft which take off and land vertically (VTOL) jet controls are additionally installed which ensure stability and controllability at low velocities when conventional control surfaces (elevators and rudder) and ailerons are ineffective.

§ 1. TECHNICAL REQUIREMENTS IMPOSED ON THE ORGANS OF AIRCRAFT STABILITY AND CONTROLLABILITY

Let us dwell on the most important of these requirements.

Aerodynamic requirements: 1) a specific degree of stability and controllability and a specific combination of different types of stability and controllability are necessary.

These requirements are different for different aircraft. Thus, maneuverable aircraft (for example, sport aircraft) should be, with respect to stability, close to neutral, Nonmaneuverable aircraft, which includes all transport aircraft, should be more stable. However, too high a degree of stability has a negative effect on controllability.

The quantitative values of the stability and controllability characteristics are given in the operational and technical requirements imposed on a given type of aircraft;

2) in all flight regimes permissible for a given type of aircraft, there should be no sharp variations in stability and controllability which could lead to catastrophic consequences. It is desirable that considerable variations in the nature of the flow around the organs of stability and controllability begin later than variations in the nature of the flow around the wing and other aircraft components: for all aircraft - at an angle of attack $\alpha > \alpha_{крит}$ of the wing, and for high-speed aircraft, moreover, at a value of $M > M_{крит}$ of the wing;

3) the necessary lateral stability should be ensured, i.e., the correct combination of static directional and transverse stability.

Too great transverse stability leads to the appearance of oscillatory instability; the consequence of excessive directional stability is spiral instability.

In selecting and estimating the dimensions and the arrangement of the organs of stability and controllability, it is not possible to be limited to an examination of static stability and controllability. It is also necessary to consider dynamics.

For example, it is obvious that an aircraft which possesses with a specific weight large moments of inertia relative to the main and central axes I_x, I_y, I_z as a result of the scattered distribution of the masses from the center of gravity, will be more difficult to control.

The effectiveness of the control organs also depends on the forces which damp the oscillations - the additional forces of air resistance which hinder the rotation of the aircraft and are proportional to the angular velocity.

To satisfy the aerodynamic requirements the areas of the ailerons $S_э$, the horizontal fin (elevator unit) $S_{г.о}$ and the vertical fin (rudder unit) $S_{в.о}$, their dimensions and arrangement should be correctly selected.

In contemporary aircraft the magnitude of the load on the wing area is great and thus the wing area is relatively small. This leads to an increase in the effect of the noncarrying parts of the aircraft (the fuselage, the engine nacelles, the landing gear) on stability and controllability, which, in turn, makes it necessary to increase the relative dimensions of the empennage.

The dimensions and the arrangement of the organs of controllability and stability in many respects depend on the purpose of the aircraft and its layout.

In the designing of a new aircraft the statistics of aircraft which are near in purpose and layout which have been produced in recent years are employed in the preliminary design for selecting the dimensions and the arrangement of the organs of stability and controllability; calculation of static stability is carried out on the basis of wind-tunnel tests and partial calculation of dynamic stability is accomplished.

Layout requirements. In laying out the organs of stability and controllability, it is necessary not to allow their mutual blanketing and their blanketing by other components of the design. It is not always possible to satisfy these requirements entirely.

Strength requirements are similar to the corresponding requirements imposed on a wing. Moreover, the following specific requirements are imposed on the organs of stability and controllability:

1) increased general rigidity (wing, stabilizer, fin and fuselage) is necessary to eliminate the danger of the appearance of aileron and control surface (rudder, elevators) reversal (see Chapter 6) and to prevent a serious decrease in their effectiveness at velocities approaching reversal velocity;

2) increased local rigidity is necessary to ensure the preservation of the shape of the empennage and ailerons during their operation;

3) measures should be taken to prevent the appearance of flutter and buffeting (see Chapter 6).

The content of the other requirements is similar to the content of the corresponding requirements imposed on a wing.

§ 2. AILERONS (ROLL CONTROL SURFACES)

Ailerons are intended to ensure a transverse controllability. On aircraft of "tailless" design elevons are employed, instead of ailerons, which, when both are deflected in the same direction, ensure longitudinal control, and when deflected in different directions - ensure transverse control.

Aileron effectiveness is reduced at high flight velocities. At high subsonic velocities this is connected with the phenomenon which has been named aileron reversal (see Chapter 6), and at supersonic velocities with the fact that in a supersonic flow aileron deflection does not affect the pressure distribution along the profile shape situated ahead of the aileron (perturbations cannot be propagated at a velocity exceeding the speed of sound).

Thus, on high-speed aircraft along with ailerons interceptors are employed for roll control. An interceptor is the plate which moves forward on the upper surface of a half wing simultaneously with the deflection of the aileron upward. This plate causes flow separation and reduces lift.

1. Basic Parameters of Ailerons

Figure 5.1a shows the location of an aileron on a wing and the following designations are given: S' - the area of the wing in the section occupied by the aileron; $S_э/2$ - the area of the aileron; $l_э$ - the aileron span; $l/2$ - the semispan of the wing; $L_э$ - the distance from the center of gravity of the aileron area to the longitudinal axis of the aircraft; $b_э$ - the aileron chord; b - the wing chord.

Aileron effectiveness can be approximately estimated by the ratio: $S_э/S$, where $S_э$ - the area of two ailerons; S - the area of the entire wing. For contemporary aircraft $S_э/S=0.06-1$. Aileron

effectiveness can be estimated more accurately by the magnitude $A_э = \frac{S_э L_э}{Sl/2}$, called the coefficient of static moment, or the coefficient of aileron power.

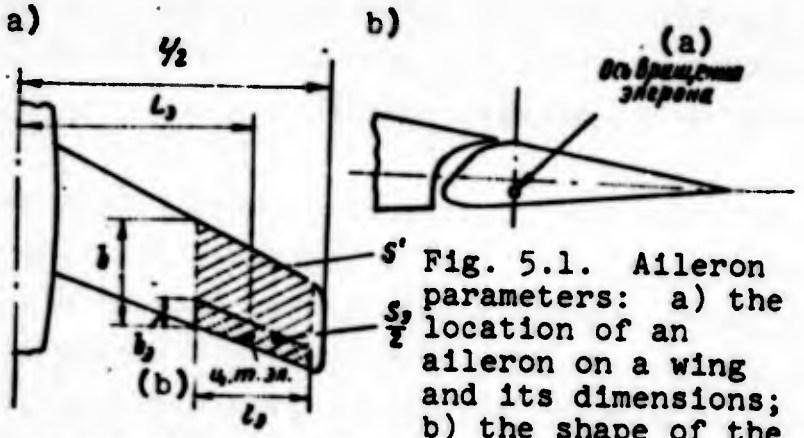

Fig. 5.1. Aileron parameters: a) the location of an aileron on a wing and its dimensions; b) the shape of the transverse cross section of an aileron of the TsAGI [ЦАГИ - Cen. Inst of Aerohydrodynamics im N. Ye. Zhukovskiy) type.
Key: (a) Aileron axis of rotation; (b) c.g. of aileron.

The usual ratios characterizing the location and the contours of ailerons are the following: $b_э/b=0.2-0.25$; $\frac{l_э}{l/2}=0{,}3\div0{,}4$.

With an increase in $b_э/b$ the working section of the wing beam is reduced. When $b_э/b>0.25$ aileron effectiveness is not increased. With an increase in $\frac{l_э}{l/2}$ the space allotted for lift-increasing devices is reduced and, moreover, the value of quantity $L_э$ drops off.

The maximum angles of aileron deflection lie within the limits of from 12 to 25°, lesser values pertain to high-speed aircraft.

2. Measures for Preventing Turning Moment During Aileron Deflection

These measures are usually employed on subsonic aircraft having unswept wings.

In flight, especially at large angles of attack, the deflection of ailerons upward and downward at identical angles produces a different drag increment: it is large on the half wing with the downward deflected aileron.

As a result of this a moment arises which turns the aircraft in the direction opposite to the bank. Measures for eliminating this deficiency are the following:

a) the application of differential aileron deflection, i.e., deflection of the aileron downward at angles less than the deflection upward. The ratio of the deflection angles of the aileron upward and downward can be as high as two;

b) profiling the leading edge of the aileron. Figure 5.1b shows the profiled leading edge of an aileron of the TsAGI type.

In the case of the deflection of the aileron upward due to the fact that its leading edge projects under the wing, wing drag is increased more than in the case of downward deflection.

3. Loads on an Aileron

An aileron is rated for two types of loads:

for loads acting on an undeflected aileron as on a wing part, in the main cases of wing loading (A, A', D, D'):

for loads applied to a deflected aileron in cases B and C, in this case the safety factor is taken equal to 2.

The load distribution to the latter cases is determined from wind-tunnel tests; it approximately corresponds to that shown in Fig. 5.2.

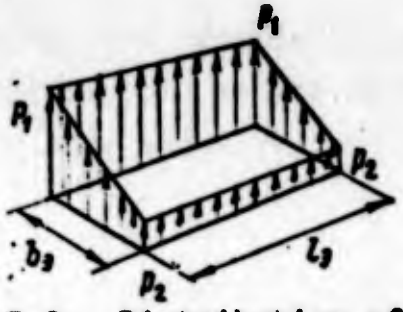

Fig. 5.2. Distribution of an air load acting on an aileron.

Operational values p_1 and p_2 (kgf/m^2) are determined via the operational impact pressure of the loading case in question.

For example in case B:

$$q_B = \frac{n_B^2}{c_{yB}} \frac{G}{S},$$

then

$$p_1 = \bar{p}_1 q_B, \quad p_2 = \bar{p}_2 q_B,$$

where $\bar{p}_1$, $\bar{p}_2$ are taken from the wind tunnel tests.

The operational value of a linear load along the length of an aileron is determined by the following formula

$$q = \frac{p_1 + p_2}{2} b_э.$$

4. Aileron Design and Operation

The aileron is a beam usually consisting of a spar, a set of ribs and the skin.

The design and operation of aileron elements are similar to the design and operation of corresponding wing elements. The skin receives the air load and transmits it to the ribs. The ribs transmit the loads to the spar, operating in flexure in its plane. The spar transmits the loads to the supports.

Since in the general case the center-of-pressure line of an aileron and its axis of rigidity do not coincide, then each rib loads the aileron with torsional moment $\Delta M_{кр}$.

To reduce the deformations of long-span ailerons and to increase the reliability the number of supports is usually made greater than two.

To reduce the great value of torsional moment it is advantageous to place the horn of the control rod nearer to the middle of the aileron. For this purpose two horns are sometimes mounted on long-span ailerons.

If an aileron is long, and the rigidity of the wing is low, then the following phenomena can become noticeable.

1. In the event of considerable wing flexure the aileron supports cease to lie in one straight line, which leads to the possibility of jamming of the assemblies. To eliminate this the following measures are taken:

a) spherical bearings are placed in the hinge assemblies;

b) the aileron is made sectional, i.e., it is divided into two (or more) parts between which hinges with a horizontal axis or universal joints are placed capable of transmitting torsional moment. The presence of a universal joint or an assembly with a horizontal axis facilitates the installation, makes it possible to remove the consequences of aileron manufacturing inaccuracy.

2. Since as a result of the bending of the aileron axis of rotation the distance between the supporting cross sections tends to be reduced, to eliminate additional loads on assemblies along the aileron axis part of the supports in this direction is made mobile.

If the aileron is comparatively short or the wing is rather rigid, then of the indicated design measures only the inserting of radial-spherical ball bearing is employed.

On aircraft with low flight velocities ailerons and control surfaces with linen have been employed. These types of designs were advantageous in a weight regard. In this case the weight of not only the control surface design was reduced, but the weight of the compensators necessary for preventing natural oscillations was also reduced (the details on weight balancing will be discussed in chapter 6). However, at high flight velocities the linen skin, being deformed, greatly distorts the profile of the aileron or control surface, and it is difficult to ensure its adequate strength. For this reason metallic skin is employed on contemporary high-speed aircraft in ailerons and control surface designs.

The transverse cross section of an aileron is a closed contour capable of receiving torsional moment (Fig. 5.3, tech. the I-I). A considerable part of this moment is received by the leading edge contour. But for installing suspension assemblies it is necessary to make cutouts in the leading edge (cross section II-II), which weaken the torsional strength of the aileron. Compensation for the cutouts is usually accomplished by reinforcing the trailing edge part of the contour (cross section II-II) by installing an additional beam between the ribs which limit the cutout, and additional skin plates (knee plates).

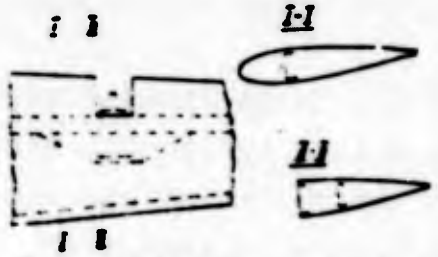

Fig. 5.3. Design concept of an aileron.

The aileron is rated for strength like a beam (the axis of which - the axis of rigidity) loaded with forces reduced towards the axis of rigidity. The aileron beam operates in flexure and shear in two planes and in torsion.

The aileron is reduced to a setup which makes it possible for its rating to employ the methods of wing rating.

Figure 5.4 shows as an example the design diagram of a three-support slotted aileron. Line ABC - the axis of rotation; D - the universal joint.

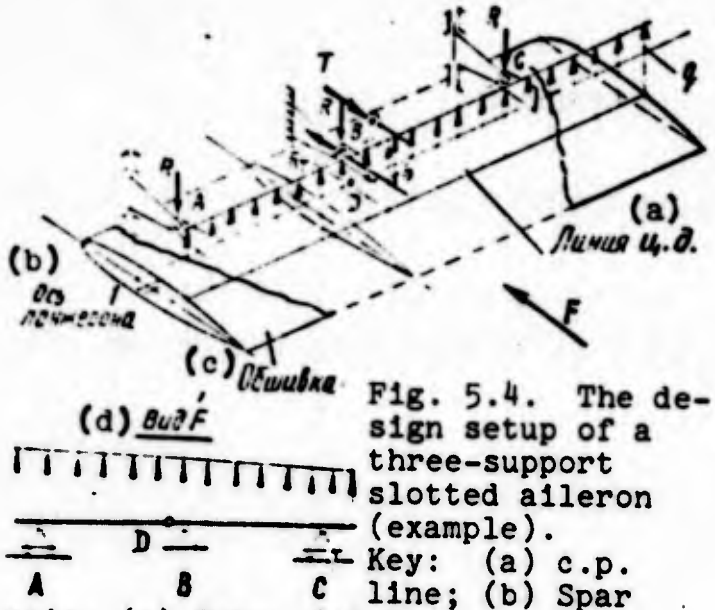

Fig. 5.4. The design setup of a three-support slotted aileron (example). Key: (a) c.p. line; (b) Spar axis; (c) Skin; (d) View.

The rating is carried out in the following sequence.

1. Determination of the distributed air load q.

2. Determination of the support reactions R and of the force in the control rod T. In the case when the aileron not slotted, and the number of supports is more than two, then for determining the reactions the methods of rating an unslotted beam are employed.

3. Determination of the forces in aileron cross sections, perpendicular to the axes of rigidity (plotting diagrams of transverse forces, bending moments and the torsional moments).

4. Determination of the stresses in aileron elements and strength testing.

§ 3. TAIL UNIT (EMPENNAGE)

The tail unit (empennage) is divided into the horizontal tail surfaces (h.t.s) [г.о] and the vertical tail surfaces (v.t.s) and consists of the stabilizer with the elevator and the fin with the rudder. The horizontal tail surfaces ensure longitudinal (relative to the z-axis) balance, stability and controllability; the vertical

tail surfaces ensure directional (relative to the y-axis) balance, stability and controllability.

1. Arrangement, External Shapes and Parameters

Empennage effectiveness is determined:

a) by the ratio of the empennage area and the wing area S_{on}/S;

b) by the location of the empennage relative to other components of the aircraft and by its distance from the center of gravity of the aircraft.

For determining, in a first approximation, the areas of the horizontal and vertical tail surfaces $S_{г.о}$, $S_{в.о}$ (Fig. 5.5) and the values of the distances of the empennage from the center of gravity of the aircraft $L_{г.о}$, $L_{в.о}$ it is necessary to employ the statistics of power factors.

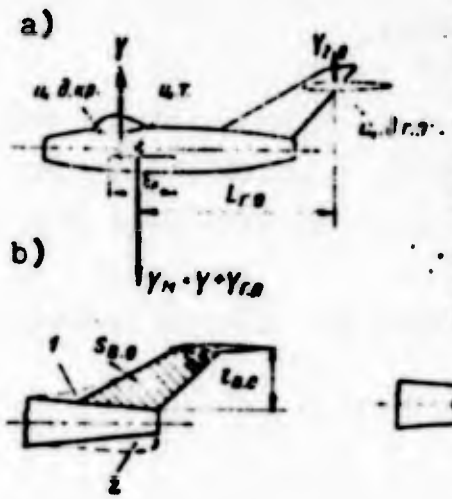

Fig. 5.5. Towards determining the parameters of an empennage: a) diagram of the balancing of an aircraft relative to the transverse axis; b) the areas and spans of an empennage: 1 - fin ridge; (forefin); 2 - additional fin (false fin).

For the horizontal tail surfaces:

$$A_{г.о} = \frac{S_{г.о} L_{г.о}}{S b_A},$$

where $A_{г.о}$ - the power factor of the horizontal tail surfaces, or the static coefficient of the horizontal tail surfaces; $L_{г.о}$ - the distance from the center of pressure of the horizontal tail surfaces to the center of gravity of the aircraft; b_A - the mean aerodynamic chord.

Power factor $A_{г.о}$ represents the product $S_{г.о}/S \times L_{г.о}/b_A$, from which it is evident that the effectiveness of an empennage is determined both by its area as well as by its arm - the distance from the center of gravity of the aircraft.

It is necessary to find the values of the coefficients from the data on aircraft, close in purpose and layout to the aircraft being designed, because statistics gives a very broad spread of these values:

$$\frac{S_{г.о}}{S} = 0{,}19 \div 0{,}28; \quad \frac{L_{г.о}}{b} = 2{,}6 \div 4{,}8,$$

$$A_{г.о} = 0{,}5 \div 1{,}0.$$

The following ratio serves for estimating elevator effectiveness

$$\frac{S_{р.в}}{S_{г.о}} = 0{,}2 \div 0{,}4.$$

The effectiveness of the vertical tail surfaces is estimated by the magnitude

$$A_{в.о} = \frac{S_{в.о} L_{в.о}}{Sl}.$$

According to statistics

$$A_{в.о} = 0{,}01 \div 0{,}08; \quad \frac{S_{в.о}}{S} = 0{,}1 \div 0{,}19; \quad \frac{S_{р.н}}{S_{в.о}} = 0{,}21 \div 0{,}35,$$

where $A_{в.о}$ - the power factor of the vertical tail surfaces, or the static coefficient of the vertical tail surfaces; l - the wing span; $L_{в.о}$ - the distance from the center of pressure of the vertical tail surfaces to the center of gravity of the aircraft; $S_{в.о}$ - the area of the vertical tail surfaces; $S_{р.н}$ - the area of the rudder.

The required vertical tail surface area is to a considerable extent determined by the length of the part of the fuselage located in front of the center of gravity of the aircraft. The longer is the nose part of the fuselage, then, other conditions being equal, the greater is the area of the vertical tail surfaces necessary for eliminating destabilizing moment.

How the areas and the spans of vertical and horizontal tail surfaces are determined is evident from Fig. 5.5b.

In the case of the attaching of horizontal tail surfaces to the fuselage $S_{в.о}$ it is determined in the same way as for a wing, taking the subfuselage part into account.

To increase the effectiveness of vertical tail surfaces in the case of large angles of sideslip fin ridges (forefins) 1 and additional fins (false fins) 2 (Fig. 5.5b) are employed. In this case the adjoining part of the lateral projection of the fuselage is included in $S_{в.о}$.

Usually it is assumed that the center of pressure of horizontal and vertical tail surfaces is located at 0.25b of the empennage.

The contours of the horizontal tail surfaces in plan and the vertical tail surfaces in a side view are a combination of trapezoids with curvatures.

The aspect ratio of an empennage has the following values

$$\lambda_{г.о} = 3 \div 5; \quad \lambda_{в.о} = 0{,}8 \div 2.$$

As is evident, the aspect ratio of an empennage is less than the aspect ratio of wings. This is beneficial for reducing the weight of the empennage and for increasing its rigidity. Moreover, with a low aspect ratio the $\alpha_{крит}$ of the empennage is increased - the angle of attack, at which flow separation begins by which the effectiveness of the empennage is ensured at large angles of attack exceeding the $\alpha_{крит}$ of the wing.

Sweep. The critical $M_{крит}$ number of the empennage should be greater than the $M_{крит}$ of the wing so as to ensure in all possible flight regimes of the aircraft sufficient stability and controllability for the aircraft. Moreover, upon deflection of the control surfaces the concavity of the empennage is increased, which leads to decrease in the $M_{крит}$ of the empennage. All this makes it necessary to employ empennage with larger sweep angles and a smaller thickness ratio than for a wing.

Empennage profiles. As a rule, the profiles of an empennage are symmetrical. When selecting the thickness ratio of an empennage ($\bar{c}$) the following considerations are taken into account:

1. The effect of $\bar{c}$ on c_x and $M_{крит}$. The smaller is $\bar{c}$, the smaller is c_x and the greater is $M_{крит}$.

2. The effect of $\bar{c}$ on the rigidity and the weight of the empennage. At a small value of $\bar{c}$ the rigidity is less. A decrease in $\bar{c}$ can lead to an increase in the weight of the empennage.

3. A small value of $\bar{c}$ makes it difficult to accomplish axial aerodynamic compensation of the control surfaces.

The control surface deflection range is usually:

$$\Sigma\delta_p = 40^\circ \div 50^\circ.$$

Empennage layout. Let us examine certain general rules of the layout of an empennage.

1. Beyond the wing the flow is slowed down. This leads, especially at large angles of attack and with large M numbers, to a reduction in empennage effectiveness, and the vortices from the wing can cause buffeting (see Chapter 6, § 4).

To eliminate this the horizontal tail surfaces should be situated below or above the zone of the wing "wake".

2. The blanketing of the vertical tail surfaces by the horizontal surfaces should be eliminated as far as possible. It is especially important that this requirement be fulfilled for maneuverable aircraft during flight at large angles of attack, for the purpose of ensuring controllability in a spin.

3. On jet aircraft the empennage should be removed from the exhuast jets of engines to prevent the effect on the empennage of heating and fluctuating loads.

4. In the layout of vertical and horizontal tail surfaces of high-speed aircraft in order that $M_{крит}$ not be reduced, it is not necessary to allow the coincidence of their maximum thicknesses.

Figure 5.6 shows the variants in the positioning of the horizontal tail surfaces relative to fuselage and the vertical tail surfaces, which are employed.

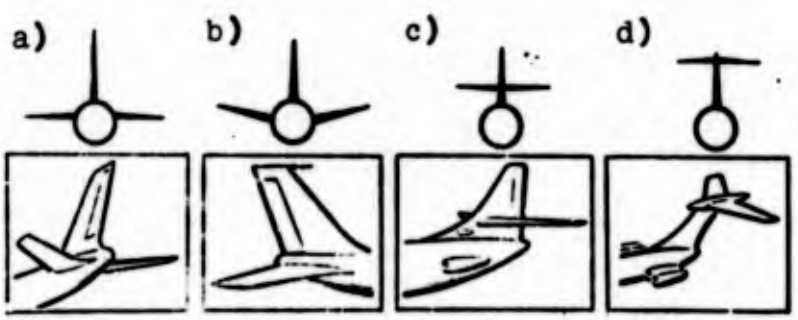

Fig. 5.6. Variants in the positioning of the horizontal tail surfaces relative to the fuselage and the fin: a, b) low (Tu-104 and Boeing-707); c) intermediate (Caravelle); d) high (VC.10).

In the low position the horizontal tail surfaces have less weight and greater rigidity. In many respects the setup with high positioning of the horizontal tail surfaces - the T-shaped setup - is advantageous. Its most significant advantages are:

a) the horizontal tail surfaces are outside the effect of the flow beyond the wing;

b) the arm of the horizontal tail surfaces is increased;

c) the horizontal tail surfaces play the role of the "end plate: on the fin which increases the effective aspect ratio of the vertical tail surfaces; this makes it possible to decrease its geometric aspect ratio;

d) the horizontal tail surfaces are removed from the zone of the effect of exhaust gases.

The deficiencies of this type of setup are the complexity of design, greater weight and less rigidity.

The intermediate layout setup is the setup with intermediate positioning of the horizontal tail surfaces with respect to height ("cruciform setup"). This setup does not have any significant advantages.

Sometimes, especially on propeller aircraft, spaced vertical tail surfaces with two or three fins are finding application. In this case the height of the fins is decreased, and the positioning of the vertical tail surfaces in the form of plates at the ends of the stabilizer increases the effective aspect ratio of the horizontal tail surfaces. If the plates are positioned in the propeller slipstreams, the effectiveness of the empennage is increased at low flight speeds.

In sport aircraft and gliders a V-shaped empennage is encountered which consists of two symmetrical stabilizing surfaces with control surfaces which simultaneously perform the role of the horizontal and vertical tail surfaces. The control surfaces are simultaneously connected with the control stick and with the pedals.

This type of empennage setup has not received broad application in aircraft.

2. Empennage Loads

In all cases of empennage loading specified by the strength standards, it is assumed, that the linear air load along the span is distributed proportional to the chords. The diagrams of load distribution along a chord are different for the different cases.

The loads on an empennage are divided into three groups: balancing, maneuvering and loads during flight in turbulence.

1. The balancing loads on an empennage are determined from the condition of the static equilibrium of the moments of the air forces relative to the y- and z-axes in different flight regimes.

Let us examine, as an example, the determination of a balancing horizontal tail surface $Y_{г.о}$ (see Fig. 5.5a). For all cases of loading from A to D' the values of $Y_{г.о}$ are found from the condition of equilibrium relative to the z-axis passing through the center of gravity:

$$Y_{г.о} = \frac{Y(\bar{x}_{ц.т.} - \bar{x}_{д})b_A}{L_{г.о}},$$

where $\bar{x}_{ц.т}$ - the position of the center of gravity in an aircraft; $\bar{x}_{д}$ - the relative coordinate of the center of pressure of the wing (with respect to MAC).

The greatest of the loads $Y_{r.o}$ is also calculated for the horizontal tail surfaces.

2. Manuevering loads act on the empennage upon sharp deflection of the control surfaces at the initial moment of a maneuver.

This group includes the load on vertical tail surfaces in the case of an engine cutoff on one side of the plane of symmetry of the aircraft. It is determined from condition of equilibrium of the moments relative to the y-axis passing through the center of gravity of the aircraft.

3. Loads during flight in turbulence arise as a result of the effect of vertical and horizontal airflows (gusts), perpendicular to the direction of flight.

The strength standards provide for, moreover, the effect of combined loads on the empennage (for example a combination of balancing and maneuvering loads), unsymmetrical loading of the horizontal tail surfaces and simultaneous loading of the vertical and horizontal tail surfaces.

3. Design and Load-Bearing Setup of an Empennage

In external shape, in the type of loads and in design empennages and wings have much in common. Thus, the load-bearing setups of stabilizers and fins are similar to the load-bearing setups of a wing. The purpose, operation and design of stabilizer and fin elements are similar to the purpose, operation and design of corresponding wing components. The elevator and the rudder designwise are similar to the aileron.

Laminar skin panels are finding application in control surface (rudder and elevator) design (and also in ailerons) of contemporary aircraft. In case of control surfaces with small

dimensions designs are being employed, where filler (foam plastic or honeycombs cell) occupies the entire space between the upper and lower skin. In such designs the skin is well reinforced for receiving of flexural and torsional moment and the shape of the profile is preserved better. Furthermore, such designs have good resistance to variable fluctuating loads due to sound pressures created by the jets of turbujet engines.

The effectiveness of control surfaces is diminished in supersonic flow. The deflection of a control surface no longer affects the air force of the fixed surface located in front of it - the stabilizer or fin. Therefore on supersonic aircraft the empennage should be made completely rotatable. This, primarily, pertains to the horizontal tail surfaces which ensure longitudinal controllability.

The absence of elevators simplifies the design of a completely rotatable horizontal tail surface - controlled stabilizer. The most responsible and complex element in this case is the axis relative to which the empennage is turned, and the fixing of this axis in the fuselage.

The control surfaces and the designs of a completely rotatable empennage are rated for strength from the effect of the air loads. The order of calculation is the same as for an aileron.

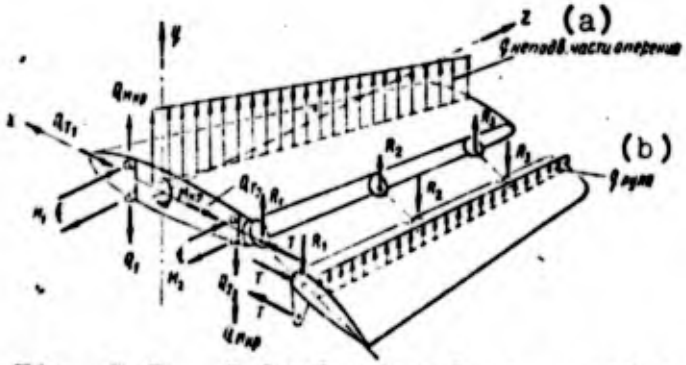

Fig. 5.7. Calculational setup of a tail surface.
Key: (a) fixed part of tail surface; (b) control surface.

The fixed parts of a tail surface are designed for the simultaneous effect of the air loads and the loads from the control surface attachment assemblies incident on them (Fig. 5.7). The order of calculation is the same as for a wing (Chapters 3 and

4). However, the mass forces are usually not considered in the calculation of a tail surface.

As a rule, the loads (mass balancing) are placed in the front part of control surface and aileron design, to prevent flutter (see Chapter 6).

§ 4. AERODYNAMIC COMPENSATION AND BALANCE DEVICES

To reduce the forces on the main levers controlling the roll control surfaces (ailerons), elevators and rudders, arising as a result of the appearance of aerodynamic hinged moments of the elevators and rudders during their deflection, aerodynamic compensation of various types is employed.

Axial aerodynamic compensation is at the present time the most widely employed type. To accomplish it the axis of rotation of the control surface is displaced backwards with respect to its leading edge (Fig. 5.8a), which decreases the arm of aerodynamic force P_p relative to the axis of rotation and, consequently, also the magnitude of hinged moment:

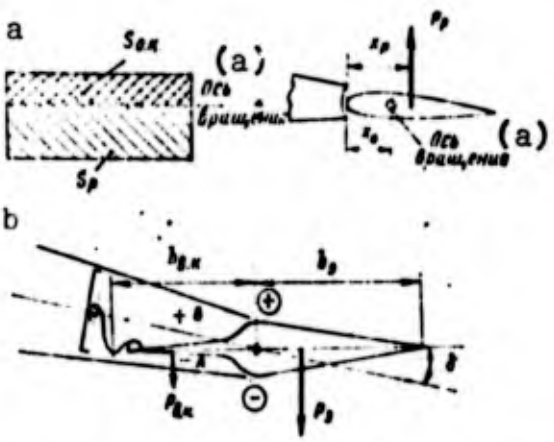

Fig. 5.8. Axial (a) and internal (b) aerodynamic compensations.
Key: (a) The axis of rotation.

$$M_ш = P_p(x_p - x_0).$$

A measure of the effectiveness of axial compensation - the ratio of the area of axial compensation $S_{o.к}$ to the area of the control surface $S_{o.к}/S_p$, or the ratio of the chords $b_{o.к}/b_p$.

Axial compensation whose area exceeds 28% of the area of the control surface, is rarely employed, since this leads to the fact that the leading edges of the control surfaces (ailerons) project beyond the dimensions of the wing and negatively affect its aerodynamics. Moreover, so-called overcompensation can also arise - change in the sign of hinged moment. If the line of the leading edges of the ailerons or other control surfaces is outlined by a radius drawn from the axis of rotation R=c/2, where c - the maximum thickness of the control surface, then it is assumed that the compensative effect does not arise. A deficiency of conventional axial compensations is the presence of slots which produce air flowing over from a region of elevated pressure into a region of low pressure. This leads to a reduction in the effectiveness of axial compensation and to the appearance of additional drag.

Sealed internal balance. This type of axial balance is employed in ailerons. The leading nose of an aileron is equipped with a sealed balance which is connected with the wing wall by an airproof diaphragm made from rubber-impregnated fabric or from canvas. The chord of the sealed balance $b_{в.к}$ can be arbitrarily measured from the axis of rotation of the aileron to the middle of the diaphragm.

Upon aileron deflection the pressure on the sides of the balance changes just as on the adjoining sides of the aileron. Thus, in Fig. 5.8b (the aileron is deflected upward) the pressure in lower cavity A decreases, and in upper cavity B increases.

The pressure differential acting on the sealed internal balance gear creates force $P_{в.к}$ which is included in the load on aileron $P_э$ displacing it forward and decreasing the hinge moment $M_ш$.

The most important advantage of this type of balancing is the absence of slots and, therefore, the absence of air flowing over from the zone of increased pressure into the zone of low pressure.

In this way great balance effectiveness is attained and also a decrease in wing drag, since the application of sealed internal balancing eliminates the jutting out of the leading edge beyond the dimensions of the wing upon aileron deflection.

The sealed internal balance limits the amount of aileron deflection; this hampers its application in thin wings.

Stabilizers and fins are considerably thinner than wings, and the required angles of deflection of the control surface (rudder and elevators) are greater than that of ailerons. Thus the application of sealed internal balancing on these control surfaces cannot ensure their deflection by the necessary angles.

Servo compensation. A servo tab (Flettner tab) is the part of the surface of the control surface at the trailing edge which is automatically deflected upon deflection of the control surface (Fig. 5.9a). A servo tab is deflected in the direction opposite to the deflection of the control surface. In this case the moment of aerodynamic force of the servo tab has the opposite sign as compared with the moment of the aerodynamic force of the control surface. As a result the hinge moment of the control surface decreases.

A conventional servo tab, like axial aerodynamic balancing, upon a specific deflection of a control surface decreases the hinge moment and the loads on the main levers at all flight velocities of an identical degree (by an identical percent). Moreover, it is desirable that with great values of hinge moment the degree of compensation (balancing) be greater. This property is possessed by a spring servo tab (Fig. 5.9b). It is deflected only upon overcoming the pretensioning in the spring by great forces in the control system. At large hinge moments the magnitude of deflection of a servo tab is greater and it yields a more considerable decrease in the loads on the main levers.

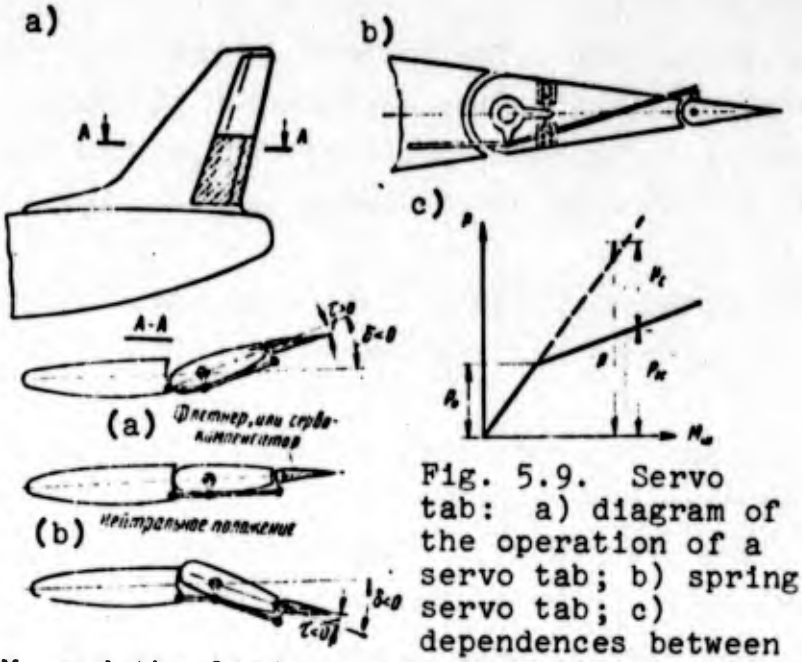

Fig. 5.9. Servo tab: a) diagram of the operation of a servo tab; b) spring servo tab; c) dependences between $M_ш$ and the load on main lever in a spring tab.
Key: (a) Flettner, or servo tab; (b) Neutral position.

The diagram (Fig. 5.9c) shows the dependence between $M_ш$ and the load on the main lever. The load corresponding to the pretensioning of springs is designated via P_0, P - the load acting on the main lever in the absence of a servo tab, $P_н$ - the load acting on the main lever in a spring servo tab setup, P_c - the decrease in the load on the main lever as a result of a decrease in $M_ш$ by the servo tab.

Deficiencies in servo compensations (balancing):

a) a decrease in the the effectiveness of the control surface, since the force on the tab is opposite to the force on the control surface;

b) an increase in the danger of the appearance of flutter.

In contrast to aerodynamic compensation (balancing) which decreases the loads on the main levers of the main control

automatically, without the pilot's intervention, means are employed, with the aid of which the pilot can remove the load as he sees fit. These types of means have individual control and are utilized during prolonged flight in a steady-state regime. They are called balancing (trimming) devices.

Included among balancing (trimming) devices are the stabilizer with the setting angle being varied in flight and the trim tab.

For varying the stabilizer setting angle in flight, one of its attachments (for example the rear one) is made hinged, and the other attachment is connected with a mechanism capable of moving this attachment along the vertical. The variation in the stabilizer setting angle in flight serves for longitudinal balancing of the aircraft.

Designwise a trim tab is made just like a servo tab, but it can be independently controlled from the flight deck. Upon deflection of the control surface the trim tab remains fixed relative to the control surface. The air force acting on a trim tab deflected by the pilot, overcoming the hinge moment of the control surface, holds the control surface in the deflected position which corresponds to a given flight regime, relieving the control column or pedal.

The trim tab - a means of balancing and the servo trim tab - a means of aerodynamic compensation (balancing), can be joined in one unit. This can be done, if we include the mechanism controlling the trim tab directly in the mechanism for automatic deflection of the servo trim tab. This type of assembly is called a trim tab-servo tab (trim tab-Flettner).

CHAPTER 6

OSCILLATIONS AND AEROELASTICITY IN AIRCRAFT DESIGNS

Aviation designs planned under the condition of ensuring strength with the least weight, especially wing and empennage design, have low rigidity, less than in the designs of general mechanical engineering and building construction.

Because of this under the conditions of the operation of flight vehicles it is necessary to consider the possibility of the appearance of different types of oscillations and other phenomena connected with the elastic deformations of the design and the interaction of aerodynamic, elastic and inertial forces.

The phenomena which are produced during the interaction of only elastic and inertia forces: free and forced mechanical oscillations are examined in the present chapter on the basis of the general methods of oscillation theory.

The joint effect of aerodynamic and inertial forces is examined in the theory of the dynamic stability of flight vehicles.

Especially characteristic for aircraft designs are the phenomena which arise in an elastic-deformed design during the effect of aerodynamic forces. They are analyzed by the methods of a special section of mechanics, i.e., the theory of aeroelasticity. Also included here are phenomena connected with the

interaction of aerodynamic and elastic forces - divergence, reversal, or aerodynamic, elastic and inertial forces - buffeting, flutter, etc.

A portion of these type of phenomena is examined in the aerodynamics of flight vehicles (static stability and the dynamics of the motion of a flight vehicle as an elastic system). In the present chapter phenomena pertaining to aeroelasticity dangerous to aircraft design strength are examined.

§ 1. TYPES OF OSCILLATIONS OF FLIGHT VEHICLE COMPONENTS

The components of an aircraft design can experience the following types of oscillations:

1. Free oscillations are the oscillations occurring after a single aberration from the state of equilibrium.

2. Forced oscillations are oscillations caused by external periodic forces acting independently of the oscillations of the system. The main causes of forced oscillations are: the lack of balance of a piston engine, a propeller, a rotor of a turbojet engine, the separation of vortices from the components of a structure situated in front of the empennage (oscillations of the "buffeting" type), random periodic effects.

3. Self-sustained oscillations (auto-oscillations) occurring in the absence of independent periodic forces; periodic forces, which support oscillations, arise in a system as a result of the presence of the oscillations themselves. Most frequently self-sustained oscillations are encountered in a wing or empennage (flutter), in the front strut of a landing gear (shimmy).

Let us recall the main aspects of oscillation theory which pertain to natural and forced oscillations for a system with a single-degree-of-freedom (figure 6.1a).

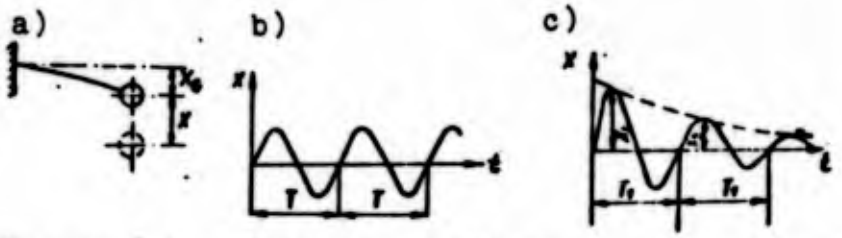

Figure 6.1. Natural oscillations of a system with a single-degree-of-freedom.

Free oscillations of a system without damping - are harmonic (sinusoidal) oscillations. In the case of these types of oscillations deviation from the position of equilibrium is depicted as dependence (figure 6.1b):

$$x = x_{max} \sin(\omega t + \varphi),$$

where x_{max} - is the amplitude; φ - the phase (it is determined by the initial conditions); $\omega=\sqrt{c/m}$ - is the natural circular frequency of the oscillations. Here c - is the rigidity of the elastic coupling of the system, cm/kg, and m=G/g - is the mass of the load.

The period of the free oscillations is:

$$T = \frac{1}{\nu} = 2\pi\sqrt{\frac{x_G}{g}}\ \text{s}$$

where $\nu = \frac{\omega}{2\pi} = \frac{1}{2\pi}\sqrt{\frac{g}{x_G}}$ Hz - is the natural frequency of the oscillations; $x_G=G/c$ - is the static deformation of the system under the load of its own weight.

Any part of an aircraft design after an external effect (shock) can begin to perform oscillations which will always gradually be damped. The reserve of the mechanical energy

(obtained under an effect) in the process of oscillations as a result of the presence of internal and external resistance will be dissipated, being converted into irreversible forms of energy, and this occurs faster, the greater is the magnitude of the logarithmic decrement of the system.

The logarithmic decrement δ of a system characterizes the decrease in the ranges of the oscillations and is equal to the natural logarithm of the ratio of two consecutive amplitudes of the oscillations in one direction:

$$\delta = \ln \frac{x_1}{x_2}.$$

It is possible to assume that the decrement for a given design is constant and does not depend on the magnitude of the initial shock of the oscillation produced, and the period of the oscillation T_1 also does not depend on the magnitude of this shock and during the entire time of the oscillatory process remains constant (figure 6.1c). At small magnitudes δ characteristic for aircraft designs, it is possible to assume that the period of the natural oscillations of the system with damping is equal to the period of the system without damping, $T_1=T$ (see figure 6.1b). In accordance with this it is assumed that, $\nu_1=\nu$.

The magnitudes of the natural frequencies and the oscillatory periods of the system are determined by the rigid and mass characteristics of the system.

The nature of the forced oscillations of a system is determined by its decrement and by the ratio of the frequencies of the perturbing forces $\omega_{вын}(\nu_{вын})$ to the natural frequencies.

The nature of the course of the self-sustained oscillations of a system also depends on the natural frequencies of the system and the decrement.

§ 2. FORCED OSCILLATIONS IN THE CASE OF RANDOM EFFECTS

Flight vehicle operating conditions are characterized by the fact that many parameters which determine the design loads are random. Also included among them are the amplitudes and the frequencies of the forces causing the oscillations.

Examples of the application to a design of forces which bear a random character are: flight in a turbulent atmosphere, motion along a dirt airfield.

The frequency of load application is determined by the rate of motion of a flight vehicle V and by the random distances L which characterize the intervals between the shocks, for example by the distances between vertical gusts and the bumpy areas on an airfield:

$$\nu_{выч} = \frac{V}{L}, \quad \omega_{выч} = 2\pi\nu_{выч}.$$

Under these conditions the intensity of the shocks is also random and is a statistical function of the frequency.

For analyzing the operation of designs under random effects let us first examine the simplest elastic system with a single-degree-of-freedom (see figure 6.1a), which undergoes damping. The static deformation of a system under the effect of force P

$$x_P = \frac{P}{c},$$

where c - is the rigidity.

Under the effect of a periodic load P(t), characterized by circular frequency $\omega_{выч}$ and by amplitude A_p, the amplitude of the oscillations is

$$A_x = HA_P,$$

$$H = \frac{1}{c\sqrt{1-\left(\frac{\omega_{вын}}{\omega}\right)^2 + \left(\frac{\omega_{вын}}{\omega}\right)^2\left(\frac{\delta}{\pi}\right)^2}},$$

where H - is the mechanical conductivity or the amplitude-frequency characteristic of the system.

The ratio of A_x to static deformation x_P due to force $P=A_P$ is called the dynamic coefficient μ

$$\mu = \frac{A_x}{x_P} = cH.$$

Functions $\mu(\omega_{вын})$ and $H(\omega_{вын})$ characterize the effect of the ratio $\frac{\omega_{вын}}{\omega} = \frac{\nu_{вын}}{\nu}$ on the amplitudes of the oscillations.

If a load is characterized by random amplitude A_P at a constant circular frequency $\omega_{вын}$, the connection of the random amplitudes of the displacement and the load is expressed by the same type of dependence.

The dependences connecting mathematical expectations $\bar{A}$ and the standard deviations s of the displacements and the loads have the same form:

$$\bar{A}_x = H\bar{A}_P;$$
$$s_x = Hs_P.$$

In the general case, if an oscillating design is a dynamic system with distributed masses and is loaded with forces having random amplitudes and frequencies, the spectral density $S_p(\omega_{вын})$ is the characteristic of the dependence of the amplitudes of the exciting forces on the frequencies.

The function of the spectral density of the amplitudes of the displacements is found from the expression

$$S_x(\omega_{вын}) = H^2 S_p(\omega_{вын}).$$

Figure 6.2 gives an example of the determination of S_x via S_p for a design, the mechanical conductivity of which is represented by the function $H(\omega_{вын})$, determined by the distribution of the masses, rigidities and other properties of the design.

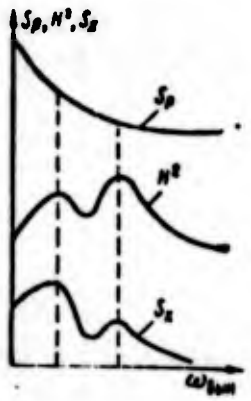

Figure 6.2. Effect of a random load on a dynamic system.

If an oscillating design in its dynamic properties is close to a system with a finite number of degrees of freedom, function $H(\omega_{вын})$ has clearly expressed maxima. The frequencies corresponding to these maxima are natural frequencies. The greatest value of H is obtained at the smallest natural frequency and at the first form of the oscillations corresponding to it.

Finally, if the amplitudes of the load do not strongly depend on frequency, i.e., the function of the spectral density of the load is flat and does not have sharply pronounced maxima, the most noticeable oscillations of the design occur when $\omega_{вын}$ is equal to the lowest natural frequency.

Oscillations under the effect of random shocks manifest themselves especially perceptibly with considerable amplitudes, when several random shocks or gusts act in succession over nearly equal time intervals with a frequency close to the natural frequency of the design.

This phenomenon is encountered, for example, during flight in turbulence and is called "cyclic turbulence."

§ 3. ACOUSTIC VIBRATIONS

Acoustic loads, producing vibrations in a design, are created by noise - by the random oscillations of air or reactive jets whose frequencies lie in the sonic range (from 16 to 20,000 Hz).

The noise intensity is characterized by the rms sound pressure (kgf/cm^2) or by the noise level in decibels. One decibel (dB) corresponds to the least increase in noise level capable of being distinguished by the human ear.

A noise of 150 dB is hard for a man to endure, 180 dB produces fatigue in metal, 190 dB can cause the failure of riveted joints.

The main constant sources of acoustic vibrations on a flight vehicle are the jet engines, the propellers and boundary layer separations, especially at supersonic flight velocities.

The noise level created by these sources, attains 160-200 dB.

The effect of acoustic loads is dangerous with a large number of repetitions of them in operation (hundreds of millions of times). The result of this is the weakening of riveted joints and the appearance of fatigue cracks in elements whose natural frequencies are close to resonance with the frequencies of the most intense acoustic loads.

It is necessary to keep in mind that this can be both the elements of the external structure - the skin belongs to these (in the zones of a reactive jet and boundary layer separation), the trailing edges of ailerons and other control surfaces, etc., as well as internal components which are inaccessible for inspection.

As measures for preventing the dangerous consequences of acoustic vibrations the elimination of the resonance of the natural frequencies of the elements by varying their rigidity and by introducing damping layers (honeycomb fillers, vibration-isolating packing with great internal friction) is employed.

§ 4. FORCED OSCILLATIONS IN AN EMPENNAGE - BUFFETING

One of the most common types of forced oscillations[1] of aircraft components in flight is the jolting (buffeting) of them caused by the air flow which is turned into vortices when flowing around the parts situated ahead of the affected parts.

Especially dangerous is the buffeting of the empennage. A vortex flow, impinging on an empennage, creates air shock loads of a periodic nature, producing oscillations in the empennage.

Two types of empennage buffeting are distinguished: low-speed and high-speed buffeting.

Low-speed buffeting is the jolting of the empennage as a result of the periodic effect on it of vortices which are separating from aircraft components located ahead of the empennage, during flight at low speeds. Flow separation can occur from a wing during flight at angles of attack, close to critical (stalling), from various secondary structures on a wing or fuselage, from a type of wing-fuselage attachment whose shape is unsuitable.

High-speed buffeting is jolting of the empennage in flight at high velocities, when as a result of the appearance of shock

---

[1]The forced oscillations of aircraft components, the cause of which is the lack of balance of the engine or the propeller, are examined in chapters 8 and 9.

stall during supersonic flow around the wing and other aircraft components situated ahead of the empennage, flow separation occurs after the shock wave.

Experimental and theoretical studies show that in all types of buffeting during flow separation from a wing or another aircraft component a vortex street of drag is formed after them with the staggered arrangement of the vortices. In figure 6.3 h designates the height of the vortex street, l designates the vortex interval.

With an increase in M number the height of the eddy zone increases as a result of air compressibility. An especially sharp increase in the height of a vortex street and in the intensity of the vortices occurs at the moment of the onset of shock stall.

Figure 6.3. Diagram of the formation of a vortex street.

Buffeting is perceived in the form of periodic shocks on the empennage, which have random amplitudes and frequencies causing jerks on the controls and quivering of the aircraft structure.

The predominant frequency of vortex formation is expressed by the formula

$$\nu_{\text{вихр}} = k\frac{V}{c},$$

where k - a constant determined from experiment which depends on the shape of the streamlined body; V - is the flow velocity, m/s; c - is the linear dimension of the streamlined body taken perpendicular to the direction of the flow; for a wing c=bsinα (here b - is the wing chord).

In the case of intense vortex formation, especially when the frequency $\nu_{вын}$ is close to the least natural oscillation frequency of the empennage $\nu_{оп}$ (taking fuselage elasticity into account), the amplitudes of the oscillations of the empennage and the fuselage can be so great that they will cause residual structural deformations.

If $\nu_{вын}=\nu_{оп}$, then resonance arises.

For contemporary aircraft, as a rule, $\gamma_{оп}>>\gamma_{вын}$, which is caused by the necessity for increasing the rigidity of the empennage and the fuselage to avoid the appearance of the phenomenon of empennage reversal whose essence will be subsequently examined. However, the natural oscillation frequency of the control surfaces relative to the axis of rotation (the controls are elastically fixed, since the controls are pressed by pilot) can be close to the frequency of vortex formation.

It should be noted that along with buffeting the entrance of the empennage into the vortex region where the flow velocity is decelerated and the air flowing around is negatively affected, also causes a decrease in empennage effectiveness.

The following measures exist for eliminating and preventing buffeting.

1) in the planning of a new aircraft special attention is given to improving the flow about the aircraft. As was already mentioned, at the sites of the joining of the wing and the fuselage fairings are installed, the external shapes of the canopies and other secondary structures are carefully selected. Furthermore, an attempt is made to remove the empennage from the vortex affected zone.

The presence of separations and the impingement of a vortex flow on the empennage is detected by the simplest method during wind tunnel testing of aircraft models from the oscillation of ribbons stuck on their surface.

It is necessary to keep in mind that the vortices which produce buffeting, can also appear as a result of distortions of the external contours of an aircraft (for example, a wing profile) manifesting themselves under operating conditions.

2) upon the appearance of buffeting it is necessary to change the flight regime. Thus, if buffeting arose during flight at a large angle of attack, it is necessary to change over to a smaller angle. If buffeting arises at a high flight velocity, it is necessary to immediately reduce speed.

§ 5. FLUTTER

Flutter - is the self-sustained oscillations of carrying surfaces in an air flow.[2]

Aviation practice confronted researchers and designers with the problem of studying and preventing flutter especially acutely in the beginning of the 30's when as a result of the transfer to the monoplane aircraft design and as a result of increased engine thrust flight velocities sharply increased. Since that time combatting flutter has become one of the most important problems being solved in the designing and construction of any new high-speed aircraft.

---

[2]The self-sustained oscillations of the nose wheel, known by the name "shimmy," and the ground resonance of helicopters will be examined in chapter 10.

In the USSR V. N. Belyayev, Ye. N. Grossman, M. V. Keldysh, et al. have worked on the problem of wing and empennage flutter. Their investigations form the basis of the contemporary methods of calculating aircraft for flutter.

The flight velocity, at which flutter appears - V_ϕ, is called the critical flutter velocity. In accordance with the stress standard requirements it is necessary that

$$V_\phi \geqslant kV_{\max \max},$$

where $V_{\max \max}$ - is the velocity which corresponds to $q_{\max \max}$; $k>1$ - is the coefficient assigned by the stress standards; for low-speed aircraft $k=1, 2$.

There is a number of types of wing and empennage flutter. Let us breakdown the physical pattern of the course of oscillations as illustrated by the most frequently encountered types of wing flutter: torsional and flexural-aileron flutter. For greater clarity let us examine the simplest setup of an unswept rectangular wing in plan in which the center line of gravity T, the axis of the rigidity Ж and the aerodynamic center line Ф - are straight lines, perpendicular to the attachment cross section (figure 6.4).

Usually in wing cross sections the center of gravity of a design is situated at 43-50% of the chord, the center of rigidity is located approximately at 30-36% of the chord, and the aerodynamic center is usually considered lying at 25% of the chord.

Let us assume that the aerodynamic forces acting on a wing, can be expressed through the aerodynamic characteristics of a certain mean cross section of the wing A-A. We will characterize the oscillatory motion of the wing by the displacements of this cross section from the equilibrium position (by deflection y and by angle of twist φ).

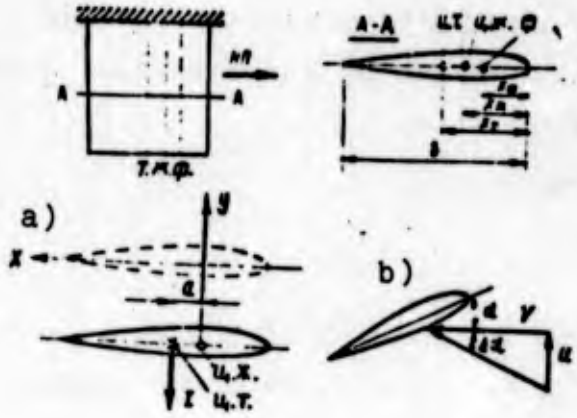

Figure 6.4. Diagram of a deformed wing. During flexural oscillations there arise: a) inertial force 1; b) variation in the angle of attack $\Delta\alpha$.
[ц.т. = center of gravity; ц.ж. = center of rigidity; ф = aerodynamic center]

The conclusions from the examination of the indicated simplest setup are also valid for conventional designs of unswept and swept wings.

Certain characteristics of the flutter of a swept wing are illuminated at the end of this chapter.

1. Torsional Wing Flutter

In the mechanism of the appearance and the course of torsional self-sustained oscillations of a wing, great significance is attached to the existence of a connection between the flexural and torsion motions of a wing, the possibility of combined flexural and torsional oscillations.

In the event of conventional positioning of the axis of rigidity and center of gravity line purely flexural or purely torsional oscillations cannot exist in a wing even in such a case, when the initial impulse which caused the motion, was purely flexural or purely torsional. In both cases the oscillation will be mandatorily combined, i.e., the initiated flexure will lead to twisting of the wing and vice versa. Let us demonstrate this.

If a wing located in a vacuum, is bent downwards, and then left to itself, then under the effect of elastic forces it will

begin to return to the position of equilibrium (axis x-x) with acceleration $j=d^2y/dt^2$. Then the resultant of the inertial forces I is directed downward and will be equal to

$$I = mj,$$

where m - is the mass of the wing.

Disregarding the natural moment of inertia of the wing relative to the axis of rigidity, we will assume, that this force passes through the center of gravity.

The inertial force arising during the motion (figure 6.4a) will yield moment relative to the axis of rigidity

$$M = Ia = maj,$$

where a - is the distance from the center of rigidity to the center of gravity of the cross section.

This moment will cause twisting of the wing. Thus, flexural motion will occur in conjunction with torsional motion.

It is easy to show in a similar manner; that with the indicated positioning of the axis of rigidity and the center of gravity line the initial torsional impulse which caused the torsional oscillations, will lead to the appearance of a periodic flexural inertial force, i.e., flexural oscillations will appear. Only in the case when a=0, i.e., the center of gravity line coincides with the axis of rigidity, are separate, purely flexural and purely torsional oscillations possible.

The frequency of combined flexural oscillations $\nu_{изг}$ is always somewhat less than the frequency of purely flexural oscillations $\nu_{изг\ 1}$, and the frequency of combined torsional oscillations $\nu_{кр}$ is somewhat greater than the frequency of purely torsional oscillations $\nu_{кр\ 1}$, i.e.

$$\nu_{изг} < \nu_{изг1};\quad \nu_{кр} > \nu_{кр1}.$$

Since these differences are small, the characteristics of separate oscillations are usually taken as the frequency characteristics of combined oscillations.

As a result of the presence of internal friction in the design the oscillations of a wing in a vacuum, which begun after the jolt, will always be damped. Damping of the oscillations will occur even faster, if the wing is placed in an air medium.

In order that the oscillations of a wing design located in a flow, be undamped, there should be constant replenishment of the energy which is being scattered during the oscillations. Steady-state oscillations are possible, when the input of energy during the oscillatory period is equal to the energy loss during the same time. If this energy balance is disturbed, then the oscillations will be either damped or increasing.

In theoretical analysis flutter is examined as steady self-sustained oscillations, although in real designs failure can occur at the very beginning of the oscillatory motion.

Let us examine the most important of the aerodynamic forces arising during wing oscillations[3] shown in figure 6.4.

Flexural oscillations in an air flow by themselves at wing angles of attack, remote from the critical (stalling) angle, always create damping forces. Let the wing in the flow impinging on it move downward at a rate of $u=|dy/dt|$. The relative air velocity is directed upward and is equal to u. By summing up the flow rate V with the velocity of u, we will obtain the resultant velocity deflected at angle $\Delta\alpha \sim u/V$ (see figure 6.4b).

---

[3]These forces are added to the main aerodynamic force acting on a wing in flight, which we will not subsequently mention.

Consequently, during the motion of the wing downward the angle of attack will increase and an increase in lift directed against the motion - upward - will appear, i.e., aerodynamic force $P_д$ damping the oscillations will appear. During the motion of the wing upward the pattern is reversed: a damping force directed downward appears. The damping aerodynamic force $P_д$ is proportional to velocity V in the first power

$$P_д = \Delta c_y \frac{\rho V^2}{2} S = \frac{dc_y}{d\alpha} \Delta\alpha \frac{\rho V^2}{2} S = \frac{dc_y}{d\alpha} \cdot \frac{u}{V} \cdot \frac{\rho V^2}{2} S = k_1 u V.$$

Variation in the angle of attack during torsional oscillations leads to the appearance of an air force proportional to the angle of twist φ and to the square of the flight velocity V

$$P_в = \frac{dc_y}{d\alpha} \varphi \frac{\rho V^2}{2} S = k_2 V^2.$$

Both aerodynamic forces $P_д$ and $P_в$, which are increases in lift, are caused by a variation in the wing angle of attack, are applied at the aerodynamic center of the wing.

Let us examine combined flexural and torsional oscillations in the absence of a phase shift between flexure and torsion (ψ=0°), corresponding to figure 6.5 (T - is the oscillatory period, A - is the flexure, B - is the torsion).

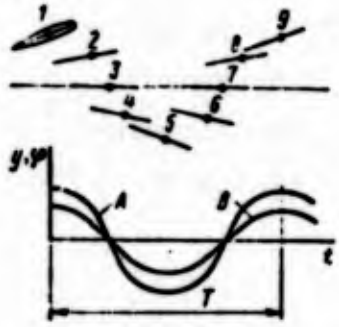

Figure 6.5. Combined flexural and torsional oscillations: 1-9 - consecutive positions of the wing tip during oscillations; A - is the variation in sag y; B - is the variation in the angle of twist φ.

In the absence of a phase shift the air forces arising due to the

torsional oscillations will not maintain the flexural oscillations. And since the air forces $P_д$ caused by flexure are damped, then the oscillations are damped.

The pattern sharply changes, if the phase shift between flexure and torsion is equal or close to 90°. Let us examine the case when ψ=90°, i.e., the zero position of the flexural oscillations is delayed in comparison with the torsional oscillation in the fourth of period. Figure 6.6a depicts the positions of cross section A-A of an oscillating wing in flight through each eighth period. Let the wing as a result of the effect of any random cause, for example, encountering a vertical flow or a sharp motion of an aileron, pass from the neutral position into position 1.

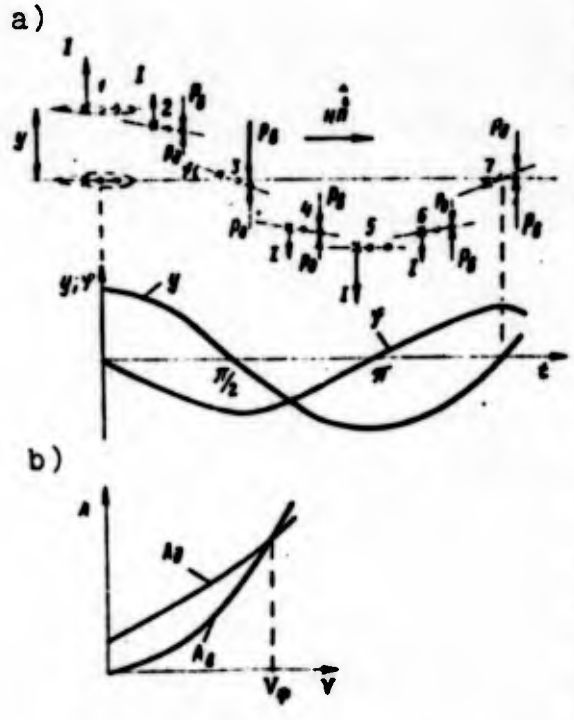

Figure 6.6. Flexural and torsional flutter of a wing: a) oscillations of a wing in flight; b) the dependence of the operation of exciting $A_в$ and damping $A_д$ forces taken over one cycle of oscillations on velocity.
[нп = neutral position]

Under the effect of elastic forces the wing will begin to move from position 1 to its neutral position. In this case the wing in moving from position 1 to position 3 will be twisted at a negative angle relative to the axis of rigidity under the effect of torsional moment $M_{кр}$ due to inertial force I passing through the center of gravity and directed upwards in the direction opposite to the acceleration of the flexural oscillations. In passing

through neutral position 3 the linear acceleration j and, consequently, inertial force I pass through zero and change direction. Thus, during the subsequent motion of the wing from position 3 to position 5 a decrease in the angle of twist of the wing will occur as a result of the presence of the inertial force directed downwards. In position 3 the velocity of the flexural oscillations of the wing $u=dy/dt$ attains the extremum, and the angular velocity of the torsional oscillations $\omega=d\varphi/dt$ changes sign, passing through zero.

Since from position 1 to position 5 the wing has a negative additive of angle of attack, caused by torsion, then in this section there is an additional aerodynamic force $P_в$ directed downward in the direction of the flexural motion, - the exciting force.

During the subsequent motion of the wing the pattern is repeated in the reverse order. In this whole section the wing has a positive increase in angle of attack caused by torsion, which causes the appearance of additional aerodynamic force $P_в$ directed upward, again in the direction of the flexural motion.

Consequently, with a phase shift $\psi=90°$ additional lift $P_в$ arising due to wing torsion amplifies the flexural oscillations, since it is always directed in the direction of the flexural motion of the wing, and is the exciting force.

At low flight velocities the energy obtained by the wing during one oscillatory period from the effect of the exciting forces is less than the energy spent on overcoming the damping effect of the flow and the internal friction, in consequence of which the arising oscillations are damped.

With an increase of flight velocity the exciting forces increase more rapidly than the damping forces, since $P_д$ is proportional V, and $P_в$ is proportional V^2. Consequently, the

energy due to the exciting forces also increases more rapidly than the energy due to the damping forces. Figure 6.6b shows approximately how the operation of exciting forces $A_в$ and the operation of the damping forces $A_д$ change with respect to flight velocity during one oscillatory period. At a flight velocity equal to the critical flutter velocity ($V=V_ф$), equality of the operations sets in. When $V=V_ф$, the operation of the exciting forces is greater than the operation of the damping forces. In this case randomly arising oscillations begin to build up right up to structural failure.

Flexural and torsional self-sustained oscillations of a wing are also observed in the case of a phase shift between flexure and torsion, close to 90°.

2. FLEXURAL-AILERON WING FLUTTER

Flexural-aileron flutter can arise in wings equipped with ailerons unbalanced in a weight regard, i.e., by those, in which the center of gravity is situated behind the axis of rotation.

The development of oscillations is shown in figure 6.7. For simplicity's sake we will consider that the aileron is completely aerodynamically balanced. Aileron deflection arises in the event of a pressed knob due to the elasticity of the control line and play.

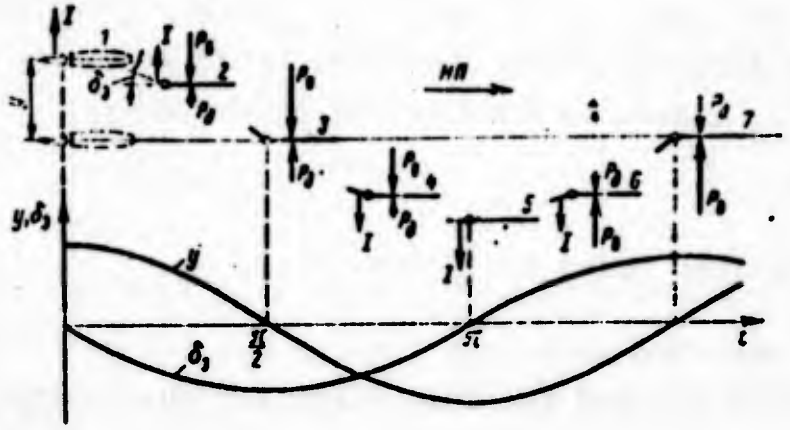

Figure 6.7. Oscillations during flexural-aileron wing flutter. [НП = neutral position]

With an aileron unbalanced in a weight regard, if under the effect of an external impulse the wing is bent upward (position 1) and then under the effect of elastic forces begins to move downwards towards the neutral position, then the center of gravity of the aileron due to inertia will lag behind the wing and aileron will be deflected upward (position 2). This will cause additional aerodynamic force $P_в$, proportional to the square of flight speed, directed downwards

$$P_в = \frac{\partial c_y}{\partial \delta_э} \delta_э \frac{\rho V^2}{2} S = kV^2,$$

where $\delta_э$ - is the aileron deflection.

During the motion of the wing upward the center of gravity of the aileron will again lag behind the wing, which will lead to the deflection of the aileron downwards and to the appearance of an additional aerodynamic force directed upwards.

Thus, as in the case of flexural-torsional flutter, aerodynamic force $P_в$ is actuating.

Along with this as a result of the presence of a vertical rate of flexural oscillations (u=dy/dt), as in the case of flexural-torsional flutter, damping air forces $P_д$ arise, proportional to velocity V in the first power.

If the flight velocity is such, that the operation of the exciting forces during one oscillatory period is greater or equal to the operation of the damping forces (internal friction forces and aerodynamic forces $P_д$ caused by the bending of the wing), then flutter arises.

Flexural-aileron flutter takes two forms:

a) <u>symmetrical</u>, connected with wing flexure and the deflection of each of the ailerons in one and the same direction due to the elasticity of the control line going to the ailerons (figure 6.8a);

b) asymmetric, when the deflections of each of the ailerons occur in different directions; here aileron deflections are possible both due to the elasticity of the control cable, and due to the fact that the pilot does not hold the control stick rigidly (figure 6.8b).

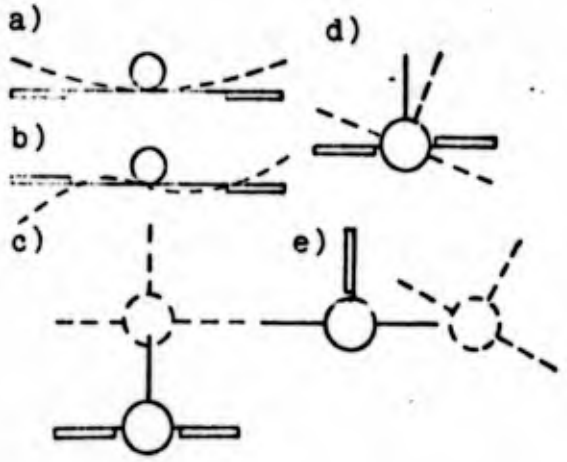

Figure 6.8. Types of wing and empennage flutter: a) symmetrical flexural-aileron flutter of a wing; by b) asymmetric flexural-aileron wing flutter; c) flexural-control surface flutter of the horizontal tail surfaces; d) the torsional-control surface flutter of the horizontal tail surfaces; e) flutter of the vertical tail surfaces.

In the diagrams presented the solid lines show the neutral position of the wing with random aileron deflection which caused the beginning of the oscillations, and the broken lines show the deformed state of the wing.

It is obvious that if an aileron is balanced, i.e., the center of gravity of the aileron is positioned on the axis of rotation, then flexural-aileron flutter will not arise, since in the case of flexural oscillations of the wing initiated as a result of a random external effect the aileron will not be deflected. Flutter will be even less possible, if the center of gravity of the aileron is situated ahead of the axis of rotation (the aileron is "rebalanced" ["retrimmed"]), since in this case during flexural oscillations of the wing the deflection of the aileron will create aerodynamic forces, which damp the oscillations.

3. Basic Types of Empennage Flutter

The physical pattern of the flutter of the vertical and horizontal tail surfaces is similar to the above examined pattern of flexural-aileron wing flutter.

The displacements caused by the deformations of the fuselage play a large role in these oscillations, since in view of the short span of the fixed parts of the empennage (fin and the stabilizer), to which control surfaces are fastened, their deformations are small.

The following types of aircraft empennage flutter are the most frequently encountered.

1. Flutter of the horizontal tail surfaces:

a) flexural-control surface flutter (fuselage flexure, symmetrical deflection of the elevator - figure 6.8c);

b) torsional-control surface flutter (fuselage torsion, asymmetric deflection of the elevator - figure 6.8d).

2. Flutter of the vertical tail surfaces is a combination of the flexural-control surface and torsional-control surface types: flexure and torsion of the fuselage in conjunction with rudder deflection (figure 6.8e).

The diagrams presented depict the neutral and deflected positions of the tail section of a fuselage during oscillations caused by the initial deflection of the control surfaces.

3. Flutter of a helicopter rotor. The flutter of helicopter rotor blades with respect to the conditions of its appearance and its course is similar to flexural-torsional wing flutter.

The flow around a blade is determined by the circular speed of rotation and the translatory flight velocity. Thus, the conditions of the appearance of flutter are characterized by critical combinations of rotor rpm and flight velocity.

Stall flutter is also encountered on helicopters - self-sustained blade oscillations, the cause of which are vortex stalls.

Stalls occur at maximum twistings of the blade due to randomly arising torsional oscillations. The periodic variations in the air forces caused by these stalls maintain the oscillations.

Stall flutter is characterized by considerable amplitudes of the torsional oscillation (the amplitudes of flexural oscillations are small).

The investigations show that the possible types of flutter of flight vehicle components are numerous.

Only those basic types of flutter were examined here, which have lesser critical velocities, close to the velocities of flight operation.

§ 6. THE EFFECT OF DESIGN PARAMETERS ON CRITICAL VELOCITY AND THE MEASURES FOR PREVENTING WING AND EMPENNAGE FLUTTER

Let us examine the effect of the basic design parameters on the most frequently encountered types of flutter and the basic measures for preventing them.

1. The Effect of the Mutual Positioning of the Axis of Rigidity, the Center of Gravity Line of Cross Sections and the Aerodynamic Center Line on Flexural-Torsional Flutter

As follows from an examination of the physical pattern of flexural-torsional flutter, in the case of the coincidence of the axis of rigidity, the center of gravity line and the aerodynamic center line the appearance of this type of flutter is impossible since flexural and torsional oscillations are separated.

This type of oscillation is also impossible in the case of the positioning of the centers of gravity ahead of the axis of rigidity, since in this case the aerodynamic forces arising as a result of reverse twisting of the wing will quench the oscillations.

However, a wing design meeting these conditions is difficult to accomplish and there is no need for this. To prevent the possibility of the appearance of torsional flutter it is sufficient to design a wing so that flutter does not arise up to velocities exceeding $V_{max\ max}$.

As investigations show, for this it is sufficient to shift the center-of-gravity of the wing somewhat forward as compared with its usual position.

The shifting of the center-of-gravity of a wing design forward is the most important measure for preventing torsional wing flutter. It is accomplished by the possible lightening of the rear section of the wing (for example, by employing light magnesium alloys in the design), and sometimes by artificially increasing the weight of the front part by accommodating the assemblies to be located in the wing in it.

In a number of cases special anti-flutter weights are placed in the wing. To increase the effectiveness of these weights, they, as a rule, are placed in the forward part of the end section of the wing. At the wing tip the amplitudes and the accelerations

of the flexural oscillations are greatest, and consequently, the inertial forces acting on the anti-flutter weights will be the greatest.

Just as in flexural-torsional wing flutter, the main measure for preventing the emergence of helicopter rotor flutter in flight regimes is by displacing the centers-of-gravity of the cross sections of the blade design forward with respect to its axis of rigidity.

2. The Effect of the Rigidity of Wing Design on Flexural-Torsional Flutter

An examination of the physical pattern of the emergence and the course of flexural-torsional flutter of an unswept wing shows that the main role in these oscillations is played by torsional deformation. Thus, a change in the torsional rigidity of a wing substantially affects critical velocity.

As investigations show, the effect of torsional rigidity on V_ϕ is described by the following analytical dependence

$$V_\phi = V_{\phi 0}\sqrt{n},$$

where $V_{\phi 0}$ - is the critical flutter velocity of the original wing; n - is the magnitude which shows, by how many times the torsional rigidity of the wing was changed.

On the basis of what has been indicated, the most rational, from the point of view of obtaining high critical velocity, are monocoque wings which have high torsional rigidity.

An increase in the flexural rigidity of an unswept wing can lead to a reduction in V_ϕ. This is explained by the fact, that usually frequency $\nu_{изг} < \nu_{кр}$ and the flutter oscillation frequency lie between them. With an increase in flexural rigidity an

increase occurs in $\nu_{изг}$ and equalization of the frequencies can occur. When $\nu_{изг}=\nu_{кр}$ the flutter oscillations will have a resonance nature, and the critical velocity $V_{ф}$ will attain its minimum.

Thus, not only the absolute values of the wing rigidities affect $V_{ф}$ but also the relationship between them.

3. Measures for Preventing Flexural-Aileron Wing Flutter and Empennage Flutter

As follows from the examined physical pattern of flexural-aileron wing flutter and empennage flutter, the main measures for preventing these types of flutter are as follows:

increasing the rigidity of the design parts deformed during the oscillations, to which the ailerons and the control surfaces are fastened;

positioning the weight compensators.

Aileron and control surface compensators are positioned so as to prevent these types of aileron or control surface deflections during the oscillations of the structure to which they are fastened (wing, stabilizer, fin), in which the aerodynamic forces producing the oscillations will be created.

When installing the compensators the following aspects are observed:

a) the weight of a compensator should be selected so that during the oscillations caused by the structural distortions characteristic for the type of flutter in question, the moment of mass forces of the compensators balance or exceed the moment

of the mass forces of the aileron or control surface design relative to its axis of rotation, i.e., (figure 6.9a)

$$\sum_{k=1}^{k=r} \frac{G_k}{g} j_k x_k \geqslant \sum_{i=1}^{i=n} m_i j_i x_i; \qquad (6.1)$$

b) it is desirable to install the compensators at the sites where large accelerations act during the oscillations; this increases the effectiveness of the compensator, and its required weight is less. An example of this type of positioning of a compensator for eliminating flutter in the vertical tail surfaces is shown in figure 6.9b;

c) compensators are employed either concentrated - positioned outside, or distributed - placed within the front part of the aileron or control surface. Concentrated compensators are convenient because it is possible to place them in the most favorable sites, and because of the possibility of placing them at a greater distance from the axis of rotation the weight of a compensator is low. However, these types of compensators when positioned in flow yield additional drag, and as a result of deformation of the attachments and the structure of the aileron or control surface itself, their effectiveness can be considerably reduced.

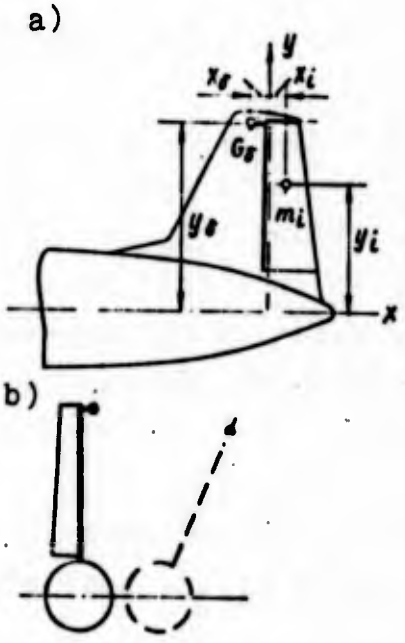

Figure 6.9. Vertical tail surfaces with the rudder compensator. Displacement of the compensator during flutter.

Let us examine as an example the determination of the position of a rudder compensator which has a weight G_p and a coordinate of the center of gravity of the structure x_p.

During flutter of the vertical tail surfaces the flexural and torsional oscillations of the fuselage occur in conjunction with the deflection of the control surface (see figure 6.9b).

Let us discuss each type of oscillation separately.

1. As a result of flexural oscillations in the fuselage the fin is displaced together with the end of the fuselage, and the axis of rotation of the fin is moved parallel to itself.

If the chord of the control surface is small, and the intrinsic deformations of the fin and the control surface are also small, then the accelerations of all points of the control surface and the compensator can be considered identical ($j_б=j_1=j$) and condition (6.1) takes the form

$$\frac{G_б}{g} j x_б \geqslant \Sigma m_i j x_i.$$

Whence $G_б x_б > \Sigma m_i g x_i$. Since $\Sigma m_i g x_i = G_p x_p$, then to prevent the type of flutter being examined it is necessary to fulfill the following conditions

$$G_б x_б \geqslant G_p x_p$$

or

$$x_б \geqslant \frac{G_p}{G_б} x_p. \qquad (6.2)$$

If the chord of the control surface is long, then, since during fuselage flexure the vertical tail surface is turned together with the end of the fuselage, the difference between j_1 and $j_б$ can be considerable, and $j_1 > j_б$. The taking of this fact into account leads to the fact that to prevent flutter it is necessary that $G_б x_б > G_p x_p$, i.e., it is necessary to rebalance (retrim) the rudder.

2. During torsional oscillations of fuselage the axis of rotation of control surface y is turned relative to the axis of

the rigidity of the fuselage x. If we disregard the intrinsic deformations of the control surface and fin, then the accelerations of the points of the control surface are

$$j_i = \varepsilon y_i,$$

where ε - is the angular acceleration of the rotation of axis y; y_i - is the coordinate of a point.

For a compensator

$$j_б = \varepsilon y_б.$$

The condition of preventing this type of flutter is:

$$\frac{G_б}{g} \varepsilon y_б x_б \geqslant \varepsilon \Sigma m_i x_i y_i.$$

Since

$$\Sigma m_i x_i y_i = I_{xy},$$

where I_{xy} - is the centrifugal moment of inertia of the control surface structure relative to the x and y axes, then the condition takes the form:

$$G_б y_б x_б \geqslant g I_{xy}.$$

Here $x_б$ is determined from the condition of the absence of the flexural-control surface type of flutter.

To prevent the torsional-control surface type of flutter of the vertical tail surface it is necessary that

$$y_б \geqslant \frac{g I_{xy}}{G_б x_б}. \qquad (6.3)$$

From this expression it is evident that to reduce the necessary weight of the compensator it is advantageous to place it at a greater distance $y_б$ from the torsional axis of the fuselage, i.e., at the location, where the accelerations of the compensator due to the torsional oscillations will be greater.

Frequently in technical descriptions of aircraft and in educational literature the degree of mass balancing is characterized

by the percentage ratio of the static moment of the balancing weights to the static moment of control surface or an aileron without weights

$$\zeta = \frac{G_6 x_6}{G_p x_p} 100\%.$$

However, as follows from the example in question, this characteristic is insufficient for a complete judgement of the properties of a system with regard to the different types of flutter. One and the same load placed at different cross sections of a control surface or aileron creates a different effect.

4. Preventing the Development of Flutter in Flight

Contemporary flight vehicles are designed and constructed in such a way that the values of critical velocity for all types of flutter would certainly exceed the velocities encountered in aircraft operation. However, in flight practice cases are known of the appearance of flutter due to the exceeding of the permissible flight velocity, damage to the airframe structure and the attachments of the balancing weights or of the formation of play in the suspensi assemblies and the control hinges. The play reduces the natural oscillation frequencies of the control surfaces and the ailerons and reduces the critical flutter speed.

If oscillations arose, then pilot should sharply reduce speed, by decreasing engine thrust and by increasing the wing angle of attack.

§ 7. WING OVERTWISTING AND DIVERGENCE

An increase in aerodynamic torsional wing moments always occurs in flight as a result of an increase in its twist angles

under the effect of these moments. At high flight velocity this phenomenon can lead to wing failure or the formation of impermissible deformations.

Usually the deformations are characterized by the twist angle of a certain specific wing cross section. The maximum value of this angle $\varphi_{пр}$ can be established from the condition of limiting the magnitude of wing deformation due to aerodynamic considerations or due to the loss in stability of design elements, or their transition beyond the yield point.

The flight velocity, at which wing twisting up to $\varphi_{пр}$ begins, is called the <u>maximum overtwisting velocity</u> $V_{пр}$. This velocity should be greater than or equal to the velocity $V_{max\ max}$.

The first profound theoretical and experimental study on this question was V. P. Vetchinkin's work the results of which were presented at TsAGI (Cen. Inst. of Aerohydrodynamics im N. Ye. Zhukovskiy) in 1929 in a report under the name "concerning wing overtwisting in an air flow."

Let us discuss the physical pattern of this phenomenon on the basis of a simple setup of a rigid rectangular wing elastically fixed to a fuselage (figure 6.10). The wing is mounted at a positive angle of attack to the impinging air flow, having velocity V. The aerodynamic force P_0 which tends to turn it around the axis of rigidity acts on the wing.

If wing deformations were absent, then the aerodynamic moment would equal $M_{A0}=P_0a_0$ and for a specific impact pressure q_1 would be a constant value.

As a result of the elasticity of the system the wing under the effect of force P_0 will begin to be twisted in the direction of an increase in the angle of attack. This will lead to an

increase in force P_0. For convex profiles in the case of an increase in the angle of attack the center of pressure is shifted forward; thus arm a also increases.

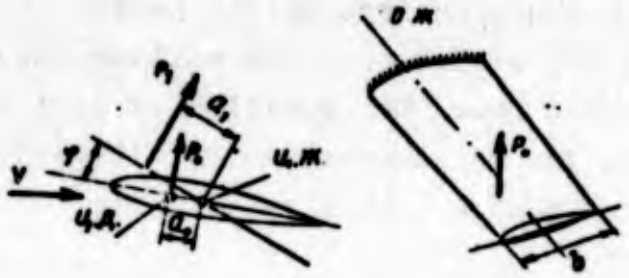

Figure 6.10. Forces acting on a wing during divergence. [ц.д. = center of pressure; ц.м. = center of rigidity; а.м. = axis of rigidity]

The twisting will continue until wing is broken or until the moment of the elastic forces of the wing M_E counterbalances the aerodynamic moment, which has become equal to $M_{A1}=P_1a_1$.

Since with a variation in the angle of attack an increase in air force is applied to the aerodynamic center of the wing, then an additional moment of air forces arising due to the variation in the angle of attack of the wing due to torsion by angle φ is equal to:

$$M_A = (x_a - x_F)\frac{dc_y}{d\alpha} q q S = k_A q q.$$

The total aerodynamic moment which corresponds to the position of equilibrium is

$$M_A = M_{A0} + k_A q q,$$

where k_A - is the coefficient which characterizes the variation in moment relative to the axis of rigidity due to the angle of attack and the impact pressure.

The torsional moment (opposite in direction) of the elastic forces up to the limit of proportionality of the wing design will vary according to the following law

$$M_E = k_E \varphi,$$

where k_E - characterizes the wing rigidity during torsion, kg-m/rad; φ - is the variation in the angle of attack due to the effect of the aerodynamic moment, rad.

The equilibrium condition is

$$M_A = M_E.$$

The curves of $M_A=f(\varphi)$ plotted for one and the same setting angle[*] and different impact pressures q, and the curve of $M_E=\psi(\varphi)$ are plotted in figure 6.11. The point of intersection of curve M_{A1} with M_E will determine the angle $\varphi=\varphi_1$, at which the wing is twisted under the effect of aerodynamic forces at flight velocity V_1 and impact pressure q_1.

An increase in flight velocity V will lead to an increase in the slope of the curve of aerodynamic moment M_A.

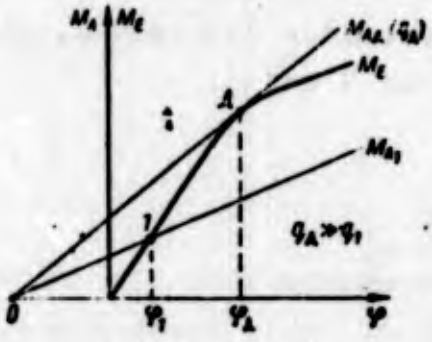

Figure 6.11. Conditions of the emergence of divergence.

Divergence is the state of a wing at which any infinitesimal increase in the twisted nature of wing leads to a more rapid increase in aerodynamic moment than elastic moment, i.e., after receiving small additional deformation the twisted nature of the wing will build right up to wing failure. The diagram in figure 6.11 illustrates the conditions of the appearance of divergence.

At a certain impact pressure $q_д$ the curve of aerodynamic moment will occupy the position of a tangent to curve M_E at point Д. Point Д corresponds to wing divergence. The velocity at which this unstable equilibrium between aerodynamic and elastic moment occurs is called the critical divergence velocity, which should satisfy the following condition

[*]The diagrams in figure 6.11 are given for an unsymmetric profile. Point 0 corresponds to wing twisting at that negative angle at which $M_A=0$, i.e., the center of pressure lies on the axis of rigidity.

$$V_д \geqslant k_д V_{max\ max},$$

where $k_д > 1$.

G. Rostovtsev, who gave the solution of the problem of calculating divergence in his work "concerning the stability of the torsion of a rectangular spar wing", was involved in the investigation of questions of the divergence of wing design in flight as early as 1932. Later this question was investigated at TsAGI by Ye. P. Grossman, V. N. Belyayev et al.

For the wings of contemporary aircraft $V_д$ is high and the conditions of the absence of flutter, reversal, and the limitation of twist angle with overtwisting which precedes divergence, give the lower bounds of the maximum values for V and q.

§ 8. REVERSAL

Reversal is the phenomenon of the complete loss of control effectiveness as a result of deformation of their fixed parts.

Questions connected with the reversal of control organs were investigated by the Soviet scientists, V. S. Pyshnov, by S. N. Shishkin, A. I. Makarevskiy, Ya. M. Serebriyskiy, S. N. Kan, who developed the methods of calculating reversal velocity.

Aileron reversal - the loss of aileron effectiveness in connection with wing twisting - is encountered more frequently than other types of reversal.

To explain the physical pattern of the phenomenon of reversal let us examine aileron reversal on the same setup of a rectangular wing with elastic attachment (see figure 6.4a), which was employed for examining wing flutter.

Upon the deflection of an aileron downward (figure 6.12) the aerodynamic force which acts on the wing ($P_2 > P_1$) increases, and as a result of the increase in the curvature of the profile the center of pressure is displaced backward.

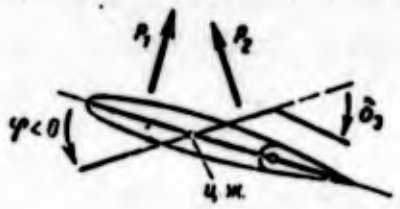

Figure 6.12. Forces acting on a wing during aileron reversal. [ц.ж. = center of rigidity]

This leads to the fact that the torsional wing moment increases and causes in the case of an insufficiently rigid wing in torsion a considerable deformation (in our case - negative angle of twist).

As a result the effect of the aileron deflected downward is reduced due to a decrease in the angle of attack as a result of wing twisting.

With an increase in flight velocity V the rolling moment due to wing twisting M^{Φ}, opposite in direction to the rolling moment due to the effect of the aileron $M_э$, will increase more rapidly than $M_э$ (figure 6.13a). This is explained by the fact that, since moment M_φ is proportional to the product φV^2, and φ in turn is determined by the load on the aileron proportional to V^2, M_φ is proportional to V^4, i.e., $M_\varphi = k_\varphi V^4$. At the same time $M_э$ is proportional to V^2, i.e., $M_э = k_э V^2$.

Aileron reversal (complete loss of aileron effectiveness) begins when a change in the rolling moment of the wing directly caused by aileron deflection, is completely damped by oppositely directed rolling wing moment due to wing twisting caused by aileron deflection, i.e., when $M_\varphi \geq M_э$.

Aileron reversal, just like overtwisting, can occur at high flight velocity. For an unswept wing - with insufficient rigidity

of the wing in torsion, and for swept wings (as will be shown subsequently) - with insufficient rigidity of the wing in flexure and torsion.

The stress standards require for impact pressure q_p, at which reversal arises, fulfillment of the following condition

$$q_p \geqslant kq_{\max \max},$$

where k>1 - is the coefficient assigned by the standards.

Value q_p should be significantly higher than the impact pressure of flight in order to insure sufficient effectiveness of the control organs also at velocities less than the reversal velocity.

The reduction in aileron effectiveness observed at flight velocities less than reversal velocity V_p is explained by the above examined wing deformations upon aileron deflection. Aileron effectiveness is characterized by magnitude ω_x - by the angular velocity of rotation of the aircraft relative to the x-x axis. As is evident from figure 6.13b, for an elastic wing ω_x with an increase in flight velocity at first increases, and then begins to drop off. At a velocity equal to V_p, aileron effectiveness is equal to zero.

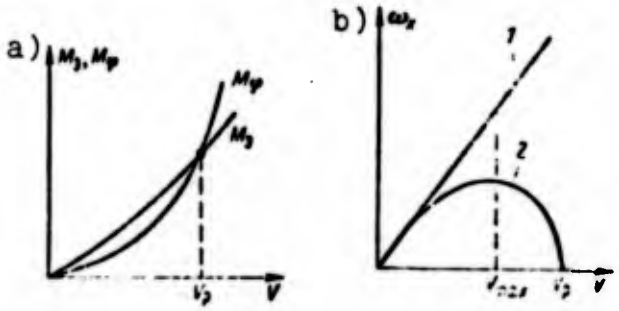

Figure 6.13. Manifestations of aileron reversal: a) a decrease in the rolling moment; b) the effect of wing deformation on ω_x; 1 - rigid wing; 2 - elastic wing.

The causes of the phenomena of elevator and rudder reversal are the same: the effect of control surface deflection is reduced due to the change to the reverse direction of the angle

of attack of the fixed part of the empennage, to which it is fastened. Thus, for instance, elevator reversal - is a loss in elevator effectiveness due to stabilizer twisting and fuselage flexure.

To ensure elevator effectiveness it is necessary to make the stabilizer sufficiently rigid in torsion, and the fuselage - in flexure.

§ 9. THE EFFECT OF WING SWEEP

Let us examine how the characteristics of the deformation of a swept wing affect the phenomena of wing divergence, reversal and flutter.

For a wing section, the tip and middle effects do not affect the flow around the section, as is known, the aerodynamic characteristics are determined by the profiles of the cross sections, normal to the aerodynamic center line (figure 6.14, cross sections cd). Thus, here the torsional deformations have an effect on the aerodynamic characteristics, just as for an unswept wing: these torsional deformations lead directly to a change in the angles of attack α in these cross sections. With regard to wing sections, close to the wing root and the wing tip, then their aerodynamic properties are determined by the profiles of the cross sections situated with respect to the direction of flight.

In the phenomena of divergence, reversal and flutter the main role is played by the deformations of the tip sections of a wing.

For a swept wing it is characteristic that the angles of attack of the cross sections (situated with respect to the direction of flight) of these sections are determined not only by torsional deformations φ(twist angle), but also by flexural deformations δ (deviation).

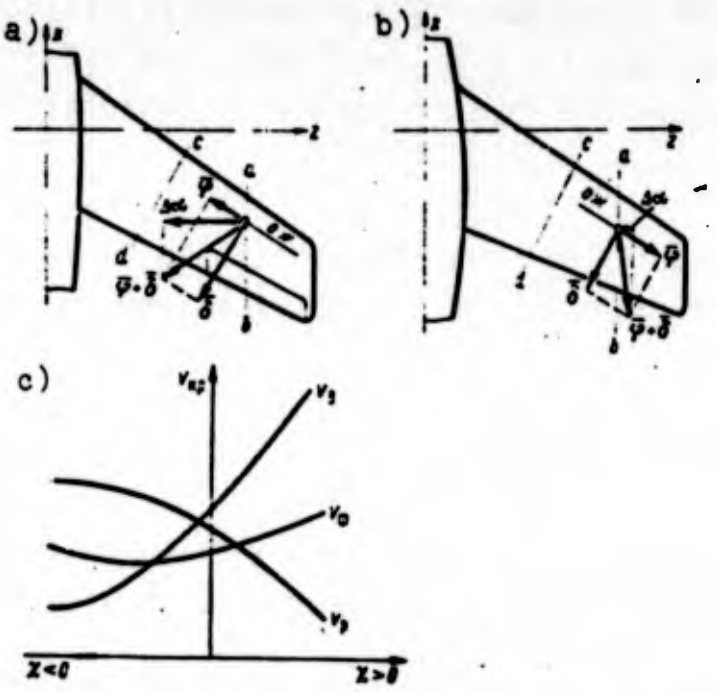

Figure 6.14. The effect of sweep on the phenomena of wing aeroelasticity: a) deformations of a swept wing during aileron reversal; b) deformations during divergence; c) the dependence of critical velocities on sweep χ; V_σ - is velocity of divergence; V_ϕ - is the flutter velocity (flexural-torsional); V_p - is the velocity of aileron reversal. [ось = axis of rigidity]

Let us examine the effect of sweep on reversal, assuming the sweep angle to be $\chi>0$.

During aileron deflection downwards, for example, displacement of the center-of-pressure backwards and an increase in the aerodynamic force on the wing section in the region of the aileron occur.

As a result of this turning of the cross sections of this part of the wing due to twisting occurs at an angle φ and due to flexure at an angle δ. As is evident from figure 6.14a, the variation (in this case - the decrease) in the angle of attack of cross section ab will constitute

$$\Delta\alpha = -(\varphi\cos\chi - \delta\sin\chi).$$

It follows from the formula that the wing flexure with $\chi>0$ upward leads to a decrease in the angle of attack and, consequently, to a reduction in the effect due to aileron deflection. Thus, when $\chi>0$ bending equally with wing torsion contributes to a reduction in the critical reversal velocity.

Thus, for combatting swept wing reversal it is necessary to increase not only the rigidity of the wing in torsion, but also its rigidity in flexure.

For an unswept wing ($\chi=0$), where $\Delta\alpha=-\varphi$, it is sufficient to increase the rigidity of the wing in torsion.

If the wing lift is positive and the center-of-pressure line lies ahead of the axis of rigidity (which usually occurs for contemporary low-moment or symmetrical shapes), then during the divergence or flutter of a swept wing with $\chi>0$ the torsional deformation due to the aerodynamic forces leads to an increase in the angles of attack of the wing sections.

In this case the pattern of the deformations and the variation in the angle of attack of cross section ab will correspond to figure 6.14b.

It follows from this, that:

$$\Delta\alpha = \varphi\cos\chi - \delta\sin\chi.$$

As is evident from this formula, during flexure of the wing upward a decrease occurs in the angle of attack, during flexure downward an increase occurs. This leads to the appearance of stabilizing aerodynamic forces and moments which impede divergence and which prevent the emergence of flutter.

In flexural deformations of a swept wing, greater in comparison with the torsional deformations, divergence is impossible.

However, in low aspect ratio swept wings ($\lambda<4$) the flexural deformations are small and the change in the angle of attack due to twisting can be greater than the change in the angle of attack due to flexure; therefore at high velocity divergence becomes possible.

In a swept wing with $\chi<0$ the effect of flexural deformation is opposite to that examined above.

Figure 6.14c shows an example of the dependence of the critical velocities of divergence, flutter and reversal on sweep.

CHAPTER 7

MEANS OF IMPROVING THE TAKEOFF AND LANDING CHARACTERISTICS OF AIRCRAFT

§ 1. CLASSIFICATION

The takeoff and landing properties of aircraft are characterized by the lengths of the takeoff run and the landing run, by the takeoff and landing velocities, by the takeoff and landing distance. Improving these characteristics increases flight safety and, by reducing the required dimensions and the cost of airfields, makes it possible to expand the airline network.

A reduction in the length of the takeoff run and the landing run as follows from formulas (7.1) and (7.2):

$$L_{\text{разб}} = \frac{V^2_{\text{отр}}}{2j_{x\,\text{ср.разб}}}; \tag{7.1}$$

$$L_{\text{пр}} = \frac{V^2_{\text{пос}}}{2j_{x\,\text{ср.пр}}}, \tag{7.2}$$

based on the assumption, that the motion is uniformly accelerated, can be obtained, by reducing velocities $V_{\text{отр}}$ and $V_{\text{пос}}$ and by increasing average values of accelerations $j_{x\ \text{ср.разб}}$ and $j_{x\ \text{ср.пр}}$ during acceleration and deceleration of the aircraft.

Velocities $V_{отр}$ and $V_{пос}$ are expressed by the following formulas (which are of the same type):

$$V_{отр} = \sqrt{\frac{2(G_0 - P_{y\,в})}{\rho c_{y\,отр} S}}; \qquad (7.3)$$

$$V_{пос} = \sqrt{\frac{2(G_{пос} - P_{y\,п})}{\rho c_{y\,пос} S}}, \qquad (7.4)$$

where G_0 and $G_{пос}$ - are the weight of an aircraft during takeoff and during landing; $c_{y\,отр}$ and $c_{y\,пос}$ - are the corresponding lift coefficients which depend on $c_{y\,max}$; S - is the wing area; $P_{y\,в}$ and $P_{y\,п}$ - are the vertical component of engine thrust during takeoff and during landing. For conventional aircraft $P_y \approx 0$, but it can attain large values for short takeoff and landing aircraft.

It follows from formulas (7.3) and (7.4) that at a given weight of an aircraft G_0 or $G_{пос}$ it is possible to reduce $V_{отр}$ and $V_{пос}$, by increasing the carrying capacity of the wing (product $c_y S$) and by employing the power plants which give vertical thrust.

A classification of the means which improve the takeoff and landing characteristics of an aircraft is given in table 7.1.

§ 2. WING LIFT-INCREASING DEVICES WHICH INCREASE c_y

Wing lift-increasing devices which increase its c_y have received broad application on the contemporary aircraft of civil aviation.

The concept of wing lift-increasing devices was first theoretically established as early as 1910 by S. A. Chaplygin. Their practical realization came about towards the end of the 20's and the beginning of the 30's when the increase in flight velocities led to the necessity for increasing wing loading

G/S and made it necessary to look for ways to reduce the landing velocity of aircraft and the liftoff velocity during takeoff.

In the design of the existing means of lift-increasing devices of this group (figure 7.1) the following basic principles are employed:

1) increasing the airfoil camber. This measure leads to a shift in the curve of $c_y = f(\alpha)$ to the left and to an increase up to known limits of $c_{y\ max}$;

2) the blowing away or sucking away of the boundary layer. These methods are employed for the purpose of delaying the beginning of flow separation up to large values of wing angle of attack. For blowing away the boundary layer from the upper wing surface slot effect is usually employed - the action of an air jet being discharged from a slot connecting the lower wing surface with the upper surface. Rarefaction formed beyond a deflected flap is employed for sucking the boundary layer away;

3) increasing the wing area by making the wing extensible either in the direction of the span, or along the chord.

All three principles lead to an increase in c_y due to an increase in the rate of flow circulation along the wing contour in accordance with Joukowski's theorem.

Figure 7.2 schematically shows the effect on the c_y of a wing (relative to initial value of S) of the sequential application of these principles. Figure 7.2b gives examples of the curves of c_y with respect to α for a wing with certain types of lift-increasing devices;

4) decreasing the wing sweep angle in flight, which eliminates the reduction in $c_{y\ max}$ and the lift/drag ratio caused by the sweep.

Table 1

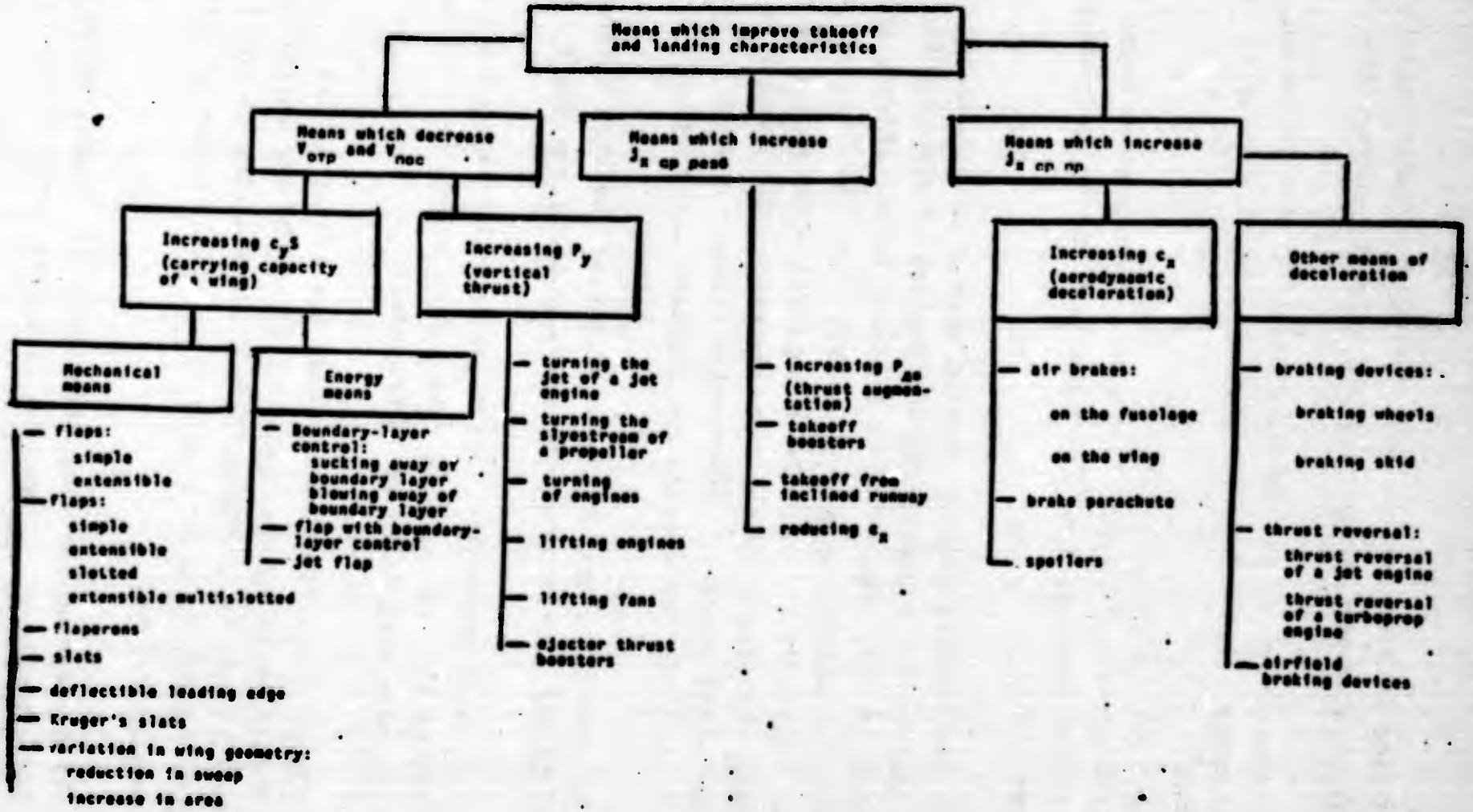
Means which improve takeoff and landing characteristics
Means which decrease V_{otp} and V_{nac}
Means which increase j_x on pass
Means which increase j_x on np
Increasing $c_y S$ (carrying capacity of a wing)
Increasing P_y (vertical thrust)
Increasing c_x (aerodynamic deceleration)
Other means of deceleration
Mechanical means
Energy means
flaps:
simple
extensible
flaps:
simple
extensible
slotted
extensible multislotted
flaperons
slats
deflectible leading edge
Kruger's slats
variation in wing geometry:
reduction in sweep
increase in area
Boundary-layer control:
sucking away of boundary layer
blowing away of boundary layer
flap with boundary-layer control
jet flap
turning the jet of a jet engine
turning the slyestream of a propeller
turning of engines
lifting engines
lifting fans
ejector thrust boosters
increasing P_{aa} (thrust augmentation)
takeoff boosters
takeoff from inclined runway
reducing c_x
air brakes:
on the fuselage
on the wing
brake parachute
spoilers
braking devices:
braking wheels
braking skid
thrust reversal:
thrust reversal of a jet engine
thrust reversal of a turboprop engine
airfield braking devices

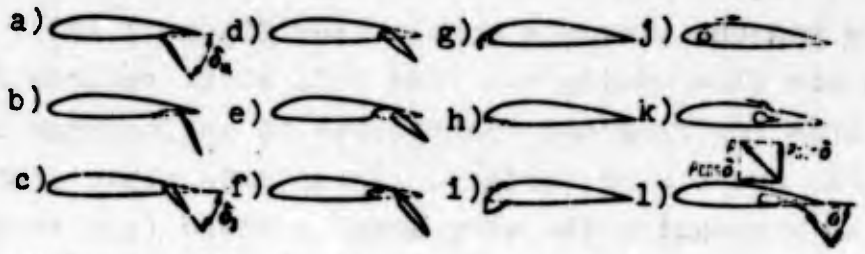

Figure 7.1. Types of wing lift-increasing devices, which increase c_y.

The lift-increasing devices, in which several principles are combined, give the greatest effect. However, designwise these means are considerably more complex.

Split flaps are made in the form of a deflected downward part of the lower wing surface situated along its trailing edge (see figure 7.1a). Upon deflection of the flap the camber is increased and, moreover, boundary-layer bleeding occurs from the upper wing surface into the rarefaction zone between the wing and the flap. As a result $c_{y\ max}$ is increased and $\alpha_{крит}$ is somewhat decreased.

More effective, but designwise more complex are extensible flaps (see figure 7.1b), which upon being deflected downward are simultaneously displaced towards the trailing edge of the wing, increasing its area.

Deflected flaps substantially increase the drag of an aircraft; thus when employing flaps in takeoff it is necessary to considerably decrease the angle of their deflection, thereby also reducing the increase in c_y.

Flaps are the tail part of a wing deflected downwards. Flaps of different types are employed.

In a wing with simple flaps (see figure 7.1c) an increase in $c_{y\ max}$ occurs only due to a change in the camber of the original profile, and therefore their effectiveness is comparatively slight.

Upon the deflection of slotted flaps a shaped slot is formed between them and the wing - a nozzle (see figure 7.1d). The accelerated air flow coming out from this slot retards flow separation from the flap and contributes to an increase in rarefaction on the upper wing surface. In an extensible slotted flap the effect of increasing the wing area is added (see figure 7.1e).

An important advantage of extensible flaps is the fact that when they are deflected by small angles a considerable increase in c_y is accompanied by a small increase in c_x.

This makes it possible to effectively employ flaps not only during landing, but also during takeoff.

The effectiveness of flaps increases with the increase in the angle of their deflection. However, at large angles of deflection of single-slotted flaps (more than 35-40°) flow separation arises leading to a drop off in c_y and causing flap vibration. In connection with this highly efficient double-slotted and three-slotted extensible flaps are employed on the majority of contemporary aircraft which operate without flow separation up to deflection angles of 50-60° (see figure 7.1f).

The employment of split flaps and flaps of all types leads to a certain reduction in the critical angle of attack and to an increase (in the absolute value) in angle α_0.

Slats. A slat is located along the leading edge of a wing, forming a shaped slot (see figure 7.1g).

Slats with a fixed slot, automatic slats and controllable slats are distinguished.

A fixed slat has a constant slot between the wing and the slat and is employed on low-speed aircraft (Yak-12). An automatic

slat is opened only at large angles of attack, its opening occurs under the action of aerodynamic forces. A controllable slat is activated by the pilot.

The effect of a slat manifests itself in the following manner.

At large angles of attack the air flow, flowing through the slot between the slat and the wing, increases speed of the boundary layer above the wing. Boundary layer blowing occurs.

As a result of the comparatively high value of the inherent lift of a slat a noticeable downwash is formed after it. The downwash and the increase in the speed of the boundary layer impede boundary-layer separation and lead to an increase in the $\alpha_{крит}$ and $c_{y\ max}$ of the wing.

Figure 7.2 depicts the curves of $c_y=f(\alpha)$ for the case of a slat (5) forced against the wing, for the open position of a slat (8) situated along the entire span of the wing and for a slat situated only opposite an aileron, a so-called tip slat (6).

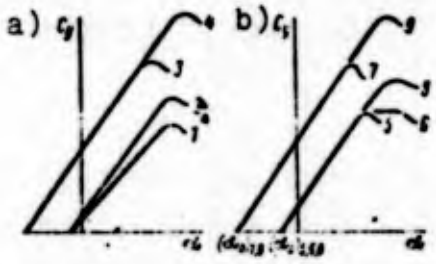

Figure 7.2. Dependence $c_y=f(\alpha)$ of a wing: a) the effect of various factors (total); b) the effect of various types of lift-increasing devices; 1 - original wing; 2 - the wing area is increased; 3 - the camber is increased; 4 - stall delay is introduced; 5 - wing without lift-increasing devices; 6 - tip slat; 7 - wing with deflected flap or split flap; 8 - slat along entire span; 9 - combined employment slat and flap.

Tip slats increase $\alpha_{крит}$ and, by preventing flow separation from the tip part of the wing, ensure aileron effectiveness at large angles of attack. The employment of tip slats virtually does not increase the carrying capacity of a wing. This is explained by the fact that slats, by increasing the $c_{y\ max}$ of the

tip sections of a wing, in front of which they are located, compensate for the lift loss in the middle part of the wing where flow separation begins.

For a swept back wing, in which the tendency towards tip stall is especially significant, it is advantageous to install slats over a larger part of the wing span.

On some passenger aircraft Kruger (simple in design) slats are installed sometimes called leading-edge flaps (see figure 7.1h). Kruger slats increase the effective camber of the leading-edge part of a profile and increase its $\alpha_{крит}$. The leading edges of a wing deflected downwards yield a similar effect (see figure 7.1i).

Usually slats are employed together with split flaps or flaps.

As experimental studies show, in this case the increase in the $\Delta c_{y\ max}$ of a wing is less than the sum of the increase in $\Delta c_{y\ max}$ obtained in the case of the deflection of one split flap or one flap and one slat taken separately. This is explained by the fact that in the case of a simultaneously opened flap and slat the separation can begin earlier than in the case of an open slat and closed flap.

A correctly selected setup of wing lift-increasing devices and the combined deflection of flaps and slats can insure values of $c_{y\ max}$ of a swept wing (when $\chi \approx 35°$) within the limits of from 2.5 to 2.8.

Flaperons. Conventional ailerons, occupying part of the wing span, reduce the effectiveness of the flaps. To eliminate this phenomenon certain aircraft (for example the An-2) employ flaperons or flap ailerons which can be additionally deflected at angle $\delta_э < \delta_{крит}$, where $\delta_{крит}$ - the critical aileron deflection angle which leads to flow separation. The difference $\delta_{крит} - \delta_э$ is employed

for deflecting the flap ailerons as ailerons and should ensure the required transverse controllability.

Variable geometry wings. The geometry of a wing can be changed as a result of varying the wing area and the sweep angle.

Varying wing area. By reducing the wing area of an aircraft in flight at high velocity, it is possible to achieve a considerable decrease in $c_x S$ and thereby an increase in V_{max}. By increasing the wing area during landing, $G_{пос}/S$ is decreased and thereby the value of the landing speed is reduced.

Varying the wing area in flight can be accomplished by varying the span or the chord of the wing. This type of wing with a variable area was employed by the Soviet designer G. I. Bakshaev in 1937 on the telescopic wing (PH=RK) aircraft constructed at the Leningrad Institute of Engineers of the Civil Air Fleet. However, as a result of the extreme complexity in designing telescopic wings they were not broadly employed and variation in the wing area is only employed on contemporary series aircraft with the aid of extensible flaps.

Variation in the sweep angle of a wing. It is only advantageous to impart sweep to a wing for flight at high transonic and supersonic flight velocities, and at low flight velocities sweep decreases the $\alpha_{крит}$ and $c_{y\ max}$. In connection with this mechanisms have been developed which make it possible during flight at low velocities to decrease the sweep angle of a wing. This operation also beneficially affects the effectiveness of the conventional lift-increasing devices installed on a wing. However, the great weight and the complexity of design impede the application of similar devices on civil aviation aircraft.

Table 7.2[1] gives a comparison of the different types of lift-increasing devices when they are positioned along the entire span of an unswept wing having an aspect ratio of $\lambda=6$, a thickness ratio of $\bar{c}=0.17$, $\alpha_{крит}=17°$, $c_{y\ max}=1.4$, $c_x=0.14$ (when $c_{y\ max}$). The relative chord of the flaps and split flaps is $\bar{b}=0.3$, of the slats - $\bar{b}=0.05$.

Table 7.2

Type of lift-increasing devices	$\delta^0_{опт}$	$\alpha^0_{кр}$	$\Delta c_{y\ max}$	Δc_x when $c_{y\ max}$
Split:				
simple	50	14	0,87	0,05
extensible	60	13	1,10	0,06
Flaps:				
simple	45	12	0,66	0,02
slotted	45	18	0,70	0,01
extensible single-slotted	40	13	1,54	0,01
double-slotted	60	12	1,70	0,085
Slat	—	28	0,4	0,02
Extensible double-slotted flap and slat	50	21	1,95	0,045

Note. $\delta^0_{опт}$ - is the optimum split flap or flap deflection angle. Values $\alpha_{кр}$, $\Delta c_{y\ max}$ and Δc_x are given when $\delta_{опт}$.

Energetic means of imparting high-lift to a wing. Decreasing the thickness ratio of the wings of contemporary high-speed aircraft and increasing the sweep reduce the effectiveness of conventional wing lift-increasing devices. Thus of great interest are the energetic means of imparting high-lift characteristics to an aircraft employing the energy of the aircraft's power plant and which make it possible to considerably raise the carrying capacity of the wing even when a large sweep angle is present. Included among these are various wing boundary layer control systems and jet flaps. On the basis of their effect, just as in

[1]The materials employed in the table were taken from F. P. Kurochkin's book "Bases of VTOL aircraft design." M., "Mashinostroyeniye," 1970.

conventional lift-increasing devices, lies the increase in flow circulation over the airfoil contour.

Boundary layer control can be accomplished by artificial (due to the expenditure of engine power) sucking or blowing away of the boundary layer from the upper surface of a wing, slats or flaps at large angles of attack (see figure 7.1j, k).

The effect of systems for the sucking and the blowing away of the boundary layer is approximately identical and is determined by the flow rate of the air through the slot. By increasing the air flow rate (by increasing the power of the boundary-layer control system), it is possible to obtain values of $c_{y\ max}$ of up to 5. It should be noted that more simple in design, not requiring the application of special pumps, are the systems which blow away the boundary layer with the compressed air from the compressors of turbojet engines or from the second stage of ducted-fan engines.

Jet (reactive) flaps. A jet flap is a shaped slot situated along the trailing-edge of a wing, through which at a certain angle δ an air jet emerges taken from a jet-engine compressor, or the engine exhaust-gas jet (see figure 7.1, 1). The jet coming out carries along after itself the air which flows around the wing, and increases its rate of motion. In summation, the circulation of the flow around the profile is increased and the lift is increased.

Additional lift is furnished by the vertical component of reactive thrust $P\sin\delta$. Accordingly the lift coefficient of a wing with a jet flap $c_{y\ p.з}$ is equal to the sum of coefficients c_{y1} due to the effect of the aerodynamic forces and c_{y2} due to the effect of the thrust. The value of $c_{y\ max\ p.з}$ can be as high as 10-12, considerably improving the takeoff and landing characteristics of an aircraft. However, the application of a jet flap is hampered by the design difficulties connected with arrangement

in the wing of channels for supplying a large quantity of air or gas and aerodynamic difficulties connected with the breakdown of longitudinal balancing (by appearance of considerable diving moment).

The general deficiencies of the energetic high-lift devices of a wing are the considerable increase in the design weight of an aircraft and the dependence of the lift-increasing devices on the aircraft's power plant; when the engines fail the lift-increasing devices do not operate.

§ 3. THE EMPLOYMENT OF VERTICAL THRUST

A considerable improvement in the takeoff and landing characteristics of an aircraft right up to the transition to vertical takeoff and landing can be attained by creating sufficiently great vertical thrust which during takeoff and landing supplements the lift from the wing or completely replaces it.

Increasing the vertical thrust of the power plant is equivalent to decreasing wing loading ($p=G-P_y/S$) leads, according to formulas (1-4), to a decrease in $V_{отр}$ and $V_{пос}$ and to a reduction in $L_{разб}$ and $L_{пр}$. When employing jet engines the vertical component of thrust can be obtained either by the gas flow downward employing rotary exhaust nozzles, or by rotating the engines themselves.

On aircraft with turboprop engines multislotted flaps are employed for this purpose (with the chord comprising up to 40-50% of the wing chord) which deflect the air flow from the propeller downwards (figure 7.3), or systems which ensure the inclination of the propeller shafts (sometimes together with the engines).

The angle of rotation of the vector of the total thrust of the engines should be selected in such a way that a considerable

decrease in its horizontal component does not occur which provides the acceleration of the aircraft during the takeoff run.

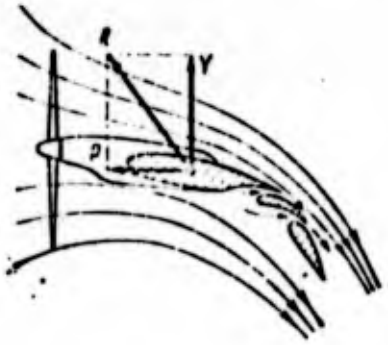

Figure 7.3. Intense air flow forced by a propeller around a wing with powerful lift-increasing devices ensures the creation of lift.

The thrust-weight ratio $\mu = \frac{\Sigma P}{G_0}$ of STOL and VTOL aircraft considerably exceeds the thrust-weight ratio required for flight in cruising regimes. This leads in comparison with conventional aircraft to an increase in the thrust and the weight of the engines and to considerable throttling in flight which increases the fuel consumption. It is possible to improve efficiency by deflecting a part of the engines after takeoff; however, for a VTOL it can be more advantageous to employ separate power plants for creating vertical and horizontal thrust (figure 7.4a). The employment of special lifting engines rated for short-term operation and which have a low specific weight ensures the creation of vertical thrust with a comparatively small increase in takeoff weight (at a given payload).

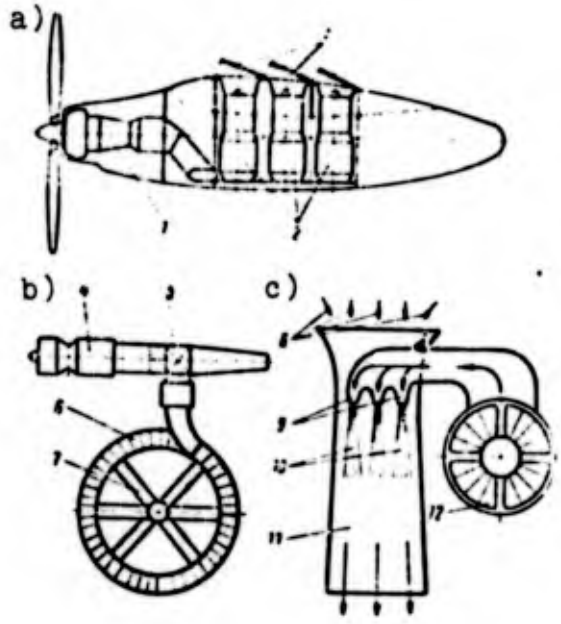

Figure 7.4. Creating vertical thrust: a) the employment of separate lifting engines and turning of the thrust of the main engine; b) turbofan unit; c) diagram of a thrust ejector booster; 1 - main engine; 2 - lifting engines; 3 - bucket-shaped retractible air intakes; 4 - turbojet engine; 5 - gas changeover valve; 6 - fan turbine; 7 - fan; 8 - air being sucked in; 9 - ejector nozzles; 10 - gas jets; 11 - mixing chamber; 12 - turbojet engine.

The main deficiency in employing jet engines with a vertical thrust component is the harmful effect of the gas jet on the surface of the airfield, especially a dirt airfield. A reduction in this effect can be ensured by employing power plants with the vertical thrust units in the form of lifting turbofans and ejectors (figure 7.4b, c).

When employing lifting turbofans the main engines of the aircraft during takeoff and landing serve as gas generators which turn the fans mounted in the wing or fuselage. The thrust of the fans can exceed the thrust of the main engines by more than 3 times, which limits the required dimensions and the weight of the engines.

Similar results can also be obtained with the multislotted ejector thrust boosters which ensure due to the sucking down of the gas jet an additional mass of air passing through the lifting device, an increase in the thrust of the main engine by 2-2.4 times.

§ 4. INCREASING ACCELERATION DURING TAKEOFF RUN

An increase in $j_{x\ ср.разб}$ - the average value of the acceleration of an aircraft during the takeoff run, as follows from expressions (7.1) and (7.3), does not affect unstick speed, (lift-off velocity), but leads to a decrease in the time and the length of the takeoff run. The most widely employed means of increasing acceleration is increasing the thrust-weight ratio of the aircraft $\Sigma P/G_0$ during the takeoff run. A takeoff engine operating regime is employed for this purpose: afterburners are employed with additional injection of fuel beyond the turbine of the engine. Rato (rocket-assisted takeoff) units, attached to the fuselage or wing and jettisonable after the takeoff of the aircraft, can also be employed. The operating time of the RATO units, operating on solid propellant, does not exceed 15-20 s. With their aid short takeoff distances can be obtained.

An increase in acceleration during takeoff can also be attained with the aid of airport takeoff boosters - various types of catapulting devices, but due to their unwieldiness and complexity, especially for heavy aircraft, these types of devices are not finding application in civil aviation.

Decreasing the drag of an aircraft also favorably affects the takeoff run length, which is taken into account when employing wing lift-increasing devices (the angle of deflection of the split flaps and flaps during takeoff is less than during landing). For this purpose the majority of contemporary aircraft are equipped with landing gear wells covered with doors both with the landing gear retracted and extended.

To facilitate the takeoff of heavily loaded aircraft with a low thrust-weight ratio the use of an inclined take-off runway for the takeoff run has found employment, in particular in the record flights of Chkalov's and Gromov's crews on ANT-25 aircraft in 1936-1937.

§ 5. AIRCRAFT BRAKING

The following means are employed for aircraft braking.

Air brakes. Gliding angle is determined by the magnitude of aerodynamic efficiency of an aircraft $tg\theta_{пл}=1/K$. The possibility of varying angle $\theta_{пл}$ over a broad range at a relatively slightly varying flight velocity increases flight safety (makes it possible to easily correct errors in landing calculations) and makes it possible to land on airfields with poor approaches. To reduce aerodynamic efficiency air brakes, made in the form of the flaps situated under the wing or on the fuselage, are employed. One of the requirements imposed on air brakes is the least possible variation in c_y and m_z during their employment in order to simplify aircraft handling near the ground before touchdown.

Speed brakes on the tail section of the fuselage (figure 7.5) completely meet this requirement. Speed brakes are also employed for the braking of an aircraft during its landing run.

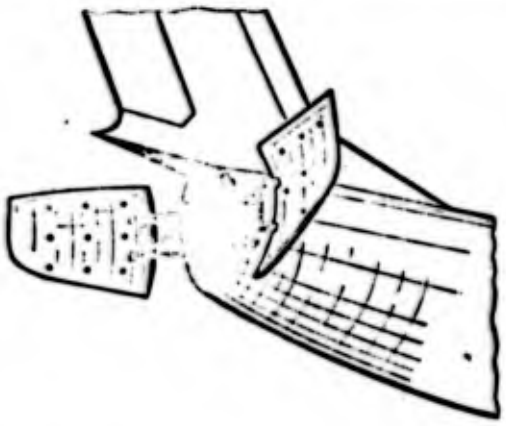

Figure 7.5. The arrangement of speed brakes on the tail section of the fuselage.

Brake parachutes are installed in the tail section of the fuselage and are deployed after touchdown. Their employment is especially advantageous when landing on a wet or icy runway, when the effectiveness of wheel braking is diminished.

On heavy aircraft due to the operational complexity of a parachute of large size and weight brake parachute systems consisting of two, three and more canopies are employed.

The most common brake parachutes are those with ribbon canopies which have a drag coefficient with respect to the area of the canopy, $c_{x\ п}$=0.5-0.6.

Spoilers, intended for application during landing, are made in the form of split flaps on the upper surface of a wing (figure 7.6). Upon the deployment of the spoilers there is flow separation from the wing which leads to a sharp drop in lift and to a certain increase in drag. The main purpose of the employment of spoilers immediately after the touchdown of an aircraft is to insure an increase in the loads on the landing gear wheels and effective employment of wheel braking over the entire distance of the landing run.

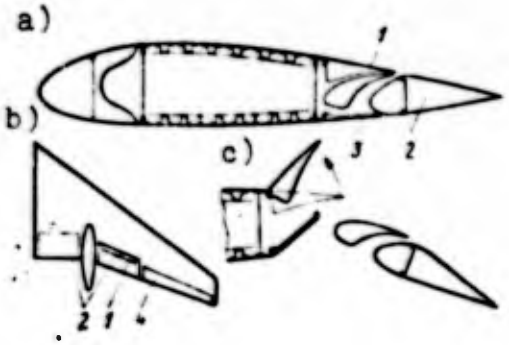

Figure 7.6. Spoiler: a) position in flight; b) placement on a wing; c) a spoiler is deployed after touchdown; 1 - spoiler; 2 - flaps; 3 - mobile cover; 4 - aileron.

Wheel braking by the landing gear is the main means of reducing the translatory velocity of an aircraft during its landing run and its motion along the taxiways of an airfield. However, during landing on a wet runway the effectiveness of this type of braking is sharply diminished. The design and operation of landing gear wheel brakes are examined in § 6 chapter 10.

Thrust reversal is an arrangement which makes it possible to change by 180° the direction of thrust of aircraft engines. The comparatively simple conversion of the blades to negative angles of attack ensures the reversing of the thrust of turboprop engines. The thrust reversal of turbojet engines is accomplished by turning the gas jet by an angle of more than 90°. An example of a thrust reversal setup is shown in figure 7.7. In practice it is possible to obtain a magnitude of reverse thrust of not more than 35-40% of the magnitude of engine thrust. As a result of the employment of reverse engine thrust effective braking of an aircraft occurs independently of the condition or state of the runway.

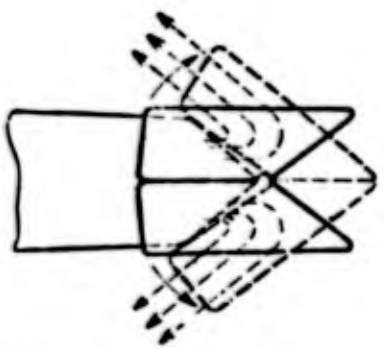

Figure 7.7 Thrust reversal.

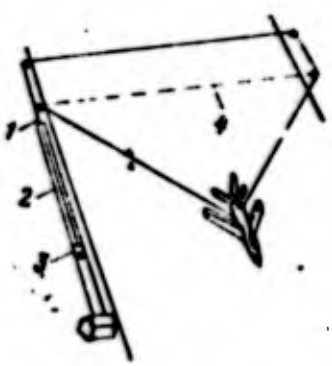

Figure 7.8. Airport braking device: 1 - cable; 2 - tube with water; 3 - piston; 4 - position of the cable before the beginning of braking.

Airport braking devices employed for carrier-based aircraft, stop aircraft over a section of several tens of meters. An aircraft having a special hook on the tail section of the fuselage, is caught by it after touchdown by one of the cables stretched at a low height across the deck and, by tugging on the cable, moves the piston in the hydraulic brake cylinder. Similar devices can also be employed for braking aircraft on short airfields (figure 7.8).

§ 6. DESIGN AND STRESS ANALYSIS OF FLAPS AND SPLIT FLAPS

The load-bearing setup and the design of flaps are not fundamentally different from the load-bearing setup and the design of an aileron (see figure 5.4).

As an example of stress analysis, let us examine the stress analysis of an extensible split flap.

Rated loads. Loads can act on lift-increasing devices both in the closed position - these are air loads incident on the surface of a closed split flap (flap suction) as well as in the open position.

Let us examine as illustrated by a simple split flap how in accordance with the stress standards the loads acting on a split flap in the open position are determined (figure 7.9).

Coefficient c_n and safety factor f=2 are assigned. Then

$$P_{\text{щ}}^{\text{р}} = f c_n S_{\text{щ}} q^{\text{э}}. \qquad (7.5)$$

For high-lift devices intended for reducing $V_{\text{отр}}$ and $V_{\text{пос}}$, the ram pressure $q^{\text{э}}$ is determined in accordance with the greatest rated flight velocity with the high-lift devices deployed and retracted.

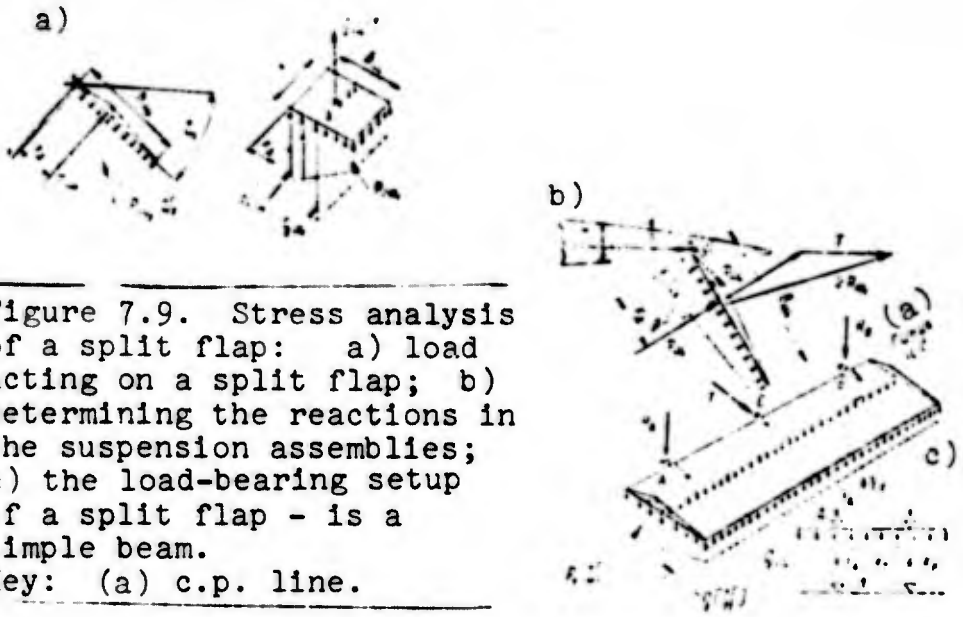

Figure 7.9. Stress analysis of a split flap: a) load acting on a split flap; b) determining the reactions in the suspension assemblies; c) the load-bearing setup of a split flap - is a simple beam.
Key: (a) c.p. line.

For high-lift devices the distribution of air loads is determined from wind-tunnel test data.

Upon a deflection of a split flap by $\delta_{щ}=60°$ it is possible to assume that $c_n=1.1-1.2$, and the center-of-pressure coefficient is $\bar{x}_д=x_д/b_{щ}=0.4-0.5$.

The distribution of the air load along the span of the split flap is assumed proportional to the chords. Then the rated linear load is

$$q_1^p = \frac{P_щ^p}{S_щ} b_щ \frac{kgf}{м}. \qquad (7.6)$$

Along the chord the air load is distributed in shape of a trapezoid the center of the area of which is situated under the center of pressure.

Sequence of stress analysis. Let us examine the sequence of the stress analyzing of an extensible flap. The analysis is carried out for calculated destructive loads (henceforth we will not write superscript "p").

A split flap consists of a spar, a set of ribs and a lower skin.

To a split flap are attached two carriages A and B and bracket C which serve for connecting the control rod (Fig. 7.9b). When a split flap is extended the carriages slide along guides. In this case the split flap is deflected downwards and extended backwards.

With respect to its load-bearing setup a split flap is a beam which operates in flexure and torsion.

The determination and the distribution of the air load is made in this sequence.

1. Determination of the total load on a split flap in accordance with the stress standards - see formula (7.5).

2. Determination of linear load with formula (7.6).

3. Determination of the values of load per unit area - $p_{1щ}$ and $p_{2щ}$ (kgf/m^2). For this a section of the three-dimensional diagram of the air load is singled out which has a length equal to unity (Fig. 7.9a).

For determination of $p_{1щ}$ and $p_{2щ}$ the following two conditions are employed:

$$q_{щ1} = \frac{p_{1щ} + p_{2щ}}{2} b_{щ1}; \tag{7.7}$$

$$x_A = \frac{b_щ}{3} \cdot \frac{p_{1щ} + 2p_{2щ}}{p_{1щ} + p_{2щ}}. \tag{7.8}$$

Condition (7.7) corresponds to the situation in which the volume of the diagram for a unit length of a split flap is equal to $q_{щ1}$.

Condition (7.8) expresses, that the center of gravity of the diagram should be located opposite the center-of-pressure line.

In equations (7.7) and (7.8) ratios $q_{щ}/b_{щ}$ (calculated) and $x_{д}/b_{щ}$ (taken in accordance with the indications of the stress standards) are known, constant for all split flap cross sections.

By simultaneously solving equations (7.7) and (7.8), $p_{1щ}$ and $p_{2ш}$ are determined, also constants for all cross sections.

Linear load $q_{щ}$ found from the calculation is necessary for rating the split flap beam (determining the support reactions, $M_{изг}$, Q), loads per unit area p_1 and p_2 are employed for rating the skin and the ribs.

Determination of the reaction of a split flap attachment includes the following.

1. Determination of the total reaction $\Sigma R_{щ}$ of assemblies A and B and of force T in the control rod. Figure 7.9b shows the graphic determination of forces of T and $\Sigma R_{щ}$ from force $P^{р}_{щ}$ calculated previously applied at the center of pressure of a split flap perpendicular to the split flap chord.

The total reaction should pass through point O - a projection of the centers of curvature of the rail guides.

2. Determination of the projections of force T and of reactions R of assemblies A and B in directions, parallel and perpendicular to $P_{щ}$. Figure 7.9c depicts a diagram of split flap loading as a simple beam in the direction of the y- and x-axes. By knowing $q_{щ}$ and $Y_{т}$, Y_{A} and Y_{B} are determined - projections of the reactions of assemblies A and B in the direction, parallel to $q_{щ}$.

Reactions X_A and X_B are similarly determined - projections of the reactions of assemblies A and B in the direction, perpendicular to $q_ш$.

3. Determination of the reactions of assemblies R_A and R_B and of their components (reactions of the rollers) R_{A1}; R_{A2}; R_{B1}; R_{B2}.

By knowing Y_A, X_A or Y_B and X_B, reactions R_A and R_B are first determined by graphic plottings, and then their components R_{A1}, R_{A2} and R_{B1}, R_{B2} whose directions are parallel to radii 0-1 and 0-2.

Strength testing of a split flap is carried out similarly to the testing of aileron strength. A flap as a whole is rated as a beam operating in flexure and torsion. Testing of the local strength of the individual elements and assemblies is also carried out.

CHAPTER 8

ARRANGEMENT AND ATTACHMENT OF ENGINES ON FLIGHT VEHICLES

§ 1. BASIC REQUIREMENTS IMPOSED ON THE ARRANGEMENT AND ATTACHMENT OF ENGINES AND UNITS CONNECTED TO THEM

The aerodynamic requirements reduce to the fact that the mounting of engines on a flight vehicle:

1) not produce a large increase in parasite drag. For this purpose an attempt is made, for example, to reduce the values of $c_{xг}S_{вг}$ of the engine nacelles ($c_{xг}$ - is the drag coefficient of a nacelle, $S_{мг}$ - is the area of the midsection cross section of a nacelle) and to obtain high value of $M_{кр}$ of the nacelles in coupling them with the wing;

2) ensure the best employment of the ram pressure for the engines;

3) not negatively affect the stability and controllability characteristics of the aircraft.

The arrangement requirements:

1) the arrangement of the engines and the fuel should satisfy the center of gravity position requirements; it is desirable to

arrange them nearer to the center of gravity to reduce the mass inertial moments which affect the maneuvering properties of the flight vehicle;

2) the arrangement of the engines should not disrupt the load-bearing setup of adjacent parts;

3) in arranging the engines it is necessary to specify measures directed at preventing the heating of components and units situated near the engines and their exhaust devices;

4) the positioning of the engines and the design of the suction and exhaust devices should ensure the least losses of engine thrust power.

Strength requirements:

1) ensuring the strength of the elements attaching the engines, nacelles, etc.;

2) ensuring sufficient durability of all elements having oscillatory loads and the damping of the vibrations of the power plant so that they are not transmitted to the airframe structure;

3) the attachments of the engines and the exhaust devices should not permit the emergence of thermal stresses in them.

Operational requirements:

1) good access for the inspection, adjustment and the repair of engines and their units; the possibility of rapid assembly and disassembly;

2) fire safety;

3) the engine gases should exit at a specific distance from the surface of the airfield;

4) sand, stones and other foreign objects should not get into the suction intakes from the surface of the airfield.

§ 2. ARRANGEMENT OF ENGINES ON AN AIRCRAFT

In the arrangement of turbojet engines on an aircraft an attempt is made to ensure the minimum external drag of the power plant, and also the least possible losses of pressure in the air intakes supplying the intake and exhaust ducts.

The site of the installation of a turbojet engine depends on the general design of the flight vehicle. At the present time three methods (setups) of arranging turbojet engines are mainly employed: at the root section of the wing, on the wing cantilevers, in the tail section of the fuselage.

In arranging engines at the root part of the wing turbojet engines can be situated behind the load-bearing part of the wing (Fig. 8.1d) or within it (Fig. 8.1e).

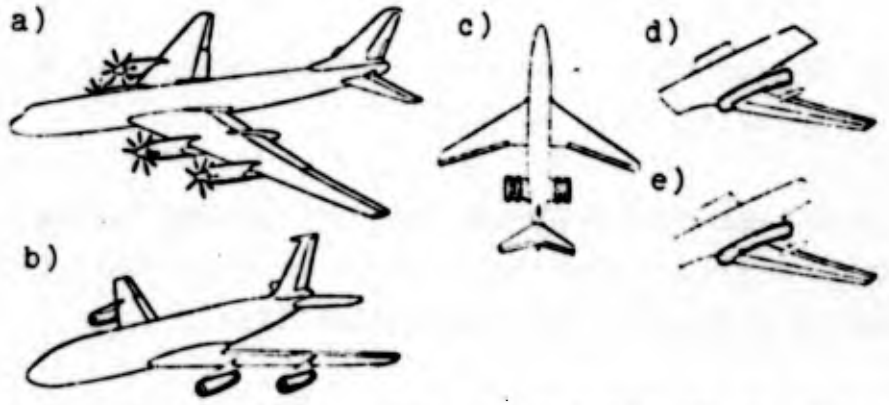

Figure 8.1. Arrangement of engines on an aircraft: a) turboprop engines on a wing; b) turbojet engines on pylons; c) in the tail section of the fuselage; d) turbojet engines on a wing beyond the load-bearing section; e) on the wing in the load-bearing section.

The arranging of engines beyond the load-bearing part of the wing makes it possible to install not only turbojet engines, but also turbofan engines and turboprop engines, having a considerably larger diameter: in this case there is no need to lengthen the exhaust duct of the engines, the continuity of the load-bearing setup of the wing is not impaired with hatches.

The installation of engines in the load-bearing section of a wing makes it possible to make the midsection of nacelles small, air ducts of short length.

The setup of positioning engines in the root part of a wing has the following advantages:

the aerodynamic drag of the power plants is considerably lower than in the positioning of these under the wing or in the tail section of the fuselage;

reducing the interference between the fuselage and the wing. During engine operation an "active" fillet is formed, in which instead of deceleration of the air flow an increase in its velocity and a reduction in the pressure occur in the direction of the flow. As a result the total drag coefficient is reduced;

engine failure on the one side of the wing does not cause sharp turning or rolling moments;

the arrangement of engines does not affect the selection of the dihedral angle of the wing, it is selected only from the conditions of stability and controllability;

the air intakes are located rather high above the surface of the earth, which prevents the entry of water, dust and small objects during engine operation;

during an emergency landing with retracted landing gear the engines are protected against impact with the earth by the wing and the fuselage.

Included among the deficiencies in this type of engine positioning arrangement are:

the high noise level in the passenger compartment;

the danger of the effect on the fuselage skin and the horizontal tail surfaces skin of powerful reactive gas jets;

the possibility of damage to the pressurized cabins and fuel tanks in the case of the failure of turbine blades or a compressor;

increasing the thickness ratio of the root section of the wing profile for accommodating engines negatively affects the aerodynamic characteristics of the wing;

the creating of systems for engine thrust reversal complicated by the fact that the output of a turned reactive jet is only possible forward - upward and forward - downward. The portion of the jet directed forward - downward, being reflected from the surface of the airfield, can get into an air intake and disrupt normal engine operation;

the entry into air intakes of stones and other small objects from under the wheels of the front landing gear strut is possible.

The positioning of engines on wing centilevers has become common, in the majority of cases - on pylons under the wing (Fig. 8.1b). This type of engine arrangement setup has the following advantages:

the weight of the engines is relieved from the wing during flight (the flexural stresses are reduced);

the critical flutter velocity is increased as a result of the arrangement of the center of gravity of the engines in front of the axis of rigidity of the wing;

the maintenance conditions are improved;

fire safety is increased;

the noise from the engines in the passenger compartment is reduced;

also possible is the installation on engines of devices for reversing thrust and devices for noise suppression.

The deficiencies of this type of engine arrangement are the following:

suspended power plants on pylons considerably increase aircraft drag, including the negative interference of the wing with the pylons;

it is necessary to create large wing dihedral in a low wing monoplane, which affects the stability and controllability characteristics;

in case of the failure of one of the engines a large turning moment in the horizontal plane is created;

the entry of water, dust and small objects into the air intakes is possible during engine operation on the ground;

increased fire hazard when landing with retracted landing gear (belly landing).

Recently the arrangement of engines in the tail section of the fuselage has obtained broad application (Fig. 8.1c).

The advantages of this setup are the following:

the possibility of creating an aerodynamically "pure" wing with maximum possible employment of the span for the accommodation of high-lift devices;

good conditions are created for the operation of the air intakes (by positioning the engines at a distance from the fuselage sufficient to ensure a boundary-layer control by suction);

the characteristics of longitudinal, directional and lateral stability are improved as a result of: the operation of the engine nacelles and their pylons as an aditional stabilizer; the placing of the horizontal tail surfaces on the upper part of the fin out of the zone of wing downwash; increasing the effectiveness of the vertical tail surfaces by making it T-shaped; slight engine turning moment when one of them stops operating;

the comfort is improved as a result of decreasing the noise in the cabin;

fire safety is increased;

the possibility of replacing an entire nacelle together with the engine is ensured and good conditions of access to the engines are created;

the effect of the reactive jet of the engines on the fuselage is reduced;

the engines are protected against the entry into them of water, dust and stones during operation on the ground and from the entry

of stones from under the landing gear as a result of the shielding of the air intakes by the wing and the flaps (Fig. 8.2).

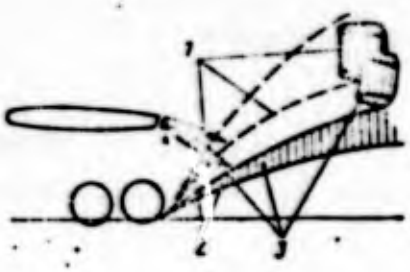

Figure 8.2. Diagram of the protection of engines against the entry of stones: 1 - zone of protection by flaps in the upper position; 2 - zone of protection with flaps down; 3 - unprotected zone.

The deficiencies of this type of engine setup are the following:

an increase in the weight of the fuselage (in connection with increasing the loads on its tail section), of the vertical tail surfaces (carrying the horizontal tail surfaces on it), of the wing (unrelieved of the mass forces of the engines);

the considerable aerodynamic drag of the engine nacelles;

the necessity for passing the fuel lines from the tanks to the engines through the passenger compartment;

the difficulties in maintaining and servicing the high-positioned engines.

Significant improvement in the aerodynamic characteristics of this setup can be attained by mounting the engines not on pylons, but on the contours of the fuselage.

The positioning of piston and turboprop engines. Piston and turboprop engines are usually mounted on the wing of aircraft (Fig. 8.1a) and more rarely in the nose or tail section of the fuselage.

The position of engine nacelles along the span of a wing is mainly determined by the diameters of the propellers. The

distance between the inboard engines and the fuselage can also be dictated by the permissible noise level in the passenger cabin or by the dimensions of the landing gear track width, since the main landing gear are retracted into the nacelles of inboard engines.

The dimensions of engine nacelles and their position relative to the wing have a considerable effect on propeller effectiveness and the aerodynamics of the wing and the aircraft as a whole. The positioning of the nacelle within the wing is best in this respect. However, this case considerable design difficulties arise. Thus, most frequently, especially on high-wing monoplane aircraft, the engines are installed ahead of the load-bearing section of the wing (box) on a level with its upper contour (Fig. 8.3a). This type of arrangement of turboprop engines insignificantly increases the frontal area of the aircraft, makes it possible to completely equip the wing trailing edge section with high-lift devices, and also to divert the reactive jet downward under the wing with minimum losses in thrust. In the low-wing monoplane setup a similar arrangement turboprop engines can be unacceptable due to the short distance of the propeller from the ground. In this case the engine is placed above the wing and the reactive jet is diverted above the wing beyond its trailing edge (Fig. 8.3b).

Figure 8.3. Installation setup of a turboprop engine on a wing.

The rotation planes of the adjacent propellers should not coincide with each other and pass through the flight deck.

Power plants with tractor propellers increase wing drag as a result of the blowing around and turbulization of the flow and

thereby eliminate the employment of laminar profiles on a wing. Pusher propellers, on the contrary, reduce its drag, since they suck air from the boundary layer and supply energy to the trailing vortex. However, the production of turboprop engines with pusher propellers is fraught with great design difficulties.

Other advantages and deficiencies of the arrangement of piston and turboprop engines being examined connected with their layout on wing cantilevers are the same as those which were noted in analyzing the arrangement of turbojet engines on pylons under a wing.

Auxiliary power plants are usually placed in the tail section of the fuselage. This type of arrangement is most rational for the following reasons:

An auxiliary power plant is installed in the nonpressurized section and it does not occupy the volume of the pressurized section;

it is possible to completely isolate an auxiliary power plant from the passenger compartment in the event of a fire;

convenience in maintenance;

convenience in connecting it to the air conditioning system of the pressurized cabin.

Auxiliary power plants on main-line long- and intermediate-range aircraft based at and making landings at 1st class airfields are used mainly for air conditioning passenger compartments after landing and when getting ready to take off.

Auxiliary power plants on regional airline aircraft which are operated on dirt airfields, not equipped for the maintenance of flight vehicles, are employed for:

refueling the aircraft;

starting engines;

heating the wing and empennage;

conditioning the air in the passenger compartment.

§ 3. ENGINE NACELLES AND COWLINGS

For reducing drag engines and units connected to them are enclosed in streamlined nacelles which are smoothly connected to the fuselage or wing. The nacelles protect the engine and its units from corrosion and contamination. Simultaneously with this the nacelles ensure the supply of air to the engine at a uniform rate for normal operation and cooling of the engine. The nacelles should ensure minimum engine drag and convenient access to the engine and the units located on it, for inspection and replacement.

An engine nacelle includes a cowling which consists of a system of easily removable or hinged covers.

Engine nacelles are thin-walled structures, similar to the fuselage structure.

The load-bearing setups of cowlings and nacelles can be frame and panel.

The frame design of a nacelle consists of a powerful framework, light covers which are fastened to the framework, and the skin reinforced with a longitudinal and transverse assembly. A nacelle of this type of design receives loads from the engine and transmits them to the wing.

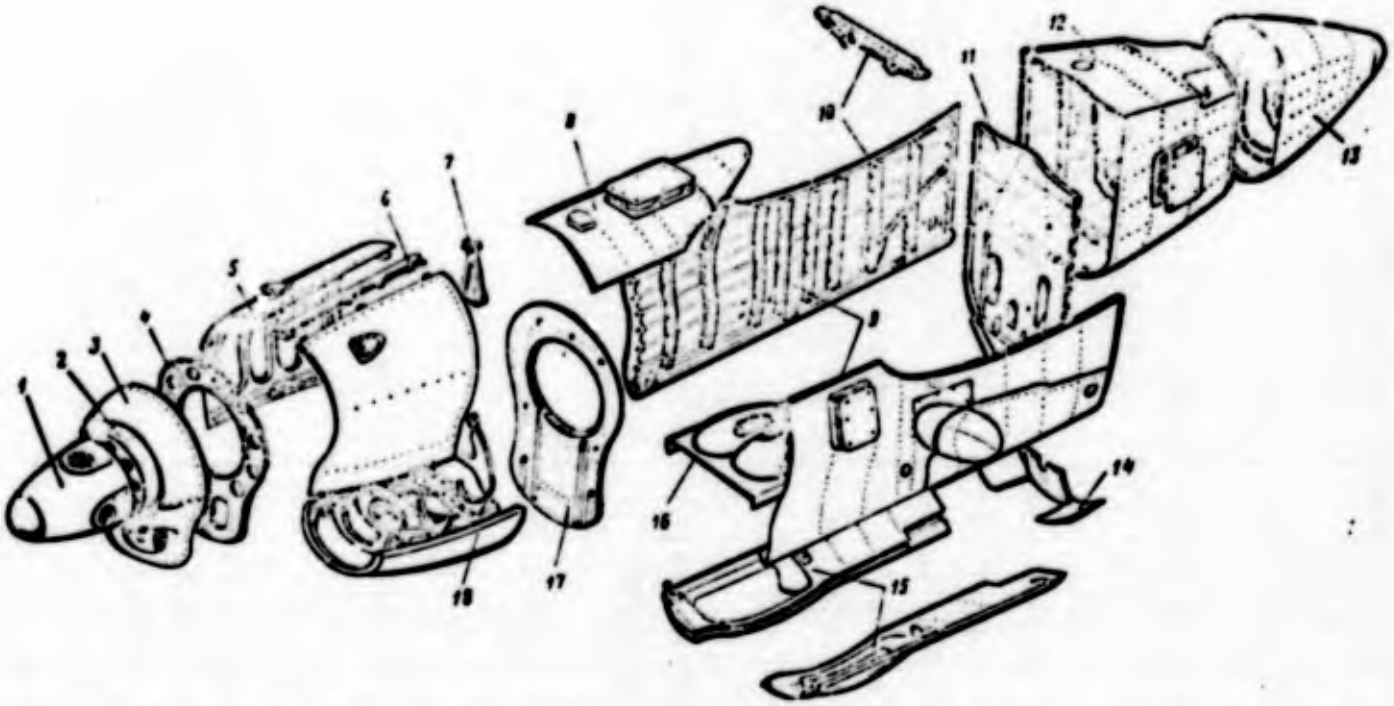

Figure 8.4. Design of a turboprop engine nacelle: 1 - propeller hub; 2 - reducer fairing; 3 - engine air intake; 4 - air intake frame; 5 - side cowling cover; 6 - upper beam; 7 - cowling attachment bracket; 8 - upper panel; 9 - side panels; 10 - horizontal and vertical beams of the middle load-bearing frame; 11 - rear load-bearing frame; 12 - forward compartment of rear section of the nacelle; 13 - fairing; 14 - split flap with cover; 15 - landing gear door; 16 - landing gear wheel screen; 17 - front load-bearing frame; 18 - lower cowling cover.

The panel design of a nacelle consists of rigid panels connected with each other with fast-acting securing locks and forming a closed load-bearing shell. This type of design receives air loads. The loads from the engine in this case are transmitted by special attachments directly to the wing or fuselage.

The turboprop engine nacelle design shown in Fig. 8.4, consists of the fairings of the propeller hub and the reducer, the air intake, the cowlings, the tail section of the nacelle, the duct leading away the exhaust gases, load-bearing beams and frames.

The propeller hub fairing serves to decrease engine drag, profiling of the intake duct of the air scoop and for protecting the propeller hub from contamination.

The front frame together with the nose of the skin forms the circular chamber of the air intake deicer into which warm air is supplied. Figure 8.5 shows the layout of another type of turboprop engine nacelle.

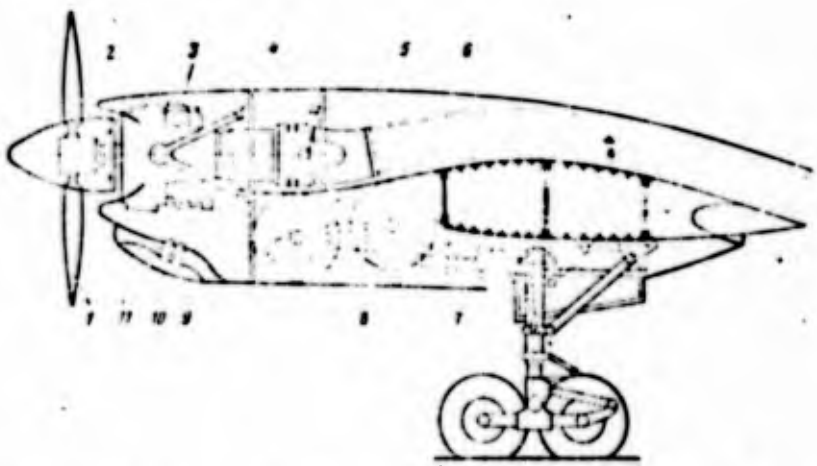

Figure 8.5. Layout of a turboprop engine nacelle: 1 - propeller; 2 - engine air intake; 3 - engine; 4 - nacelle and fire wall frames; 5 - rear cowling; 6 - exhaust duct; 7 - wing; 8 - landing gear; 9 - oil cooler; 10 - oil cooler air intake; 11 - front cowling.

The turboprop engine nacelles on pylons (Fig. 8.6) (sic) are similar in design to the one examined above.

Figure 8.6. Nacelle of a turbojet engine mounted on a pylon.

Turbojet engines located on a wing, are completely or partially accommodated within the wing (see Fig. 8.1d, e). In these cases the wing spars in the section where the engine is located have an annular shape and are simultaneously reinforcing frames of the nacelle.

§ 4. DESIGN OF ATTACHMENTS FASTERNING ENGINES TO FLIGHT VEHICLES

Let us examine some typical designs of engine attachment set-ups.

The attachment of a radial piston engine (Fig. 8.7) consists of tubular ring to which the engine crankcase, and rods welded-on to it which are connected with the airframe, is fastened. This type of design is a three-dimensional system. To hold the engine attachment, connected to the ring, firmly in position to the airframe, the number of rods should not be less than six. The ring and rods are made from high-strength steel and are connected at points with the aid of welded knee plates (see cross section B-B).

The points of attachment of engine mounts to a fuselage or wing are lugs or fittings welded to the rods. In the eye connections the bolts operate in shear. In the fitting connections - mainly in tension.

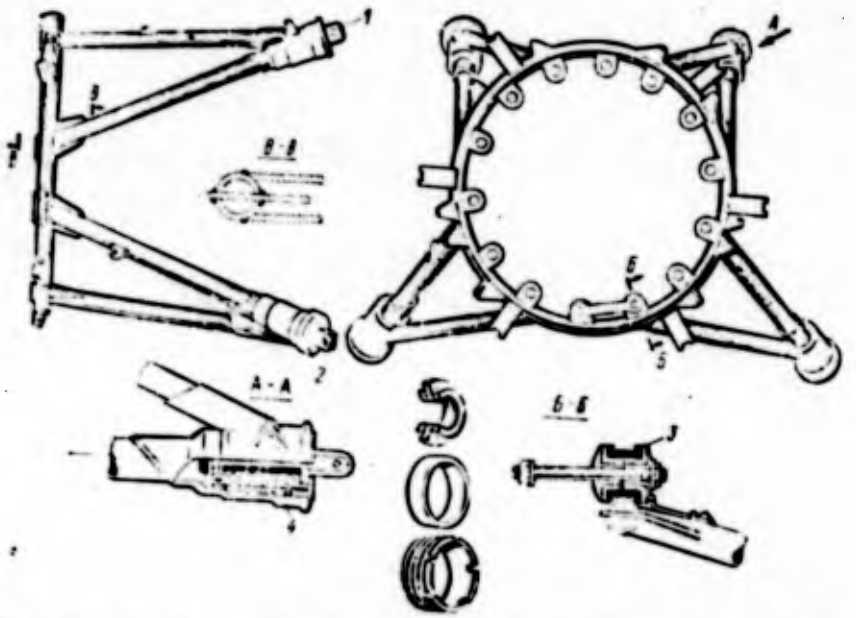

Figure 8.7. Design of the engine mount of a radial engine: 1 - upper points with shock absorbers; 2 - lower points with shock absorbers; 3 - bushing for attaching the engine to the engine mount; 4 - shock absorber of the sub-engine mount.

The engine crankcase is fastened with stud bolts to bushings 3, which are welded to the ring (cross section B-B). Rubber shock absorbers are inserted in the bushings. The rear ends of the rods connected in pairs and welded with the sleeve of the mount attachment point to wing. Shock absorbers are placed in the sleeves.

Turboprop engines are fastened to a wing with three-dimensional rod system connected with the engine assemblies. The attachment can be of the truss type, with the rods operating in tension and compression, and the truss-beam type, in which some elements in the form of beams operate in flexure.

Figure 8.8 shows the setup for attaching a turboprop engine to an aircraft wing. The assembly connects the engine to the center section of the wing.

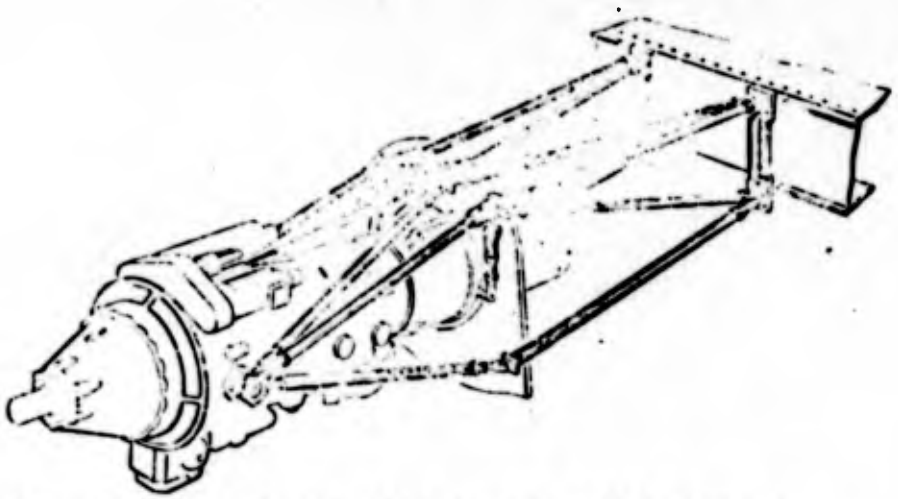

Figure 8.8. Truss attachment fastening a turboprop engine to a wing.

The assembly consists of a front truss connecting the engine with the intermediate load-bearing frame, and of a rear truss connecting the frame with the wing.

The rods of the front truss form a statically determinable fixed attachment to the frame of two assemblies with the front (plane) rubber dampers; each point is fastened with three rods.

The engine rests on two front and two rear (rod) dampers, with the aid of two front and two rear journals. The load due to propeller thrust and part of the load from the mass forces of the engine are received by the front dampers. The rear dampers receive only part of the mass forces of the engine. The upper and lower struts of the front truss have prongs on the ends with threaded points for regulating the position of the engine.

The rear truss consisting of eight rods connects the frame with the engine connected to it to the center section. The load-bearing frame is installed for the purpose of ensuring more efficient arrangement of the rods and for reducing their lengths, which is important when operating in longitudinal flexure.

Figure 8.9 depicts the design of a truss-beam type of attachment (Fig. 8.9a) consisting of two beams and six struts. Beam 5 supported at two points - on the nacelle frame and internal strut 6 - operates in flexure. The remaining elements operate only for axial loads.

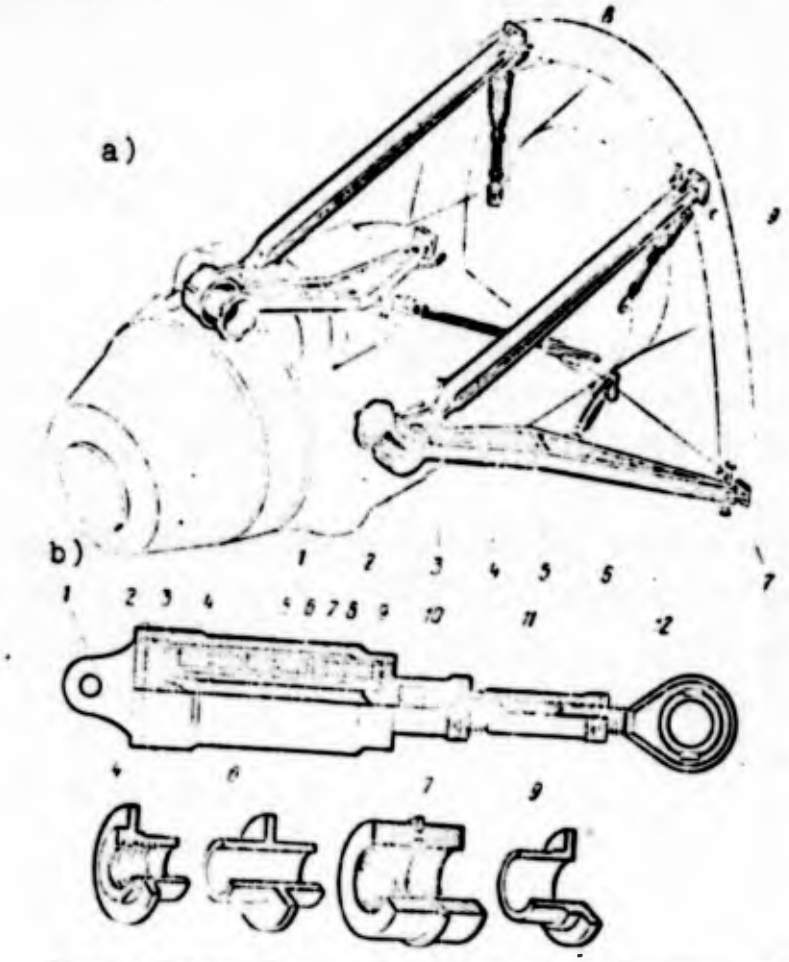

Figure 8.9. Truss-beam for attaching a turboprop engine to a nacelle: a) general view: 1 - front journal; 2 - front damper; 3 - connecting link; 4 - upper strut; 5 - beam; 6 - internal strut; 7 - bracket; 8 - electrical bonding short-circuiting connector; 9 - rear strut - rod damper; b) rear strut - the damper: 1 - bracket; 2 - stop screw; 3 - housing; 4 - nut; 5, 6 and 9 - bushings; 7 - disk damper; 8 - ring; 10 - central rod; 11 - transfer bushing; 12 - eye.

The engine is fastened to four journals. The front journals 1 are inserted into the front dampers 2 of beams 5. With the aid

of these beams and the upper struts 4 the journals 1 transmit loads to points located on the load-bearing frame of the engine nacelle. The load from the rear journals is transmitted to the points of the load-bearing frame through struts - rod dampers 9 the parts of which are shown in Fig. 8.9b. The position of the engine can be varied by adjusting the length of internal struts 6 and of the rear shock absorbers.

The attachment of a turbojet engine to a flight vehicle is carried out in the form of a three-dimensional system of rods and assemblies.

A characteristic of the attaching of a turbojet engine is the presence on the engine itself of load-bearing strips, or lugs for attaching the journals or pronged (eye) points.

The presence of several possible attachment points makes it possible to employ different variants of attaching an engine depending on the characteristics of the aircraft layout on which the engine is being installed.

The housing of a turbojet engine is subjected to considerable heating; thus the engine attachments should ensure the free displacement of the housing assemblies produced by the change in the temperature.

Figure 8.10 shows the attachment of a turbojet engine to the load-bearing frames of the fuselage. A characteristic of this setup is its asymmetry. Within the rod system consisting of six main rods 2-3, 4-5, 6-10, 11-12, 9-13, 1-8 and one additional rod 7-9, is a plane assembly reinforced to the engine strip by rods 2-2', 2-2''.

The correct positioning of the engine on an aircraft is attained by adjusting the length of the six main rods.

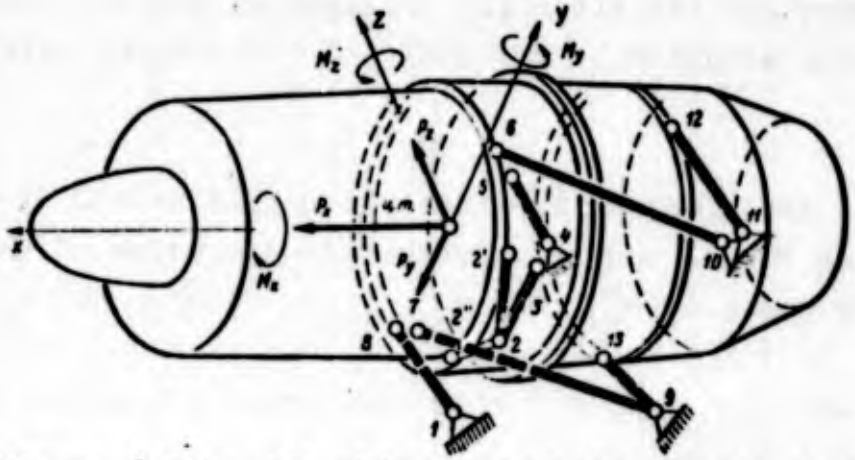

Figure 8.10. Attaching a turbojet engine to the load-bearing frames of a fuselage and the types of loads on it: forces P_x, P_y, P_z and moments M_x, M_y, M_z.

In all cases of loading both in the air and on the ground the rod system of the engine mount receives all the forces impinging on it by means of the operation of the rods in pure tension and compression.

The attaching of a turbojet engine to a pylon under a wing or in the tail section of the fuselage is accomplished with the aid of pronged assemblies located on top of the engine housing.

The dampers in the constructing of turbojet engine attachments are sometimes not installed, if the vibrations caused by its operation, are insignificant.

§ 5. LOADS ACTING ON ENGINE ATTACHING ASSEMBLIES, AND THE BASES OF STRESS ANALYSIS

1. Loads Acting on Engine Attaching Assemblies

Loading cases stipulated by the stress standards for engine attaching devices have been compiled taking into account all loading variants, possible in operation.

The engine and the attaching arrangement are the part of a flight vehicle situated in the state of the loading case in question.

The most important with respect to magnitude and direction of the acting forces and with respect to the value of impact pressure are cases A'($n^э_{max}$ and $q_{max\ max}$), D'($n^э_{min}$ and $q_{max\ max}$, see chapter 1, § 7), H (the effect of lateral acceleration and sideslip with $q_{max\ max}$), and also the cases of landing and takeoff E and others (see chapter 10, § 3).

The mass loads are the main ones.

Figure 8.11a shows the directions of the mass loads in cases A', D', H, E.

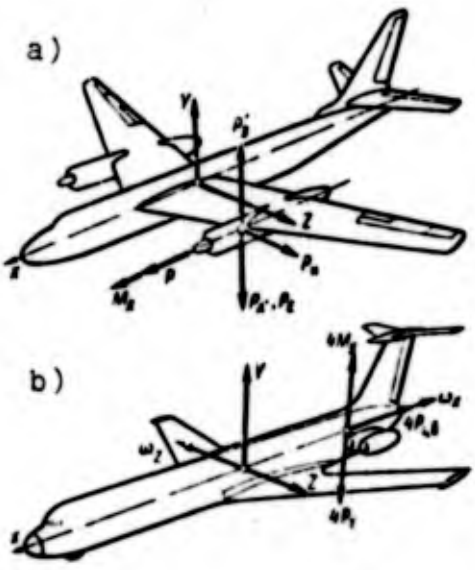

Figure 8.11. Loads on engine wing attaching devices: a) the main mass and surface loads; b) additional mass forces and gyroscopic moment during the rotation of the aircraft with ω_z, ε_z (transmitted from pylons attaching four engines to an aircraft).

The operational values of the mass forces are defined as $P=n^э G_{ду}$, where $G_{ду}$ is the weight of an engine, the attachment assemblies and the nacelle. The safety factor f is taken for the case in question.

To these mass forces determined by the weight and the inertial forces of the curvilinear translational motion of a flight vehicle, it is necessary to add the additional inertial forces arising during the rotation of the aircraft relative to its center of gravity with an angular velocity ω and an acceleration

ε, in the case of the positioning of the engines beyond the center of gravity of the aircraft. If an engine is located at a distance r from the center of gravity and the rotation occurs relative to z, then the centrigugal force is $P_{ц6} = \frac{G_{дв}}{g} r\omega_z^2$, the tangential force is $P_т = \frac{G_{дв}}{g} r\varepsilon_z$ (Fig. 8.11b). It is also necessary to take the gyroscopic moments into account.

Here the parts of the engine and the propeller, rotating relative to the x-axis, for a turbojet engine - its rotor - are the gyroscope.

Gyroscopic moment arises during the rotation of the aircraft relative to the z- or y-axes.

During the rotation of the aircraft, for example, relative to the z-axis, at angular velocity ω_x moment M_y arises which tends to turn the gyroscope axis in the shortest way so that vector ω_x coincides in its direction with vector ω_z (see Fig. 8.11b)

$$M_y = I_x \omega_x \omega_z \text{ кгс м},$$

where I_x is the moment of inertia of the rotating part of the engine relative to the axis of rotation, kgf s^2m; ω_x - is the angular velocity of the rotating part of the engine, 1/s; ω_z - is the angular rate of rotation of the aircraft, 1/s.

The values of moment of inertia I_x and of angular velocity ω_x depend on the engine design and its operating regime. The angular velocities of an aircraft ω_z can be determined in accordance with the loading case.

Included among the surface forces are engine thrust P and reactive moment (directed in the direction opposite to the rotation of the propeller)

$$M_x = 716{,}2 \frac{N}{n} \text{ кгс м},$$

where N - is the engine power on the propeller shaft, hp; n - is the rpm of the propeller.

These loads are also depicted in Fig. 8.11a.

For helicopters, the rotational speed of the rotors of which is approximately 10 times less than aircraft propellers, the value of the reactive moment can be very great. To eliminate reactive moment on helicopters with one rotor special steering rotors are employed, in twin-rotor helicopters - opposite rotation of the propellers.

For aircraft with jet engines in which there is virtually no twisting of the gas jet after exiting from the nozzle, moment $M_x=0$.

The air forces acting on a nacelle, cowlings and pylons, are less in value. The loads on the pylons of an engine mount under a wing arising during sideslip are the most significant.

2. Bases for Rating Engine Attachment Devices

It is necessary to take engine attachment into account in all cases specified by the stress standards, for which it is necessary to determine the loads which correspond to loading cases.

The load-bearing setup of an engine attachment device is usually statically indeterminable. The order of static indeterminacy in this case is determined by the number of excess, over those necessary for ensuring inalterability of the structure of the connections (rods).

The order of carrying out the rating is as follows.

1. Determination of the weight and the center-of-gravity position of the engine, truss and the units fastened to them.

2. Determination of the rated destructive loads in accordance with the stress standards.

3. Establishing the design setup. Determination of the dimensions of the rods and the direction cosines of the rods:

$$\cos(l_i,x)=\frac{x_i}{l_i};\quad \cos(l_i,y)=\frac{y_i}{l_i};\quad \cos(l_i,z)=\frac{z_i}{l_i},$$

where x_i, y_i, z_i - are the projections of a rod; $l_i=\sqrt{x_i^2+y_i^2+z_i^2}$ - is the length of a rod.

4. Determination of the degree of static indeterminacy and selection of the basic system.

The basic system is formed by a section (cut) of the excess connections (rods).

5. Determination of forces.

Types of load on the device and an example of its design setup are shown in Fig. 8.10.

In a symmetrical design the forces in symmetrical elements with a symmetrical load are equal in magnitude and in sign, in an asymmetric load they are equal in magnitude, but opposite in sign.

Symmetry of the system makes it possible during the rating for each type of load to take as the "excess" symmetrical elements the forces in which are identical.

Let us examine as an example the truss design of an engine attachment device.

The forces in the rods can be represented in the following form

$$S = S_0 + \Sigma S_i X_i,$$

where S - is the total force in the rod, kgf; S_0 - is the force in a rod of a statically determinable system due to an external load; S_i - are the forces in the rods of a statically determinable system due to the unit forces acting in the sections of the "excess" rods; X_i - are the forces in the "excess" rods during the effect of the external load.

The values of the forces X are determined from canonical equations of deformation of the following type

$$X_1\delta_{11} + X_2\delta_{12} + \ldots + \Delta_{10} = 0,$$

where Δ_{10} - the mutual displacement of the sides of the section due to the external loads; $X_1\delta_{11}$; $X_2\delta_{12}$ - are the mutual displacements of the sides the section due to the effect of the forces X_i in the "excess" rods.

Displacements δ_{12} and Δ_{10} are calculated as for any trusses, with formulas:

$$\delta_{12} = \Sigma S_1 S_2 \frac{l}{EF};$$

$$\Delta_{10} = \Sigma S_1 S_0 \frac{l}{EF},$$

where l - is the length of the rod; E - is the elastic modulus; F - is the cross-sectional area.

Sums Σ are taken for all rods, including the sectioned ones.

6. Strength testing.

As a result of the calculations the rated destructive forces in the rods with different load cases are obtained. The greatest tensile and compressive forces are summarized in the table of rated forces.

The compressed rods are checked for longitudinal flexure (from the graphs). The strength condition is: $S \leq P_к$.

For rods with hinged attached ends $\mu=1$.

For rods with welded or fastened points it is assumed that $\mu = \frac{\sqrt{2}}{2} = 0{,}707$.

The tensioned rods are checked for tension with respect to the strength condition: $\sigma = \frac{S_{раст}}{F} \leqslant k\sigma_в$; $k = 0{,}9 \div 0{,}95$.

The coefficient k takes into account the weakening of rod strength by welding or holes for rivets.

In a number of cases to reveal the static indeterminacy it is not necessary to formulate and to solve canonical deformation equations. If the number of excess unknowns does not exceed two, and the design is symmetrical, then for determining them it is sufficient to employ the rules for determining forces due to symmetrical and antisymmetric loads based on the analysis of deformations.

§ 6. CHARACTERISTICS OF THE POSITIONING AND ATTACHING OF ENGINES ON HELICOPTERS

The basic technical requirements imposed on the positioning and the attaching of engines on helicopters, are similar to the requirements imposed for arranging and attaching engines on aircraft.

The arrangement of engines on helicopters depends on the types of engines.

The load-bearing setups of helicopters depending on arrangement are divided into two groups: internal setups, those arranged within the fuselage, and external setups, those arranged in individual nacelles or on top of the fuselage.

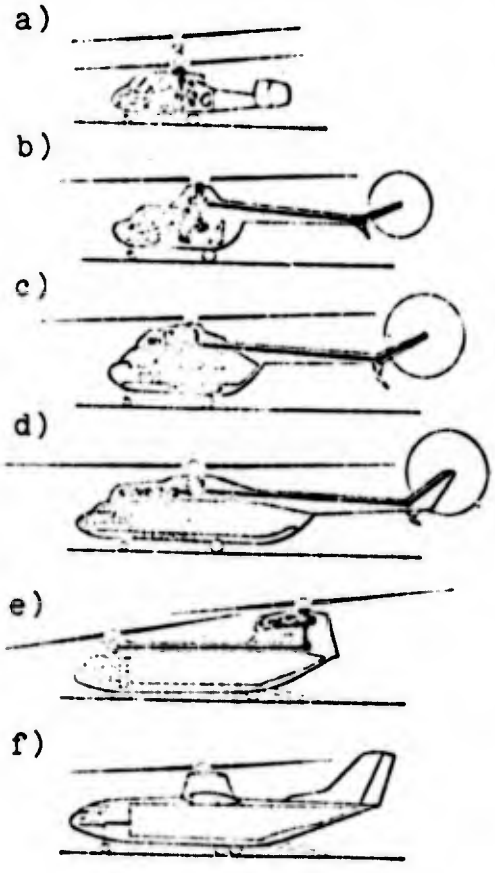

Figure 8.12. Arrangement of engines on helicopters

Piston engines are mainly positioned within the fuselage (Fig. 8.12a, b). With this type of arrangement the volume of fuselage for the accommodation of loads is considerably reduced and the necessity installing an engine cooling system arises. Piston engines can also be positioned on pylons attached to the beam of a transverse helicopter design (Fig. 8.12f).

Gas turbine engines are positioned on the fuselage on top both in front of and behind the rotor (Fig. 8.12c, d). This type of engine arrangement makes it possible to free additional volumes in the fuselage for the accommodation of loads.

On Twin-rotor helicopters with a longitudinal setup gas turbine engines can be positioned both within the fuselage (Fig. 8.13) and outside of it (Fig. 8.12e).

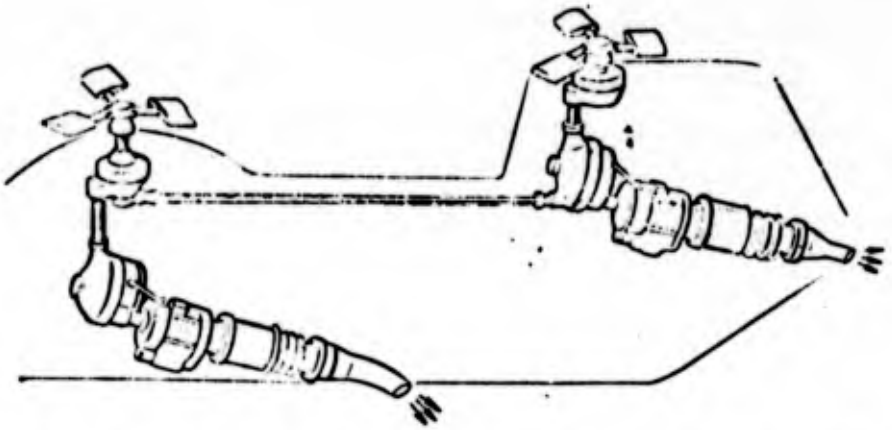

Figure 8.13 Arrangement of engines within the fuselage of a helicopter.

The designs of the arrangements for attaching engines to helicopters are similar to the designs of the arrangements for attaching engines on aircraft.

In this case the possibility of regulating the engine attachments for connecting the engine shaft with the reducer should be provided for.

§ 7. FORCED OSCILLATIONS OF LOAD-BEARING SETUPS AND THE DAMPING OF THEM

The main causes of forced oscillations in load-bearing setups are the lack of rotor balance, the rotating and the translationally moving parts of the engine, and also the periodically changing aerodynamic forces acting on the rotor blades during their passage ahead of the other parts of the design.

The vibrations during the operation of turboprop and piston engines are especially significant.

For turbojet engines the vibration are explained by the lack of balance of the rotor. Since the lack of balance is slight, and the number of revolutions is considerable, than the vibrations are perceived in the form of jittering with low amplitudes.

The harmful consequences of vibrations are: the play in the attachment assemblies arising as a result of the effect on the assemblies of dynamic loads, the failure of individual elements due to alternating loads (for example fatigue cracks in welded assemblies), the disruption of the proper operation of the instruments, the unpleasant sensations of the crew and passengers.

The following measures are taken to reduce the vibrations:

1) reducing the magnitudes of the perturbing forces by improving the balance of the engine and the rotor;

2) employing special devices - oscillation quenchers (dampers) which diffuse a considerable portion of the vibrational energy;

3) varying the rigidity of the oscillating system and its elements for the purpose keeping them away from resonance.

The latter measure is especially important. The rigidities should be selected so that its natural oscillation frequency relative to the remaining structure of the airframe of the system consisting of the engine, the rotor, the units and the structures for engine attachment, and also the natural oscillation frequencies of the individual elements of the truss (for example, flexural oscillations of a rod relative to their supports) be sufficiently remote from the frequencies most significant with respect to amplitude, acting for a long time during the operation of the exciting forces, differing from them by ±300-400 osc./min. Such frequencies of the exciting forces are: for rotors with i blades: $n_{эв}$, $in_{эв}$; for piston engines; $n_{эд}$, $2n_{эд}$; for turbojet engines: $n_{эд}$, where $n_э$ - are the operational (most frequently used) numbers of revolutions of the engine or rotor.

Two methods of fulfilling these requirements are possible:

1) the selection of the rigidity of the oscillating system is carried out so that natural vibration frequencies are higher than the dangerous forced frequencies;

2) the selection of the rigidity is carried out so that natural vibration frequencies are lower than the dangerous forced frequencies.

The diagram of the dependence of dynamic coefficient $\mu = \frac{A_x}{x_p}$ on the ratio of the frequencies $\frac{\nu_{вын}}{\nu}$ (Fig. 8.14b) is known from vibration theory, where A_x - is the amplitude of the oscillations; x_p - is the static deformation under the effect of the statically applied amplitude value of the exciting force A_p; ν - is the natural oscillation frequency; $\nu_{вын}$ - is the frequency of the forced oscillations.

The frequency of the forced oscillations $\nu_{вын}$ is given.

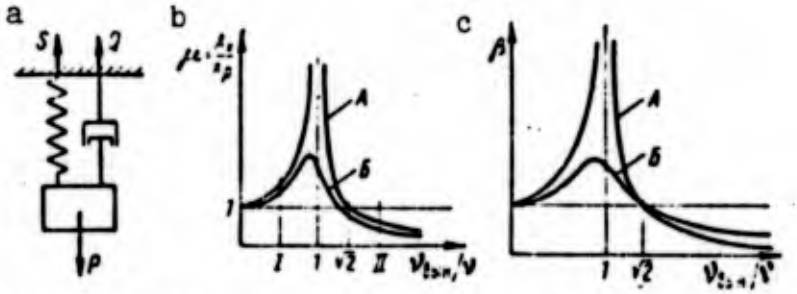

Figure 8.14. Dynamic setup of an engine mount (a), its frequency characteristics (b) and transmission coefficients (c): A - oscillations of an elastic system (without damping); B - oscillations of a system with inelastic resistance (with attenuation).

It follows from the diagram, that removing from resonance by means of lowering the natural frequency ν (second method) is advantageous due to the fact that μ becomes less than unity.

In designing an aircraft it is very important to know, with which force the engine arrangement fixed to the aircraft structure,

acts during oscillations on its support points. The real connections by which the engine setup is connected with the aircraft structure, create both elastic (force S) and inelastic (force Q) resistance (Fig. 8.14a). Force S is proportional to the displacement, and force Q - is proportional to the rate of displacement; thus the force being transmitted to the support is

$$N = Q + S = k\dot{x} + cx,$$

where k - is the attenuation factor of the oscillating system;
c - is the rigidity of the flexible coupling.

According to d' Alembert's principle for a body on which exciting force P is acting, it is possible to write

$$P = N + I,$$

where $I = m\ddot{x}$ - is the force of inertia.

If exciting force P is periodic

$$P = A_p \sin \nu_{вын} t,$$

then forces Q, S and N will be periodic.

The ratio of the amplitude value of force N being transmitted to the support to the amplitude of applied force P is called the force transmission coefficient

$$\beta = \frac{A_N}{A_p} = \frac{(S+Q)_{max}}{P_{max}}.$$

Thus, force N transmitted from the system to the support is β times greater than applied force P_{max}.

Since the dynamic coefficient is

$$\mu = \frac{A_x}{x_p} = \frac{S_{max}}{P_{max}},$$

then in the absence of viscous resistance in the connections coefficient β is equal to μ.

Figure 8.14c shows the curve of the dependence of β on $\nu_{вын}/\nu$. It is evident from it that when employing the second method of the removal of resonance too significant inelastic resistance is not advantageous.

For the rods of the truss of the engine mount the first method of removing resonance is employed. For attaching the engine to the truss and the entire arrangement to the aircraft structure the second method is usually employed. This is explained by the following considerations.

The natural frequency of the flexural oscillations of a rod is unavoidably rather high. It is calculated by the formula

$$\nu = \frac{30\pi}{l^2}\sqrt{\frac{EI}{m}} \text{ osc/min},$$

where m - is the mass of a unit length of rod, $kG \cdot s^2/cm$; l - is the length of a rod, cm.

The rods for the trusses of the engine attachment are selected mainly on the basis of their operating condition in longitudinal flexure with compression. For long rods the critical force is

$$P_к = \frac{\pi^2 EI}{(\mu l)^2},$$

where I - is the moment of inertia of the rod area, cm^4; E - is the elastic modulus, kgf/cm^2.

Thus, reducing their flexural rigidity EI to decrease ν is impossible, since this decreases $P_к$. For removing resonance it is necessary to select the truss rods by the first method so that the frequency of their inherent oscillations is higher than the frequency of the dangerous forced oscillations. For this purpose the rods are made more rigid.

It is not possible to make the attachments of the engine to the truss and of the truss to the aircraft airframe sufficiently rigid to remove resonance, this would lead to the considerable

weight increase in the design. Thus, they are made more pliable, so that the natural vibration frequencies of the fixed system is lower than the dangerous forced oscillations (second method of removing resonance). For this rubber oscillation quenchers (dampers) are included in the attachment assemblies.

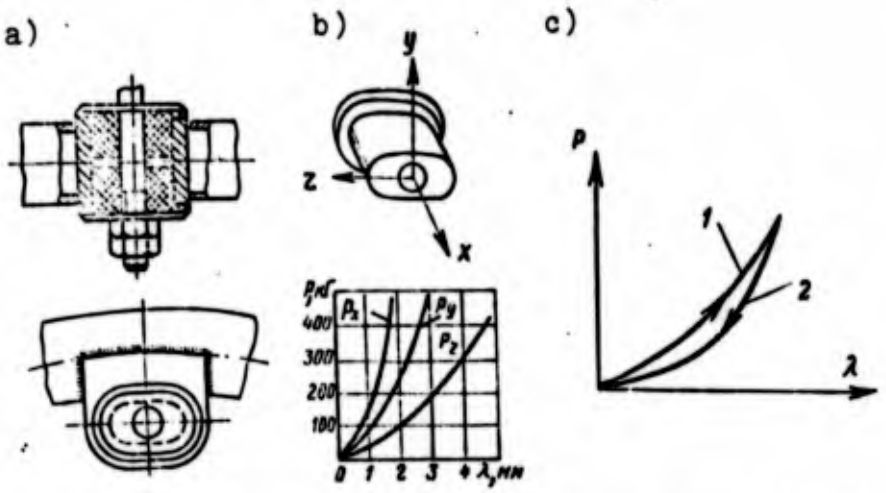

Figure 8.15. Rubber damper for attaching a piston engine: a) structure; b) mechanical characteristics; c) hysteresis during cyclic loading; 1 - loading; 2 - relieving.

Rubber possesses a low elastic modulus, especially in shear, and sufficient inelastic resistance characterized by the hysteresis loop (Fig. 8.15c), which ensures good absorption of the oscillational energy. The energy received by the rubber is converted into thermal energy. The metal parts of the damper structures should ensure good thermal conductivity for removing it.

When selecting the rigidities of the dampers it is assumed that the greatest perturbing pulses act in the yz plane.

Thus, in this plane and around the x-axis the most effective damping is required. In other directions the rigidity of the damper system should be greater, otherwise for propeller engine arrangements during the rotations of the rotating propeller

relative to the y- and z-axes undesirable precessional oscillations arise caused by the gyroscopic effect of the propeller.

The different rigidities of the dampers in different directions are attained by the following two methods.

1. The employment of a shock-absorbing bushing with a different thickness of rubber in the different directions. The damper depicted in Fig. 8.15a is employed for attaching radial piston engines to engine mounts and ensures: great angular displacements of the engine relative to the x-axis, moderating the pulses of the reactive moment, sufficient displacements in the radial direction (in the yz plane); small displacements along the x-axis and during the rotation of the engine around the y- and z-axes.

2. The employment of the properties of rubber which has a considerable difference in elastic moduli in shear and in compression (the elastic modulus of rubber in shear is 6-10 times less than in compression). Deformation λ of the damper under the effect of force P in different directions are shown in Fig. 8.15b.

The dampers are equipped with rests for preventing large deformations of the rubber and its failure in the case of large loads (in case A, etc.).

CHAPTER 9

§ 1. PURPOSE OF THE FUSELAGE AND THE MOST IMPORTANT TECHNICAL REQUIREMENTS IMPOSED ON IT. EXTERNAL SHAPES OF FUSELAGES

The fuselage is intended for accommodating the crew, passengers, loads, equipment, sometimes power plants devices and fuel, and also for connecting the basic aircraft components: wing, empennage, landing gear with each other.

The most important technical requirements imposed on a fuselage can be combined into the following four main groups.

The following layout requirements specified:

the obtaining of the greatest free volumes with the assigned overall dimensions for accommodating loads and creating comfort for the passengers;

slight variation in the center-of-gravity position of the flight vehicle in the case of different loading variants, fuel combustion and other variations in the weight of the loads contained within the fuselage so that the longitudinal stability is not disrupted;

compact arrangement of loads - closer to the center of gravity for reducing the mass moments of inertia of the flight vehicle I_z and I_y;

coordination of the load-bearing setups of the fuselage and the parts adjoining it in the section where they are joined together.

Aerodynamic requirements:

the obtaining of the least possible coefficient c_x of the fuselage and of the least destabilizing moment (for example, the moment created by the long nose part of the fuselage).

Strength requirements:

sufficient strength, service life and rigidity with the least weight (fulfillment of the stress standard requirements);

ensuring survivability of the structure in the event of partial failures.

Operational requirements:

ensuring the necessary life-support conditions and comfort for the passengers and the crew members;

convenience and rapidity in loading and unloading and the possibility of emergency exit from the flight vehicle in the event of crashes;

ensuring the field of view from the crew's cabin and the passenger compartments.

The enumerated requirements mainly determine the design and the external shapes of fuselages.

The external shapes of the fuselage of high-speed aircraft should be well streamlined, and the area of the greatest transverse

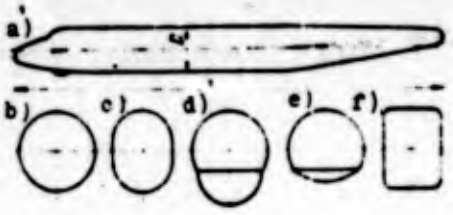

Figure 9.1. The shape of the fuselage (side view) of a contemporary passenger aircraft and shapes of transverse fuselage sections.

(midsection) cross section of the fuselage should be as small as possible. From the point of view of aerodynamics the best shape of a fuselage is a solid of revolution with outlines, close to the outlines of a symmetric profile.

The protruding canopies of the cockpits and, the installation radar equipment determine the need for deviating the shapes of a fuselage from a solid of revolution (Fig. 9.1a). Moreover, sometimes the axis of the nose part of the fuselage is deflected downward to improve the field of view from the crew's cabin, and the axis of the tail section is deflected upward to increase the tilting angle (see Chapter 10, § 1).

The nose part of a supersonic fuselage is made elongated and pointed to form oblique shock waves for the purpose of reducing the wave drag. Sometimes, this type of nose section (for example on the Tu-144 aircraft) is equipped with a mechanism for deflecting it downward for the purpose of improving the field of view from the flight deck during takeoff and landing.

The shape of the transverse section of the fuselage is determined by the purpose of aircraft, by the flight velocity, by the number of passengers, by the overall dimensions of the loads being transported, etc.

From the point of view of aerodynamics the most advantageous shape of the transverse section is circular (Fig. 9.1b). However, because of assembly and operating requirements other shapes of the cross section can be more advisable. Thus, an oval shape (Fig. 9.1c) makes it possible to better employ the internal volumes of the fuselage. But an oval fuselage is inconvenient for production and its panels undergo flexure with the presence of excess

pressure in the pressurized section. Thus for passenger aircraft the more advantageous is the section formed by two intersecting circles (Fig. 9.1d, e). At the level where the circles forming the cross section come together it is advantageous to place the floor of the flight deck or of the passenger compartment.

For special cargo and assault aircraft and helicopters, for which the operational and layout requirements are of first priority, the shape of the fuselage should be convenient for the loading, accommodating and unloading of bulky and heavy loads. In this case the most expedient shape of the transverse cross section can be rectangular with rounded corners (Fig. 9.1f).

The most important parameter of a fuselage is its fineness ratio

$$\lambda_\Phi = \frac{L_\Phi}{D},$$

where L_Φ - is the length of the fuselage; D - is the diameter of its midsection section.

When the cross section is noncircular D is taken to be the diameter of a circle equal in area to the midsection section.

Sometimes the fineness ratio of the fuselage is determined by the formula

$$\lambda_\Phi = \frac{2L_\Phi}{B+H},$$

where B and H - are the greatest width and height of the fuselage.

In contemporary subsonic aircraft λ_Φ=7-11, while for supersonic λ_Φ =12-15.

An important parameter of an aircraft is the distance from the center of gravity of the aircraft to the center of pressure

of the horizontal tail surfaces determined by the length of the tail section of the fuselage: $L_{г.о}=kb_A$. For aircraft of conventional designs k=2.6-4.8.

The transverse dimensions of a fuselage are selected depending on the purpose of the flight vehicle. Thus, the diameter of the fuselage of a passenger aircraft is determined by the minimum height of the passenger compartment in the center isle (not less than 1.8-2.0 m) and by the number of seats in a row:

D=3.0 m with four seats in a row;
D=3.4 m with five seats in a row;
D=3.8 m with six seats in a row.

For cargo aircraft the transverse dimensions of the fuselage are determined by the type and the quantity of cargo intended to be transported on the aircraft in question.

For example, for the An-22 aircraft intended for the transportation of large-dimension cargo, B=H=4.4 m.

§ 2. CONDITIONS OF FUSELAGE LOADING

The following loads can act on a fuselage under different operating conditions:

the forces transmitted to the fuselage from the parts of the flight vehicle attached to it (wing, empennage, power-plants, landing gear);

the mass forces of the cargo and units situated within the fuselage, and also the mass forces of its intrinsic design;

the reactions of the earth or water in an emergency situation applied directly to the fuselage;

the aerodynamic forces (rarefaction or pressure) distributed over the surface of the fuselage;

the pressure (or rarefaction) in pressurized compartments.

In the fuselage design of supersonic flight vehicles significant internal forces (thermal stresses) can also arise due to kinetic heating.

In contrast to a wing, the aerodynamic forces applied to the surface of a fuselage are distributed in such a way that they do not exert a substantial effect on the operation of the fuselage design as beams. But these forces can be decisive in the rating of individual parts (for example, the cockpit canopy) for local strength.

The loading cases of the fuselage of an aircraft specified by the stress standards can be broken down into three groups.

1st group. Loading cases of aircraft components adjoining the fuselage. An aircraft is examined as a solid located in equilibrium under the effect of the surface and mass loads of the fuselage and the parts adjoining the fuselage.

The safety factors f for a fuselage are assumed to be the same as for the parts adjoining it. An exception is case E. In this case for the landing gear f-1.5, and for fuselage f=1.65.

1st sub-group. Cases in which accelerated rotation of the aircraft relative to the center of gravity is absent. Let us examine, for example, case A, when the following surface forces, parallel to the y-axis (Fig. 9.2a) are acting on the aircraft:

a) the lift of the wing $Y=n_A G$ determined in accordance with the stress standards for case A of a wing;

b) the balancing load on the horizontal tail surfaces $Y_{г.о}$, determined from the condition of equilibrium of the moments relative to the center of gravity of the aircraft.

The g-force at the center of gravity of the aircraft n_y is different in magnitude from g-force n_A assigned by the stress standards for a wing:

$$n_y = \frac{Y + Y_{г.о}}{G} = n_A + \frac{Y_{г.о}}{G}. \qquad (9.1)$$

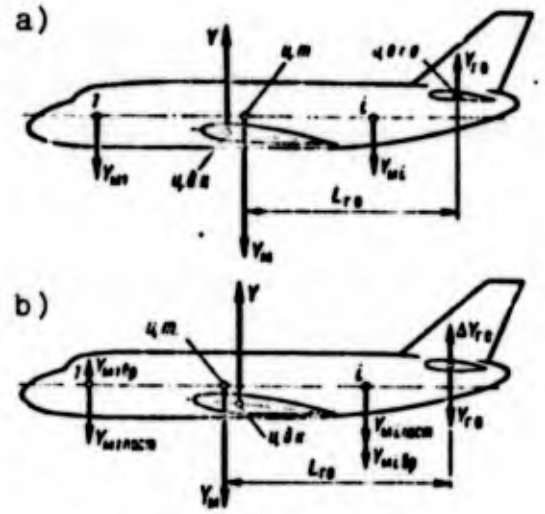

Figure 9.2. Forces acting on an aircraft: a) in loading case A; b) in loading case B. [ц.т. = c.g. (center of gravity); ц.д.к. = c.p. (center of pressure)]

As a result of the absence of accelerated rotation of the aircraft the magnitude of n_y for all loads is identical. Thus, the mass force of a load or a unit which has a weight G_i, is equal to

$$Y_{мi} = n_y G_i. \qquad (9.2)$$

2nd sub-group. Cases connected with the accelerated rotation of an aircraft relative to its center of gravity. As an example let us examine the effect of a maneuvering load on the horizontal tail surfaces in case B. Surface forces, parallel to the y-axis act on the aircraft (Fig. 9.2b):

a) the lift of the wing $Y=n_B G$;

b) the balancing load on the horizontal tail surfaces $Y_{г.о}$;

c) the maneuvering load on the horizontal tail surfaces $\Delta Y_{г.о}$.

Let us introduce the absolute values of $Y_{г.о}$, $\Delta Y_{г.о}$ and x_i into the calculation.

Under the effect of unbalanced force $\Delta Y_{г.о}$ the aircraft accomplishes rotation relative to the center of gravity with angular acceleration

$$\varepsilon_z = \frac{\Delta Y_{г.о} L_{г.о}}{I_z}, \tag{9.3}$$

where I_z - is the mass moment of inertia of the aircraft relative to the z-axis;

$$I_z \approx \frac{1}{g} \Sigma G_i x_i^2. \tag{9.4}$$

The g-force at the center of gravity of the aircraft is

$$n_{y\,пост} = n_{y_1} = \frac{Y_п}{G} = \frac{Y - Y_{г.о} + \Delta Y_{г.о}}{G} = \\ = n_в - \frac{Y_{г.о} - \Delta Y_{г.о}}{G}. \tag{9.5}$$

The g-force at a point not lying at the center of gravity is,

$$n_{yi} = n_{y_1} + n_{y\,вр\,i} = n_{y_1} \pm \frac{\varepsilon_z x_i}{g}. \tag{9.6}$$

Here plus or minus signs are taken depending on the directions of mass forces $Y_{M_i\,пост}$ and $Y_{M_i\,вр}$ at the point in question (Fig. 9.2b).

The mass force of arbitrary load i is

$$Y_{xi} = n_{yi} G_i. \qquad (9.7)$$

2nd group. Cases of direct loading of the fuselage. The main cases of this group are H_ϕ, P_ϕ, $П_\phi$, M_ϕ, H_ϕ.

Case H_ϕ - is an incomplete noseover (Fig. 9.3a). This case is examined only for an aircraft with a tail wheel.

Case P_ϕ - is a complete noseover (Fig. 9.3b). This case is examined only for aircraft with $G_0 \leq 10{,}000$ kgf.

Case $П_\phi$ - is a forced (belly) landing with the landing gear retracted (Fig. 9.3c).

The load from the earth is transmitted to the fuselage in the sector designated in Fig. 9.3c by angles 60° and 30°.

Case M_ϕ - is a forced landing on water (ditching). The effect of the hydrodynamic load upon impacting on the water is examined.

In fuselage design special load-bearing elements should be specified, which possess sufficient strength for receiving the loads and protecting the crew and passengers in the enumerated loading cases, and also in case M_ϕ for ensuring buoyancy.

Case H_ϕ - is a lateral load on the front section of the fuselage (for example, a turn with sideslip). Taken as the "front" section of the fuselage is that part of the fuselage from fuselage nose to the front wing spar.

Loading of the nose section of the fuselage is examined only with mass forces in the direction of the z-axis.

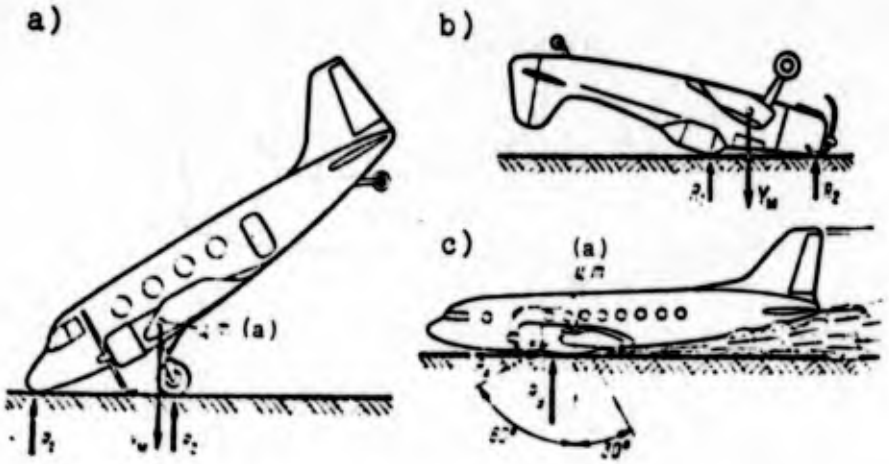

Figure 9.3. Cases of direct loading of the fuselage: a) incomplete noseover; b) complete noseover; c) forced (belly) landing with landing gear retracted.
Key: (a) c.g. (center of gravity).

3rd group. Loading with distributed aerodynamic forces and forces of pressure and rarefaction in pressurized compartments.

The calculation of air loads on the surface of a fuselage can be carried out in accordance with the results of wind-tunnel tests or in accordance with the recommendations of the stress standards. As an example Fig. 9.4 depicts diagrams of the distribution of the surplus pressure coefficient $\bar{p}=p_{изб}/q$ (where q - is the impact pressure in flight) on the surface of fuselages of different contours when $M<<M_{крит}$. Considerable lateral loads also act on the nose section of a fuselage during the sideslip of an aircraft.

Knowledge of the excess pressure on the surface of a fuselage is necessary for calculating hatch covers, windows and canopies, for the correct positioning of the outlet of vent tubes. Air loads are also taken into account in calculating the design of air intakes and air ducts.

In the stress analysis of pressurized compartments of a fuselage two variants of loads due to pressure and rarefaction in the compartments should be examined.

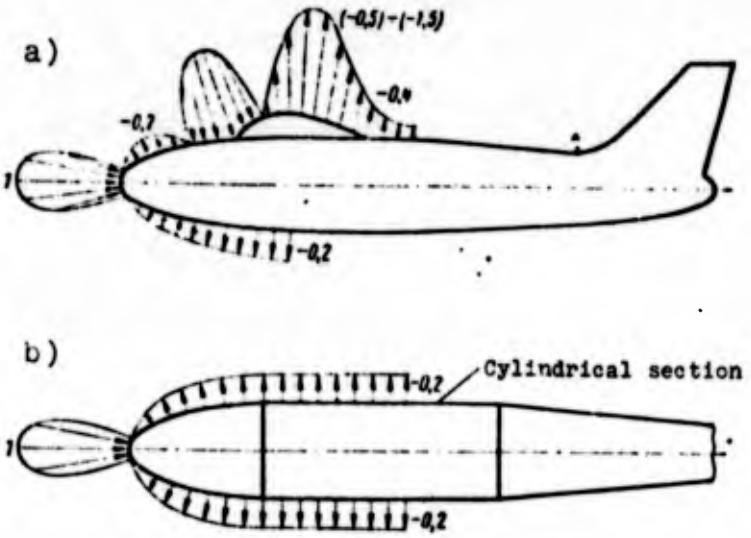

Figure 9.4. Diagrams of pressure distribution on the surface of a fuselage (example): a) fuselage with protruding canopy; b) fuselage made in the shape of a solid of revolution with cylindrical insert.

1. The effect of the maximum excess pressure and the maximum excess rarefaction (in the event of an extreme descent of the aircraft when the internal pressure can be less than the external - atmospheric pressure).

2. The joint effect of loads due to pressure and rarefaction and loads acting on a pressurized compartment in the main flight loading cases as on part of the fuselage.

When examining the joint effect of aerodynamic loads and pressure or rarefaction in pressurized compartments it is necessary to keep in mind that the actual conditions of skin loading correspond to those indicated in Fig. 9.5.

The forces of complete (absolute) pressure, external $p_{нар}$ and internal $p_{вн}$, act in opposite directions. Deformations of the skin and the load on its attachments are determined by the excess pressure $p_{изб}$, which is the difference in the absolute pressures: $p_{изб} = p_{нар} - p_{вн}$ or manometric pressures (excess in comparison with

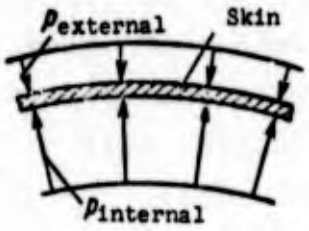

Figure 9.5. Loading of the fuselage skin.

atmospheric pressure $p_{ат}$) of the aerodynamic pressure and the pressure in cabin $p_{каб}$, i.e., $p_{изб}=\bar{p}q-p_{каб}$.

Hence, it follows that the conditions of skin (and window panes) loading will be especially unfavorable, if:

the aerodynamic excess pressure $\bar{p}>0$ and the rarefaction in the cabin $p_{каб}<0$; the aerodynamic rarefaction $\bar{p}<0$ and the pressure in the cabin $p_{каб}>0$.

§ 3. DESIGN AND STRESS ANALYSIS OF A FUSELAGE

1. Load-Bearing Setups of Fuselages

A conventional fuselage setup (monofuselage or monocoque fuselage) is a beam supported on a wing and operating in flexure and torsion (Fig. 9.6a).

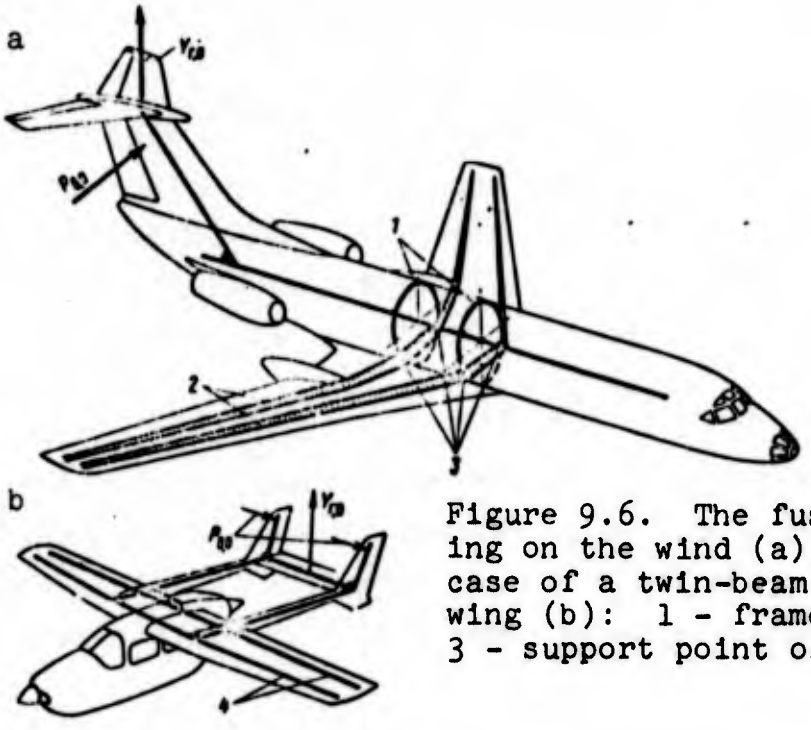

Figure 9.6. The fuselage is a beam resting on the wind (a), or a frame (in the case of a twin-beam setup) sealed in the wing (b): 1 - frames; 2, 4 - wing spars; 3 - support point of the fuselage.

If an aircraft is made in accordance with the twin-beam setup with a gondola, then the gondola also rests on the wing and operates as a beam, and the tail beams together with the horizontal tail surfaces form a rigid frame sealed in the wing (Fig. 9.6b).

Fuselage framework designs are divided in accordance with the load-bearing setup into truss and beam designs.

Truss design. The main load-bearing elements of a truss design are the rods which form a three-dimensional truss (Fig. 9.7a). The skin imparts a streamlined shape to the fuselage, receives the air loads and transmits them to the truss. The increase in the flight velocity of aircraft led to the fact that the secondary structures for attaching the skin to the truss and the skin itself began to become so heavy that truss fuselages turned out to be unfavorable in a weight regard. At the present time they are employed only on some light low-speed aircraft and helicopters.

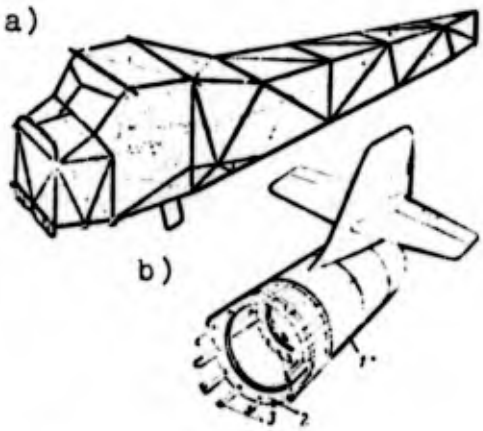

Figure 9.7. Load-bearing setups of fuselages: a) the truss fuselage of the Yak-12 aircraft; b) a beam fuselage and its main load-bearing members; 1 - skin; 2 - frames; 3 - stringers.

Beam design. The fuselages of contemporary aircraft and the majority of helicopters are made in accordance with this load-bearing setup. Thus only beam-type fuselages are subsequently examined.

In a beam-type fuselage the main load-bearing elements are (Fig. 9.7b): the working skin; the load-bearing elements of the longitudinal assembly - are normal and reinforced stringers; the load-bearing members of the transverse assembly - are normal and reinforced frames.

Depending on which load-bearing members are included in the design, two types of it are distinguished.

1. Semimonocoque, or beam-stringer fuselage. The operating skin of this design is supported by normal stringers and frames (Fig. 9.8a) or by normal and reinforced stringers (the reinforced stringers are sometimes called longerons) and frames (Fig. 9.8b).

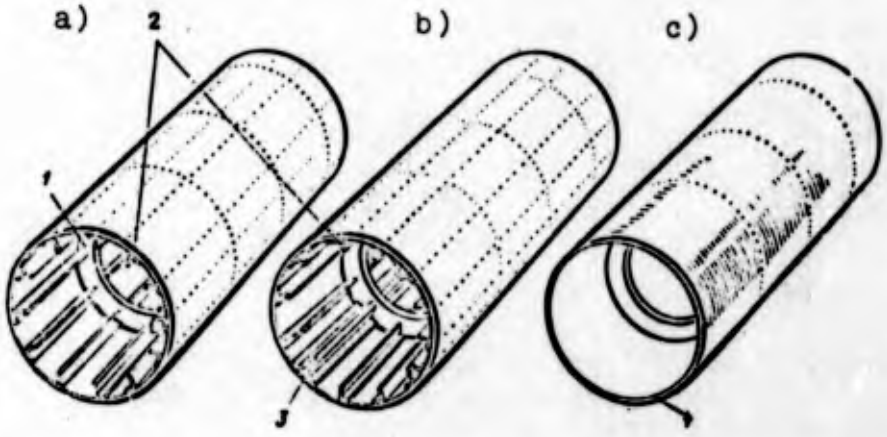

Figure 9.8. Types of beam fuselages: a) semimonocoque with normal stringers; b) semimonocoque with reinforced stringers; c) monocoque; 1 - frame; 2 - normal stringers; 3 - reinforced stringer; 4 - thick skin.

2. Monocoque, or beam-shell fuselage. The thick operating skin of this type is supported only by frames (Fig. 9.8c).

Individual sections of aircraft and helicopter fuselages are made in accordance with the monocoque setup, not having cut-outs in the skin. Fuselages completely made in accordance with the monocoque setup are rarely encountered. This is explained by the fact that for compensating a cut-out in a stringerless skin it is necessary to install reinforcements which considerably increase the design weight.

2. Forces in Fuselage Cross Sections

In the general case in the transverse cross section of a fuselage vertical or horizontal transverse forces, flexural and torsional moments are acting (Fig. 9.9).

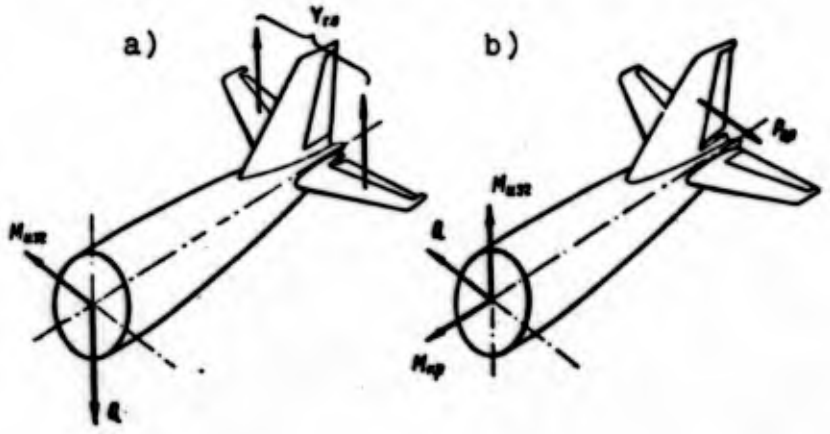

Figure 9.9. Forces in a fuselage cross section: a) during vertical flexure; b) during horizontal flexure and torsion.

Transverse forces, flexural and torsional moments are determined by the usual methods. For this in the loading case in question the surface forces in the wing and empennage are determined; the g-forces are calculated with formula (9.1) or (9.6); the mass forces of the loads and units and the linear mass forces of the design q_ϕ are determined with formula (9.2) or (9.7). In the approximation calculations the fuselage is broken down into a number of sections whose number depends on the required accuracy. The mass loads from the design and the loads in each section are represented in the form of a concentrated force applied at the center of gravity of the section.

A fuselage is examined as a beam, located in equilibrium under the effect of mass and surface forces. The surface forces from the wing and empennage are applied at their attachment points and can be examined as reactions.

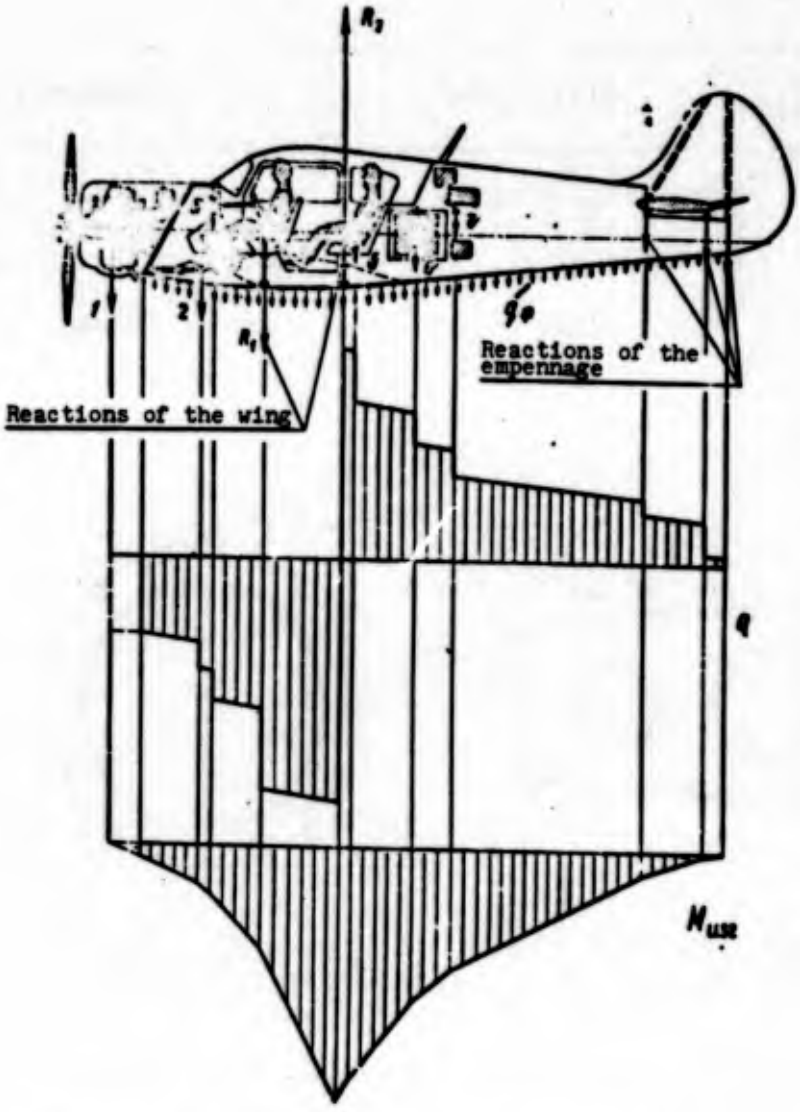

Figure 9.10. Diagrams of the transverse forces and flexural moments of a fuselage during its flexure in the vertical plane.

As an example diagrams of transverse forces and flexural moments of the fuselage are depicted in Fig. 9.10 in the case of its flexure in the vertical plane.

As a result of the similarity of the load-bearing setups of the wing and the fuselage there is an analogy in the purpose and the operation of the elements of a beam fuselage and wing. Table 9.1 and Fig. 9.11 explain this analogy.

Table 9.1

No. of the position in Fig. 9.11	Wing beam	Fuselage beam
1	Operating wing skin	Operating fuselage skin
2	Normal wing stringers	Normal fuselage stringers
3	Spar flanges	Reinforced stringers
4	Webs	Lateral skin panels
5	Normal ribs	Normal frames

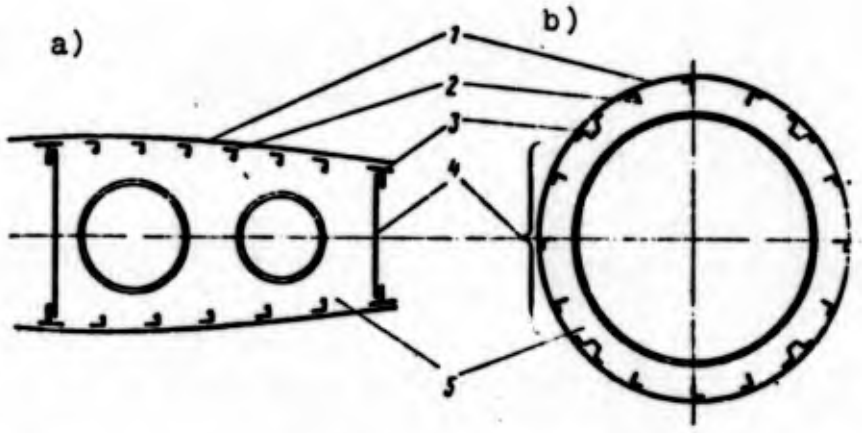

Figure 9.11. Analogy in the purpose and operation of elements: a) wing; b) beam fuselage.

The analogy in the operation of a beam fuselage and wing makes it possible to employ the same methods of calculation in the strength calculation of the fuselage, as for a wing.

Let us examine the approximate strength calculation of a fuselage.

3. Determination of the Stresses in Fuselage Cross Sections and Checking the Strength of the Longitudinal Assembly and Skin

Calculation in vertical flexure. Calculation for flexure in the vertical plane is main one for selecting the longitudinal assembly cross sections.

The most significant loads causing fuselage flexure in the vertical plane are the loads in flight cases A, A' and B and in landing case E.

The fuselage cross section is schematized as a cross section of a two-flange beam (Fig. 9.12). The arches of a cross section are examined as beam flanges, the side members - as webs.

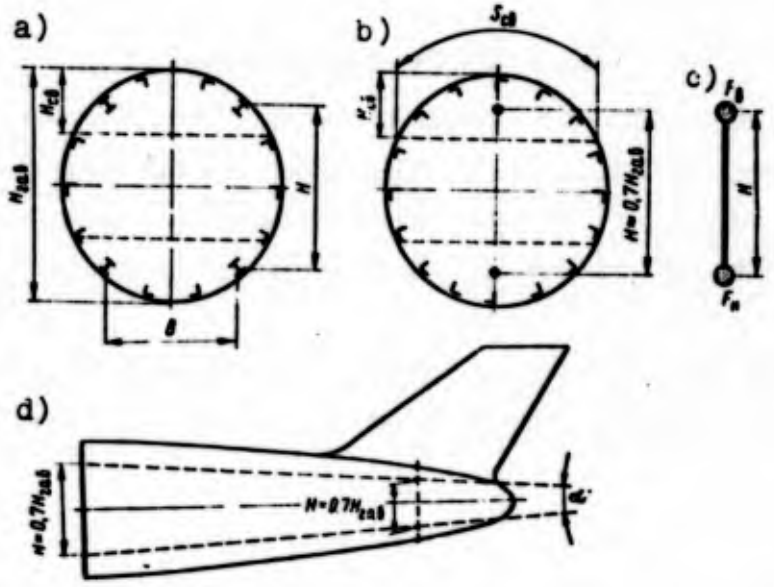

Figure 9.12. Rating a fuselage for vertical flexure: a, b, c - schematization of the cross section; d - the angle of taper considered in rating for shear in the vertical plane.

As the operating height H of a two-flange beam it is assumed:

1) in a design with reinforced stringers - the distance between them (Fig. 9.12a);

2) in stringer design for circular and elliptical sections cross $H \approx 0.7\ H_{габ}$ (Fig. 9.12b); the height of the arch for them is assumed equal to $H_{св} \approx 0.3\ H$ (in Fig. 9.12 the arches are distinguished by broken lines).

The fictitious normal stress in an arch is

$$\sigma_{\phi} = \frac{M_{изг}}{HF_{ред}}, \qquad (9.8)$$

where $F_{ред}$ - is the reduced area of the arch cross section.

The reduced area of an arch cross section (upper or lower) is determined just as was done in rating wing panels. Thus, for instance, for a fuselage with reinforced stringers

$$F_{ред} = 2f + \Sigma f_{стр}\varphi_{стр} + f_{обш}\varphi_{обш}, \qquad (9.9)$$

where f - is the cross-sectional area of a reinforced stringer (for the arch in question; $f_{стр}$ - is the cross-sectional area of a normal stringer; $f_{обш}=S_{св}\delta_{обш}$ - is the cross-sectional area of the skin ($S_{св}$ - is the length of the arc in the arch in question).

The actual values of the normal stresses in the arch elements can be obtained from the expression

$$\sigma_i = \sigma_{\phi}\varphi_i. \qquad (9.10)$$

The magnitude of the reduction coefficient ϕ_1 is selected in the same manner as in approximate wing rating. If the stresses are close to destructive, then

$$\varphi_i = \frac{\sigma_{разр\,i}}{\sigma_{разр.ус.стр}}.$$

If the stresses are small (for a compressed zone less than $\sigma_к$, and for a tensioned zone less than $\sigma_т$), then

$$\varphi_i = \frac{E_i}{E_{ус.стр}}.$$

Notes: 1. In rating fuselage cross sections situated within the limits of pressurized compartments, the loading of these compartments with internal pressure should be taken into account. Additional normal stresses are developed from this pressure in the elements of the fuselage. For a cylindrical circular shell the additional axial stress is

$$\Delta\sigma = \frac{\Delta pR}{2\delta_{пр}},$$

where Δp - is the rated excess pressure; R - is the radius of the cylinder; $\delta_{пр}$ - is the reduced skin thickness.

Since

$$\delta_{пр} = \frac{F_{ред}}{S_{св}},$$

then formula (9.8) taking the internal excess pressure into account in pressurized fuselage compartment will take the form

$$\sigma_{\phi} = \frac{1}{F_{ред}}\left(\frac{M_{изг}}{H} \pm \frac{\Delta pRS_{св}}{2}\right). \qquad (9.8')$$

where the sign "+" is taken for the tensioned arch, and "-" for the compressed arch.

2. During determining the normal stresses in the elements of an arch with formula $\sigma_i = \phi_i \sigma_{\phi}$ the different positioning of the load-bearing elements with respect to height, and their different distance from the neutral axis are not considered. The error will be insignificant, if all elements operate in the zone of plastic deformations (Fig. 9.13b). With small stresses (Fig. 9.13a) the calculation is inaccurate. It is possible to introduce a correction for the elements most distant from the neutral axis, using a formula analogous to that employed in the approximate rating of the wing

$$\sigma_i = \varphi_i \sigma_{\phi} \frac{H_i}{H},$$

where H_i - is the distance of the element from the neutral axis.

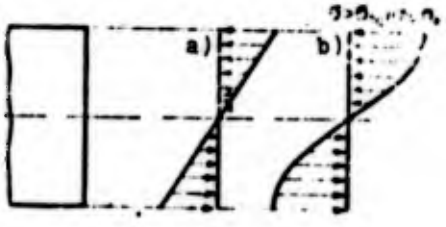

Figure 9.13. Distribution of normal stresses with respect to the height of the fuselage cross section during the operation of the elements in the zone of elastic (a) and in the zone of plastic (b) deformations.

The tangential stresses in the side skin walls of the fuselage during vertical flexure are determined with the formulas

$$\tau = \frac{Q}{F_{ст}} = \frac{q}{\delta_{общ.б}}; \qquad (9.11)$$

$$q=\frac{Q}{2H},$$

where $\delta_{\text{обш.б}}$ - is the thickness of the lateral skin.

In determining τ the curvature of the sidewalls is not considered.

The given value of force Q in the rated cross section is found by taking into account the taper of the fuselage in a side view with the formula

$$Q=Q_{\text{эп}}-\frac{M_{\text{изг}}}{H}\alpha, \qquad (9.12)$$

where $Q_{\text{эп}}$ - is the value of the transverse force obtained in calculating the diagram of Q, not allowing for taper; α - is the angle of taper; it is defined as the angle between the axes of the reinforced stringers or the lines connecting the points which correspond to $H=0.7\ H_{\text{габ}}$ (Fig. 9.12d).

Under the effect of the stresses found from calculating for vertical flexural, the elements of fuselage are checked for strength, just as are analogous elements of the wing: the skin and the normal stringers of the upper and lower arches - just as are the skin and the stringers of wing during operation in normal stresses, the skin of the sidewalls - in shear as are the spar webs, the reinforced stringers - as are spar flanges.

Calculating horizontal flexure and torsion. The loads which cause horizontal flexure and torsion in the fuselage are the lateral surface and mass forces. The most significant of these for the nose section - are the loads during sideslip, for the tail section - the loading cases of the vertical tail surfaces during a maneuver, in turbulence, and for aircraft with several engines also the case of engine cutoff on one side of the plane of symmetry.

In rating for horizontal flexure, a beam fuselage as also in examining of vertical flexure, is schematized in the form of

a two-flange beam (Fig. 9.14a). The sidewalls of the cross section are considered the beam flanges, the arches - as the webs. In determining the operating height of a two-flange beam B the same rules are employed as for H in the case of vertical flexure of a fuselage.

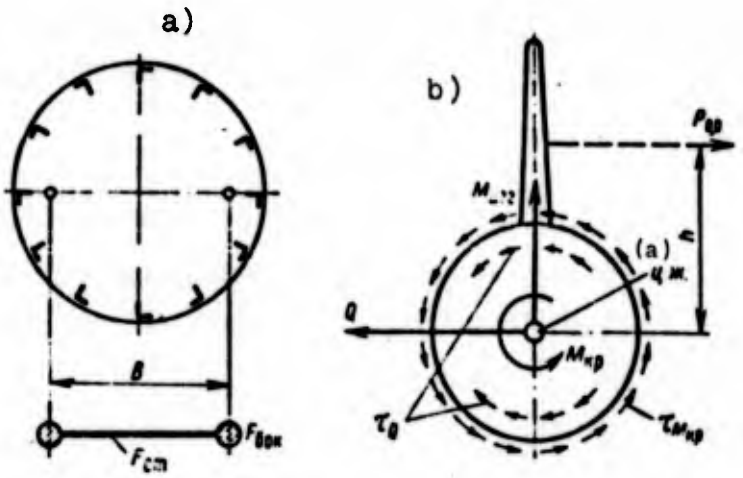

Figure 9.14. Rating a fuselage for horizontal flexure and torsion: a) schematization of the cross section; b) forces in the cross section and tangential stresses in the skin.
Key: (a) c.r. (center of rigidity).

The normal stresses in the elements of the lateral arches are determined as in the rating for vertical flexure, with formulas (9.8) and (9.10). In this case the reduced area of the lateral arch is found with an expression analogous to expression (9.9), in which the dimensions of the elements of the lateral arch are included

$$F_{\text{прив}} = 2f + \Sigma f_{\text{стр.б}} \varphi_{\text{стр.б}} + f_{\text{обш.б}} \varphi_{\text{обш.б}}. \qquad (9.13)$$

During horizontal flexure and torsion of the fuselage large tangential stresses are received in the skin caused by the transverse force and the torsional moment.

Since the sidewalls of a fuselage are symmetrical, then the center of rigidity of the cross section is located on its vertical

axis. The position of the center of rigidity with respect to height is approximately defined by the relationship of the cross-sectional areas of the skin as the center-of-gravity position of the areas of the upper and lower arches.

In calculating the torsional moment it is assumed, that the axis of the rigidity of the cross section is perpendicular to the plane of the frame.

The magnitude of the torsional moment is computed as the sum of the moments of all forces (surface and mass) acting on a cut-off part of the fuselage, relative to the axis of the rigidity of the cross section in question. Thus, during the effect on the cut-off tail section of only force $P_{в.о}$ (Fig. 9.14b)

$$M_{кр} = P_{в.о}h.$$

The linear tangential forces due to the transverse force applied at the center of rigidity, are found in a manner analogous to that in the case of vertical flexure

$$q_Q = \frac{Q}{2B}. \tag{9.14}$$

The given value of force Q taking into account the taper of the fuselage is determined with the formula

$$Q = Q_{ск} - \frac{M_{изг}}{B}\beta, \tag{9.15}$$

where β - is the angle of taper in a top view, determined analogously to the angle of taper α in a side view (Fig. 9.12d).

The tangential forces in the closed contour of the cross section due to torsional moment are found with the formula

$$q_{M_{кр}} = \frac{M_{кр}}{2F_к}, \tag{9.16}$$

where $F_к$ - is the area of the contour of the cross section.

The total tangential forces and stresses are computed with the formulas:

$$q = q_Q \pm q_{M_{кр}}; \quad \tau = \frac{q_Q \pm q_{M_{кр}}}{\delta}, \qquad (9.17)$$

in this case the thicknesses of the upper and lower skin - $\delta_{обш.в}$ and $\delta_{обш.н}$ - are introduced into the calculation.

Since the vertical tail surfaces are situated above the fuselage, then the forces q_Q and $q_{M_{кр}}$ in the skin of the upper arch caused by the load on these surfaces are always summed (see Fig. 9.14b).

During the horizontal flexure and torsion the skin of the sidewalls of the fuselage operates in normal and tangential stresses. Thus, it is necessary to carry out its strength testing just as for a wing skin during the joint action σ and τ.

§ 4. DESIGN ELEMENTS OF THE FUSELAGE. CHARACTERISTICS OF THE OPERATION OF THE FUSELAGE IN THE REGION OF CUTOUTS

1. Design and Operation of the Basic Elements of a Beam Fuselage

Figure 9.15 shows sections of a fuselage of a contemporary passenger aircraft.

Let us examine the design and the operation of the basic elements of a beam fuselage - of the skin, stringers and frames.

The sheathing skin of a beam fuselage operates in normal stresses due to $M_{изг}$ and in tangential stresses due to Q and $M_{кр}$. The local air loads and the radial forces tending to flatten the fuselage during flexure, cause, moreover, transverse flexure of the skin. However, here the air loads and the stresses of transverse flexure due to them are small (considerably less than in a wing skin).

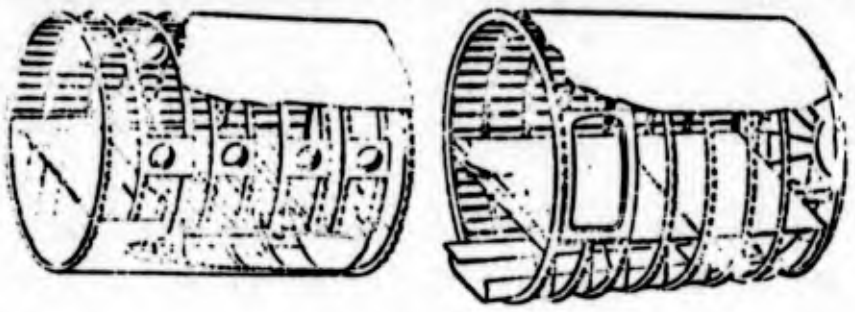

Figure 9.15. Beam-stringer fuselage of a contemporary passenger aircraft.

The skin of fuselages of contemporary aircraft consists of duralumin sheets stamped in accordance with the shape of the fuselage surface. The sheets are connected with each other and with the elements of the framework by riveted, glued or welded seams.

The sections of the skin subjected to the effect of hot gases from the engines or to intense kinetic heating, are made from stainless steel or titanium alloy.

In fuselage design, just as in wing design, instead of the conventional skin sheets monolithic panels and panels with a filler (laminar panels) can be employed.

The stringers (normal and reinforced) in conjunction with the skin operate in normal stresses due to $M_{изг.}$. At the same time they reinforce the skin during transverse flexure and increase its critical stresses $\sigma_к$ and $\tau_к$. After the loss of stability of the skin due to shear the transverse forces, which cause transverse flexure of the stringers resting in this case on the frames begin to act on the stringers.

With respect to their design the stringers of a fuselage are similar to the stringers of a wing. Usually they are metal profiles: bent (Fig. 9.16a, b, c, d, e), pressed (Fig. 9.16f, g, h, i) or composite (Fig. 9.16j). For longitudinal joining of panels

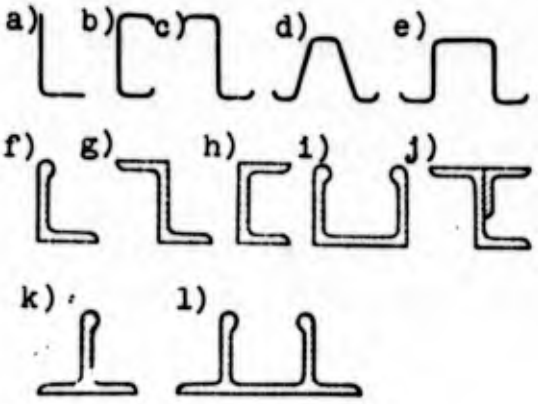

Figure 9.16. Transverse cross sections of fuselage stringers (examples).

are the profiles shown in Fig. 9.16k, l are employed. Stringers pass along the entire length of the fuselage or a considerable part of it; an attempt is made to make them one-piece.

The distance between stringers (stringer interval) is within the limits of from 150 to 200 mm. On the upper and lower arches of the fuselage stringers are positioned more frequently.

The frames (formers) of a fuselage are divided into normal and reinforced.

Normal frames just like wing ribs, preserve the shape of the fuselage and, being supports of the stringers and the skin, increase their critical stresses.

Frames (formers) are loaded with the following types of loads acting in their plane:

1) with radial forces during flexure of the fuselage; the longitudinal elements of the tensioned and compressed zones bent during flexure, tending to come together, compress the frames, in a direction normal to the neutral plane of the beam;

2) with loads due to the tensioning of the skin after its loss of stability during shear;

3) with local air loads.

All these loads are transmitted to the frames (formers) by the skin and the stringers.

As an example let us examine the loading conditions of a frame during vertical flexure of the fuselage. The following forces from the elements adjacent to it act on a frame (Fig. 9.17a):

R' - are the radial forces which tend during vertical flexure to bring the skin and the stringers of the upper and lower arches nearer to the neutral axis of the fuselage cross section;

R" - are the forces due to the tensioning of the skin after its loss of stability (on the lateral panels).

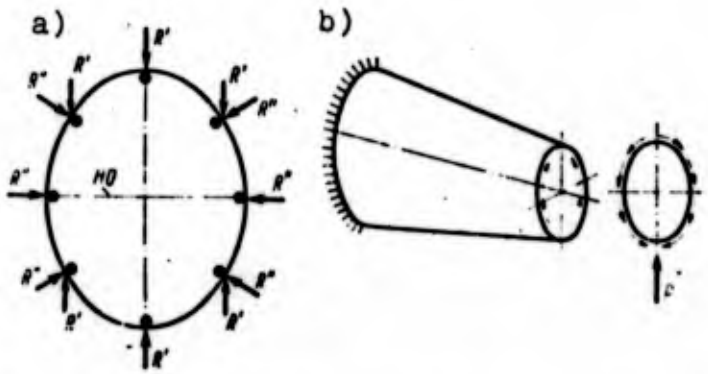

Figure 9.17. Examples of the loading of frames (formers): a) forces acting on a frame during vertical flexure of the fuselage; b) diagram of the balancing of a reinforced frame (former) loaded with a vertical force.

Under the effect of each group of these loads a frame (former) is in equilibrium.

Air loads play a small role in the tensioning of frames.

Normal frames (formers) are made in the form of thin-walled frameworks usually of channel or Z-shaped cross section. Riveted frames consisting of two or several profiles are sometimes employed. Figure 9.18 depicts examples of the design of normal frames.

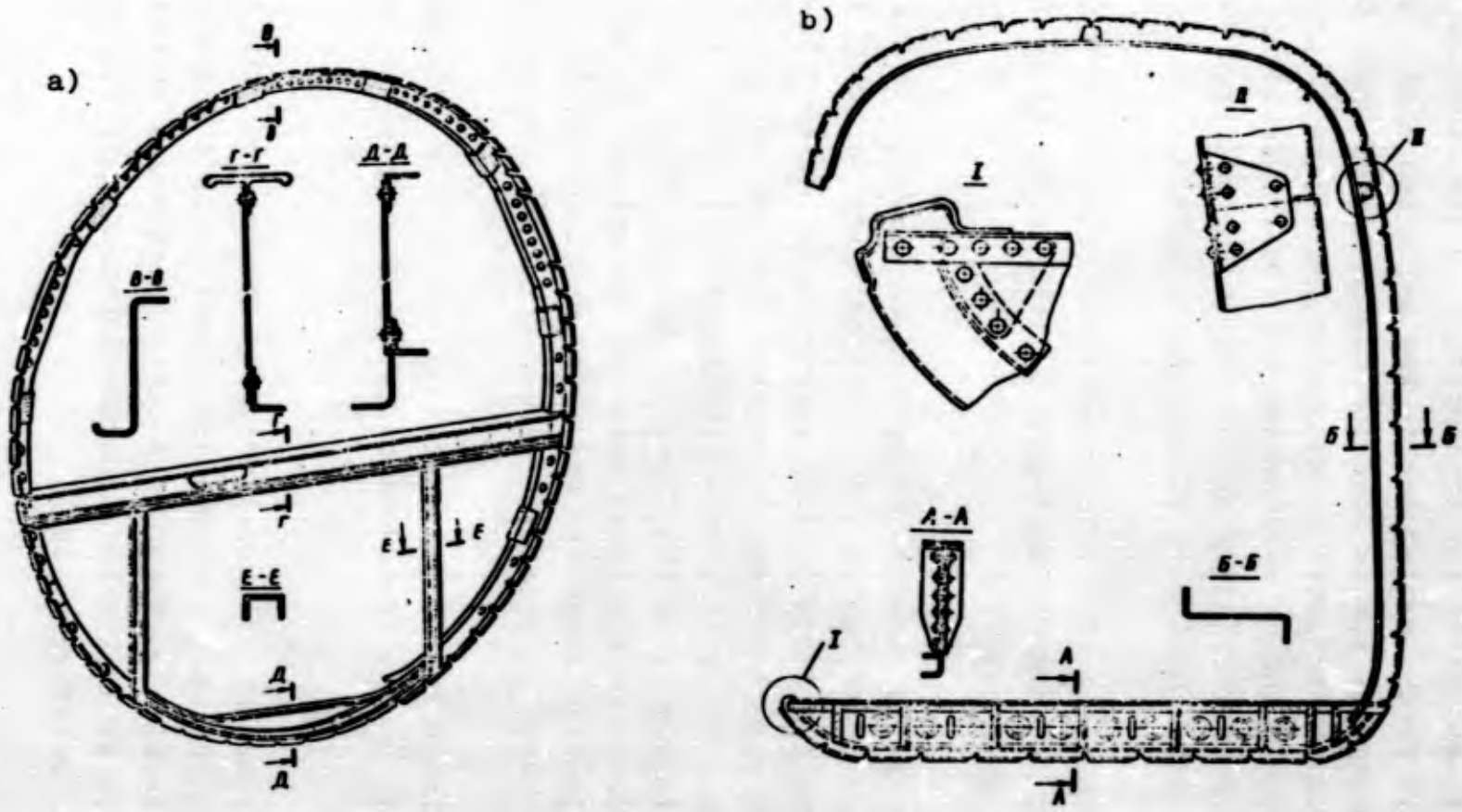

Figure 9.18. Designs of normal frames (formers) (examples).

Reinforced frames (formers) along with fulfilling the functions of normal frames serve for transmitting to the fuselage design the concentrated forces acting due to the units and loads, and also for redistributing the forces near the boundaries of large cutouts in the skin and at the sites of change in the angles of taper (for example, at a joint of cylindrical and conical sections). The reinforced frames standing at the ends of pressurized compartments, are loaded with the forces of internal pressure.

The balancing of a reinforced frame (former) for its rating is carried out in a manner analogous to that in the balancing of a reinforced wing rib.

Figure 9.17b shows an example of the setup of the balancing of a reinforced frame loaded with a concentrated vertical force (for example from the front landing gear strut). Force P is transmitted to the skin via rivets and is balanced by the reactions on the part of the skin. The reactions are tangential forces transmitted from the skin via rivets to the frame (former) contour. It is assumed, that the forces in a riveted seam are distributed in the same manner as the tangential forces in the cross section of a fuselage due to transverse force Q, equal to the resultant load on the frame.

Reinforced frames are made in the form of a circular framework or in the form of a framework partially or completely covered with a sheet.

The framework is usually made by forging or by injection molding and in the transverse cross section is a powerful profile, i.e., a channel bar, T-bar or I-bar. Sometimes a framework is manufactured as a riveted structure consisting of flanges and a web with struts reinforcing it.

Both the normal and reinforced frame (former) of the circular type are in the general case a three times statically indeterminable system. Flexural moment M, transverse force Q and axial force N

appear in the transverse cross section of frame (former) during its loading. The expansion of static indeterminability and the plotting of diagrams of M, Q and N are accomplished by known methods structural mechanics.

Calculations show that strength of frame (former) cross sections, as a rule, is determined by flexure.

Figure 9.19 depicts design setups and diagrams of the flexural moments of a rectangular frame (former) of a cargo aircraft (a), of a circular frame (former) of the attachment of engines to the tail section of a fuselage (b) and of a circular frame (former) of the attachment of vertical tail surfaces (c). Given in the same place are approximate design setups of sections of frames (formers) which facilitate the understanding of the nature the diagram of the flexural moments.

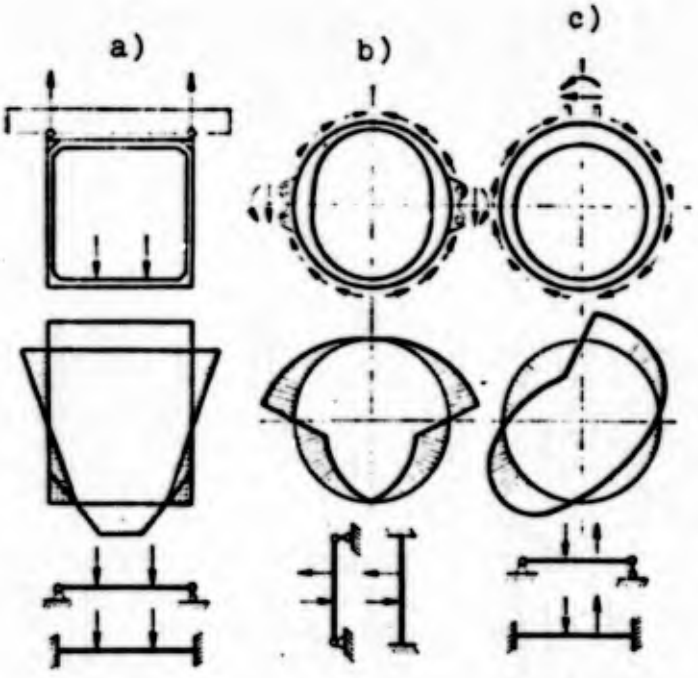

Figure 9.19. Design setups and diagrams of the flexural moments of reinforced frames (formers) (examples).

The actual supporting conditions for these sections are intermediates - elastic jamming.

The distance between frames (formers) (frame interval) in the fuselages of contemporary passenger aircraft is located within the limits of from 400 to 500 mm.

Coupling of frames (formers) with stringers. The tendency is to make stringers continuous. However, during coupling with the most loaded reinforced frames (formers) (for example, with frames (formers) for attaching a landing gear, wing, empennage) the stringers, as a rule, are cut.

This is explained by the fact that the cutouts for the passage of continuous stringers would considerably weaken a reinforced frame (former).

Two types of mutual coupling of normal frames (formers), continuous stringers and skin can be employed.

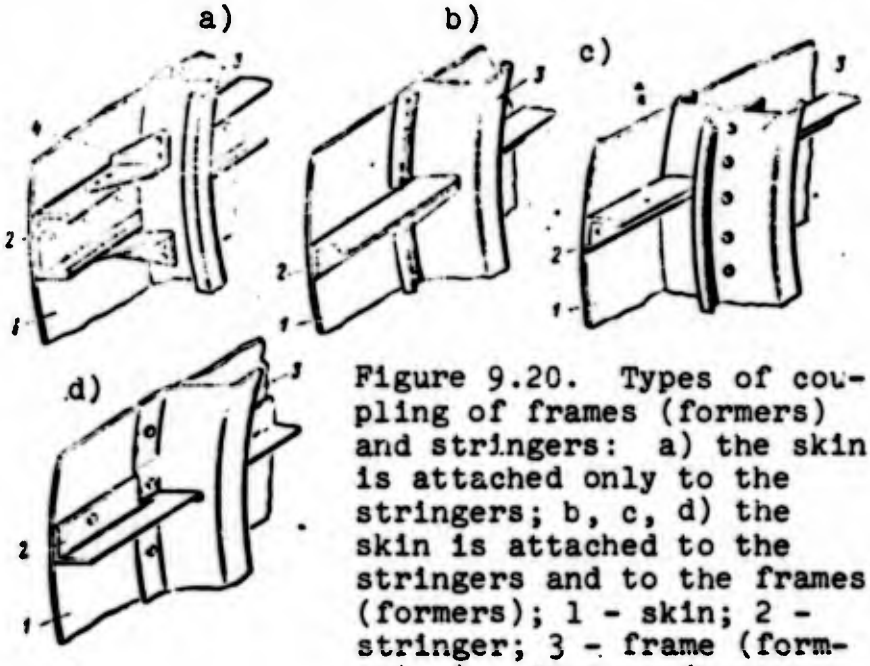

Figure 9.20. Types of coupling of frames (formers) and stringers: a) the skin is attached only to the stringers; b, c, d) the skin is attached to the stringers and to the frames (formers); 1 - skin; 2 - stringer; 3 - frame (former); 4 - fitting (technological compensator).

1. The frames (formers) are connected with the skin not directly, but via stringers (Fig. 9.20a). The stringers are attached to the frames (formers) with the aid of compensators. This type of coupling makes it possible to simplify the technology of fuselage assembly.

2. The frames (formers) are directly connected to the skin (Fig. 9.20b, c, d). Cutouts are made for positioning the stringers in the frame (former).

These types of frames (formers) more completely reinforce the skin (increase its critical stresses).

Moreover, in this case the frames (formers) are capable of restricting the propagation of fatigue cracks, thus increasing the durability of the design. Thus on contemporary passenger aircraft, in spite of a certain increase in weight, precisely this type of coupling is most frequently employed.

2. The Joining Together of the Parts of a Fuselage

For operational and technological considerations the fuselage is usually broken into parts which will be joined with the aid of detachable joints. The detachable joining of parts should ensure as far as possible the direct transmission of the forces acting on the elements being united, without changing the nature of their operation. Thus the joining of the parts of a beam fuselage is accomplished along the contour by means of joining angles and the bolts installed with a small interval (Fig. 9.21). In this case the stringers are connected with each other by special fittings which transmit the forces of the joined parts of the stringer and the skin adjacent to them.

3. Joining the Fuselage with the Wing

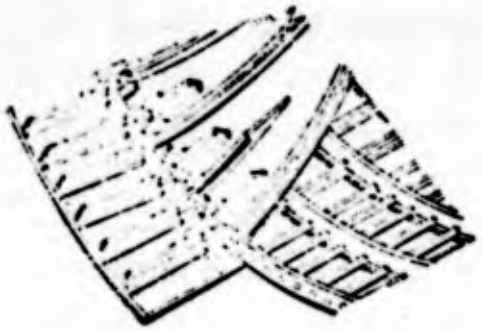

Figure 9.21. Design of a detachable joint of the parts of a beam fuselage (example).

A fuselage rests on a wing like a beam. Reinforced frames (formers) are installed at the sites where the wings are attached. The elements of a wing which operate in flexure, are also extended at the section occupied by the fuselage. The flexural moments of the two halves of a wing are balanced in the central (fuselage) part of the wing and, consequently, are not transmitted to the fuselage elements. Only vertical reactions from the spar webs are transmitted to the reinforced frames (formers) of the fuselage. Thus, joining units connected with the flanges and the webs of the spars are installed at the sites of the joining of the reinforced frames (formers) and the spars.

Figure 9.22 shows examples of the design of fuselage and wing joints.

Joining angles which connect the skin of the center section of the wing with the skin and the fuselage stringers are installed for transmitting the torsional moment from a wing of monocoque design to the fuselage. These angles transmit the horizontal reactions of the wing to the fuselage skin.

4. Characteristics of the Operation of the Fuselage in the Region of Cutouts

Cutouts are made in the fuselage skin for doors, windows, cockpit hoods, cargo, inspection and assembly hatches, etc.

Small cutouts (for example, cutouts for windows and inspection hatches) do not affect the operation of the general load-bearing

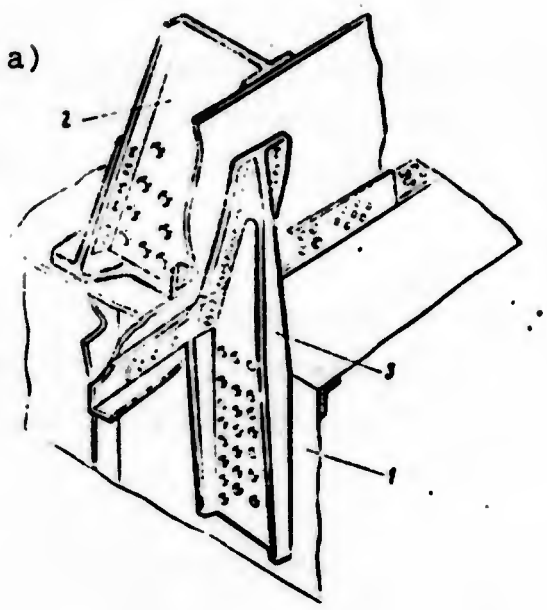

Figure 9.22. Joining of a fuselage with a wing (examples): a) in a low wing monoplane setup; b) in a high wing monoplane setup; 1 - wing spar (center section); 2 - a reinforced frame (former) of the fuselage; 3 - joining unit.

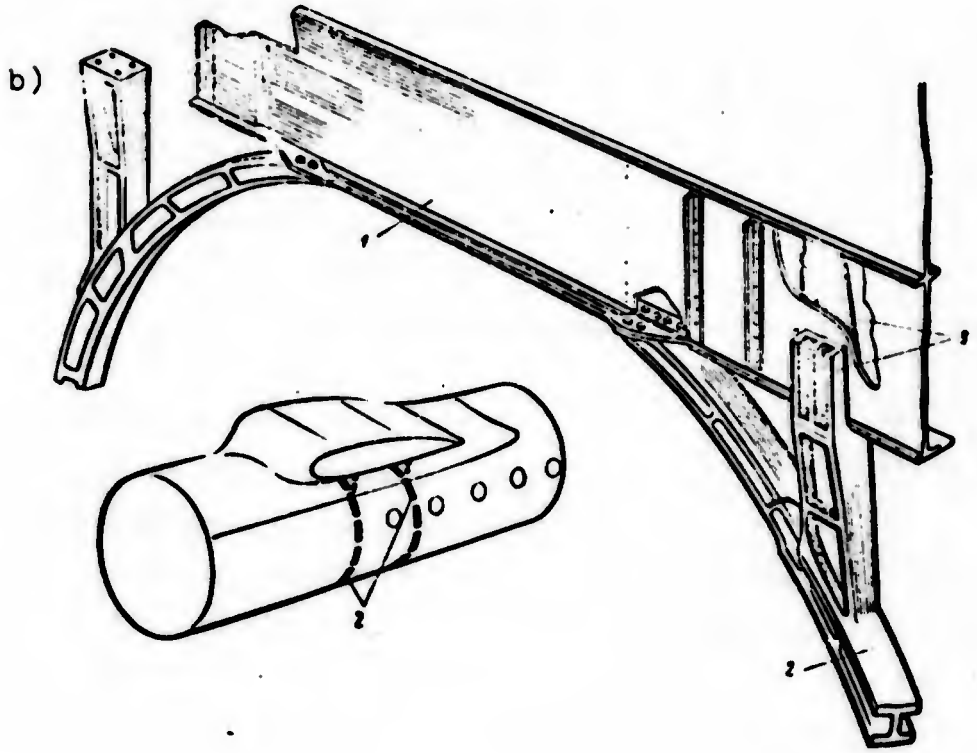

setup of the fuselage. As in wing design, these types of cutouts are compensated for either by surrounding them with frameworks, or by including the hatch covers in the operation of the load-bearing setup of the fuselage.

When there are large cutouts (for example, cutouts for a canopy, a cargo hatch, landing gear struts) for economizing on weight it is more advantageous to create another load-bearing setup in the region of the cutout.

Let us examine the characteristics of the operation of a fuselage in the region of a large cutout by the example presented in Fig. 9.23 (cutout at the bottom for a landing gear strut or a cargo hatch).

During vertical flexure of the fuselage the elements of the upper and lower arches operate in normal stresses. In the example in question a lower arch is cut out in a section with a length l. In the region of a cutout for receiving the axial forces from the skin and the stringers interrupted by the cutout powerful reinforced stringers are installed on the longitudinal edges of the cutout.

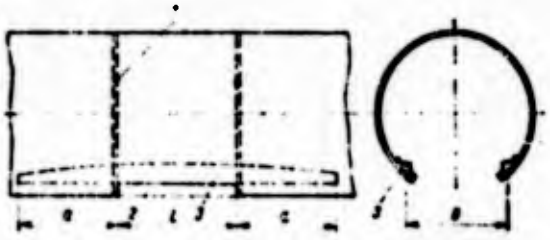

Figure 9.23. The load-bearing setup of a beam fuselage in the region of a large cutout: 1 - reinforced frames (formers); 2 - cutout; 3 - reinforced stringers.

In the sections adjoining a cutout, the lower arch is included in the operation in normal stresses not at the boundary of the cutout, but at a certain distance, at a distance a, approximately equal to the width cutout B. Thus, the reinforced stringers do not end near the boundaries of the cutout, but continue a length a, compensating for the incomplete operating value of the arches in normal stresses near the cutout.

Since the lateral panels are continuous, then the transverse force of vertical flexure is transmitted through the cutout zone in the form of tangential stresses τ_Q, of the same kinds as outside of the cutout.

During horizontal flexure and torsion the flexural moment in the cutout zone is received by the lateral panels just as outside the cutout.

The horizontal transverse force in the cutout section is received only by the upper panel. In transmitting the torsional moment only the lateral panels participate, since only they are capable of receiving it in the form of a pair of forces (like the spars of a two-spar wing).

In this case the lateral panels are additionally loaded with flexural moment, i.e., the fuselage, just like the wing, in the region of an uncompensated cutout operates in flexural torsion.

Thus, during horizontal flexure and torsion of a fuselage the distribution of the tangential forces in the region of the cutout considerably differs from their distribution in cross sections with a closed contour. For redistributing the forces in the skin reinforced frames (formers) are installed on the boundaries of the cutouts. In the example in question the reinforced frame (former) at the boundary of the cutout removes from the lower panel its share of the transverse force and transmits it to the upper panel, and also removes from the horizontal panels the part of the torsional moment received by them and transmits it to the lateral panels. A diagram of the loading of a frame (former) is shown in Fig. 9.24.

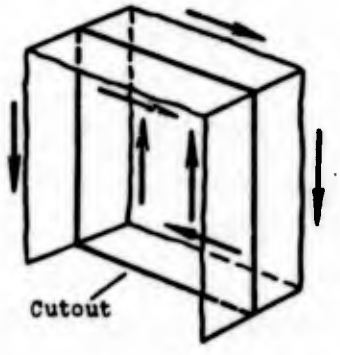

Figure 9.24. Diagram of the loading of a reinforced frame (former) situated near the edge of a cutout.

§ 5. FLIGHT DECKS, PASSENGER COMPARTMENTS AND AUXILIARY AREAS

Flight decks are intended for accommodating the members of the crew (pilots, navigators, flight engineers, radio operators, etc.), and also the instruments, units and devices which ensure control of the aircraft and constant monitoring during flight.

The dimensions and layout of the flight deck depend on the composition of the crew, and the composition is determined by the type of aircraft and by the type of power plants. Thus, domestic long- and intermediate-range main-line aircraft at first had a crew composed of five people: two pilots, a navigator, a radio operator and a flight engineer. At the present time the tendency is towards decreasing the number of crew members on aircraft of these types to three people - two pilots and a flight engineer. This possibility is provided by the perfection both of the onboard equipment of the aircraft and the ground-based equipment of the air lines. On short-range main-line aircraft the crew consists of two pilots, sometimes in the composition of the crew there is also a flight mechanic or navigator-radio operator. On aircraft of regional airlines the crew consists of one-two pilots.

Each of the crew members has his own working area equipped with the appropriate equipment. The dimensions of the working areas of the flight engineer, the navigator and the radio operator are determined by the overall dimensions of their panels and by the average dimensions of the human body. The seats of these crew members are frequently made rotating relative to the vertical axis for working convenience and to provide visual communication between the crew members.

Stricter requirements are imposed on the working areas of pilots. The pilot's position in the cabin should ensure minimum fatigability, the possibility of applying maximum forces on the main

control levers, convenience in observing the instruments and the possibility for rapid activation of all the control elements. Usually the dimensions of the pilot's working area are specified during the designing of an aircraft in the technical specifications of the customer. The pilots' seats are made adjustable with the possibility of changing position both in height and with respect to the length of the cabin.

Special attention is given to ensuring a good field of vision to the pilots from the cabin. The pilot should have the following minimum angles of view with the position of the aircraft in the line of flight

forward-downward - 15-20°,
forward - upward - 30°;
laterally in both directions - ±90°.

The field of vision from the cabin is ensured by the presence of a canopy. On light single-seat aircraft it is necessary to make the canopy in the form of a superstructure on the fuselage which considerably increases drag. Figure 9.25 shows an external view of the flight deck window area (canopy) of a contemporary passenger aircraft.

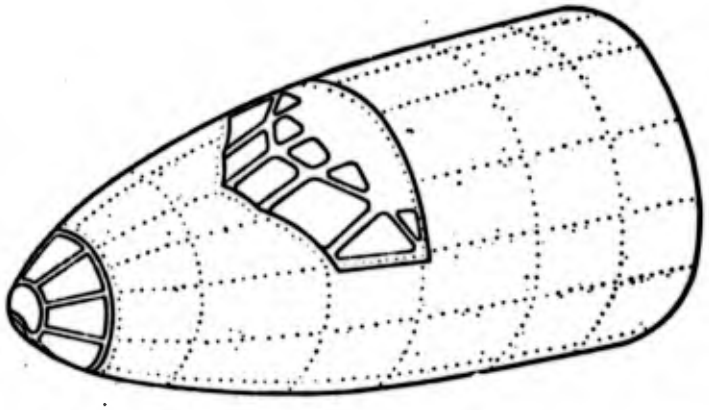

Figure 9.25. Flight deck window area (canopy) of a contemporary passenger aircraft.

The framework of the flight deck window area is made in the form of frames cast from magnesium alloy or welded frames made from forged Chromansil sheets. The cockpit windows usually consist of single or double organic glass. The pilots' viewing windows are frequently made from silicate glass with internal electrical heating. When double glass is employed the inter-glass space is connected with the cabin via a drying system (receptacles with a moisture-absorbing compound) which prevents the misting up and the icing over of the glass.

Passenger compartments are intended for accommodating passengers. One of the main requirements imposed on passenger compartments is the requirement for comfort. Passenger compartment comfort includes the following elements:

1) sufficient room for accommodating the passengers;

2) comfortable seats of sufficient dimensions;

3) an effective airconditioning system;

4) convenient positioning and proper equipment for the galley, cloakrooms and toilet facilities;

5) soundproofing which reduces noise to permissible limits;

6) sufficient natural and artificial illumination;

7) pleasant internal decorative furnishing of the passenger compartment.

The required volume for passenger accomodation is determined by the number of passengers and by the size of the specific volume. The specific volume of passenger accommodation is the volume which is required for one passenger. The size of the specific volume

depends on the class of the passenger compartment. At the present time four classes of passenger compartments are in existence: "luxury" class, 1st class, tourist or 2-1 class, and economy or 3rd class. The specific volume for the indicated classes varies within the following limits: for "luxury" class it is 1.8-2.0 m^3/man; 1st class is 1.5-1.6 m^3/man; tourist class is 1.2-1.3 m^3/man; economy class is 0.9-1.0 m^3/man.

The linear dimensions of the passenger compartment depend on the number of passengers, the specific volume and the class of the passenger compartment.

The most important element of a passenger compartment are the passenger seats. The dimensions, the design and the convenience of a seat first of all determine its comfort. Thus, precisely these indices are employed as the basis for dividing the passenger compartments into classes. Table 9.2 gives the basic dimensions of the passenger seat of all four classes. Indicated there also is the distance between the rows of seats (the seat interval) and the width of the center aisle.

Table 9.2

Class	Distance between elbow-rests, mm	Length of the back from the cushion of the seat, mm	Angle of deflection of the back from the vertical, deg	Total hgt of the seat, mm	Distance between the rows of seats (seat interval), mm	Width of the center aisle (not less than), mm
"Luxury"	400—500	730—770	55—65	1 012—1 094	1 200—1 500	500
1st	450—480	710—730	40—50	993—1 055	930—1 110	500
2nd	420—440	650—700	30—40	954—1 056	870—960	450
3rd	400—420	610—650	18—30	965—1 007	712—870	350

The seats of the "luxury" class are usually made separate or joined in two units. The seats of the remaining classes are joined in two or three units.

To ensure passenger safety the design of the seats, the safety belts and the elements attaching the seats to the floor is rated along with other loading cases for g-forces during a forced landing: $n_x^p=9$, $n_y^p=4$, $n_z^p=1.5$.

The devices attaching the seat units to the floor should ensure the possibility of rapid conversion of the passenger compartment from one class to another. Thus, the devices attaching the seat units are standardized: each unit is fastened to the floor with the aid of two standard rails situated at a distance of 805±0.5 mm from each other (international standard).

The entrance doors to the passenger compartments and the flight decks are situated on the left lateral surface of the fuselage, and in certain cases - at the bottom (the Yak-40). The door width usually does not exceed 800 mm, and the height - 1,500 mm. On passenger aircraft with pressurized compartments the doors open, as a rule, inward; in this case it is simpler to ensure the air-tightness of the door in the closed position. Designwise the door is, as a rule, forged from a sheet duralumin cup reinforced with a frame. The cutouts in the fuselage skin for the doors are compensated for with riveted or cast frames which rim the cutouts. In these cases when the dimensions of the cutout are great in comparison with the dimensions of the transverse cross section of the fuselage, the positioning on the edges of the cutout of reinforced frames (formers) and reinforced stringers can be more advisable.

The windows of passenger compartment have diverse shapes. The most frequently employed shape is circular windows and rectangular with rounded corners. The dimensions and the interval of the windows vary within broad limits. The window glass is usually double, and the inter-glass space is connected with interior of the compartment via a receptacle with a moisture absorber. The cutouts in the fuselage skin for the windows are compensated for by rim frames.

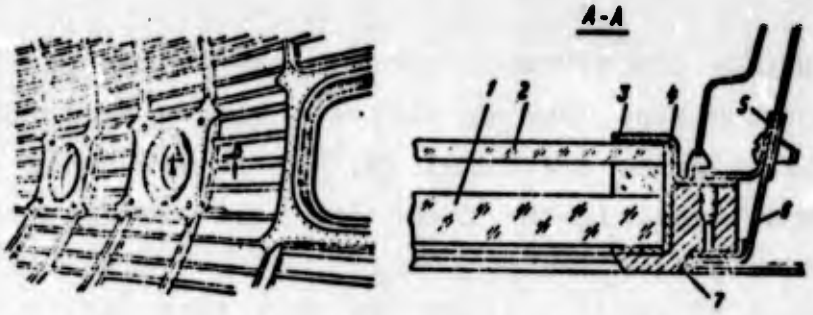

Figure 9.26. Window design of a passenger compartment (example): 1 - exterior glass; 2 - interior glass; 3 - circular holder; 4 - rubber profile; 5 - semi-ring clamps; 6 - forged cup; 7 - sealing cement.

Figure 9.26 shows an example of window design.

Included among the auxiliary areas the galleys, cloakrooms, baggage compartments and rest room facilities.

It is advantageious to locate the galley up front, near the front entrance, between the flight deck and the passenger compartment. It is prohibited to place the galley near the rest rooms and it is not recommended placing it together with the cloakrooms. The dimensions of the sections for the galleys and their equipment depend on the type of aircraft.

It is necessary to position the cloakrooms near the doors intended for the entry and exiting of the passengers. As the experience in passenger aircraft design shows, the dimensions of the areas for cloakrooms are determined from calculating that for each coat it is necessary to have 0.045-0.05 m^2 of cloakroom floor space.

The baggage compartments should be separated from the passenger compartments and have separate doors for loading.

The location of the baggage compartments depends on the dimensions of the aircraft. On aircraft with a large-diameter

fuselage the baggage compartments are situated under the floor of the passenger compartment, and on aircraft with a small-diameter fuselage - in sections of the fuselage. It is desirable to locate the baggage compartments in the front and tail sections of the fuselage in order to have the capability of obtaining the necessary position of center of gravity in an aircraft (with an incomplete number of passengers) by appropriate distribution of the luggage and cargo. The baggage compartments should be equipped with devices for holding down the baggage and cargo and with mechanisms for facilitating loading-unloading operations and reducing the time for carrying out these operations. Promising in this regard is the use of baggage containers.

The required volume of baggage compartments can be approximately estimated by employing the following dependence:

$$V_{бар} \approx 0{,}25n \text{ м}^3,$$

where n - is the number of passengers.

The rest room facilities are usually situated behind the passenger compartment. The floor area of one rest room is equal to 1.5-1.6 m^2 with a width of not less than 1 m. The number of rest rooms in a passenger aircraft depends on the number of passengers and the nonstop flight duration. Thus, with a flight duration of more than 4 h it is necessary to have one rest room for each 30 passengers; 2-4 h - one rest room for each 40 passengers; with a flight duration of less than 2 h - one rest room for each 50 passengers.

Noise on aircraft is the cause of the rapid fatigability of the crew members and passengers and of reducing the working efficiency of the crew members.

The noise sources within the flight decks and the passenger compartments are the engines, the propellers, the vibrating parts

of the structure and boundary air layer which flows around the fuselage. If special measures are not taken, then the noise level in the flight decks and passenger compartments of contemporary aircraft will considerably exceed the maximum permissible level. At the present time the maximum permissible noise level[1] is approximately equal to 100 dB.

To reduce the noise level in the flight decks and the passenger compartments of contemporary aircraft soundproofing is employed, which is simultaneously thermal insulation. It consists of several layers of sound-proofing material and an air space between them and the external decorative finishing of the flight deck and passenger compartment. Foamy material from the thinnest fiberglass with a light specific weight is employed as sound-proofing material. Furthermore, the presence of dampers in the engine attachments, elastic attachment of the floor panels and partitions, the employment of double and triple window glass, the application of sound suppressors in the airconditioning systems, etc., contributes to reducing the noise level.

§ 6. PRESSURIZED COMPARTMENTS

Contemporary aircraft accomplish flights at high altitudes. The advisability of flights at high altitudes is determined by the following reasons:

by increasing the economic effectiveness of air transport as a result of decreasing the kilometer fuel consumption and increasing the flight velocity;

by increasing flight safety as a result of greater uniformity in the meteorological conditions in the upper layers of the troposphere and in the stratosphere, than at low altitudes.

[1]Whispered conversation creates a noise level of 30 dB, normal conversation - 65 dB, loud conversation - 70-80 dB.

Furthermore, supersonic aircraft should fly at high altitudes due to the condition of the limited permissible intensity of sonic boom on the earth's surface (7-8 kgf/m^2).

There is a number of difficulties connected with flights at high altitudes. With respect to transport aircraft the main difficulties are as follow.

1. The flight altitude affects the vital activity of the human organism. At high altitudes functional disorders connected with oxygen deficiency occur in the human body.

Oxygen deficiency is caused by a drop in the partial pressure of oxygen in the alveoli of the lungs with an increase in altitude. Physiological investigations have demonstrated that by the minimum value of partial oxygen pressure in the alveoli of the lungs, at which the blood is still saturated with 80-85% oxygen, is a pressure of 47-50 mm Hg. This pressure corresponds to an altitude of 4.5 km, which, consequently, is the physiological altitude limit of flight in an open cockpit.

The manifestations of oxygen deficiency can be the diverse: headache, sleepiness, decrease in reaction speed, deterioration of vision and hearing, deterioration of metabolism, sad mood, and sometimes, vice versa, unjustified gaiety, black-out and even death in the event of prolonged oxygen deficiency or in the event of a sharp drop in pressure - decompression.

It is possible to increase the partial oxygen pressure in the alveoli of the lungs by increasing the percent of oxygen content in the air being inhaled or by increasing the pressure of the ambient air. The first method is combined with the employment of individual oxygen instruments and can be applied only up to an altitude of 13.5 km.

The basic method of ensuring the conditions essential for life on passenger aircraft is the second method - increasing the pressure on the flight decks and in the passenger compartments in comparison with the atmospheric pressure at a given altitude.

For this the flight decks and the passenger compartments should accommodated in pressurized sections of the fuselage. Measures should be taken for reducing the danger of decompression in the event of the failure of airtightness.

2. With an increase in altitude the operation of a number of the units of the aircraft, the engines and the equipment deteriorates due to the reduction in pressure and temperature. The appearance of cavitation is possible due to low suction pressure in the fuel, oil and hydraulic systems, also possible are deterioration in the operation of the seals, and a reduction in toughness of metals at low temperatures, etc. Some of these difficulties can be overcome in the working out of the design of the aircraft and its units. However, the reliable operation of many units of special equipment can be ensured only by creating the necessary pressures and air temperatures around them. This can be accomplished by placing them in pressurized sections.

3. Baggage and cargo can be damaged at high altitudes. To avoid this the baggage sections should be mandatorily placed in pressurized compartments.

4. In the flight of supersonic aircraft at altitudes of 20 km and more the intensity of the irradiation of people with cosmic rays becomes significant.

The pressurized sections of a fuselage, in which flight decks and passenger compartments are situated are usually called pressurized compartments. Let us examine them in more detail, keeping in mind, that in accordance with the nature of loading and in accordance

with design other pressurized sections are similar to pressurized compartments.

1. The Basic Physiological and Hygienic Requirements Imposed on Pressurized Compartments

1. The pressure in a compartment should not be less than 0.75-0.70 of the normal pressure at H=0, which corresponds to a "cabin altitude" of 2,400-2,800 m ("cabin altitude" - is the altitude at which atmospheric pressure corresponds to the pressure in a compartment).

2. The rate of change of pressure in a compartment $dp_к/dt$ should not be more than 0.18 mm Hg/s. At a greater rate pain arises in the ears, frontal sinuses, joints and in the lungs. A short-term increase in the rate of change in the pressure is possible up to 2.0 mm Hg/s in the event of an extreme descent of the aircraft.

Since

$$\frac{dp_к}{dt} = \frac{dp_к}{dH} \cdot \frac{dH}{dt} = \frac{dp_к}{dH} V_y,$$

this requirement imposes a restriction on the vertical rate of an aircraft V_y depending on the law of pressure change in the cabin with altitude.

3. The air temperature in a cabin should be within the limits of from 18 to 22°C.

4. The rate of air movement in a cabin should not exceed 0.5 m/s to avoid the sensation of a draft.

5. The air in a cabin should be fresh and clean, for which it is necessary to accomplish a 20-30-fold air exchange per hour.

6. The relative humidity in a cabin should be within the limits of from 25 to 60%.

2. Laws for Regulating Air Pressure in Pressurized Cabin

For accomplishing the first of the above enumerated requirements in a pressurized cabin an excess pressure, should be created the greater, the greater is the flight altitude. From the point of view of the second requirement the law is very important, in accordance with which the pressure in a cabin will change with an increase in the altitude of the aircraft or with a decrease in it.

Three laws for regulating air pressure in a cabin are possible (Fig. 9.27).

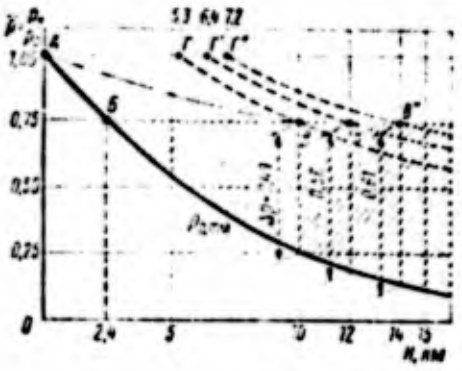

Figure 9.27. Laws for regulating air pressure in pressurized cabins.

1) The pressure in a cabin up to an altitude of 2,400-2,800 m varies just as the atmospheric pressure, and then it is held constant (law A-Б-B). This law limits the rate of climb to a magnitude of V_y=2-2.5 m/s in the A-Б section. Moreover, it is desirable here to have the greatest possible vertical rate to reduce the time of the engine noise effect in the region of the airfield. Thus, law A-Б-B is not employed on passenger aircraft.

2) The pressure in a cabin up to a certain height, which corresponds to the rated pressure differential, remains constant, and then decreases in such a way that the pressure differential remains constant between the cabin and the atmosphere (law A-Г-B). This law makes it possible to gain considerable altitude (points Г, Г' and Г") without limiting the vertical rate. A subsequent gain in altitude should be accomplished at a vertical rate of from

3.5 m/s at a height of 5,500 m to 5.9 m/s at a height of 10,000 m.

The rated pressure differential between the cabin and the atmosphere is defined as the difference between the atmospheric pressure at a calculated flight altitude (maximum operational altitude) and the pressure at an altitude of 2.4-2.8 km. Figure 9.27 gives the values of the calculated differential for altitudes of 10, 12 and 14 km.

Law A-Г-B is ensured by comparatively simple regulating devices and is finding broad application on passenger aircraft.

3) The pressure in a cabin with a gain in altitude continuously decreases up to the rated altitude (law A-B). This law makes it possible to gain altitude at a great vertical rate over the entire altitude range (for example when $H_{расч}$=10,000 m, V_y=9.5 m/s). Law A-B is promising. However, its realization requires more complex regulating devices.

3. Basic Types of Pressurized Cabins

Three basic types pressurized cabins are distinguished: ventilation, regeneration and oxygen-ventilation.

Let us examine the basic setups of these types of cabin.

Ventilation cabins. A continuous flow of air is created in the cabin. The air enters from the atmosphere into a supercharger: from the supercharger where its pressure is increased it goes into the cabin: from the cabin through a pressure regulator valve it goes back into the atmosphere.

Figure 9.28a depicts the simplified diagram of cabin ventilation. Engine compressors are employed as the supercharger 1 on contemporary

aircraft with GTD (gas-turbine engine). Since the air is heated in the engine compressors, in this case the airconditioning system is a complex system ensuring pressurization, ventilation and cabin heating. From the compressor the air is fed into the cabin along conduits, passing in this case through check valve 2, heat regulator distributor 3, absolute pressure limiters 4, heat exchanger 5, turborefrigerating unit 6, noise suppressor 7 and return valve 8. The heat regulator distributor 3 together with heat regulator sensor 9 is intended for the automatic maintenance of the air temperature within the assigned limits. In the case of an increase in temperature the distributor increases air supply through heat exchanger 5 and turborefrigerating unit 6, which is the second cooling stage; in the event of a temperature drop the air supply through these units is reduced and more hot air is supplied into the cabin. The air comes out of the cabin through automatic pressure regulator (APR) 10, which ensures the assigned law of pressure change with altitude. For the event of the operational failure of the APR safety valve 11 is installed, which usually carries out the following functions:

it secures the cabin against vacuum (negative pressure differential);

it secures the cabin against excessive surplus pressure;

it ensures the pressure balance as desired by the crew (manual pressure drop).

Regeneration cabins. The feed is carried out with compressed oxygen which enters into the cabin from cylinders; it is also possible to employ liquid oxygen. The respiratory products are removed by passing the air through a regenerative (reducing) device which absorbs the carbon dioxide and water vapor.

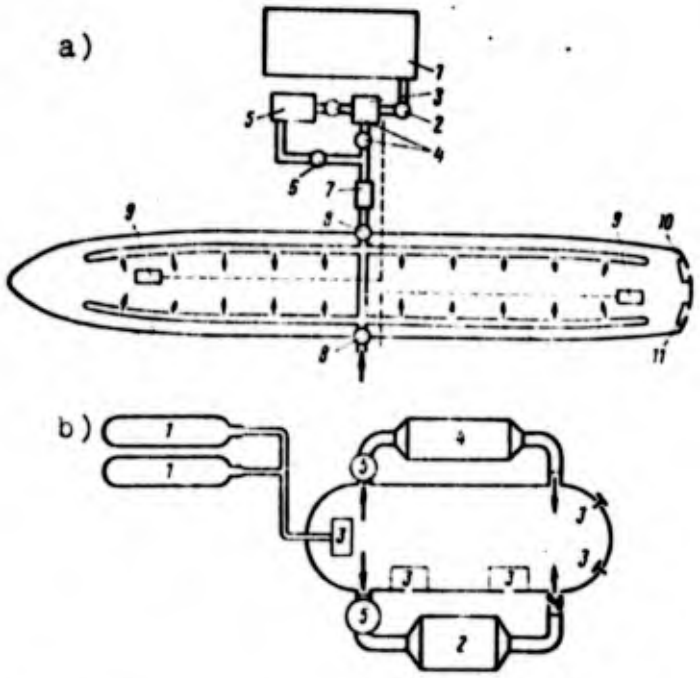

Figure 9.28. Simplified diagrams of cabin ventilation (a) and regeneration (b) types.

The necessary partial oxygen pressure in the alveoli is ensured by an increase in the air pressure in the cabin and by an increase in the volumetric oxygen content.

Regeneration cabins, in comparison with other types of pressurized cabins, have the following deficiencies:

1) they require the presence onboard the flight vehicle of a large oxygen reserve or a considerable limitation of the duration of flight of the flight vehicle;

2) they require special instruments for heating or cooling the cabin air;

3) they have great weight (cylinders, regenerative device);

4) they increase the danger of fire due to the presence of a large quantity of oxygen.

The basic advantage of a regeneration cabin is the possibility of their employment at high altitudes and in extraterrestrial space.

Figure 9.28b gives a diagram of a regeneration cabin. Its basic units are: cylinders with compressed oxygen 1, regenerative device 2, a system of pressure control valves and safety valves 3, heater or cooler of cabin air 4, ventilators 5. The regenerative setup has carbon dioxide absorber and a moisture absorber.

Oxygen-ventilation cabins. These types of cabins are mixed and have both a supercharger which uses atmospheric air and oxygen feed from the cylinders into the cabins. During continuous ventilation oxygen consumption is too great. In the case of separate employment of a cabin as a ventilation cabin at low altitudes and as a regeneration cabin at high altitudes these types of cabins are promising for application.

Pressurized ventilation cabins are employed on contemporary passenger aircraft.

4. Design Characteristics and Stress Analysis of Pressurized Cabins

On contemporary aircraft pressurized cabins are made as pressurized sections of the fuselage.

The design of the pressurized sections should ensure its strength under the effect of surplus pressure and also that there are no considerable air losses through the walls of the sections into the atmosphere.

To reduce the stresses from excess pressure pressurized sections should be made as combination cylindrical, spherical and conical sections with reinforced frames (formers) at the sites of coupling.

In the process of creating a pressurized section it is necessary to ensure the airtightness of riveted joints, the windows, the movable parts (doors, hatch covers, etc.) and the outlets of aircraft control lines and their units.

The airtightness of riveted joints is ensured with Thiokol sealing strips which are placed under riveted joints. The rivet heads are coated with Thiokol cement or with other sealing compounds.

Windows, doors and hatches are sealed employing rubber packing or rubber tubes. An example of the sealing of the windows of a passenger compartment is presented in Fig. 9.26.

The outlets of the control lines (rods and cables) are sealed employing special assemblies. For the outlet of rigid wiring assemblies are employed with translational motion of the rods or assemblies with rotary motion of the shafts. In both cases the packing of the mobile elements is carried out with packing glands which consist of felt and rubber rings. The outlets of cables are accomplished via rubber cores. The loading conditions of pressurized sections were examined in § 2 of the present chapter.

For strength testing of the cabin framework the loads from pressure differences are first of all determined. In strength testing for the first load variant (see § 2) these stresses are examined by themselves, in calculating for the second load variant - in the sum with the stresses from the loads acting on a fuselage in flight loading cases. In determining the stresses from the pressure difference the skin of a section is examined as a momentless shell. The design setup of a section is a thin-walled vessel with the walls flexible in flexure.

For a momentless shell, which is a body of revolution (Fig. 9.29), the normal stresses are calculated with the following formula

$$\frac{\sigma_1}{\rho_1}+\frac{\sigma_2}{\rho_2}=\frac{\Delta p}{\delta},$$

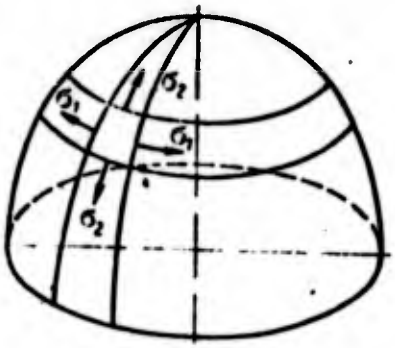

Figure 9.29. Towards determining the stresses due to excess pressure in a momentless shell.

where ρ_2 and ρ_1 - are the radii of the curvature in meridianal and in the circular cross sections; σ_2 and σ_1 - are the corresponding normal stresses; Δ_p - is the calculated excess pressure determined with respect to the stress standards; δ - is the thickness of the skin.

In the particular case for a spherical cabin section (for example, a spherical end plate) $\rho_1=\rho_2=\rho$ and $\sigma_1=\sigma_2=\sigma$; thus

$$\sigma = \frac{\Delta p \rho}{2\delta}.$$

For a design section, which is a circular cylinder, $\rho_2=\infty$; thus

$$\sigma_1 = \frac{\Delta p \rho_1}{\delta}.$$

The magnitude of σ_2 is found from the equilibrium condition of the cut off part of the cabin

$$\sigma_2 = \frac{\Delta p \pi \rho_1^2}{2\pi\rho_1\delta} = \frac{\Delta p \rho_1}{2\delta}.$$

If the design of the section ensures the inclusion in the operation for the normal stresses of the stringers, then

$$\sigma_2 = \frac{\Delta p \rho_1}{2\delta_{пр}},$$

where $\delta_{пр} = \frac{F_{пред}}{2\pi\rho_1}$ - is the given thickness of the skin.

It is necessary to keep in mind that reinforced frames (formers) or frameworks should be placed at the sites of the coupling of surfaces of different curvature, otherwise considerable additional flexural stresses arise in the skin

§ 7. ENSURING CREW AND PASSENGER SAFETY IN EMERGENCY SITUATIONS

The employment of pressurized cabins is connected with the possibility of decompression in the event of a sudden loss of cabin pressure as a result of some type of failure.

Sudden ("explosive") decompression can have the following consequences (depending on the flight altitude, at which it occurred):

1) damage to the internal organs of people as a result of a rapid change in pressure, including hemorrhages in the lungs, under the meninx and in the ears;

2) loss of consciousness and even death as a result of the onset of acute oxygen deficiency;

3) freezing of people as a result of a reduction in the air temperature in the cabin to the temperature of the ambient air at the particular altitude.

Moreover, in the event of sudden decompression the formation of fog in the cabin is possible as a result of the precipitation of moisture and the appearance of strong air flows, which, entraining individual unfastened objects along with them, can cause contusions and injuries to passengers.

From what has been stated it is clear, how important is the problem of ensuring crew and passenger safety during flights on contemporary aircraft with pressurized cabins.

To eliminate the possibility of decompression or to reduce its dangerous consequences, if it should nevertheless occur, the following measures are employed.

1. The high static and fatigue design strength of a pressurized cabin in its operation due to the forces of internal pressure and due to external aerodynamic forces is ensured. In this case special attention is given to such elements as the windows, doors, and hatches. The flight deck windows where the pilot is situated, furthermore, should withstand the impact of a bird weighing up to 2 kg.

2. The engines should be situated so that in the event of a failure of a turbine of a gas-turbine engine the fragments of the turbine do not damage the pressurized cabin.

3. The window, door and hatch areas should be selected so that in the event of the failure of these elements the rate of decompression can attain a magnitude dangerous to internal human organs.

4. If decompression should nevertheless occur, then to save the people an extreme descent of the aircraft should be employed to safe altitudes (3,000-4,500 m).

The fact is, that loss of consciousness as a result of the onset of acute oxygen deficiency does not occur instantly, but only after a specific time called the time of useful consciousness. The time of useful consciousness depends on the flight altitude, at which the decompression occurs. The greater is the height, the shorter is the time of useful consciousness. Thus, at an altitude of 10 km the time of useful consciousness approximately 50 s.

It was noted above that it is possible to allow a rate of pressure change in a cabin of up to 2 mm Hg/s over a short time period. This makes it possible to ensure an extreme descent from

an altitude of 11 km to an altitude of 4.5 km over a period of 2.5-3 min. At this rate of descent the time of useful consciousness is not exceeded at one of the altitudes.

In order that an extreme descent begin immediately after the beginning of decompression, light and sound signaling systems with respect to a pressure drop in a cabin is provided for on aircraft which automatically operates at the beginning of a pressure drop. Moreover, oxygen equipment is provided for the crew members. One of the pilots should always have an oxygen mask on with the oxygen supply switched on.

Crew and passenger safety in the cases of an emergency forced landings is ensured by the following means.

1. Emergency exits are provided for the rapid abandonment of a aircraft after a forced belly (with landing gear retracted) landing on both sides of the fuselage. The number of emergency exits (including the main doors) is determined from a calculation of the abandonment of an aircraft by its passengers within a period of 30 s (under favorable facts one passenger can exit from an aircraft in approximately 1 s). Not less than two emergency exits are made on top for abandoning an aircraft in the event of a forced landing on water (ditching).

2. For exiting from an aircraft during an emergency landing with extended gear on an aircraft with the doors situated high above the ground onboard emergency ramps are provided. An onboard emergency ramp is a tarpaulin chute or an inflatable rubber ramp, which at one end is fastened to the door and, at the other - to the ground.

3. On aircraft which fly over oceans, measures for saving the passengers and crew after an emergency landing on the water are provided for. First, the aircraft should possess buoyancy sufficient

for supporting the aircraft until the people have exited from the cabin (up to several tens of minutes). Secondly, the passengers and the crew are supplied with individual inflatable life jackets or group rescue devices are provided for in the form of inflatable life rafts.

CHAPTER 10

LANDING GEAR

§ 1. PURPOSE AND BASIC TECHNICAL SPECIFICATIONS

The landing gear is a system of struts employed for supporting a flight vehicle on the ground and for carrying out takeoff and landing. The landing gear weight constitutes a considerable part of the weight of the aircraft. Thus, for contemporary passenger aircraft

$$G_{ш} = (0.035 \div 0.06) G_0 = (0.17 \div 0.22) G_{кн},$$

where G_0 and $G_{кн}$ - are the takeoff weight and the design weight of an aircraft.

The following basic technical specifications are imposed on landing gear:

1. The design and the positioning of the landing gear on a flight vehicle should ensure the stability and controllability of the aircraft during motion along ground and when parked and the possibility of retraction during flight. The employment of non-retractable landing gear is possible for low-speed aircraft.

The design and the lay-out setup of the landing gear should ensure the necessary ground surface performance - the

possibility of moving along the surface of an airfield corresponding to the conditions under which the flight vehicle is employed.

2. In designing a landing gear shock absorption should be included for softening the landing shocks and during movement over uneven or rough areas of an airfield.

3. The design of a landing gear should correspond to the stress standards specifications with the least possible weight and have an assigned service life.

The problems of landing-gear designing and rating have been worked out by domestic (Soviet) designers and scientists. The first investigations with respect to shock absorption operation were carried out by V. P. Vetchinkin.

§ 2. THE BASIC ARRANGEMENT SETUPS OF LANDING GEAR ON AN AIRCRAFT

The positional arrangement of a landing gear characterized by the number of struts (supports) and by their location relative to the center of gravity of the aircraft to a considerable degree predetermines the takeoff and landing properties of the aircraft. Thus, the selection of all the parameters characterizing the arrangement of the landing gear should be based on considerations of the operating conditions of the aircraft.

Let us examine the basic parameters of the landing gear and the principles of their selection for those landing-gear setups most commonly employed at the present time, and then let us dwell on a comparison of these setups.

1. Landing-Gear with a Nose Strut (Nose Support)

The nose-wheel landing gear includes two main struts: the front (nose) and the safety tail support.

Figure 10.1 shows the basic parameters characterizing the nose-wheel landing gear setup. The fuselage center line, which is taken as the basis for aircraft levelling, is arbitrarily taken as the aircraft axis.

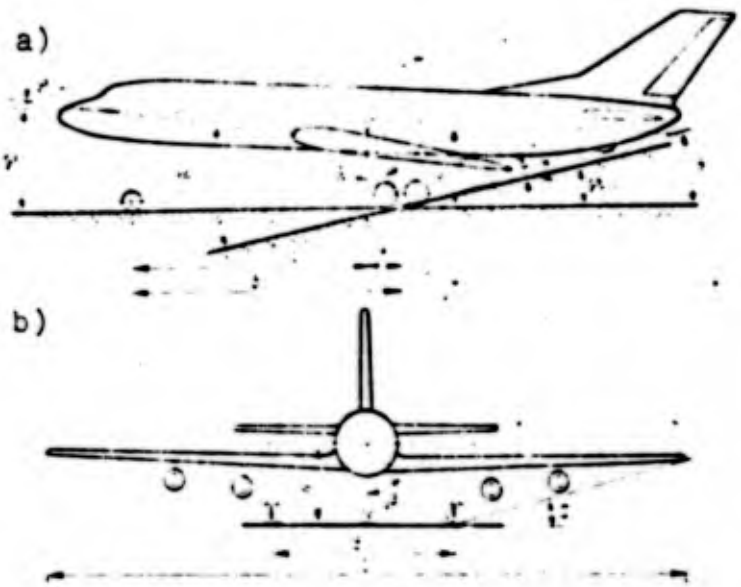

Figure 10.1. Parameters of a landing gear with a nose-wheel (nose strut): a) side view; b) front view.
[ц.т. = c.g. (center of gravity)].

The take-off run of an aircraft starts first in the three-point position, and then with the front strut elevated slightly.

During a normal landing an aircraft will approach the ground at an angle of attack $\alpha_{\text{пос}}$ with the tail dropped, touch the ground with the wheels of the main struts and during the landing run tilt over onto the front strut.

From an examination of the takeoff run and the landing the following conditions ensue, which relate to the angular parameters of the landing gear setup.

1. In order that the aircraft drop down onto the front landing gear strut under the effect of gravitational force even

from the position with the tail strut dropped to the ground, it is necessary that the angle of forward projection λ be greater than the tilting angle θ, i.e.,

$$\lambda > \theta.$$

2. In order that at the first moment of a landing an aircraft can have a wing angle of attack $\alpha=\alpha_{\text{пос}}$, with the tail strut not touching the ground, it is necessary that

$$\varphi_{\text{уст}} + \varphi + \theta \geqslant \alpha_{\text{пос}}.$$

3. It is necessary that the wing angle of attack with the aircraft in the three-point position not exceed the smallest value of the angle during the take-off run:

$$\varphi_{\text{уст}} + \varphi \leqslant \alpha_{\text{[illegible]}}.$$

Under this condition the pilot can control the takeoff run angle, by lifting the aircraft nose.

In the case of the layout of an aircraft for a wing with a normal aspect ratio it is taken that

$$\alpha_{\text{пос}} = \alpha_{\text{крит}} - \Delta\alpha,$$

where $\alpha_{\text{крит}}$ - is the critical angle of attack of a wing with the high-lift devices deflected in the landing position: $\Delta\alpha=2-3°$.

Since in a low aspect-ratio wing value $\alpha_{\text{крит}}$ is great, value $\alpha_{\text{пос}}$ can be limited designwise to permissible values of the height of the front support and angle ϕ.

As was noted in Chapter 2, an attempt is made to take the angle of incidence [angle of wing setting] $\theta_{\text{уст}}$ equal to the angle of attack in the basic flight regime of an aircraft. With respect

to statistics ϕ=0-6°. Large values of ϕ lead to an increase in the height of the front strut and the impingement of engine exhaust streams on the airfield surface.

For obtaining a minimum sum of drag and wheel friction the angle of attack during the takeoff run $\alpha_{разб}$ should satisfy the condition

$$\frac{dc_y}{dc_x} = \frac{1}{\mu_т},$$

where $\mu_т$ - is the coefficient of wheel friction.

In aircraft layout the following sequence of determining angular parameters is usually followed:

a) by knowing $\phi_{уст}$ - $\alpha_{пос}$ and $\alpha_{разб}$ are selected;

b) by means of the above examined dependences ϕ, θ and λ are established taking landing gear layout into account.

The dimension of y characterizes the smallest distances from the surface of an aircraft component (or from a propeller) to the ground. Distance y should not be less than 200 mm at an average height of the uneven areas of the airfield taken to be equal to 120 mm.

The conditions limiting the parameters of landing gear positioning should be checked in the cases of all adverse combinations of the shock absorption stroke.

The value of the landing gear base (dimension b in Fig. 10.1a) is estimated by the ratio b/L_ϕ, where L_ϕ - is the length of the fuselage. Usually b/L_ϕ=0.25-0.4.

If the base is small, the aircraft during its movement over uneven areas has considerable longitudinal rocking. A large base value is difficult to carry out designwise, since this requires elongation of the nose part of the fuselage and displacement of the main landing gear struts backwards.

The displacement of the main struts backwards is e=h tg λ.

Ratio e/b determines the part of the weight which is situated on the front strut when the aircraft is parked. Usually for passenger aircraft

$$\frac{e}{b} = 0{,}05 - 0{,}1.$$

At large values of e/b it is difficult to separate the front strut from the ground and to control the variation in the angle of attack during the takeoff run. In the case of small e/b due to the decrease in the load on the front wheel strut the control of the aircraft movement by the turning of these wheels becomes not too effective; moreover, in the case of small e λ decreases and the danger of the tilting of the aircraft on the tail support arises.

Let us go on to an examination of the parameters characterizing the positioning of the landing gear in the front view of the aircraft in (Fig. 10.1b).

On contemporary aircraft the size of the landing gear track B mainly depends on the attachment site and the method of landing gear retraction.

The magnitude of B affects the transverse stability of the aircraft during its movement over the ground. A decrease in the track in the case of other constant dimensions increases the tendency of the aircraft to tilt onto a wing during lateral sideslip or during a steep turn and leads to the transverse

rocking of the aircraft during movement over uneven areas and during unsymmetric shock absorption stroke. On the other hand, an excessively large track is also undesirable, since in the case of unsymmetric front shocks considerable turning moments arise.

Angle β also characterizes the tendency of an aircraft to tilt on its wing and determines the maximum slope of the airfield on which the landing of an aircraft is possible without tilting. It should not be less than 15°.

Angle ε - is the maximum roll angle at which the wing of an aircraft or the engine nacelles clear the surface of an airfield. Usually it is required that angle ε be not less than 10°.

The greater is the height of the center of gravity of an aircraft h (with the retention of the other dimensions), the greater is the effect on the aircraft of the inertia forces.

During acceleration and during deceleration with acceleration j a longitudinal moment of inertial force equal to G h/g varies the loads which are situated on the front and the main struts. During sideslip or turning the transverse moment tends to incline the aircraft sideways.

During aircraft motion with drift (Fig. 10.2) the danger of its tilting relative to the ADC line arises.

The safety margin against tipping over sideways can be indirectly estimated by the magnitude of angle β and more strictly - by the magnitude of angle β': a decrease in these angles increases the danger of tipping over.

2. Tail Wheel Landing Gear (Tail Strut)

The two main landing gear of this type of setup on which the main part of the weight of the aircraft is located when parked are

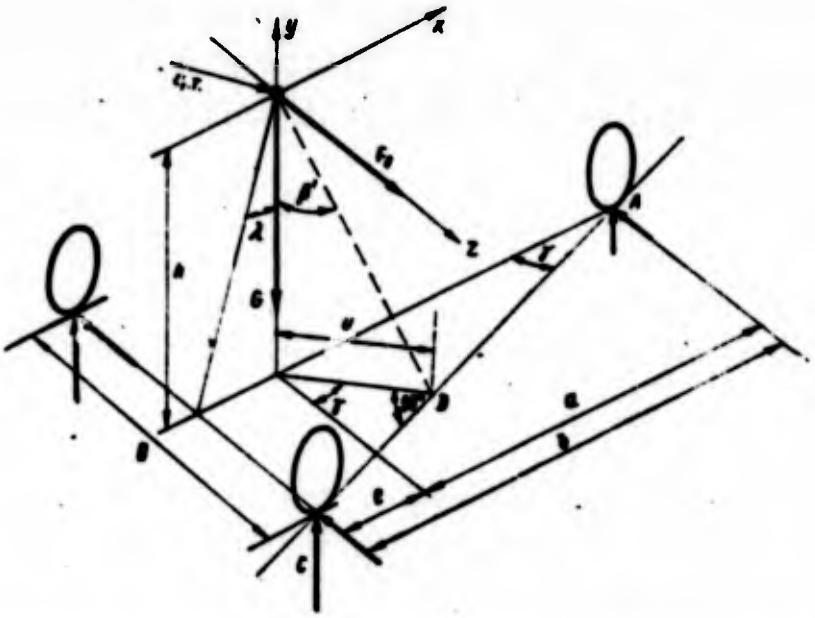

Figure 10.2. Concerning the question of the nosing over of an aircraft which has a nose-wheel landing gear (a nose strut).
[ц.т. = c.g. (center of gravity)].

situated ahead of the center of gravity of the aircraft and are attached to the wing or to the fuselage. The third strut is installed in the tail section of the fuselage.

The basic parameters which characterize the positioning on an aircraft of landing gear with a tail strut are shown in Fig. 10.3.

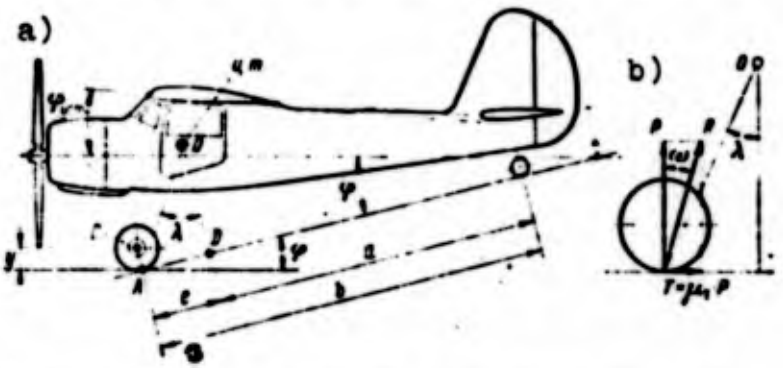

Figure 10.3. Landing gear with a rear wheel (tail strut): a) positioning setup; b) loading of the main struts which does not lead to tipping over.
[ц.т. = c.g. (center of gravity)].

During a normal landing an aircraft with a landing gear of this type of setup should touch the ground with the wheels of all the struts simultaneously (a three point landing). For this it is necessary that

$$\varphi_{уст} + \varphi = \alpha_{пос}.$$

The parking angle of the aircraft axis ϕ is determined from this condition.

The angle of overhang λ characterizes the safety against the tilting of an aircraft on its nose - "nosing-over" during motion in the three-point position.

In order that nosing-over does not occur during landing, the reaction of the main landing gear struts should pass ahead of the center of gravity of the aircraft (Fig. 10.3b). For this it is necessary to fulfill the following conditions:

$$\lambda > \omega, \quad \operatorname{tg}\lambda > \operatorname{tg}\omega = \frac{T}{P} = \mu_T.$$

In contemporary aircraft λ=27-31°. An excessive increase in the angle of overhang is undesirable, since it leads to an increase in the dimension of e, and at large values of e an aircraft has the tendency towards turning during lateral shocks on the main wheels. Moreover, with an increase in e the load on the tail wheel increases, which negatively affects the takeoff conditions - hampers the liftoff of the tail, as a consequence of which the length and the time of the takeoff run are increased. With regard to the remaining parameters which characterize the arrangement of landing gear of this type of setup on aircraft (B, ε, β), the same considerations are valid which were given in the examination of landing gear with a nose strut.

3. Bicycle Landing Gear

An aircraft with bicycle landing gear has two main struts situated one behind the other in the plane of symmetry of the aircraft on different sides of its center of gravity, and two auxiliary subwing struts.

Usually the positioning of the front and rear strut along the axis of an aircraft relative to its center of gravity obeys the same rules as landing gear with a nose strut e/b=0.05-0.10.

There are designs where the bicycle landing gear is situated with the main strut located at a distance from the center of gravity of the aircraft c/b~0.5.

Subwing struts situated at the tips of a swept wing can during a landing touch the ground first. This requires the presence on them of soft shock absorption with a large stroke.

4. A Comparison of the Positioning Setups of Landing Gear on Aircraft

For a long time aviation most frequently employed landing gear with a skid setup, or with a tail wheel. This type of landing gear setup was convenient for single-engine propeller aircraft.

Landing gear with a tail strut are also employed at the present time on some low-speed aircraft.

The basic deficiency of the landing gear setup with a tail strut is the complication of the landing: for a correct three point landing high accuracy of aircraft handling is required (touchdown only on the main struts can lead to the ballooning of the aircraft - "bouncing"); it is necessary to limit the braking

intensity due to the danger of aircraft nose-over; the considerable inclination of the fuselage center line during the landing run and taxiing negatively effects the field of vision from the flight deck.

Moreover, an aircraft with a tail strut has directional instability during its motion along the ground (Fig. 10.4a). During motion with drift the forces of the wheel friction of the main landing gear struts form a turning moment which tends to increase the drift angle and to turn the aircraft crosswise to its direction of motion. The tendency toward turning decreases with the locking of the orienting tail strut, since the moment of lateral frictional force of the tail wheel arising in this case impedes turning.

An increase in the takeoff and landing velocities and the introduction of jet engines led to greater application of landing gear with a nose strut. Its application makes it possible to reduce the length of the landing run as a result of the possibility of intense wheel braking without the danger of nosing-over and ensures the directional stability of motion. With an orienting nose wheel in the case of a landing with drift the forces of wheel friction of the main struts created restorative moment which decreases the drift angle (Fig. 10.4b).

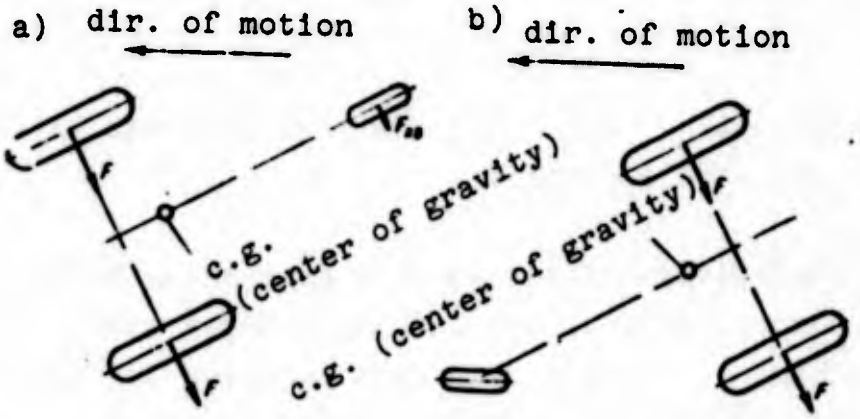

Figure 10.4. Motion along the ground with aircraft drift: a) landing gear with tail strut; b) landing gear with nose strut.

A setup with a nose strut is convenient due to the fact that in the three-point position of the aircraft the gas exhaust jets are ejected almost parallel to the airfield surface.

Included among the deficiencies in this type of landing gear setup are:

1) the great loads acting on the nose strut during the descent of the aircraft onto its nose after touchdown, during braking and during an increase in engine thrust, during motion along uneven or miry ground. Because of this, and also due to the greater design height the nose strut is heavier than the tail strut;

2) poor ground performance on soft dirt due to the miring of the wheels of the nose strut in it. Breakage of the nose strut results in a severe aircraft crash;

3) the possibility of the emergence at high velocity of aircraft motion along the ground of self-excited vibrations in the wheels of the nose strut relative to the axis of orientation (the axis of rotation of the strut). Hydraulic vibration dampers are built in to stop these oscillations.

The practice of operating aircraft which have landing gear with a nose strut, has shown that the deficiencies characteristic to this landing gear setup in comparison with its advantages are not considerable. This landing gear setup is employed in the majority of contemporary aircraft.

A bicycle landing gear can be employed on high-speed aircraft with thin wings which does not provide for the retraction of the main struts into it. Aircraft with bicycle landing gear are equipped with subwing struts for attaining transverse stability of motion along the ground.

The deficiencies in the bicycle landing gear they are:

1) a decrease in the useful volume of the fuselage due to the retraction of the main struts into the fuselage;

2) a reduction in the service life of the design of the pressurized part of the fuselage to which considerable alternating loads are directly transmitted from the struts fixed to it.

For aircraft having bicycle landing gear with the main strut situated at a distance from the center of gravity, the following deficiencies are added:

1) complication of the design (control of the change in the height of one of the main supports, or control of the angle of incidence [angle of wing setting]) and a corresponding increase in weight;

2) complication of the piloting technique during landing connected with the requirement for the simultaneous touchdown of the wheels of front and rear struts. The indicated deficiencies of the bicycle landing gear prevent its broad application.

For improving the ground performance of heavy aircraft multiple-strut landing gear (having more than two main struts) can be employed.

§ 3. REQUIREMENTS IMPOSED ON LANDING GEAR STRENGTH AND THE BASIC LOADING CASES OF AN AIRCRAFT ON THE GROUND

To ensure the strength, the rigidity and the service life of both landing gear units and other aircraft components the stress standards examine a number of loading cases in which the basic variants of loads acting on an aircraft on the ground are reflected.

Before going on to an examination of the basic loading cases, let us note the following general aspects.

1. In all loading cases, except $M_ш$, the geometric relationships of an aircraft are examined during shock absorption compressed [the stroke] by a magnitude which corresponds to the operational g-force of the case in question. In case $M_ш$ the parking compression [the stroke] of shock absorption is employed.

2. With paired wheels nonuniform wheel loading is examined in all cases.

3. For landing gear struts having a four-wheeled carriage, the vertical loads on a strut are distributed between the front and rear pairs of wheels inversely proportional to the distance from them to the axis of the rotation of the carriage.

4. In all loading cases of an aircraft of civil aviation on the ground the safety factor for a landing gear is f=1.5, for all other aircraft components it is f=1.65.

5. Landing-gear loads are assigned as surface forces acting on the wheels from the ground.

The rated destructive value of a vertical load on a strut is determined with the formula

$$P^{р} = n^{р}\Delta G = fn^{э}\Delta G.$$

where $n^{р}$, $n^{э}$ - are the rated and operational g-forces[1] in the loading case in question; ΔG - is the part of the landing or takeoff weight located on a strut.

---

[1] $n^{р}$ and $n^{э}$ - are called arbitrarily "g-force," since of the surface forces they connect only the reaction of the ground with the weight, without taking into account the lift ΔY located on a strut. If $\Delta Y^{э}=\Delta G$, then the actual g-force shown by an accelerometer, will be

$$n_{э} = \frac{P^{э} - \Delta Y^{э}}{\Delta G} = \frac{n^{э}\Delta G - \Delta G}{\Delta G} = n^{э} - 1.$$

Longitudinal force T and lateral force F are usually expressed via P.

The basic loading cases in connection with the main landing gear struts are examined below. For employing these cases for front and tail struts additional instructions are given in the stress standards.

Case $E_ш$ - is a three point landing and the takeoff run. Lift is assumed to be equal to the weight of the aircraft.

A <u>three point landing</u> (with the landing weight). Here only the vertical reactions of the ground are examined (Fig. 10.5a).

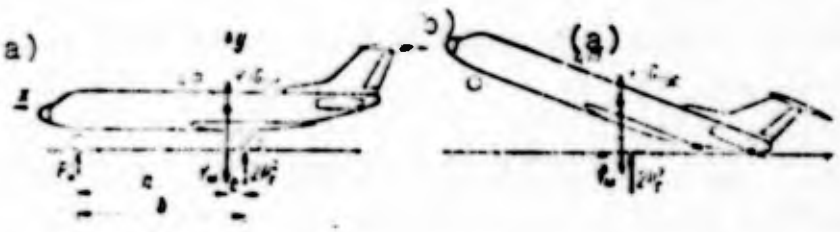

Figure 10.5. Landing cases: a) case $E_ш$ is a three point landing; b) case $E'_ш$ is a landing on the main struts.
Key: (a) c.g. (center of gravity).

<u>For the main strut</u> ΔG is taken as the parking load, and g-force $n^э$ - from the calculation of the shock absorption for this case.

<u>The takeoff run</u>. An aircraft with its takeoff weight is examined in its parked position. Forces P and T from the uneven areas of the airfield simultaneously act on each strut. The loads and the g-forces during motion over uneven areas depend on the state of the ground and the dimensions of the tires. They are the lesser, the harder is the soil and the greater is the possible value of the complete compression of the tires.

Case $E'_ш$ - landing on main struts. This case is examined for landing gear with a front strut. Here it is assumed, that the tail safety strut does not touch the ground, but is located in immediate proximity to it (Fig. 10.5b). The loads are vertical.

Cases $E_ш$ and $E'_ш$ reflect the most frequently encountered takeoff run and landing conditions.

Case $G_ш$ - front shock in the wheels of both main struts. The position of the aircraft corresponds to that of being parked on the ground.

Force P_G applied to the center of the wheel from the front and from below at an angle of α acts on each landing gear strut (Fig. 10.6a).

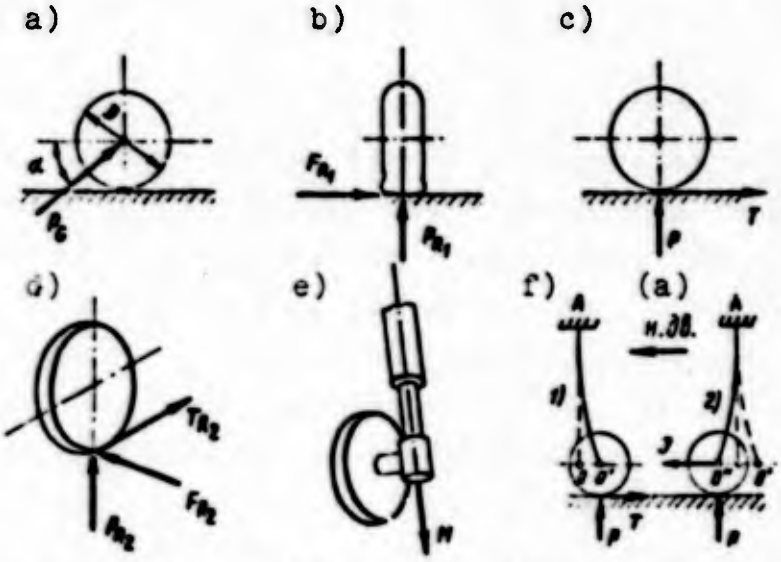

Figure 10.6. Landing-gear loads: a) case $G_ш$; b) case $R_{1ш}$, c) case $T_ш$; d) case $R_{2ш}$; e) case $M_ш$; f) landing-gear loads during acceleration of the wheels.
Key: (a) Direction of motion.

Case $R_{1ш}$ - landing with lateral shock in the wheels of the main struts (Fig. 10.6b). The aircraft is examined in the position which corresponds case $E'_ш$. Vertical and lateral loads act on each strut.

Case $T_ш$ - landing with braking. The aircraft is situated in the three-point parking position. The strut is loaded with the vertical reaction of the ground P and with friction force T (Fig. 10.6c).

Case $R_{2ш}$ - turning during taxiing. A sharp turn is examined during which one main landing gear strut is loaded with lateral force, friction force and vertical reaction (Fig. 10.6d); the second main strut and the front or tail strut are considered as not touching the ground.

Case $M_ш$ - torsioning of the landing gear. This case is introduced to ensure the torsional strength of a landing gear, if the wheels get into a rut or in soft ground. The aircraft is situated in the three-point position. The main landing gear strut is loaded with torsional moment M and vertical reaction P (Fig. 10.6e).

Case $E'_ш+G'_ш$ - landing with unaccelerated wheels. The landing gear is loaded with vertical reaction and the horizontal forces which arise in the process of accelerating the wheels (Fig. 10.6f): 1) the great friction force T acting in the beginning of the acceleration of a wheel, causes loading of the strut in the direction opposite to its motion and also its elastic deformation O-O'; 2) when the circular velocity of the wheel becomes equal to the velocity of the aircraft motion relative to the earth the friction force T sharply drops off and the strut begins to experience vibrations in which in position AO" inertial force J loads it in the direction of motion of the aircraft.

§ 4. THE PURPOSE OF SHOCK ABSORPTION AND THE TECHNICAL REQUIREMENTS IMPOSED ON IT

1. The Purpose and the Conditions of Shock Absorption Operation

Shock absorption is designed to reduce landing-gear loads and to receive and dissipate the energy from the shocks arising during the landing of an aircraft and during its motion over uneven areas of an airfield.

On contemporary aircraft and helicopters shock absorption usually consists of pneumatic aviation tires and shock absorbers.

The pneumatic tires receive energy in an shock direction, but its capacity to receive energy is limited. Moreover, the energy is received in reversible form and thus is almost completely returned to the aircraft.

If shock absorption consisted only of pneumatic tires, then an aircraft after the landing impact would vibrate for a long time or would jump. In order that the vibrations are rapidly damped, the shock absorption system should dissipate part of the energy received by it.

A shock strut serves to receive the main portion of impact energy and also to transfer part of it into irreversible form and to dissipate it. The shock absorber receives the energy during the effect of the force along its axis.

In investigating the operation of a shock absorption system the complex motion of the aircraft on the three struts during a landing is approximately examined as the veritcal motion of three separate reduced masses. By reduced mass $m_{ред}$ is understood the mass of the aircraft which is situated on the strut in question; $m_{ред}$ is assigned by the stress standards.

In the moment when an aircraft touches the ground during a landing the reduced masses possess a vertical velocity and, consequently, the kinetic energy of vertical motion.

Upon the compression (direct stroke) of the shock absorption system the vertical velocity is gradually decreased; this should occur with a small magnitude of negative acceleration a, otherwise the inertial force $m_{ред}a$ and the g-force will be great.

The kinetic energy is converted into shock absorption energy. In this case, in order that shock absorption system is able to straighten itself out and receive the next shock, part of the energy should be received in potential form.

2. Technical Requirements Imposed on a Shock Absorption System

Let us examine the requirements imposed on a shock absorption system based on the stress standards and on design and operational experience.

1. The shock absorption system of each of the main landing gear struts should be capable of receiving the standardized operational energy during a landing

$$A^{э} = 0{,}5 m_{пред} V_y^2 .$$

where V_y - is the reduced vertical velocity; $V_y = f(G, V_{пос}) \geq 2.8$ m/s; $m_{ред}$ - is the reduced mass located on a strut.

For each of the main landing gear struts

$$m_{пред} = 0{,}5 \frac{G_{пос}}{g} .$$

For the nose strut the reduced mass is determined from the greatest dynamic load on this strut $P_{оп.дин}$ during takeoff run and during a landing (see § 13 below)

$$m_{пред} = \frac{P_{оп.дин}}{g} .$$

When a shock absorption system receives energy $A^э$ the operational g-force $n^э$ should not be greater than the load-bearing factor of the wheel $n_{г.р}$.

For the main struts

$$n_{гр} = \frac{P_{м.д}}{P_{к.ст.пос}},$$

where $P_{к.ст.пос}$ - is the parking load acting on a wheel with the landing weight; $P_{м.д}$ - is the maximum permissible load on a wheel, which is a characteristic of its strength.

For the nose struts

$$n_{гр} = \frac{P_{м.д}}{P_{к.дин}},$$

where $P_{к.дин}$ - is the dynamic load on a wheel of a nose strut.[2]

The safety factor f in the receiving by a shock absorption system of operational energy $A^э$ for a landing gear is equal to 1.5, for all remaining aircraft components - 1.65.

2. The shock absorption system of each of the main struts should be capable during a rough landing of receiving in the case of complete compression of the system a maximum energy of

$$A^{max} = \frac{G_0}{G_{пос}} A^э \leqslant 1{,}5A^э,$$

---

[2]For the maximum employment of the energy receiving capacity of pneumatic tires it is necessary that $n^э = n_{гр}$. However, these types of g-forces are great and for heavy passenger aircraft can exceed $n^э$ in flight cases. Thus, it is usually assumed that $n^э < n_{гр}$.

For landing gear of passenger aircraft $n^э = 2\text{-}2.5$; lesser values of $n^э$ are taken for heavy aircraft.

where G_0 - is the takeoff weight of the aircraft.

Upon receiving A^{max} there should not be any structurals failure of landing gear and other parts. For this it is necessary that

$$n^{max} f_{n^{max}} \leqslant n^{p}, \; n^{max} \leqslant \frac{n^{p}}{f_{n^{max}}},$$

where $f_{n^{max}}$ - is the safety factor with respect to g-force n^{max}. It is necessary that $f_{n^{max}} \geqslant 1.3$.

3. A shock absorption system should possess hysteresis, i.e., a considerable part of the impact energy should be received by the shock absorption system in irreversible form, mainly on the reverse stroke of the shock absorber. In this case, however, the total time of the forward and reverse strokes should not exceed 0.8 s so that the shock absorption system has time to straighten itself out for the next shock.

4. The rigidity of a shock absorption system should be such that the inherent oscillational frequency of an aircraft on an elastic landing gear is far away from the shock frequencies during the motion of the aircraft over uneven areas.

5. The rating of a shock absorption system should be carried out both by taking into account and disregarding the drag forces due to the acceleration of the wheels.

6. The capacity of a shock absorption system to absorb $A^{э}$ and A^{max} should be checked by testing for failure on an impact tester.

A shock absorption system is rated and tested for case $E_{ш}$ - "three-point landing"; however, it is also necessary to ensure the possibility of its operation under other loading conditions (front and lateral shocks, etc.).

7. The properties of a shock absorption system should depend as little as possible on the external conditions (temperature, atmospheric conditions, duration of operation, shock absorber loading with flexure).

§ 5. AVIATION WHEELS

The designs of the aviation wheels of domestic (Soviet) aircraft conform to standards which in the course of time undergo review. All the data are contained in the aviation wheel catalogs.

The weight of aviation wheels is 35-55% of the landing gear weight.

An aviation wheel consists of an aircraft tire - a pneumatic tire, a [wheel] drum and brakes. The wheels mounted in the nose, tail, subwing and rear safety struts usually do not have brakes. The strength of wheels, their reliability and service life should be checked by plant tests reproducing the operational loading conditions.

1. Pneumatic Tires and Their Characteristics

A pneumatic tire (Fig. 10.7a) consists of an outer casing 1 and an inner tube 2. Tubeless pneumatic tires are also finding application. For increasing the strength, rigidity and wear resistance, the outer casing 3 is made multilayer. An external layer (the tread) 4 is made from vulcanized rubber; over the external surface it has a tread pattern (recesses) for creating resistance to lateral slipping. The internal part of the casing (the cords) 5 consists of many layers of weftless rubberized filaments. The cords are made from cotton or high-strength synthetic filaments.

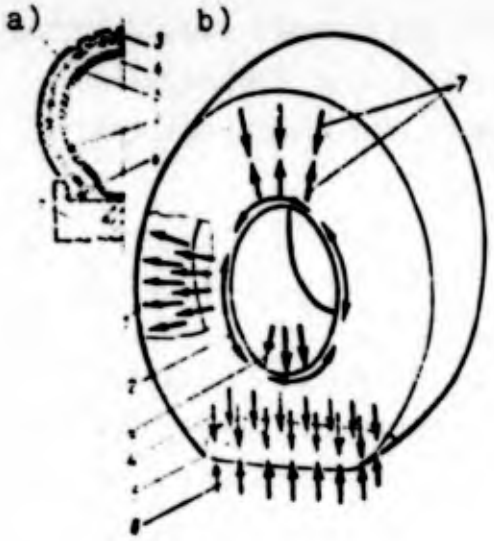

Figure 10.7. Pneumatic tire: a) cross section of a pneumatic tire; b) diagram of the loading of the casing elements: 1, 4 - excess internal pressure; 2 - tension in the core; 3 - reaction of the [wheel] drum; 5 - contact area; 6 - reaction of the ground; 7 - tension of the casing walls.

For increasing its strength the casing has a core 6 - a ring made from metal wires or cable. The normal load from the ground on a pneumatic tire is balanced mainly by the effect of the excess air pressure from within the pneumatic tire on the contact area which is formed as a result of the flattening of the pneumatic tire. The casing elements, nearest to the ground, are bent and compressed, its remaining sections operate mainly in tension. The overall dimensions of wheels are characterized by the ratio B/D (Fig. 10.8a).

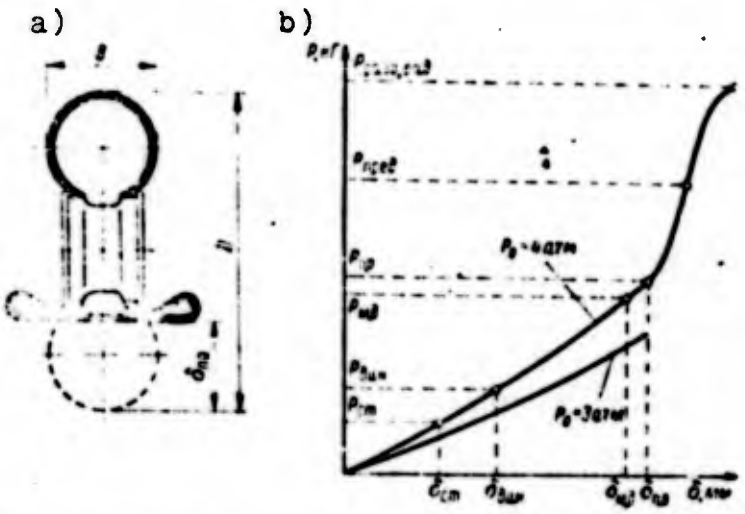

Figure 10.8. Aviation wheels: a) overall dimensions of wheels; b) diagram of pneumatic tire compression.

Aviation wheels in accordance with the type of pneumatic tires being employed are divided into semi-balloon, arched, high and ultrahigh pressure tires.

Table 10.1 gives tentative maximum values of the internal pressure p_{0max} and of the takeoff velocity $V_{отр}$, and also shows the properties and the conditions of application of the different types of wheels.

Table 10.1

Type of wheels	Maximum P_{0max}, atm	Maximum $V_{отр}$, km/h	Properties and conditions of application
Semi-balloon	5	200	Increased B/D, good ground performance
Arched	7	300	Casing with increased rigidity. Employed on hard dirt runways.
High pressure	15	400	For runways with artificial surface
Ultrahigh pressure	17 and higher	450	For airfields with great surface thickness. For highly loaded landing gear of high-speed aircraft. Casings with a large number of layers of cord of increased strength.

An increase in the takeoff and landing velocities and an increase in the loads on a wheel made it necessary to increase p_{0max} and to increase the number of layers and the strength of the cord in pneumatic tires.

The energy spent on compressing a wheel is converted into the potential energy of air compression (main part) and the elastic deformation of the casing (lesser part).

Arched pneumatic tires possess somewhat greater flexural rigidity, since the cross section of the casing has the shape of an arch.

When selecting wheels which are to be employed on dirt airfields, it is necessary to consider the requirement for aircraft ground performance - the capacity to move from a site under the thrust of its own engines and to move along the airfield without forming deep ruts. To ensure good ground performance the pressure in the pneumatic tires should not exceed 3-3.5 atm for soft and wet soil, 5-6 atm for dry soil.

The strength of rubber diminishes with the passage of time and under the effect of high and low temperatures.

Centrifugal forces during turning cause radial tensioning of pneumatic tires; it becomes more rigid under compression.

The forces of internal pressure and centrifugal forces with the passage of time increase the external dimensions of pneumatic tires (the pneumatic tires "expand"), which can interfere with the retraction and the lowering of the landing gear.

2. Characteristics of the Strength and Energy Bearing Capacity of Wheels

Figure 10.8b shows a diagram of the radial static compression of a wheel - curve $P=f(\delta)$, where P - is the radial load on a wheel, and δ - is the compression of a tire.

In the aviation wheel catalog diagrams at different pressures p_0 of filling of pneumatic tires are given for each wheel.

Let us examine the characteristic points of these diagrams:

$P_{разр.рад}$ - (destructive radial load) - corresponds to the structural failure of a wheel;

$P_{пред}=0.75\ P_{разр.рад}$ - is the maximum load - the load, which still does not represent the danger of wheel failure and which is permissible in receiving energy A^{max}; by the shock absorption system; $P_{разр.рад}$ and $P_{пред}$ practically do not depend on the initial pressure p_0 in a pneumatic tire.

The remaining load bearing characteristics of P are determined by the magnitude of the compression δ corresponding to them and by the magnitude of the pressure of filling p_0:

$\delta_{п.о}$ and $P_{п.о}$ - are the deformation and the load during complete pneumatic tire compression (flattening to the rim); $\delta_{м.д}=(0.95\text{-}1)\delta_{п.о}$ and $P_{м.д}$ - the maximum permissible compression and the maximum permissible load; $\delta_{дин}=0.5\delta_{п.о}$ and $P_{дин}$ - are the dynamic compression and the radial dynamic load, permissible of a pneumatic tire of a front strut under the effect on the aircraft of the landing weight and the braking forces; $\delta_{ст.взл}$ $\delta_{ст.пос}$ and $P_{ст.взл}$ and $P_{ст.пос}$ - are the permissible values of parking compression and parking load under takeoff and landing weights.

A large part of the service life of pneumatic tires takes place under conditions of parking compression. To ensure the life of a pneumatic tire it is assumed that $\delta_{ст}$ is considerably less than $\delta_{п.о}$. Usually $\delta_{ст.пос}=(02\text{-}04)\delta_{п.о}$.

Wheel loads P which correspond to specific compression δ are proportional to the initial pressure p_0 in a pneumatic tire.

The loads which correspond to p_{0max}, are designated by the subscript "max.", for example $P_{м.д\ max}$.

Formulas for converting the characteristics of a pneumatic tire from one pressure to another take the form

$$P_{м.д} = P_{м.д\,max}\frac{p_0}{p_{0\,max}}.$$

The energy received by a pneumatic tire during its compression is found as the area of diagram $P=f(\delta)$, i.e.

$$A_к = \int_0^{\delta} p d\delta.$$

Energy $A_к$ is also proportional to p_0. The conversion of the received energy $A_к$ to another pressure is carried out in accordance with formula

$$A_{м.д} = A_{м.д\,max}\frac{p_0}{p_{0\,max}},$$

where $A_{м.д}$ - is the energy received by a pneumatic tire during compression by a value of $\delta=\delta_{м.д}$.

In approximate calculations the initial section of the compression diagram of a tire (when $\delta<\delta_{дин}$) is assumed to be a straight line. Then it is possible to write

$$A_к \approx \frac{1}{2} P\delta.$$

In the case $\delta>\delta_{дин}$ it is better to approximately determine the value of $A_к$ with the formula

$$A_к \approx 0{,}91\frac{P\delta}{2}.$$

3. Wheel Drum Design

A [wheel] drum is cast from light magnesium, aluminum or titanium alloy. This simplifies production and makes it possible to manufacture a [wheel] drum sufficiently durable and rigid with light weight. Good heat removal from the brakes is ensured by the high specific heat capacity of the drum material and by the finned shape of the surface of its parts.

Figure 10.9 shows a typical design of a [wheel] drum of a contemporary wheel with disk brakes. The drum flanges prevent the lateral separation of the pneumatic tire. For convenience in replacing a pneumatic tire one flange is made detachable. To reduce the turning friction when radial and lateral wheel loads are present, the drum is mounted on radial-thrust tapered roller bearings. The internal part of the [wheel] drum is employed for accommodating the brake.

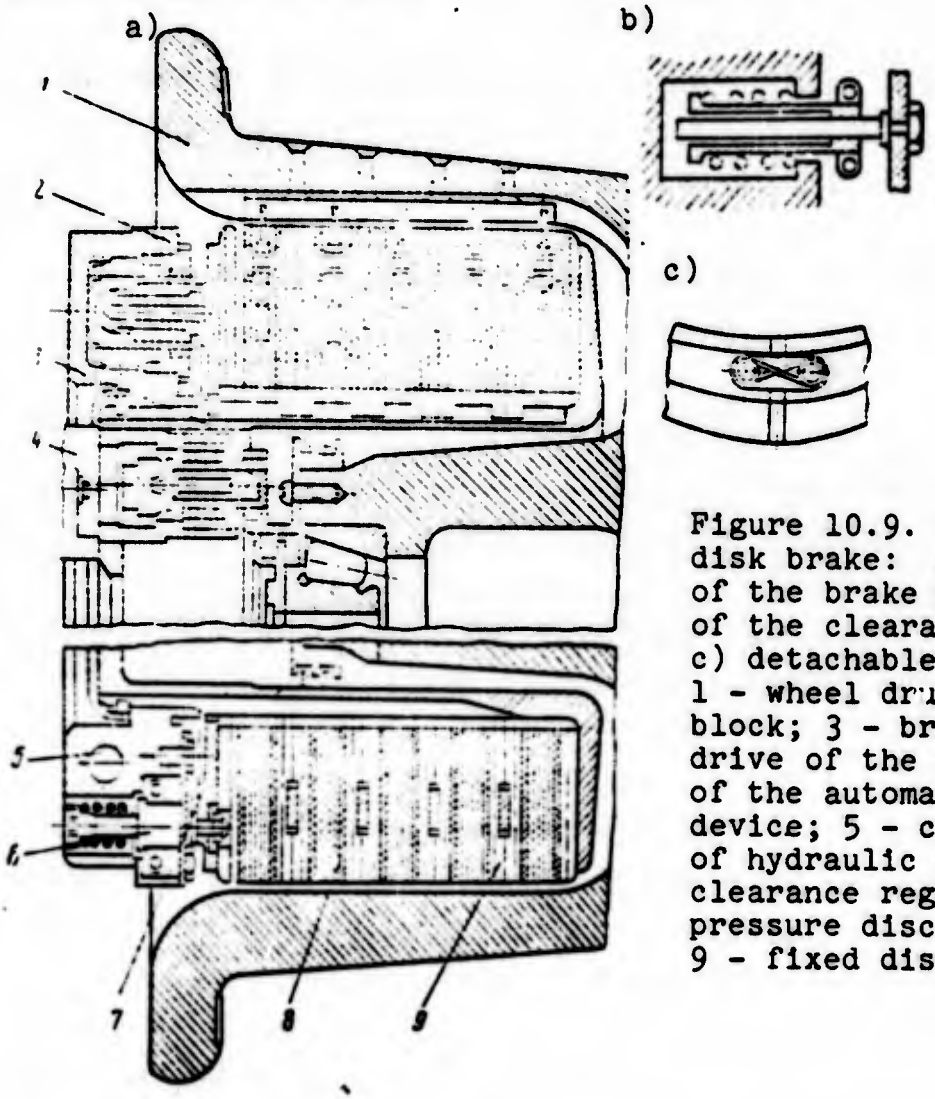

Figure 10.9. Wheel drum with disk brake: a) general view of the brake parts; b) diagram of the clearance regulator; c) detachable semiflange joint: 1 - wheel drum; 2 - cylinder block; 3 - brake housing; 4 - drive of the inertia sensor of the automatic antiskid device; 5 - circular channel of hydraulic system; 6 - clearance regulator; 7 - pressure disc; 8 - mobile disc; 9 - fixed disc.

§ 6. AVIATION WHEEL BRAKES

Aviation wheel brakes, by receiving and dissipating the kinetic energy of the aircraft moving over the airfield, make it

possible to considerably decrease the length of the post-landing landing run. They are also employed in the testing of engines and in the maneuvering of an aircraft on the ground.

The kinetic energy of an aircraft, which it has during a landing, is determined with the formula

$$A_{кин} = \frac{G_{пос} V_{пос}^2}{2g}.$$

Toward the end of a landing run $A_{кин}$ is expended on overcoming aerodynamic drag, the reversive thrust of the engines and the braking power of the wheels (sic).

The braking wheels receive a considerable portion of the kinetic energy.

The skidding of the wheels during braking (sliding) reduces braking effectiveness and can lead to the failure of a pneumatic tire as a result of local heating and wear.

To prevent skidding automatic antiskid devices (automatic antislide devices) are installed in the wheel braking control system.

The automatic devices cause releasing of the brakes during an abrupt deceleration of wheel rotation characterized by a specific value of negative angular acceleration. As a result braking occurs with variable magnitudes of braking moment, but close to the maximum permissible under the condition of the absence of sliding. Braking effectiveness and the conservation of the pneumatic tires are ensured in this way.

On a wet or icy airfield the braking effectiveness of the wheels is sharply reduced.

The sliding of wheels can occur on a snow or water covered airfield surface at high aircraft speeds. The cause of the sliding consists in the fact that a layer of water builds up directly ahead of the wheel. The force of the hydrodynamic pressure of the water creates moment which stops the turning even of unbraked wheels (Fig. 10.10a) and raises them slightly (Fig. 10.10b). The wheel begins to slip on the water layer. The coefficient of adhesion becomes greater than during rolling, but remains less than during braking on a dry surface. This leads to elongation of the takeoff run and the landing run, and as a result of difference and the instability of the adhesion conditions of the different wheels - to the yawing of the aircraft. The heating due to slipping leads to the formation of water vapor and the softening of the rubber of the pneumatic tire tread, which is noted by the appearance of white streaks on the surface of the airfield.

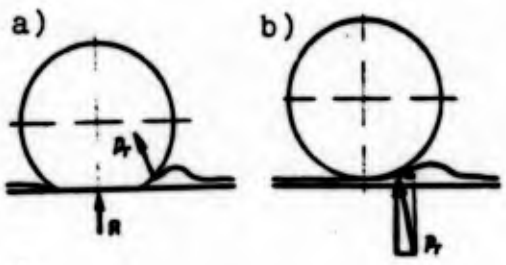

Figure 10.10. The effect of the forces of the hydrodynamic pressure of water during the motion of a wheel over the surface of an airfield covered with water or snow: a) before sliding; b) during sliding; R - reactions of the ground; $P_г$ - the force of the hydrodynamic pressure.

The water layer has the possibility of exiting from under the wheel through the longitudinal grooves of the tread: thus the wearing of the tread which smoothes out the grooves can contribute to the occurrence of sliding at a lower speed.

Aviation Wheel Brake Design

A brake wheel should possess a high energy bearing capacity. A brake design during the course of a short time period of the post-landing landing run (15-25 s) converts into heat and dissipates a considerable amount of energy. In this case brake elements

operating at high temperatures and under considerable loads, should retain their frictional properties and strength during the course of the required service life.

Three types of aviation wheel brakes are employed: shoe (Fig. 10.11a), bag [drum] (Fig. 10.11b) and disk brakes (see Fig. 10.9).

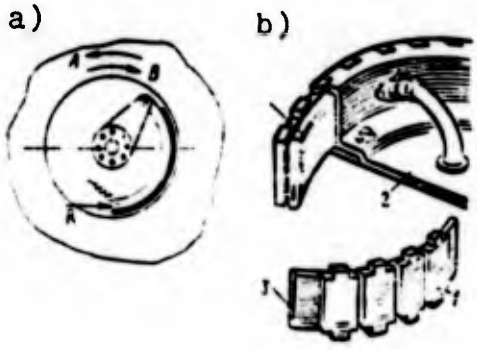

Figure 10.11. Diagrams of brakes: a) shoe brake; b) bag (drum) brake.

Shoe brakes consist of the metal shoes covered with friction plastomer - a heat-resistant material with a high coefficient of friction containing asbestos. To accomplish braking the shoes are pressed against the surface of the wheel drum brake jacket (see Fig. 10.11a). Thrust force R which presses the shoe to the drum, is created with the aid of a hydro- or pneumatic actuator. The magnitude of required force depends on the direction of wheel rotation.

Shoe brakes with positive servo action, in which the friction forces aid in the pressing of the shoes, require less thrust force, but can when improperly adjusted cause spontaneous braking of a wheel. Springs are installed to withdraw the shoes after force R is removed.

Shoe brakes have the following deficiences:

the operation of the brakes is disrupted due to errors in assembling;

due to nonuniform wear of the shoes frequent gap adjustment is necessary;

intense heating causes deformations and cracks in the brake jacket.

The bag [drum] brake (see Fig. 10.11b) has a housing 2 with a large number of brake shoes 1, faced with a friction plastomer. The shoes are pressed against the surface of the brake jacket by the pressure of circular rubber chamber 3 filled during braking with liquid or air, and are kept from turning by splined projections on the sides of the housing.

Upon a reduction in the pressure leaf springs return the shoes to the original position.

In comparison with shoe brakes, bag [drum] brake have the following advantages:

uniform fitting of the shoes to the drum and as a consequence of this they experience uniform wear;

there is no need for frequent checking and adjustment of the gaps;

great effectiveness, since the brake shoes are situated over the entire periphery of the brake;

less weight.

The deficiencies of the bag [drum] brakes:

diminished responsiveness, since a specific time is required for filling the large volume of the bag with liquid or air (1-1.5 s). The responsiveness deteriorates in proportion to the wear of the brake shoes;

the possibility of the failure of the rubber bag in the event of overheating of the brake. This deficiency leads to the necessity for limiting the thermal regime and thus to a reduction in the energy bearing capacity of the brakes,

during intense heating deformations and cracking of the brake jacket are possible.

The disk brake (see Fig. 10.9) consists of fixed discs 9 mounted on splines of brake housing 3, mobile discs 8 connected with the wheel drum 1, pressure disc 7, cylinder unit 2 and return springs. The spline joint of the fixed discs with the housing and of the mobile discs with the drum ensures the possibility of the axial displacement of the discs. Upon feeding fluid pressure into the piston cylinder unit, by overcoming the resistance of the return springs, pressure disc moves which presses the fixed discs to the turning discs. The wheel is braked.

To increase the coefficient of friction and to decrease wear, the friction surfaces of the rotating steel discs are coated with a special ferro-alloy, and the fixed discs are made from cermet or with linings of friction plastomer. To reduce the warping during heating and for the best fitting of the friction surfaces the rotating disks are made in the form of individual segments connected by hinge-joints.

The radial clearances between the frictional lining-segments of the fixed discs ensures ventilation and cooling of the friction surfaces and the removal of the dust which is formed during the operation of the brake.

In brake design gap adjustors 6 are specified which compensates for the increase in the axial clearance between the discs as the frictional coverings wear.

The advantages of disk brakes in comparison with shoe and bag [drum] brakes are:

smaller overall brake dimensions with identical energy bearing capacity and effectiveness, which simplifies the accommodation of the brake in the wheel;

better cooling of the friction surfaces;

low contact heat transfer from the brake discs to the wheel drum decreases the danger of the failure of the pneumatic tire in the event of the overheating of the brake.

Included among the deficiencies in disk brakes are the design complexity and the presence of constant friction between the contiguous discs in the released state.

§ 7. TYPES OF SHOCK ABSORBERS

At the present time the majority of aircraft employ liquid-gas shock absorbers. The simplest setup of a shock absorber of this type is shown in Fig. 10.12a.

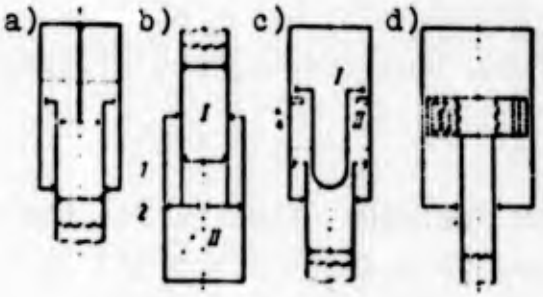

Figure 10.12. Diagrams of shock absorbers: a) liquid-gas conventional setup; b) liquid-gas shock absorber with isolated chambers for the gas and for the liquid; c) liquid-gas shock absorber with two gas chambers; d) liquid shock absorber.

The basic working elements of a liquid-gas shock absorber are the gas - nitrogen[3] or air and the liquid - hydraulic fluid.

---

[3]Nitrogen is employed because an emulsion of hydraulic fluid with air is dangerously explosive at high pressures. The nitrogen should not contain an oxygen admixture.

Upon the operation of the shock absorber (direct stroke) part of the impact energy is expended on compressing the nitrogen. The nitrogen is an elastic element, and the shock absorber due to its compression like a pneumatic tire received energy in the reversible form. In the reverse stroke the energy of the compressed gas sets the shock absorber in its operating position preparing it to receive the next shock.

At the same time it is necessary that part of the received impact energy be converted into the irreversible form and be dissipated. In a liquid-gas shock absorber this is ensured by the second working element, i.e., the liquid.

In the forward and reverse stroke the liquid in the shock absorber is forced through small apertures, as a result of which part of the impact energy due to the effect of the forces of hydraulic resistance of the liquid is converted into thermal energy and is dissipated. Part of the impact energy in the forward and reverse stroke is converted into heat and is also dissipated as a result of the expenditure of energy on overcoming the forces of friction of the parts the shock absorber (the rod and the cylinder) during their relative motion.

Let us examine some other frequently employed types of liquid-gas shock absorbers.

The liquid-gas shock absorber with isolated chambers for the gas and for the liquid makes it possible to eliminate the mixing of the liquid with the gas - the formation of an emulsion and ensures the wetting of the packing with liquid with the shock absorber in any position. Figure 10.12b shows a diagram of this type of shock absorber with chambers: I - for the air, II - for the liquid; 1 - floating piston, 2 - packing.

The liquid-gas shock absorber with two gas chambers (Fig. 10.12c) reduces the rigidity of the shock absorber under the effect of small loads: compression of the shock absorber occurs as a result of the compressing of the gas in low-pressure chamber II. In the event of the occurence of heavy loads the gas is compressed in the high-pressure chamber I.

The hydraulic (pure liquid) shock absorber (Fig. 10.12d). In liquid shock absorbers the liquid is the elastic element which accumulates energy on the forward stroke. The reverse stroke is accomplished as a result of this energy. In order that the magnitude of the stroke be sufficient, such liquids are selected as the working liquids, which possess a low bulk modulus, and employ high pressures. Just as in liquid-gas shock absorbers, part of the energy in a hydraulic shock absorber is converted into the irreversible form due to the effect of hydraulic friction during the course of the passage of the liquid through small apertures and the friction forces of the parts of the shock absorber during their mutual slipping.

The advantages of liquid shock absorbers are their small overall dimensions and low weight. The basic deficiency which prevents their broad application is the difficulty in creating packing seals which operate reliably at very high pressures.

There are also other varieties of shock absorbers, for example, rubber and spring-friction shock absorbers. However as operational practice has shown the liquid-gas shock absorbers are the most successful.

§ 8. THE ARRANGEMENT OF SHOCK ABSORBERS IN LANDING GEAR DESIGN. TRANSFER CONSTANT ψ

The operating conditions of a shock absorber to a considerable degree depend on its arrangement in the landing gear design.

Depending on the mutual positioning of the wheels and the shock absorber, two types of strut design are distinguished:

1) with direct attachment of the wheels or carriage to the shock absorber (the so-called telescopic strut);

2) with lever suspension of the wheels.

Let us examine the operating conditions of a shock absorber with a telescopic strut (Fig. 10.13a).

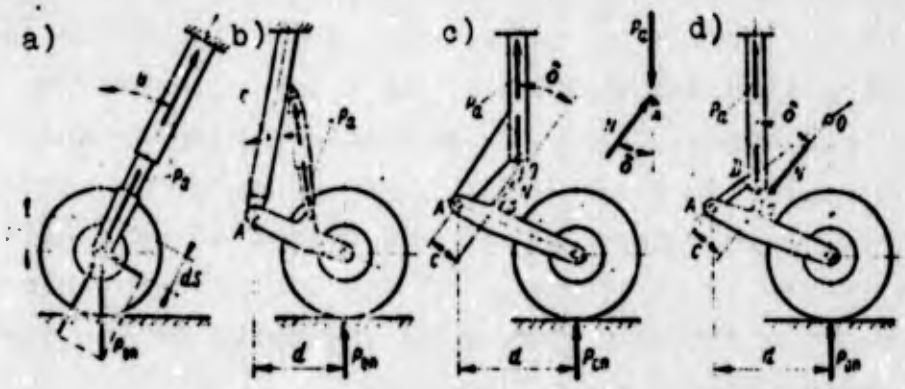

Figure 10.13. The positioning of shock absorbers in landing gear design: a) telescopic strut; b, c, d) strut with lever suspension of the wheels.

Load $P_{оп}=iP_к$ acting on the wheels of the strut causes both compression of the shock absorber and its flexure. The flexure of the shock absorber and the friction forces connected with this are greater, the greater is angle θ - the angle of inclination of the axis of the landing gear strut. To avoid considerable flexure and great friction this angle is taken in the design to be not more than 20°. However, with small θ the shock absorber will poorly receive the front shock.

Let us determine the transfer coefficient for a shock absorber with a telescopic strut. By transfer coefficient ψ is understood the ratios of the force acting on shock absorber P_a to the corresponding load on the wheels of the strut $P_{оп}=iP_к$.

As is evident from Fig. 10.13a, this relation takes the form

$$\psi = \frac{P_a}{P_{ш}} = \frac{P_{ш}\cos\theta}{P_{ш}} = \cos\theta.$$

It is possible to disregard the change in angle θ during the compression of a shock absorption and to assume the transfer coefficient constant

$$\psi = \cos\theta = \text{const.}$$

By employing the principle of possible displacements, it is possible to obtain another expression for the transfer coefficient ψ - via the ratio dh/ds of the increase in the vertical displacement of the wheels to the increase in the rod's stroke with respect to the axis of the shock absorber. According to the principle of the possible displacements the sum of the operations of all forces, under the effect of which the body is in equilibrium, during the possible displacements, is equal to zero

$$P_{ш}dh = P_a ds = 0,$$

hence

$$\psi = \frac{P_a}{P_{ш}} = \frac{dh}{ds}.$$

This expression is valid for all shock-absorber positioning setups.

For a telescopic strut, since ψ=const., it is obtained, that

$$\psi = \frac{h}{s}.$$

In strut setups with a lever suspension ψ>1 changes during shock absorption compression (Fig. 10.13b, c, d). For calculating h - the vertical displacement of the axis of a wheel (or a carriage) the following expression is employed

$$h = \psi_{ср} s,$$

where ψ_{cp} - the average value of ψ during the section of the shock absorber stroke from 0 to s.

Struts with a lever suspension of the wheels are usually made in accordance with one of the setups shown in Fig. 10.13.

The transfer coefficient ψ for a strut having an external shock absorber (see Fig. 10.13b) can be determined at each value of the shock absorber stroke s from the condition of the equality to zero of the sum of the moments with respect to pivotal axis A:

$$\Sigma M_A = 0;$$

$$\psi = \frac{P_a}{P_{on}}.$$

Similarly, ψ is found for landing gear struts with lever-suspension of the wheels and with an internal shock absorber (see Fig. 10.13c, d).

For the landing gear strut shown in Fig. 10.13d, the value of angle δ can be determined graphically, by employing for this the theorem concerning the intersection of three forces, which are in equilibrium, at one point. In this setup this is point O of the intersection of the axial line of mobile link AD with the line of the effect of force P_{on}. Straight line OB is the line of the effect of total force N applied to the rod at point B, and angle δ characterizes the inclination of this force. For the setups (see Fig. 10.13c and d) from equation $\Sigma M_A=0$ we obtain $N=P_{on}(d/c)$. Since $P_a=N \cos \delta$, then

$$\psi = \frac{P_a}{P_{on}} = \frac{d}{c} \cos \delta.$$

Landing gear with lever-suspension of the wheels possess the following essential advantages over telescopic struts:

1) the shock absorber of this type of strut also damps well the loads due to drag forces;

2) in the case of external positioning of a shock absorber (see Fig. 10.13b) it is completely relieved of flexure; in a landing gear with an internal shock absorber (see Fig. 10.13c) the rod of the shock absorber is considerably relieved of flexure:

3) at great values of ψ the shock absorber is more compact, since the energy transmitted to it is received with large forces $P_a=\psi P_{on}$ in a short stroke. At the same time with large ψ the short stroke s ensures a rather large vertical displacement of the wheel $h=\psi_{cp}s$, necessary during its motion over uneven areas.

However, a landing gear with lever suspension of the wheels has mobile highly loaded articulations which make the design heavier and they are susceptible to wear.

§ 9. OPERATION OF A LIQUID-GAS SHOCK ABSORBER

Let us examine the operation of the typical liquid-gas shock absorber depicted in Fig. 10.14a.

1. Shock Absorber Operational Setup

Figure 10.15a shows a setup of a liquid-gas shock absorber. The rod stroke of the shock absorber s is applied along the abscissa axis, and force P_a, acting on the shock absorber with a given value s, is applied along the ordinate axis.

Force P_a is balanced by the forces: of the resistance of the gas - $P_г$, of the liquid - $P_ж$ and of friction - $P_т$. In the forward stroke force P_a, which must be applied to compress the shock absorber, is equal to the sum of the resisting forces.

$$P_a = P_г + P_ж + P_т.$$

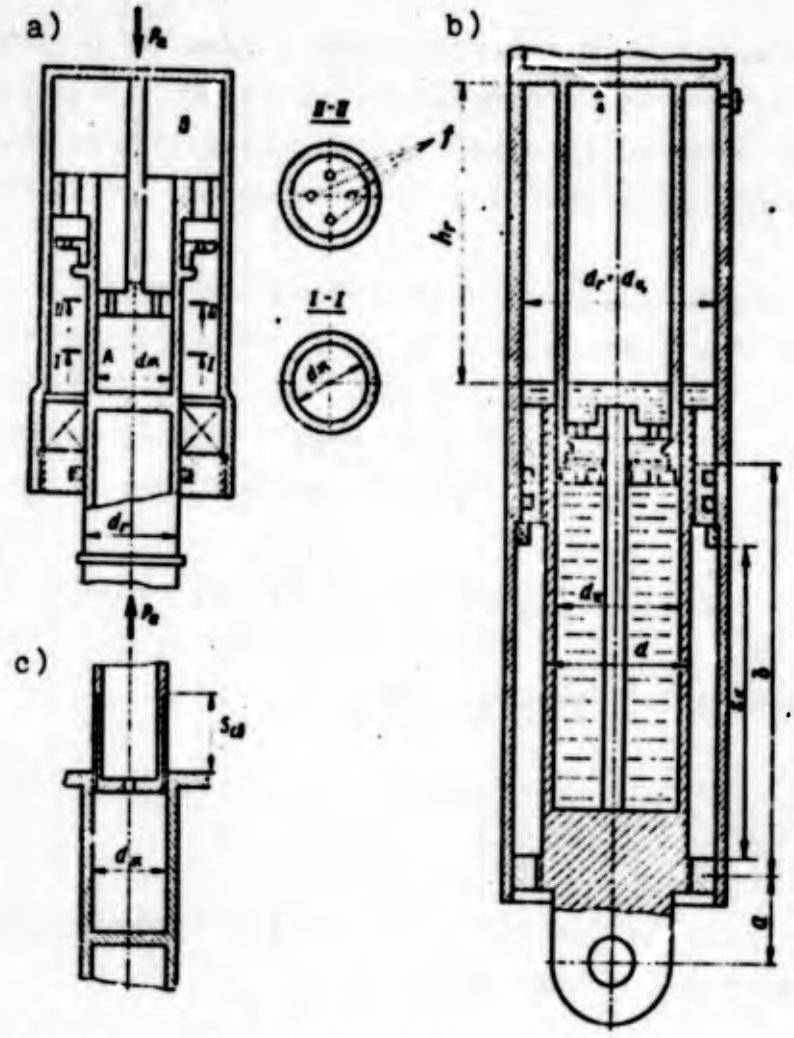

Figure 10.14. Setups of typical liquid-gas shock absorbers: a) with the packing attached non-moving to the cylinder; b) with the packing attached to the upper rod bushing; c) with a free stroke with respect to the liquid.

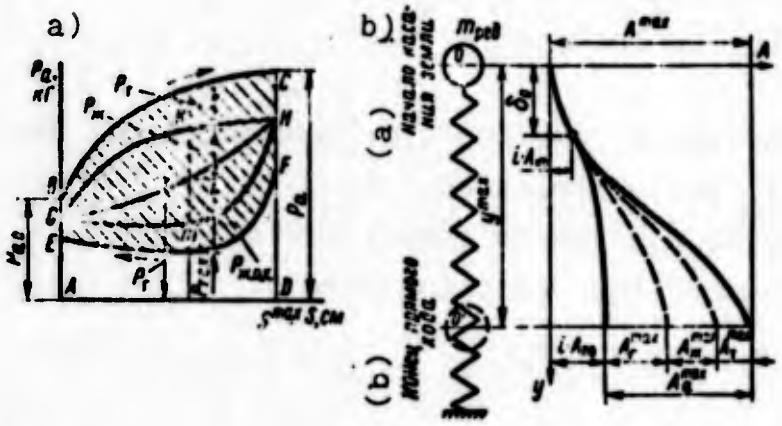

Figure 10.15. Shock absorption operation of a landing gear strut: a) diagram of a shock absorber; b) diagram of energy balance.
Key: (a) Beginning of touchdown; (b) End of the forward stroke.

On the diagram of the **forward stroke** (curve BC) the magnitude of the force of pretensioning of the shock absorber P_{ao} is noted, equal to the load, which must be applied to the shock absorber in order that it begin to be compressed, and of the maximum force of the shock absorber P_a^{max} acting in the shock absorber upon the receiving by it of maximum energy A_a^{max}.

The area of diagram ABCD represents in scale the energy of A_a^{max} received by the shock absorber in the forward stroke. The ratio of this area to the area of a rectangle with sides P_a^{max} and s^{max} is called the <u>diagram efficiency factor</u> η

$$\eta = \frac{A_a^{max}}{P_a^{max} s^{max}}.$$

The greater is η, the greater is the magnitude of the energy the shock absorber absorbs in the forward stroke at given values of P_a^{max} (and this also means the g-forces) and stroke s^{max}.

The **reverse stroke** (curve FE on the shock absorber diagram) is realized due to the energy accumulated in the compressed gas.

With the straightening out of the shock absorber the force of the compressed gas $P_г$ forces the shock absorber to straighten out in order to be prepared for receiving the next shock.

The resisting forces of the liquid $P_{ж.о.х}$ and of the friction $P_{т.о.х}$ impede the straightening out of the shock absorber, thus in the reverse stroke, force $P_{а.о.х}$ which keeps the shock absorber from straightening out is equal to the difference between the force of the gas and the resisting forces of the liquid and the friction

$$P_{а.о.х} = P_г - P_{ж.о.х} - P_{т.о.х}.$$

Curve GH of the resistance of the gas $P_г$ is plotted on the diagram; in examining the operation of a shock absorber it is possible to consider that these curves during compression and straightening out practically coincide.

In accordance with the expressions of P_a for the forward and the reverse stroke the ordinates of the curves of $P_ж$-s (from the curve of $P_г$-s) and $P_т$-s (from curves of $P_ж$-s) for the forward and reverse stroke) are plotted.

The area of the hysteresis loop of diagram BCFE represents the energy which is dissipated during one cycle. The area of diagram AEFD expresses the energy returned to the aircraft and expended on its bouncing.

Let us examine the principles by which the dependences of resisting forces $P_г$, $P_ж$ and $P_т$ on s are determined.

2. Resisting Force of the Gas

The resisting force of a compressed gas is proportional to its pressure[4]

$$P_г = p_г F_г = p_г \frac{\pi d_г^2}{4},$$

where $F_г$ and $d_г$ - are the area and the diameter of the gas piston.

In the general case as the diameter of the gas piston it is necessary to take the diameter of the surface over which the seals slide preventing the leakage of the liquid and gas from the shock absorber.

---

[4]Since the pressure of a gas in a shock absorber is considerably greater than atmospheric pressure, let us disregard the difference between the values of the absolute and excess pressures.

Figure 10.14 shows the diameters of the gas pistons of two varieties of liquid-gas shock absorbers.

In the case of the rapid compression of a shock absorber gas pressure $p_г$ changes in accordance with politropic curve

$$p_г v^{\kappa} = \text{const},$$

where v - is the volume of the gas chamber; κ - is the polytropic exponent.

For liquid-gas shock absorbers in which during the compression process heat exchange occurs between the gas and the atomized liquid (the gas cavity is not isolated from the liquid), κ=1, 0-1.1 for shock absorbers with slight atomization or with gas chambers isolated from the liquid, κ=1.2-1.3, i.e., the politropic curve is close to the adiabatic curve.

The following dependences are then derived from the equation of polytropic curve $p_г v^{\kappa}$=const.

During the compression of a shock absorber in stroke s the initial volume v_0 of the gas chamber in which the pressure $p_{г0}$ was will vary by magnitude $F_г s$. The current magnitude of the resisting force of the gas in stroke s will be

$$P_г = \frac{P_{г0}}{\left(1 - \frac{F_г s}{v_0}\right)^{\kappa}},$$

where $P_{г0}=p_{г0}F_г$ - is the force of gas in the case of prestressing.

The energy received by the gas (potential energy) during stroke s^{max} will be

$$A_г^{max} = \int_{p_г^{max}}^{p_{г0}} p_г dv = \frac{p_{г0} v_0}{\kappa - 1}\left[\frac{1}{\left(1 - \frac{F_г s^{max}}{v_0}\right)^{\kappa-1}} - 1\right].$$

where $p_г^{max}$ - is the gas pressure during stroke s^{max}.

The accepted position concerning the fact that curves of $P_г$-s during the forward and the reverse stroke coincide is equivalent to the assumption that the gas operates according to an adiabatic curve - without heat exchange between the gas and the other parts of the shock absorber. Thus, in examining the operation of a liquid-gas shock absorber it is usually assumed, that energy $A_г^{max}$ is received by the gas in the reversible form.

3. Resisting Force of the Liquid

The hydraulic resisting force of a liquid $P_ж$ depends on the rate of compression of the shock absorber and on the dimensions and the number of small apertures through which the liquid is forced.

In the forward stroke the liquid passes through these apertures in moving from cavity A into cavity B (see Fig. 10.14). In this case additional dynamic pressure of the liquid $p_ж$ is developed in cavity A. The resisting force of the liquid is

$$P_ж = p_ж F_ж, \qquad (10.1)$$

where $F_ж$ - is the area of the liquid piston, equal to the cross-sectional area of the liquid column, in which pressure $p_ж$ acts; in the shock absorber shown in Fig. 10.14, $F_ж=(\pi d_ж^2/4)$.

The additional pressure is connected with the rate $V_ж$ of outflow of the liquid through the small apertures by dependence

$$p_ж = \frac{\gamma V_ж^2}{2g}, \qquad (10.2)$$

where γ - is the specific weight of the liquid (for AMG-10 γ=0.8-0.85 g/cm^3).

From the equation of the constancy of the fluid flow rate in cross sections I-I and II-II (see Fig. 10.14a)

$$F_ж W = \mu f V_ж$$

it is possible to determine

$$V_ж = \frac{F_ж W}{\mu f}, \qquad (10.3)$$

where μ - is the outflow coefficient; usually it is assumed that μ=0.7-0.8; W=ds/dt - is the rate of shock absorber compression; f - is the area of the small apertures serving to create the resisting forces of the liquid.

It follows that from expressions (10.1), (10.2) and (10.3) that

$$P_ж = \frac{\gamma F_ж^3 W^2}{2g\mu^2 f^2}.$$

Thus, the resisting force of the liquid depends on the rate of its compression W varying in accordance with the stroke of the shock absorber on the area of the small apertures f and on the shape (through μ).

If the area of the apertures f is constant, then the variation in $P_ж$ in accordance with stroke s is determined by the variation in the rate of compression W.

When s=0 and at the end of the stroke when $s^э$ of $s^{max} P_ж = 0$ (Fig. 10.15a).

The law of the variation in W(s) can be found from an examination of the dynamics of the vertical motion of the reduced mass of the strut taking its shock absorption resistance into account.

In order to affect the nature of dependence $P_ж(s)$ sometimes is made variable.

In certain designs f varies in accordance with the stroke s, - in others, depending on the magnitude of $P_{ж}$ (designs with a safety valve).

The value of $f/F_{ж}$ affects $p_{ж}$ directly also via W. With an increase in $f/F_{ж}$ the value of W also increases; thus, in the case of large values of $f/F_{ж}$ it is possible to disregard the liquid resistance.

The parameters of a shock absorber, including the magnitude of f, are determined mainly by the conditions of the reception of the maximum impact energy during a landing - A_a^{max}. However, it is also necessary to ensure good properties of a shock absorber during the motion of an aircraft over the airfield surface.

In the case of the passage of the wheels over highly uneven areas, if the dimensions of the wheels are small, a great rate of the motion of the rod can arise and cause a sharp increase in the hydraulic resistance of the shock absorber.

The diagram in Fig. 10.16 shows that for the passage over an uneven area $h_н$ of an uncompressed wheel with a maximum permissible compression of $\delta_{м.д}$ a vertical displacement of the wheel axis as follows is necessary

$$h = h_н - \delta_{м.д}.$$

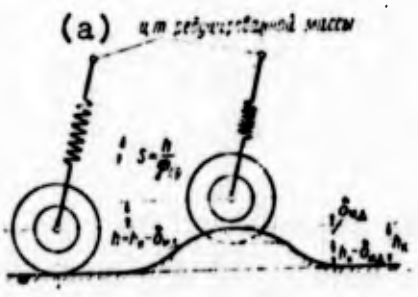

Figure 10.16. Towards an explanation of the need for a free stroke. Key: (a) c.g. of the reduced mass.

In order that during the passage of the strut over the uneven area the aircraft does not heave, it is necessary that the compression [stroke] of the shock absorber be not less than

$$s = \frac{h}{\psi_{ср}}.$$

This compression will not cause liquid resistance if a free stroke as follows below is ensured in the shock absorber

$$s_{св} = \frac{1}{\psi_{ср}}(l_ж - \delta_{м.д}),$$

within the limits of which the liquid passes through enlarged apertures. In this case

$$P_ж \approx 0, \text{ while } P_а \approx P_г + P_т.$$

Figure 10.14c shows an example of a design which gives an increase in $f/F_ж$ in stroke $s_{св}$ - longitudinal cross section.

The energy received by the liquid in stroke s^{max},

$$A_ж^{max} = \int_0^{s^{max}} P_ж ds$$

can be expressed in the following manner:

$$A_ж^{max} = \eta_ж P_{ж\,max} s^{max},$$

where $\eta_ж$ - is the coefficient of the efficiency of the diagram of the liquid ($\eta_ж < 1$); $P_{ж\,max}$ - is the greatest resisting force of the liquid. At a constant value of f it corresponds to the maximum rate of shock absorber compression W_{max}, which occurs near the middle of the stroke (when s=0 and at the end of the stroke W=0).

Energy $A_ж$ is received in irreversible form (compression energy of the liquid can be disregarded in comparison with the compression energy of the gas); it is converted into thermal energy which is dissipated.[5]

---

[5]In a liquid shock absorber the energy of the elastic compression of the liquid must be considered.

The large value of the coefficient of efficiency of the diagram of the forward stroke of the shock absorber η attests to the fact that in the forward stroke a considerable role is played by the liquid resistance. This can lead to the appearance of a peak load at the moment when the wheel hits against an obstruction during the takeoff or landing run.

In order that the g-forces during a landing and during the motion along the uneven areas of an airfield are not great, the apertures for the passage of the liquid in the forward stroke should not be too small. Thus, to ensure sufficient hysteresis (energy dissipation) contemporary shock absorbers have an additional braking of the motion of the rod in the reverse stroke. For this a valve is usually installed which ensures a decrease in the passage apertures and creates great liquid resistance in the reverse stroke (see Fig. 10.14). The dimensions of the apertures for the passage of the liquid is found by the calculations and are more precisely determined by the subjecting of an experimental shock absorber to tests.

4. Friction Force $P_т$

The friction force in a shock absorber is represented by the sum of two terms: the friction force in the seals $P_{уп}$ and the friction force in the sleeves $P_б$, i.e.,

$$P_т = P_{уп} + P_б.$$

The magnitude of $P_{уп}$ depends on the design and the material of the sealing rings and on the liquid pressure applied to them.

The friction force in the sleeves $P_б$ depends on the flexural loads acting on the rod, on the magnitude of the strut base b (Fig. 10.17) and on the material and the state of the friction surfaces.

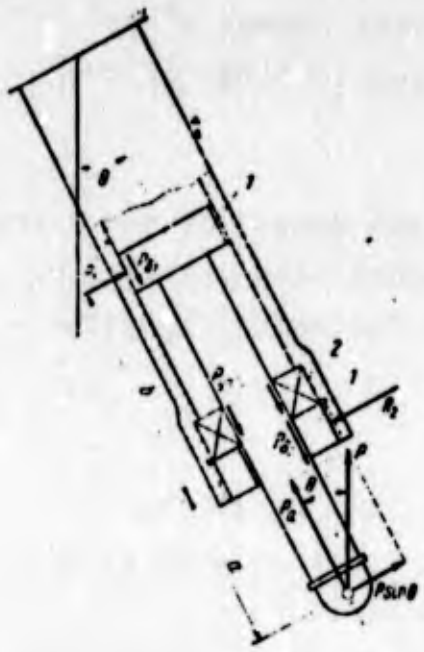

Figure 10.17. Diagram of the effect of friction forces in a shock absorber: 1 - guide sleeve; 2 - sealing package.

In such a case when the friction parts are made from different materials (steel and bronze), the friction is less, and during axial loading of a shock absorber the friction force in the sleeves can be disregarded.

During approximate calculation the total friction force (in the seals and sleeves) is considered proportional to the total force acting on the shock absorber, and is found with the following formula

$$P_т = \chi P_а,$$

where the coefficient χ for different loading conditions of a shock absorber varies within the limits of from 0.1 to 0.2.

The energy which is expended in overcoming the friction forces in a maximum stroke s^{max} is determined with the following formula

$$A_т^{max} = \int_0^{s^{max}} P_т ds.$$

If we assume χ constant, then

$$A_т^{max} = \chi A_а^{max},$$

where A_a^{max} - is the total energy received by a shock absorber in a forward stroke s^{max}.

5. The Joint Operation of a Shock Absorber and the Pneumatic Tires of the Wheels

In examining the operation of the shock absorption of a landing gear strut it is necessary to consider the joint

participation in the reception of the supplied energy $A^{э}$ of A^{max} of both the shock absorber and the pneumatic tires of the wheels.

During shock absorption operation at each moment of the stroke the force in the shock absorber P_a is connected with the load on the strut $P_{оп}$ and the wheel loads $P_к$ by the following expression

$$P_a = \psi P_{оп} = \psi i P_к.$$

The wheel load $P_{к0}$ which corresponds to the beginning of shock absorber compression is expressed via the load when parked $P_{к.ст}$ in the following manner:

$$P_{к0} = n_0 P_{к.ст},$$

where n_0 - is the coefficient of prestressing of the shock absorber.

Hence, the force of prestressing when s=0, when the shock absorber begins to be compressed is equal to

$$P_{a0} = n_0 \psi_0 i P_{к.ст},$$

where ψ_0 - is the value of the transfer constant when s=0.

Accordingly, in the case of stroke s^{max} the maximum force is

$$P_a^{max} = n^{max} \psi_{s^{max}} i P_{к.ст}.$$

where n^{max} and $\psi_{s^{max}}$ - are the g-force and transfer constant when s^{max}.

The distribution of the energy received by strut shock absorption between its components is shown in the energy balance diagram (see Fig. 10.15b). The ordinates of the diagram correspond to the vertical stroke of strut shock absorption due to shock absorption stroke s and the compression δ of the pneumatic tire.

The reduced mass $m_{ред}$ is the portion of the mass of the flight vehicle impinging on the strut.

At first before the stroke $y=\delta_0$, when $P_a=P_{a0}$, $P_к=P_{к0}$, only the pneumatic tires of the wheels are compressed. Energy $iA_{к0}$ is received at this moment by them.

Toward the end of the stroke $y^{max}=\delta_{п.о}+\psi_{ср}s^{max}$ energy A^{max} is completely received by strut shock absorption.

Energy distribution A_a received by a shock absorber is shown on the diagram of the shock absorber in Fig. 10.15a

$$A_a^{max}=A_г^{max}+A_ж^{max}+A_т^{max}.$$

The pneumatic tire at this moment has complete compression $\delta_{п.о}$ and receives energy $A_{п.о}$

As is evident from the energy balance diagram (Fig. 10.15b), the energy A^{max} supplied toward the end of stroke y^{max} which corresponds to s^{max} and $\delta_{п.о}$, is completely absorbed by the shock absorption of the strut. In this case part of it is received in the form of the potential energy of the gas and the air in the pneumatic tires

$$A_{пот}=A_г^{max}+iA_{п.о.}$$

The remaining part $A_{необ}=A_ж^{max}+A_т^{max}$ is received in irreversible form and is dissipated, being converted into heat.

In the diagram of the shock absorber (Fig. 10.15a) the types of energy are reflected by the appropriate areas. For example, $A_{необ}$ corresponds to the shaded area BCFE, and $A_ж^{max}$ - corresponds to the area GKHm.

In intermediate positions from the moment of touchdown until complete compression the mass $m_{\text{пред}}$ possesses the following kinetic energy

$$A_{\text{кин}} = A^{\max} - A_{\text{а}} - iA_{\text{п}},$$

which is connected with the rate of compression of the strut $\dot{y}$ by the following dependence

$$A_{\text{кин}} = \frac{m_{\text{пред}}(\dot{y})^2}{2}.$$

In its turn $\dot{y}$ is determined by the formula

$$\dot{y} = \dot{\delta} + \psi_{\text{ср}}\dot{s},$$

where $\dot{\delta}$ and $\dot{s}$ - are the rates of compression of the tires and the shock absorber.

6. Determining the Basic Parameters and Dimensions of Shock Absroption

The technical specifications imposed on shock absorption, the characteristics of aviation wheels and the principles governing the operation of a liquid-gas shock absorber determine the necessary parameters of shock absorption.

In order to show the effect of different factors on these parameters, let us present the approximate design calculations of the shock absorption of a main landing gear strut. The loading conditions correspond to the case $E_{\text{Ш}}$ - "a three-point landing."

In examining the calculation sequence Figs. 10.8, 10.13 and 10.14 are employed.

Selecting the wheels. The parking load on one wheel of a main landing gear strut of an aircraft being designed with the rated takeoff weight is

$$P_{\text{к.ст.взл}} = \frac{G_{\text{взл}}}{2i}\frac{a}{b}.$$

where a - is the distance of the front strut from the center of gravity of the aircraft; b - is the landing gear base; i - is the number of wheels on each of the main landing gear struts.

The parking load on one wheel with a rated landing weight is

$$P_{к.ст\,пос} = \frac{G_{пос}}{2i} \cdot \frac{a}{b}.$$

A wheel selected from the catalog for the main landing gear struts should correspond to the following conditions:

1) $P_{к.ст.взл} \geq P_{ст.взл.max}$;
2) $P_{к.ст.пос} \geq P_{ст.пос.max}$;
3) $V_{взл} \leq V_{взл.max}$;
4) $V_{пос} \leq V_{пос.max}$.

where $P_{ст.взл.max}$ and $P_{ст.пос.max}$ - are the static (parking) load on a wheel permissible with p_{0max} respectively with the weight of aircraft at the beginning of takeoff and during landing; p_{0max} - is the maximum operating pressure in a pneumatic tire; $V_{взл.max}$ and $V_{пос.max}$ - are respectively the maximum takeoff and maximum landing velocities permissible in accordance with the catalog for the wheel in question; $V_{взл}$ and $V_{пос}$ - are respectively the takeoff and landing velocitys of the aircraft being designed.

If for a selected wheel $P_{к.ст.взл}$ is substantially less than $P_{к.ст.взл.max}$ then to retain the parking compression indicated in the catalog at a rated takeoff weight, the pressure in the pneumatic tire should be decreased, employing the following relationship:

$$p_0 = p_{0max} \frac{P_{к.ст.взл}}{P_{к.ст.взл.max}}.$$

Subsequently the calculation is set forth on the assumption that this recommendation was fulfilled.

For the obtained p_0 the maximum permissible value of impact load $P_{м.д}$ and the operation of pneumatic tire $A_{м.д}$ with respect to it are determined.

Determining the energy and the g-forces which shock absorption should receive. The operational energy $A^э$ - is the operation which the shock absorption (shock absorber and pneumatic tires) of each of the landing gear struts should receive with an operational g-force of $n^э$ in the forward stroke

$$A^э = \frac{m_{рез} V_y^2}{2},$$

where V_y - is the cited vertical velocity of the reduced mass both for the main and for the front landing gear struts. It can be determined with the following formula

$$V_y = \sqrt{0{,}5\,(0{,}25V_{пос} + 0{,}01G_{пос}^{0{,}5} + 8)}.$$

Here $V_{пос}$ - is the landing velocity, m/s. V_y - is taken to be not less than 2.8 m/s.

For each of the main landing gear struts

$$m_{рез} = \frac{G_{пос}}{2g}.$$

To ensure the strength and the prologned reliable operation of aviation wheels it is necessary that for the main landing gear struts the value of operational g-force $n^э$ not be greater than ratio $P_{м.д}/P_{к.ст.пос}$. For passenger aircraft landing gear shock absorption $n^э$=2-2.5; lesser values of $n^э$ are taken for heavier aircraft.

The maximum energy is determined with the formula

$$A^{max} = \frac{G_{взл}}{G_{пос}} A^э,$$

but it is not taken less than 1.5 $A^э$.

The value of the maximum g-force n^{max} during the receiving of A^{max} by the shock adsorption can be determined from the equation

$$n^р = fn^э = f_{n\,max} n^{max},$$

where $n^р$ - is the calculated g-force; f - is the safety factor (for a landing gear f=1.5); $f_{n\ max} \approx 1.3$.

It is necessary to check that value n^{max} not be greater than the value

$$\frac{P_{пред}}{P_{к.ст.пос}} \text{ or } \frac{P_{пред}}{P_{к.ин}};$$

where $P_{пред}=0.75\ P_{разр.рад}$.

The maximum energy on a shock absorber is,

$$A_a^{max} = A^{max} - iA_{п.о},$$

where $A_{п.о}\approx 1.1A_{м.д}$ - is the energy received by a pneumatic tire during its complete compression.

The shock absorber stroke s^{max} upon the receiving of energy A_a^{max} by it is determined with the formula

$$s^{max} = \frac{A_a^{max}}{P_a^{max}\eta},$$

where $\eta=0.65-0.80$ - is the coefficient of efficiency of the diagram of the shock absorber stroke; P_a^{max} - is the resisting force of the shock absorber upon the receiving of energy A_a^{max} by it.

For the main landing gear strut $P_a^{max}=iP_{к.ст.пос}n^{max}\psi_s max$. Thus,

$$s^{max} = \frac{A_a^{max}}{iP_{к.ст.пос}n^{max}\psi_s max\,\eta},$$

where $\psi_s max$ - is the transfer constant in the case s^{max}.

Determining the area $F_г$ and diameter $d_г$ of a shock absorber gas piston.

The area of a shock absorber gas piston is found with the expression

$$F_г = \frac{P_{г0}}{p_{г0}} = \frac{P_{a0}(1-\gamma)}{p_{г0}},$$

where $p_{г0}$ - is the gas pressure in a shock absorber when s=0 (loading pressure of the shock absorber); $P_{г0}$ - is the resisting

force of the gas in the shock absorber when s=0; χ - is the coefficient which considers the resisting forces of friction in the seal and in the guide sleeves of the shock absorber; P_{a0} - is the force of the prestressing of the shock absorber - the force on the shock absorber rod which corresponds to the beginning of its compression. For the shock absorbers of main landing gear struts

$$P_{a0} = n_0 i P_{\text{к.ст.нос}} \psi_0,$$

where n_0 - is the coefficient of the prestressing of the shock absorber; ψ_0 - is the transfer constant when s=0.

The diameter of the gas piston of a shock absorber is found with the expression

$$d_г = 2\sqrt{\frac{F_г}{\pi}}.$$

The diameter of a cross section for which sealing of a high pressure cavity is accomplished is accepted as the diameter of the gas piston.

The rigidity of the shock absorber and the magnitude of the volume of its gas chamber depends on the magnitude of coefficient n_0.

Usually for landing gear struts with direct attachment of the wheels or the carriages to the shock absorber n_0=0.4-0.7; for landing gear struts with a lever suspension of the wheels n_0=0.7-1.0.

In the case of polytropic law variation in the parameters of a gas during the compression of a liquid-gas shock absorber the **required initial volume v_0 of the gas chamber** is determined with the formula

$$v_0 = \frac{F_г s^{\max}}{1 - \left(\frac{n_0 i - n}{n^{\max} \psi_{\max}}\right)^{\frac{1}{n}}}.$$

Plotting the diagram of shock absorber compression. The ordinates of the politropic curve of gas compression $P_г=f(s)$ are determined with the expression

$$P_г = \frac{P_{г0}}{\left(1-\frac{F_г s}{\omega_0}\right)^n}.$$

For the plotting of a graph which characterizes the variation in the total resisting force of a shock absorber in the forward stroke through points P_{a0} when s=0 and P_a^{max} when s^{max} a smooth curve is drawn so that the area of the diagram corresponded to A_a^{max} in scale.

By deducting the friction forces, we will obtain a curve which characterizes the variation of the shock absorber in the sum of the resisting forces of the gas and the liquid in accordance with the stroke of the shock absorber rod

$$P_г + P_ж = P_a(1-\gamma).$$

A smooth curve is drawn through points $P_{г0}$ when s=0 and $P_г^{max}$ when s^{max} and the points obtained by calculating according to this formula.

Determining the cross-sectional area of the apertures for creating the resisting force of the liquid in the forward stroke. The resisting force of the liquid is

$$P_ж = \frac{\gamma F_ж^3 W^2}{2g\mu^2 f^2},$$

where $F_ж$ - is the area of the liquid piston - the cross-sectional area, on which the excess pressure of the liquid resistance acts: $F_ж = \frac{\pi d_ж^2}{4}$; W - is the rate of shock absorber compression; μ - is the discharge coefficient of the liquid; f - is the cross-sectional area of the passage apertures; γ/g - is the mass density of the liquid.

Hence the required value is

$$f = \sqrt{\frac{\gamma F_{ш}^{3} W^{2}}{2g P_{ш}}} = \frac{F_{ш} W}{\mu} \sqrt{\frac{\gamma F_{ш}}{2g P_{ш}}}.$$

The value of f, if the area of the apertures is assumed constant, is approximately determined from an examination of $P_{ш}$ and W when $s=0.5s^{max}$.

Let us take the value of $P_{ш}$ for $s=0.5s^{max}$ from the diagram.

Let us determine the value of W with the formula

$$W = \frac{W_{ц.т.} - W_{пн}}{\psi},$$

where $W_{ц.т.}$, $W_{пн}$ and ψ - are the velocity of the vertical displacement of the center of gravity of the reduced mass, the rate of tire compression and the transfer constant which correspond $s=0.5s^{max}$.

When $s=0.5s^{max}$, the rate of tire compression is short; thus

$$W \approx \frac{W_{ц.т.}}{\psi}.$$

The rate of vertical displacement of the center of gravity of the reduced mass is

$$W_{ц.т.} = \sqrt{\frac{2A}{m_{прив}}}.$$

where A - is the kinematic energy of the reduced mass remaining unabsorbed by shock absorption; its magnitude is determined by the formula

$$A = A^{max} - A_{а} - iA_{к},$$

where $A_{а}$ and $A_{к}$ - are respectively the energy received by the shock absorber and the pneumatic tires of the wheels at the moment in question:

$$A_{а} = (1,1 \div 1,2)\frac{(P_{а0} + P_{а})\, s^{max}}{4};$$

$$A_{к} = \left(\frac{P_{к}}{P_{к}^{0}}\right)^{2} A_{к}^{0}.$$

here P_a - is the total resisting force of the shock absorber at $0.5s^{max}$. It is taken from the diagram of $P_a=f(s)$; $P_к^э=n^э P_{к.ст.пос}$.

7. The Effect of Incorrect Filling and of the Operating Conditions of Liquid-Gas Shock Absorber on its Operation

All parameters of landing gear shock absorption - the dimensions and the pressure of the tires of the wheels, the pressure and the volume of the liquid in shock absorbers and other values are selected during designing so that the shock absorption system can receive standardized values of energy $A^э$ and A^{max} with g-forces not greater than those accepted during calculation and at stroke values s, not exceeding the maximum design stroke s_k.

Thus, deviations during the operation of an aircraft from the established rules of filling of the shock absorber with gas and liquid and from the normal pressure in the pneumatic tires. These types of deviations sometimes can in the case of slight compressions even improve the operation of a shock absorption system, but, as a rule, they lead to the breakdown of the landing gear or its attachment units in such cases when to the shock absorption system during a rough landing impact energy, close in magnitude to the standardized value of A^{max} is delivered.

Let us examine certain cases of the incorrect filling of a shock absorber. These cases can be broken down depending on the nature of their effect on the diagram of gas operation into two groups.

1. Cases which lead to a reduction in the curve of $P_г=f(s)$ (Fig. 10.18a):

a) the initial pressure in the shock absorber is $p_{г0}<p_{г.норм}$, and the volume of liquid corresponds the rated; thus $v_0=v_{0норм}$;

b) $p_{г0}=p_{г0норм}$, but the volume of liquid is less than normal; thus the initial volume of gas is $v_0>v_{0норм}$.

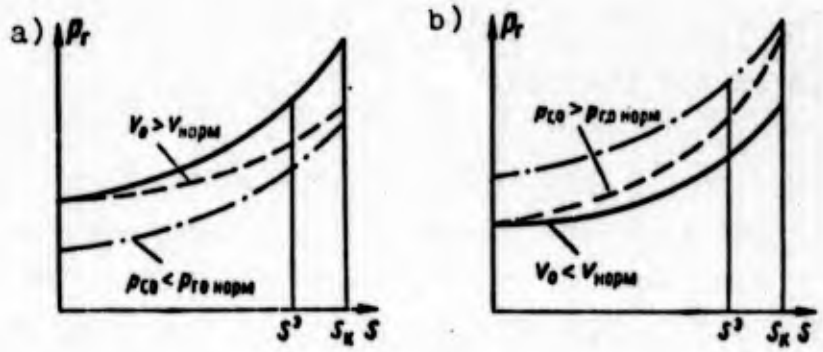

Figure 10.18. Cases of the incorrect filling of a shock absorber: a) leading to a drop in the curve of $p_г=f(S)$; b) leading to an increase in the curve or $p_г=f(S)$.

In these cases the gas resistance diagrams $P_г$ with respect to the stroke are below normal. Experiments show that in this case the diagram of the total resistance of a shock absorber P_a is accordingly reduced.

The compression of a shock absorber under given loads (including parking compression, if $n_0<1$) increases. The shock absorption system turns out to be more pliable ("soft"), but for receiving $A^э$ a stroke greater than the normal value of $s^э$ is required, and for receiving A^{max} stroke $s_к$ will turn out to be insufficient, as a result of which at the end of the stroke a rigid impact and breakage of the landing gear can occur.

2. Cases which lead to increase in the curve of $P_г=f(s)$ (Fig. 10.18b):

a) the initial gas pressure in a shock absorber is $p_{г0}>p_{г0\ норм}$, and the volume of the liquid corresponds to the rated volume thus $v_0=v_{0\ норм}$;

b) $p_{г0}=p_{г0\ норм}$, but the volume of the liquid is greater than the normal volume, thus the initial volume of the gas is $v_0<v_{0\ норм}$.

In these cases of the diagrams of gas resistance $P_г$ and as experiments show, the diagrams of P_a are higher than corresponding diagrams with the correct filling of the shock absorber. The compression of the shock absorber under given loads is reduced. The shock absorption becomes more "rigid." Energies $A^э$ and A^{max} are received at lesser magnitudes of the stroke, than $s^э$ and s^{max}, but with greater values of g-forces and forces dangerous for the strength of the landing gear and other components of the aircraft.

The state of a shock absorber changes during operation. This can also be reflected in the properties of shock absorption. Let us dwell on certain examples.

1. When an aircraft is parked after landing the temperature of a shock absorber gradually changes to the value of the temperature of the air. In this case the pressure and the volume of the gas in a shock absorber follow the law of $p_г v=RT$. When parked the load on a shock absorber is constant: $P_a=P_{a.ст}$.

If $P_{a.ст}>P_{a0}$, then a shock absorber when the aircraft is parked is compressed by $s_{ст}$. In this case $p_г=const$, and with an increase in the temperature the volume of the gas increases and, thus, compression is reduced.

If $P_{a.ст}\leq P_{a0}$, then in a shock absorber the initial gas pressure increases and its characteristic change as in the case of an increase in pressure during filling.

2. A shock absorber with non-isolated gas and liquid chambers changes its properties somewhat after the first compression. The liquid, passing through the small apertures, becomes foamy, and

its resistance is reduced; a shock absorber with low compressions s becomes "softer." However, with large s (upon encountering uneven areas), when all the froth passes through the apertures, the impact of the driving piston occurs against the liquid.

3. After a large number of landings in shock absorbers highly loaded with flexure, the frictional resistance can be increased. This is explained by the deterioration in the state of the friction surfaces of the shock absorber - by scoring and corrosion.

§ 10. DESIGN AND LOAD-BEARING SETUPS OF LANDING GEAR

The load-bearing setup of a landing gear determines the method of receiving and transmitting the loads acting on it. In accordance with this criterion all types of landing gear can be divided into three groups:

truss (pyramidal);

beam;

semicantilever-beam or truss-beam.

Wheel axles of **truss landing gear** are attached to the rods of the truss and are loaded with flexure and torsion. The remaining rods operate in axial forces; the shock absorber is usually included among the rods (Fig. 10.19).

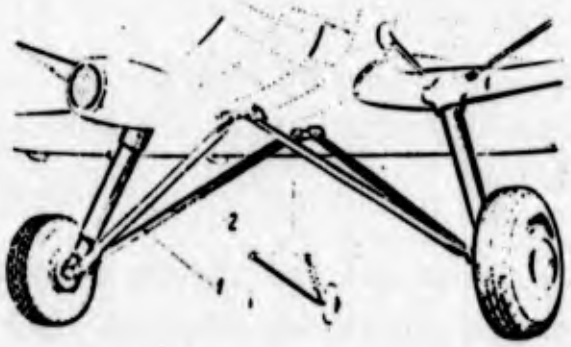

Figure 10.19. Truss landing gear of the An-2 aircraft: 1 - shock absorber; 2 - struts.

The advantage of a truss landing gear is the simplicity of its design and its light weight. However, to make this type of landing gear retractable in flight is difficult, and sometimes even impossible. Thus the truss type landing gear is finding application at the present time only for light low-speed aircraft and helicopters.

The beam landing gear is made with a strut in the form of a cantilever beam (Fig. 10.20). The design of a beam landing gear is simple and compact, but it has increased weight due to the loading with great flexural and torsional moments. In the case of the direct attachment of the wheels to the shock absorber rod its flexure leads to a considerable increase in the friction between the rod and the cylinder. Thus for a beam landing gear the lever suspension of the wheels is frequently employed which makes it possible (completely or partially) to relieve the shock absorber of flexure (see Fig. 10.13b, c, d).

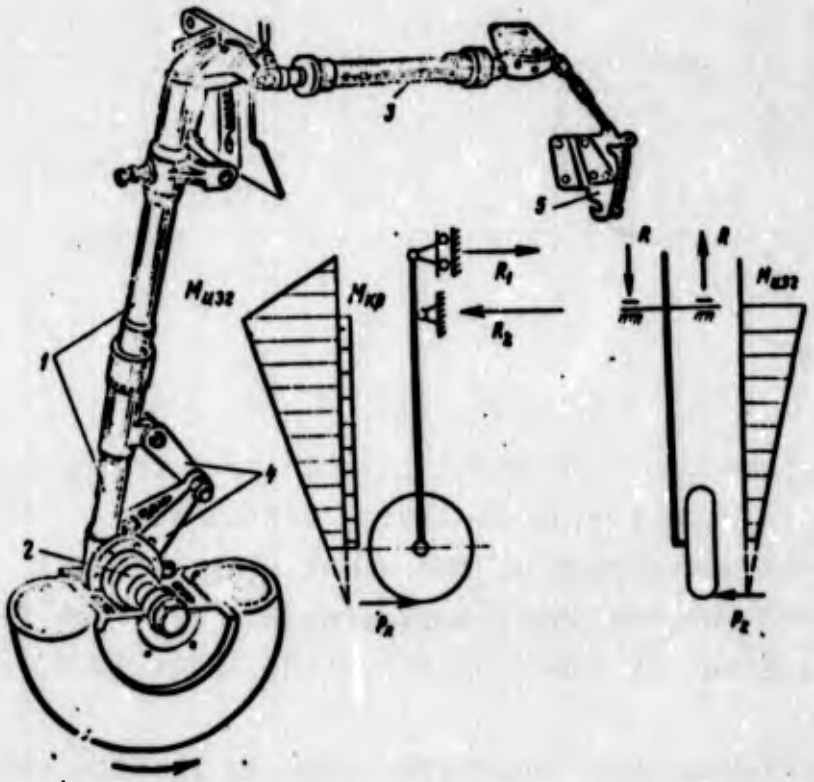

Figure 10.20. The beam landing gear of the Yak-18 aircraft: 1 - shock absorber; 2 - semi-axle; 3 - retractor; 4 - torsion link (torque arms); 5 - the retracted position lock.

The design of landing gear of medium and heavy aircraft in the majority of cases is made in accordance with a semicantilever-beam load-bearing setup. In it the beam-strut of the landing gear for reducing the flexural moments rests on lateral and front or rear struts (Fig. 10.21). The setup with the front strut which operates in the case of braking and frontal impacts in tension, is more favorable in a weight regard. However, the conditions of the arrangement of the landing gear on an aircraft and the kinematics of its retraction frequently lead to the need for installing a rear strut.

Figure 10.21. Semicantilever-beam landing gear of the Il-18 aircraft: 1 - carriage; 2 - shock absorber; 3 - lateral struts; 4 - cross piece; 5 - rod; 6 - retractor; 7 - rear strut; 8 - stabilizing damper of the carriage.

The attachment of the wheel to the strut or the lever of the landing gear is made in the following variants:

cantilever attachment of the wheel (Fig. 10.22a);

attachment of the wheel employing a wheel fork (Fig. 10.22b);

the attachment of wheel on poluvilke (Fig. 10.22c).

These variants are encountered both in landing gear with direct attachment of the wheel to the shock absorber as well as

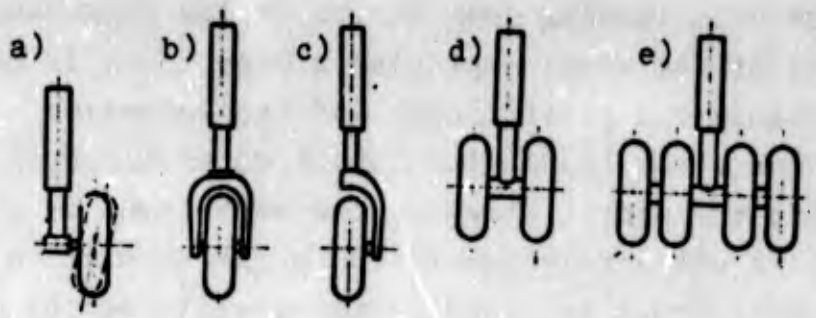

Figure 10.22. Setups for the attaching of wheel to the shock absorber rod.

in landing gear with a lever setup. Each of them has its advantages and disadvantages.

In the case of the cantilever attachement of the wheel to the shock absorber rod the height of landing gear can be minimum, since the rod begins at the wheel axle. At the same time the forces acting in the plane of the wheel cause additional flexure of the strut in the lateral plane, and if they are not parallel to the strut, then they also twist it. To reduce the flexural moment (reduce the vertical force arm) the arrangement of a wheel with a slight inclination to the strut axis is sometimes employed - "tilting of the wheels" (this is indicated with the broken line in Fig. 10.22a). For this purpose it is more advantageous to install the wheel on the external side of the strut, since during a landing with lateral impact or during sharp turning of the aircraft during taxiing (load cases $R_{1ш}$ and $R_{2ш}$) the moment from the lateral force F will counteract the flexural moment from the effect of force P.

The attachment of a wheel employing a wheel fork is broadly employed for the orienting nose and tail landing gear struts of light aircraft. This type of wheel attachment does not cause additional flexure and torsion due to the forces acting in the plane of the wheel. Its deficiency is the great length of the strut, since the shock absorber is positioned above the wheel

fork. For the main landing gear struts of low wing monoplanes the attachment of the wheel employing a wheel fork is more rarely encountered, since the great length and the increased transverse dimension of the strut impede its layout on an aircraft and its retraction into the wing. However, the employment of this type of attachment is completely justified by the retraction of the main landing gear strut into the engine nacelle on the wing of a high wing monoplane, for example on the Be-30 aircraft.

The attachment of a wheel on a half-fork, ensuring the minimum transverse dimensions of the landing gear strut, facilitates its retraction; however, the more severe conditions of the operation of the half-fork in flexure and torsion as a result of the cantilever attachment of the wheel axle lead to an increase in weight.

For medium and heavy aircraft the employment of multiwheel landing gear is characteristic.

This is due to the following reasons:

increasing the number of wheels with the same load on a landing gear strut leads to a reduction in their dimensions and weight, and makes it possible to decrease the overall dimensions of the landing gear and also simplifies its retraction;

a multiwheel landing gear distributes the load incident on it over a large area; this makes it possible to reduce the thickness of the artificial covering on runway surfaces;

as a result of the better cooling of the braking systems of smaller wheels the conditions of heat transfer from the brakes are improved; thus, their total energy bearing capacity is increased, which makes it possible to decrease the landing run of the aircraft;

the failure of one of the pneumatic tires of a multiwheel landing gear does not result in an airplane crash.

Different variants of multiwheel struts are encountered. Thus, for the nose and main landing gear struts of aircraft of medium weight the paried arrangement of wheels on a common axle is broadly practiced (Fig. 10.22d). In the landing gear of heavier aircraft carriages are employed (see Fig. 10.21) and more rarely a quadrupled wheel arrangement (Fig. 10.22e).

The usually employed biaxial carriages with a paired wheel setup on each axle have a rigid frame attached hingewise to the shock-absorbing strut, for uniform load distribution between the front and rear wheels (see Fig. 10.21). In flight the carriage is fixed relative to the strut with the aid of a stabilizing shock absorber. Its prestressing should be sufficient in order to keep the carriage from rotating in flight under the effect of the moments due to the aerodynamic and mass forces. At the same time the stabilizing shock absorber should make it possible for the carriage to be turned to maintain the constant contact of the front and rear pair of wheels with an uneven airfield surface.

Another characteristic element of the design of landing-gear carriages is the compensation mechanism. In its absence the moment of friction forces T relative to joint O, which arises during the braking of the wheels or during motion over sloppy ground (Fig. 10.23a), leads to an increase in the ΔP of the load on the front wheels and to the relieving of the same force from the rear wheels. Depending on the braking intensity, the magnitude of the foces $\Delta P = \Sigma Th/l$ can be 0.3-0.8 of the parking wheel load. This type of load redistribution increases the wear on the pneumatic tires, reduces braking effectiveness and has a negative effect on the ground performance of the aircraft on a dirt airfield.

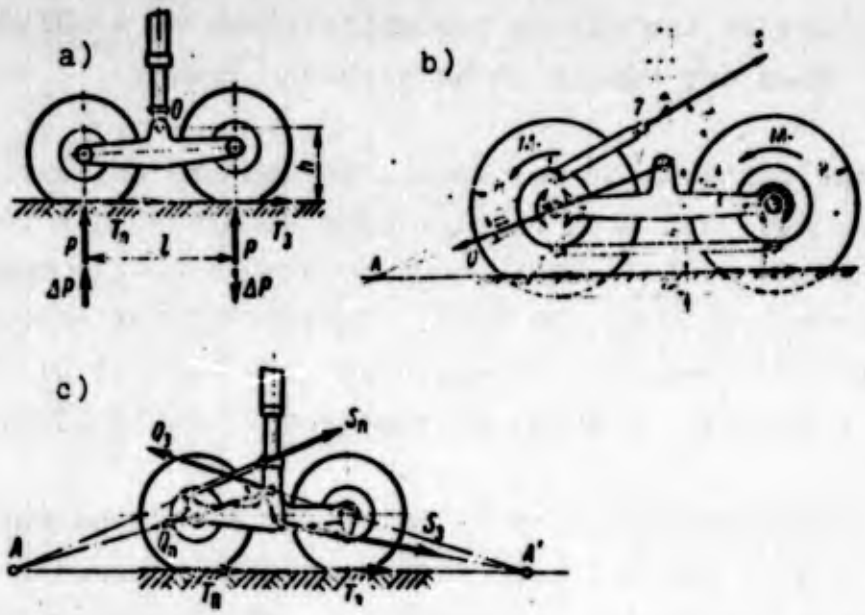

Figure 10.23. Explanation of the operation of a landing-gear carriage: a) in the absence of a compensation mechanism the moment of the friction forces increases the load on the front wheels of the carriage and decreases the load on the rear wheels; b) carriage compensation mechanism. The moments of friction forces T relative to joint O are balanced by the moment of the reaction force applied to point 2; c) carriage with separate compensation mechanisms for the front and rear pair of wheels.

The compensation mechanism operates in the following manner (Fig. 10.23b). The wheel axles together with the braking mechanisms are freely mounted in the carriage frame assembly and are kept from twisting and turning by the rods and levers of the compensation mechanism. During braking reaction S arises in the upper rod 1-2 whose moment counteracts the moment of friction forces T.

By equating to zero the sum of the moments relative to joint O and considering that the moments from vertical forces P are mutually balanced, we obtain the equation of the equilibrium of the carriage $\Sigma Th-Sb=0$. If it is considered that

$$h=R-\delta+c;\quad \Sigma T=\frac{\Sigma M_T}{R-\delta}\quad \text{and}\quad S=\frac{\Sigma M_T}{a},$$

where R is the radius of an uncompressed pneumatic tire; δ is the magnitude of tire compression; ΣM_T is the total braking moment, then it follows from the equation of equilibrium that the condition of uniform loading of the carriage wheels under the effect of forces T will be

$$\frac{b}{a} = 1 + \frac{c}{R - \delta}.$$

By analyzing this expression, it is possible to draw the following conclusions.

1. The operation of the compensation mechanism does not depend on the magnitude of the braking forces and is determined only by the geometric relationships of the elements of the carriage and mechanism.

2. Complete uniformity of wheel loading under the effect of forces T occurs only at a specific magnitude of tire compression.

The required position of rod 1-2 can also be determined graphically by examining the equilibrium of the carriage under the effect of three forces - the friction forces ΣT, forces and the reactions Q of the carriage axis of rotation O. In order that the lever attaching the front brakes does not turn, the resultant of the forces ΣT and S should pass through the axis of the front wheels.

At the same time in order that the carriage does not turn, this force should also pass through axis O. The equilibrium condition of the carriage is the intersection of the line of the effect of these three forces at one point A.

Other variants of the positioning of the rods and levers of the compensation mechanism are also possible. One of them is shown in Fig. 10.23c. Here the transfer of the braking moments to the shock absorber rod is carried out separately from the front and rear wheels of the carriage.

§ 11. CALCULATING LANDING GEAR STRENGTH

The rating of a landing gear for strength is carried out, as a rule, for the case of landing and the motion of an aircraft over the ground (E, R_1, G, R_2, M, etc.).

Flight cases are examined in rating the landing-gear retraction mechanisms.

The initial data for rating a landing gear for strength are:
the loads determined in accordance with the stress standards;
drawings of landing gear in the lowered position.

The rating of landing gear for strength is carried out in the following sequence.

1. The drawing of the landing gear design with an indication of the axes of the rods, joints and units. Figure 10.24 depicts a very simple example of a rated landing gear setup.

Figure 10.24. For determining the reactions and the forces in landing gear design.

2. Determination of the reactions and the breakdown of the reactions and loads along the axes, connected with the design setup.

3. Determination of the forces and drawing of the diagram of the axial and transverse forces N and Q, of flexural and torsional moments $M_{изг}$ and $M_{кр}$ for the elements of the design setup. The main forces are $M_{изг}$ and $M_{кр}$, since the greatest loading arises from them.

In determining the reactions and forces and in drawing the diagram of the flexural and torsional moments known methods of structural mechanics and strength of materials are employed.

4. Strength testing.

Let us examine certain characteristics of determining the reactions and forces for the individual parts of a landing gear design.

1. Figure 10.24a shows a graphic determination of the reactions of the units attaching a landing-gear strut. First point c is found - the intersection of the known directions of forces P and R_A. Reaction R_B should pass also through c, since the three forces in equilibrium should intersect at one point. The magnitudes of the reactions are found by plotting an equilibrium triangle.

2. The directions and the magnitudes of the reactions of the lever of the lever suspension are found in a similar manner (Fig. 10.24b).

3. If the joint attaching the brace to the strut lies on the strut axis at F, then the diagram of $M_{изг}$ it has a break at this point f. If the joint is positioned with eccentricity at E, then the upper part of the diagram remains without changes up to the level DE (up to d), and the lower part, since in section FD no forces are applied, continues linearly up to e, where $M_{изг}$ is varied by an abrupt change (see Fig. 10.24a).

4. The flexural moment in the cross section of the shock-absorbing strut is

$$M_{изг} = M_{ш} + M_{ц},$$

where $M_{ш}$ and $M_{ц}$ are the flexural moments in the cross sections of the rod and cylinder.

Accordingly the diagram of $M_{изг}$ of the strut in Fig. 10.24c is divided into diagrams of the rod and the cylinder.

The dividing line ab is drawn on the basis of the following considerations:

in cross sections A and B, where the rod rests against the cylinder, concentrated forces of interaction act; thus the diagram of the rod opposite these cross sections has a break; the diagram of $M_ш$ in section AB is rectilinear (ab), since no transverses are applied to the rod;

below cross section A we have $M_{изг}=M_ш$; this determines the position of point a;

above B everywhere $M_{изг}=M_ц$, and $M_ш=0$; this determines point b.

The ordinates of diagram $M_ш$ are counted from break abc along the normal to bc.

5. Torque line BDE (Fig. 10.25) serves to transmit moment M_y from the rod to the cylinder which tends to turn the rod.

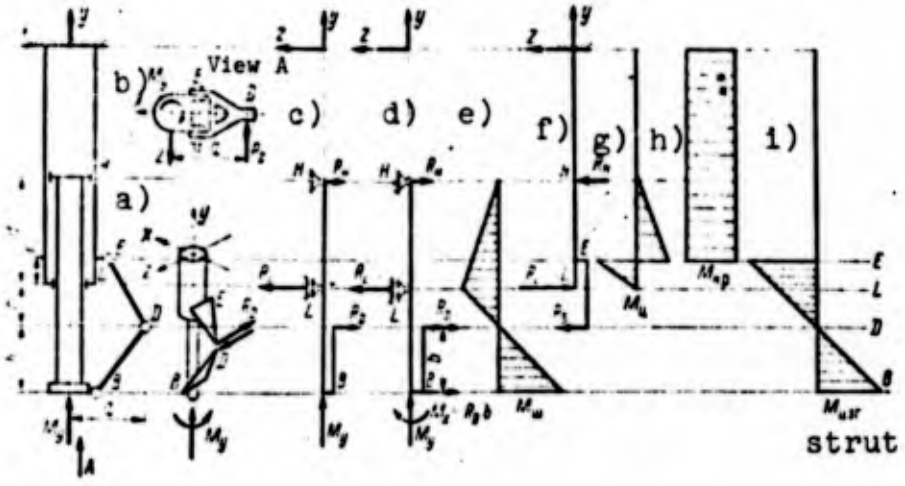

Figure 10.25. The transmission of M_y through the torsion link.

The forces of interaction of the links (Fig. 10.25a)

$$R_D = \frac{M_y}{a}$$

cause the flexure of the links in their planes and the flexure of the rod and the cylinder in plane yz (relative to x).

Figure 10.25c and d shows rod loading diagrams, and Fig. 10.25f - a cylinder loading diagram. Figure 10.25 also depicts their projection diagrams (e, g, h, i).

The projection diagram (i) of the total $M_{изг}$ of a strut is placed in section BE of the strut, where M_y is transmitted through the flexure of the strut and the links. Above cross section E moment M_y loads the cylinder with torsion $M_{кр}=M_y$ (projection diagram h).

The projection diagrams of rod flexural moments $M_ш$(e) and of cylinder flexual moments $M_ц$(g) are continued above E up to the cross section at level H where the flexure caused by the transmission of M_y ends.

In section EH

$$M_{изг} = M_ш + M_ц = 0; \quad M_ц = -M_ш; \quad M_{кр} = M_y.$$

Let us examine the characteristics of the strength testing of a landing gear design.

A landing gear shock absorber with direct wheel attachment is found in the most complex stress case; it is subjected to the effect of flexure, torsion and internal pressure.

If we cut an element of the wall from a shock absorber cylinder, then the normal and tangential stresses shown in Fig. 10.26 will act on its faces:

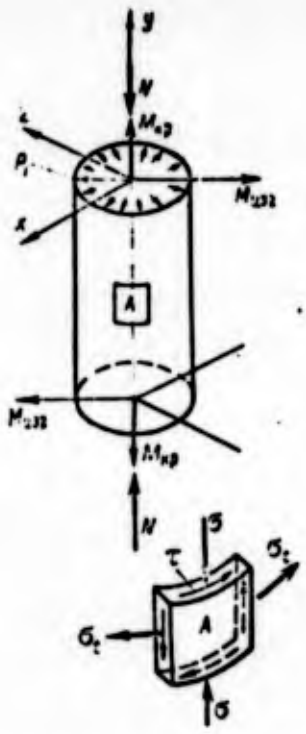

Figure 10.26. The loading and the stressed state of a shock absorber cylinder of a telescopic strut.

σ - the normal stress in the cylinder walls due to $M_{изг}$; τ - the tangential stress due to $M_{кр}$; σ_t - the tangential normal stress arising as a result of the effect of the internal gas pressure $p_г$.

Their magnitude is computed with the following formula

$$\sigma_t = p_г \frac{D}{2\delta},$$

where D - the diameter of the cylinder along the center line; δ - the cylinder wall thickness.

From the found stresses σ, σ_t and τ it is possible to determine the main stresses σ_1 and σ_2 (σ_3 is taken as equal to zero).

$$\left.\begin{matrix}\sigma_1\\ \sigma_2\end{matrix}\right\} = \frac{1}{2}\left[(\sigma_t + \sigma) \pm \sqrt{(\sigma_t - \sigma)^2 + 4\tau^2}\right].$$

It is possible to carry out strength testing in accordance with the third theory of strength. The following inequality will be a condition of strength in its employment

$$\tau_{max} = \frac{\sigma_1 - \sigma_2}{2} \leqslant \tau_в.$$

In this case σ_1 and σ_2 are taken from calculated destructive loads.

Since according to the third theory of strength $\tau_в = \frac{\sigma_в}{2}$, then the condition of strength can be represented in the following form

$$\sigma_{прив.} \leqslant \sigma_в,$$

where $\sigma_{прив} = \sigma_1 - \sigma_2$.

The greatest value of $\sigma_{прив}$ will be in the cylinder where compressive stresses act $\sigma_{изг}<0$ (see Fig. 10.26).

§ 12. KINEMATIC SETUPS AND ELEMENTS OF THE MECHANISMS FOR RETRACTING AND LOWERING LANDING GEAR

The majority of contemporary aircraft has landing gear which retract in flight. The kinematic setups of its retraction and lowering are worked out taking into account the general layout of the aircraft, the permissible range of the operational positioning of the center of gravity of the aircraft, the presence of sufficient of free volume for accommodating the landing gear in the wing or fuselage, the arrangement of the basic load-bearing elements of the airframe, etc.

Two setups for the retraction of the main landing gear struts are most broadly employed (Fig. 10.27):

retraction in the transverse plane (retraction sideways);

retraction in the longitudinal plane, parallel to the plane of symmetry of the aircraft.

In the case of retraction in the transverse plane the position of the center of gravity of the aircraft barely changes, but the presence of large free sections in the wing is required (Fig. 10.27c) or nonhermetic sections in the fuselage which decrease the volume for accommodating cargo (Fig. 10.27a, e).

Retraction of the landing gear in the direction of the wing tip (see Fig. 10.27c) requires a sufficient height of the wing profile and, as a rule, is employed only in those cases when retraction in the direction of the fuselage is not possible (for example, in the case of installing engines in the root part of the wing).

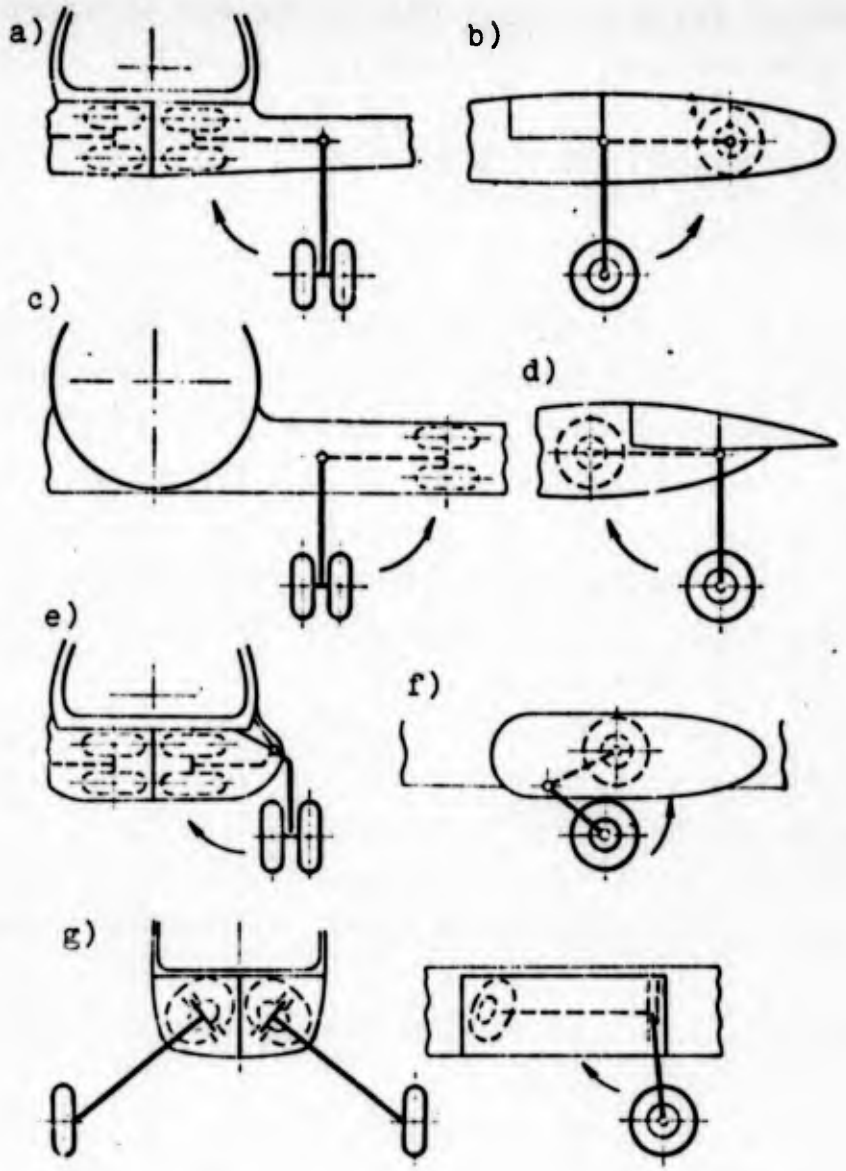

Figure 10.27. Setups of the retraction of main landing gear struts.

Retraction of the landing gear forward (Fig. 10.27d) in the direction of the nose of the aircraft is more rational for the following reasons:

the position of the center of gravity is favorably changed. The displacement of the center of gravity forward improves the longitudinal stability of the aircraft in cruising flight, and at the same time the more rearward positioning of the center of gravity (within permissible limits) with the landing gear lowered decreases the required deflection of the elevator during landing;

the system of emergency lowering of the landing gear is simplified. The impinging air flow assists in the lowering of the landing gear and to the locking of the landing gear in the lowered position;

in the case of the positioning of the landing gear in the wing after retraction it forwards it plays the role of an anti-flutter weight.

The landing gear setups shown in Fig. 10.27e, f, are applied in high wing monoplane aircraft, when the attaching of the landing gear to the load-bearing elements of the wing framework is undesirable due to an increase in the height and weight of the strut. However, in this case it is not possible to obtain large track landing gear.

The landing gear setup shown in Fig. 10.27g is encountered on light aircraft with upper and intermediate positioning of the wing. The direction of the axis of rotation of the landing gear is selected so that during longitudinal motion the retraction of the wheel into the fuselage occurs.

The examined retraction setups for the main landing gear struts (see Fig. 10.27) are simple, since the rotation of the strut occurs only relative to one axis. However, the layout conditions which require reducing the overall dimensions of the landing gear bays in the retracted position also lead to the need for employing more complex kinematic setups in which retraction is accompanied by the rotation of the wheels or carriage relative to the shock-absorbing strut. This rotation can take the place either due to the kinematic connection of the elements being rotated with other parts of the strut or with the design of the aircraft, or by employing individed hydraulic power cylinders.

The front and tail landing gear struts are retracted into the fuselage by rotating in the plane of symmetry of the aircraft. For the front struts as for the main struts, it is more advisable to retract them forward, although this also leads to a certain decrease in the landing gear base.

The retraction and lowering of landing gear are accomplished employing the hydraulic, gas and electrical power systems of the aircraft. The power of the system should ensure the retraction and the lowering of the landing gear in a given time and at a given flight velocity in turbulent air. In order to eliminate the possibility of the "sticking" of the landing gear, the power calculation of the retraction and lowering mechanisms should encompass both the extreme and intermediate positions of the strut.

The retractor of the landing gear strut cannot be included in its load-bearing setup and can be employed only for the retraction and lowering of the landing gear (Fig. 10.28). In such a case when the retractor performs the role of a load-bearing brace (Fig. 10.28c), the design of the support is somewhat simplified, but the dimensions and the weight of the retractor are increased, since during a landing and motion over an airfield large loads will be transmitted to it.

Landing-gear should be held in the retracted and lowered position by mechanical locks mounted on the load-bearing elements of the airframe adjoining the landing gear, or by locks which lock the retractor rod (Fig. 10.28).

The load-bearing lock which holds the shock-absorbing strut (Fig. 10.28a) or brace (Fig. 10.28b), the lock which locks the retractor rod (Fig. 10.28c), the locks and the devices which maintain the extended position of the collapsible brace (Fig. 10.28d, e, f) can be the lowered-position lock preventing the folding up [collapse] of the landing gear on the ground.

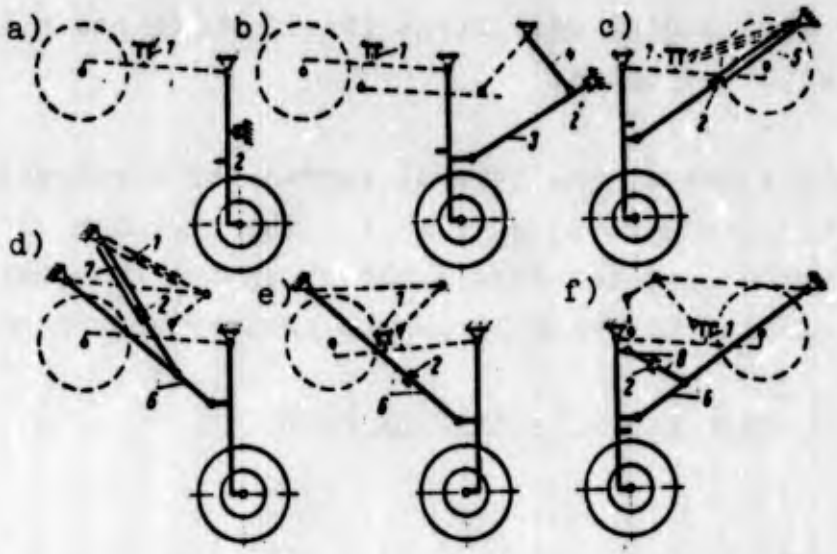

Figure 10.28. Kinematic setups of landing gear retraction and the positioning of locks: 1 - retracted position lock; 2 - lowered position lock; 3 - strut; 4 - guide rod; 5 - strut retractor; 6 - articulated strut; 7 - retractor, also serving for the thrusting on articulated strut; 8 - mechanism for thrusting on articulated strut (retractors which are not included in the load-bearing setup and which do not play the role of locks, on setups not shown).

The retracted-position locks and the design elements, to which they are attached are rated for the effect of the mass forces due to the weight of the landing gear in loading cases A and D, and the lowered-position locks are rated for the loads acting during landing and during motion over the ground. During flight sections of the wing, the fuselage or special fairings into which the landing gear struts are retracted, are covered with doors. To reduce drag during takeoff and to protect the internal volumes of these sections from becoming dirty the doors are also usually closed when the landing gear are extended and they are opened only during the retraction or the lowering of the landing gear. The control of the movement of the doors is interconnected with the control of the retraction and the lowering of the landing gear and is accomplished either with power mechanisms of the aircraft power system (by power cylinders, electric motors), or

directly by the landing gear strut itself which has a kinematic connection with the doors.

Beside the doors, the lateral surface of a retracted wheel can also cover the landing gear well. The circular clearance between the wheel and the framed cutout in the fuselage or wing is pressurized in this case by shaped pressurized chambers.

§ 13. FRONT, TAIL AND AUXILIARY LANDING GEAR STRUTS

The front, tail, subwing, safety tail wheel struts of landing gear are loaded with smaller loads, than the main landing gear strut, but the functions performed by them are the same: they support the flight vehicle on the ground and receive the landing shocks and the shocks due to the aircraft's motion over the ground.

By virture this their design in the majority of cases contains the same basic elements: wheels, shock-absorbing struts, retraction mechanisms. At the same time the conditions of loading and attachment affect their load-bearing setups and design shapes.

Let us note the basic design characteristics of these struts.

In the design of tail struts, due to their low height, the lever suspension is more frequently encountered with the attachment of a wheel or a ski to it. The struts are oriented and have a stop.

The designs of subwing struts of aircraft with bicycle landing gear are made with soft shock absorbers, which is ensured by a low coefficient of prestressing n_0 (n_0 pertains to the load on a strut when parked with bank). This is especially important for struts located on the types of swept wings, because in the case of landing with a high angle of attack they can touch the ground together with the main struts.

The loading characteristics are taken into account in designing a shock absorption system and in selecting the wheels for the front struts. The initial load is that load acting dynamically on strut $P_{оп.дин.}$ In accordance with the strength standards this load is taken to be greater than the parking load and consists of up to 0.25 $G_{пос}$. It is determined from examining the types of loading shown in Fig. 10.29, and also (with large e/b) from examining the tilting over onto the front strut during a landing.

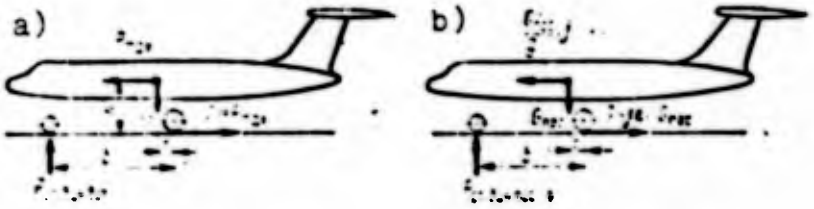

Figure 10.29. Conditions of loading of the front landing gear strut: a) at the beginning of the takeoff run; b) at the end of the landing run with braking.

At the beginning of the takeoff run (Fig. 10.29a)

$$P_{оп.дин.взл} = G_0 \frac{e}{b} + \frac{Th}{b},$$

where $T=P_{max}$; P_{max} - the maximum engine thrust when the aircraft is still parked or at rest.

At the end of the landing run with braking (Fig. 10.29b)

$$P_{оп.дин.пос} = G_{пос} \frac{e}{b} + \frac{Th}{b},$$

where $T=\frac{G_{пос}}{g} j \leq \mu_т G_{пос}$; $\mu_т$ - the coefficient of friction; j - the braking acceleration.

The lower part of the front strut with the wheels should be made oriented. In this case the advange of a landing gear with a front strut is realized - mobile stability. The control of the turning of the front strut is employed for controlling the aircraft during taxiing.

The front landing gear strut can be made both in accordance with a setup with direct attachment of the wheels to the shock absorber and with lever suspension of the wheels.

The setup with direct attachment of the wheel to the shock absorber is advisable when a high landing gear is employed (in propeller aircraft). Lever suspension ensures the possibility of impact shock absorption in any direction in the wheel plane.

The basic parameters characterizing the positioning of the wheels of a front landing gear strut are as follow:

the angle of inclination of the axis of rotation (orientation axis) α;

the projection of the wheels t (Fig. 10.30a).

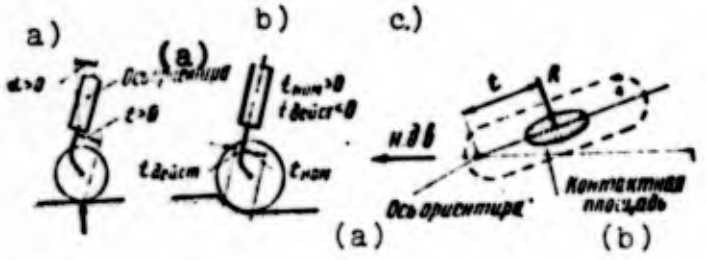

Figure 10.30. Front landing gear strut: a) setup; b) the projection is displaced during motion over soft ground; c) the effect of the projection on stability.
Key: (a) Axis of orientation; (b) Contact area.

In the case of the direct attachment of the wheels to the shock absorber the axis of the shock-absorbing strut can be inclined forward at an angle of α. However, at a positive angle of inclination α the wheel has the tendency to turn when the aircraft is parked or at rest.

In contemporary setups of front struts in all types of wheel attachment the axis of orientation is positioned vertically.

Magnitude t is called the projection of the wheels of the front strut, or the stability arm. Positive projection corresponds to the positioning of the point of contact of the wheels against the earth behind the axis of orientation.

Positive projection ensures stability during the motion of the wheels over the ground (Fig. 10.30c). In the case of the deflection of the wheel plane at a certain angle from the direction of movement lateral force R arises, which creates a restorive moment on arm t, which tends to return the wheel to the previous position, which coincides with the direction of movement. Upon the designation of magnitude t it is assumed that in the case of movement over soft and uneven ground the point of contact of the wheel is displaced forward and at a nominal value of $t_{ном}>0$ the actual value of $t_{дейст}$ can become even negative (Fig. 10.30b). In this case the turning of the wheel crosswise to the motion is possible.

During the operation of aircraft on airfields with concrete runways and taxiways or with grass covering a value of relative projection $\bar{t}=\frac{t}{D}=0.08-0.1$ is sufficient to ensure stability of motion, where D - the wheel diameter.

During aircraft motion over an airfield the emergence of self-excited oscillations of the wheels relative to the axis of orientation is possible.

These types of oscillations are called "shimmy." Usually vibrations arise at high velocities of translatory motion of an aircraft over an airfield surface.

The nature of the oscillations and the velocity at which they appear depend substantially on the inertia forces of the oscillating masses. Front landing gear wheel strut shimmy is reminiscent by its nature of the self-excited oscillations of a wing and empennage - flutter - and it is an extremely dangerous type of oscillation, since it can lead to the breaking of the landing gear and as a result of this to a severe airplane crackup.

A number of works of Soviet scientists has been dedicated to the study of the vibrations of oriented wheels of a front landing gear strut. The purpose of these investigations was to establish the effect of different factors on the nature of the course of the phenomenon of self-excited vibrations, to determine the velocities at which they arise, i.e., the critical shimmy velocity $V_{кр}$ and to discovering the most effective measures for combatting this phenomenon.

M. V. Keldysh created the theory of self-excited vibrations of oriented wheels and derived the following formula for determining the critical shimmy velocity

$$V_{кр} = \sqrt{\frac{2C\bar{t}}{I}},$$

where C - the coefficeint characterizing the effect of the rigidity of a pneumatic tire in torsion; $\bar{t}$ - the relative projection; I - the mass moment of inertia of the parts of a front landing gear strut, turning relative to the axis of orientation.

Increasing the rigidity of pneumatic tires in torsion C and the projection of the wheel $\bar{t}$ contributes to an increase in the critical shimmy velocity. When $\bar{t} \geq 0.5$, oscillations practically do not arise.

For the purpose of increasing $V_{кр}$ the pneumatic tires with increased rigidity in torsion or paired wheels (rigidly sitting on one axle mounted in bearings) are employed; however, this somewhat negatively affects the controllability of an aircraft during its motion over the ground.

The most convenient and most effective means of combatting shimmy is by installing dampers - shimmy or oscillation dampers. Hydraulic oscillation [shimmy] dampers have received the greatest application. Their important advantage in comparision with other types of dampers (for example, dry friction dampers) is the fact that the moment created by them is proportional to the square of the angular velocity of the oscillations $\dot{\theta}$. Thus, hydraulic oscillation dampers have only a slight effect during taxiing (when $\dot{\theta}$ is small), but create considerable effective moment when wheel oscillations set in as $\dot{\theta}$ increases.

At the present time hydraulic piston dampers are mainly employed (Fig. 10.31).

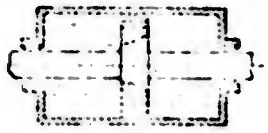

Figure 10.31. Shimmy damper.

Investigations show that the critical shimmy velocity decreases with an increase in wheel loading, with an increase in the coefficient of adhesion, with a decrease in the rigidity of the wheels and the strut, when play is present and in the case of incorrect filling of the damper (insufficient amount of liquid).

In contemporary designs of front landing gear struts in the case of the inclusion of turning control in the lower part of the strut the possibility of free orientation of the wheels is eliminated. In this case the damper is employed as a power control cylinder.

§ 14. HELICOPTER LANDING GEAR

1. Design Characteristics and Power and Load-Bearing Setups

The landing gear employed on helicopters and fulfilling the same function, as aircraft landing gear, have different setups.

Three-strut landing gear with two main and one front or tail struts, four-strut landing gear two main and two front, or landing gear, in which all four struts are main struts are encountered.

With respect to the load-bearing setup helicopter landing gear, just like those of aircraft, can be truss (pyramidal), beam and beam-semicantilever landing gear.

On single-rotor helicopters the main landing gear struts are frequently of the pyramidal type (see Fig. 10.19).

In the loading of this type of landing gear the shock absorber is compressed and all sides of the pyramid change their position in space; thus the joining of the landing gear rods with each other and the fuselage is accomplished employing hinge joints.

The front landing gear struts are most frequently made in accordance with the beam setup with lever attachment of the wheel (Fig. 10.13b, c, d).

The wheels of the front strut are always made self-orienting; this ensures maneuvering freedom during taxiing. Automatic positioning of the wheels with respect to flight direction after the lift off of the helicopter from the ground is provided for.

Depending on the purpose and the weight of the helicopter semiballoon type tires or arched tires and more rarely high-pressure tires are mounted on the landing-gear wheels.

The wheels of the main landing gear struts of helicopters have brakes for shortening the landing run after a nonvertical landing and for preventing the rolling of the helicopter upon landing on an inclined site.

The landing gear of helicopters are mainly made nonretractable in flight and the parts are covered with fairings to reduce parasite drag. But in connection with increasing the maximum velocity of helicopters retractable landing gear are beginning to be installed on them.

On light helicopters, for their landing on water, snow or moisture-saturated ground instead of wheeled landing gear floats or pontoons are being installed. Skid or ski landing gear are now finding application.

There are cases of the employment of mixed takeoff-landing devices (wheel and float types), as a result of which the possibilities for the employment of helicopters are being considerably expanded.

2. The Positioning of Landing Gear on Helicopters

The basic parameters characterizing the positioning of landing gear on helicopters, in connection with the two most broadly employed helicopter setups with one and two rotors (see Fig. 10.32a, b), are given in Table 10.2.

3. Helicopter Ground Resonance

The shock absorbers of the main landing gear struts, besides carrying out their basic purpose - the receiving of the impact energy of a helicopter against the ground during a landing, during taxiing, takeoff run and landing run, should also damp the auto-oscillations of the helicopter; called ground resonance.

Ground resonance is self-excited oscillations of a helicopter arising as a result of the interaction of two oscillating systems: the helicopter on its elastic landing gear and the blades of the rotor relative to the drag hinges.

Table 10.2

Parameters		Single-rotor helicopter, three-strut landing gear with a nose strut (Fig. 10.32a)	Double-rotor helicopter with tandem arrangement, four-strut landing gear (Fig. 10.32b)
Angles of forward projection of the landing gear, deg.	$\lambda_н$	30–45	0–20
	$\lambda_г$	12–25	27–48
Tilting angle θ, deg		8–15	10–35
e/b		0,15–0,25	0,4–0,5
Landing gear track B		(0,2–0,25) $D_{н.в}$ (0,75–0,95) H	(0,7–1,3) $H_н$
Height of the rotor above the ground H, $H_п$		(0,2–0,3) $D_{н.в}$	(0,2–0,3) $D_{н.в}$
Landing gear base b		--	(0,4–0,75) $l_{ос}$
Distance between rotor axes $l_{ос}$		—	(0,6–0,98) $D_{н.в}$

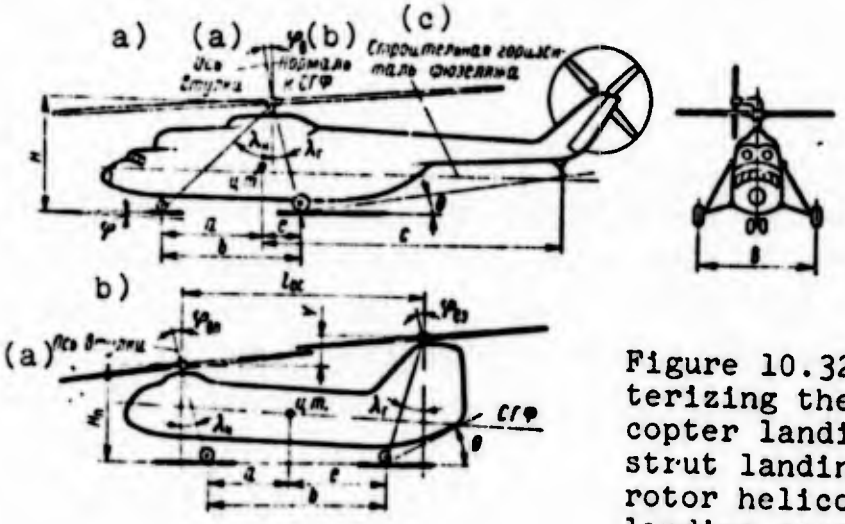

Figure 10.32. Parameters characterizing the positioning of helicopter landing gear: a) three-strut landing gear of a single-rotor helicopter; b) four-strut landing gear of a twin-rotor helicopter with a tandem setup. Key: (a) Hub axis; (b) Normal to fuselage center line; (c) Fuselage center line; (d) c.g.

Ground resonance arises in the following manner. In the event of an unsymmetric impact of a helicopter landing gear against the ground the blades receive different angular displacements relative to the drag hinges. The general center of gravity of the rotor in this case is displaced relative to the axis of rotation. A large magnitude unbalanced centrifugal rotor force arises, - a perturbing force,- which bounces the helicopter. If the frequency of the perturbing force is equal to the natural frequency (or close to it) of the oscillations of the helicopter on the landing gear, then the phenomenon of ground resonance arises. In this case the bouncing of the helicopter (amplitude of oscillations) increases, the unbalanced centrifugal force on the rotor is increased and the prerequisite is created for increasing the oscillations. Oscillations with increasing amplitude in the presence of ground resonance can lead to the destruction of the helicopter.

There are two basic methods of combatting ground resonance:

1) damping of these oscillations;

2) varying the natural oscillatory frequencies of the helicopter on the landing gear for the purpose of bringing out of the zones of instabilities, in which the emergence of ground resonance is possible, beyond the limits of the operating revolutions of the rotor.

Oscillation damping is provided for by placing oscillation dampers in oscillatory systems. In an oscillatory system the "suspended rotating vanes of the rotor" dampers are the oscillation dampers of the drag hinges.

In a "fuselage on an elastic landing gear" system the dampers are the landing gear shock absorbers, which damp the fuselage oscillations during the compression of the shock absorber as a

result of the overflowing of the fluid in the shock-absorbing struts through the apertures and as a result of the friction forces in the seals.

4. Design Characteristics of Helicopter Shock Struts

In designing a helicopter the rating of the shock absorbers is usually carried out for the landing case with the subsequent checking for the possibility of ensuring damping by them during the oscillations of the helicopter.

The rating of a shock absorption system for the landing case is determined by the stress standards of the helicopter and in content is mainly analogous to the rating of a shock absorption system of an aircraft landing gear.

The main difficulty arising in the designing of a helicopter landing gear is the creation of a shock absorber with parameters which ensure both the receiving of standardized operation during landing and the necessary damping of the auto-oscillations of the helicopter.

It can be that the dimensions of the apertures through which the liquid flows in the operation of a shock absorber, rated (the apertures) for landings conditions, will be unsuitable for damping the transverse oscillations of the helicopter, i.e., for preventing ground resonance.

In this case into the landing gear system whose shock absorber was selected for helicopter landing conditions, special devices are introduced which make it possible to obtain additional damping or to change the natural oscillatory frequency of the helicopter on the landing gear removing in this way the critical revolutions $n_{крит}$ from the operating range of the rotor revolutions.

Certain recommendations and design measures employed in landing gear design for eliminating ground resonance are examined below.

The employment of shock-absorbing struts with a small prestressing force. For a helicopter landing gear it is desirable to have as small as possible prestressing forces P_{a0}, since with great rotor thrust the forces P on the landing gear are reduced and when $P<P_{a0}$ the shock absorbers are straightened out and do not operate as dampers. This can lead to the appearance of ground resonance during the landing run.

Thus, for a helicopter landing gear it is recommended that the parameters be selected so that the prestressing force is not more than 10% of the parking load on the shock absorber with zero rotor thrust.

Shock absorbers with this type of prestressing will have low initial pressure in the gas chamber and a considerable rod stroke.

Increasing the damping in the reverse shock absorber stroke. The dimensions of the apertures through which the liquid flows in the forward stroke of a shock absorber (compression), are selected with respect to landing conditions, and the dimensions of the apertures through which it flows in the reverse stroke (straightening) - are selected from the conditions of ground resonance.

Since with oscillations of a helicopter at each moment in time one of the shock-absorbing struts (right or left) is accomplishing a reverse stroke, then the necessary damping of the helicopter can be ensured.

However, it is possible to increase the damping in the reverse stroke only within certain limits, otherwise the

straightening of the shock-absorbing strut form the compressed state after an impact on the earth will be very slow and it will not have time to prepare for the subsequent impact.

The installing of special valves in a shock absorber design (Fig. 10.33b). A special spring valve is installed in a shock absorber which is opens only when the compression force in the shock absorber exceeds (upon impacting with the earth) a certain critical value $P_{крит}$. When $P_a < P_{крит}$ additional large-diameter apertures, selected from conditions of g-forces during landing, open.

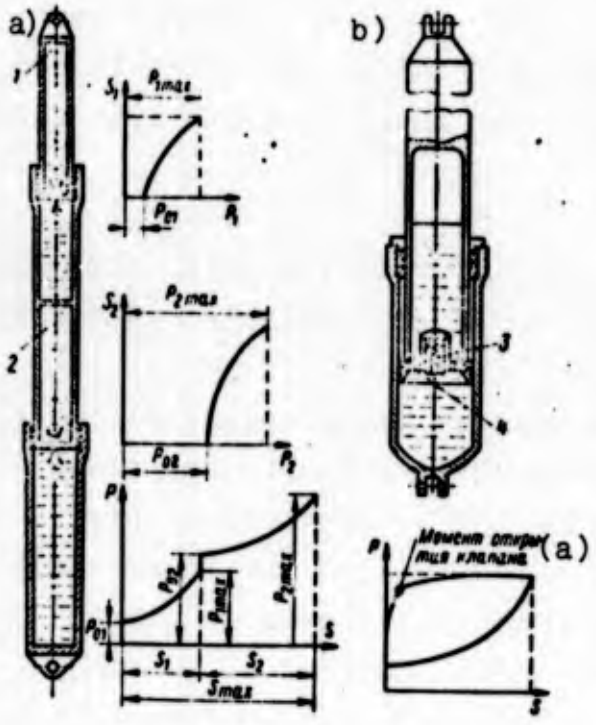

Figure 10.33. Shock absorbers setups: a) two-chamber shock absorber; b) the installing of special valves in shock absorber design: 1 - low-pressure chamber; 2 - high-pressure chamber; 3 - a valve which opens only during a landing at a time of high g-force; 4 - apertures for damping ground resonance. Key: (1) Moment of valve opening.

The employment of a two-chamber shock absorber. In those cases when the creation of shock absorber with a low initial pressure causes difficulties, it is recommended that so-called two-chamber shock absorbers be employed.

An additional shock absorber with low pressure in the gas chamber is installed on the shock-absorbing strut of the main landing gear support (Fig. 10.33a).

The low-pressure chamber is intended to ensure damping properties of a shock absorber at the very beginning of the stroke with small loads on the landing gear (at the moment of the lift off of the helicopter from the ground during takeoff or upon touchdown during landing and in the event of oscillations under ground resonance conditions).

The high-pressure chamber is intended mainly for receiving the impact energy during a landing; in the case of light loads on the landing gear it does not operate. Figure 10.12c gives another setup of a two-chamber shock absorber.

A two-chamber shock absorber as a device for eliminating ground resonance is finding extensive application on new domestic [Soviet] helicopters.

The installation of a spring damper which connects the liquid high-pressure chambers of two-chamber shock absorbers of both struts of main landing gear supports (Fig. 10.34). A spring damper is installed between the liquid high-pressure chambers of a two-chamber shock absorber. The spring damper device is such, that it does not change the landing gear characteristics during a landing on both main wheels simultaneously (without bank). But if a helicopter begins to oscillate on its landing gear, then the pressure in the compressed strut is greater than the pressure in the straightened strut.

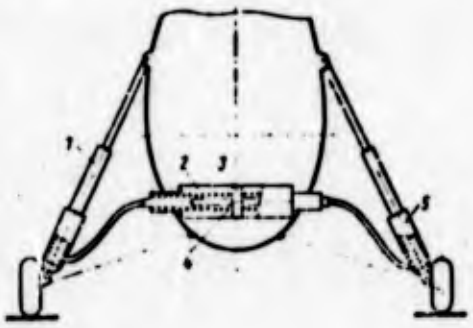

Figure 10.34. Spring damper installation setup: 1 - low-pressure chamber; 2 - spring damper; 3 - floating piston; 4 - spring; 5 - high-pressure chamber.

Under the effect of the pressure differential the floating piston of the spring damper will move. The overflowing of the liquid from the compressed shock absorber in the direction of the uncompressed shock absorber is equivalent to reducing the rigidity of the shock absorber, and this reduces the natural oscillatory frequency of the helicopter on landing gear, bringing it away from the number of rotor revolutions.

CHAPTER 11

HYDRAULIC AND PNEUMATIC POWER SYSTEMS

Energy (power) systems are employed to vary the position of flight vehicle units and to control their motion.

Hydraulic systems which always operate in conjunction with mechanical and electrical sections play the leading role on contemporary flight vehicles.

Hydraulic systems are examined in detail in the present chapter; since pneumatic systems have an auxiliary significance, special courses are dedicated to electrical systems, and mechanical systems are covered in chapter 12.

§ 1. HYDRAULIC SYSTEMS

A hydraulic system (hydraulic drive) is a complex of devices intended for transmitting mechanical energy over distance and for controlling motion by the employment of a fluid.

A hydraulic system includes:

pumps which convert the energy applied to them into the energy of fluid flow;

hydraulic engines (power cylinders, hydraulic motors) which convert the energy of fluid flow into the mechanical energy of translatory or rotary motion for controlling units;

working fluid;

the elements which ensure the connection between the pumps and the hydraulic engines and their regulation (conduits, distributors, throttles, valves, etc.);

auxiliary devices (reservoirs for the working fluid, filters, hydraulic accumulators, safety valves, working fluid coolants, etc.).

The major advantages of hydraulic systems which have resulted in their broad application are:

the evenness of the motion being accomplished, good responsiveness and the short delay in the motion of the units being controlled;

the practical incompressibility of a liquid, which ensures a very short lag in control and the possibility of installing hydraulic locks.

The compressibility of a liquid can be estimated by the magnitude

$$\frac{\Delta W}{W} = \beta p,$$

where ΔW - is the elastic reduction in the liquid volume, cm^3; W - is the volume of liquid at atmospheric pressure, cm^3; p - is the acting pressure, kgf/cm^2; β - is the coefficient of compressibility of the liquid, cm^2/kgf.

When $p=150-250$ kgf/cm^2 for liquids which are employed in aircraft hydraulics, it is possible to assume $\beta=50\cdot10^{-6}$ cm^2/kgf. For comparison let us point out that steel has $\beta=0.6\cdot10^{-6}$ cm^2/kgf;

light weights and small volumes of the main units per unit of power being transmitted;

high reliability of operation and long service life.

The basic deficiencies of hydraulic systems are:

fire hazard in connection with the possibility of the ignition of working liquids;

the dependence of the operation of a hydraulic system on external conditions - the ambient temperature and pressure.

1. The Basic Technical Requirements Imposed on Hydraulic Systems

The following requirements are imposed on hydraulic systems:

the response time should conform to the technical specifications;

operational reliability under all flight conditions and conditions of motion over the ground (height, velocity, maneuver, operational regimes of an aircraft engine), characteristic of a flight vehicle;

the employment of redundancy, duplication and the greatest amount of automation possible;

tightness of the non-moving joints and units in a temperature range of the surrounding medium and of the working fluid of from -55°C up to the greatest positive temperature which is encountered during the operation of the flight vehicle;

elimination of the possibility of extraneous solid particles getting into the hydraulic system and thorough cleaning of the working liquid during operation.

The working liquid should possess the following properties: a specific lubricating capacity, a slight variation in viscosity due to temperature and a freezing point not less than 15°C below the lowest temperature which is encountered in the operating conditions of the flight vehicle; neutrality to the sealing materials, anticorrosiveness, nontoxicity, a high flash point; stability of the above mentioned properties.

In the hydraulic systems of the aircraft and helicopters of civil aviation AMG-10 oil is employed as the working liquid in accordance with GOST (state standard) 6794-53 - it is the product of the distillation of petroleum, to which a thickener, an antioxidant and a dye have been added.

The basic characteristics of AMG-10 are: a kinematic viscosity at 50°C - of not less than 10 centistokes; at -50°C - of not more than 1,250 centistokes; a solidification point - not higher than -70°C; flash point - not lower than +92°C; the density at a temperature of +20°C is not more than 0.85.

2. Types of Hydraulic Systems and Their Operation

It is possible to divide hydraulic systems into feed section (from the pump to the liquid distributor) and into user sections.

The most frequently employed types of flight vehicle hydraulic systems are distinguished by the feed sections:

a) with unadjustable pumps driven by the aircraft engines;

b) with adjustable pumps driven by the aircraft engines;

c) with unadjustable pumps driven by electric motors.

On contemporary passenger aircraft, as a rule, hydraulic system feed sections of two types are employed simultaneously. For example, on the An-24 aircraft hydraulic systems of types "a" and "c" are employed, on the Tu-124 - types "b" and "c", and on the An-10 - types "a" and "b".

A hydraulic system with an unadjustable pump driven by an aircraft engine is presented in Fig. 11.1. Let us examine the purpose and the principles of the structure of its basic units and elements.

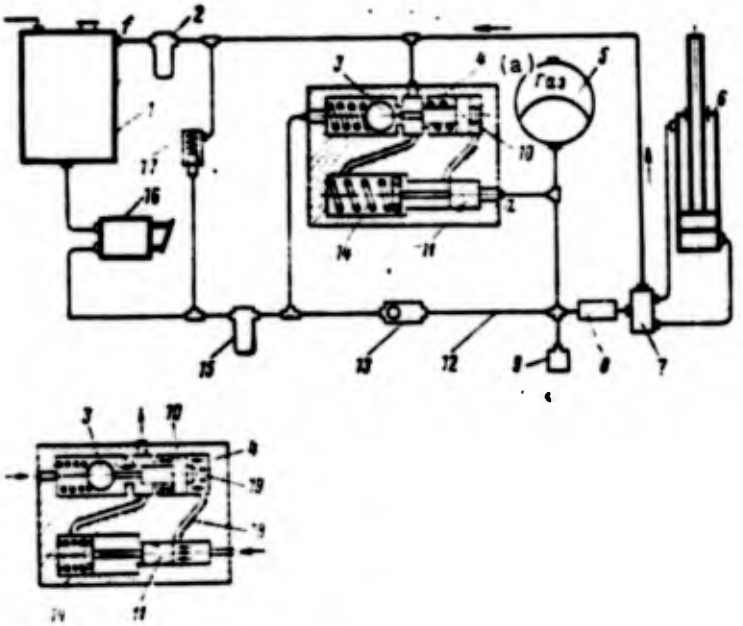

Figure 11.1. Diagram of a hydraulic system with unadjustable pump feed driven by an aircraft engine.
Key: (a) gas.

Tank 1 is a reservoir for the working liquid which feeds the pump and which flows from the system. Provided in it are devices for sediment, filtration and the preventing of the foaming of the liquid, the feeding of the liquid from the tank into the pump during maneuvers characteristic of the given flight vehicle. To prevent cavitation during pump operation at high altitudes tank pressurization with an excess pressure of $\Delta p=0.7-1.2$ kgf/cm^2 is employed. To keep the working liquid free from moisture and dust which can get

into the tank with air, special filters are provided.

The tank volume is made greater than the volume of the liquid poured into it by approximately 50% for receiving the additional volume of liquid which is formed upon increasing the temperature in the system, upon the discharging of the hydraulic accumulators and as a result of the difference in the liquid volumes which coming and going from the cylinders cavities.

Unadjustable pump 16 in the system in question is driven by one of the shafts of the engine gear-box. The gear-type and piston pumps which work at high speeds (n=2,000-4,000 r.p.m.) and at high pressures ($p_н$=150-300 kgf/cm^2) are most frequently employed. These types of pumps have light weights and small volumes per unit of transmitted power.

The most important characteristic of a pump is the dependence of its productivity on pressure $Q_н=f(p_н)$ (Fig. 11.2). Productivity $Q_н$ depends on the parameters of the working organs of the pump, on the perfection of its design and manufacture, the rotational speed of the shaft, the viscosity of the working liquid, and the pressures in the suction and forcing cavities.

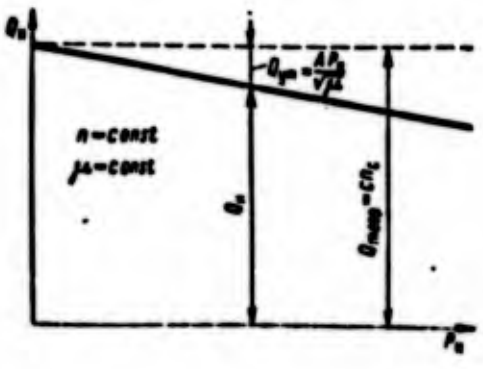

Figure 11.2. The characteristics of unadjustable pump feed - the dependence of productivity on pressure.

The real productivity of an unadjustable pump with sufficient pressure at its input can be approximately expressed by the following formula

$$Q_н = cn_c - \frac{Ap_н}{\sqrt{\mu}} \cdot см^3/с,$$

where cn_c - is the theoretical pump capacity, cm^3/s; $Ap_н/\sqrt{\mu}$ - is the reduction in productivity due to internal leaks in the pump through gaps and fissures between the elements separating the high- and low-pressure cavities;

c - is the theoretical feed during one revolution of the pump shaft, cm^3/rev; n_c - is the number of pump shaft revolutions in 1 s; A - is the coefficient which characterizes the internal leakage of the pump; p_H - is the pressure at the output from the pump forcing chamber; μ - is the dynamic coefficient of viscosity of the liquid going into the pump suction chamber.

Power cylinder 6 (see Fig. 11.1) serves to convert the energy of liquid pressure into the mechanical kinetic energy of a moving rod.

In a number of cases mechanical locks are employed in hydraulic power cylinders for fixing the rod in a specific position. Dampers are provided in hydraulic cylinders to prevent shocks in the case of the abrupt stopping of the piston at the end of its stroke.

Liquid distributor 7 (cock or valve) setup in question ensures the alternating connection of one of the cavities of the power cylinder with the fluid flow from the pump, and of the other - with the overflow line leading into the tank.

Safety valve 17 is intended for limiting the fluid pressure; it opens for the overflow of liquid into the tank, remains opened in the case of the exceeding of the specified pressure level and closes upon the restoration of the latter. The safety valve operates only occasionally.

Automatic pump relieving device 4 is a device for the automatic switching of the pump into the idle regime (in Fig. 11.1 below) - for connecting the pressure line of the pump with the tank, if the pressure in the system in the section beyond the automatic device attains a higher maximum magnitude (for example, after the liquid fills the power cylinder) $p_{авт_1}$. The automatic device switches off the pump from the tank and transfers it again to the working regime (in Fig. 11.1 above), when the pressure in the system (for example, due to leakage) drops to a lower maximum magnitude $p_{авт_2}$.

A hydroaccumulator is necessary to ensure the operation of the automatic relief device.

Hydroaccumulator 5 (usually liquid-gas) is employed to accumulate the potential energy of a compressed gas (nitrogen) and to return the energy to the working liquid; it has an isolated gas cavity pre-filled with compressed nitrogen, and a liquid cavity isolated from the gas cavity by a diaphragm or a floating piston and connected with the hydraulic system.

The accumulation of energy occurs, when the working liquid supplied by the pump, entering into the hydroaccumulator, reduces the gas volume and increases its pressure; the expenditure of energy occurs when the compressed nitrogen, upon expanding, ejects the liquid from the hydroaccumulator into the system.

In the hydraulic system setup in question the hydroaccumulator makes up for the leakage of working liquid from the high-pressure line in the interval between operations, when the pump is operating in the idle regime. Without this the automatic relief device would switch on the pump considerably more frequently, which is undesirable due to the pressure pulsations and the hydraulic shocks connected with this which cause fatigue loading of the hydraulic system structure.

The law of the variation in gas parameters in hydroaccumulators is polytropic. It is approximately possible to examine it as an isothermal law

$$p_{a0}W_{a0} = p_{ai}W_{ai} = \text{const},$$

where p_{a0}, $p_{a\,i}$ is the pressure in the gas cavity; W_{a0}, $W_{a\,i}$ is the volume of the gas cavity.

The accumulated energy reserve at the end of the charging is

$$A_a = p_{a0}W_{a0}\ln\frac{p_{ai}}{p_{a0}},$$

where W_{a0} and p_{a0} are the initial volume of the gas cavity and the pressure of the precharging of the hydroaccumulator; p_{a1} is the gas pressure at the end of the charging.

As a result of the expansion of a comparatively large volume of gas a reduction in the pressure in the hydroaccumulator and in the system occurs due to leakages from $p_{авт_1}$ to $P_{авт_2}$ over the course of a prolonged time interval.

According to isothermal law

$$p_{авт_2} = p_{авт_1} \frac{W_{авт_1}}{W_{авт_1} + \Delta W},$$

where ΔW is the increase in the volume of the gas cavity due to liquid leakages.

Usually $p_{авт_1}$, the upper maximum pressure, is assumed to be equal to the maximum working pressure $p_{раб}$ selected for the hydraulic system in question and $p_{авт_2}=(0.7-0.8)p_{авт_1}$.

In a number of cases the energy of the hydroaccumulators is employed as a reserve at the moments of the greatest demand for liquid or for supplying liquids when the pumps are not operating, for example, in the case of the necessity of emergency control of the landing gear wheel brakes.

The presence of hydroaccumulators in the system contributes to reducing the pressure pulsation caused by the nonuniformity of liquid feed by the pump, and to the softening of the hydraulic shocks which arise during sharp variations in the rate of motion of the liquid.

Unidirectional restrictor valve 13 is a locking device for the transmission of the fluid flow in one direction and the stopping of this flow in the case of its motion in the reverse direction.

Filters 2 and 15 are necessary for cleaning extraneous particles from the fluid, which get into the hydraulic system.

Conduits 12 ensure the supply of working liquid to the different units and devices and its removal from them.

The wall thickness and the material of the conduits are selected depending on the magnitude and the oscillations in the maximum pressure in the section of the system in question. Rigid jointless tubes manufactured from steel and duralumin, and from other alloys, and also flexible tubes, made from rubber reinforced with cotton fabric or with metal braiding are employed in the hydraulic systems of flight vehicles.

Hydraulic shock damper 8 helps to prevent hydraulic shock in the event of the rapid opening of the liquid distributor.

Pressure sensor 9 serves to measure the pressure in the system.

Let us examine the operation of a hydraulic system with an unadjustable pump (see Fig. 11.1).

In the starting of a aircraft engine the pump installed in it begins to operate. The liquid from tank 1 goes into pump 16, and from it through filter 15 and unidirectional restrictor valve 13 goes into hydroaccumulator 5; in this case as a result of the increase in the volume of the liquid chamber the volume of the gas cavity is decreased, which is accompanied by an increase in the gas and liquid pressure. When the liquid pressure becomes sufficient to overcome the prestressing of spring 14 of the automatic relief device, the displacement of plunger 11 begins. Upon attaining the upper maximum value of liquid pressure $p_{\text{авт}_1}$ the plunger is displaced so, that the access of the liquid through channel 18 into cavity 19 is ensured. Under the effect of the excess pressure piston 10 is displaced whose needle opens locking ball valve 3.

In this case the pump is switched over to the idle regime: the pressure in the pump pressure line drops sharply, since the liquid from the pump through the automatic relief device is being returned to the tank, by overcoming only slight hydraulic resistance. In the operating period in the idle regime, the unswitched-off unadjustable pump is relieved as a result of a considerable decrease in pressure p to p_{min}; under the effect of the pressure differential which occurs along the sides of unidirectional restrictor valve 13, the latter is closed and the high-pressure section is isolated from the low-pressure section by the hydroaccumulator. In this case the pump operates at minimum power $N_{min}=p_{min}Q$.

In the period when the pump is operating in the idle regime the liquid from the hydroaccumulator goes to make up for the leakages through gaps and the slot in the unidirectional restrictor valve, in the automatic pump relief device and in the liquid distributor. In this case the volume of the gas cavity is increased, and the pressure in both cavities of the hydroaccumulator is reduced. With a decrease in the liquid pressure plunger 11 of the automatic pump relief device under the effect of spring 14 is gradually displaced towards its initial position. When the pressure in fitting a descends to the lower maximum value of the liquid pressure, plunger 11 is located in such a position that channel 18 is opened and cavity 19 is connected with the overflow line, and piston 10 under the effect of the spring returns to the initial position, the needle of piston 10 releases the ball of valve 3, which is sitting in a seat and shuts off the access of the liquid from the pump into the tank. The period of the idle pump operating regime has finished. The liquid from the pump again goes through the unidirectional restrictor valve into the hydroaccumulator and charges it.

The moment of the switching on of the liquid distributor to the working condition can randomly coincide with any stage of charging or discharging of the hydroaccumulator. Let us examine the nature of the pressure change in the hydraulic system upon the

switching on of the distributor for feed into the power cylinder at the moment which corresponds to the discharging of the hydroaccumulator. Upon the switching on of the distributor the pressure cavity of the power cylinder is connected with the hydroaccumulator, the motion of the piston in the cylinder begins. It must be noted that piston motion is possible only under the condition that the pressure in the hydroaccumulator

$$p_a > \frac{P}{F} + p_{гидр},$$

where P is the force in the rod of the power cylinder due to the external load; $p_{гидр}$ is the hydraulic resistance to the motion of the working liquid in the section from the hydroaccumulator to the power cylinder.

The pressure in the hydroaccumulator is decreased, and it is increased in the pressure and in the overflow cavities of the power cylinder. During time interval τ_1 up to moment, when the pressure in the hydroaccumulator drops to $p_{авт_2}$, the piston stroke is accomplished under the effect of the hydroaccumulator.

For timely switching of the pump to the working regime it is necessary that the parameters of the hydraulic system ensure the fulfillment of the following condition:

$$\frac{P}{F} + p_{гидр} < p_{авт_2}.$$

Otherwise the rod of the power cylinder will stop its motion, until the pressure in the hydroaccumulator is reduced to $p_{авт_2}$ due to leakages. At this moment the automatic relief device switches the pump over into the working regime, the liquid pressure at the pump output is sharply increased and the operation during time interval τ_2 is continued mainly due to the pump energy.

Thus, the total time for the operation of the filling of the power cylinder and the displacement of the rod is $\tau = \tau_1 + \tau_2$.

Then ensue the stages of the charging of the hydroaccumulator, the switching of the pump over into the idle regime and the slow discharging of the hydroaccumulator due to leakages.

A hydraulic system with an unadjustable (sic) pump driven by an aircraft engine is shown in Fig. 11.3.

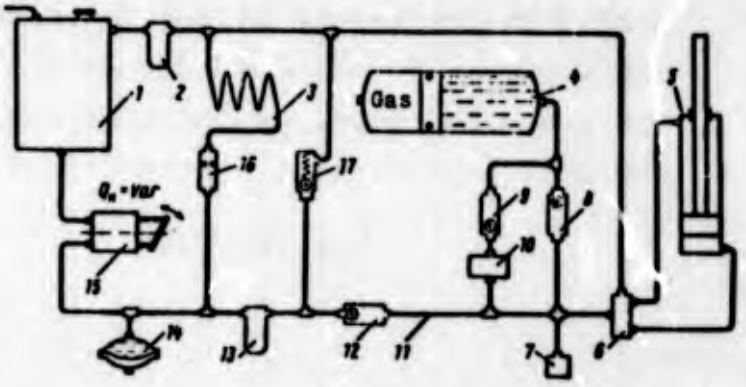

Figure 11.3. Diagram of a hydraulic system with an adjustable feed pump.

Tank 1, power cylinder 5, liquid distributors 6 and 10, filters 2 and 13, safety valve 17, sensor 7 and other units have in the hydraulic system in question the same purpose and can have the same structure as in a hydraulic system with an unadjustable pump.

Let us examine the purpose and the operating principle of some basic units, differing in purpose and design, characteristic for hydraulic systems with an adjustable pump.

Pump 15 differs by the presence of automatic devices for adjusting productivity. Figure 11.4 gives the characteristic $Q_н = f(p)$ of a pump with adjustable productivity. In the pressure range from $p=0$ up to the working pressure $p_{раб}$ in the first - the working regime - the pump productivity at constant revolutions is somewhat decreased as a result of internal leakages (section AB).

When the pressure at the pump output becomes higher than $p_{раб}$, an automatic gradual decrease in the working volume of the pump and

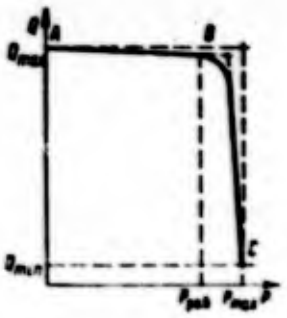

Figure 11.4. The performance of an adjustable-feed pump is the dependence of productivity on the forcing pressure.

its productivity (section BC) is attained. At a pressure $p=p_{max}$ the pump productivity $Q_н$ decreases to the minimum value Q_{min} necessary to compensate for leakages, for lubricating and cooling the pump.

The relieving of the pump in the operating period in the second regime in which $p=p_{max}$, and $Q_н=Q_{min}$, is attained due to the fact that the power developed by the pump becomes minimum due to a considerable decrease in feed $Q_н$:

$$N_{min} = p_{max} Q_{min}.$$

Throttle 16 (see Fig. 11.3), installed in the line which connects the delivery and the run-off main lines, ensures the small constant circulation of hydraulic fluid through the pump necessary for cooling the pump in that period when the units making a demand on the hydraulic system are opened.

Heat exchanger 3 is intended for cooling the liquid which is circulating through throttle 16 and pump 15.

Hydraulic accumulator 14 fulfills the functions of the pressure pulsation damper in the fluid caused by the operation of the piston pump. It usually has a small capacity and is installed in immediate proximity to the pump.

Hydraulic accumulator 4 is an additional energy source which is employed in activating distributor 10. In the diagram the hydraulic accumulator is connected with the system in such a way that upon activation of distributor 6 unidirectional restrictor valves 8 and 9 and liquid distributor 10 ensure the expenditure of the energy of the hydraulic accumulator and prevent its charging during this period.

Let us examine the operation of this particular hydraulic system. The fluid from tank 1 goes into pump 15. During the operation of the aircraft engine the fluid being supplied by the pump charges hydraulic accumulator 14 - the pulsation damper - is cleaned in filter 13 and through unidirectional restrictor valve 12, distributor 10 and unidirectional restrictor valve 9 goes to charge hydraulic accumulator 4. Along with this part of the working fluid (approximately 0.1 $Q_н$) through throttle 16, heat exchanger 3 and filter 2 of the run-off line goes back into the tank.

At first the pump operates in the first regime, then, when the pressure in the hydraulic accumulators becomes greater than $p_{раб}$, - in the second regime.

Upon the activation of liquid distributor 6 in power cylinder 5 the pressure in the system usually drops. The working fluid goes into power cylinder 5 both from pump 15 and from hydraulic accumulator 4. At the end of the operation distributor 6 is placed in the neutral position, and distributor 10 interlocked with it is placed in the position in which hydraulic accumulator 4 can be charged up to p_{max}.

A hydraulic system with an unadjustable pump driven by an electric motor is shown in Fig. 11.5.

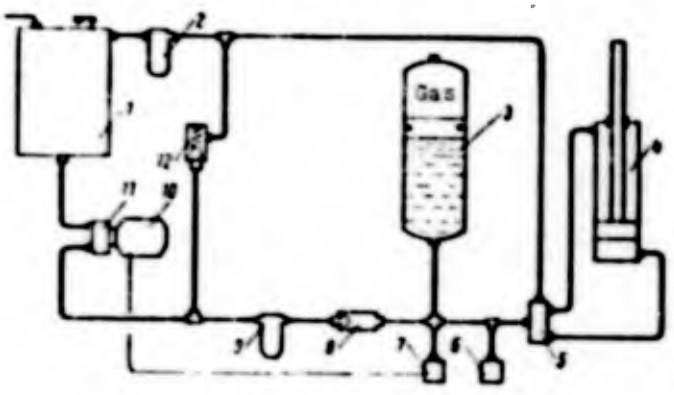

Figure 11.5. Diagram of a hydraulic system with an unadjustable pump driven by an electric motor.

A characteristic feature of this hydraulic system is the presence in it of pressure switch 7, the main purpose of which consists in the automatic switching off of electric motor 10 which drives pump 11, when the pressure in the system attains the upper maximum value $p_{верх}$, and the switching on of engine 10, when the pressure drops to the lower maximum value $p_{нижн}$.

All remaining units in this hydraulic system, for example tank 1, pump 11, unidirectional restrictor valve 8, filters 2 and 9, pressure sensor 6, power cylinder 4 and others, are similar to the corresponding units of the systems examined above.

Let us examine the operation of this hydraulic system. Upon the activation of electric motor 10 pump 11 begins to operate. The fluid from tank 1 goes into pump 11 and through unidirectional restrictor valve 8 is forced into hydraulic accumulator 3. When the pressure in hydraulic accumulator 3 attains an upper maximum value of $p_{верх}$, pressure switch 7 operates and switches off the feed circuit of the electrical pump drive. Pump 11 stops. Safety valve 12 goes into operation when pressure switch 7 malfunctions.

Upon the activation of fluid distributor 5 for the units making a demand a pressure drop occurs in hydraulic accumulator 3; when the pressure in the system drops to a specific lower maximum value $p_{нижн}$, pressure switch 7 switches on the feed circuit of the pump electric drive.

3. Selecting the Parameters and the Basis for the Development of Hydraulic Systems

In developing hydraulic systems and perfecting them it is necessary to select the parameters and to seek design solutions, taking into account the experience in creating such systems and the results of contemporary research.

Let us examine the general sequence of the development of a hydraulic system.

1. The development of a general functional setup of power systems intended for controlling an aircraft, its units and devices taking into account the requirements for ensuring reliability, by the employment of duplication, redundancy and emergency control. At this stage of design a number of basic, auxiliary and emergency hydraulic systems and the operations performed by them are established; the types of pumps (unadjustable or adjustable) and their drives (from an aircraft engine, from an electric motor, etc.) are selected.

In solving these problems the conditions under which the hydraulic system as a whole and its individual sections will operate, taken into account, for example:

the altitude at which the aircraft is employed (it is necessary to know this in order to ensure the maximum operational altitude of the hydraulic system);

the revolutions of an aircraft engine during the different flight stages (to ensure the possibility of controlling certain units during the operation of aircraft engines at low rpm's or in the case when aircraft engines are not operative);

the necessary level of reliability of a hydraulic system is estimated for the purpose of justified designation of duplication, emergency control, etc.

2. The development of a block diagram. It is necessary to project the sequence of the motion of the mechanisms controlled by the individual sections of the hydraulic system. For the section of the hydraulic system employed for retracting and lowering landing gear and their doors this sequence of motion of the individual mechanisms can be developed, for example: the opening of the

landing gear door locks and their deployment; the opening of the upper locks of the landing gear struts and the extending of the struts; the shutting of the strut locks in the lowered position and the closing of part of the landing gear doors. Methods and means of ensuring a specific sequence of the motion of hydraulic system units (hydraulic matching devices, electromagnetic cranes and valves, etc.) are selected; methods and means of relieving pumps in the interim period between operations and of synchronizing the motion of individual controlled devices. Methods of fixing the controlled mechanisms in the intermediate and extreme positions are also developed. For sections of units which create a demand that can operate from two and more hydraulic systems, reliable methods of switching from one system to another, etc., are projected.

On the basis of these materials and the content of the general functional setup a drawing of the block diagram of the hydraulic system is developed, on which all units, mechanisms and conduits are schematically shown.

3. The development of the kinematics of the controlled units and the determination of the loads on the rods of the hydraulic power cylinders. The loads on the rods of the hydraulic power cylinders are determined for the extreme and several intermediate positions of the unit being controlled. In this case the loads from the mass forces, air loads, frictional forces and the loads required for overcoming the resistance of the locks of the extreme positions of the unit being controlled are taken into account.

4. Determination of the parameters of the main units and conduits. The pump productivity should be sufficient to ensure the necessary rate of control of the mechanisms which are simultaneously activated.

At first the areas of the pistons of the power cylinders of the units creating demand are determined

$$F_i = \frac{P_i}{\eta_r p},$$

where η_r - is the efficiency which considers in the first approximation the losses in overcoming the hydraulic resistance; P_i - is the greatest load on the rod of the hydraulic power cylinder; p - is the working pressure.

The employment of high pressures leads to a reduction in the weight of a hydraulic system and in the overall dimensions of power cylinders and conduits. However, the maximum working pressure is limited to the value at which the pumps, units, flexible hoses and the fixtures for joining the conduits adopted by industry operate reliably.

The volumes of the power cylinders are determined

$$W_i = F_i S_i,$$

where S_i - is the power cylinder rod stroke taken from the kinematic calculation.

The necessary average pump productivity is determined

$$Q = \frac{\Sigma W_i}{\tau},$$

where ΣW_i - is the sum of the volumes of the power cylinders connected in parallel and acting simultaneously (for example, two power cylinders of the main landing gear struts and one power cylinder of the front strut); τ - is the operating time, for example, of the complete retraction of a landing gear or another aircraft mechanism, assigned by the technical specifications.

The required pump power at the output is found with the formula

$$N = \frac{Qp}{7500}.$$

In selecting feed sources, as a rule, the power and productivity reserve are taken and several pumps are placed to ensure duplication.

Another approach to determining the required values of N and Q is possible, if there are data on the maximum resisting forces P_{max} and hinged moments $M_{ш\ max}$, of the units being controlled and about the required maximum speeds of their motion - linear S and angular $\delta_{max\ j}$.

In this case the maximum required pump power at the output is

$$N_{max} = \frac{\sum_i P_{max\ i} \dot{S}_{max\ i} + \sum_j M_{ш\ max\ j} \dot{\delta}_{max\ j}}{75\eta},$$

where $\eta = \eta_м \eta_г$; $\eta_м$ - is the efficiency of the mechanical parts of the system; $\eta_г$ - is the efficiency of the hydraulic system from the pumps to the power cylinders.

The maximum required productivity is

$$Q_{max} = \frac{7500 V_{max}}{p}.$$

To ensure comparatively low hydraulic losses the internal diameter of the conduits in aircraft hydraulic systems is selected so that the average rate of fluid flow in the suction and run-off lines would be 2-3 m/s, in the forcing lines - 5-8 m/s. This diameter is determined with the formula

$$d = \sqrt{\frac{4Q}{\pi v}},$$

where v - the average rate of fluid flow, cm/s; Q - is the greatest fluid flow rate possible in the conduit section in question, cm^3/s.

The value of d determined with the formula is rounded off to the dimension recommended GOST (state standard).

Then the calculation and the development of the design of other units (power cylinders, cranes, valves, etc.) and accessories are carried out or the selection of standard articles is made.

5. Development of the assembly setup. In developing the assembly setup the technical specifications with respect to ensuring durability, ease of operation and maintenance of the system are realized.

The arrangement and the methods of attaching the units, conduits and their connections to the aircraft are shown on the assembly setup.

6. Verifying calculation and testing. During the verifying calculation the amount of time τ, during which the movement of the devices being controlled by the hydraulic system from one position to another under the different operation conditions of the hydraulic system primarily depending on the speed of the pump, the flight altitude and the temperature of the working liquid is determined.

For the experimental checking of the operational efficiency of a designed hydraulic system a stand is made on which all the units and conduits are positioned with maximum approximation to their proposed arrangement on the aircraft. The operational efficiency of the hydraulic system, of its individual sections and units is checked under conditions, close to operating conditions.

§ 2. PNEUMATIC SYSTEMS

On contemporary flight vehicles pneumatic power systems are applied mainly as auxiliary - emergency systems.

As the main power systems pneumatic systems are encountered only on light aircraft.

For driving different devices and units in a pneumatic system the energy is employed which is liberated during the expansion of a precompressed gas - air or nitrogen. The physical properties inherent to gases - their compressibility and low viscosity determine the characteristics of a pneumatic power system and finally its advantages and deficiencies.

Like hydraulic systems, pneumatic systems also have feed sections and sections which have a demand for energy. On aircraft and helicopters of Civil Aviation two feed section setups are employed - gas cylinder and gas cylinder-compressor. In the gas cylinder setup the energy of the compressed gas located in cylinders charged on the ground is employed. The energy capacity of this type of system is low, and its application is usually limited to emergency control tasks.

The gas cylinder feed setup is only possible in systems which operate on compressed nitrogen employed as an emergency drive for units normally controlled by a hydraulic system.

The employment of compressed air for this purpose is dangerous, since the vapors of AMG-10 oil at high pressures can form an explosive mixture with air.

The gas cylinder-compressor feed setup is employed only in pneumatic systems in those cases when it is necessary to increase their energy capacity without a significant increase in the volume and the weight of the gas cylinders. Since aviation compressors have relatively low productivity and cannot ensure normal operation of the system, the main energy source as in the gas cylinder feed setup is gas cylinders with compressed air. The role of the compressor is the recharging of the cylinders.

The positive qualities of the pneumatic systems employed on flight vehicles are the following:

the low dependence of the characteristics of the system on external conditions and, in particular, on temperature whose effect on the viscosity of the working medium (air or nitrogen) is absent in practice;

non-inflammobility;

the possibility of employing a system in inoperative engines - autonomy as a result of the employment of the energy of the compressed gas located in cylinders;

the absence of pressure pulsations and hydraulic shocks;

less weight;

speed of operation.

The last property of a pneumatic system is valuable, when rapid operation is required, in other cases it becomes a deficiency, since the abruptness of its operation can, if special measures are not taken, lead to breakages.

Also included among the deficiencies of a pneumatic system are the following:

the low energy capacity which at a given pressure depends on the volume of the cylinders, and increasing the volume of the cylinders leads to a sharp increase in their weight;

the increased requirements for the airtightness of the units and joints;

the compressibility of the gas is a disadvantage for employing pneumatic systems for servo drives and complicates design, if the placing of a unit being controlled in any intermediate position should be specified.

A schematic diagram of a gas cylinder-compressor pneumatic system is shown in Fig. 11.6. The working pressure in the cylinders is usually 50-150 kgf/cm^2.

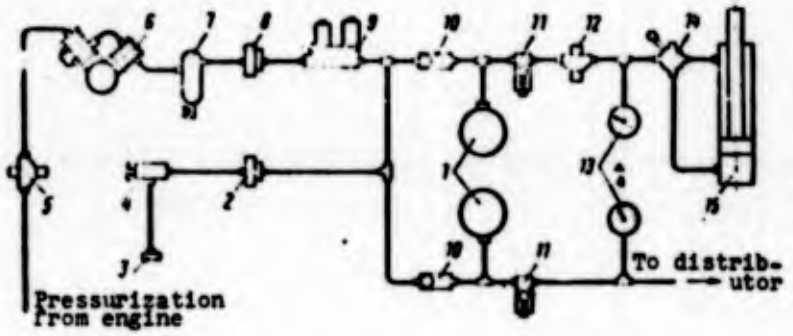

Figure 11.6. Schematic diagram of a pneumatic (air) power system: 1 - cylinders; 2 - filter; 3 - onboard charging fitting; 4 - charging cock; 5 - reducer; 6 - compressor; 7 - filter trap; 8 - felt filter; 9 - automatic pressure control (relieves the compressor, as an automatic relief device); 10 - unidirectional restrictor valve; 11 - safety valve; 12 - reducer for units and devices requiring low pressure; 13 - manometer; 14 - distributor; 15 - power cylinder.

To reduce the weight cylinders of spherical shape are frequently employed.

A certain weight saving can be attained by employing load-bearing design elements as compressed air cylinders, for example, the free (not occupied by a shock absorber) volumes of landing gear struts.

The compressor which recharges cylinders in flight is driven by an aircraft engine.

CHAPTER 12

THE CONTROL OF FLIGHT VEHICLES

§ 1. THE PURPOSE OF CONTROL SYSTEMS AND THEIR TECHNICAL SPECIFICATIONS

Control systems are the totality of onboard devices which ensure the control of a flight vehicle and the displacement of its different units and parts.

Changing the position of a flight vehicle in space is accomplished for an aircraft by deflecting the elevators, rudder and ailerons, and for a helicopter - by means of the cyclic-pitch control and the tail rotor. The devices which ensure the continuous control of these units, are called the main control system.

The principles of creating the forces and moments which change the position of an aircraft during the operation of the main control system are examined for an aircraft in chapter 5, and for a helicopter in chapter 2, § 3.

All the remaining control units (devices for the retraction and the lowering of the landing gear and takeoff and landing high-lift devices, devices for braking aviation wheels, etc.) are called the supplementary control system.

In this chapter the greatest attention is allotted to the main control system, since an examination of this responsible and complex system makes it possible to clarify the majority of the questions pertaining to the supplementary control systems.

The characteristics of the supplementary control system are examined in § 5.

Included in the main control system are the following:

a) the controls - are the parts of the main control system which are directly operated by the pilot, by applying forces to them and by displacing them (control columns, control sticks, and pedals);

b) the control line which connects the controls with the elevators and rudder, the ailerons, the adjustable stabilizer, the cyclic-pitch control, the tail rotor pitch-changing mechanism and consisting of rods, shafts, cables, levers, rockers, rollers and other elements.

The main control accomplished only by the pilot's muscular energy can be called direct main control. This type of control is usually installed on low-speed aircraft.

On helicopters, on heavy and on low-speed aircraft such large loads can arise on the controls, that the pilot's strength is insufficient for overcoming them. In these cases control of the elevators, rudder and ailerons, the cyclic-pitch stick and other units is accomplished partially or completely as a result of the energy developed by boosters (hydraulic amplifiers) connected in the main control line. This type of control is called main control boostering.

To assist the pilot during a prolonged flight control actuators controlled by autopilots are connected in the main control line.

Figure 12.1 gives a functional diagram of the control of aircraft as an automatic system. It follows from the diagram that the pilot is the most important link in both systems. He receives and interprets the information concerning the position of the control surfaces and the flight vehicle, concerning the g-forces, makes a decision and creates the controlling action. Thus, the number of special technical specification imposed on the main control system takes into account the characteristics of the work and of the possibility of a man as a link in this system. Let us examine the most important of these specifications imposed on the main control system.

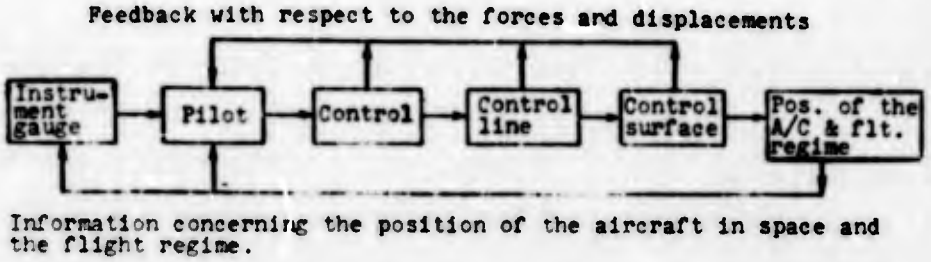

Figure 12.1. A functional setup of aircraft control.

1. In controlling a flight vehicle the motions of the hands and feet of the pilot for deflecting the controls should correspond to the natural reflexes of a man in maintaining his equilibrium. The displacement of a control by a pilot in a specific direction should cause the desired turning of the flight vehicle in the same direction.

2. The short delay in the movement of the control surfaces and of the reaction of the flight vehicle to the deflection of the controls (less than 0.15-0.25 s - the delay time of a human reaction).

3. To give the pilot a "control feel" - a sensation for him of the loads on the controls coordinated with the flight regime, it is necessary that in proportion to the displacement of the controls from the neutral position the resisting forces increase and be

directed in the direction opposite to the displacement. These forces should also increase with an increase in the impact pressure. It is desirable to employ a ratio of loads for controlling the ailerons - the elevator - the rudder - equal to 1:2:5.

The acceptable loads on the controls of the main control system are attained by aerodynamic compensation of the control surfaces, by ensuring low friction in the control line, by the selection of the kinematic control setup and by the employment of booster control.

4. The strength specifications imposed on the control system are covered in the stress standards.

A characteristic of them is the fact that in testing the structural strength of a control system the loads created by the pilot should be examined. In connection with this by stress standards the calculated destructive values of loads caused by the pilot are assigned. For aircraft with a flight weight $\geq$10,000 kg they have the following values (kgf):

The load on the control column or the elevator control stick.....	240
The load on the rudder control pedal.	250
The load on the aileron control column.....	160
The load on the aileron control stick	130

The components of a double control system should be checked for the isolated effect of a pilot (right and left) on the controls and for the simultaneous effect of two pilots both in one direction and in opposite directions; in this case the calculated load due to each pilot is assumed to be equal to 75% of the calculated load indicated above.

5. The following operational specifications should be met; they ensue from the necessity for ensuring the reliability of the functioning and the convenience in maintaining the main control system:

all the control links and mechanisms should be accessible for inspection and maintenance;

devices should be provided for the locking of the elevators, rudder and ailerons when the aircraft is parked; they should be controlled from the cockpit or flight deck.

In the main control system there should not be any units, the incorrect installation of which would lead to reverse operation of the control surfaces;

the extreme positions of the control surfaces should be limited by stops located near the control surfaces or on boosters.

§ 2. THE DESIGN AND STRENGTH OF THE COMPONENTS OF A CONTROL SYSTEM

1. The Kinematics of a Control System and the Gear Ratio

The control gear ratio $d\delta/d\theta$ is an important characteristic of the kinematic setup of a main control system. Here δ - is the angle of deflection of the elevator or aileron, θ - is the angle of deflection of the control.

Figure 12.2a presents a setup of elevator control.

On the basis of the principle of possible displacements, by disregarding friction it is possible to write $M_ш d\delta = PH d\theta$, whence

$$\frac{d\delta}{d\theta} = \frac{PH}{M_ш}.$$

On contemporary aircraft the range of variation in δ is determined by the conditions of controllability, and the range of θ - by the layout of the controls in the cockpit or on the flight deck.

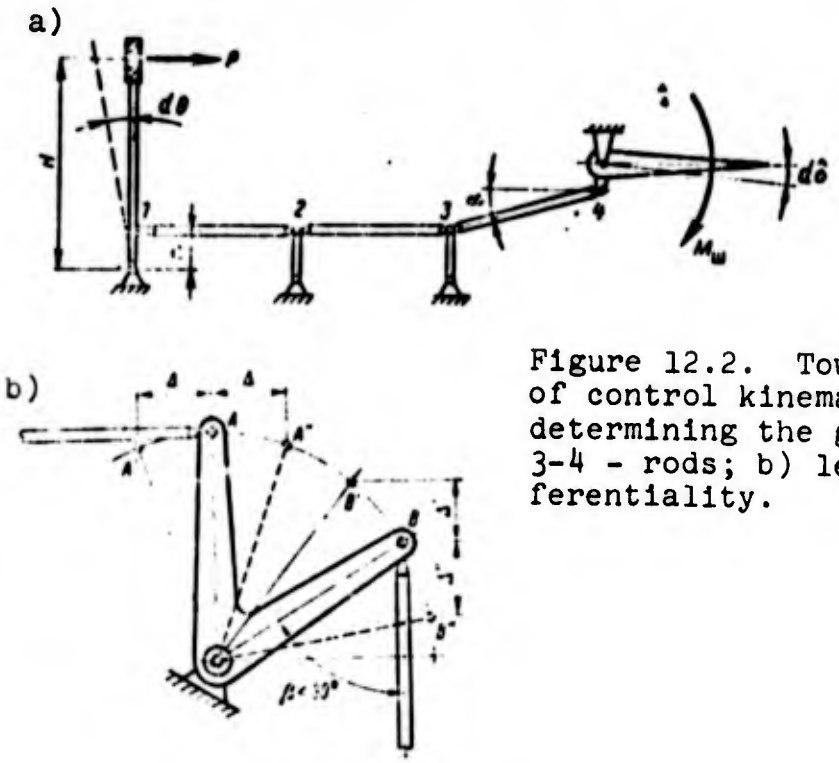

Figure 12.2. Towards an examination of control kinematics: a) diagram for determining the gear ratio: 1-2, 2-3, 3-4 - rods; b) lever for creating differentiality.

To ensure ease of control it is necessary that for deflecting the control surfaces by the maximum angle the required deflection of the controls have the following values:

a) the control column (control stick): forward - 10-18°, backward - 15-23°;

b) the control stick in both directions ±15-18°;

c) the wheel - turning by ±70-180°;

d) the pedals - a stroke of 100-130 mm in each direction.

Thus for elevator and rudder control systems $\frac{d\delta}{d\theta}$=1-2, for an aileron control system employing a wheel $\frac{d\delta}{d\theta}$=0.15-0.3.

The dependence of the force applied to the control on the gear ratio can be expressed by the formula

$$P = \frac{d\delta}{d\theta} \cdot \frac{M_m}{l}.$$

It follows from this formula that a decrease in the gear ratio, other conditions being equal, leads to a decrease in the force on the control.

A change in $d\delta/d\theta$ is possible due to a change in the kinematics and the ratio of the dimensions of the control elements.

As the means of changing the value of gear ratio $d\delta/d\theta$ depending on the deflection of the controls control differentiality is employed.

To provide differentiality angular levers are installed in a control system. To obtain differentiality it is necessary that not all the angles between the lever arms and the rods be right angles. Then, if in the event of the displacement of a control in different directions BB'=BB", we will obtain $\Delta' < \Delta''$. As a measure of differentiality the following ratio is employed $\bar{\Delta} = \frac{\Delta''}{\Delta'}$.

Differentiality is employed for varying, in proportion to the deflection of the control, the ratio between hinge moment $M_ш$ and the load on lever P.

Differentiality is also employed in the aileron control of subsonic aircraft in order that the aileron is deflected upward at a larger angle, than the other aileron is deflected downward. This is necessary because in the case of their deflection by equal angles a greater increase in drag is obtained on the half-wing with the downward deflected aileron, which creates an undesirable turning moment in the direction opposite to the bank.

2. Rigid Control Line

A rigid control line (Fig. 12.3) consists of control columns 1, rods 2, rockers 3, levers 4 and roller guides 5.

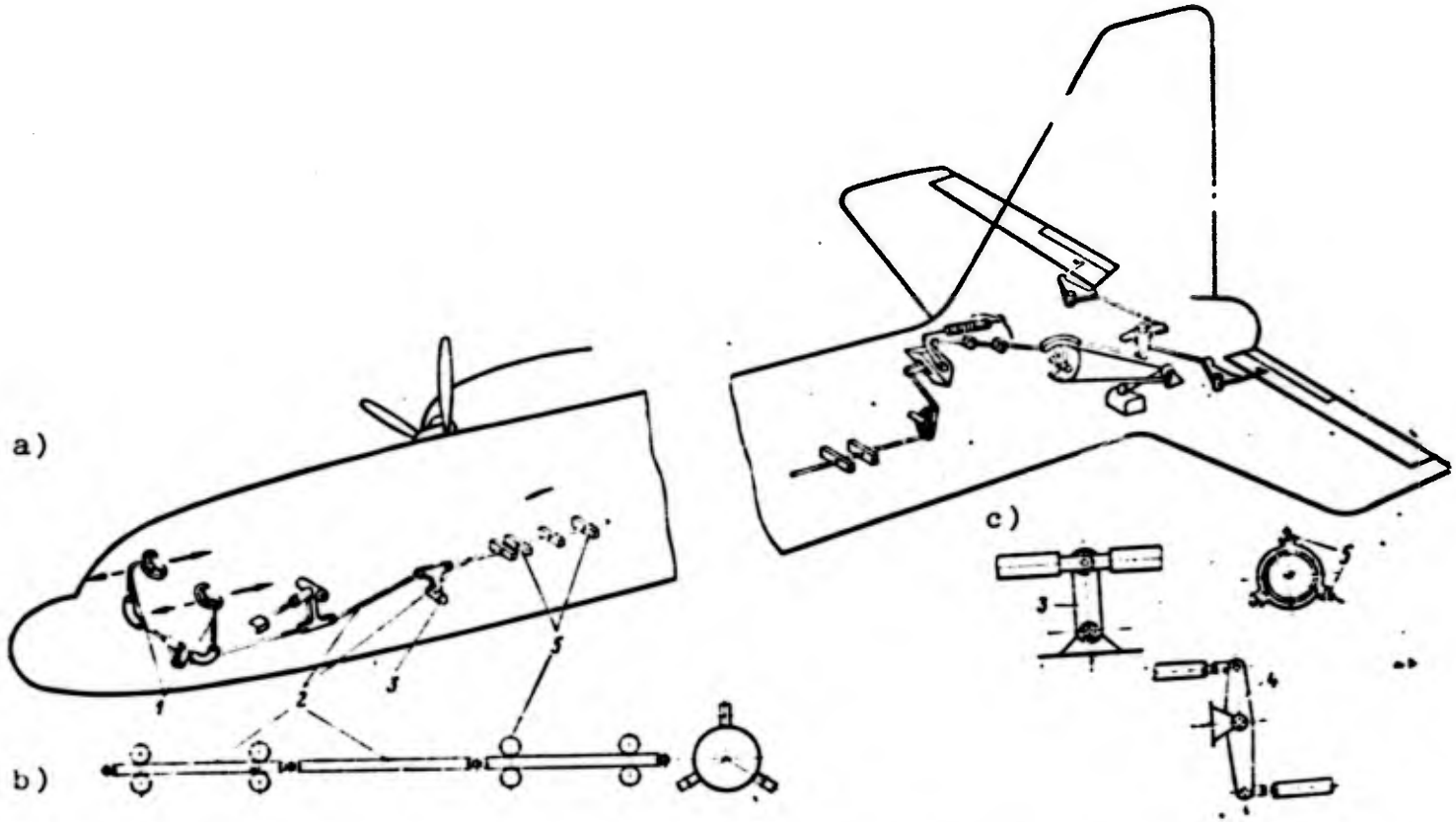

Figure 12.3. Elevator controls: a) control line; b) the resting of rods on roller supports; c) design components.

The ball bearings employed in a rigid control line are, as a rule, radial spherical-race thrust bearings. These are heavily loaded slow-speed bearings selected from the catalog of aviation bearings in accordance with the magnitude of the acting loads.

Figure 12.4 shows an example of the design of a control column.

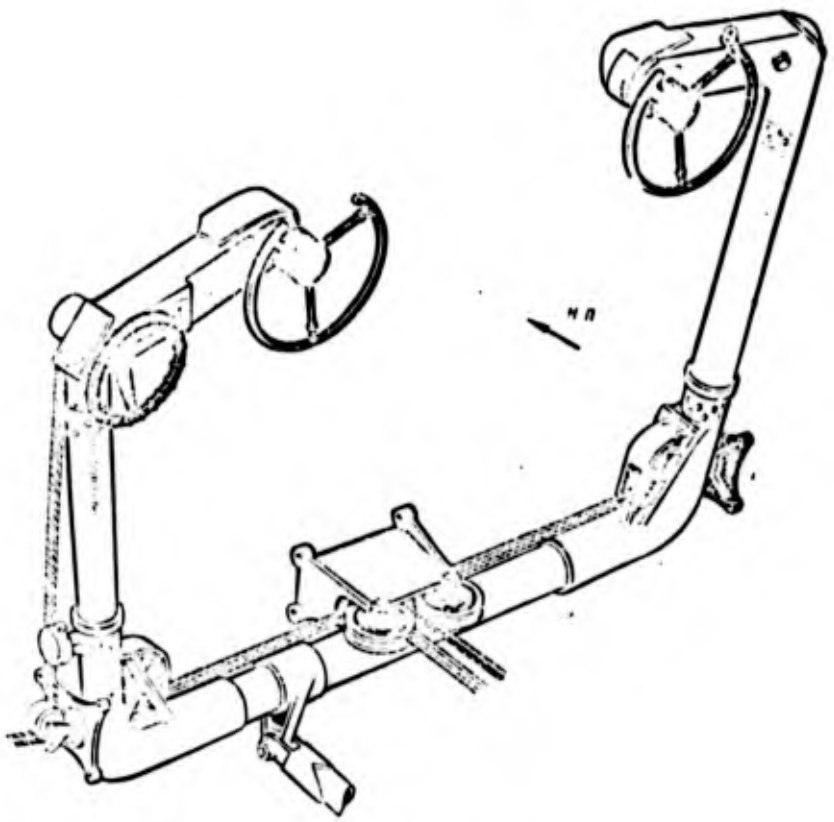

Figure 12.4. Control column.

The rockers, which are intermediate supports of the line divide it into rather short rods. This is necessary for increasing the stability of the rods during compression and for preventing vibrations in them. The lever serves for varying the direction of motion of the rods.

In such a case, when a line is made from rods installed in roller guides it is necessary that the line be divided into sections as is shown in Fig. 12.3b to avoid jamming of the rods in the event structural deformation of the airframe.

3. Flexible Control Line

A flexible control line is broadly employed for a main control system, and also for controlling trim-tabs and engines.

The design elements of a flexible control line (Fig. 12.5) are as follows: steel cables 1, rollers 2, grooved sectors 3, levers 4, stretchers 5, eye rings 6. Chain drives are also sometimes employed in its individual links.

In a flexible control line cables in accordance with GOST 2172-47 and KSAN (steel aviation untwisted cable) are employed.

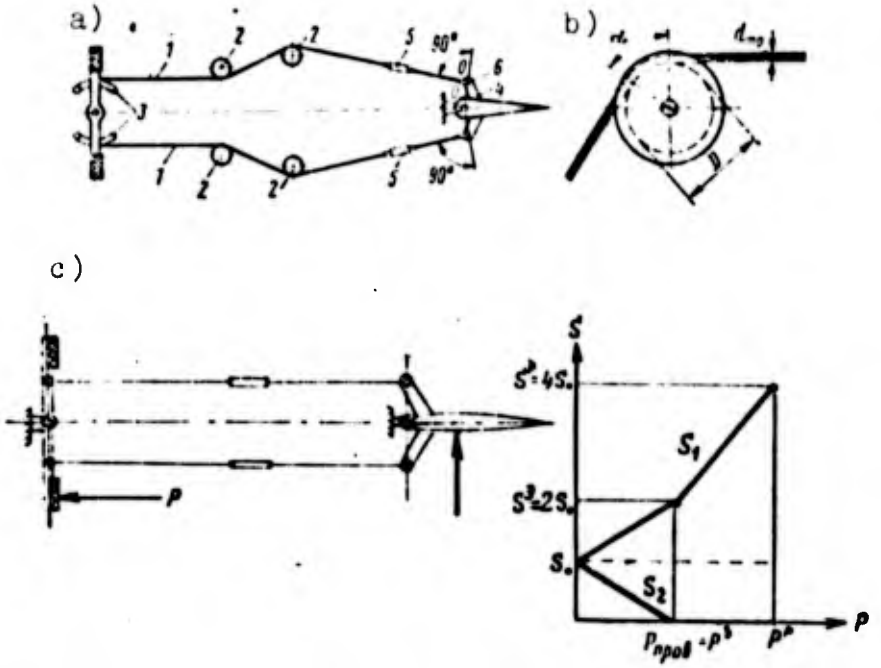

Figure 12.5. Rudder control with a flexible control line: a) control setup; b) arrangement of the cable on a roller; c) variation in the forces in the cables with prestressing in the case of an increase in the load on the control.

The cable consists of strands, and the strands consist of 7-19 fine zinc-coated wires. This makes it flexible. Wire 0.2-0.4 mm

in diameter is manufactured from carbon steel and has $\sigma_в$=170-220 kgf/mm^2 (the high $\sigma_в$ is due to cold hardening). Cables from 1.8 to 6 mm in diameter are employed.

The destructive forces for the cables are assigned by the standards.

To ensure a sufficient service life of the cables it is desirable that the force in a cable during aircraft control does not exceed 10% of the destructive force.

Before positioning cables in a flexible control line it is necessary to prestress then under a load of approximately 50% of the destructive load for a period of 20-50 min.

This prevents the elongation of the cables during operation.

The attaching of the cables to rockers, sectors, etc., is accomplished by means of eye rings, end caps and balls. Stretchers are employed for tensioning the cables. An example of the cable characteristics is given below.

Brand of cable	7×19-3 in accordance with GOST 2172-47
Nominal diameter, mm.....	3
Cross-sectional area of all the wires of the cable, mm^2.....	4.18
Rated tensile strength, kgf/mm^2.....	210
The breaking load of a cable is not less than, kgf.....	750
The weight of 1 linear m of cable is not more than, kgf.	0.044

The weakening of the strength of a cable when it is attached to an eye ring is approximately 15%.

The rollers of a control line serve to support the cable and to change the direction of the cable control line. They are manufactured from Textolite or duralumin and have ball bearing.

To ensure the fatigue life and low wear of a cable the diameter of roller D should be the greater, the greater is the diameter of cable $d_{тр}$ and the greater is the angle α of contact of the roller with the cable (Fig. 12.5b). When α=0-40° it is recommended assuming $D/(d_{тр})$=10-20, when α=40-90° value $D/(d_{тр})$=20-30.

To ensure the normal operation of a flexible control line without weakening and excess tensioning of cables they should be attached to the levers employing sectors 3 (Fig. 12.5a). In the case of the direct attachment of the cables to the levers with bolts it is necessary that the angle between the axis of the lever in its neutral position and the direction of the cable be equal to 90° (see Fig. 12.5b).

In a flexible control line it is mandatory to carry out pretensioning (stressing) of the cables employing stretchers.

When there is no pretensioning and loading a pedal, one cable will be tensioned, and the other cable will sag. If in this case a load is rapidly applied to the other pedal, then dynamic loading of the sagging cable will occur.

When there has been pretensioning and unsymmetrical loading exists one cable is additionally tensioned, and in the other cable the force of prestressing is reduced, but if the tensioning is sufficient, the cable will not sag.

The diagram in Fig. 12.5c shows how the forces change in cables with an increase in the load on the control, if the force of the

prestressing of the cables in flexible control line S_0 is selected so that before the exceeding of operational load $P^э$ sagging of the cables does not occur. For this at a safety factor of f=2 the magnitude of prestressing should be not less than $0.5\ S^э=0.25\ S^р \times P_{пров}$ - the load at which one of the cables sags.

For cables which are held on drums by means of friction, prestressing should not decline up to $P^р$, i.e., for them it should be

$$S_0 \geqslant \frac{S^р}{2}.$$

Strain gauges are employed for measuring prestressing.

A variation in temperature affects the tensioning of the cables of a flexible control line.

It is known that the coefficient of linear expansion for carbon steel is $\alpha_{ст}=11\cdot10^{-6}$, and for duralumin $\alpha_д=22\cdot10^{-6}$.

Since $\Delta l=\alpha t l$, where t - is the temperature differential; l - is the initial length of the cable, then the tensioning of a control line made from steel cable installed in a duralumin framework, with an increase in temperature increases, and with a decrease - decreases (Fig. 12.6b).

The temperature effect on the tensioning of a flexible control line must be taken into account when designating the magnitude of prestressing. In the case of T_{min} condition $S_{от}\geq 0.25\ S^р$ should be observed, in the case of T_{max} - condition $S_{от}+S^э\leq(S_{разр})/2$ where $S_{разр}$ the force which destroys the cable.

Excess tensioning of cables at elevated temperatures increases their tensioning in operation and reduces their service life. To reduce the variations in the tensioning of it control line it is

advantageous to insert a spring compensator.

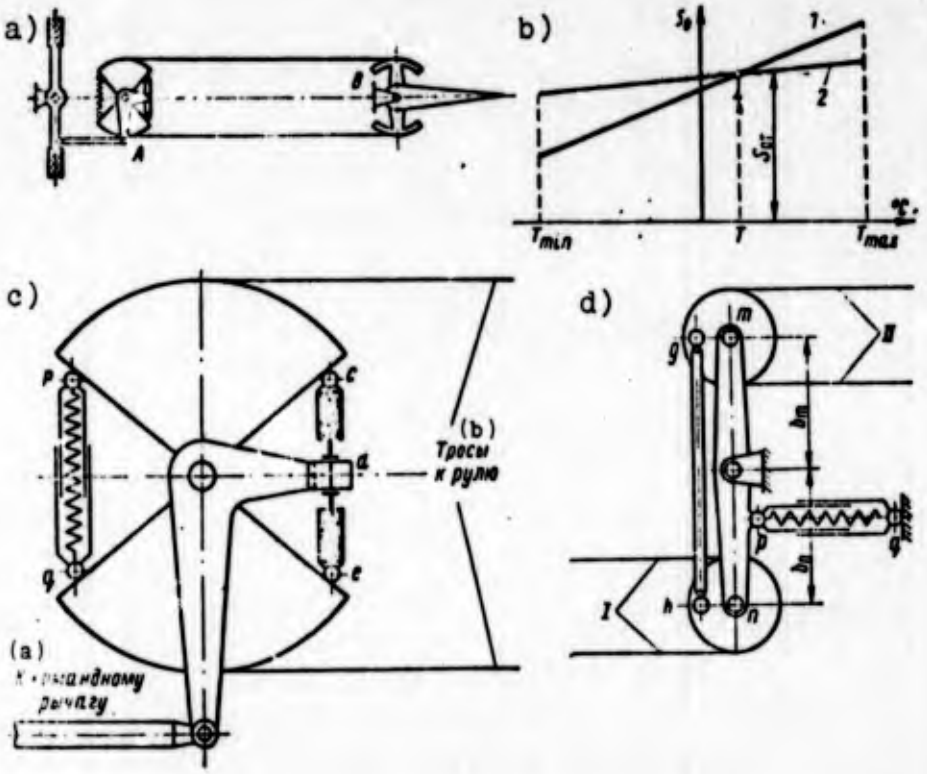

Figure 12.6. Inserting a compensator into a control line to reduce the effect of temperature on the tensioning of the cables: a) insertion diagram; b) the effect of temperature on the tensioning of a cable control line: 1 - without a compensator; 2 - with a compensator; c and d) two types of compensators.
Key: (a) cables to control surface; (b) to control.

For the purpose of explaining the role of the compensator let us examine the deformations of a fuselage $\Delta l_{ф}$ and of a control line $\Delta l_{п}$ in section AB of fuselage with a length $l_{ф}$ between the extreme supports of the control line (Fig. 12.6a). They are respectively equal to $\Delta l_{ф}=\alpha_{д} t l_{ф}$ (let us disregard the deformation of the fuselage due to the tensioning of the control line) and $\Delta l_{п}= \alpha_{ст} t \frac{l_{п}}{2}+\Delta S \frac{l_{п}}{2E_{ст}F}+$ $+\Delta Sr$, where $E_{ст}F$ - is the rigidity of the cable during tensioning;

$l_п$ - the total length of the control line (of two symmetrical halves); r - is the pliability coefficient of the compensator; ΔS - is the variation in tensioning. Since $\Delta l_ф = \Delta l_п$, то $\alpha_д t l_ф = \alpha_{ст} t \frac{l_п}{2} + \Delta S \frac{l_п}{2E_{ст}F} +$ $+\Delta Sr$, hence

$$\Delta S = \frac{\left(\alpha_д l_ф - \alpha_{ст}\frac{l_п}{2}\right)t}{\frac{l_п}{2E_{ст}F} + r}.$$

It is evident from this expression that the pliability of a spring compensator ensures a reduction in ΔS. As is shown in Fig. 12.6b the diagram of S with respect to T becomes flatter.

The pliability of a compensator should reduce the rigidity of a control line only in the case of a change in its tensioning under the effect of temperature. A compensator spring should not be deformed during unsymmetric tensioning of a cable arising from the loads on the controls and control surfaces.

Figure 12.6c shows a diagram of a compensator on a Vickers VC-10 aircraft, and Fig. 12.6d - a diagram of a compensator on an Il-62.

In the diagram in Fig. 12.6c rod cde has two screws with a steep pitch without self-locking with the opposite direction of the thread. As a result of this the rod ensures the displacement of points c and d and of the turning of the sectors only symmetrically relative to d; pq - is the spring.

For the diagram in Fig. 12.6d the ratio of arm b_m and b_n should be such that the tensioning of cables I (to the control) and II (to the control surface) of the sections of the cable control line during heating would be changed equally; gh - is the rod connecting the rollers to which the cables are fastened; pq - is the spring.

4. Advantages and Deficiencies of Rigid and Flexible Control Lines. Checking Their State in Operation

The advantages of a rigid control line - are the rigidity which ensures slight elastic deformations; the deficiencies - are the great weight and the complexity of manufacture, the danger of failure due to vibrations.

The advantages of a flexible control line - are the convenience in the layout, light weight, lower cost; the deficiencies - are the increased friction and wear, the residual deformation which increases in the course of time, the effect of temperature on the state of the adjustment.

The loading conditions of control components require special attention to the state of the surface of the parts, to friction and gaps in the control system, to the tensioning of the flexible control line during operation.

The presence of dents and nonrectilinearity of control rods lead to a decrease in the values of their critical compressive force of $P_{крит}$.

The jamming of the bearings of the rollers causes an increase in cable friction and increased wear.

Friction in a control system increases the pilot's fatigability.

The presence of gaps increases the danger of vibrations in a control line, by reducing the natural frequency and increasing the amplitude of the transverse oscillations.

Gaps and insufficient rigidity lead to a kinematic lag in the displacements of a control surface which correspond to specific deflections of the control (as a result of the pliability of the

control line the gear ratio $d\delta/d\theta$ is reduced in comparison with its nominal value). Insufficient rigidity of the structure, to which the control line is fastened, contributes to this.

Insufficient rigidity of aircraft design leads to a reduction in the effectiveness of the control elements and can contribute to the appearance of aileron reversal at great flight velocities.

For determining the gaps in a control system the stroke $S_{люфт}$ of the appropriate control caused by the gaps is measured with the control surface activated.

For the characteristic of rigidity of a flexible control line the magnitude of stroke $S_{упр}$ of the control due to the elastic deformation of the control line with the control surface activated and with loading of control with a specific assigned load P is measured.

To evaluate the friction in a control system the load on control $P_{тр}$ necessary for overcoming the friction as the average of the values found during the motion of the lever in one and the other direction is determined.

The normal values $S_{люфт}$, $S_{упр}$ and $P_{тр}$ permissible for each aircraft are indicated in the instructions on the operation of the aircraft.

With the purpose of ensuring the correspondence of the angles of deflection of the control surfaces and the controls to their established values (indicated in the description of the aircraft) there are adjustable detents and special adjustable parts in the control system design: in a cable control line - there are stretchers, in a rigid control line - there are adjustable rod ends.

5. Strength Rating of Control System Components

The rating of the forces in the elements of a main control system of an elevator, a rudder and ailerons is carried out from the rated destructive loads acting on the controls by the pilot determined from the stress standards.

Strength rating and vibration rating of the elements of rigid control line is accomplished in the following sequence.

1. Determining the load on a control in accordance with the stress standards.

2. The forces in the rods are determined from the values of P^{P}.

The equilibrium of a control and other units is examined in sequence. For example, in the diagram in Fig. 12.2 we examine the equilibrium of a control stick and obtain

$$S_{2-1} = S_{1-2}; \quad S_{2-4} = \frac{S_{2-1}}{\cos\alpha}; \quad S_{1-2} = \frac{P'l'}{r_1}.$$

The forces in the rods are determined in the different positions of the controls (for example in the two extreme positions and in the neutral position).

3. Selection of the cross sections or of the strength testing of the rods in longitudinal flexure and tension.

4. The stress analysis of the remaining elements of a control line (joints (hinges), rockers, levers, etc.). The forces in the levers and rockers are determined in accordance with the loads from the rods adjoining them.

The joint (hinge) bolts are selected in accordance with the shear and buckling rating, and a bearing is selected which corresponds in diameter to a bolt with respect to the catalog.

5. Vibration testing of rods. The causes of rod vibrations are the periodic exciting forces created by the power plants. The vibrations caused by the lack of balance of a piston engine and a propeller are the most significant. Thus for propeller aircraft the dimensions of the rods are selected not only from the condition of their operation in longitudinal flexure and tension, but also from the condition of the absence of resonance oscillations in the main operational regimes of engine operation.

The oscillations of the rods belong to the type of transverse (flexural) oscillations and thus can occur without considerable displacement of the ends of the rods (unnoticed by the pilot).

The harmful consequences of rod vibrations are the following:

a) the appearance of cracks and rod failure due to metal fatigue;

b) the formation of gaps in the joints (hinges);

c) the formation of hollows in control rods due to impact against roller guides when there are large clearances between the thrusts and the guides.

To get sufficiently away from resonance caused by the lack of balance of a engine, the natural oscillational frequencies of the rods should not lie within the ranges:

$$n_э \pm 300 \text{ osc/min}, \quad 2n_э \pm 400 \text{ osc/min},$$

where $n_э$ - is the number of revolutions of an engine or a propeller in the main operational regime.

The natural oscillational frequency of a rod is determined as for a beam on hinged supports

$$\nu = \frac{\pi}{2l^2}\sqrt{\frac{EI}{m}} = \frac{30\pi}{l^2}\sqrt{\frac{EI}{m}},$$

where l - is the length of the rod, cm; E - is the elastic modulus, kgf/cm^2; I - is the moment of inertia of the rod cross section, cm^4; $m=\frac{\gamma}{g}F$ - is the mass of a unit length of the rod, $kg\cdot s^2/cm^2$; γ - the specific gravity of the rod material, kg/cm^3; F - is the cross-sectional area of the rod, cm^2.

It is necessary to note that, since

$$\left(\frac{E}{\gamma}\right) \text{ of steel} \approx \left(\frac{E}{\gamma}\right) \text{ of duralumin} \sim 2.6\cdot 10^9 \text{ cm},$$

then the values of ν of tubes manufactured from these metals with equal dimensions differ very slightly. If we take this circumstance into account, and then that for thin-walled tubes $F=\pi D_{cp}\delta$: $I=\frac{\pi D_{cp}^3\delta}{8}$, then ν for duralumin and steel tubes can be expressed by the approximate formula

$$\nu = 170\frac{D_{cp}}{l^2} \text{ osc/min},$$

where D_{cp} - is in millimeters; l - is in meters.

The longitudinal force compressing or tensioning a rod changes the natural oscillational frequency; however, this effect is small and is considered by the width of the ranges: ±300 and ±400 osc/min.

The effect of the longitudinal force on ν is expressed by the formula

$$\nu_p = \nu\sqrt{1 \pm \frac{P}{P_0}} \text{ osc/min},$$

where P - is the force acting in the rod; $P_0=\frac{\pi^2 EI}{(\mu l)^2}$ - is the critical force in accordance with the Euler formula; $\mu=1$.

In the formula in the event of compression the sign "-" is employed, in the event of tension the sign "+" is employed.

In order that ν is not reduced due to the elastic displacements of the supports, the rockers and supporting units should have considerable rigidity.

Characteristics of the stress analysis of a cable control line. The sequence of the stress analysis of the elements of a cable control line is the same for a rigid control line. The difference consists in the necessity for also taking into account the forces due to prestressing.

§ 3. MEASURES FOR REDUCING THE LOADS ON THE CONTROLS OF THE MAIN CONTROL SYSTEM OF HIGH-SPEED AND HEAVY AIRCRAFT

As was found earlier, the dependence of the load on the controls P on hinge moment $M_ш$ and gear ratio $d\delta/d\theta$ is expressed by the formula

$$P = \frac{d\delta}{d\theta}\frac{M_ш}{H}.$$

The magnitude of hinge moment for a control surface is

$$M_ш = m_ш S_p b_p q,$$

where $m_ш$ - is the hinge-moment coefficient of the control surface; S_p and b_p - are respectively the area and the chord of the control surface; q - is the impact pressure of the flow impinging on the empennage.

It is evident from these expressions that the value of hinged moment depends on the dimensions of control surfaces S_p and b_p. Thus on heavy aircraft large hinge moments and excessive loads P on the controls are possible.

An increase in flight velocity when $M<M_{крит}$ brings about an increase in $M_ш$ and P due to an increase in impact pressure q. In the case of flight at $M>M_{крит}$ upon surpassing the speed of sound and at supersonic velocity the magnitude of hinge moment changes both as a result of the increase in q, and also as a result of the sharp change in the hinge-moment coefficient $m_ш$.

The following measures are employed for reducing the loads on the controls:

reducing the hinge moment on the control surfaces;

the employment of small gear ratios in the control system;

the employment of boosters (auxiliary drives), directly reducing the magnitude of P.

1. **Reducing $M_ш$.** The reducing of $M_ш$ by employing aerodynamic compensation for the control surfaces was examined in chapter 5. Practice has shown that the possibilities of employing aerodynamic compensation for reducing the loads on the controls of the main control system of high-speed and heavy aircraft are limited.

2. **Reducing the gear ratio** $d\delta/d\theta$. A simple decrease in the gear ratio due to an increase in the range of the deflection angles of the controls is limited by the overall dimensions of the cockpit or flight deck and is connected with control inconvenience.

The employment of control systems with variable $d\delta/d\theta$ is possible. This is attained by introducing into a control system such kinematic links which ensure a nonlinear dependence between θ and δ, which gives in the region of average angles of deflection of the control surfaces (6-10°) small values of the gear ratios, and in the region of large angles of deflection - conventional values. In this case the following aspects should be taken into account:

a) the deflection angles of the control surfaces at high speeds are small, and the hinge moments are large; thus in these regimes it is desirable to have smaller $\frac{PH}{M_ш}\frac{d\delta}{d\theta}$;

b) the control surfaces have considerable deflections at comparatively low flight velocities, thus in this case the employment of conventional or even increased values of $d\delta/d\theta$ is possible.

A variable gear ratio is sometimes employed for reducing the loads on the controls of subsonic aircraft. Transmission mechanisms for attaining variable $d\delta/d\theta$ are also employed on some supersonic aircraft with booster control for reducing the loads on a control depending on the velocity and flight altitude and in the event of an emergency changeover to manual control.

3. **The inclusion of boosters in a control line** - is a radical means which ensures acceptable loads on the controls of the main control system on contemporary high-speed and heavy aircraft.

The boosters are usually made in the form of hydraulic amplifiers. The following specifications are usually imposed on them: operational reliability at all operational temperatures; the power developed by a hydraulic booster should be sufficient to displace the control elements at the necessary speed.

A hydraulic booster consists of a power cylinder driven by a special continuously acting hydraulic system, and a servo mechanism. Recently electromechanical units have also been finding application as boosters.

Booster control systems are divided into two groups depending on the method of providing the pilot with a "control feel":

a) reversible systems, in which the force on a control is determined by the hinge moment of the control surfaces, and the

role of the booster reduces to decreasing the magnitude of this force;

b) irreversible systems, in which the force on a control does not depend on the hinge moment of the control surfaces.

Figure 12.7 shows a schematic diagram of a hydraulic booster connected in a control system in accordance with an irreversible setup. For irreversible systems the "control feel" can be ensured by artificial means - by special artificial feel devices.

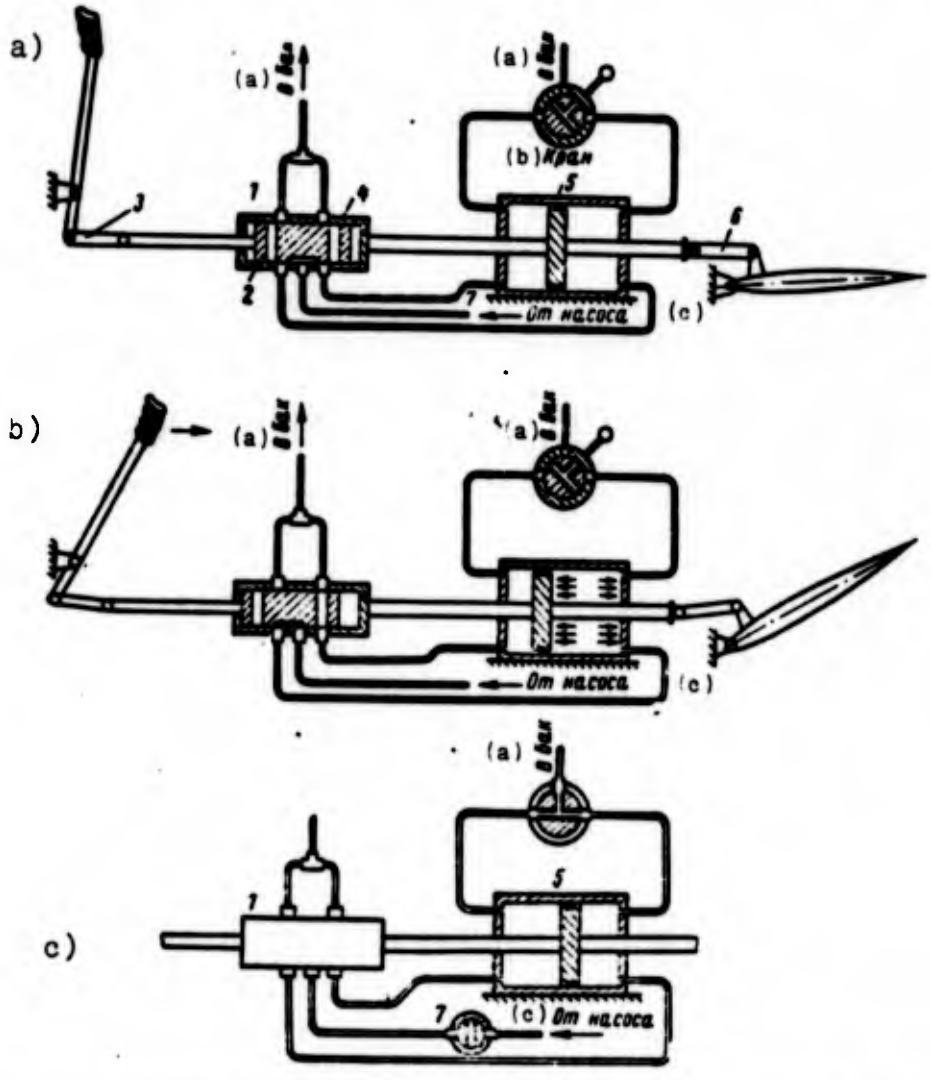

Figure 12.7. Schematic diagram of a hydraulic booster inserted in accordance with an irreversible setup: a) neutral position; b) motion of the control backward; c) changeover to manual control: 1 - run-off line; 2 - valve shaft; 3, 6 - rods; 4 - valve housing; 5 - power cylinder; 7 - fluid feed line.
Key: (a) to the tank; (b) cock; (c) from the pump.

A feel device is usually made so that it creates for a pilot control resistance corresponding to the sensations customary for him in different flight regimes in the subsonic region. The simplest type of feel device is a spring. Figure 12.8 shows a diagram of an irreversible booster control with a spring feel device which varies the load on the control with a change in the impact pressure and with a trimmer effect mechanism. For example, with an increase in impact pressure $q=(\rho V^2)/2$ ratio a/b decreases, rocker 2 is displaced upward and the forces on the stick from the load mechanism increase. The trimmer effect mechanism is a system of springs connected with the control whose tension is varied by employing a conventional button or trim tab control handle, which affects the force on the control just as does trim-tab deflection (the trim tab in this case is not necessary).

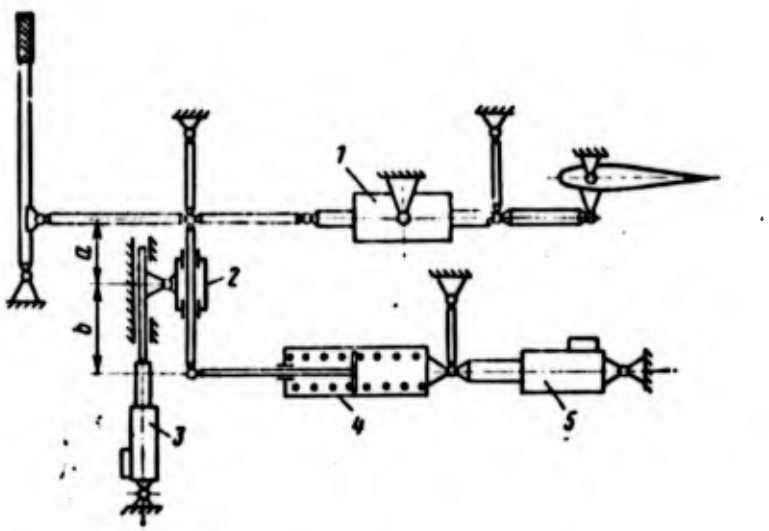

Figure 12.8. Diagram of a control line with an irreversible hydraulic booster and a feel device: 1 - hydraulic booster; 2 - adjustable rocker; 3 - electrical mechanism; 4 - spring loader - load imitator; 5 - electrical trimmer effect mechanism.

Let us examine the schematic diagram (Fig. 12.9).

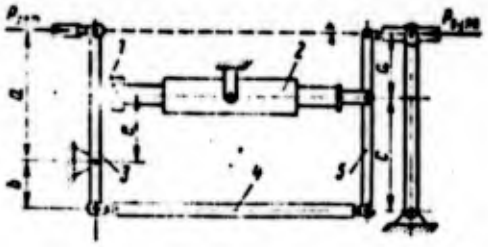

Figure 12.9. The inclusion of a hydraulic booster in accordance with the reversible setup.

A hydraulic booster consists of a distributor 1 and a power cylinder 2. The system of levers 3, 4, 5 ensures the transmission to the control of a portion of the force from the hinge moment of the control surface characterized by the magnitude of the amplification factor.

Amplification factor i is the magnitude which shows, by how many times with a given $M_ш$ the force on the control with the booster switched off is greater than the force on the control with the booster working. For the setup shown in Fig. 12.9,

$$i = \frac{a}{b} \cdot \frac{c}{d}.$$

It is possible to vary magnitude i, by varying e. When e=0, a=d, b=c, i=1. In the designs of reversible booster systems with hydraulic amplifiers the magnitude of the amplification factor is 2-10.

Irreversible booster systems are especially promising for supersonic aircraft. Their application is necessary, when the compressibility of air can strongly influence the magnitude and the sign of the hinge moment.

As was shown in chapter 11 the required power of a hydraulic drive is expressed by the formula

$$N = \frac{pQ}{7500} \text{ hp},$$

where p - is the average working pressure, kgf/cm^2; Q - is the required feed, cm^3/s.

For an irreversible booster control system the required feed is determined by the formula

$$Q = \frac{M_ш \omega}{p\eta}.$$

For a reversible booster control system taking into account the energy applied by the pilot, the required feed is determined by the expression

$$Q = \frac{M_ш \omega}{p\eta} \cdot \frac{i-1}{i},$$

where ω - is the required angular rate of deflection of the control surface, 1/s; η - is the efficiency of the entire system; $M_ш$ - is the hinge moment, kgf·sm.

§ 4. HELICOPTER CONTROL

1. The Concept of the Control of a Helicopter in Flight

Helicopter control is accomplished by varying the forces and moments acting on a helicopter in flight relative to all three of its axes.

They distinguish vertical control (along the y-axis) directional control (turning relative to the y-axis) transverse control (banking relative to x) and longitudinal (turning relative to z).

For varying the forces and moments which determine the position of a helicopter in space, the direction and the flight velocity it is necessary to vary the magnitude and the inclination of the rotor thrust force.

The magnitude of the thrust vector is changed in the case of varying the collective pitch, the inclination of the vector of this force is varied in the case of a cyclic change in the pitch of the rotor (successive variation in blade pitch with respect to azimuth).

During cyclic variation in pitch the thrust of the blade and its moment relative to the flapping hinge is periodically changed. This leads to a change in the flapping motions (flapping motion due to a cyclic variation in pitch is imposed on the flapping motion due to unsymmetric flow) and to the (backward and sideward) tilting of the axis of the cone of rotation of the rotor. In this case deviation in the thrust force vector T occurs (Fig. 12.10). Its vertical component yields lift Y which balances gravitational force G, and the horizontal component - yields the thrust P for the motion of the helicopter in the assigned direction. Moment of force T relative to the center of gravity of a helicopter causes its turning.

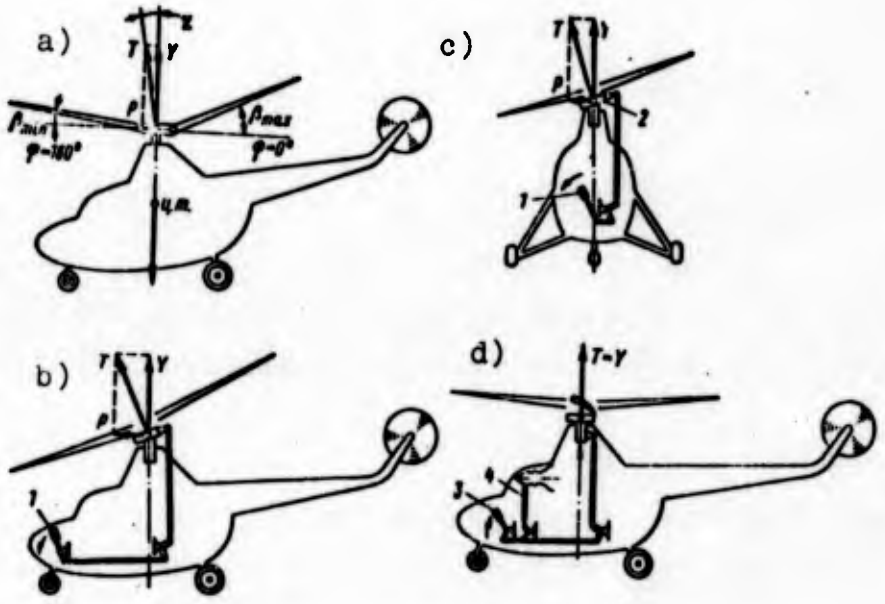

Figure 12.10. Helicopter control: a) thrust force and flapping angles; b) longitudinal control; c) transverse control; d) helicopter lift: 1 - cyclic-pitch stick; 2 - cyclic-pitch control; 3 - collective pitch-throttle stick; 4 - engine control rod.
Key: (a) c.g. (center of gravity).

The forces in question correspond to the case of the forward flight of a helicopter.

The collective and cyclic changes in pitch, and consequently, in the magnitude and the direction of the thrust force of the rotor

are accomplished with the aid of a special unit - the cyclic-pitch control.

2. Design Characteristics and the Operating Principle of the Rotor Cyclic-Pitch Control

Cyclic-pitch control was invented in 1910 by B. N. Yur'yev, the creator of the first Soviet helicopter design.

Cyclic-pitch control of the swashplate type has received the greatest application.

The basic parts of cyclic-pitch control are shown in Fig. 12.11a. With the aid of the collective pitch-throttle stick 14 and the control line components 11 and 3 collective pitch slider 2 together with the fixed 5 and mobile 4 swashplates of the cyclic-pitch control move upward or downward. In this case rods 7 connected with the blades move, equally increasing or decreasing the setting angles of all the blades, which leads to a change in the magnitude of rotor thrust. A change in thrust in a given case is employed for moving the helicopter upward or downward (see Fig. 12.10d).

Upon the deflection of control stick 13 (the "cyclic-pitch stick") the fixed 5 and mobile 4 swashplates of the cyclic-pitch control turn around the axis of the universal joint (Fig. 12.11). The mobile swashplate, turning together with shaft 1 and having the slope of the plane of rotation, via guides 8 causes repeated turning of the blades relative to their longitudinal axes in each revolution of the rotor. Each blade varies its pitch cyclically.

Let with the aid of control stick 13 and control line components 10 and 3 the plane of the swashplates be deflected forward in the direction of helicopter motion (see Fig. 12.11a, b). Then from an azimuth of 0° to 180° the rods move downward and the blade pitch is decreased; from an azimuth of 180° to 360° the rods move upward and the pitch is increased.

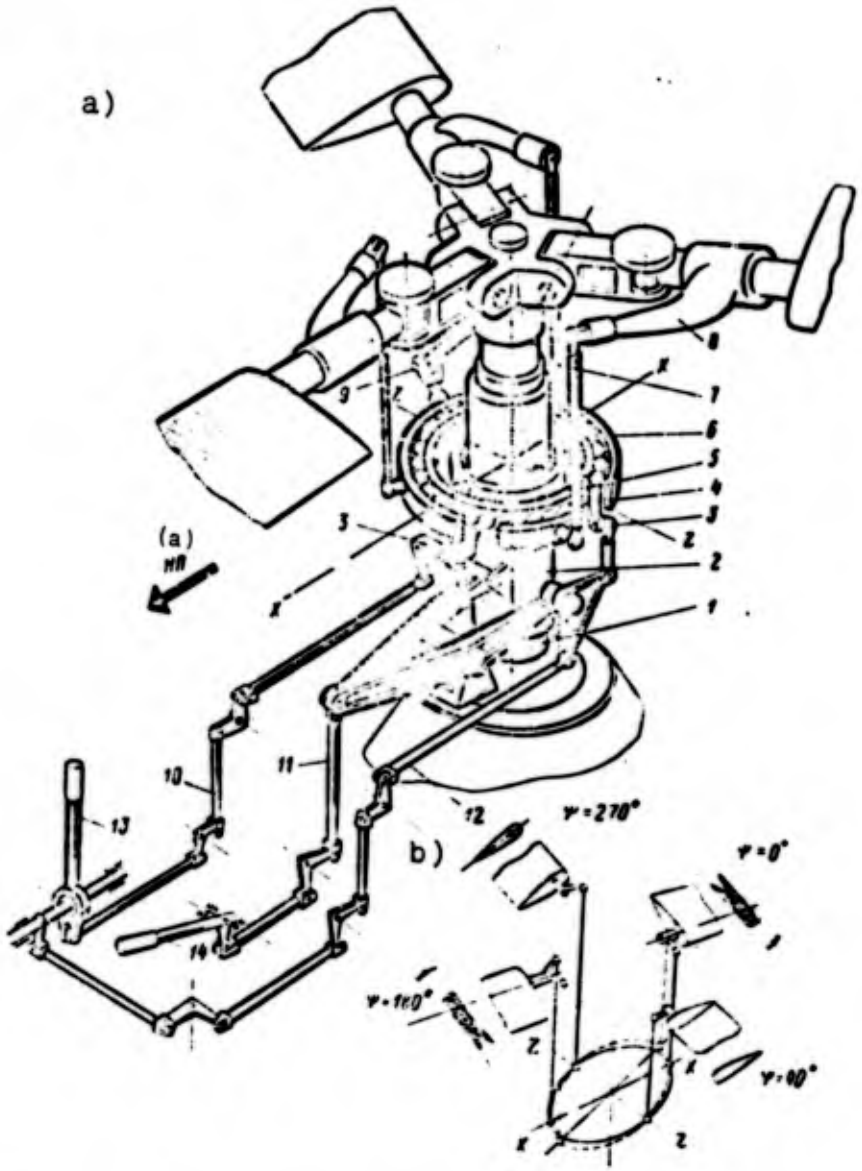

Figure 12.11. Cyclic-pitch control of the rotor hub: a) design; b) schematic diagram. Key: (a) NP (neutral plane).

As a result of the cyclic change in pitch the axis of the cone of the blades is inclined in the direction of minimum pitch. In this case the rotor rod is inclined and a thrust component directed forward appears, which balances the parasite drag and creates longitudinal motion of the helicopter.

With the aid of cyclic-pitch control it is possible to incline the rotor rod in any direction and to realize control of the

helicopter both in the longitudinal (see Fig. 12.10b), as well as in the transverse directions (Fig. 12.10c).

3. Design Characteristics of Single-Rotor Helicopter Control Systems

An entire helicopter control system can be represented in the form of four circuits independent of one another which ensure longitudinal, transverse and directional control, and also control of the magnitude of rotor thrust (displacement of the helicopter upward and downward).

These circuits constitute the main control system of a helicopter. The remaining control units (landing gear wheel braking, main rotor and tail rotor brake control, etc.) are called the supplementary control system of a helicopter.

Included in a main helicopter control system as on an aircraft are the following: the controls on which the pilot acts in order to change the flight regime (the cyclic-pitch stick, the collective pitch-throttle stick, the pedals), and the control line.

Figure 12.12 depicts a standard setup of the control system of a single-rotor helicopter. The control of the cyclic and the collective variation in pitch (longitudinal, transverse control and control of the movement of the helicopter upward and downward) was examined earlier.

Directional control of a single-rotor helicopter is accomplished by varying the thrust of the tail rotor by deflecting pedal 4 of the foot controls.

The directional control line is made so that when the pedals going to the tail rotor are not moved the control line is not loaded.

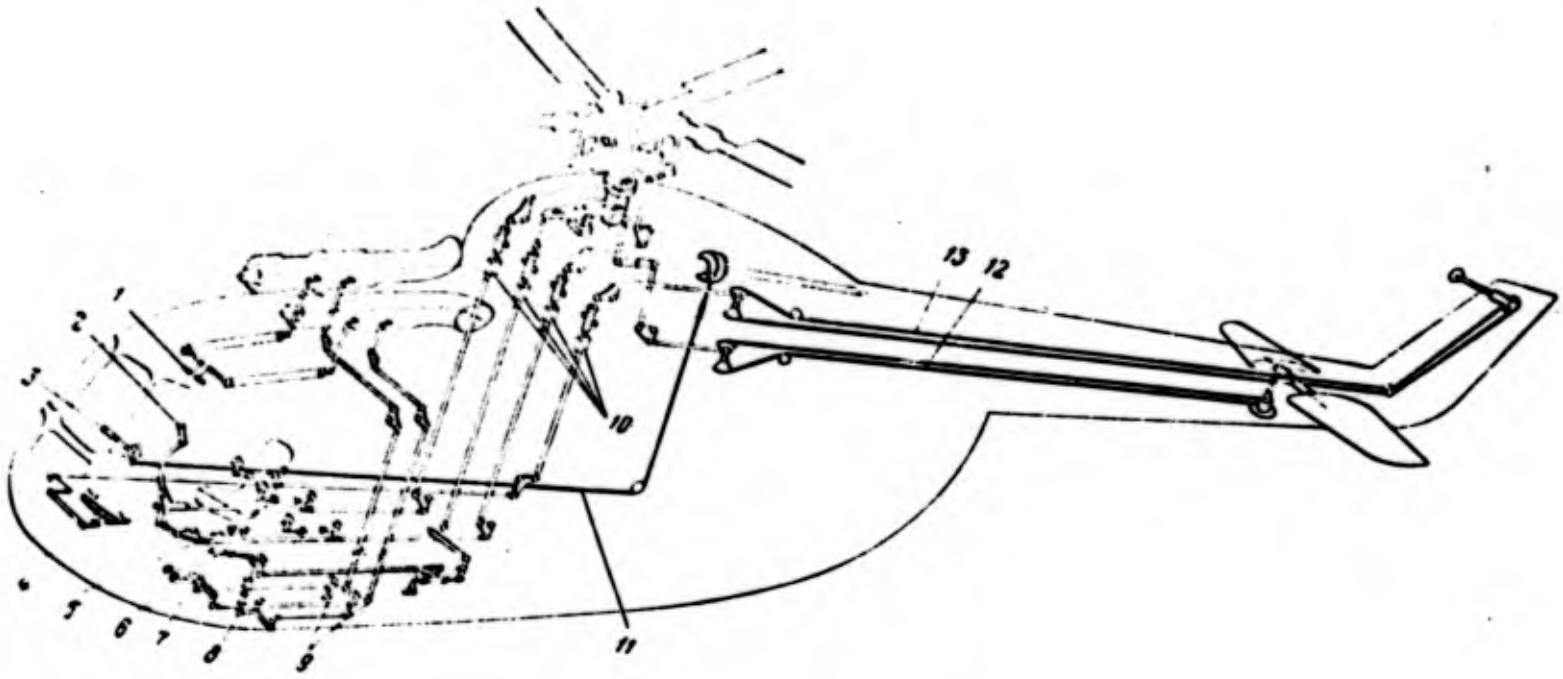

Figure 12.12. Control setup of a single-rotor helicopter: 1 - lever for stopping the engine; 2 - cyclic-pitch stick; 3 - knob for controlling the braking of the rotor; 4 - pedals; 5 - knob for controlling the fire cocks; 6 - collective pitch-throttle stick; 7 - lever for separate engine control; 8 - hydraulic engine control booster; 9 - differential mechanism for separate engine control; 10 - hydraulic control system boosters; 11, 12, 13 - cable lines for controlling the rotor brake, the stabilizer and the tail rotor.

This is achieved by installing a self-braking rotor couple directly on the rotor hub. When moving the pedals it is necessary for the pilot to overcome the force from the hinge moments of the tail rotor blades and the friction force in the rotor couple.

Considerable forces determined by the hinge moments of the blades act on the control elements. Thus, at the present time almost all helicopters have hydraulic boosters 10 (as a rule, irreversible) in their control systems.

The hydraulic boosters are placed directly in front of the cyclic-pitch control: in this case the length of the power part of the control circuit will be minimum. The hydraulic boosters are fastened, as a rule, to the housing of the main reducer. As a result the high rigidity of their mounting necessary for eliminating control auto-oscillations is ensured.

The collective-pitch control of the rotor is accomplished by employing the collective pitch-throttle stick 6, connected with the helicopter engine power control system. This type of connection ensures the maintaining of the assigned rpm's of the rotor in the case of varying of the collective pitch. On the collective pitch-throttle stick this is a turning handle which makes it possible to carry out independent throttle control.

To improve the balancing characteristics of single-rotor helicopters the collective-pitch control is usually connected with the stabilizer control.

When irreversible hydraulic boosters exist in the control system the forces are not transmitted to the control stick.

For creating the necessary stick force gradient, and also for eliminating the forces from the stick in the case of different steady flight regimes flight spring loading devices and trimmer effect mechanisms can be included in the manual and foot control systems.

The requirement for maximum reliability is imposed on the hydraulic system of helicopter hydraulic boosters, since its malfunction would result in the total loss of helicopter controllability.

4. Design Characteristics of the Control of Twin-Rotor Helicopters with Transverse, Longitudinal and Coaxial Positioning of the Rotors

Just as for single-rotor helicopters all moments necessary for helicopter control are created by the rotors.

On a tandem-rotor designed helicopter the longitudinal control is accomplished cyclic variation in pitch, and also by differential variation in the collective pitch when the thrust of one rotor is increased, and the other is decreased.

Transverse control for helicopters with transverse positioning of the rotors takes place as a result of differential collective-pitch control.

On helicopters with transverse and longitudinal positioning of the rotors pedal deflection causes a differential change in the cyclic pitch of the rotors. The axes of the cones of rotation are deflected in different directions, forming the directional control moment.

Directional control of a twin-rotor helicopter with coaxial rotors is accomplished as a result of a differential variation in the collective pitch of the rotors. This leads to a variation in the reactive moments of the upper and lower rotors and the helicopter is turned in the direction of the effect of the greater reactive moment.

For purposes of ensuring flight safety the equipping of a helicopter with an autopilot and other means of automation which facilitate the pilot's work is acquiring great importance.

§ 5. SUPPLEMENTARY CONTROL SYSTEMS

Included among the supplementary control systems is the control of the high-lift devices and of the landing gear struts, of the wheel brakes, of trim tabs, etc.

Characteristic of the supplementary control systems are the short duration of the effect and irreversibility - the load acting on a unit being controlled, is not transferred to the controls. The pilot does not directly feel the resistance of the unit being controlled and thus does not sense its positions. In order for the pilot to know the position of a unit special indicators are installed.

The following requirements are imposed on the supplementary control system:

1) synchronization of the motion of parts of the split flaps, the flaps, the air brakes, etc., positioned in different directions from the aircraft axis;

2) the rated destructive forces for the cock handles, etc., should not be less than 30 kgf;

3) the presence of emergency duplicating (redundancy) systems for landing gear lowering, for opening the landing high-left devices and for the braking system;

4) limitation of the time of the variation in the position of a unit being controlled;

5) in their extreme positions the landing gear and the high-lift devices should be held in place with locks. During flight also during motion over the ground of the systems for controlling the landing gear and the high-lift devices should be as unloaded as possible;

6) in rating the mechanisms for controlling the landing gear the operational g-forces are determined from the flight condition in turbulence, the safety factor is f=2.

The maximum flight velocity, at which it is permissible to carry out retraction and lowering of the landing gear or of landing high-lift devices is introduced into the calculation as the operational velocity.

The design elements of the control line of the supplementary control system are the same as for the main control system.

As a rule, the supplementary control system is driven by energy sources available on the flight vehicle.

Let us examine the characteristics of the employment of different types of power systems in the supplementary control systems.

A hydraulic system is most frequently employed for the remote control of the retraction and the lowering of landing gear, of the high-lift devices, of units of the equipment, etc. Hydraulic circuits were examined in detail in chapter 11.

A pneumatic system is rarely employed at present, in spite of the lesser weight as compared with hydraulic or electrical systems, the invariability of its properties during a change in temperature, the possibility of its functioning when the engine is inoperative. This system was examined in chapter 11.

Electrical systems of the supplementary control system are employed in conjunction with mechanical and sometimes hydraulic sections.

The operating principle of electromechanical systems consists in the fact that an electric motor by means of mechanical units

(reducers, frictional coupling clutches, transmissions, helical or worm gears, sometimes by means of a cable line) is related with the units being controlled.

The advantages of the electrical systems of the supplementary control system are: the simplicity of control, the great possibilities for automating control, the low dependence of the properties of the system on low temperatures.

The deficiencies are the complexity of design and the great weight.

CHAPTER 13

RELIABILITY, DURABILITY AND DESIGN SERVICE LIFE OF FLIGHT VEHICLES

§ 1. VARIATION IN THE STRUCTURAL STATE OF FLIGHT VEHICLES UNDER OPERATING CONDITIONS

The structural state of flight vehicles changes with the passage of time.

Changes occur more intensely during flight operation; however, they also occur when flight vehicles are parked or in storage. Thus, for structural components along with service life which determines the permissible operational duration expressed in flight hours or the number of flights, in a number of cases the maximum calendar service life is ascertained.

1. The Causes and the Manifestations of Variations

Let us examine the basic factors which bring about variations in structural state, and their consequences.

The multiple repetition of loading effects causes:

the appearance and the development of fatigue cracks, wearing of movable joints;

the formation of gaps, the weakening of riveted seams and joints which were made with great tightness (negative allowance).

Thermal effects cause:

the appearance of the thermal stresses in statically indeterminable structures which combine with stresses due to conventional loads and act in the same way as they do;

a reduction in the strength of materials, metal creep at high temperatures, brittleness at low temperatures.

Physicochemical effects of the environment cause:

progressive corrosive failure of materials, a reduction in the cross sections of structural elements;

a reduction in strength, especially under alternating loads.

2. Operational Strength, Reliability and Durability

An examination of the effect of operation on structural state shows that the duration and the conditions of operation mainly affect strength. Structural strength determined by taking into account the conditions of operation and its duration is sometimes called operational strength.

The characteristics of operational strength are a function of the history of the loading of an airframe structure during the time of its service life. Figure 13.1 explains this. It shows the random process of the variation in operational load S acting on a structure whose strength taking into account the effect of its loading history is characterized by the random functions U (the beginning of the development of cracks) and R (failure).

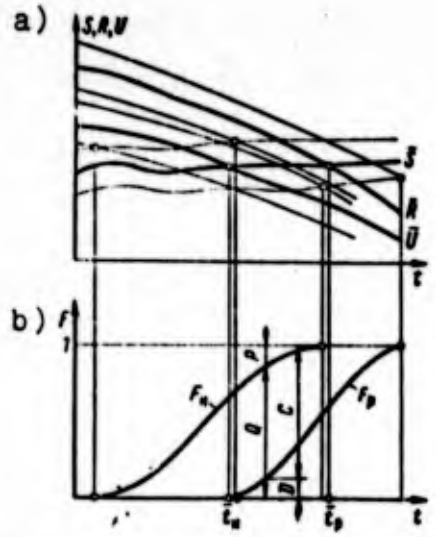

Figure 13.1. The effect of loading history on the characteristics of operational strength.

Figure 13.1a shows the mathematical expectations $\bar{S}$, $\bar{U}$, $\bar{R}$ and the dispersion boundaries (which correspond for example, to values of probability density function 0.99). of processes S, U, R.

If function U(t) is mainly defined by the properties of the material and by the form of concentrator, then the connection of the element in which the crack is developing, with the remaining structure greatly affects the form of function R(t).

The following distribution functions (Fig. 13.1b):

$$F_{\text{н}} = P\{S \geqslant U\} = Q(t);$$
$$F_{\text{р}} = P\{S \geqslant R\} = D(t)$$

characterize the probability of the breakdown of the structure in the time interval from 0 to t.

Here Q(t) - is the probability of the onset of the beginning of cracking; D(t) - is the probability of complete failure.

In accordance with this, function P(t)=1-Q(t) characterizes the reliability of the structure, and function C(t)=1-D(t) is a characteristic of the durability of the structure.

Durability - is the capacity of a structure after the beginning of failure over the course of a specific time period to work under operating conditions.

In the case of a specific t the corresponding value of ordinate R represents the level of operational strength, and intervals $\bar{t}_н$-t and $\bar{t}_р$-t - are the average values of the residual longevity up to the beginning and up to the end of failure, which the structure in question possesses after service life t.

Value $\bar{t}_р$-$\bar{t}_н$ - is the average time period of durability of the structure, over the course of which its carrying capacity is retained.

3. Service Life of a Structure and Current Evaluation of Its State

Safe service life of a structure with increased durability. In creating aviation designs the requirement for ensuring safe service life is realized. In accordance with it within the limits of a service life which does not exceed the established general technical lifetime $\tau_{рес}$, structural failure should not begin. This condition is written in the following manner:

$$\tau_{рес} = \frac{\bar{t}_н}{\eta_{рес}},$$

where $\eta_{рес}$>1 - is the coefficient of reliability.

It should be fulfilled with a high level of reliability P.

Lifetime is measured by the number of flight hours or by the number of flights. The expenditure of lifetime is estimated with these units. The inadequacy of this method of measurement is connected with considerable differences in the operating conditions of individual flight vehicles.

The dispersion of the characteristics of operational strength is determined both by these differences and the heterogeneity of the properties of the different models of the design itself. This

leads to the fact that there exists, although small, a probability Q of the appearance of the beginning of structural failure during a service life which does not exceed the lifetime.

Therefore it is also necessary to impose on a structure a requirement for increased durability which is expressed for the parts of the airframe by a slow grow in the fatigue cracks and by the prolonged retention of a sufficiently high level of durability C.

This requirement can be fulfilled, by employing statically indeterminable, in particular, monocoque designs, and by employing special design procedures which ensure a limitation on the growth cracks and the possibility of their development.

The period of durability of a structure after the beginning of failure chracterized by $\bar{t}_p - \bar{t}_н$ (see Fig. 13.1) should be sufficient so that a crack does not have time to develop to failure and can be detected in the next inspection. Thus, the interval between inspections or for parts of a design which are highly inaccessible for purposes of inspection the inter-repair lifetime should be less than period of durability

$$\tau_0 = \frac{\bar{t}_p - \bar{t}_н}{\eta_0},$$

where $\eta_0 > 1$ - is the coefficient of reliability.

Evaluation of structural state. Until recently the basic criterion for replacing units in a flight vehicle structure was the accrued operating time of the lifetime established for them.

The determination of the real state of a unit can make it possible to prolong its service life beyond the limits of its lifetime, if signs of the failure of the structure have not manifested themselves.

For units of the airframe, the general and inter-repair lifetime of which is determined by the operational strength, current evaluation of the level of their strength as a criterion of their state is necessary.

For this type of evaluation inspections of the units are employed for the purpose of detecting fatigue cracks, various manifestations of wear, corrosion and other signs of defective structural state.

Investigations are being conducted with respect to the creation of special indicators which note the approach of fatigue failure.

§ 2. BASES FOR DETERMINING THE FATIGUE LIFETIME OF A STRUCTURE

Conventional stress analysis ensures the determination of the structural dimensions with respect to the condition of strength under the effect of large, but single or rarely repeated loads.

Operational experience, especially of those who have serviced passenger aircraft for a long period of time, has shown that the maximum service life of an airframe structure (general technical lifetime) is determined by metal fatigue. To substantiate the fatigue lifetime it is necessary to evaluate the effect of smaller, but of frequently encountered loads.

1. Strength Characteristics in the Case of Cyclic Loading

These types of characteristics (Fig. 13.2) are those in the diagrams σ-N (maximum stress - destructive number of cycles) obtained during tests with the cyclic load depicted by the diagram (Fig. 13.3) of σ-τ (stress-time). The <u>fatigue limit</u> σ_w - is the stress at which a model can endure any number of load changes (it is assumed in practice, that this occurs, if the model endures $N>10^7$ without failure).

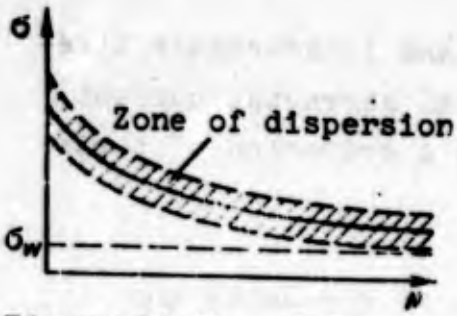

Figure 13.2. Fatigue diagram.

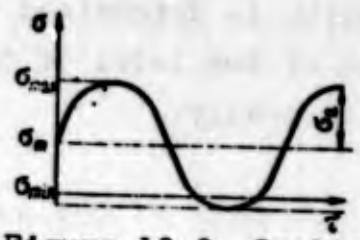

Figure 13.3. Cyclic load.

Since aviation structures work in a range of stresses greater than the fatigue limit the stress at which failure occurs after a specific number of cycles can be called by the limit of cyclic strength at a number of cycles N. The magnitude of this stress depends:

on the properties of the material (Fig. 13.4);

on the cycle frequency. For a lesser frequency the limit of cyclic strength of less (in accordance with the loading conditions in operation the frequency in the testing of aviation structures is taken within the limits of from 3 to 25 cycles/min);

on the type of cycle. For a symmetrical cycle the limit of cyclic strength is less.

As the initial experimental data for calculating the effect of repeated loads diagrams (Fig. 13.5) are employed at coordinates K-N, where $K = \sigma_{max}/\sigma_в$ - is the coefficient of load. The diagrams are plotted from the results of tests carried out with different types of cycles on models similar to the elements of

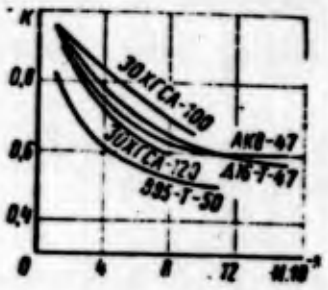

Figure 13.4. Fatigue diagrams (next to the designation of the material is shown the ultimate strength in kilograms per square millimeter).

aircraft designs with respect to the nature of their operation under fatigue loads.

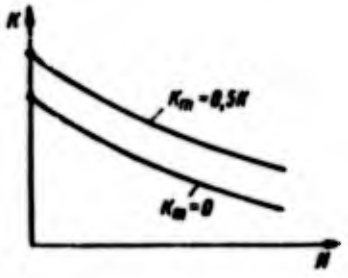

Figure 13.5. Fatigue diagrams for symmetrical ($K_m=0$) and pulsating ($K_m=0.5K$) cyclic loads.

In evaluating the effect of different factors on fatigue life it is necessary to consider the following:

experimental studies show that the fatigue life is lower, if the loads are repeatedly static loads, i.e., they change slowly with time;

the application of acoustic loads on slower basic oscillations also leads to a reduction in longevity.

2. Characteristics of the Repeated Loading of an Airframe Structure

The level of the loads and the number of their repetitions are determined mainly from statistics (maneuverable and landing loads, loads during flight in turbulence).

The loading characteristics of a structure are found on the basis of the following aspects.

1. With sufficient rigidity of an airframe design the loads on it can be evaluated by the g-force at the center of gravity; the most important is g-force n_y.

2. The strength of an aircraft design under repeated loads is determined by strength of its weakest element.

Let us assume that the dimensions of an element are taken in accordance with the strength requirements from a failure rating at a g-force of n^p, i.e., in accordance with condition $\sigma^p \leq \sigma_в$, with a coefficient of excess strength of m, i.e., $\sigma^p = \sigma_в/m$.

3. We will consider that the acting stresses in this element depend only on the magnitude of n_y. This corresponds to the assumption concerning the invariability of the nature of the distribution of loads acting on a flight vehicle.

Then at g-force n_{yi} the maximum stress in the element is

$$\sigma_i = \frac{n_{yi}}{mn^p} \sigma_в.$$

The characteristic of the load level - the coefficient of load is connected with the g-force by the expression

$$K_i = \frac{n_{yi}}{mn^p}.$$

Statistics show that the negative and positive increases in g-force during flight in turbulent air are positioned approximately symmetrically relative to $n_y = 1$.

In this case the average coefficient of the load of a cycle is constant and is equal to

$$K_m = \frac{1}{mn^p}.$$

The laws of the variation in g-forces with time during maneuvering flight are close to pulsating, when the average coefficient of the load of the cycle is

$$K_m = 0{,}5K = 0{,}5\frac{n_{yi}}{mn^p}.$$

The buildup of fatigue damages in a material is connected with the variable directions of the deformations of the structural

elements caused by the transitions of the load through extreme values.

Thus, the numbers of the repetitions N during the specific time of the maximums of the function of variation in g-force n_y with τ, lying within the specific ranges of its values are taken as the characteristics of the recurrence of fatigue loads.

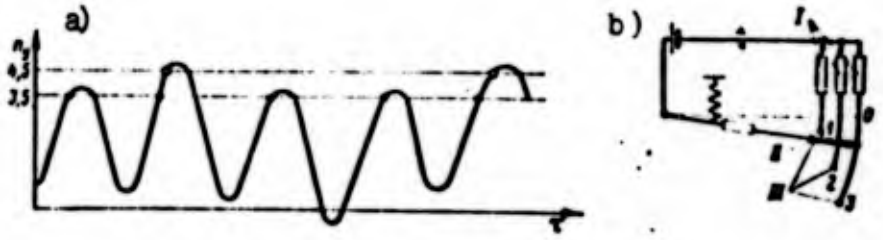

Figure 13.6. Determining the number of exceedings of the g-force level: a) from a curve of variation in g-force; b) by means of a g-force counter; I - pulse counters; II - sliding contact; III - points of the breaking of contact at g-forces 1, 2, 3.

The data on the number of exceedings of overload level n_{yi} during a specific period (for example, during an hour of flight operation) can be found from a recording obtained on an accelerograph (Fig. 13.6a). The number of cases when, for example, the g-force exceeds the value 3.5 is equal to the number of points marked on the diagram with small black circles. The exceeding of level 4.5 is noted by small white circles.

It is not difficult to see that the number of repetitions of maximums n_y in Fig. 13.6a lying in the interval which corresponds to $n_y=4$ (between 3.5 and 4.5) is equal to the difference in the numbers of the exceedings of the levels of the interval boundaries

$$\Delta N_4 = N_{3,5} - N_{4,5}.$$

For measuring the number of exceedings of g-forces a g-force counter is also employed.

For example, let us present a diagram of a g-force counter (Fig. 13.6b) which considers positive g-forces. Included in it are electrical pulse counters which operate during the breaking of the electric current circuit.

The g-forces during the flight operation of a flight vehicle are characterized by the statistical integral curve of the exceedings of overload level $H\text{-}n_y$ (Fig. 13.7a) during a specific time τ.

Shown on it is the determination of ΔH_i - the number of repetitions of the g-force maximums lying in interval i with an average value of n_{yi}, having a width Δn_y, with respect to $H\text{-}n_y$.

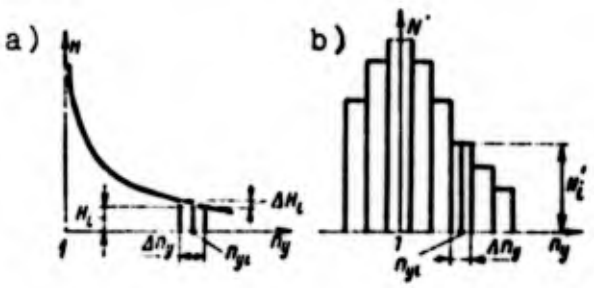

Figure 13.7. Characteristics of the recurrence of g-forces: a) the integral curve of the exceedings of overload level n_y; b) diagram of the repetition frequency of the maximums for different levels of n_y.

Diagram N' of the repetition frequency during one hour of values of the maximums of g-forces n_y lying at different intervals Δn_y (Fig. 13.7b) $N_i=\Delta H_i/\tau$ is plotted on curve $H\text{-}n_y$.

3. Longevity in the Case of Alternating Repeated Loads

The calculation of the longevity of an aircraft design under the effect of repeated loads is carried out on the basis of the linear theory of the summation of damages.

At the basis of this theory is the hypothesis concerning the fact that structural failure under the effect of repeated cyclic loads begins when a specific magnitude of deformation energy

characterized by the magnitude of specific work A_p (kgf·cm/cm^3) is supplied in irreversible form to the most stressed structural element.

If with each form of cyclic load the buildup of fatigue damages depends linearly on the number of cycles, a failure condition as a result of loading m with different cycles can be written in the following form:

$$\Sigma N_i a_i = A_p,$$

where a_i - is the energy supplied in irreversible form during one cycle of the type i; N_i - is the number of cycles of the type i.

During loading with one form of cyclic load i before failure which occurs at the number of cycles $N_{i\,p}$,

$$N_{ip} a_i = A_p.$$

Hence $a_i = \frac{A_p}{N_{i\,p}}$.

After substituting this expression for a_i in the failure condition, we will obtain

$$\Sigma \frac{N_i}{N_{ip}} = 1.$$

Experiments show that this theory can be employed for an approximate evaluation of longevity in the case of alternating repeated loads; however, the law of summation of damages is better represented in the following form

$$\Sigma \frac{N_i}{N_{ip}} = \alpha.$$

Magnitude α has considerable variance and greatly depends on the sequence of the application of loads of different levels (for

example, in accordance with different experiments for structural steels α=0.5-3).

In determining the longevity of aircraft designs, by taking into account the random nature of load alternation, it is assumed that α=1, and the variance is considered by the coefficient of reliability η.

4. The Order of Calculating the Fatigue Service Life of a Structure

The initial data for calculating fatigue service life τ are:

for the element in question (the weakest) the dependence of K_i on n_{yi};

diagram N'-n_y (the sign of the g-forces is identical) (see Fig. 13.7b);

diagram of K with respect to N (see Fig. 13.5) of the element in question for K_m, which corresponds to the loading conditions for which curve N'-n_y was obtained.

The calculation is carried in the following sequence.

1. For a series of values n_{yi} lying at intervals Δn_y, the numbers of loading N_i' during 1 h which correspond to g-forces n_{yi} are found from the diagram of the repetition frequency: $N_i'=\frac{N_i}{\tau}$ (τ is still unknown).

2. The values of K_i are calculated for the same n_{yi}.

3. The values of $N_{i\ p}$ are found from diagram K-N for each K_i.

4. The values of $\frac{N_i}{N_{i\,p}}$ are determined for each value of K_1 which exceeds $K=\frac{\sigma_w^*}{\sigma_в}$.

5. Then $\Sigma\frac{N_i'}{N_{i\,p}}$ is calculated. Since in accordance with the law of the summation of damages during period τ the following condition should be fulfilled

$$\Sigma\frac{\tau N_i'}{N_{ip}}=a,$$

then the average value of the fatigue service life is

$$\tau=\frac{a}{\Sigma\frac{N_i'}{N_{ip}}}.$$

5. Evaluation of Design Lifetime

In evaluating the lifetime of a structure it is necessary to take into consideration the great dispersion of the experimental data on the connection between N_p and K.

If there is a differential law p of the distribution of the values of N_p with a specific form of loading cycle K (Fig. 13.8), then the probability that N_p will be $\geq N_{p\,min}$, is equal tc

$$P=\int_{N_{p\,min}}^{\infty}pdN.$$

If it is assumed that the dispersion corresponds to the

---

*Let us approximately disregard the effect of stresses less than fatigue limit σ_w on the buildup of the fatigue damages.

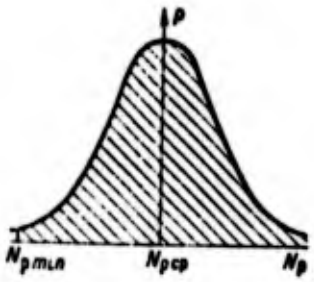

Figure 13.8. Differential distribution law N_p.

normal distribution law (Gauss'), then 99.7% of the test results will lie in the range ±3s of the average value of N_p, where $s=\sqrt{\frac{\Sigma(N_p-N_{p\ cp})^2}{n-1}}$ - is the standard deviation; n - is the number of tests.

Assuming a probability of failure of 0.3%, it is possible to take as the guaranteed number of cycles, which the structure can endure without failure, $N_{min}=N_{p\ cp}-3s$.

If it is possible to assume ratio $\frac{N_{p\ min}}{N_{p\ cp}}$ identical for different values of K, then the minimum coefficient of reliability, which must be introduced in ascertaining the lifetime of the structure is,

$$\eta_{min}=\frac{N_{p\,cp}}{N_{min}}.$$

For evaluating a number of negligible facts (in the calculation - an inaccuracy in the law of summation, the possibility of loads not encompassed by statistics, in the experiment - a limited number of tested samples, the difficulty for a systematic inspection of the structure) an additional factor $\eta'>1$ is introduced into the coefficient of reliability. Then $\eta=\eta_{min}\eta'$.

Finally, the lifetime is determined with the following formula

$$\tau_{rec}=\frac{\tau}{\eta}.$$

6. Fatigue Testing of Structures

The approximate calculation examined above is necessary in designing a structure, since it makes it possible to evaluate the

effect of a number of factors on fatigue life: values n^p, m, the characteristics of the material and the loading conditions.

To be certain of the fact that there are no structural and technological defects in a structure which could cause its premature failure, experimental models of the structure should be subjected to a certain minimum number of tests to evaluate the effect of repeated loads.

These types of tests, for example, could be the following:

testing the wing structure with a pulsating cyclic load which corresponds to 0.5 n_A^p;

testing of the landing gear by repeated dropping on an impact tester with a g-force which corresponds each time to the absorption of the operational energy assigned by the stress standards.

The determining of fatigue lifetime is mainly based at present on the testing of a full-scale structure with repeated loads simulating the conditions of its loading in operation.

Loads are applied to the structure in cycles in which loads are included which act on the structure over the duration of a typical flight (also including takeoff, landing and taxiing). Figure 13.9 gives an example of a cycle program which corresponds to a typical flight for the structure of the "Caravelle" aircraft.

The destructive number of cycles N_p is the number of flights which leads to structural fatigue failure. The corresponding flying time in hours - is a fatigue life of $\tau = N_p \tau_n$.

In determining lifetime with the formula

$$\tau_{рес} = \frac{\tau}{\eta}$$

the magnitude of η is taken larger, the lesser the number of tested models of the structure.

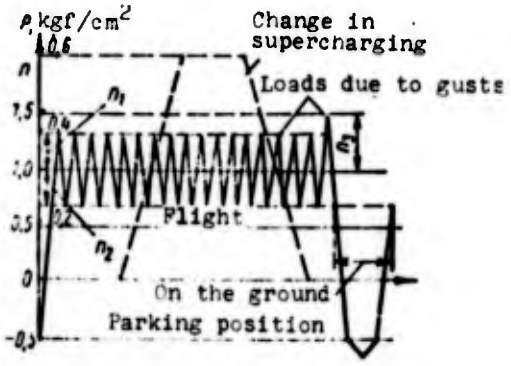

Figure 13.9. Diagram of the loading program of the "Caravelle" aircraft during one cycle which corresponds to a typical flight. Here n_1 - is a g-force which corresponds to an ascending gust $W_{э\phi}$=3 m/s; n_2 - is a g-force which corresponds to a descending gust $W_{э\phi}$=3 m/s; n_3 - is a g-force which corresponds to the ascending gust $W_{э\phi}$=5 m/s; ($W_{э\phi}$ - is the effective velocity of a hypothetical gust which causes the same g-force as a real gust).

The duration of a test cycle is considerably shorter than the duration of an actual flight $\tau_п$; however, full-scale fatigue tests take up much time and they are continued even after the introduction of the flight vehicle into operation.

The testing of designs which come from the factory, are subsequently supplemented by the testing of models which have accrued operating time (flying time) in operation.

The continuation of testing gives the grounds for a periodic increase in the initially established value of lifetime. In this case it is necessary that the lifetime indicated by the tests which have been conducted and ensured by the necessary changes in the design sufficiently exceed the level of flying time of the type of flight vehicles being tested.

§ 3. THE EFFECT OF A KINETIC HEATING AND COOLING OF A STRUCTURE

In projecting the designs of contemporary flight vehicles it is necessary to take into account their kinetic heating in flight at great velocities.

Kinetic heating leads to a decrease in the strength and the rigidity of the structure and to the limitation of its service life. It causes thermal stresses in the structure, a decrease in the physico-mechanical properties of the material and also creep.

1. Maximum Velocities with Respect to Kinetic Heating

For supersonic aircraft kinetic heating can limit the greatest flight velocities.

It is possible to approximately estimate kinetic heating by the temperature of the surface of a streamlined body in the stagnation region by employing the following formula:

$$T_{\text{торм}} = T\left(1 - r\frac{k-1}{2}M^2\right),$$

where T - is the air temperature (in degrees Kelvin); k=1.41 - is the adiabatic index; r - is the temperature recovery factor (for a laminar boundary-layer flow r=0.85; for turbulent flow - 0.88-0.89).

If we pose the condition of limiting velocity by the maximum stagnation temperature $T_{\text{торм.пред}}$=const, then expression $T_{\text{торм}}$ makes it possible to obtain the dependence of $V_{\text{пред. T}}$ on H.

Taking into account that V=Ma and the speed of sound $a=20.1\sqrt{T}$, we will obtain

$$V_{\text{пред.т}} = 20{,}1\sqrt{\frac{2}{r(k-1)}(T_{\text{торм}} - T)},$$

where T=f(H) is determined from the International Standard Atmosphere (ISA).

The temperature of heated structural elements, for example, sections of the skin in the zone of flow stagnation $T_{\text{общ}}$ differs from $T_{\text{торм}}$ and is determined by taking heat exchange with other adjoining parts of the design and with the external medium into account.

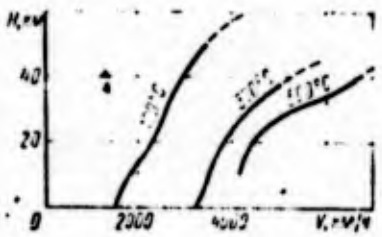

Figure 13.10. Limitation of flight velocities by kinetic heating of the skin.
Abbreviation: км/ч = km/h.

If the maximum permissible temperature for a structure is equal to $T_{\text{пред}}$, then the limitation of velocity is determined by the condition

$$T_{\text{общ}} = f(V, H) = T_{\text{пред}} = 273^\circ + t_{\text{пред}},$$

where $t_{\text{пред}}$ - is the maximum temperature in degrees Celsius.

Hence the dependence $V_{\text{пред } T}(H)$.

Figure 3.10 gives an example of these types dependences for the skin. The three curves correspond to $V_{\text{пред } T}(H)$ in the application of duralumin (100°C), titanium alloy (370°C) and stainless steel (500°C).

For increasing the values of $V_{\text{пред. } T}$ along with the application of heat-resistant materials it is also possible to use coatings and layers which retard the flow of heat to structural elements.

2. Thermal Stresses

The simplest example of the appearance of thermal stresses is given in Fig. 13.11a.

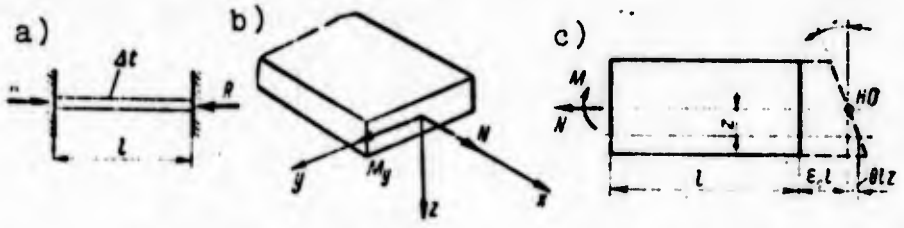

Figure 13.11. Diagrams explaining the appearance of thermal stresses: a) the appearance of reactions during heating; b) forces in the rod cross section; c) deformation of the rod ($\varepsilon_0 l$ - axial elongation; $\theta l z$ - elongation due to the turning of cross sections, $\theta = d\sigma/dx$, δ - is the angle of rotation of a cross section during flexure).

In the heating to Δt of rod rigidly supported at the ends, three types of deformations arise in it:

1) thermal deformation - elongation $\Delta l_t = \alpha \Delta t l$;

2) elastic deformation due to stresses $\sigma < 0$ caused by arising supporting reactions R,

$$\Delta l_t = \frac{\sigma}{E} l < 0;$$

3) plastic creep deformation under the effect of temperature and compressive stresses

$$\Delta l_p = \varepsilon_p l < 0.$$

Due to the rigidity of the supports the total strain is equal to zero

$$\Delta l = \Delta l_t + \Delta l_t + \Delta l_p = \alpha \Delta t l + \frac{\sigma}{E} l + \varepsilon_p l = 0.$$

Hence

$$\sigma = -E(\alpha\Delta t + \varepsilon_p).$$

At first $\varepsilon_p=0$ and thermal stress σ has the greatest value. In proportion to the increase in creep deformation the stress drops off.

Let us examine a more general case - the effect of temperature and creep on the stresses in a rod load with axial force N and flexural moment $M_y=M$ (Fig. 13.11b); the stressed state of a rod is linear $\sigma_x\neq 0$, $\sigma_y=\sigma_z=0$. In this case let us make the following assumptions:

a) the distribution of temperature t over the cross section does not depend on x; t=f(z) - the temperature reckoned from the value at which the thermal stresses are equal to zero;

b) in the temperature range in question the coefficients of linear expansion α for each material are constant, the values of E correspond to the values of t;

c) deformations obey the law of plane cross sections.

The stress at a point with coordinate z for any cross section sufficiently distant from the ends of the rod is found with the following formula

$$\sigma = \frac{E}{E_\phi F_{\text{рез}}}\left[N + E_\phi \int_{F_{\text{рез}}} (\alpha t + \varepsilon_p)\, dF_{\text{рез}}\right] + \frac{E_z}{E_\phi I_{\text{рез}}}\left[M + E_\phi \int_{F_{\text{рез}}} (\alpha t + \varepsilon_p)\, z\, dF_{\text{рез}}\right] - E(\alpha t + \varepsilon_p), \qquad (13.1)$$

where E_ϕ - is the value of E taken as the main value; ε_p - is creep deformation; z - is the coordinate of the point reckoned from the center of gravity of the reduced cross section; $dF_{\text{рез}}=(E/E_\phi)dF$.

Let us examine the derivation of this formula. According to the law of plane cross sections (Fig. 13.11c) $\Delta l=\varepsilon_0 l+\theta l z$; $\varepsilon=\Delta l/l=\varepsilon_0+\theta z$.

Moreover, $\varepsilon=\frac{\sigma}{E}+\varepsilon_p+\alpha t$.

Hence

$$\sigma = E\varepsilon_0 + E\theta z - E\varepsilon_p - Eat. \tag{13.2}$$

According to equilibrium conditions, we have:

$$\int_F \sigma dF = N, \tag{13.3}$$

$$\int_F \sigma z dF = M. \tag{13.4}$$

By substituting expression (13.2) in formula (13.3), we will obtain

$$\varepsilon_0 \int_F E dF + \theta \int_F E z dF - \int_F E\varepsilon_p dF - \int_F Eat dF = N.$$

Let us introduce the substitution

$$\int_F E dF = E_\phi \int_F \frac{E}{E_\phi} dF = E_\phi \int_{F_{\text{пед}}} dF_{\text{пед}} = E_\phi F_{\text{пед}}.$$

Since coordinate z is reckoned from the center of gravity of the reduced cross section, then $\int_F E z dF = E_\phi \int_F z dF_{\text{пед}} = 0$ and

$$E_\phi \varepsilon_0 F_{\text{пед}} = N + E_\phi \int_{F_{\text{пед}}} (at + \varepsilon_p) dF_{\text{пед}}. \tag{13.5}$$

In the same manner, by substituting expression (13.2) in formula (13.4), we obtain

$$E_\phi \theta I_{\text{пед}} = M + E_\phi \int_{F_{\text{пед}}} (at + \varepsilon_p) z dF_{\text{пед}}. \tag{13.6}$$

After determining from formulas (13.5) and (13.6) the values

of ε_0 and θ and after substituting them in expression (13.2), we will obtain formula (13.1).

As an example of the application of dependence (13.1), let us examine the determination of purely thermal stresses in a beam cross section (wing, rib, longeron or spar) with a temperature distribution symmetrical relatively to y (see Fig. 13.11b and Fig. 13.12). The values of E are constant within the limits of each element; thus integration is replaced by summation.

Let us assume $E_\phi = E_\Pi$ and $F_{прив} = 2F_п + \frac{E_c}{E_п}F_c$, then

$$\sigma_п = \frac{1}{2F_п + \frac{E_c}{F}F_c} E_п \left(2\alpha_п t_п F_п + \frac{E_c}{E_п}\alpha_c t_c F_c\right) -$$

$$- E_п \alpha_п t_п = \frac{E_c F_c}{2F_c + \frac{E_c}{E_п}F_c}(\alpha_c t_c - \alpha_п t_п) =$$

$$= \frac{E_п}{1 + 2\frac{E_п F_п}{E_c F_c}}(\alpha_c t_c - \alpha_п t_п). \qquad (13.7)$$

By analyzing formulas (13.1) and (13.7), it is possible to note the following conditions:

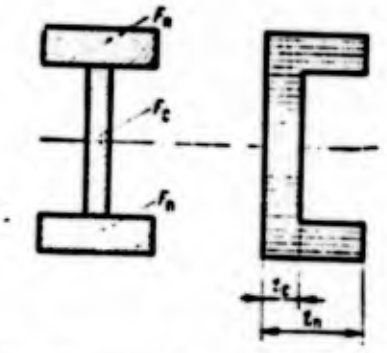

Figure 13.12. Temperature distribution over a rod cross section.

1. The thermal stresses are great in those cases when a structure is made from different materials, and in the warm-up period, when the non-uniformity of the temperature distribution over the cross section is great (Fig. 13.12).

2. It follows from formula (13.1) that temperature also affects the stresses due to loads, since a change in E causes changes in the nature of the stress distribution. The dependence of σ on z can be nonlinear.

3. It is evident from formula (13.1) that in connection with the increase in creep deformation the stresses vary with time.

The total stresses should be compared with the ultimate strength $\sigma_в^t$ found at the temperature in question and taking into account the duration of the time period at this temperature. As an example values of $\sigma_в$ are given for stainless chrome-nickel steel EYalT:

Temperature, °C.....	20	600	600	700	700
Time at the temperature, h...	0	0	100	0	100
Ultimate strength of EYalT steel, kgf/mm^2.....	66	40	25	28	14

3. Creep

Creep - is the phenomenon of an increase in plastic strain with the passage of time, which occurs under the effect of a constant or even a reduced load.

The creep curve obtained during tests takes the form shown in Fig. 13.13a.

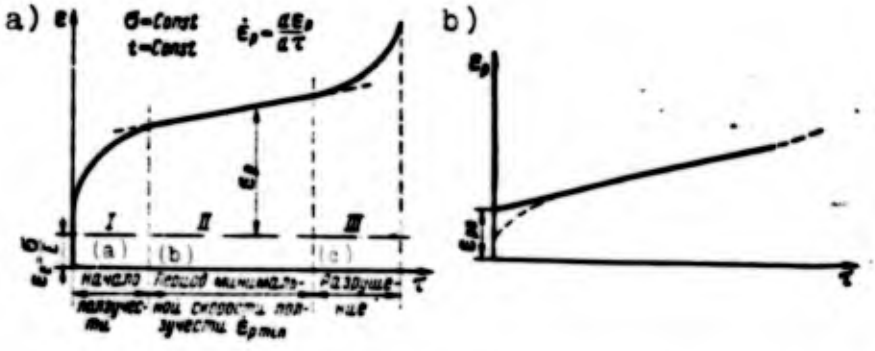

Figure 13.13. Creep curve: a) creep periods; b) schematization of the curve.
Key: (a) Beginning of creep; (b) Period of minimum creep rate $\dot{\varepsilon}_{p\ min}$; (c) Failure.

Metal creep manifests itself more intensely the higher are the values of ratios $t/t_{пл}$ and $\sigma/\sigma_в$, where $t_{пл}$ - is the melting point of the metal.

The characteristics of creep obtained from tests are:

σ_{τ}^{t} - is the rupture stress - the stress at which failure due to creep occurs during time τ;

$\sigma_{\varepsilon_p}^{\tau}$ - is the hypothetical creep limit - the stress at which during time τ the creep deformation attains the value ε_p.

When employing metal in a structure it is necessary that the following be within the limits of the service life:

a) creep deformation proceeds in the I and II zone (failure should not begin, i.e., it should be that $\sigma<\sigma_{\tau}^{t}$);

b) plastic strain does not exceed the limit permissible with respect to the conditions of the geometry of the component; usually ε_p=0.1-0.2% is taken as the limit;

c) the total structural deformation (for example, the change in wing profile) caused by creep in the components does not exceed the permissible deformation;

d) weakening of the joints made with negative allowance (relaxation of the negative allowance stresses) cannot occur.

The experimental creep curves or the empirical formulas obtained as a result of their processing are employed in the calculations as the initial data.

The minimum creep rate can be expressed by the empirical dependence

$$\dot{\varepsilon}_{p\,\min} = A\sigma^{n}e^{\alpha t},$$

where A, n, α - are coefficients which depend on the properties of the metal.

Within the limits of zone II it is possible to approximately represent the creep deformation by the expression (Fig. 13.13b)

$$\varepsilon_p = \varepsilon_{p0} + \dot{\varepsilon}_{p\,min}\tau,$$

where

$$\dot{\varepsilon}_{p0} = f(\sigma, t).$$

Relaxation of stresses. As an example let us examine structural creep which has prenegative allowance. Rigid flanges connected by a bolt are tensioned by a force of P. The rated setup of the joint is shown in Fig. 13.14. Pretightening of the bolt is characterized by relative negative allowance Δ - by axial displacement of the nut due to elongation of the bolt and compression of the flanges relative to the length of bolt shank l.

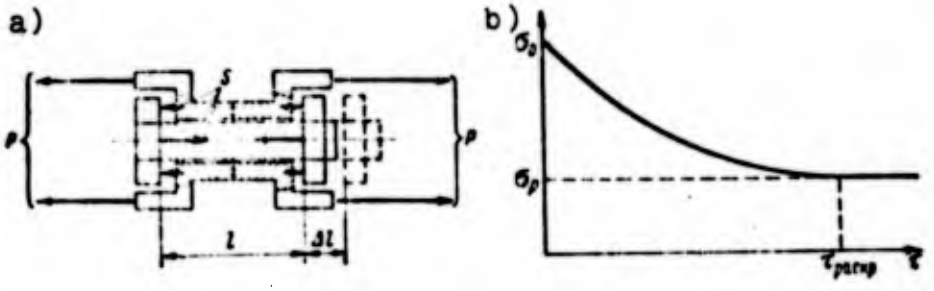

Figure 13.14. Joint with prenegative allowance: a) rated setup of the joint; b) relaxation of the tightening stresses.

A connecting bolt under the effect of tightening and force P is tensioned by force S.

The stress in a bolt shank is determined with the formula

$$\sigma_c = \frac{S}{F_c},$$

where F_c - is the cross-sectional area of the shank.

The relative change in the distance between the head and the nut is found with the expression

$$\varepsilon_c = \frac{\sigma_c}{E_c} - \Delta + \alpha_c t_c + \varepsilon_{p.c},$$

where α_c - is the coefficient of linear expansion of the shank material; t_c - is the shank temperature; $\varepsilon_{p.c}$ - is the creep deformation of the shank.

If the connection is tightened, force P-S<0 acts on the flange. The stress in the flange (compressive) is determined with the formula

$$\sigma_{фл} = \frac{P-S}{F_{фл}} = \sigma_p \frac{F_c}{F_{фл}} - \sigma_c \frac{F_c}{F_{фл}} = \frac{F_c}{F_{фл}}(\sigma_p - \sigma_c),$$

where $F_{фл}$ - is the cross-sectional area of the part of the flange between the faces of the nut and the bolt-head (shaded in Fig. 13.14a), to which force P-S is transmitted.

The stress in a bolt due to P is computed with the formula

$$\sigma_p = \frac{P}{F_c}.$$

The relative deformation of the flange is found with the expression

$$\varepsilon_{фл} = \frac{1}{E_{фл}} \cdot \frac{F_c}{F_{фл}}(\sigma_p - \sigma_c) + \alpha_{фл} t_{фл} + \varepsilon_{p\,фл},$$

where $\alpha_{фл}$ - is the coefficient of linear expansion of the flange material; $t_{фл}$ - is the flange temperature; $\varepsilon_{p.фл}$ - the creep deformation of the flange.

From the condition of the equality $\varepsilon_c = \varepsilon_{фл}$ we will obtain

$$\frac{\sigma_c}{E_c} - \Delta + \alpha_c t_c + \varepsilon_{p\,c} = \frac{1}{E_{фл}} \cdot \frac{F_c}{F_{фл}}(\sigma_p - \sigma_c) + \alpha_{фл} t_{фл} + \varepsilon_{p.фл}.$$

Hence

$$\sigma_c = \frac{1}{1+\frac{E_c}{E_{\phi л}}\cdot\frac{F_c}{F_{\phi л}}}\left[\frac{E_c}{E_{\phi л}}\cdot\frac{F_c}{F_{\phi л}}\sigma_p + E_c\Delta - \right.$$
$$\left. - E_c(\alpha_c l_c - \alpha_{\phi л} l_{\phi л}) - E_c(\varepsilon_{p.c} - \varepsilon_{p.\phi л})\right],$$

or after the transformations

$$\sigma_c = \sigma_p \frac{\frac{E_c}{E_{\phi л}}\cdot\frac{F_c}{F_{\phi л}}}{1+\frac{E_c}{E_{\phi л}}\cdot\frac{F_c}{F_{\phi л}}} + \frac{E_c}{1+\frac{E_c}{E_{\phi л}}\cdot\frac{F_c}{F_{\phi л}}}\Delta -$$
$$- \frac{E_c}{1+\frac{E_c}{E_{\phi л}}\cdot\frac{F_c}{F_{\phi л}}}\left[(\alpha_c l_c - \alpha_{\phi л} l_{\phi л}) + (\varepsilon_{p.c} - \varepsilon_{p.\phi л})\right]. \qquad (13.8)$$

Before the loading and the heating of the connection (P=0; t=0; ε_p=0) the stress in the bolt shank due to pretightening will be

$$\sigma_{c\,пред} = \frac{E_{c0}}{1+\frac{E_{c0}}{E_{\phi л 0}}\cdot\frac{F_c}{F_{\phi л}}}\Delta.$$

Let us examine the particular case of the effect of force P, when tightening is performed in the heated state and E_0=E. Let us also assume, that the material and the temperatures of the shank and the flanges are identical, i.e., E_c=$E_{\phi л}$=E, t_c=$t_{\phi л}$, and let us disregard the flange creep (the stresses which are usually small in comparison with σ_c). Then formula (13.8) will take the form

$$\sigma_c = \sigma_p \frac{\frac{F_c}{F_{\phi л}}}{1+\frac{F_c}{F_{\phi л}}} + \frac{F_c}{1+\frac{F_c}{F_{\phi л}}}\Delta - \frac{E}{1+\frac{F_c}{F_{\phi л}}}\varepsilon_{p.c} =$$
$$= \sigma_0 - \frac{E}{1+\frac{F_c}{F_{\phi л}}}\varepsilon_{p.c}, \qquad (13.9)$$

where σ_0 - is the stress before the beginning of creep.

The nature of change σ_c with time τ is shown in Fig. 13.14b.

At the moment of the opening of the flanges at $\tau_{раскр}$ (the beginning of the formation of clearance) $\sigma_c=\sigma_p$, since load P on the section between the head and the nut is transmitted only via the bolt shank.

This corresponds to the expression

$$\varepsilon_{p.c} = \Delta - \frac{\sigma_p}{E}. \qquad (13.10)$$

Expression (13.10) can be obtained both from formula (13.9) under the condition $\sigma_c=\sigma_p$ and directly from an examination of the bolt shank deformations at the moment of the opening of the flanges.

The rate of the relaxation (dropping off) of stress is determined with the expression

$$\dot{\sigma}_c = \frac{E}{1+\frac{E_c}{F_{фл}}}\dot{\varepsilon}_{p.c.}$$

From the last expression it is possible to make the following conclusions:

1) the rate of relaxation of stress is determined by the creep rate;

2) the rate of relaxation slows down with an increase in $F_c/F_{фл}$ due to an increase in the portion of elastic deformation in the flanges in the total sum of pretightening deformation. Designwise it is more convenient to slow down relaxation by employing elastic packing between the head and the nut of the bolt and flanges.

4. Effect of Low Temperatures

Structural elements can be highly cooled under the prolonged effect of low temperatures (down to -50°C and below) in flight and also when parked.

Nonuniformity of cooling also causes the appearance of thermal stresses determined by the same method, as in heating. Moreover, cooling can lead to a reduction in the strength of a metal and brittle fracture in the event of impact loads, especially in the zone of stress concentrators.

CHAPTER 14

THE BASES OF DESIGNING AND EVALUATING THE EFFECTIVENESS OF FLIGHT VEHICLES

The problems of designing and evaluating the effectiveness of flight vehicles are the subject of a number of scientific investigations. They include the works of the Soviet aviation designers and scientists V. F. Bolkhovitinov, S. M. Yeger, M. L. Mil' et al.

In the present chapter these problems are examined in connection with the development of preliminary design, since precisely at this stage the initial decisions are made which subsequently determine the aviation engineering data, the operational characteristics and the effectiveness of a flight vehicle.

The materials in this chapter can be used to fulfill the course and diploma academic designs of flight vehicles.

§ 1. EXISTENCE EQUATION OF A FLIGHT VEHICLE. THE BASES OF EVALUATING EFFECTIVENESS

The basic purpose of any flight vehicle is the delivery of a specific load, for a transport aircraft - a payload over a given distance under specific conditions (at a given altitude, flight velocity, etc.). To fulfill this task a flight vehicle should have a fuselage (body), a unit for creating left (a wing, a rotor), organs of stability and controllability, takeoff and landing

devices, a power plant, and a fuel reserve. Furthermore, the crew is accommodated in it and the necessary equipment is installed in it.

Each of the above enumerated objects possesses an initial weight whose magnitude is due to the specific properties of the flight vehicle.

The sum of these weights constitutes the takeoff weight of the aircraft

$$G_0 = G_{эк} + G_{об} + G_{ком} + G_{т.с} + G_{д.у} + G_{кн}, \qquad (14.1)$$

where $G_{эк}$ - is the weight of the crew; $G_{об}$ - is the weight of the equipment; $G_{ком}$ - the weight of the payload; $G_{т.с}$ - is the weight of the fuel and the fuel system; $G_{д.у}$ - is the weight of the power plant; $G_{кн}$ - is the structural weight of the aircraft (the weight of the airframe).

Expression (14.1) is the weight balance equation of a flight vehicle.

After dividing the terms of equation (14.1) by the takeoff weight of the aircraft, we will obtain the weight balance equation in the relative form

$$1 = \frac{G_{эк} + G_{ком}}{G_0} + \bar{G}_{об} + \bar{G}_{т.с} + \bar{G}_{д.у} + \bar{G}_{кн}. \qquad (14.2)$$

From it the following formula is obtained

$$G_0 = \frac{G_{эк} + G_{ком}}{1 - (\bar{G}_{об} + \bar{G}_{т.с} + \bar{G}_{д.у} + \bar{G}_{кн})} \qquad (14.3)$$

where $\bar{G}_{об} = \frac{G_{об}}{G_0}$ - is the relative weight of equipment; $\bar{G}_{т.с} = \frac{G_{т.с}}{G_0}$ - is the relative weight of the fuel and the fuel system; $\bar{G}_{д.у} = \frac{G_{д.у}}{G_0}$ - is the relative weight of the power plant; $\bar{G}_{кн} = G_{кн}/G_0$ -

is the relative structural weight of the aircraft.

As V. F. Bolkhovitinov showed, the weight balance equation, if we express its terms by the parameters of the flight vehicle and the engine, the aerodynamic and aviation engineering characteristics, is converted into an equation which reflects the connection and the mutual dependence of the properties of the flight vehicle.

Each of the terms of equation (14.2) is connected with those or other parameters and properties of the flight vehicle. Thus, for instance, for an aircraft $G_{ком}$ and $G_{эк}$ are determined by the purpose of the aircraft:

$$\bar{G}_{об} = f(m, L, H, V_{крейс}, \Delta h, l, \ldots);$$
$$\bar{G}_{т.с} = \varphi(C_{уд}, K, L, H, V_{крейс}, \ldots, \ldots);$$
$$\bar{G}_{д.у} = \psi(\gamma_{дв}, \mu, \ldots);$$
$$\bar{G}_{кн} = \nu(n^{p}, \tau_{рес}, \lambda, \bar{c}, \chi, \eta, V_{max}, p_0, \ldots),$$

where L - is the flight range; H - is the flight altitude; $V_{крейс}$ - is the cruising flight velocity; $C_{уд}$ - is the specific fuel consumption; $\gamma_{дв}$ - the specific weight of the engine; K - is the lift/drag ratio of the aircraft; n^{p} - is the rated g-force; $\tau_{рес}$ - the lifetime of the airframe structure; Δh, l - are the minimum weather characteristics, under which operation of the aircraft is specified (respectively, the height of the lower boundary of cloud cover and horizontal visibility); m - is the number of crew members and passengers; λ, $\bar{c}$, χ, η - are the wing parameters; p_0 - is the specific wing loading; μ - is the required power-weight ratio.

By employing these expressions, it is possible to write

$$1 = \frac{G_{эк} + G_{ком}}{G_0} + f(m, L, H, V_{крейс}, \Delta h, l, \ldots) + \varphi(C_{уд}, K, L, H, V_{крейс}, \ldots) + \psi(\gamma_{дв}, \mu, \ldots) + \nu(n^{p}, \tau_{рес}, \lambda, \bar{c}, \chi, \eta, V_{max}, p_0, \ldots). \quad (14.4)$$

Equation (14.4) connects in a single whole all the parameters and properties of the flight vehicle and can be called by the existence equation of the flight vehicle. It follows from this equation that it is possible to create a flight vehicle not with any combinations of its properties, but only with specific ones which satisfy equation (14.4). The form of the functions going into the equation varies with the advancement in science and technology, but an improvement in some properties will unavoidably entail deterioration in some other properties.

An analysis of equation (14.4) makes it possible at the very beginning of designing to resolve an important question: which combinations of properties can actually be implemented in one aircraft.

But this raises another important question: which of these calculations is the most advantageous for the flight vehicle being designed.

The problem of selecting the most advantageous combination of properties can be solved on the basis of evaluating the effectiveness of the application of the flight vehicle.

For military aviation by effectiveness of application is understood combat effectiveness. It is usually estimated as the probability of the fulfillment of an assigned mission taking into account the opposition of an enemy in an actual combat situation.

By the effectivness of the application of civil aviation is usually understood economic effectiveness - the expenditures of live and embodied labor on carrying out transportation or other types of work.

A quantitative evaluation of the effectiveness of flight vehicles in comparing them can be accomplished by employing effectiveness criteria. Their selection depends on the purpose

and the properties of the aircrafts being compared.

In some cases the simplest criteria can be used for a comparative evaluation of the effectiveness of transport flight vehicles:

the weight coefficient with respect to payload

$$\bar{G}_{\text{пол}} = \frac{G_{\text{пол}}}{G_0};$$

the weight coefficient with respect to full load

$$\bar{G}_{\text{п.н}} = \frac{G_{\text{п.н}}}{G_0},$$

where $G_{\text{п.н}}$ - is the weight of a full load (the total weight of the payload, crew, fuel and oil);

relative structural weight (design refinement)

$$\bar{G}_{\text{кн}} = \frac{G_{\text{кн}}}{G_0}, \text{ etc.}$$

The specified criteria make it possible to compare similar types of flight vehicles with each other which differ from one another only in some one single property (payload, or full load or relative structural (design) weight).

For a comparative evaluation of the effectiveness of various flight vehicles with different groups of properties more general criteria are necessary.

The selection of a criterion is determined by which characteristics of a flight vehicle we want to most completely describe employing this criterion.

For a comparative evaluation of the economic effectiveness of civil flight vehicles several criteria are utilized at present. The most important of these are:

where $A_ч$ - are the flight expenditures on one flight vehicle per hour, ruble/hour; $G_{ком}$ - is the payload; t; $V_{рейс}$ - is the flight velocity, km/h.

Flight expenditures can be represented in the following form:

for a flight vehicle with a turbojet engine

$$A_{час} \approx \alpha P_0 + \sigma Q_{ср} + \beta G_{пуст};$$

for a flight vehicle with a turboprop engine

$$A_{час} \approx \alpha N_0 + \sigma Q_{ср} + \beta G_{пуст},$$

where P_0 and N_0 - are the total takeoff thrust in tons and the takeoff power in thousands of equivalent horse powers; $Q_{ср}$ - is the mean hourly consumption of fuel on a flight vehicle during the time from takeoff to landing, ton/hr; $G_{пуст}$ - is the weight of an empty flight vehicle, ton; α - is the total hourly expenditure rate for operation, repair and depreciation of the engines in rubles per 1 ton of takeoff thrust per hour or 1000 engine hp of takeoff power per hour; σ - the coefficient which considers the cost of fuel and its consumption during engine operation on the ground; β - is the total hourly expenditure rate for operation, repair and depreciation of the airframe with the equipment, which considers the flight expenditures in rubles for 1 ton of weight of an empty flight vehicle per hour.

Let us divide the numerator and the denominator of the obtained expressions by the takeoff weight G_0 and let us designate:

μ_0 - the takeoff thrust-weight ratio $\frac{P_0}{G_0}$ or the power-weight ratio $\frac{N_0}{G_0}$ of the flight vehicle; $\bar{Q}_{ср}=\frac{Q_{ср}}{G_0}$ - is the relative mean hourly consumption of fuel; $\bar{G}_{пуст}=\frac{G_{пуст}}{G_0}$ - is the relative weight of an empty flight vehicle.

By substituting in formulas (14.6) and (14.5) we will obtain

$$a' = \frac{k}{\varepsilon} \cdot \frac{a\mu_0 + \sigma \bar{Q}_{cp} + \beta \bar{G}_{пуст}}{\bar{G}_{max} V_{рейс}}. \qquad (14.7)$$

The values going into formula (14.7), can be expressed via aviation engineering data and the parameters of the flight vehicle and its engine by means of the existence equation of the flight vehicle (14.4) and the thrust-weight ratio and relative weight formulas given in § 4.

If we substitute the expressions of these values in formula (14.7), the obtained dependence will make it possible to investigate the questions of selecting the parameters of the flight vehicle with respect to the condition of ensuring economic effectiveness - a lesser prime cost of transportation.

§ 2. THE DEVELOPMENT OF OPERATIONAL TECHNICAL REQUIREMENTS

The first stage in designing a flight vehicle is the rough design draft. Here all the most important properties of the aircraft being designed are revealed, its setup, parameters and layout, and also the most important structural units are worked out. From the preliminary design draft the conclusion is made about the advisability of further work on creating the flight vehicle.

Thus in the beginning of the rough design draft special attention should be allotted to the operational technical requirements imposed on the flight vehicle being designed. These requirements are developed and are given by organization-customer.

In the summary of the operational technical requirements the following most important questions are explained with the necessary substantiation.

the prime cost of transportation (in special aviation use - the prime cost of labor);

the required capital investments;

the period of compensability of supplementary capital investments;

the annual economic effect from the implementation of a new model into operation.

The methods of calculation the enumerated criteria are examined in specialized literature.

In the initial designing stage when comparative evaluation of different variants of flight vehicles is carried out, it is convenient to use some one criterion. For transport (passenger and cargo) aircraft the most suitable criterion is the prime cost of transportation a'.

Let us examine an approximate expression of the prime cost of transportation

$$a' = \frac{ka}{\varepsilon}, \tag{14.5}$$

where a - are the flight expenditures per 1 ton-kilometer, ruble/ton-kilometer; ε is the payload coefficient - the ratio of the weight of the actual payload onboard a flight vehicle to the maximum permissible load at a given flight range; k - is a coefficient which considers the expenditures not directly connected with flight operation.

Flight expenditures per 1 ton-kilometer

$$a = \frac{A_ч}{G_{ном} V_{рейс}} \text{ ruble/ton-kilometer}, \tag{14.6}$$

1. The purpose of the flight vehicle being designed, the basic and additional variants of its application.

2. The conditions and the characteristics of application: the basing conditions (geographical latitude, relief of the area, the quality of airfields, etc.), the limitations on operation with respect to weather, etc.

3. The types and quantities of payloads.

4. Required flight properties: flight range L, cruising flight velocity $V_{крейс}$, working flight altitude H, landing speed $V_{пос}$ and landing run $L_{пр}$, unstick (lift-off) velocity $V_{отр}$ and takeoff run length $L_{разб}$, etc.

5. Necessary equipment complement.

6. Required crew complement (with respect to number of members and qualifications).

7. Requirements connected with ensuring economy of transportation, safety and comfort of the passengers.

8. Special technical requirements imposed on the structure and layout, the power plant and units of equipment owing to the specific features of the flight vehicle being designed. Included here are various operational, technological, strength requirements, requirements imposed on stability and controllability, etc.

The general technical requirements necessary for all aircraft of civil aviation are formulated in the Standards of Flight Fitness and Civil Aircraft of the USSR.

In working out the operational and technical requirements and the technical assignment variants of certain technical flight data of the flight vehicle are examined for the purpose of ascertaining their optimum values.

Let us examine this question as illustrated by a passenger aircraft.

The size of the payload and the flight range of an aircraft being designed are selected depending on the class of the aircraft by means of analyzing the passenger and cargo traffic on different air lines.

If the quantity of passenger and cargo traffic G_i is known and the number of flights ω_i during a specific time on line is assigned, it is possible to determine the size of the payload of the aircraft being designed with the following formula

$$G_{\text{ном}} = \frac{G_i}{\omega_i}.$$

The dependence of payload on the number of passenger seats for a passenger aircraft takes the form

$$G_{\text{ном}} = 75n + g_{\text{л.б}}n + G_{\text{гр}},$$

where n - is the number of passenger seats; 75 - is the average weight of one passenger without luggage; $g_{\text{л.б}}$ - is the average weight of the personal luggage of one passenger; $G_{\text{гр}}$ - is the weight of the mail and the cargo which, as revealed by operating experience, should be not more than 25-30% of the weight of the passengers with luggage.

Each aircraft can operate on lines of different length. The rated flight range (average range, taking into account the amounts of cargo traffics) L_0 can be determined with the formula

$$L_0 = \frac{\sum_{i=1}^{m} L_i G_i}{\sum_{i=1}^{m} G_i},$$

where m - is the number of lines on which the employment of the aircraft being designed is being proposed; L_i - is the nonstop distance on each line; G_i - is the average passenger and cargo traffic on each line.

An analysis of the passenger and cargo on different lines makes it possible to substantiate the classification and the main characteristics of civil aircraft and helicopters.

Main-line aricraft are classed in the following manner:

1. Long-distance main-line aircraft (LDMLA) [ДМС] - the rated distance is L_0=6000-7000 km, the number of passenger seats is n=180-220. Supersonic passenger aircraft (SPA) [СРС] belong to this same class.

2. Intermediate-range main-line aircraft (IRMLA) [СМС] - L_0=3000 km, n=160-180 (on lines with heavy passenger traffic n=240-250).

3. Short-range main line aircraft (SRMLA) [БМС] - L_0=1500 km, n=70-80.

Aircraft of regional air lines (RAL) [МВЛ]:

1. Heavy aircraft of RAL - L_0=300-400 km, n=60-70.

2. Medium aircraft of RAL - L_0=300-400 km, n=24-30.

3. Light aircraft of RAL - L_0=500-600 km, n=15-20.

The length of regional air lines varies over broad limits (from 50 to 1500 km). Thus the capacity of the fuel systems of aircraft of regional air lines should ensure flight at least over double the distance as compared with the rated range with the takeoff weight increased by 10-12%.

The rated values of range, velocity and flight altitude selected during designing have a considerable effect on the prime cost of transportation. Thus, in working out the requirements it is advantageous to plan a number of variants of the aircraft being designed differing from one another in range, velocity and flight altitude, and to carry out for each of them, at least approximately, a weight rating in the order examined subsequently in § 4, and to find the prime cost of transportation a' with formula (14.7).

Figure 14.1 shows the curves obtained as a reuslt of such calculations for the aircraft variants differing from the adopted values of V and H. From the curves it is possible to ascertain the optimum aircraft variant with a flight altitude $H_{опт}$ and a velocity $V_{опт}$, that ensure the least prime cost of transportation a'.

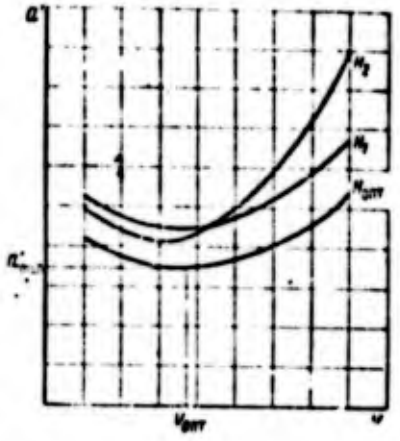

Figure 14.1. Curves which make it possible to ascertain the optimum aircraft variant.

The requirements imposed on the takeoff and landing properties should correspond to the conditions under which the aircraft is based.

It is necessary to give special attention to these questions in designing aircraft for regional lines which should operate from dirt airfields of limited dimensions and with a ground hardness of 3.5-4 kgf/cm^2.

The problem of selecting the optimum values of takeoff and landing characteristics of an aircraft and of the economic evaluation of the advisability of employing an aircraft with vertical or short takeoff and landing characteristics can be examined in working out the operational and technical requirements.

In this case the possible capital investments in the construction of airfields should be taken into account.

§ 3. GENERAL PRINCIPLES OF THE SELECTING OF THE LAYOUT DIAGRAM AND THE PARAMETERS OF A FLIGHT VEHICLE

The layout of a flight vehicle is the coordinating of the mutual positioning of its structural components and all types of loads (passengers, luggage, cargo, fuel, etc.).

The selecting of the layout setup and the parameters of a flight vehicle, including the selecting of the type and the parameters of the engine, is subordinated to the condition of the best fulfillment of the operationally technical requirements.

The problem of determining the optimum parameters for each of the variants of the layout setups being investigated can be examined as a problem of finding the parameter values which correspond to the minimum prime cost of transportation, i.e., to the extremum of the function, which represents the expression of the prime cost of transportation a' as criteria of the effectiveness through aviation engineering data and the parameters. The method of this type of representation was examined in § 1.

The employment of this method is made difficult by the fact that the possibilities of design realization superimpose a number of limitations on the unknown parameters which prevent the acceptance of their theoretically optimum values. After the takeoff weight of a flight vehicle and the dimensions of its main units have been determined, the layout drawing and the positioning of the center of gravity are carried out.

In this case the following particular layout problems are solved:

1. The external, aerodynamic, layout: the selecting of the

shapes and mutual positioning of the wings, control elements, fuselage and power plants.

2. The layout of the power plants and of the fuel system and the providing of fire-fighting measures.

3. The layout of the premises: the compartments for accommodating the crew, the passengers and the cargo; providing for passenger and crew comfort, safety in emergencies, convenience in loading and unloading.

4. The selecting of the parameters and the layout of the takeoff-and-landing units - the landing gear and high-lift devices taking the type of airfields into account.

5. The layout of the load-bearing structural design: the forming and the joining together of the load-bearing setup of the components.

6. The technological layout of the design: the arrangement of technological and operational joints; the ensuring of convenience in repair, adjustment and inspection.

7. The weight layout - is the arrangement of the structural components and cargo which satisfies the requirements of center of gravity positioning.

The order of determining center of gravity positioning and the carrying out of the layout drawing is examined in further detail in § 5.

In working out the layout and in analyzing the adopted solutions a many-sided approach to it is necessary taking into account the conditions of production, operation and repair and all factors affecting the effectiveness of a flight vehicle.

The selecting of the setup and the characteristics of the layout is determined by the imposed operational technical requirements.

Depending on the purpose of a flight vehicle specific requirements and the aviation engineering data and parameters connected with them are more important, more urgent for ensuring economic effectiveness.

This is manifested in the following manner.

1. If it is necessary to increase a specific aviation engineering index, then the components $\bar{G}$ connected with it entering into the expression for takeoff weight (14.3)

$$G_0 = \frac{G_{\text{пс}} + G_{\text{пом}}}{1 - (\bar{G}_{\text{об}} + \bar{G}_{\text{т.с}} + \bar{G}_{\text{д.у}} + \bar{G}_{\text{сн}})}$$

and the components μ_0, $\bar{Q}_{\text{ср}}$, going together with G_0 into the prime cost of transportation (14.7)

$$a' = \frac{k}{e} \cdot \frac{a_{\text{нр}} + \sigma \bar{Q}_{\text{ср}} + \beta \bar{G}_{\text{нуст}}}{\bar{G}_{\text{пом}} V_{\text{рейс}}},$$

have a tendency to vary in such a way that this leads to an increase in G_0 and a'.

2. The parameters are selected so as to limit the increase in G_0 and a' even at the expense of certain losses in other indices, which are secondary for the type of flight vehicle in question.

3. The selection of the setup and the development of the layout and the design primarily satisfy these requirements. In this case, certainly, the fulfillment of these requirements cannot proceed due to the incomplete satisfaction of the necessary requirements for flight fitness.

Let us give some examples which explain the examined aspects.

1. In creating a supersonic aircraft the main problem is ensuring the required high value of $V_{крейс}$ with the assigned values of L and of the number of passengers and at a low prime cost of transportation.

The setup of the external layout and many design parameters of an aircraft are determined by the aerodynamic specifications: by the necessity for first of all obtaining a high value of lift/drag ratio at supersonic cruising velocity (Fig. 14.2).

2. The designing of a transport aircraft intended for the transportation of large-dimension cargo, machines and other technological equipment, first of all requires the solving of design layout problems to ensure convenient loading, positioning and attachment of the cargo.

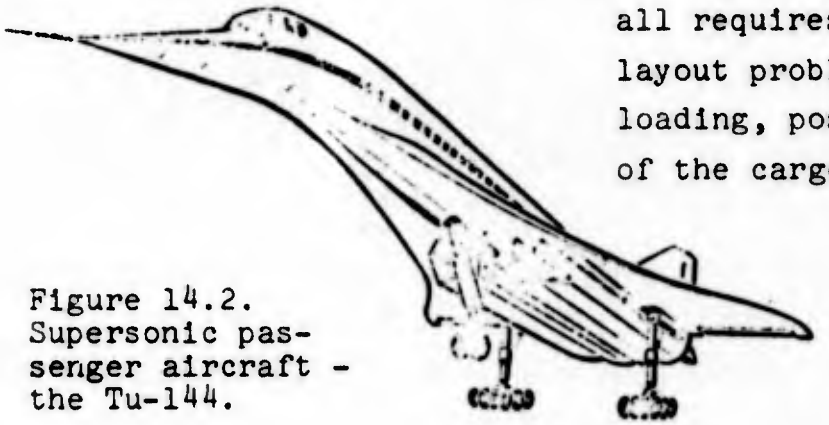

Figure 14.2. Supersonic passenger aircraft - the Tu-144.

Good takeoff and landing properties are necessary for application on small airfields; therefore effective wing high-lift devices and landing gear with good ground performance are necessary.

As an example of an aircraft for the transportation of large-dimension cargo Fig. 14.3 shows the An-22 aircraft.

3. The problem of selecting the setup and the parameters of an aircraft for regional air lines can be solved in a number of variants. Thus for instance, the layout of the Be-30 aircraft (Fig. 14.4) reflects the specific character of the requirements connected with its purpsoe.

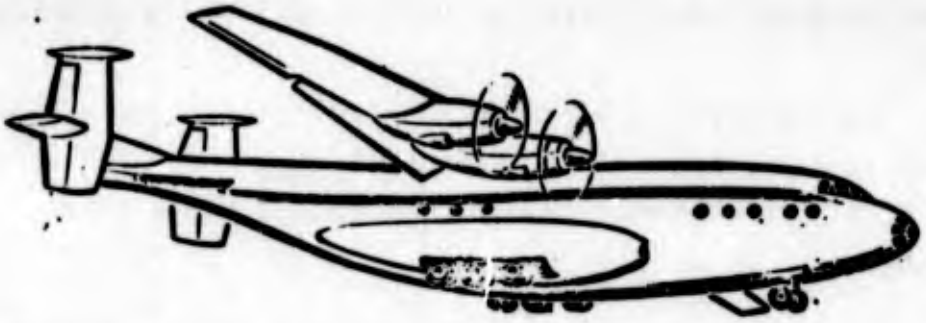

Figure 14.3. The cargo aircraft - the An-22.

Figure 14.4. The light aircraft - Be-30 for regional air lines.

In spite of the low power-weight ratio required for a horizontal flight two turboprop engines are placed on this aircraft. This is done in accordance with the recommendations of the Standards of Flight Fitness for the possibility of continuing takeoff and flight when one of the engines has failed. The increase in $G_{д.у}$ caused by this can be reduced, if in the event of the stopping of one engine both propellers connected with the transmission shaft will operate creating a thrust greater than an engine with one propeller.

Landing gear with semi-balloon pneumatic tires and effective high-lift devices make it possible to apply the aircraft on dirt landing fields.

Its short range led to a reduction in its flight altitude, which made it possible to get by without employing a pressurized cabin.

In the present chapter the types of flight vehicles, up to this time have not found application civil aviation are not examined.

Let us briefly dwell on vertical takeoff and landing aircraft (VTOL)[1].

The prospects of flight vehicles of this type for civil aviation are connected with the possibility of their operation not only on airfields with short takeoff and landing strips, but also on unequipped sites. Investigations show that as a result of the reduction in expenditures for creating airfields VTOL's with series construction can have economic advantages over conventional aircraft.

§ 4. WEIGHT CALCULATION AND THE DETERMININATION OF THE BASIC DIMENSIONS OF AN AIRCRAFT

Weight calculation. In developing the preliminary design of a flight vehicle the weight calculation is made - the determination of the takeoff weight and the weights of the individual structural components. The knowledge of weights is necessary for evaluating effectiveness, for determining center of gravity positioning and carrying out stress analyses.

1. The takeoff weight of an aircraft G_0 is determined with formula (14.3).

The weights of the crew and the payload are assigned by the requirements imposed on the aircraft being designed.

---

[1]Questions on VTOL design are examined in detail in F. P. Furochkin's book "The bases of designing VTOL aircraft". M., "Mashinostroyenie", 1970.

The values of the terms of the denominator of formula (14.3), as was noted above, are connected with the properties and the parameters of the aircraft. Let us examine the procedure for compiling the actual forms of this connection and for determining the relative weights using a transport aircraft as an example. We consider the following flight properties (L_0, $V_{крейс}$, H, $V_{пос}$, $L_{розб}$, ...), the parameters of the aircraft (p_0, λ, χ, $\bar{c}$, η, ...), the type and parameters of the engine ($\pi_к^*$, $T_з^*$, y ...) for the variant in question known.

2. Determination of the relative weight of the fuel and the fuel system. The total fuel reserve on an aircraft is found with the following formula

$$G_т = G_{т.г.п} + G_{т.в.в.п} + G_{т.а.з},$$

where $G_{т.г.п}$ - is the weight of the fuel necessary for ensuring an assigned horizontal flight range; $G_{т.в.в.п}$ - is the weight of the fuel required for the takeoff, the climb, the landing and the operation of the engine on the ground; $G_{т.а.з}$ - is the aeronautical fuel reserve.

In accordance with this the total relative fuel reserve is

$$\bar{G}_т = \bar{G}_{т.г.п} + \bar{G}_{т.в.в.п} + \bar{G}_{т.а.з}.$$

The horizontal flight range is determined with the formula

$$L_{г.п} = 3{,}6 \frac{KV_{крейс}}{C_{уд\ крейс}} \cdot \ln \frac{G_0}{G_{кон}}, \qquad (14.8)$$

which is derived assuming that $KV_{крейс}/C_{уд\ крейс}$=const and that the initial weight of the aircraft (the weight at the beginning of horizontal flight) is equal to the takeoff weight.

Since the horizontal flight $K=1/u_{крейс}$, and the final weight of an aircraft is $G_{кон}=G_0-G_{т.г.п}$, formula (14.8) can be

represented in the form[2]

$$L_{г.п} = \frac{3{,}6V_{крейс}}{C_{уд.крейс}\mu_{крейс}} \cdot \ln \frac{1}{1 - \bar{G}_{т.г.п}}.$$

Hence

$$\bar{G}_{т.г.п} = 1 - e^{-x},$$

where

$$x = \frac{L_{г.п}C_{уд.крейс}}{3{,}6V_{крейс}} \mu_{крейс};$$

$\mu_{крейс}$ - is the required thrust-weight ratio (power-weight ratio) of an aircraft in the cruising flight regime; $C_{ус.крейс}$ - is the specific fuel consumption at a given flight velocity and flight altitude in the cruising regime of engine operation.

The horizontal flight range is

$$L_{г.п} = L_0 - (L_{н.в} + L_{сп}),$$

where $L_{н.в}$ - is the distance along the horizontal during climb; $L_{сп}$ - is the distance along the horizontal during descent.

The required thrust-weight ratio of an aircraft with a turbojet engine (turbofan engine) in the cruising flight regime is

$$\mu_{крейс} = \frac{q_{крейс}c_x}{p_{ср}},$$

and the required power-weight ratio of an aircraft with a turboprop engine

---

[2]In this form the formula is also valid for an aircraft with a turboprop engine, if we introduce in it values connected with equivalent power $N_{экв}$:

$$C_{уд.N} = C_{уд}\frac{P}{N_{экв}} \quad \text{and} \quad \mu_N = \frac{N_{экв}}{G_0}.$$

$$\mu_{\text{крейс}} = \frac{q_{\text{крейс}} V_{\text{крейс}} c_x}{75 \eta_в p_{ср}},$$

where $q_{\text{крейс}}$ - is the cruising impact pressure; $p_{ср}$ - is the load on the wing with an average flight weight; $\eta_в$ - is the propeller efficiency; c_x - is the drag coefficient of the aircraft in the cruising regime.

The specific fuel consumption $C_{\text{уд.крейс}}$ is determined by the altitude-speed characteristics of the engine with the selected parameters ($\pi_к^*$, $T_з^*$, y, etc.) taking throttling into account in the cruising flight regime

$$C_{\text{уд крейс}} = C_{\text{уд}} \bar{C}_{\text{уд.п}},$$

where $C_{\text{уд}}$ - is the specific consumption with respect to the altitude-speed characteristics for a given velocity (Mach number) and flight altitude; $\bar{C}_{\text{уд.п}} = C_{\text{уд.п}} / C_{\text{уд}\, n_{max}}$ - is the relative fuel consumption during engine throttling.

Examples of altitude-speed and throttle characteristics are presented in Figs. 14.5 and 14.6.

In the initial design stage the relative weight of the fuel $\bar{G}_{\text{т.н.в.п}}$ is estimated from the data of aircraft which are similar to the aircraft being designed.

The relative aeronautical fuel reserve $\bar{G}_{\text{т.а.з}}$ is determined from the flight condition during the course of the reserve time t, h brought about by the operational technical requirements.

Then

$$\bar{G}_{\text{т.а.з}} = C_{\text{уд крейс}} \mu_{\text{крейс}} t \frac{p_{ср}}{p_0}.$$

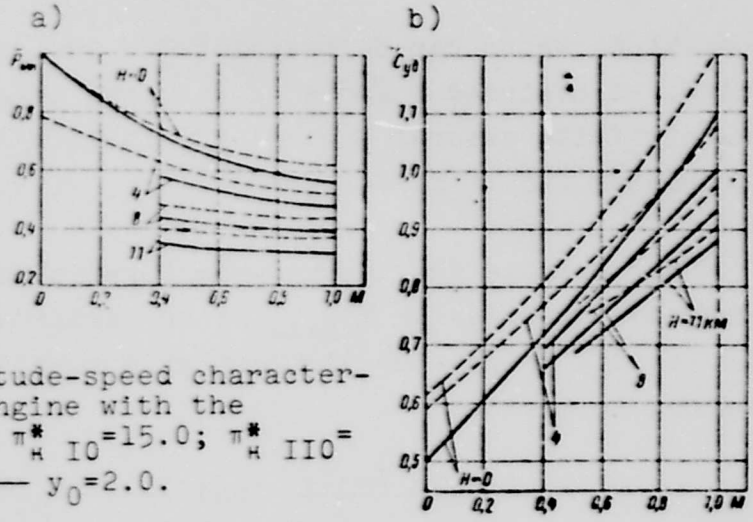

Figure 14.5. The altitude-speed characteristics of a turbofan engine with the parameters: $T_з^*$=1200°; $\pi_{н\ II0}^*$=15.0; $\pi_{н\ II0}^*$= =2.15; --- y_0=1.0; ——— y_0=2.0.

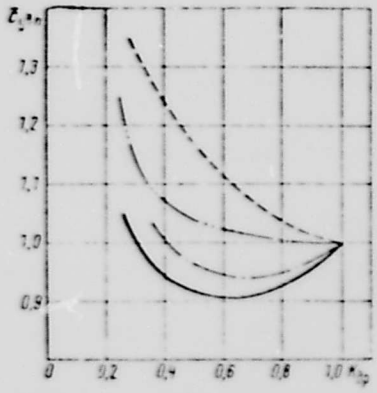

Figure 14.6. Tentative throttle characteristics of engine: ---- turboprop engine; —··— single-shaft turbofan engine; —·—·— turn-shaft turbofan engine; ——— turbojet engine.

The relative weight of the fuel and the fuel system is

$$\bar{G}_{т.с} = k_{т.с}\bar{G}_т,$$

where $k_{т.с}$ is the coefficient which considers the weight of the units of the fuel system, the fuel lines and tanks.

3. The relative weight of a power plant $G_{д.у}$ - is determined by the expression

$$\bar{G}_{д\,у} = \frac{G_{д\,у}}{G_0} = \frac{k_\gamma \gamma_{дв.0} P_{0\,max}}{G_0} = k_\gamma \gamma_{дв.0} \mu_0,$$

where $\gamma_{дв.0}$ - is the specific bench weight of an engine; μ_0 - is the required takeoff thrust-weight ratio (power-weight ratio) of the aircraft; k_γ - is the coefficient which considers the weight of the engine nacelles, the propellers (turboprop engine), the control and cooling units.

The value of μ_0 is determined from the condition of ensuring the necessary values of engine thrust under all operating

conditions which can be decisive for their selection: in cruising flight at assigned V and H, during the takeoff run and during takeoff (with several engines the failure of one is considered), at ceiling (if it is assigned).

For example the thrust-weight ratio (power-weight ratio) required for ensuring $V_{крейс}$ at an assigned altitude relative to the takeoff weight for aircraft with turbojet and turboprop engines is equal to

$$\mu_V = \frac{q_{крейс} c_x}{p_0} \quad \text{and} \quad \mu_V = \frac{q_{крейс} V_{крейс} c_x}{75 \eta_в p_0}.$$

The takeoff thrust-weight ratio (power-weight ratio) for aircraft with turbojet and turboprop engines is $\mu_{0V} = \frac{\mu_V}{k_{др} k_P \bar{P}_{МН}}$ and $\mu_{0V} = \frac{\mu_V}{k_{др} k_N \bar{N}_{МН}}$ where $\bar{P}_{МН} = \frac{P}{P_{0max}}$ - is the relative engine thrust in flight at a given velocity (Mach number) and altitude (at maximum rpm); $N_{МН} = \frac{N}{N_{экв\ 0max}}$ - is the relative equivalent power under the same conditions; $k_{др} = \frac{P}{P_{max}}$ or $\frac{N}{N_{max}}$ - is the degree of engine throttling in the flight regime in question k_P and k_N - are coefficients of thrust and power loss.

The values of $\bar{P}_{МН}$ and $\bar{N}_{МН}$ are determined from the altitude-speed characteristics engines with the selected parameters. An example of this type of characteristic for turbofan engines is presented in Fig. 14.5.

As a calculated value μ_0 is selected large from the values found for the indicated engine operating conditions.

4. The relative design weight of an aircraft $\bar{G}_{кн}$ is comprised from the following components

$$\bar{G}_{пл} = \bar{G}_к + \bar{G}_ф + \bar{G}_{оп} + \bar{G}_{упр} + \bar{G}_ш, \qquad (14.9)$$

where $\bar{G}_к$ - is the relative design weight of the wing; $\bar{G}_ф$ - is the relative design weight of the fuselage; $\bar{G}_{оп}$ - is the relative design weight of the empennage; $\bar{G}_{упр}$ - is the relative design weight of the control system (including the weight of the hydraulic and pneumatic system); $\bar{G}_ш$ - is the relative weight of the landing gear.

For each term on the right side of expression (14.9) dependences can be obtained which reflect the effect of the basic parameters of a unit on its weight. Thus, for instance, the relative weight of a wing can be determined by a formula of the type

$$\bar{G}_к = k\left(0{,}0033\,\frac{n^{эк}_{э}\left(\frac{1}{\eta_к}+1\right)}{\bar{p}_0\bar{c}_0\cos^2\chi_к} + \frac{q_{к.э}}{p_0}\right),$$

where k - is a statistical coefficient equal to 1.07 for unswept and 1.24 for swept wings; $\bar{c}_0$ - is the wing thickness ratio in the root cross section along flow; $q_{к.э}$ - is the specific weight of the structural elements of a wing which are not included in the main load-bearing setup, kgf/m^2 (local reinforcements, leading-edge assembly, trailing-edge assembly, flaps, ailerons). For transport aircraft $q_{к.э}$=10-20.

Let us note that the values of the relative weights of a fuselage, an empennage, a control system and a landing gear are quite similar for each class of aircraft. Thus, they can be determined from the data on aircraft similar to the one being designed. Tentative values of relative weights $\bar{G}$ are given below:

Fuselage.....	0.08-0.12
Empennage.....	0.015-0.028
Control system.....	0.013-0.028
Landing gear.....	0.035-0.065

5. Determination of the relative weight of the equipment $\bar{G}_{об}$. In the initial stage of drafting a design the relative weight of the equipment can be determined from data on aircraft similar in purpose and properties to the one being designed.

Determining the weights and the dimensions of aircraft components. From the found value of G_0 the following are calculated:

a) the weight of the units and of the systems $G_i=\bar{G}_i G_0$;

b) the dimensions of the wing: area $S=G_0/p_0$; the span $l=\sqrt{\lambda S}$; the tip chord $b_{конц}=\frac{2S}{l(\eta+1)}$; the axial chord $b_0=b_{конц}\eta$; the tip thickness and the thickness along the axial chord $c_{конц}=\bar{c}_{конц}=b_{конц}$; $c_0=\bar{c}_0 b_0$;

c) the dimensions of the fuselage;

the dimensions of the midsection (diameter $d_ф$ or height and width) are determined by the overall dimensions of the passenger or cargo compartment;

the length of the fuselage

$$l_ф=d_ф\lambda_ф,$$

where $\lambda_ф$ - is the fineness ratio of the fuselage;

d) the dimensions of the empennage

the areas of the horizontal and vertical tail surfaces are

$$S_{г.о}=\frac{A_{г.о}b_A}{l_{г.о}}S;\quad S_{в.о}=\frac{A_{в.о}l}{l_{в.о}}S,$$

where $A_{г.о}$, $A_{в.о}$ - are the static moments of the horizontal and vertical tail surfaces; b_A - is the mean aerodynamic chord of the

wing; $L_{г.о}$, $L_{в.о}$ - are the arms of the horizontal and vertical tail surfaces. The remaining dimensions of the empennage are determined in the same way as the dimensions of the wing;

e) the thrust (power) and the overall dimensions of the engine:

the thrust is $P_{0max}=\frac{\mu_0 G_0}{i}$;

where i - is the number of engines on the aircraft;

the power is $N_{эквв0max}=\frac{\mu_0 G_0}{i}$;

the area of the engine midsection is

$$F_{дв}=\frac{P_{0max}}{P_{удо6}} \text{ or } F_{дв}=\frac{N_{эквв0max}}{N_{удо6}},$$

where $P_{удо6}(N_{удо6})$ - is the frontal thrust (power) of an engine;

the overall diameter of an engine $d_{дв}=\sqrt{\frac{4F_{дв}}{\pi}}$; the length of an engine is $l_{дв}=d_{дв}\lambda_{дв}$,

where $\lambda_{дв}$ - is the fineness ratio of an engine.

Note. Values i, $P_{удо6}(N_{удо6})$ and $\lambda_{дв}$ are taken from the data on existing engines.

The dependences given above give an idea about the diversity of the interconnections of the properties and the parameters of an aircraft, which must be considered in designing.

§ 5. LAYOUT AND THE POSITION OF THE CENTER OF GRAVITY OF AN AIRCRAFT

The term "center of gravity positioning" denotes both the process itself of the positioning of weights (weight layout) and the determining of the center-of-gravity position of an aircraft

(c.g.), as well as the numerical value of the coordinates of the c.g. relative to the mean aerodynamic chord (MAC) of a wing expressed in fractions or percentages of the length of the MAC.

The layout of an aircraft and the positioning of the center of gravity are carried out together in designing.

In all the specified variants of loading, in the combustion of fuel, in retracting and lowering of the landing gear the values of the c.g. positions in operation must be located within the limits of the permissible c.g. position range (between the maximum forward and the maximum rearward c.g. positions), defined by the conditions of stability and controllability of the aircraft.

Thus, in approaching layout and center of gravity positioning, it is necessary to plan beforehand the permissible c.g. position range.

It is necessary at first to determine the position of the aerodynamic center of the aircraft along the x-axis and, after assigning the minimum value of the reserve of longitudinal static stability with respect to g-force $m_z^{c_y}$, to find the maximum rearward c.g. position from the following relationship

$$m_z^{c_y} = -(\bar{x}_F - \bar{x}_{ц.т}),$$

where $\bar{x}_F$ - is the distance from the MAC leading edge to the aerodynamic center of the aircraft expressed in fractions of b_A;
$\bar{x}_{ц.т}$ - is the c.g. position.

Then, having tentatively assigned the value of the permissible c.g. position range $\Delta\bar{x}_{ц.т}=0.05-0.08$, it is possible to find the maximum forward c.g. position more precisely formulated subsequently from the rating of controllability (elevator sufficiency during landing).

In the initial stage of drafting a design it is possible to employ the data on the limits of the position of the center of gravity in aircraft similar in properties and layouts to the one being designed.

For beginning the determination of c.g. positioning a rough draft layout is made. Usually it is made in two projections - in the form of a sideview and a view in plan with one half wing. The mutual arrangement of the main units (wing, fuselage, empennage, landing gear, power plants) is established in accordance with the accepted setup taking into account the requirements examined in previous chapters of this textbook. Outlined on the drawing is the position of all types of loads (the crew, the passengers, the cargo, the fuel) and the equipment. The fuel and the loads which are developed in flight should be arranged so that the change in the position of the center of gravity as a result of the depletion of the fuel and weight shifting would be as small as possible.

Even in this stage of layout, questions of the arrangement and mutual connecting of the main load-bearing structural elements - the wing spars and the empennage and the reinforced formers of the fuselage - should be solved.

For calculating the c.g. position the weight of the aircraft is broken down into a number of group loads (in approximate calculation 10-20), in which the weights of the closely arranged parts of the load and the structural components are united. Calculation is carried out with the takeoff weight and with the landing gear lowered for the basic variant of the aircraft loading. Usually the longitudinal axis of the fuselage is taken as the x-axis, and the origin of the coordinates is assumed to be in the nose of the fuselage (Fig. 14.7). Coordinates x_i, y_i of the group loads are determined and a center of gravity positioning record (Table 14.1) is compiled.

Table 14.1

No. of group loads	Designation	G_i, kgf	x_i, m	$G_i x_i$, kg-m	y_i, m	$G_i y_i$, kg-m
1 2 ...						
		$\Sigma G_i = G_0$		$\Sigma G_i x_i$		$\Sigma G_i y_i$

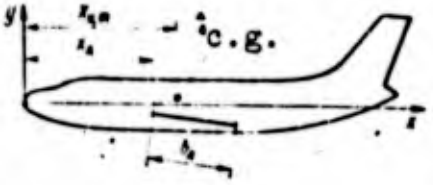

Figure 14.7. On calculating of the position of the center of gravity of an aircraft.

The coordinates of the center of gravity of an aircraft are found with the following formulas

$$x_{\text{ц.т.}} = \frac{\Sigma G_i x_i}{G_0}; \quad y_{\text{ц.т.}} = \frac{\Sigma G_i y_i}{G_0}.$$

In the initial design stage it is possible to be limited to the determining of the position of the center of gravity along the x-axis and to assume $b_A \| x$.

The value of the position of the center of gravity of an aircraft is determined with the formula

$$\bar{x}_{\text{ц.т.}} = \frac{x_{\text{ц.т.}} - x_A}{b_A},$$

where x_A - is distance from the origin of the coordinates to the MAC leading edge; b_A - is the MAC length (Fig. 14.7).

If the obtained value of c.g. position did not fall within the permissible range, then it is necessary to introduce a change

in the layout. The following simplest measures are usually employed:

individual loads are moved in the direction of the necessary displacement of the center of gravity;

the position of the MAC is changed by displacing the wing relative to the fuselage or by a slight change sweep (for an unswept wing).

Then it is necessary to check, whether the c.g. position remains in the designated range with different load variants, including in the case of the burning up of the fuel, and in the case of landing gear retracting.

For calculating the c.g. position with different load variants simple conversion formulas are employed, which are derived by compiling the sum of the moments of the loads being displaced relative to the center-of-gravity position of an aircraft in the main variant and which give the center-of-gravity displacement $\Delta x_{ц.т.}$ relative to this position.

If loads G_i, which are included in the takeoff weight G_0, are displaced by distances Δx_i from their position in the main variant, then

$$\Delta x_{ц.т.} = \frac{\Sigma G_i \Delta x_i}{G_0}.$$

If additional placement ("+") or removal ("-") of loads $G_н$ with coordinates $x_н$ is carried out, then

$$\Delta x_{ц.т.} = \frac{\Sigma (\pm G_н) x_н}{G_0 + \Sigma (\pm G_н)}.$$

Finally c.g. positioning is more precisely formulated from the layout drawing of the aircraft.

The layout drawing made on a large scale (usually a side view and in plan with a number of various sections and cross sections), is the most important preliminary design drawing. It serves to show the accommodating of the crew, cargo, equipment and for the mutual connecting of the load-bearing setups and the structure of the individual components. At the same time it is employed as proof of the rationality of the adopted layout and design of the aircraft, and also for fulfilling the operational and technical requirements imposed on the aircraft and the general requirements of the standards of flight fitness.

Sections of the design are depicted on the layout drawing, which must be considered in accommodating the cargo, and the main load-bearing elements: spars, reinforced ribs of the wing and the empennage, reinforced stringers and formers of the fuselage, hermetically sealed partitions, joint sites, etc. Outlines of the engines, units of equipment of the power plant, and the control lines, etc. are depicted on this same drawing.

The basic layout drawing can be supplemented by drawings which explain the layout and the design of the individual components of the aircraft (landing gear, wing high-lift devices, etc.).

§ 6. CHARACTERISTICS OF THE LAYOUT AND THE C.G. POSITIONING OF HELICOPTERS

The established practice of aircraft design is completely applicable to helicopters; however, it has its specific character.[3]

As for any flight vehicle in order to evaluate the possibility of realizing the operating requirements which have been worked

---

[3]The work under the editorship of M. L. Mil' "Helicopters, Calculation and Design". M., "Mashinostroyenie", 1966-1967 is dedicated to the questions of helicopter design.

out, it is necessary to determine the value of the relative weights of the structure, the power plant and the fuel system, expressing them through the basic operational and technical parameters of the helicopter being designed.

The basic parameters which determine the technical flight properties which must be assigned in designing a helicopter, are: the load on the area swept by the rotor (p kgf/m^2); the circular velocity of a blade tip (ωR m/s); the rotor solidity ratio (σ); the number of blades (z); for winged helicopters the relative wing area is $\left(\bar{c}=\frac{S_{кр}}{\pi R^2_{нв}}\right)$; the coefficient of parasite drag of a rotary-wing flight vehicle relative to the surface swept by the rotor $\left(\bar{c}_x=\frac{\Sigma c_x S}{\pi R^2_{нв}}\right)$.

For selecting the parameters and the setup of a helicopter the data of contemporary helicopters similar in purpose and class to the one being designed are employed.

The following helicopter setups are most frequently realized in contemporary designs:

single-rotor setup with a tail rotor;
twin-rotor setups: coaxial, longitudinal and transverse;
multirotor;
with jet rotor drive;
hybrid helicopters (e.g. the convertiplane).

For each of the enumerated setups variants are possible which differ by number and the positioning of the engines, the types of rotor systems, the control system setup, etc.

The helicopter setup mainly determines the method of the damping of reactive torque.

The single-rotor helicopter setup with a tail rotor (Fig. 14.8a) is the one most commonly employed at the present time. Its advantage is the relative simplicity of its design - one rotor, a simple control system, one main drive shaft. Helicopters of this design are simpler than the others in operation and manufacture. This makes it possible to obtain a relatively lower cost per flight hour for them.

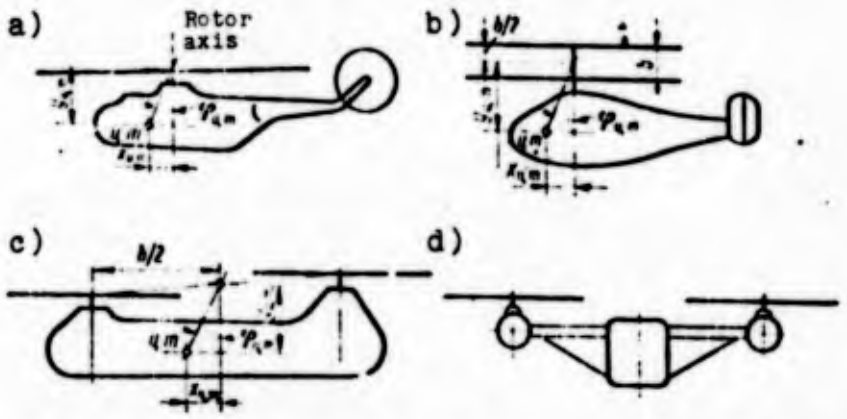

Figure 14.8. Helicopter setups: a) single-rotor; b) coaxial twin-rotor; c) longitudinal twin-rotor; d) transverse twin rotor.
[u.m. = c.g.]

The expenditures of engine power on driving the tail rotor which balances the reactive torque, the long transmission of the tail rotor and the low permissible c.g. position range are the deficiencies of the single-rotor design.

In the twin-rotor helicopter design the balancing of the reactive torque is accomplished in all cases by imparting opposite direction rotation to the rotors.

Helicopters of the twin-rotor coaxial design (Fig. 14.8b) are the most compact and maneuverable; they have a high load ratio (ratio of payload to flight weight); they do not have a tail rotor.

However, the presence of two rotors, situated one above the other and rotating on two coaxial shafts, complicates the design and control during operation. Their deficiency is the harmful mutual effect of the rotors.

The twin-rotor helicopter design with longitudinal positioning of the rotors (Fig. 14.8c) has a long fuselage within which it is possible to transport loads of great length, good longitudinal stability and a broad c.g. position range.

It is necessary to include among their deficiencies: the complexity of the transmission; high inductive losses during horizontal flight; the necessity for reliable synchronization of the rotation of the rotors.

A helicopter with a transverse twin-rotor setup has two rotors positioned in one plane on each side of the fuselage (Fig. 14.8d). From the point of view of aerodynamics, this type of setup of rotor positioning is most advisable, since the inductive losses in horizontal flight due to the positive mutual effect of the rotors is less than in other setups.

The development of this setup in the direction of increasing the dimensions of helicopters and their lifting capacity has no limitations on it. It, for example, is employed on the heavy V-12 helicopter which has a takeoff weight of the order of 100 t.

In helicopters with jet rotor drive the torque from its aerodynamic forces is balanced by the torque created by the thrust of the jet engines or nozzles located on the blade tips. In this case there is no need for the balancing of reactive torque.

Among the major advantages of these types of helicopters it is necessary to include: the absence of a complex transmission, lower cost, high load ratio.

The deficiencies of helicopters of this setup are: the high fuel consumption, the complexity of creating jet engines, operating reliably in a field of great centrifugal forces on the blade tips, the complex construction of the rotor hub and the rotor blades in the case of air feed through them.

The efficiency of a helicopter depends on a number of factors, among which the cruising flight speed plays an important role. Increasing the velocity of a helicopter is prevented by two phenomena - the increase in drag due to the effect of air compressibility on the tips of the rotor blades which are going forward, and the flow separation on the tips of the blades which are going backward.

Decreasing flow separation on the blades, and consequently, raising the permissible flight velocity of a helicopter is possible by means of relieving the rotor, i.e., by decreasing the load on the swept area. This ensures the possibility of its operation at lesser blade setting angles.

The relieving of the rotor can be accomplished by employing a wing on the helicopter, by mounting an aircraft type propeller on it (tractor or pusher) for creating horizontal thrust or by the joint application of a wing and this type of propeller.

In the latter case a helicopter on which a wing and an aircraft type propeller are mounted is called a **convertiplane**, or a **hybrid helicopter**.

In the case of low lifting capacity it is also possible to employ an **autogyro** setup - a flight vehicle on which the rotor does not have a drive and rotates due to aerodynamic forces, and the thrust is created by an aircraft type propeller.

In designing a helicopter it is necessary to consider the advantages and deficiencies of the different setups and to carry

out a comparative evaluation of them. The criteria characterizing the advantages of a setup are: the best load ratio; less power loss; more economic flight over long range; the best stability and controllability; high flight safety; technological construction and lower cost; comfort for the passengers and the crew.

The layout of a helicopter depends on the helicopter setup, its purpose, number and engines and other factors. The basic units of a helicopter (power plant, transmission, rotor, wing) are intimately connected with each other with respect to their positioning.

The layout process is accompanied by **c.g. positioning.** The calculation of helicopter c.g. positioning is carried out in a manner similar to the calculation of aircraft c.g. positioning.

The center-of-gravity position of a helicopter is determined for helicopters of the single-rotor, transverse and coaxial setups (see Fig. 14.8a, b, d) relative to the design axis of the rotor and its plane of rotation; for helicopters of the longitudinal setup (see Fig. 14.8c) - relative to the line connecting the hubs of the front and rear rotors and perpendicular to the plane of rotation of the rotor in its middle.

A change in c.g. positioning in designing can be carried out in two ways: by displacing the units and the cargo or by displacing the rotor relative to the center of gravity.

Besides the abscissa and ordinate of the center of gravity $x_{ц.т}$, $y_{ц.т}$, the c.g. position of a helicopter is conveniently expressed as the angle $\phi_{ц.т.}$ formed by the axis of the rotor and by the line connecting the center of the hub with the center of gravity of the helicopter.

The c.g. position is determined for all helicopter loading

variants, and the most forward and the most rearward position of the center of gravity are found.

BIBLIOGRAPHY

1. Александров В. Г., Майоров А. В., Пашестюк А. М. Авиационный технический справочник. М., «Транспорт». 1969, 496 с.

2. Справочная книга по расчету самолета на прочность. М., Оборонгиз, 1954, 708 с. Авт.: Астахов М. Ф., Караваев А. В., Макаров С. Я., Суздальцев Я. Я.

3. Конструкция летательных аппаратов. Под ред. Кана С. Н. М., Оборонгиз, 1963, 710 с. Авт.: Бельский В. Л., Власов Н. Б., Зайцев В. Н., Кан С. Н., Карножицкий В. Н., Коц В. М., Лизовский Д. Е.

4. Богданов А. П., Виноградов Р. И., Миртов К. Д. Сборник задач по конструкции и прочности самолетов. М., Оборонгиз, 1959, 232 с.

5. Бадягин А. А., Овруцкий Е. А. Проектирование пассажирских самолетов с учетом экономики эксплуатации. М., «Машиностроение», 1964, 295 с.

6. Братухин И. П. Проектирование и конструкция вертолетов. М., Оборонгиз, 1955, 360 с.

7. Конструкция и прочность самолетов. Под ред. Миртова К. Д., изд. РКВНАВУ, 1956, 626 с. Авт.: Виноградов Р. И., Воскобойник М. С., Миртов К. Д., Требушко О. Н.

8. Воскобойник М. С., Миленький Ю. Д., Ушаков В. С. Приближенные расчеты конструкции самолета. Изд. РКИИ ГА, 1969, 131 с.

9. Гудков А. И., Лешаков П. С. Внешние нагрузки и прочность летательных аппаратов. М., «Машиностроение», 1968, 470 с.

10. Егер С. М. Проектирование пассажирских реактивных самолетов. М., «Машиностроение», 1964, 452 с.

11. Кан С. Н., Свердлов И. А. Расчет самолета на прочность. М., «Машиностроение», 1966, 519 с.

12. Вертолеты. Ч. I и II. М., «Машиностроение», 1967. Ч. I, 455 с., ч. II, 424 с. Авт.: Миль М. Л., Некрасов А. В., Браверман А. С., Гродко Л. Н., Лейканд М. А.

13. Шульженко М. Н., Мостовой А. С. Курс конструкции самолетов. М., Машгиз, 1965, 563 с.

14. Teichmann F. K. Airplane Design Manual. Pitman Publishing Corporation. New York, 1958.